RARE ENDOCRINE AND NEUROENDOCRINE TUMORS: GENETICS AND MOLECULAR ASPECTS

EDITED BY: Barbara Altieri, Antongiulio Faggiano and Enzo Lalli
PUBLISHED IN: Frontiers in Endocrinology

frontiers Research Topics

frontiers

ISSN 1664-8714
ISBN 978-2-88976-290-3
DOI 10.3389/978-2-88976-290-3

About Frontiers

Frontiers is more than just an open-access publisher of scholarly articles: it is a pioneering approach to the world of academia, radically improving the way scholarly research is managed. The grand vision of Frontiers is a world where all people have an equal opportunity to seek, share and generate knowledge. Frontiers provides immediate and permanent online open access to all its publications, but this alone is not enough to realize our grand goals.

Frontiers Journal Series

The Frontiers Journal Series is a multi-tier and interdisciplinary set of open-access, online journals, promising a paradigm shift from the current review, selection and dissemination processes in academic publishing. All Frontiers journals are driven by researchers for researchers; therefore, they constitute a service to the scholarly community. At the same time, the Frontiers Journal Series operates on a revolutionary invention, the tiered publishing system, initially addressing specific communities of scholars, and gradually climbing up to broader public understanding, thus serving the interests of the lay society, too.

Dedication to Quality

Each Frontiers article is a landmark of the highest quality, thanks to genuinely collaborative interactions between authors and review editors, who include some of the world's best academicians. Research must be certified by peers before entering a stream of knowledge that may eventually reach the public - and shape society; therefore, Frontiers only applies the most rigorous and unbiased reviews.
Frontiers revolutionizes research publishing by freely delivering the most outstanding research, evaluated with no bias from both the academic and social point of view. By applying the most advanced information technologies, Frontiers is catapulting scholarly publishing into a new generation.

What are Frontiers Research Topics?

Frontiers Research Topics are very popular trademarks of the Frontiers Journals Series: they are collections of at least ten articles, all centered on a particular subject. With their unique mix of varied contributions from Original Research to Review Articles, Frontiers Research Topics unify the most influential researchers, the latest key findings and historical advances in a hot research area! Find out more on how to host your own Frontiers Research Topic or contribute to one as an author by contacting the Frontiers Editorial Office: frontiersin.org/about/contact

RARE ENDOCRINE AND NEUROENDOCRINE TUMORS: GENETICS AND MOLECULAR ASPECTS

Topic Editors:
Barbara Altieri, University Hospital of Wuerzburg, Germany
Antongiulio Faggiano, Sapienza University of Rome, Italy
Enzo Lalli, UMR7275 Institut de Pharmacologie Moléculaire et Cellulaire (IPMC), France

Citation: Altieri, B., Faggiano, A., Lalli, E., eds. (2022). Rare Endocrine and Neuroendocrine Tumors: Genetics and Molecular Aspects. Lausanne: Frontiers Media SA. doi: 10.3389/978-2-88976-290-3

Table of Contents

frontiers in Endocrinology

ORIGINAL RESEARCH
published: 13 November 2020
doi: 10.3389/fendo.2020.597878

Impact of the Chemokine Receptors CXCR4 and CXCR7 on Clinical Outcome in Adrenocortical Carcinoma

Irina Chifu[1†], Britta Heinze[1†], Carmina T. Fuss[1], Katharina Lang[2,3], Matthias Kroiss[1,4], Stefan Kircher[5], Cristina L. Ronchi[1,2,3], Barbara Altieri[1], Andreas Schirbel[4,6], Martin Fassnacht[1,4] and Stefanie Hahner[1,4]*

[1] Division of Endocrinology and Diabetes, Department of Medicine I, University Hospital of Wuerzburg, University of Wuerzburg, Wuerzburg, Germany, [2] Institute of Metabolism and Systems Research, University of Birmingham, Birmingham, United Kingdom, [3] Centre for Endocrinology, Diabetes and Metabolism, Birmingham Health Partners, Birmingham, United Kingdom, [4] Comprehensive Cancer Center Mainfranken, University of Wuerzburg, Wuerzburg, Germany, [5] Institute of Pathology, Interdisciplinary Bank of Biomaterials and Data (ibdw), University of Wuerzburg, Wuerzburg, Germany, [6] Department of Nuclear Medicine, University Hospital of Wuerzburg, University of Wuerzburg, Wuerzburg, Germany

OPEN ACCESS

Edited by:
Vincenzo Pezzi, University of Calabria, Italy

Reviewed by:
Yuto Yamazaki, Tohoku University Graduate School of Medicine, Japan
Sandra Sigala, University of Brescia, Italy

***Correspondence:**
Britta Heinze
heinze_b@ukw.de

[†]*These authors have contributed equally to this work*

Specialty section:
This article was submitted to Cancer Endocrinology, a section of the journal Frontiers in Endocrinology

Received: *22 August 2020*
Accepted: *20 October 2020*
Published: *13 November 2020*

Citation:
Chifu I, Heinze B, Fuss CT, Lang K, Kroiss M, Kircher S, Ronchi CL, Altieri B, Schirbel A, Fassnacht M and Hahner S (2020) Impact of the Chemokine Receptors CXCR4 and CXCR7 on Clinical Outcome in Adrenocortical Carcinoma. Front. Endocrinol. 11:597878. doi: 10.3389/fendo.2020.597878

Chemokine receptors have a negative impact on tumor progression in several human cancers and have therefore been of interest for molecular imaging and targeted therapy. However, their clinical and prognostic significance in adrenocortical carcinoma (ACC) is unknown. The aim of this study was to evaluate the chemokine receptor profile in ACC and to analyse its association with clinicopathological characteristics and clinical outcome. A chemokine receptor profile was initially evaluated by quantitative PCR in 4 normal adrenals, 18 ACC samples and human ACC cell line NCI-H295. High expression of CXCR4 and CXCR7 in both healthy and malignant adrenal tissue and ACC cells was confirmed. In the next step, we analyzed the expression and cellular localization of CXCR4 and CXCR7 in ACC by immunohistochemistry in 187 and 84 samples, respectively. These results were correlated with clinicopathological parameters and survival outcome. We detected strong membrane expression of CXCR4 and CXCR7 in 50% of ACC samples. Strong cytoplasmic CXCR4 staining was more frequent among samples derived from metastases compared to primaries (p=0.01) and local recurrences (p=0.04). CXCR4 membrane staining positively correlated with proliferation index Ki67 (r=0.17, p=0.028). CXCR7 membrane staining negatively correlated with Ki67 (r=–0.254, p=0.03) but positively with tumor size (r=0.3, p=0.02). No differences in progression-free or overall survival were observed between patients with strong and weak staining intensities for CXCR4 or CXCR7. Taken together, high expression of CXCR4 and CXCR7 in both local tumors and metastases suggests that some ACC patients might benefit from CXCR4/CXCR7-targeted therapy.

Keywords: chemokine receptor, prognosis, adrenocortical carcinoma, CXCR4, CXCR7

INTRODUCTION

Chemokines and their receptors play a major role in immune cell trafficking in both physiological and pathological settings (1, 2). They are an active component of the tumor microenvironment, driving tumor-specific immune responses and promoting invasion, metastasis, stemness and resistance to chemo- and radiotherapy (1, 2). Recently, expression of CXCR4 was reported in primary tumors and metastatic lesions of patients with ACC both at protein level *in vitro* and *in vivo* using radiolabeled CXCR4 ligands (3, 4).

CXCR4, a classical transmembrane G protein-coupled receptor, has been associated with more aggressive tumor phenotypes and poor prognosis in several cancer types (5–8). Its ligand CXCL12 (SDF-1) is highly abundant in tissues that are common sites of metastasis such as lymph nodes, lung or bone, suggesting a specific chemokine-mediated trafficking-pattern of circulating tumor cells (6, 9, 10). CXCR7, an atypical chemokine receptor with a ten times higher affinity for CXCL12 compared to CXCR4, was detected at protein level in ACC metastases and correlated with CXCR4 expression (4). CXCR7 can generate CXCL12 gradients for CXCR4 but also acts as a CXCL12 "scavenger", as it is constantly recycled to the cell membrane after ligand binding (11, 12). In cancer, CXCR7 mainly promotes local tumor growth and angiogenesis (11–13).

In recent years, CXCR4 has emerged as a potential target for cancer treatment with a particular focus on cancer stem cells that are regarded as chemotherapy-resistant (14–17) and several CXCR4 antagonists have shown promising therapeutic effects in first studies (18–20). Furthermore, radiotracers for non-invasive *in vivo* characterization of CXCR4 expression have entered clinical evaluation (21–25). However, only one CXCR4 antagonist (Plerixafor®) has been approved for therapeutic purposes for stem cell apheresis in multiple myeloma and lymphoma (26). The main limitations in developing a CXCR4 and/or CXCR7-targeted therapy are not only of biological nature due to the important roles of both chemokine receptors in the normal physiology, but also due to technical limitations. Only few antibodies are available and the prognostic impact of CXCR4 and CXCR7 is not consistent among different cellular localizations. Cell membrane localization mostly reflects the activated state of the chemokine receptor and has been associated with a worse prognosis in esophageal cancer for CXCR7 and in gastric and breast cancer for CXCR4 especially due to enhanced metastasis (27–29). On the contrary, high cytoplasmic CXCR4 localization was reported to be favorable for triple-negative breast cancer and adenocarcinoma of the lung (30, 31) but has been independently associated with lymph node metastasis of breast cancer in another analysis (32).

The aim of our study was to describe the chemokine receptor profile in ACC, focusing in particular on CXCR4 and CXCR7 and their prognostic relevance.

Abbreviations: ACC, adrenocortical carcinoma; IHC, immunohistochemistry; qRT-PCR, quantitative real-time polymerase chain reaction; RT, room temperature; FFPE, formalin fixed paraffin-embedded; ENSAT, European Network for the Study of Adrenal Tumors; OS, overall survival; PFS, progression-free survival; PET/CT, Positron Emission Tomography/Computed Tomography.

MATERIAL AND METHODS

Study Subjects

We included patients with histologically confirmed ACC and available formalin fixed paraffin-embedded (FFPE) specimens, who were treated at our center since 2004. The following clinical and histopathological characteristics were assessed: sex, age at diagnosis, tumor size, Ki67 proliferation index, Weiss score, staging according to ENSAT classification (33), hormone secretion, presence of distant metastases and specific anti-tumor treatments (**Table 1**). The study was approved by the ethics committee of the University of Wuerzburg (No. 88/11). Patients had given written informed consent for tissue collection and analysis of clinical data.

Gene Expression Analysis

Chemokine receptor mRNA expression levels were investigated by quantitative real-time polymerase chain reaction (qRT-PCR). Adrenocortical tissue is composed of different cell entities and leukocyte infiltration in tumor tissue might have influenced chemokine receptor levels detected by qRT-PCR. We therefore also analyzed the chemokine receptor profile in a total of 13 adrenocortical NCI-H295 cancer cell line samples obtained from 3 different sources. RNA was isolated from fresh frozen tissue of eighteen ACCs (not included in the IHC cohort) and four normal human adrenal glands using the RNeasy Lipid Tissue Minikit (Qiagen, Hilden, Germany) and from the human adrenocortical cancer cell line NCI-H295 using the RNeasy Mini Kit (Qiuagen). Reverse transcription of RNA was performed using the QuantiTect Reverse Transcription Kit (Qiagen), as previously described (34). The following Taqman Gene Expression assays from Applied Biosystems (Darmstadt, Germany) were used to analyze the chemokine receptor profile: *CCR1* (Hs 00928897_s1), *CCR2* (Hs 00704702_s1), *CCR3* (Hs 01847760_s1), *CCR4* (Hs 00747615_s1), *CCR5* (Hs99999149_s1), *CCR6* (Hs 10890706_s1), *CCR7* (Hs01013469_m1), *CCR8* (Hs 00174764_m1), *CCR9* (Hs01890924_s1), *CCR10* (Hs00706455_s1), *CCR11* (Hs00664347_s1), *CXCR1* (Hs 01921207_s1), *CXCR2* (Hs 01891184_s1), *CXCR3* (Hs01847760_s1), *CXCR4* (Hs00607978_s1), *CXCR5* (Hs00540548_s1), *CXCR6* (Hs01890898_s1), *CXCR7* (Hs00664172_s1) and *CX3CR1* (Hs 01922583_s1). Endogenously expressed *β-actin* (Hs9999903_m1) was used for normalization. 40 ng cDNA was used for each PCR reaction. qRT-PCR was performed three times for each cell line. Transcript levels were determined using the TaqMan Gene Expression Master Mix (Applied Biosystems), the CFX96 real-time thermocycler (Bio-rad, Hercules, CA, USA) and Bio-Rad CFX Manager 2.0 software. Cycling conditions were 95°C for three min followed by 50 cycles of 95°C for 30 s, 60°C for 30 s, and 72°C for 30 s. Using the ΔCT method, the gene expression levels were normalized to those of *β-actin*, as previously described (35).

NCI-H295 Cell Culture

The human adrenocortical cancer cell line NCI-H295 was obtained from American Type Culture Collection (ATCC, Rockville, MD, USA). NCI-H295 cells were cultured with RPMI-1640 medium supplemented with 10% FCS, insulin (5 μg/ml), transferrin (100 μg/ml) and sodium selenite (5.2 ng/ml).

TABLE 1 | Clinical parameters of ACC patients (n=187).

Sex	
Male, n (%)	62 (33)
Age at diagnosis, y (mean±SD)	49±15
ENSAT stage, n (%)	
I	12 (6)
II	85 (45)
III	40 (21)
IV	53 (28)
Unknown	5 (3)
Tumor size (cm), mean±SD	12±5.4
Hormone secretion, n (%)	
Yes	98 (52)
Cortisol	75 (77)
Androgens/estrogens/progesterone	54 (55)
Mineralocorticoids	9 (9)
No	33 (18)
Unknown	56 (30)
Ki67 (%), n (%)	
Low (<10)	38 (20)
High (≥10)	125 (67)
Unknown	24 (13)
Weiss score[a], n (%)	
Low (≤6)	100 (53)
High (>6)	52 (28)
Unknown	35 (19)
Resection status, n (%)	
R0	94 (50)
R1	16 (9)
R2	25 (13)
Rx	20 (11)
Unknown	30 (16)
Surgically not removed	2 (1)
Mitotane, n (%)	
Yes	153 (82)
No	21 (11)
Unknown	13 (7)
Chemotherapy, n (%)	
No	48 (26)
Unknown	14 (7)
Yes	125 (67)
EDP[b]	99 (79)
EP[c]	11 (9)
Gemcitabine/Capecitabine	60 (48)
Streptozotocin	68 (54)
Other	61 (49)
Radiotherapy (primary tumor and/or metastases), n (%)	
Yes	52 (28)
No	121 (65)
Unknown	14 (7)
Additional surgery, n (%)	
Yes	71 (38)
No	103 (55)
Unknown	13 (7)

[a]*Divided into low and high according to mean.*
[b]*E, etoposide; D, doxorubicin; P, platinum compound (Cisplatin/Carboplatin).*
[c]*E, etoposide; P, platinum compound (Cisplatin/Carboplatin).*

Medium was changed every 48–72 h. 30% of the conditioned culture medium was used for passaging. Cells were frozen for RNA extraction. Short tandem repeat-profiling confirmation was performed.

Immunohistochemistry

Immunohistochemistry was performed in 187 FFPE unmatched ACC specimens (159 primary tumors, 17 local recurrences, 11 metastases). Standard full slides (n=95) were available for the analysis of both chemokine receptors. Staining for CXCR7 was evaluable in n=84. The expression of CXCR4 was additionally assessed on tissue microarrays (TMA) (n=92). The tissue sections were deparaffinized in xylene and rehydrated in ethanol (100, 90, 80, and 70% each concentration for 5 min). Immunohistochemical detection was performed using an indirect immunoperoxidase technique after high temperature antigen retrieval in 10 mM citric acid monohydrate buffer (pH 6.5) in a pressure cooker for 13 min. Blocking of unspecific protein-antibody interactions was performed with 20% human AB serum in PBS for 1 h at room temperature (RT). Primary CXCR4 antibody (Abcam, UMB2; 124824) and CXCR7 antibody (Abcam, 38089) were used at a dilution of 1:100 at RT for 1 h. Signal amplification was achieved by En-Vision System Labeled Polymer-HRP (Dako) for 40 min and developed for 10 min with DAB Substrate Kit (Vector Laboratories, Burlingame, CA, USA) according to the manufacturer's instructions. Mayer's hematoxylin was used for the counterstaining of nuclei. Negative controls were carried out by treating the slides with N-Universal Negative Control Anti-Rabbit (Dako, Glostrup, Denmark) instead of the primary antibody, yielding a nearly complete loss of staining with only some faint background.

All slides were evaluated independently by three investigators blinded to patients' clinicopathological data. Staining intensity was evaluated with a grading score of 0, 1, 2, or 3, which corresponded to negative, weak, moderate, or strong staining intensity, respectively. The percentage of positive tumor cells was calculated for each specimen and scored 0 if 0% were positive, 0.1 if 1–9%, 0.5 if 10–49%, and 1 if ≥ 50%. A semi-quantitative H-score was then calculated by multiplying the staining intensity grading score with the proportion score as previously described (36). Calculation of H-score was separately performed for membrane and cytoplasmic staining. An H-score ≤ 1 was rated as low (weak staining), whereas an H-score >1 was rated as high (strong staining) for both membrane and cytoplasm, according to the median value of the staining intensity for CXCR4 and CXCR7 as previously described (30, 37). Results of the individually assessed H-scores for the TMA cores were averaged to obtain the whole-section score for each tumor sample. In case of divergent results, slides were re-evaluated by all investigators, forming the final score by consensus.

Statistical Analysis

Quantitative values were expressed as mean ± standard deviation or median and range as appropriate. Fisher's exact or chi-square tests were used to analyze dichotomic variables, whereas continuous variables were investigated with a two-sided t test or Mann-Whitney Test. *P*-values <0.05 were considered statistically significant. Correlations between the staining patterns of both chemokine receptors and the clinical and histopathological data as well as among each other were calculated by Pearson and Spearman's correlation test.

Kaplan Meier survival analysis was performed to investigate the correlation between each chemokine receptor and

prognosis. Progression-free survival (PFS) was defined as the time from the date of first surgery to the first radiological evidence of disease progression or death from ACC. Overall survival (OS) was defined as the time from the date of first diagnosis to the time of death or last follow-up. Differences between survival curves were assessed by the log-rank (Mantel-Cox) test and the factors considered to independently influence survival were analyzed by Cox proportional hazard regression.

All statistical tests were performed using SPSS Statistics Version 23 (IBM) and GraphPad Prism version 8.4.1 (GraphPad, La Jolla, CA).

RESULTS

mRNA Expression of Chemokine Receptors in Adrenal Tissues and NCI-H295 Cells

Relative mRNA expression of different CCR- and CXC-chemokine receptors in the normal adrenal glands (n=4) and in adrenocortical carcinomas (n=18) is reported in **Figure 1**. Each point represents the result obtained from the qRT-PCR analysis performed for a single cell sample. The highest mRNA expression levels in all analyzed samples were found for CXCR4 and CXCR7. Normal adrenals exhibited significantly higher mRNA levels for CXCR4 compared to ACCs (mean mRNA expression 1.5-fold higher in normal adrenals, $p<0.01$). CXCR4 mRNA levels in NCI-H295 were similar to those found in ACC ($p=0.06$) and normal adrenals ($p=0.13$), whereas CXCR7 mRNA levels in NCI-H295 were significantly lower compared to both ACC (46-fold lower, $p<0.01$) and normal adrenals (11-fold lower, $p<0.01$).

Immunohistochemical Analysis of Protein Expression of CXCR4 and CXCR7 in ACC

CXCR4 was detectable in 98% (184/187) and CXCR7 in 100% of cases (84/84). Localization at the cell membrane was preponderant for both chemokine receptors (**Figure 2**). Strong membrane staining (H-score >1) was observed in 50% of specimens both for CXCR4 (94 out 187) and CXCR7 (42 out 84 sections) (**Table 2**). Membranous and cytoplasmic staining significantly correlated for CXCR4 ($r_s=0.45$, $p<0.01$) but not for CXCR7 ($r=0.07$, $p=0.5$). A weak correlation between the two chemokine receptors could only be seen at the cytoplasmic level ($r_s=0.32$, $p<0.01$). The proportion of samples with strong CXCR4 cytoplasmic staining was higher in metastases compared to primary tumors and local recurrences ($p=0.01$ and $p=0.04$) (**Table 2**).

Correlation of CXCR4 and CXCR7 Staining Intensity and Staining Pattern With Clinicopathological Features and Clinical Outcome Data in ACC

Clinicopathological features of the 187 ACC patients with complete survival data are summarized in **Table 1**. Among the 94 patients who had an initial R0 resection status, 69 (73%) developed metastases at follow-up. ENSAT tumor stage did not correlate with the staining intensity of CXCR4 or CXCR7. At membrane level, we found a weak positive correlation between CXCR4 and Ki67 ($r_s=0.17$, $p=0.028$). In contrast, a weak negative correlation between CXCR7 and Ki67 was noted ($r_s=-0.254$,

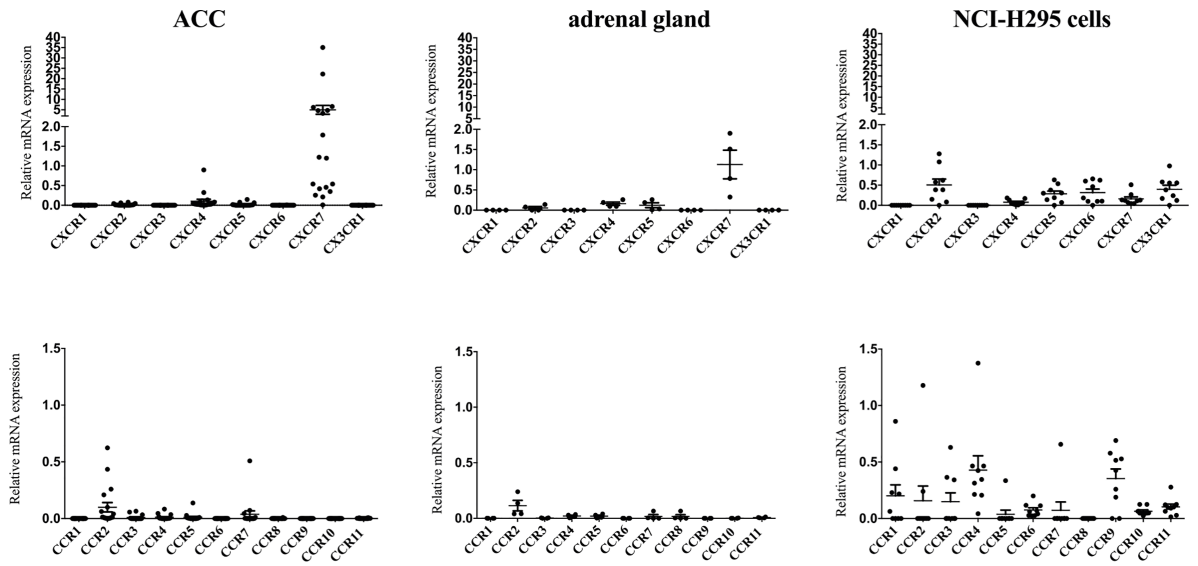

FIGURE 1 | Quantitative analysis of chemokine receptor mRNA levels in adrenal tissues and NCI-H295R cells. mRNA levels of chemokine receptors were assessed by real time PCR in 18 adrenocortical carcinomas, 4 normal adrenal glands and the human adrenocortical carcinoma cell line NCI-H295R. Levels were normalized to *β-actin*. Data are given as mean ± SEM.

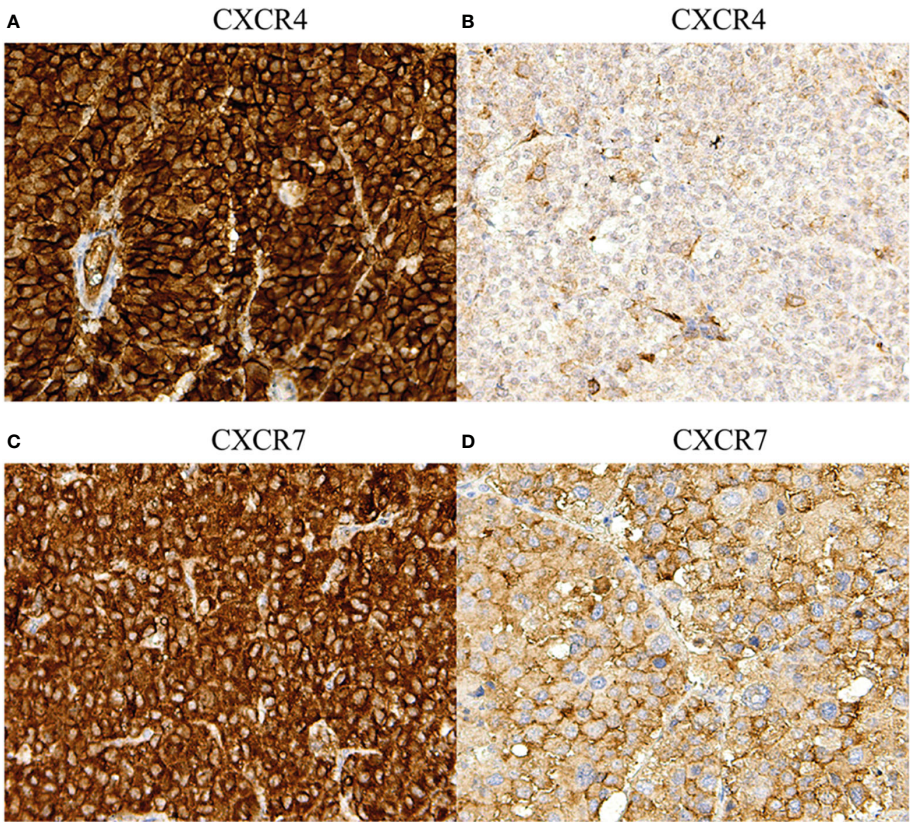

FIGURE 2 | Immunohistochemical staining of CXCR4 and CXCR7 in adrenocortical carcinoma: different staining patterns. **(A)** Primary tumor, strong membranous and cytoplasmic CXCR4 staining (magnification 20x), **(B)** primary tumor, weak membranous and cytoplasmic CXCR4 staining (magnification 20x), **(C)** primary tumor, strong membranous and cytoplasmic CXCR7 staining (magnification 20x), **(D)** primary tumor, weak membranous and cytoplasmic CXCR7 staining (magnification 20x).

TABLE 2 | Distribution of strong and weak cytoplasmic staining of CXCR4 among primary tumors (PT), local recurrences (LR) and metastases (M).

CXCR4	PT(n=159)	LR(n=17)	M(n=11)	p		
				PT vs M	LR vs M	PT vs LR
Cytoplasmic staining						
Strong	34 (21%)	3 (18%)	6 (55%)	0.01	0.01	ns
Weak	125 (79%)	14 (82%)	5 (45%)			
H-score (mean±SD)	1.0±0.8	0.9±0.5	1.6±1.3	ns	ns	ns
Membrane staining						
Strong	80 (50%)	9 (53%)	5 (46%)	ns	ns	ns
Weak	79 (50%)	8 (43%)	6 (54%)			
H-score (mean±SD)	1.4±1.0	1.1±0.9	1.1±1.2	ns	ns	ns

p=0.03), whereas membranous CXCR7 staining was positively correlated with tumor size (r=0.3, p=0.02).

Kaplan-Meier analyzes for OS and PFS revealed no significant differences between patients with high and low expression of the chemokine receptors regardless of their cellular localization, neither in the whole cohort (**Figures 3** and **4**), nor in the subgroup of patients with initial R0 resection (data not shown). In the subgroup of patients with markers of more favourable prognosis (ENSAT stage I–II, n=94; Ki67 <10%, n=38), mean PFS was significantly longer in cases with strong CXCR7 cytoplasmic staining compared to cases with weak CXCR7 cytoplasmic staining (25±21 *vs.* 12±11 months, p=0.04, for ENSAT I-II, and 34±4 *vs.* 8±6 months, p=0.02, for Ki67<10%). However, multivariate analysis did not confirm the

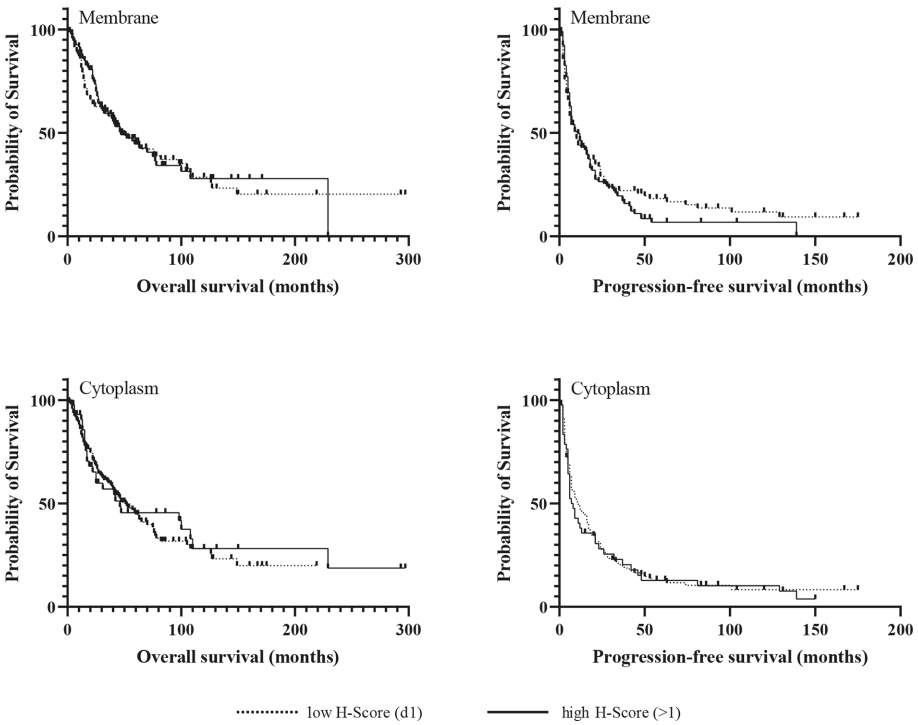

FIGURE 3 | Kaplan-Meir survival analysis for overall and progression-free survival according to membranous and cytoplasmic CXCR4 expression.

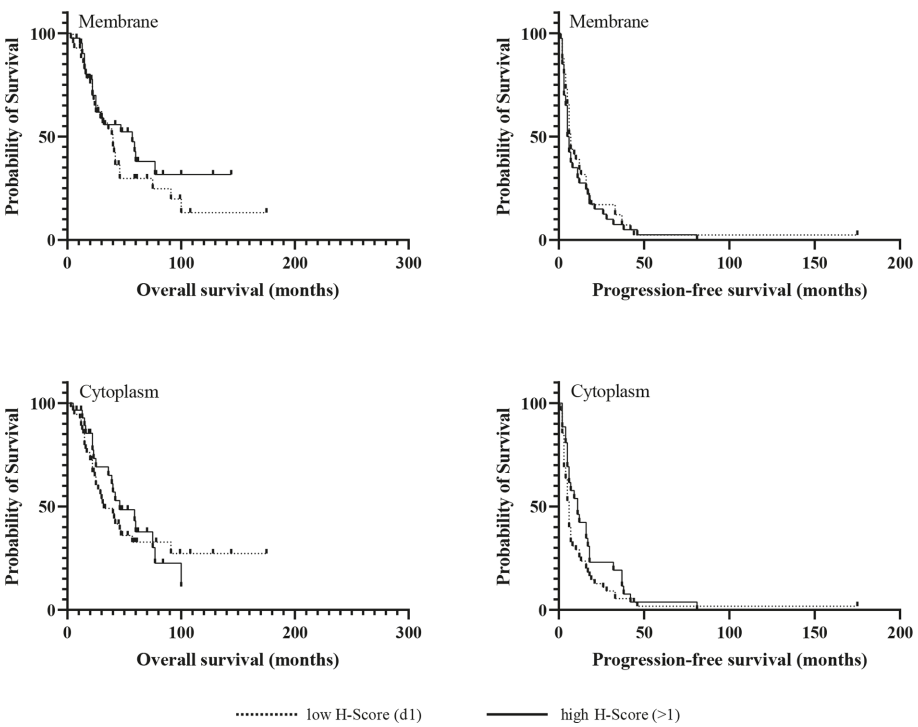

FIGURE 4 | Kaplan-Meir survival analysis for overall and progression-free survival according to membranous and cytoplasmic CXCR7 expression.

significant association between the cytoplasmic CXCR7 staining and PFS seen in the univariate analysis in this subgroup (**Table 3**).

DISCUSSION

To our knowledge, this is the largest study that describes the immunohistochemical expression pattern of both chemokine receptors CXCR4 and CXCR7 in ACC and the first one that analyzes their correlation with clinicopathological parameters and clinical outcome.

We demonstrate that both chemokine receptors are highly expressed in most ACCs especially at membrane level. However, different from observations made in other malignancies, CXCR4 nor CXCR7 expression was neither associated with the occurrence of metastases nor with survival. Since both chemokine receptors are present at high levels also in normal adrenocortical tissue, it can be assumed that CXCR4 and CXCR7 are constitutively expressed by the adrenal gland and are mainly relevant for maintaining adrenal homeostasis. A recent publication from our group revealed particularly strong CXCR4 expression in the subcapsular region of the normal adrenal cortex (38), which also hosts the adrenocortical stem/progenitor cell niche (39, 40), whereas CXCR7 was uniformly distributed within all adrenocortical zones (38). A possible role for CXCR4 in the differentiation and zonation of the adrenal cortex along complimentary CXCL12 gradients was assumed (38). CXCR7, on the other hand, might be involved in less zone-specific processes such as angiogenesis or tissue repair.

Nevertheless, CXCR4 and CXCR7 might still be of therapeutic interest for ACC in the light of upcoming theranostic concepts. Especially the predominant membrane localization is of advantage as it allows direct inactivation of the chemokine receptors by ligand binding. For CXCR4, suitable radioligands are available and have been successfully tested in lymphoproliferative malignancies (19–21). Two of these radioligands, ^{64}Cu-plerixafor and ^{68}Ga-Pentixafor, can also reliably assess the expression of CXCR4 *in vivo* in patients affected by ACC or aldosterone producing adenoma, respectively (4, 38). Bluemel et al. went a step further towards a potential theranostic use of CXCR4 and compared the performance of ^{68}Ga-pentixafor PET/CT with ^{18}F-FDG PET/CT in 30 patients with advanced ACC (3). Overall, at least two thirds of the patients were rated as suitable or potentially suitable for a CXCR4-directed endoradiotherapy based on the number of lesions identified by ^{68}Ga-pentixafor PET and the intensity of the tracer uptake (3).

The correlation between CXCR4 and Ki67 at membrane level suggests that the activated form of the chemokine receptor is preferentially upregulated in highly proliferative ACCs, that are known to have a dismal prognosis even after complete resection (41). Effectively blocking CXCR4 might therefore interfere with tumor growth and metastasis in ACC *in vivo*, as also highlighted by the inhibitory effect of the CXCR4 antagonist AMD3100 on the proliferation and migration of the human ACC cell line NCI-H295 reported by Kitawaki et al. (42).

The response to immunotherapy in ACC might also benefit from antagonizing CXCR4, as shown for hepatocellular carcinoma (43), pancreatic (44), breast (45) and ovarian cancer (46). These tumors escape immunosurveillance and respond poorly to immune checkpoint inhibitors due to their immunosuppressive milieu. One of the common mediators of cancer immunoresistance is the CXCL12/CXCR4 pathway due to enhanced recruitment of immunosuppressive cells in the tumor microenvironment (47). Combined blockade of CXCR4 and PD-1/PD-L1 increases antitumor immunity and significantly improves the response to immune checkpoint inhibitors (47). According to a recent analysis of the immune landscape in cancer, ACC also belongs to the leukocyte depleted tumors ("immunologically quiet") (48). Therefore, the modest tumor

TABLE 3 | Relationship between the immunhistochemical expression of CXCR4 and CXCR7 and progression-free survival in the subgroup of patients diagnosed at an early ENSAT stage (I–II), univariate and multivariate analysis for risk of death.

	Univariate		Multivariate	
	HR(95% CI)	**p**	**HR(95% CI)**	**p**
CXCR4 membrane expression				
weak (≤ 1)				
strong (>1)	0.8 (0.5–1.3)	ns		
CXCR4 cytoplasmic expression				
weak (≤ 1)				
strong (>1)	1.1 (0.7–1.9)	ns		
CXCR7 membrane expression				
weak (≤ 1)				
strong (>1)	1.1 (0.6–1.9)	ns		
CXCR7 cytoplasmic expression			0.5 (0.2–1.1)	0.1
weak (≤ 1)				
strong (>1)	2 (1.4–4.0)	0.04		
Ki67			1.2 (0.4–3.1)	0.7
low (<10%)				
high (≥10%)	1.8 (1.1–2.9)	0.02		
Weiss Score[a]			1.5 (0.7–3.3)	0.2
low (≤6)				
high (>6)	2.1 (1.1–3.9)	<0.01		
Tumor size[a]				
low (<12 cm)				
high (≥12 cm)	1.4 (0.9–2.3)	ns		
Resection status				
R0				
R1/2/x	1.1 (0.6–2.1)	ns		
Sex				
male				
female	1.0 (0.6–1.7)	ns		
Age	0.9 (0.9–1.0)	ns		
Cortisol secretion				
no				
yes	0.8 (0.5–1.3)	ns		

[a]*Divided into low and high according to mean.*
HR, hazard ratio; 95% CI, 95% confidence interval.

response to PD-1/PD-L1 directed therapy, with a best median overall-survival of 24.9 months, is not surprising (49–51). However, recently published data from our group identified a subset of ACCs with preserved cytotoxic T-cell infiltration and significantly improved overall survival, especially in the absence of glucocorticoid excess (52). Therefore, activating tumor immunity in leukocyte depleted ACCs could be strategical in improving the response to immune checkpoint inhibitors. Several mechanisms related to leukocyte depletion and immunoresistance in ACC, such as glucocorticoid excess, upregulation of WNT/β-catenin pathway or TP53 mutations, are also associated with upregulation of CXCR4 (49–51). Glucocorticoid excess, even if not clinically manifest, is approached in the majority of cases by adrenolytic therapy with mitotane, but pharmacological targeting of WNT/β-catenin and TP53 pathways is not yet available (49, 50). Therefore, CXCR4-targeted therapies might overcome immunoresistance in ACC by simultaneously blocking multiple pathways.

As the CXCR4-specific tracer CPCR4 can be labeled with Lutetium-177 (53) and Yttrium-90 (54), endoradiotherapy of ACC may emerge as a future treatment option for patients with ACC. However, this approach requires harvesting stem cells prior to treatment initiation due to hematologic toxicity (55). This could be compromised in patients pretreated with several myelotoxic chemotherapy regimens, as is often the case with ACC.

Opposite to CXCR4, the intensity of CXCR7 membrane staining was inversely correlated with Ki67 but positively correlated with tumor size, describing thus a rather slow-growing local tumor pattern, as also reported for CXCR7-positive breast cancer samples (56). So far, one radiolabeled highly selective antibody (ACKR3-mAb) has been tested for *in vivo* assessment of CXCR7 in mice xenografted with human cancer cells showing correlation of tracer uptake with CXCR7 immunoreactivity (57).

Our study has several strengths and limitations. We assessed the immunohistochemical expression of both CXCR4 and CXCR7 in a large series of ACC samples. We used a well validated antibody shown to identify membranous and cytoplasmic CXCR4 staining both in healthy and in malignant tissues (58). However, the same antibody failed to detect CXCR4 in 25% of the analyzed ACC metastases in the study performed by Weiss et al., despite detectable CXCR4 mRNA in all samples (4). Similarly, we cannot exclude that some samples might have been classified as false-negative. We also could not investigate an equal number of tumor samples for both CXCR4 and CXCR7 and only had access to a limited pool of metastases and local recurrences unrelated to the primary tumors. Extended analyzes of the expression of both chemokine receptors and their common ligand CXCL12 not only in primary tumors but also in matched metastases together with functional studies on ACC cell lines are warranted to receive a better insight into the impact of CXCR4 and CXCR7 on the prognosis of ACC.

In summary, we could demonstrate that CXCR4 and CXCR7 are the most abundant chemokine receptors in adrenocortical carcinoma. The lack of prognostic significance and their high expression in the normal adrenal gland rather suggest a predominant role of both chemokine receptors in adrenocortical homeostasis. Nevertheless, our study provides further evidence for the theranostic potential of CXCR4 and CXCR7 in ACC, with special emphasis on potentially improving tumor response to systemic therapies.

DATA AVAILABILITY STATEMENT

The original contributions presented in the study are included in the article/supplementary materials. Further inquiries can be directed to the corresponding author.

ETHICS STATEMENT

The studies involving human participants were reviewed and approved by Ethics committee of the medical faculty of the Julius-Maximilians University Würzburg. The patients/participants provided their written informed consent to participate in this study.

AUTHOR CONTRIBUTIONS

BH and SH wrote the study protocol, were involved in applications for authorities, and supervised the conduct of the study. IC did the literature research, performed the immunohistochemical analysis, statistical analysis, and data interpretation. CF performed the qRT-PCR analysis and contributed to the immunohistochemical analysis. SK provided materials for the immunohistochemical analysis. BH, BA, CR, and KL contributed to the statistical analysis and data interpretation. IC, BH, SH, MK, MF, AS, and SK co-wrote and edited the manuscript. All authors contributed to the article and approved the submitted version.

FUNDING

This work was supported by the Deutsche Forschungsgemeinschaft (DFG) (within the CRC/Transregio 205/1 "The Adrenal: Central Relay in Health and Disease"), IZKF Würzburg (Grant No. F 365 to AS and SH), Deutsche Forschungsgemeinschaft (DFG AL 203/11-1 to AS and SH), and the Else Kröner-Fresenius Stiftung (Grant No. 2010_EKES.29 to SH).

ACKNOWLEDGMENTS

We thank Katja Marienfeld (Dept. of Medicine I, Endocrinology and Diabetology) for excellent technical assistance.

REFERENCES

1. Mollica Poeta V, Massara M, Capucetti A, Bonecchi R. Chemokines and Chemokine Receptors: New Targets for Cancer Immunotherapy. *Front Immunol* (2019) 10:379. doi: 10.3389/fimmu.2019.00379
2. Nagarsheth N, Wicha MS, Zou W. Chemokines in the cancer microenvironment and their relevance in cancer immunotherapy. *Nat Rev Immunol* (2017) 17:559–72. doi: 10.1038/nri.2017.49
3. Bluemel C, Hahner S, Heinze B, Fassnacht M, Kroiss M, Bley TA, et al. Investigating the Chemokine Receptor 4 as Potential Theranostic Target in Adrenocortical Cancer Patients. *Clin Nucl Med* (2017) 42:e29–34. doi: 10.1097/RLU.0000000000001435
4. Weiss ID, Huff LM, Evbuomwan MO, Xu X, Dang HD, Velez DS, et al. Screening of cancer tissue arrays identifies CXCR4 on adrenocortical carcinoma: correlates with expression and quantification on metastases using (64)Cu-plerixafor PET. *Oncotarget* (2017) 8:73387–406. doi: 10.18632/oncotarget.19945
5. Chatterjee S, Behnam Azad B, Nimmagadda S. The intricate role of CXCR4 in cancer. *Adv Cancer Res* (2014) 124:31–82. doi: 10.1016/B978-0-12-411638-2.00002-1
6. Sun X, Cheng G, Hao M, Zheng J, Zhou X, Zhang J, et al. CXCL12 / CXCR4 / CXCR7 chemokine axis and cancer progression. *Cancer Metastasis Rev* (2010) 29:709–22. doi: 10.1007/s10555-010-9256-x
7. Wang J, Knaut H. Chemokine signaling in development and disease. *Development* (2014) 141:4199–205. doi: 10.1242/dev.101071
8. Zhao H, Guo L, Zhao H, Zhao J, Weng H, Zhao B. CXCR4 over-expression and survival in cancer: a system review and meta-analysis. *Oncotarget* (2015) 6:5022–40. doi: 10.18632/oncotarget.3217
9. Domanska UM, Kruizinga RC, Nagengast WB, Timmer-Bosscha H, Huls G, de Vries EGE, et al. A review on CXCR4/CXCL12 axis in oncology: No place to hide. *Eur J Cancer* (2013) 49:219–30. doi: 10.1016/j.ejca.2012.05.005
10. Janssens R, Struyf S, Proost P. The unique structural and functional features of CXCL12. *Cell Mol Immunol* (2018) 15:299–311. doi: 10.1038/cmi.2017.107
11. Sanchez-Martin L, Sanchez-Mateos P, Cabanas C. CXCR7 impact on CXCL12 biology and disease. *Trends Mol Med* (2013) 19:12–22. doi: 10.1016/j.molmed.2012.10.004
12. Asri A, Sabour J, Atashi A, Soleimani M. Homing in hematopoietic stem cells: focus on regulatory role of CXCR7 on SDF1a/CXCR4 axis. *EXCLI J* (2016) 15:134–43. doi: 10.17179/excli2014-585
13. Naumann U, Cameroni E, Pruenster M, Mahabaleshwar H, Raz E, Zerwes H-G, et al. CXCR7 functions as a scavenger for CXCL12 and CXCL11. *PloS One* (2010) 5:e9175–e. doi: 10.1371/journal.pone.0009175
14. Cojoc M, Peitzsch C, Trautmann F, Polishchuk L, Telegeev GD, Dubrovska A. Emerging targets in cancer management: role of the CXCL12/CXCR4 axis. *Onco Targets Ther* (2013) 6:1347–61. doi: 10.2147/OTT.S36109
15. Eckert F, Schilbach K, Klumpp L, Bardoscia L, Sezgin EC, Schwab M, et al. Potential Role of CXCR4 Targeting in the Context of Radiotherapy and Immunotherapy of Cancer. *Front Immunol* (2018) 9:3018:3018. doi: 10.3389/fimmu.2018.03018
16. Scala S. Molecular Pathways: Targeting the CXCR4-CXCL12 Axis–Untapped Potential in the Tumor Microenvironment. *Clin Cancer Res* (2015) 21:4278–85. doi: 10.1158/1078-0432.Ccr-14-0914
17. Trautmann F, Cojoc M, Kurth I, Melin N, Bouchez L, Dubrovska A, et al. CXCR4 as Biomarker for Radioresistant Cancer Stem Cells. *Int J Radiat Biol* (2014) 90:687–99. doi: 10.3109/09553002.2014.906766
18. Galsky MD, Vogelzang NJ, Conkling P, Raddad E, Polzer J, Roberson S, et al. A phase I trial of LY2510924, a CXCR4 peptide antagonist, in patients with advanced cancer. *Clin Cancer Res* (2014) 20:3581–8. doi: 10.1158/1078-0432.CCR-13-2686
19. Nervi B, Ramirez P, Rettig MP, Uy GL, Holt MS, Ritchey JK, et al. Chemosensitization of acute myeloid leukemia (AML) following mobilization by the CXCR4 antagonist AMD3100. *Blood* (2009) 113:6206–14. doi: 10.1182/blood-2008-06-162123
20. Uy GL, Rettig MP, Motabi IH, McFarland K, Trinkaus KM, Hladnik LM, et al. A phase 1/2 study of chemosensitization with the CXCR4 antagonist plerixafor in relapsed or refractory acute myeloid leukemia. *Blood* (2012) 119:3917–24. doi: 10.1182/blood-2011-10-383406
21. Kircher M, Herhaus P, Schottelius M, Buck AK, Werner RA, Wester HJ, et al. CXCR4-directed theranostics in oncology and inflammation. *Ann Nucl Med* (2018) 32:503–11. doi: 10.1007/s12149-018-1290-8
22. Gourni E, Demmer O, Schottelius M, D'Alessandria C, Schulz S, Dijkgraaf I, et al. PET of CXCR4 expression by a (68)Ga-labeled highly specific targeted contrast agent. *J Nucl Med* (2011) 52:1803–10. doi: 10.2967/jnumed.111.098798
23. Demmer O, Dijkgraaf I, Schumacher U, Marinelli L, Cosconati S, Gourni E, et al. Design, synthesis, and functionalization of dimeric peptides targeting chemokine receptor CXCR4. *J Med Chem* (2011) 54:7648–62. doi: 10.1021/jm2009716
24. Demmer O, Gourni E, Schumacher U, Kessler H, Wester HJ. PET imaging of CXCR4 receptors in cancer by a new optimized ligand. *ChemMedChem* (2011) 6:1789–91. doi: 10.1002/cmdc.201100320
25. George GP, Pisaneschi F, Nguyen QD, Aboagye EO. Positron emission tomographic imaging of CXCR4 in cancer: challenges and promises. *Mol Imaging* (2014) 13. doi: 10.2310/7290.2014.00041
26. De Clercq E. Mozobil® (Plerixafor, AMD3100), 10 years after its approval by the US Food and Drug Administration. *Antivir Chem Chemother* (2019) 27:2040206619829382-2040206619829382. doi: 10.1177/2040206619829382
27. Lee HJ, Kim SW, Kim HY, Li S, Yun HJ, Song KS, et al. Chemokine receptor CXCR4 expression, function, and clinical implications in gastric cancer. *Int J Oncol* (2009) 34:473–80. doi: 10.3892/IJO_00000172
28. Okuyama Kishima M, de Oliveira CE, Banin-Hirata BK, Losi-Guembarovski R, Brajao de Oliveira K, Amarante MK, et al. Immunohistochemical expression of CXCR4 on breast cancer and its clinical significance. *Anal Cell Pathol (Amst)* (2015) 2015:891020. doi: 10.1155/2015/891020
29. Tachezy M, Zander H, Gebauer F, von Loga K, Pantel K, Izbicki JR, et al. CXCR7 expression in esophageal cancer. *J Transl Med* (2013) 11:238. doi: 10.1186/1479-5876-11-238
30. Shim B, Jin MS, Moon JH, Park IA, Ryu HS. High Cytoplasmic CXCR4 Expression Predicts Prolonged Survival in Triple-Negative Breast Cancer Patients Treated with Adjuvant Chemotherapy. *J Pathol Transl Med* (2018) 52:369–77. doi: 10.4132/jptm.2018.09.19
31. Minamiya Y, Saito H, Takahashi N, Ito M, Imai K, Ono T, et al. Expression of the chemokine receptor CXCR4 correlates with a favorable prognosis in patients with adenocarcinoma of the lung. *Lung Cancer (Amsterdam Netherlands)* (2009) 68:466–71. doi: 10.1016/j.lungcan.2009.07.015
32. Yasuoka H, Tsujimoto M, Yoshidome K, Nakahara M, Kodama R, Sanke T, et al. Cytoplasmic CXCR4 expression in breast cancer: induction by nitric oxide and correlation with lymph node metastasis and poor prognosis. *BMC Cancer* (2008) 8:340–. doi: 10.1186/1471-2407-8-340
33. Fassnacht M, Johanssen S, Quinkler M, Bucsky P, Willenberg HS, Beuschlein F, et al. Limited prognostic value of the 2004 International Union Against Cancer staging classification for adrenocortical carcinoma: proposal for a Revised TNM Classification. *Cancer* (2009) 115:243–50. doi: 10.1002/cncr.24030
34. Altieri B, Sbiera S, Della Casa S, Weigand I, Wild V, Steinhauer S, et al. Livin/BIRC7 expression as malignancy marker in adrenocortical tumors. *Oncotarget* (2017) 8:9323–38. doi: 10.18632/oncotarget.14067
35. Ronchi CL, Sbiera S, Altieri B, Steinhauer S, Wild V, Bekteshi M, et al. Notch1 pathway in adrenocortical carcinomas: correlations with clinical outcome. *Endocr Relat Cancer* (2015) 22:531–43. doi: 10.1530/erc-15-0163
36. Valeria L, Barbara A, Silviu S, Stefan K, Sonja S, Felix B, et al. ERCC1 as predictive biomarker to platinum-based chemotherapy in adrenocortical carcinomas. *Eur J Endocrinol* (2018) 178:181–8. doi: 10.1530/EJE-17-0788
37. Werner TA, Forster CM, Dizdar L, Verde PE, Raba K, Schott M, et al. CXCR4/CXCR7/CXCL12 axis promotes an invasive phenotype in medullary thyroid carcinoma. *Br J Cancer* (2017) 117:1837–45. doi: 10.1038/bjc.2017.364
38. Heinze B, Fuss CT, Mulatero P, Beuschlein F, Reincke M, Mustafa M, et al. Targeting CXCR4 (CXC Chemokine Receptor Type 4) for Molecular Imaging of Aldosterone-Producing Adenoma. *Hypertension* (2018) 71:317–25. doi: 10.1161/HYPERTENSIONAHA.117.09975
39. Steenblock C, Rubin de Celis MF, Delgadillo Silva LF, Pawolski V, Brennand A, Werdermann M, et al. Isolation and characterization of adrenocortical progenitors involved in the adaptation to stress. *Proc Natl Acad Sci U S A* (2018) 115:12997–3002. doi: 10.1073/pnas.1814072115

40. Lerario AM, Finco I, LaPensee C, Hammer GD. Molecular Mechanisms of Stem/Progenitor Cell Maintenance in the Adrenal Cortex. *Front Endocrinol (Lausanne)* (2017) 8:52. doi: 10.3389/fendo.2017.00052
41. Beuschlein F, Weigel J, Saeger W, Kroiss M, Wild V, Daffara F, et al. Major prognostic role of Ki67 in localized adrenocortical carcinoma after complete resection. *J Clin Endocrinol Metab* (2015) 100:841–9. doi: 10.1210/jc.2014-3182
42. Kitawaki Y, Morimoto R, Satoh F, Sasano H. SUN-335 The Chemokine Receptor 4 (CXCR4) Plays an Important Role in Adrenocortical Carcinoma Cell Proliferation. *J Endocr Soc* (2019) 3:SUN–335. doi: 10.1210/js.2019-SUN-335
43. Chen Y, Ramjiawan RR, Reiberger T, Ng MR, Hato T, Huang Y, et al. CXCR4 inhibition in tumor microenvironment facilitates anti-programmed death receptor-1 immunotherapy in sorafenib-treated hepatocellular carcinoma in mice. *Hepatology* (2015) 61:1591–602. doi: 10.1002/hep.27665
44. Seo YD, Jiang X, Sullivan KM, Jalikis FG, Smythe KS, Abbasi A, et al. Mobilization of CD8(+) T Cells via CXCR4 Blockade Facilitates PD-1 Checkpoint Therapy in Human Pancreatic Cancer. *Clin Cancer Res an Off J Am Assoc Cancer Res* (2019) 25:3934–45. doi: 10.1158/1078-0432.CCR-19-0081
45. Chen IX, Chauhan VP, Posada J, Ng MR, Wu MW, Adstamongkonkul P, et al. Blocking CXCR4 alleviates desmoplasia, increases T-lymphocyte infiltration, and improves immunotherapy in metastatic breast cancer. *Proc Natl Acad Sci U S A* (2019) 116:4558–66. doi: 10.1073/pnas.1815515116
46. Zeng Y, Li B, Liang Y, Reeves PM, Qu X, Ran C, et al. Dual blockade of CXCL12-CXCR4 and PD-1-PD-L1 pathways prolongs survival of ovarian tumor-bearing mice by prevention of immunosuppression in the tumor microenvironment. *FASEB J* (2019) 33:6596–608. doi: 10.1096/fj.201802067RR
47. Zhou W, Guo S, Liu M, Burow ME, Wang G. Targeting CXCL12/CXCR4 Axis in Tumor Immunotherapy. *Curr Med Chem* (2019) 26:3026–41. doi: 10.2174/0929867324666170830111531
48. Thorsson V, Gibbs DL, Brown SD, Wolf D, Bortone DS, Ou Yang T-H, et al. The Immune Landscape of Cancer. *Immunity* (2018) 48:812–30. doi: 10.1016/j.immuni.2018.03.023
49. Fiorentini C, Grisanti S, Cosentini D, Abate A, Rossini E, Berruti A, et al. Molecular Drivers of Potential Immunotherapy Failure in Adrenocortical Carcinoma. *J Oncol* (2019) 2019:6072863–. doi: 10.1155/2019/6072863
50. Cosentini D, Grisanti S, Dalla Volta A, Laganà M, Fiorentini C, Perotti P, et al. Immunotherapy failure in adrenocortical cancer: where next? *Endocr Connections* (2018) 7:E5–8. doi: 10.1530/EC-18-0398
51. Altieri B, Ronchi CL, Kroiss M, Fassnacht M. Next-generation therapies for adrenocortical carcinoma. *Best Pract Res Clin Endocrinol Metab* (2020) 34:101434. doi: 10.1016/j.beem.2020.101434
52. Landwehr L-S, Altieri B, Schreiner J, Sbiera I, Weigand I, Kroiss M, et al. Interplay between glucocorticoids and tumor-infiltrating lymphocytes on the prognosis of adrenocortical carcinoma. *J Immunother Cancer* (2020) 8:e000469. doi: 10.1136/jitc-2019-000469
53. Schottelius M, Osl T, Poschenrieder A, Hoffmann F, Beykan S, Hanscheid H, et al. [(177)Lu]pentixather: Comprehensive Preclinical Characterization of a First CXCR4-directed Endoradiotherapeutic Agent. *Theranostics* (2017) 7:2350–62. doi: 10.7150/thno.19119
54. Osl T, Schmidt A, Schwaiger M, Schottelius M, Wester H-J. A new class of PentixaFor- and PentixaTher-based theranostic agents with enhanced CXCR4-targeting efficiency. *Theranostics* (2020) 10:8264–80. doi: 10.7150/thno.45537
55. Maurer S, Herhaus P, Lippenmeyer R, Hanscheid H, Kircher M, Schirbel A, et al. Side Effects of CXC-Chemokine Receptor 4-Directed Endoradiotherapy with Pentixather Before Hematopoietic Stem Cell Transplantation. *J Nucl Med* (2019) 60:1399–405. doi: 10.2967/jnumed.118.223420
56. Hernandez L, Magalhaes MAO, Coniglio SJ, Condeelis JS, Segall JE. Opposing roles of CXCR4 and CXCR7 in breast cancer metastasis. *Breast Cancer Res* (2011) 13:R128–R. doi: 10.1186/bcr3074
57. Behnam Azad B, Lisok A, Chatterjee S, Poirier JT, Pullambhatla M, Luker GD, et al. Targeted Imaging of the Atypical Chemokine Receptor 3 (ACKR3/CXCR7) in Human Cancer Xenografts. *J Nucl Med* (2016) 57:981–8. doi: 10.2967/jnumed.115.167932
58. Fischer T, Nagel F, Jacobs S, Stumm R, Schulz S. Reassessment of CXCR4 chemokine receptor expression in human normal and neoplastic tissues using the novel rabbit monoclonal antibody UMB-2. *PloS One* (2008) 3:e4069. doi: 10.1371/journal.pone.0004069

Conflict of Interest: The authors declare that the research was conducted in the absence of any commercial or financial relationships that could be construed as a potential conflict of interest.

frontiers in Endocrinology

REVIEW
published: 16 November 2020
doi: 10.3389/fendo.2020.562505

mTOR Pathway in Gastroenteropancreatic Neuroendocrine Tumor (GEP-NETs)

Sara Zanini[1], *Serena Renzi*[2], *Francesco Giovinazzo*[3]* *and Giovanna Bermano*[1]*

[1] Centre for Obesity Research and Education (CORE), School of Pharmacy and Life Sciences, Robert Gordon University, Aberdeen, United Kingdom, [2] School of Biosciences and Veterinary Medicine, University of Camerino, Camerino, Italy, [3] Fondazione Policlinico Universitario A. Gemelli Istituto di ricovero e cura a carattere scientifico (IRCCS), Department of Surgery -Transplantation Service, Rome, Italy

Gastroenteropancreatic neuroendocrine neoplasms (GEP-NENs) originate from neuroendocrine cells in the gastrointestinal tract. They are heterogeneous, and though initially considered rare tumors, the incidence of GEP-NENs has increased in the last few decades. Therapeutic approaches for the metastatic disease include surgery, radiological intervention by chemoembolisation, radiofrequency ablation, biological therapy in addition to somatostatin analogs, and PRRT therapy (177Lu-DOTATATE). The PI3K-AKT-mTOR pathway is essential in the regulation of protein translation, cell growth, and metabolism. Evidence suggests that the mTOR pathway is involved in malignant progression and resistance to treatment through over-activation of several mechanisms. PI3K, one of the main downstream of the Akt-mTOR axis, is mainly involved in the neoplastic process. This pathway is frequently deregulated in human tumors, making it a central target in the development of new anti-cancer treatments. Recent molecular studies identify potential targets within the PI3K/Akt/mTOR pathway in GEP-NENs. However, the use of target therapy has been known to lead to resistance due to several mechanisms such as feedback activation of alternative pathways, inactivation of protein kinases, and deregulation of the downstream mTOR components. Therefore, the specific role of targeted drugs for the management of GEP-NENs is yet to be well-defined. The variable clinical presentation of advanced neuroendocrine tumors is a significant challenge for designing studies. This review aims to highlight the role of the PI3K/Akt/mTOR pathway in the development of neuroendocrine tumors and further specify its potential as a therapeutic target in advanced stages.

Keywords: neuroendocrine tumor, mTOR, cancer treatment, target therapy, GEP-NENs, GEP-NETs

OPEN ACCESS

Edited by:
Enzo Lalli,
UMR7275 Institut de Pharmacologie Moléculaire et Cellulaire (IPMC), France

Reviewed by:
Marco Volante,
University of Turin, Italy
Jean-Yves Scoazec,
Institut Gustave Roussy, France

***Correspondence:**
Francesco Giovinazzo
giovinazzo_francesco@live.com
Giovanna Bermano
g.bermano@rgu.ac.uk

Specialty section:
This article was submitted to Cancer Endocrinology, a section of the journal Frontiers in Endocrinology

Received: *15 May 2020*
Accepted: *07 September 2020*
Published: *16 November 2020*

Citation:
Zanini S, Renzi S, Giovinazzo F and Bermano G (2020) mTOR Pathway in Gastroenteropancreatic Neuroendocrine Tumor (GEP-NETs). Front. Endocrinol. 11:562505. doi: 10.3389/fendo.2020.562505

INTRODUCTION

Gastroenteropancreatic neuroendocrine neoplasms (GEP-NENs) are defined as a heterogeneous group of neoplasia that originates from neuroendocrine cells widely dispersed throughout the gastrointestinal tract forming the largest group of hormone-producing cells in the body (1, 2). Although initially considered rare tumors, in the last decade, the incidence has significantly increased. Different factors may explain this increase such as a better classification with the introduction in 2010 of the World Health Organization (WHO) criteria and the ever-increasing use of screening and diagnostic methods such as the gastrointestinal endoscopy and radiological

techniques (3, 4). On the contrary, during the same period, progress in diagnosis has only been matched by a modest improvement in outcomes due to (5) GEP-NENs often being unpredictable and unusual in terms of symptoms, disease progression, and overall survival (6).

Functioning GEP-NENs release peptides and neuroamines that are implicated in specific clinical syndromes, such as carcinoid syndrome, which is relatively uncommon (10–15%) and non-specific symptoms such as irritable bowel syndrome, asthma, or food allergy response. The consequence of late diagnosis (5–7 years on average) is that 75% of tumors exhibit synchronous liver metastases at the time of diagnosis (7, 8). Moreover, 50% of the tumors are asymptomatic until late presentation with symptoms of mass effects or distant metastases, frequently hepatic, or both or tumor-induced fibrosis (9).

Most GEP-NENs are sporadic with a minor group related to inheritable genetic conditions such as multiple endocrine neoplasia type 1 (MEN1), tuberous sclerosis (TSC) and Von-Hippel Lindau (VHL) syndrome (10). Management treatment includes surgery, which at present, is the only therapeutic option in localized and locally advanced disease. Other therapeutic approaches for the metastatic disease include radiological intervention by chemoembolisation, radiofrequency ablation, biological therapy, somatostatin analogs (SSAs), and Peptide Receptor Radionuclide Therapy (PRRT) with 177Lu-DOTATATE (11). Therefore, the need to develop novel therapeutic approaches is paramount in the absence of several treatment strategies.

Frequently, an mTOR abnormal activation has been observed, likely due to inactivating mutations occurring on genes coding for negative regulators of the pathway or through indirect mechanisms. Clinically, the overexpression of mTOR and the downstream targets has been associated with the worst prognosis in different NETs (12–14). Molecularly targeted drugs are emerging as a new and promising treatment for patients affected by GEP-NENs (15).

This review aims to highlight the role of the PI3K/Akt/mTOR pathway in the development of a neuroendocrine tumor and its potential as a therapeutic target providing a biomolecular overview and reporting results from clinical trials.

OVERVIEW OF AKT-MTOR SIGNALING

The phosphatidylinositol 3-kinase (PI3K)-Akt-mTOR pathway supports the modulation of cell growth, proliferation, metabolism, survival, and angiogenesis (16). Evidence suggests that PI3K, one of the significant upstream of the Akt-mTOR axis, is involved in the neoplastic process through the receptor tyrosine kinases (RTKs) and the G protein-coupled receptors (GPCRs). Oncogenic factors such as epidermal growth factor receptor (EGFR), platelet-derived growth factor receptor (PDGFR), and mesenchymal-epithelial transition factor can activate PI3K by binding RTKs and GPCRs (17–19). PI3K is anchored to the plasmatic membrane through a lipid tail. It transduces the signals into intracellular messages by phosphorylating the 3′-OH position of the inositol ring of the lipid second messenger phosphatidylinositol (4, 5) bisphosphate (PIP_2). Subsequently, phosphatidylinositol (3–5) triphosphate (PIP_3) recruits and activates the phosphatidylinositol-dependent kinase 1 (PDK1) that phosphorylates the serine-threonine protein kinase AKT [also known as protein kinase B (PKB)] (20).

AKTs are serine-threonine kinases and comprise three different protein isoforms (AKT1, AKT2, and AKT3) acting on cellular survival, proliferation, growth, and metabolism. To be fully activated AKT needs the phosphorylation on T308 by PKD1 and S473 by mTORC2. AKT downstream effectors are implicated in the control of apoptosis (FOXO family of transcription factors, BAD or NF-κB), cell cycle regulation (GSK3β, p27kip1), and growth (TSC2) (21). AKT downstream is mTOR that plays a vital role in the regulation of cell growth and proliferation. The control is achieved by controlling cellular energy levels, nutrient availability, oxygen levels, and mitogenic signals. The protein is a serine-threonine protein kinase of the PI3K superfamily, referred to as class IV PI3Ks, frequently overactivated in cancer (22). mTOR is comprised of two complexes, mTOR complex 1 (mTORC1) and mTOR complex 2 (mTORC2), different in chemical structures and substrate specificity. mTORC1 consists of mTOR protein, the regulatory-associated protein of mTOR (raptor), deptor, mlST8, and Pras40 (16). After the stimulation with growth factors as IGF-1 and 2, PDGF and VEGF, the mTORC1 translation is increased via the ribosomal protein S6 kinase (p70S6K) and the eukaryotic initiation factor 4E binding protein (4E-BP1) (23). The function of mTORC1 is modulated within the PI3K/Akt pathway via phosphorylation alongside inactivation of the tuberous sclerosis complex (TSC1/TSC2) by inhibition of the guanosine triphosphatase activity, which controls the activity of the mTOR activator Rheb (22). Tumor suppressor genes, such as phosphatase and tensin homolog (PTEN), that antagonize the PI3K action on PIP_3 (24), NF1, the kinase LKB1 and oncogenes such as Ras and Raf, all converge on the TSC1/TSC2 complex (25). The activity of HIF1α and VEGF (26) is enhanced through the activation of the mTOR pathway. In contrast, mTORC2 complex is associated with Protor, SIN1, the rapamycin-insensitive companion of TOR protein (Rictor), LST8, Deptor which reacts to growth factor receptor binding, thus initiating full activation of Akt kinase by phosphorylation at the Ser473 (16). This pathway is frequently deregulated in human tumors, making it a central target in the development of new anti-cancer treatments (21) (**Figure 1**).

ROLE OF AKT-MTOR SIGNALING PATHWAY IN GEP-NENS

In the last decade, molecular studies (12, 27, 28) pointed to several targets of the PI3K/Akt/mTOR pathway in GEP-NENs. Shah et al. found that, respectively 76 and 96% of 98 NENs tissues analyzed by IHC display constitutive AKT phosphorylation and activated ERK, a downstream target (29). Missiaglia et al. (30) demonstrated that the expression of two endogenous inhibitors of the mTOR pathway, PTEN and TSC2, were downregulated in a large proportion of tumors, respectively 35 and 60% of cases. Further, low expression was significantly

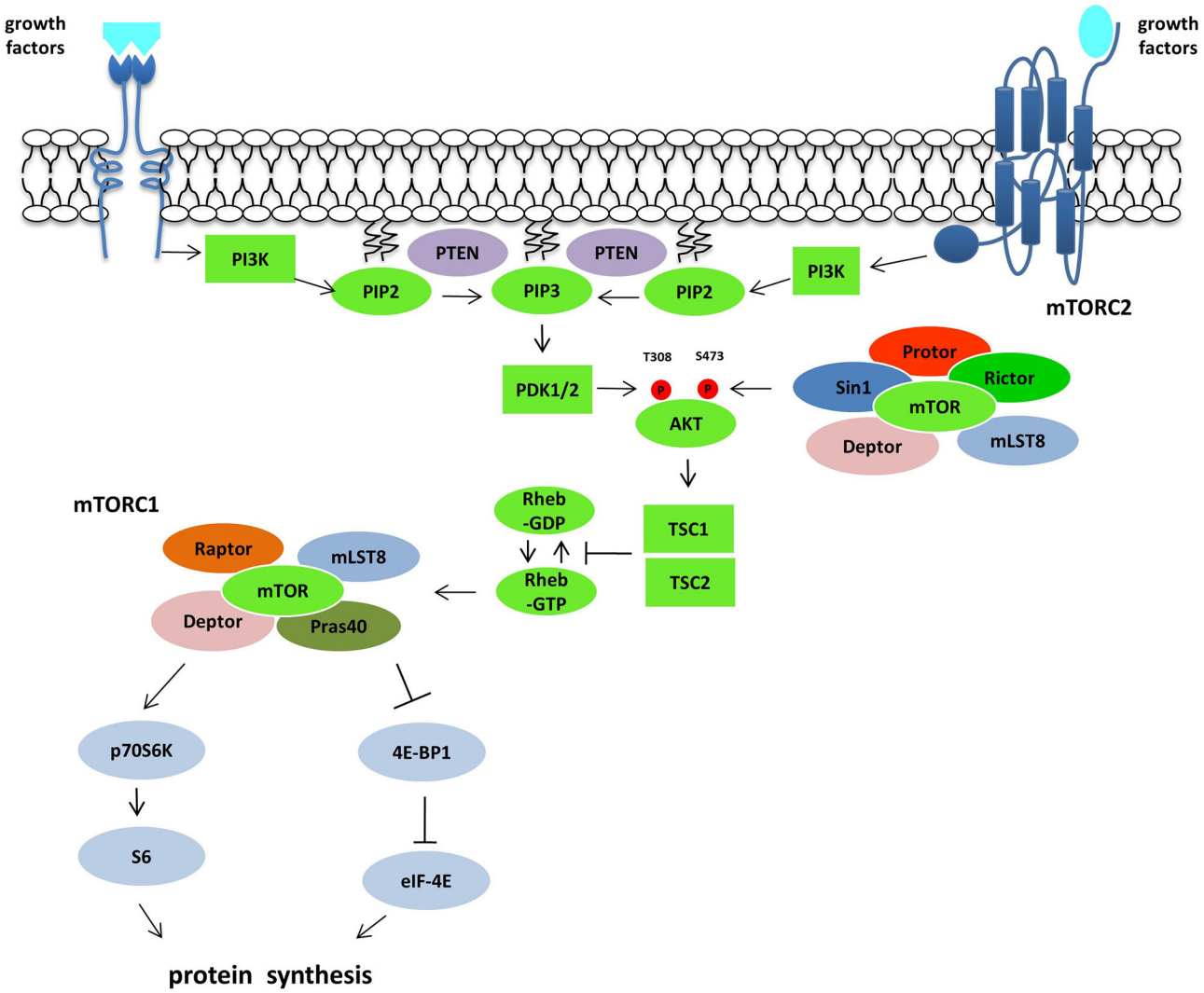

FIGURE 1 | The PI3K/Akt/mTOR pathway. Following growth factors stimulation and subsequent activation of RTKs and GPCRs, PI3K is recruited to the plasma membrane directly or through adaptor protein and phosphorylated PIP2 producing PIP3, which recruits and activates PDK1. Akt activation is mediated by PDK1 on T308 and by mTORC2 complex on S473. Akt controls the activity of mTORC1 inactivating the GTPase activity of the TSC1/TSC2 complex toward the mTORC1 activator Rheb. mTORC1 activation induces protein synthesis *via* p70S6K and 4EBP1. The tumor suppressor gene PTEN acts on this pathway antagonizing the PI3K action on PIP3.

related to both diminished disease-free and overall survival. Overexpression of mTOR has been demonstrated in poorly differentiated NENs, but the expression rate decreased in well-differentiated neuroendocrine tumors and carcinomas (67 vs. 27% of analyzed tissues by IHC) (13). In another study, Catena L. et al. showed that mTOR was expressed in 80% of patients who had poorly differentiated neuroendocrine carcinoma. They also found no relationship with tumor origin (pancreas, colon, lung, small bowel and others) or the rate of proliferation as determined by MIB-1 (>20% in all samples) (31). Molecular studies in SI-NEN cell lines (KRJ-I, H-STS) showed increased activation of AKT respective to normal Enterochromaffin (EC) cells that exhibited inferior expression of transcripts for AKT and mTORC1 as well as a lower level of Akt activation suggesting a neoplasia-related involvement of this pathway (32).

Jiao et al. analyzed the exomic sequences of 10 sporadic panNENs and screened the most frequently mutated genes in 58 pancreatic NENs. The mutations on MEN1 (44%), DAXX/ATRX (43%), TP53 (3%) were found. Notably, 15% of the tumors showed mutations in mTOR pathway-related genes (the onco-suppressor PTEN, the negative regulators TSC2, and PIK3CA, and the catalytic subunit of phosphatidylinositol 3-kinase) (33). In a clinical study, the patients with MEN-1, DAXX, and ATRX mutations had a median overall survival of 10 years in contrast with 60% of patients without mutation that died within 5 years of diagnosis. Based on the results of the study, the authors advanced

the stratification of patients for treatment with mTOR inhibitors (34). In 2017 Scarpa et al. published a study on the whole genome sequencing of 98 pancreatic NETs in which they confirm the mTOR pathway activation in 15% of the analyzed samples. They identified mTOR pathway inhibitors alterations such as PTEN mutations (7.1%), TSC1 or TSC2 (2%). The study also proposed DEPDC5 inactivating mutations (2%) and EWSR1 fusion event as a novel mechanism of mTOR activation (14).

INHIBITORS OF AKT-MTOR SIGNALING PATHWAY AS NEUROENDOCRINE TUMOR THERAPY

mTOR has been the first node of the pathway to be targeted with a drug in tumors exhibiting phosphoinositide 3-kinase (PI3K) pathway mutation or activation (35, 36). First-generation of mTOR inhibitors includes Rapamycin (Sirolimus), an immunosuppressant agent identified as a fungicide isolated from the soil bacterium Streptomyces hygroscopicus (37). Derivatives of Rapamycin, referred to as rapalogs, (Temsirolimus, Everolimus, and ridaforolimus), function similarly to inhibit mTOR, although they have better efficacy and activity which optimizes clinical use. The Food and Drug Administration (FDA) firstly approved (**Figure 2**).

Temsirolimus

Temsirolimus inhibits mTOR activity by binding the intracellular protein peptidyl-prolyl cis-trans isomerase FKBP1A (FKBP-12) (38). The inhibition results in a G1 growth arrest and in a blockade of the mTOR ability to phosphorylate S6K1 and the ribosomal protein S6, and in reduced levels of HIF-1α, HIF-2α, and VEGF expression. In a phase II trial, Duran et al. (39) evaluated the efficacy, safety, and pharmacodynamics of Temsirolimus amongst 37 patients with advanced neuroendocrine carcinoma (21 carcinoids and 15 islet cell carcinomas). Patients were treated with weekly intravenous doses of 25 mg of Temsirolimus and then evaluated on several outcomes, including tumor response rate, time to progression, adverse events, and overall survival. Data were analyzed with

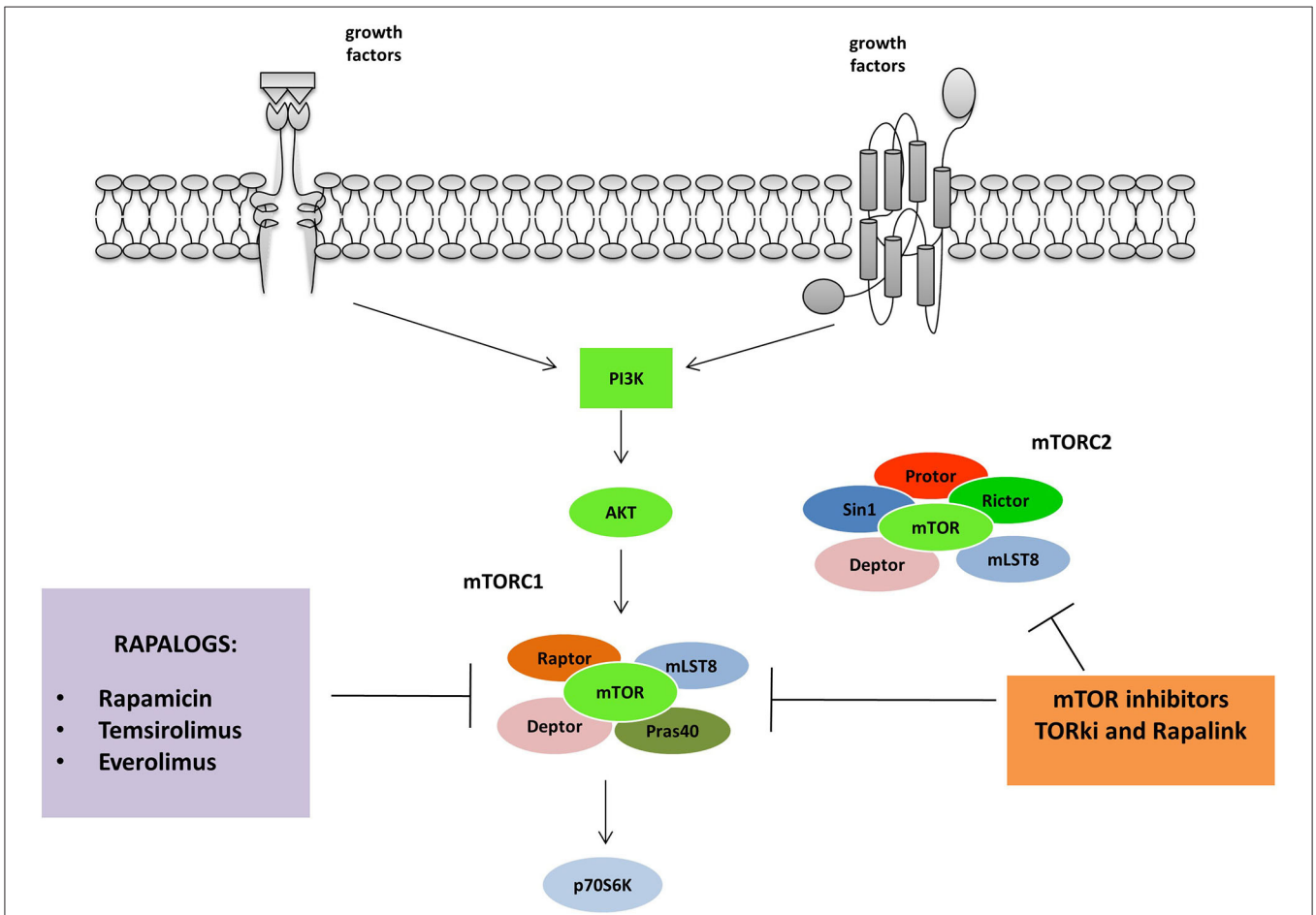

FIGURE 2 | mTORC 1 and 2 are inhibited by different classes of mTOR inhibitors: Rapalogs are the first generation mTORC inhibitors able to induce a partial inhibition of mTORC1. The second and third generation act on both mTORC1 and 2. TORki blocks the ATP binding sites of the complexes, while Rapalinks act through blocking the ATP binding site and by the inhibition of the mTORC1.

intention-to-treat modeling and revealed a response rate of 5.6% [95% confidence interval (CI), 0.6–18.7], respectively 4.8 and 6.7% in carcinoids and islet cell carcinomas. The median time to progression was 6 months. The 1-year survival rate was 71.5%. The study confirmed the inhibition of the phosphorylation of the ribosomal protein S6 in paired baseline and post-treatment biopsies ($p = 0.02$). With higher baseline levels of pS6, there was a non-significant trend toward a better response ($P = 0.097$). Higher baseline levels of phosphorylated mTOR were significantly correlated with a better response ($p = 0.01$).

On the contrary, after 2 weeks of treatment, an increase in the expression of pAKT and a decreased expression of phosphorylated mTOR were observed, both associated with increasing time to progression ($p = 0.04$ and $p = 0.05$, respectively). Given the low response rate, the authors concluded that Temsirolimus appears to have limited clinical utility as a single agent for patients with GEP-NENs. The study proposed evaluating Temsirolimus in combination with other targeted agents, for example, a multi-kinase inhibitor or an anti-angiogenic compound (39). A phase II trial involving 58 patients (56 eligible) was performed to investigate the efficacy of temsirolimus and bevacizumab association. Results showed an increased response rate (RR) of 41% exceeding the single-agent RRs measured by RECIST criteria and a PFS at 6 months of 79%. The therapy administrated to moderate-well-differentiated metastatic P-NETs showed substantial activity and no high toxicity since the most common adverse events were hypertension, fatigue, hyperglycemia and lymphopenia (40).

EVEROLIMUS

Single Therapy

Everolimus is a first-generation oral mTOR inhibitor approved by the US FDA and EMEA for the treatment of P-NENs. Everolimus similarly acts as Temsirolimus inhibiting mTOR kinase binding to FKBP-12 and reducing the activity of mTOR downstream effectors S6K1 and 4E-BP1 (41, 42). A phase I study involving 55 patients with advanced solid tumors, including NETs, evaluated Everolimus safety and pharmacodynamics. The trial aimed to establish an evidence-based dose and effective schedule for cancer treatment. A key criterion was the achievement of complete inhibition of mTOR dependent-signaling pathways on tumor and skin biopsies. Patients unresponsive to standard therapy were enrolled and treated with Everolimus with either 20, 50, or 70 mg weekly or 5 and 10 mg daily. Data suggested that Everolimus brought about both a dose- and schedule-dependent inhibition of the mTOR pathway. There was almost complete inhibition seen of the phosphorylated ribosomal protein S6 ($p < 0.001$) and further eIF4G ($p < 0.001$) expression at 10 mg/day and $\geq$50 mg/week. Although non-significant, there was a trend toward the reduction of phosphorylated 4E-BP1 expression ($p = 0.058$). Also, an overall increase in Akt phosphorylation, occurring in about 50% of patients, was observed ($p = 0.006$). This finding raises the question as to whether the upper regulation of pAKT may reduce the clinical effectiveness of the drug. The authors proposed a dose of 10 mg/day or 50 mg/week to be evaluated in further researches (43).

RADIANT-3 (44) was a phase III study aimed at evaluating Everolimus at 10 mg/day as monotherapy ($n = 207$) or placebo ($n = 203$), with a total sample size of 410 patients with progressive P-NENs, both in conjunction with best supportive care including the use of somatostatin analogs. This trial demonstrated 2.4 odds of improvement in median PFS (11.0 vs. 4.6 months; HR = 0.35; 95% CI: 0.27–0.45; $P < 0.001$) in the arm treated with Everolimus. The trial concluded that although the exact sequencing of therapies to treat of panNENs remains unclear, Everolimus can be advanced as effective in patients with prior chemotherapy or therapy-naïve prolonging PFS (44). RADIANT-4 involved 302 patients with advanced GI and Lung NET's. The Everolimus showed an increase in PFS of 7.1 months in respect to the placebo comparable along with disease stabilization similarly to the results obtained in the RADIANT 3 (45). In a prospective, randomized, pharmacokinetic, crossover trial comparing everolimus 10 mg once daily with 5 mg twice daily Verheijen et al. showed that switching everolimus from once daily to twice daily could reduce the toxicity and maintain treatment efficacy (46).

COMBINATION THERAPY

Somatostatin Analog (SSAs) Octreotide and Pasireotide

Octreotide is a first-generation SSA that is used to control the symptoms in NET's and exhibited tumor growth inhibitory function in metastatic well-differentiated midgut NET's (47). The first trial included 60 patients diagnosed with advanced low- to intermediate-grade GEP-NETs. Of these, 30 patients had carcinoid tumors, and 30 had islet cell carcinomas. All were treated with intramuscular octreotide LAR 30 mg every 28 days and oral Everolimus, 5 mg/day (patients 1 to 30) or 10 mg/day (patients 31 to 60) every 28 days. Overall response (OR) rate was 20%. In details, 70% of the patients showed stabilization of the disease, and 22% confirmed partial responses. The overall median progression-free survival (PFS) of patients treated with octreotide LAR and RAD001 was 60 weeks (95% CI, 54–66 weeks). Therefore, the trial showed that Everolimus, in combination with octreotide LAR, presented promising antitumour activity in patients with advanced NETs (48). The second phase II trial (RADIANT-1) assessed the antitumour activity of oral Everolimus at 10 mg daily in 115 patients with advanced pancreatic NETs who had disease progression during or after cytotoxic chemotherapy. The study confirmed the antitumour activity of Everolimus in panNENs in both groups, those receiving Everolimus alone (PFS was 9.7 months and ORR = 9.6%,) and Everolimus with Octreotide (PFS was 16.7 months and ORR = 4.4%) (49). Following the results of the two randomized phase II clinical trials, RADIANT-2 was planned. RADIANT-2 was a landmark and the most extensive study to have been conducted. RADIANT-2 involved 429 patients with progressive functional carcinoid tumors. The study was conducted to compare Everolimus, at a dose of 10 mg per day, plus octreotide LAR, 30 mg every 28 days, vs. placebo plus octreotide LAR at the same doses. In this trial, the primary

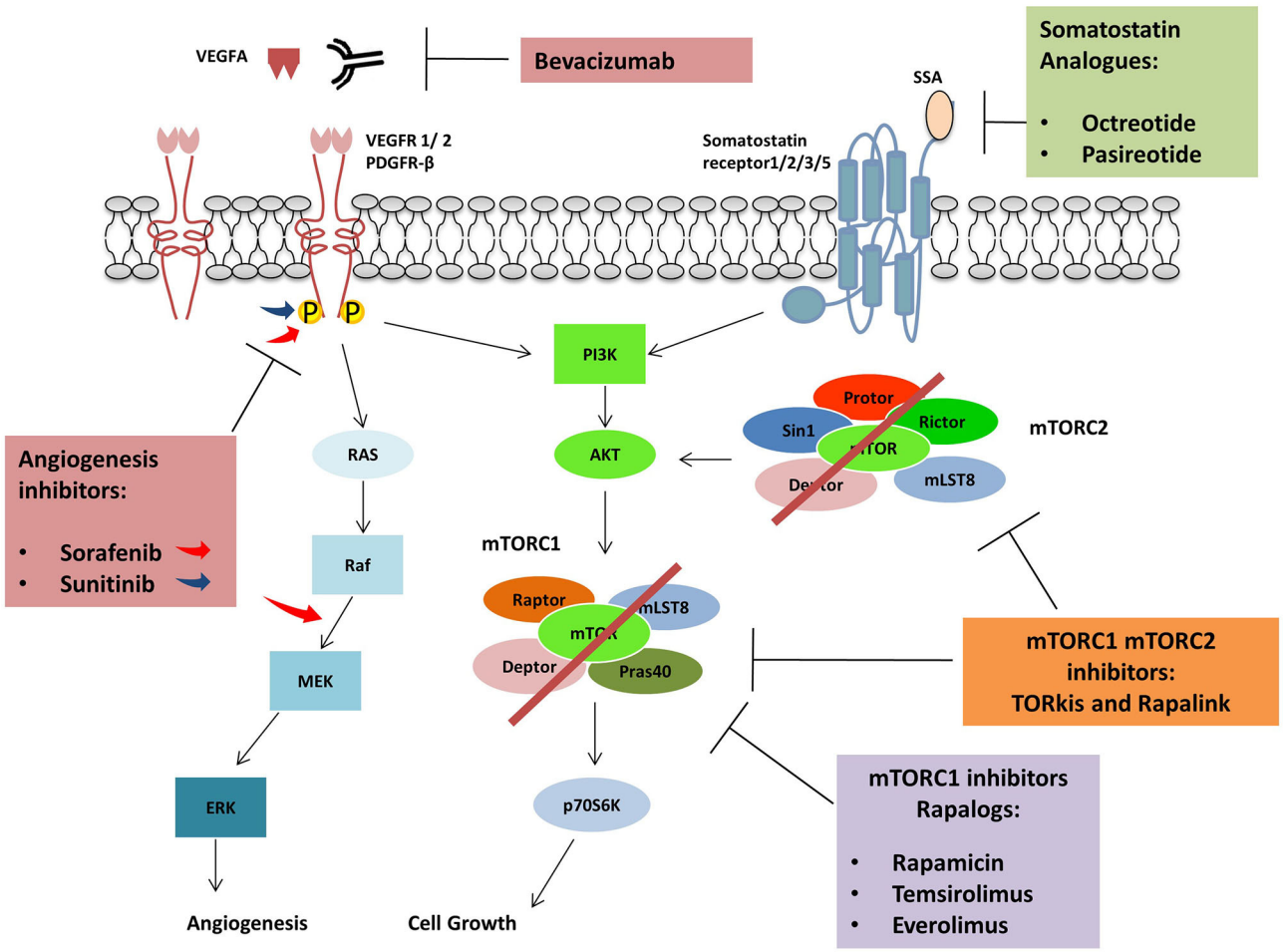

FIGURE 3 | Agents used in combination with mTORC1 inhibitors: Protein kinase inhibitors, Sorafenib and Sunitinib are active against several tyrosine kinases receptors (RTKs) including VEGFR and PDGFR. Sorafenib can also inhibit RAF kinases. The monoclonal antibody Bevacizumab inhibits angiogenic pathway binding VEGFA and avoiding VEGFRs activation. Somatostatin analogs bind somatostatin receptors impairing cell growth while Rapalogues can inhibit mTORC1.

endpoint was to evaluate PFS. PFS was 16.4 months on the Everolimus plus octreotide LAR arm vs. 11.3 months on the placebo plus octreotide LAR arm (hazard ratio = 0.77; 95% CI, 0.59–1.00; $p = 0.026$) (50). The results support the efficacy of Everolimus as an effective intervention for a broad spectrum of advanced neuroendocrine tumors. In a final analysis of the overall survival (OS) data from the RADIANT-II study, Pavel et al. showed that the median OS (95%CI) after 271 events was 29.2 months (23.8–35.9) for the everolimus arm and 35.2 months (30.0–44.7) for the placebo arm (HR, 1.17; 95% CI, 0.92–1.49) with no significant differences in OS between the two group (51). The ITMO group study was set up on 50 patients with different NETs. The results showed an objective response rate (ORR) of 18%; complete response in 4% of the patients and a partial response in 16% while 74% showed disease stabilization. Similarly to the RADIANT-2, the study suggests antitumour benefit in the use of Everolimus plus octreotide as a treatment in NETs, even if, the small number of patients included in the study must be considered in the data interpretation (52).

Pasireotide is a second-generation SSA, targeting the somatostatin receptor subtype 1,2,3 and 5 (53). In a randomized phase 2 study, Everolimus was administrated with Paoirreotide or in monotherapy to 160 NETs patients. However, no improvement of PFS was observed between the two groups, and no benefit was found in the use of drugs combination (54). Contrarily, another study made on 21 NETs patients treated with increasing doses of Pasireotide (until 60 mg monthly) and Everolimus (5–10 mg daily) confirmed the antitumour activity (81% of patient experienced a grade of tumor regression) and the tolerability in term of side effects of this therapy (55). The combination of selective internal radioembolisation (SIRT), Everolimus, and Pasireotide showed encouraging results in a study involving 13 NETs patients (median progression-free survival 18.6 months and overall survival 46.3 months) at a low level of toxicity (53) (**Figure 3**).

EVEROLIMUS AND ANTI-ANGIOGENETIC

NETs are high vascularised tumors, and this observation laid the groundwork/basis for the investigation of a synergistic effect through combined targeting of mTOR pathway and VEGF (56). A potent anti-angiogenic and antivascular effect were observed after the treatment with Everolimus of various solid tumors. The mechanism was different from those found with VEGFR targeting agents. Everolimus inhibited the proliferation of human endothelial cells and impaired VEGF release from cancer cells while VEGFR inhibitor PTK/ZK inhibited endothelial cell migration and vascular permeability. The results suggested the use of rapalog in combination with VEGF inhibitors as an effective therapeutic strategy to obtain a stronger diminishing of tumor vascularisation (57). Sorafenib is a drug inhibiting PDGFRB, and VEGFR2 also found to have modest activity in phase II study on NET's patients (58). In a phase I trial, 21 patients were treated with 10 mg daily Everolimus and two different doses of sorafenib (400 and 600 mg daily), the maximum tolerated dose (MTD) was established in 400 mg per day. A partial response was observed in one patient while a limited tumor regression in 13 out of 21 patients (62%) (56). Furthermore, the combination of Everolimus and Sunitinib to target both the PI3K/Akt/mTOR and VEGF signaling was evaluated as a therapy for different cancers. However, the treatment showed significant acute toxicity (59). Sunitinib is a multitarget tyrosine kinase inhibitor directed against different receptors such as VEGF-R1/2/3, PDGF-R α/β, Stem cell factor receptor (c-KIT-R). Also, colony-stimulating factor 1 receptor (CSF1-R), FML like tyrosine kinase three receptor (FLT3-R) and glial cell line-derived neurotrophic factor receptor (RET) (60). The drug showed comparable efficacy for Everolimus as first-line therapy in phase II study (61). Sequential administration was studied in 31 patients as high toxicity when the two drugs were simultaneously administrated. The results showed good tolerability with no differences in median PFS between the two groups (Everolimus followed by sunitinib, 36.5 months vs. Sunitinib followed by Everolimus, 31.6 months) (62). Another drug investigated to find a synergistic effect with Everolimus and to impair vascularisation in NETs was Bevacizumab in a randomized phase 2 study on 150 patients. The combination of the two drugs showed an increase of PFS (16.7 vs. 14 months), but also the adverse events were more frequent in patients receiving both drugs (63).

Everolimus Plus Target and Radionuclide-Therapy

Everolimus was also tested in phase I/II study, in combination with temozolomide in 43 pancreatic NETs, 40% of the patients (40 evaluable patients) had a partial response with median progression-free survival (PFS) of 15.4 months (64). In a phase I study (NETTLE) involving 16 NETs patients the toxicity of Everolimus in combination with PRRT (Lutetium-177-octreotate) was investigated and Everolimus 7.5 mg per day appeared to be well-tolerated (65).

Second and Third-Generation mTOR Inhibitors

To overcome the resistance phenomenon and to have a complete inhibition of the mTOR pathway, second-generation inhibitors were synthesized. These compounds are called TORkis and act binding the ATP binding site "of mTOR kinase pocket." Differently from the rapalogs, these molecules ensure a complete block of both MTORC1 and 2 preventing the Akt phosphorylation due to MTORC2 and avoiding the resistance observed in rapalogs. Different TORkis were synthesized and showed promising results in pre-clinical studies. PP242 and the derived compound MLN0128, the quinolone-derived torin1 and 2, QSI-027, ku0063792 and Ku-0068650 showed a high antiproliferative power. From the latter derived AZD8055 and AZD2014, which was primarily tested in clinical trials even in combination with other therapeutic agents in different solid tumors (66).

The mTORC1/2 kinase inhibitor named CC-223 was tested in a phase 1/2 study involving metastatic non-pancreatic GI-NETs patients treated with SSA who had failed treatment. The drug showed efficacy in induce tumor regression and carcinoid syndrome symptoms controls and led to an Improvement of median PFS (19.5 months) superior to Everolimus alone (PFS 11.0 months) (44, 67). The CC-223 safety profile was found to be comparable to currently approved mTOR inhibitors, and toxicity was well-managed by dose adjustments or treatments (67).

Third generation mTOR inhibitors were studied to address the treatment resistance issues found in the use of the rapalogs and TORkis (68). The new compounds are called RAPAlink since they are made by the conjugation of TORkis, having high affinity for ATP binding site of both MTORC1/2 and Rapamycin having the FKB12-dependent mechanism to block MTORC1. These compounds sowed increased and durable inhibitory action compared to the first and second-generation inhibitors and ability in crossing BBB in glioblastoma *in vitro* and *in vivo* (69). An *in vitro* study on the resistance to first and second-generation mTOR inhibitors showed the development of mutations in FKBP-12 (FRB domain) in Rapalogs resistant cells and mutations increasing intrinsic kinase activity of mTOR in TORkis resistance. These mechanisms have been overcome by the use of Rapalink able to establish a bivalent interaction of the two-binding site (68). Sapanisertib is an inhibitor of raptor-mTOR, and rictor-mTOR tested in several solid tumors (70). In a patient-derived xenograft model of PNET (PDX-PNET) the majority if everolimus-resistant PDX-PNETs responded to sapanisertib (71).

GEP-NENS TREATMENT RESISTANCE AND FUTURE APPROACHES (RAPALOGS RESISTANCE, MOLECULAR MECHANISMS)

GEP-NENs develop resistance to treatment, not only to standard target therapy and SSA but also to novel agents. After long-term exposition to prolonged targeted inhibition of a single pathway, cancer cells acquire therapeutic resistance activating

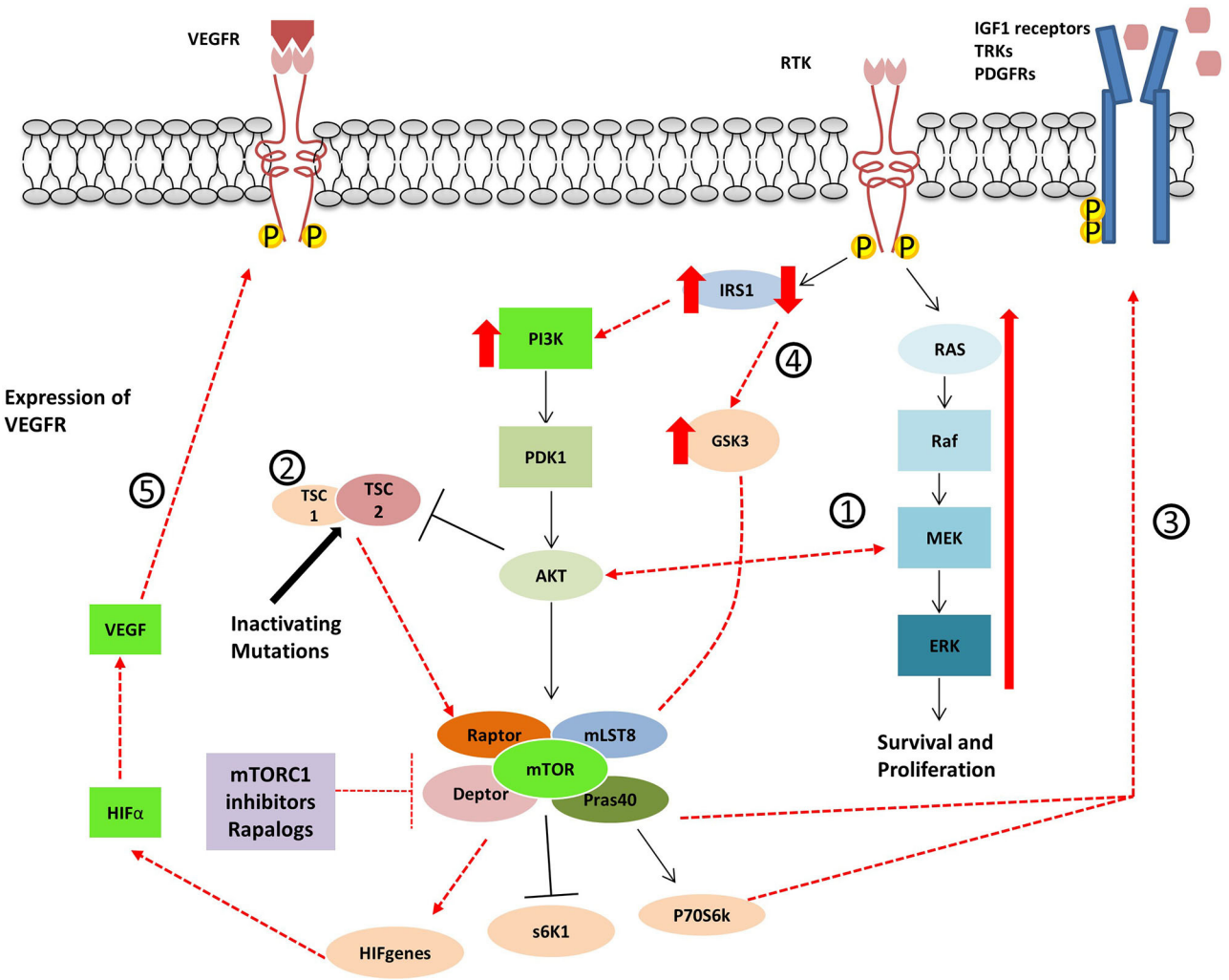

FIGURE 4 | Proposed mechanisms for resistance to Rapalogues in NET. 1- Inhibition of mTOR results in PI3k-Akt-mTOR pathway reactivation and MAPK pathway activation. 2- Inactivating mutations in TSC1/2 cause the inactivation of the TSC1/TSC2 protein complex leading to mTOR hyperactivation. 3- mTOR inhibitor treatment cause an increase in tyrosine kinase receptors and growth factor secretion. 4- GSK3 over-expression accompanied by the decrease of IRS-1 protein leads to decreased autophagy and cell resistance to Everolimus. 5- The up-regulation of angiogenic factors mTOR-independent or the re-expression of HIFα.

alternative or compensatory pathways. The PI3K-Akt-mTOR and Ras/MAPK pathway are connected at multiple levels, and both can be mutuality activated or inhibited (72, 73). In other words, activation of the mTORC1 leads to PI3K and MAPK inhibition via a negative feedback loop system, and inhibition of mTOR, inversely, results in reactivation of PI3k-Akt-mTOR pathway and MAPK pathway. The resistance of antitumour effects of mTOR inhibitors is explored in most the studies investigating the PI3K/Akt pathway. However, several studies showed that mTOR inhibition resulted in an activation of the MEK/ERK cascade through a PI3K-dependent feedback loop (32, 74–76). The phenomenon may contribute to explain the escape of drug efficacy. Thus, combination therapies of mTOR inhibitors with MEK inhibitors have been proposed as an alternative mechanism to inhibit both pathways and overcome tumor resistance (77) (**Figure 4**).

Carracedo et al. showed that tumor samples were taken from patients with biopsy-accessible solid tumors of advanced disease and treated with RAD001. The study demonstrated robust activation of the MAPK pathway at specific doses and related to the administration schedule. The researchers also described a rapamycin-induced ERK/MAPK activation in both normal cells and cancer cells lines based on an S6K/PI3K/Ras pathway (74). Mi et al. evaluated the combinatorial inhibition of mTOR and MAPK pathway in mouse Tsc2 knockout cells by administrating both Rapamycin and MEK1/2 inhibitor, PD98059. The mutations in TSC1 or TSC2 result in the inactivation of the TSC1/TSC2 protein complex that leads to hyperactivation of mTOR, causing uncontrolled cell growth and proliferation. The inhibitory

effects on proliferation in Tsc2 deficient cells were higher using the combinatorial approach (75). Ziztmann et al. studied the complex interplay between PI3K/Akt/mTOR pathway and MAPK pathway using different drugs combination in different human NET cell lines. The study showed that cells develop a mechanism of escape when using a single agent target pathway also through compensatory induction of AKT. They noted that the dual inhibition of mTOR (Everolimus) and PI3K (NVP-BEZ235) had a more significant effect than the single inhibition of mTOR in cell lines (78). However, two trials on NVP-BEZ235 were early stopped due to unmet statistical endpoint or intolerable toxicity (79).

The resistance to mTOR inhibitors has also been proposed through other potential mechanisms. O'Reilly et al. (80) reported that mTOR inhibition induces insulin receptor substrate-1 (IRS-1) expression resulting in AKT activation both in cancer cell lines and in tumor tissues treated with RAD001. AKT activation after mTORC1 inhibition has also been demonstrated depending on upregulation of RTKs such as PDGFRs (81, 82). It has been shown that SI-NEN cell lines escape from mTOR inhibitor treatment through dual feedback activation of Akt and ERK1/2 *via* an increase in tyrosine kinase receptors and growth factor secretion. Concurrent therapy with octreotide failed to overcome the escape phenomenon suggesting dual targeting of PI3K/Akt/mTOR pathway and MAPK pathway as an alternative method to reverse feedback cross-activation (32).

From an *in vitro* study on everolimus resistant panNET cell lines (BON1 RR1, BON1 RR2) Gsk3 was found to be dysregulated. In these models, the GSK3 hyperactivation was associated with reduced IRS-1 protein levels, decreased autophagy and cell cycle arrest in G1 phase due to CDK1 (cdc2) reduced expression. Interestingly, A PI3Kα-inhibitor (BLY719) used in combination with everolimus was able to re-establish the everolimus sensitivity (83).

Pro-angiogenic factors upregulation can also be involved in rapalogs resistance since mTOR inhibition has been proven to have a direct and indirect anti-angiogenetic effect (57).

NETs, especially those well-differentiated, are high vascularised tumors due to the significant HIFα up-regulation which may arise by genetic alteration of the VHL protein and to the tumor microenvironment (84, 85) PI3K/AKT/mTOR pathway regulates the angiogenesis in NETs modulating (84–87) The Aurora Kinase A (AKURA) overexpression has been observed in everolimus resistant GI adenocarcinoma cell lines. This protein can mediate elF4E phosphorylation and increase c-Myc levels. The AURKA-EIF4E-c-MYC axis can be an alternative target for everolimus resistant tumors (86, 88, 89).

Several studies have been performed to found predictive biomarkers allowing the stratification of patients that may benefit from therapy with mTOR inhibitors. Recently, mRNA-based evaluation (NETest) performed on the tumor has proven to be a useful biomarker for NETs. NETest is a gene panel analyzed from a liquid biopsy and represents an innovative non-invasive approach to disease progression evaluation that better performs in respect to conventional biomarkers such as CgA (90).

CgA and neuron-specific enolase (NSE) have been proposed as markers of (91) From the RADIANT1 trial CgA > x2 ULN, two times higher than normal levels (36,4 ng/mL) is linked to the worst prognosis and shorter PFS in panNET's. Similarly, NSE >2xULN were associated with a shorter PFS. Although baseline CgA and NSE levels failed to predict mTOR therapy responsiveness, prospective analysis on a large number of patients showed a correlation between an early decreasing in CgA or NSE levels in response to Everolimus treatment (>30% decrease from baseline or normalization after 4 weeks) and a significant improvement of PFS (48). Furthermore, 5-hydroxyinoleacetic acid (5-HIAA) was found to be related to an increase in PFS in patients receiving Everolimus (92, 93).

Correlations between rapalogs sensitivity and the levels or activation status of the mTOR pathway signaling components were found (94). Baseline Phosphorylation of mTOR signaling molecules has been related to the worst outcome in NET's patients but also with a better response to Everolimus (95). For this reason, the increase of phosphorylated Akt was proposed as a biomarker in case of reduced PTEN expression to individuate tumors responding to mTOR inhibitors. Akt phosphorylation (S473 and T308) was more likely found in patients responding to rapamycin than non-responders (96). However, as discussed in the previous chapter, Akt was also found to be phosphorylated (ser473) in case of rapalogs resistance due to MTORC2 activation (97).

PTEN mutations were investigated as a possible predictive biomarker, and several studies pointed out that PTEN null cells, as well as xenograft models with reduced PTEN activity, were more sensitive to rapalogs (prostate cancer) (94). PTEN mutations which are related to the increase of the mTOR pathway activation has been found in different diseases as well as in NET's (14).

High sensitivity to rapalogs was observed in *in vitro* and *in vivo* NET's models with mutated PIK3CA/PTEN and high p-Akt levels (96). Interestingly, response to everolimus was lost when PIK3CA mutation occurred together with KRAS mutation. However, everolimus sensitivity was re-established in HCT116 cells in which the KRAS D13 mutant allele had been genetically deleted by homologous recombination (98). Single nucleotide polymorphism is investigated in cancer and in particular, the SNP GFR4-G388R was observed in panNET patients. The fibroblast growth factor receptor 4 (FGFR4) plays a role in mitogenesis and angiogenesis and the presence of an arginine instead glycine in the codon 388 was related with shorter PFS especially in heterozygous patients compared to homozygous for the SNP (PFS 4.8 vs. 16.6 months, respectively; OS of 9.3 vs. 40 months, respectively). Also, the SNP was found to be related to a higher risk of liver metastasis and was present in patients not responding to everolimus (99). Contrarily, Cros et al. who studied the FGFR4 polymorphism (G388R) on 41 patients with NET's did not found a correlation between PFS and the presence of SNP (100). The inactivating PHLPP2-L1016S SNP was investigated as a possible predictive marker and was found to be associated with a reduced PFS in extra-pancreatic NET's patients treated with Everolimus. PFS was 16.8 months in wild type PHLPP2 patients vs. 7.7 months in those harboring SNP. Overall survival and response rate were not affected by the SNP presence. The results suggested that wild type PHLPP2 patients

TABLE 1 | Clinical trials on mTOR inhibitors in neuroendocrine tumor.

Study	Patients	Type of tumor	Progressive metastic disease	Drug	Combination therapy	Median OS (months)	Response rate	Median Progression free survival (PFS, months)	Molecular markers analyzed	References
Phase-II	37	Carcinoid 21 islet cell carcinoma 15	yes	Temsirolimus 25 mg/w	no	Not reached	5.6%	6 (TTP)	PTEN, p53, pAKT, pS6, pmTOR.	Duran et al. (45)
Phase-II	56	Well or moderately differentiated pancreatic neuroendocrine tumors	yes	Temsirolimus 25 mg/week	bevacizumab 25 mg/kg (once every 2 weeks)	34.0	41%	13.2	CgA Circulating hormones level	Hobday et al. (46)
Phase-I	55	Neuroendocrine neoplasms	Yes	Everolimus 20, 50, 70mg/w or 5,10 mg/d	No	-	-	-	pAKT and AKT, p4E-BP1 and 4EBP1, pS6, and S6	Tabernero et al. (48)
Phase-II	30 30	Low-to intermediate grade neuroendocrine neoplasms	Ns	Everolimus 5 mg/d everolimus 10 mg/d	octLAR 30 mg every 28 d	Not reached	20%	12.5 18	Ki-67	Yao et al. (52)
Phase-II	50	Advanced well-differentiated NETs	Yes	Everolimus 10 mg/d	OctLAR 30 mg every 28 d	Not reached	18%	-	CgA	Bajetta et al. (55)
RADIANT-1, Phase-II	115 45	Low-to intermediate grade pancreatic neuroendocrine neoplasms	Yes No	Everolimus 10 mg/d everolimus 10 mg/d	No octLAR 30 mg every 28 d	24.9 not reached	9.6% 4.4%	9.7 16.7	CgA NSE	Yao et al. (53)
RADIANT-2, phase-III	216 213	Low-to intermediate grade neuroendocrine neoplasms	Yes	Everolimus 10 mg/d placebo	octLAR 30 mg every 28 d octLAR 30 mg every 28 d	Not reached	-	16.4 11.3	CgA	Pavel et al. (54)
RADIANT-3, phase-III	207 203	Low-to intermediate grade pancreatic neuroendocrine tumors	yes	Everolimus 10 mg/d placebo	Best supportive care	Not reached	5% 2%	11.0 4.6	-	Yao et al. (49)
RADIANT-4 phase-III	205 97	Advanced, progressive, well-differentiated, non-functional lung or gastrointestinal neuroendocrine tumors	yes	Everolimus 10 mg/d Placebo	Best supportive care	23.7 16.5	64% 26%	11.0 3.9	-	Yao et al. (50)
Phase-I	21	Advanced neuroendocrine tumors	ns	Everolimus 5, 10 mg/d	Pasireotide s.c. 600, 900, 1,200 μg Pasireotide LAR 40,60,80 mg monthly	-	81%	-	Aminotransferase alanine-aminotransferase serum creatinine neutrophil count CgA.	Chan et al. (58)
Phase-II	160	Well-differentiated neuroendocrine tumors	yes	Everolimus 10 mg/d	PasireotideLAR 60 mg every 28 d	22.6	20%	16.8	CgA NSE IGF-1/2, IGFBP-2/3	Kulke et al. (57)
Phase I-II	7 phase I 36 phase II	Advanced pancreatic neuroendocrine tumors	ns	Everolimus 5 mg/d Everolimus 10 mg/d	Temozolomide 150 mg/m^2 Temozolomide 150 mg/m^2 (days 1 to 7 and days 15 to 21 of a 28-days cycle).	Not reached	40%	15.4	CgA	Chan et al. (66)

(Continued)

TABLE 1 | Continued

Study	Patients	Type of tumor	Progressive metastic disease	Drug	Combination therapy	Median OS (months)	Response rate	Median Progression free survival (PFS, months)	Molecular markers analyzed	References
Phase I	13	Moderately or well-differentiated neuroendocrine tumors	Yes	Everolimus 2.5, 5, 10 mg/d	Pasireotide s.c. 600 μg twice daily Along with SIRT yttrium-90 on days 9 and 37	46.3	46%	18.6	Angiopoietin 1/2, bfgf, collagen V, IGF1/2, IGFBP, IL8, PGF, VEGFR2, CgA, prolactin, HGF.	Kim et al. (56)
Phase I	21	Locally unresectable metastatic carcinoid and pancreatic neuroendocrine tumors	Yes	Everolimus 10 mg/d	Sorafenib 400 mg/d Sorafenib 600 mg/d	-	62%	Pf-6 months 79%	CgA	Chan et al. (59)
NETTLE Phase I	16	Advanced unresectable progressive well-differentiated GEP-NETs	No	Everolimus 5, 7.5, 10 mg/d	PRRT ^{177}Lu-octreotate 240 mg every 8 weeks	57	44%	-	CgA. urinary 5-HIAA	Claringbold et al. (67)
Phase-II	150	Advanced pancreatic neuroendocrine tumors		Everolimus 10 mg/d and octreotide acetate 20 mg once	Bevacizumab 10 mg/kg every 15 days	36.7	31%	16.7	-	Kulke et al. (65)

w, weekly; d, daily; ns, not specified; oct, octreotide; CgA, chromogranin A; NSE, neuron-specific enolase; bfgf, basic fibroblast growth factor; IGF, insulin like growth factor; pgf, placental growth factor; VEGFR, endothelial growth factor receptor; HGF, hepatocyte growth factor; 5-HIAA, 5-hydroxyindoleacetic acid.

may benefit more from everolimus therapy. Interestingly, PLPP2 is known as a regulator of AKT that in turn, activate the mTOR pathway (101).

Falletta et al. successfully used patients derived primary cultures as a tool to predict the sensitivity to everolimus treatment. The study showed that IGF1 is related to everolimus antiproliferative effect only in patients with higher phosphorylated IGF1R levels, p-Akt, p-mTOR, p-4EBP1 and higher Ki67 index (responders) compared to non-responders to mTOR inhibitors (102).

Another possible predictive biomarker for rapalogs sensitivity is the presence of mTOR activating mutations. A study showed the presence of missense mutations in 400 oncologic patients' samples with different cancer subtypes. The mutations were present in 6 various sites but most frequently in the C-terminal region of the protein. In a subgroup of these samples, the hyperactivation of mTOR was due to the impairment of mTOR-DEPTOR inhibitor binding. The activating mutations observed in cell culture and xenografts were linked to an increased sensitivity to Rapamicin (103). Contrarily, activating mutations of mTOR has been observed in cell resistant to TORkis targeting the ATP binding pocket (68).

Meta-Analysis

In a meta-analysis including studies performed on 1908 NET's patients, target therapies were found to be effective and improve PFS (hazard ratio = 0.59, 95% CI:0.42–0.84; $P = 0.003$) in particular in pancreatic NET's patients (HR = 0.49 95% CI: 0.29–0.83) than in non-pancreatic NET's (HR = 0.71 95% CI: 0.49–1.02). Target therapies with Everolimus and with sunitinib (monotherapies) or Everolimus and octreotide were found effective in pan NETs (104).

Recently, a meta-analysis comprising 3,895 cases of NETs evaluated the most promising therapies in panNET's. Everolimus as single therapy (0,82 P score)/(hazard ratio [HR], 0.35 [95% CI, 0.28–0.45]) appeared to be the most effective treatment followed by SSA combined with Everolimus (0,73 P score)/ (HR, 0.35 [95% CI, 0.25–0.51]). The combination therapy with interferon and SSA (P score 0.71) was also found to be effective followed by the monotherapies interferon (P score 0.62), SSA (0.54 P score)/(HR, 0.46 [95% CI, 0.33–0.66]), sunitinib (0.39 P score), Dactolisib (0.6 P score), and placebo (0.13 P score).

In 8 studies assessing the PFS after nine different therapies, Everolimus showed high effectiveness in panNETs, especially in combination with SSA (0.72 P score) as well as in monotherapy (0,72 P score). The combination of the mTOR inhibitor with bevacizumab and SSA showed lower efficacy (0.44 P score)/ (HR, 0.44 [95% CI, 0.26–0.75]). The best performing therapy improving PFS was the combination of SSA with interferon (0.77 P score)/(HR, 0.31 [95% CI, 0.13-0.71]. Differently, in GI-NET's the most efficient therapy in disease control was the combination of bevacizumab with SSA (0.93 P score)/ (HR, 0.22 [95% CI, 0.05–0.99]) followed by ^{177}Lu-dototate and SSA (0.92 P score)/(HR, 0.08 [95% CI, 0.03–0.26] and interferon plus SSA (0.66 P score)/(HR, 0.27 [95% CI, 0.07–0.96]). Everolimus with SSA (0.52 P score)/ (HR, 0.31 [95% CI, 0.11–0.90]) was found to be less effective in GI-NETs than in panNETs. Furthermore, Everolimus as monotherapy resulted to be effective comparably to SSA alone (0.39/ (HR 0.48 [95% Cl, 0.20–1.13]) vs. 0.4/(HR, 0.40 [95% CI, 0.21–0.78]) P scores, respectively) (105).

Studies on the quality of life and adverse events (AE) showed that the combination SSA with Everolimus reported one of the highest numbers of AE (82.7% of the patient), with 68% of these being grade 3–4. Similarly, Everolimus used in monotherapy caused AE in 92.1% of the patients, but 59.3% of grade 3–4. Among the therapies showing good efficacy, SSA in combination with ^{177}Lu-dototate showed a better profile in term of toxicity in respect to Everolimus (94% AE, 41% grade 3–4). Interferon and SSA caused AE in 21% of the patient and a small percentage of a grade 3–4 (3%) while SSA alone caused AE in 69.8% of the cases and 20.9% of AE of grades 3–4 (105). A meta-analysis of individual patient data showed that a 2-fold increase in Everolimus Cmin delayed NET disease progression with improved tumor size reduction. However, the protocol increased the risk of high-grade toxicity, mainly with a high number of pulmonary, metabolic and stomatitis events (106). Mujica-Mota et al. evaluated the clinical effectiveness of three interventions (everolimus, lutetium-^{177} DOTATATE, and Sunitibib). The primary limitation was that there was no RCT comparing lutetium-^{177} DOTATATE with the other treatments. The authors concluded that based on NICE guidelines, only sunitinib could be considered cost-effectiveness in England and Wales (107).

CONCLUSIONS

Treatment of advanced neuroendocrine neoplasms is an ongoing clinical challenge. RCTs are mainly focused on treatments with Everolimus and SSAs (**Table 1**). Everolimus administration in advanced NET's demonstrates its efficacy and high tolerability both as monotherapy and in combination with other drugs. However, the use of Everolimus has been known to lead to resistance due to several mechanisms such as feedback activation of alternative pathways, inactivation of protein kinases, and deregulation of the downstream mTOR components (108, 109) Next-generation mTOR inhibitors have been studied to avoid the mechanisms of resistance and reduce the drug toxicity (85). Levels of CgA and NSE can predict outcomes in patients with advanced pNETs treated with everolimus, and other circulating biomarkers have been studied. There are several limitations with treatment outcomes (e.g., lack of benefit in OS from mTOR inhibitors) and biomarkers clinical application (e.g., small study sample size). However, the present review suggests that a range of combination therapies associated with the use of predictive biomarker is available for NET patients. Therefore, new emerging compounds such as second and third-generation mTOR inhibitors and anti-angiogenetic drugs should be tested in RCTs.

AUTHOR CONTRIBUTIONS

SZ, FG and GB conceptualized the study. SZ, FG and SR identified relevant literature. SZ, FG, GB and SR wrote the manuscript. All authors contributed to the article and approved the submitted version.

ACKNOWLEDGMENTS

The authors would like to thank Dr. Shivani Sharmi (Head of Psychology Group School of Life and Medical Sciences, University of Hertfordshire; UK) for the kind review of the English language.

REFERENCES

1. Modlin IM, Lye KD, Kidd M. A 5-decade analysis of 13,715 carcinoid tumors. *Cancer*. (2003) 97:934–59. doi: 10.1002/cncr.11105
2. Rehfeld JF. The new biology of gastrointestinal hormones. *Physiol Rev*. (1998) 78:1087–108. doi: 10.1152/physrev.1998.78.4.1087
3. Anlauf M. Neuroendocrine neoplasms of the gastroenteropancreatic system : pathology and classification. *Horm Metab Res*. (2011) 43:825–31. doi: 10.1055/s-0031-1291307
4. Lawrence B, Gustafsson BI, Chan A, Svejda B, Kidd M. The epidemiology of gastroenteropancreatic neuroendocrine tumors carcinoid epidemiology incidence neuroendocrine tumor. *Endocrinol Metab Clin*. (2011) 40:1–18. doi: 10.1530/ERC-13-0125
5. Modlin IM, Champaneria MC, Chan AKCA, Kidd M. A three-decade analysis of 3,911 small intestinal neuroendocrine tumors: the rapid pace of no progress. *Am J Gastroenterol*. (2007) 102:1464–73. doi: 10.1111/j.1572-0241.2007.01185.x
6. Modlin IM, Oberg K, Chung DC, Jensen RT, Herder Wouter W de, Thakker RV, et al. Gastroenteropancreatic neuroendocrine tumors. *Lancet Oncol*. (2008) 9:61–72. doi: 10.1016/S1470-2045(07)70410-2
7. Warner PRR. Enteroendocrine tumors other than carcinoid: a review of significant advances. *Gastroenterology*. (2005) 128:1668–84. doi: 10.1053/j.gastro.2005.03.078
8. Frilling A, Akerstrom G, Falconi M, Pavel M, Ramos J, Kidd M, Modlin and I. Neuroendocrine tumor disease : an evolving landscape. *Endocr Relat Cancer*. (2012) 19:163–85. doi: 10.1530/ERC-12-0024
9. Pellikka PAAJTBKKJBS, JACHCP, and LKK. Carcinoid heart disease. Clinical and echocardiographic spectrum in 74 patients. *Circulation*. (2015) 87:1188–96. doi: 10.1161/01.CIR.87.4.1188
10. Cives M, Strosberg JR. Gastroenteropancreatic neuroendocrine tumors. *CA Cancer J Clin*. (2018) 26:29–36. doi: 10.3322/caac.21493
11. Pavel M, Öberg K, Falconi M, Krenning EP, Sundin A, Perren A, et al. Gastroenteropancreatic neuroendocrine neoplasms: ESMO Clinical Practice Guidelines for diagnosis, treatment and follow-up. *Ann Oncol*. (2020) 31:844–60. doi: 10.1016/j.annonc.2020.03.304
12. Marinoni I, Kurrer AS, Vassella E, Dettmer M, Rudolph T, Banz V, et al. Loss of DAXX and ATRX are associated with chromosome. *Gastroenterology*. (2014) 146:453–60.e5. doi: 10.1053/j.gastro.2013.10.020
13. Shida T, Kishimoto T, Furuya M, Nikaido T, Koda K, Takano S, et al. Expression of an activated mammalian target of rapamycin (mTOR) in gastroenteropancreatic neuroendocrine tumors. *Cancer Chemother Pharmacol*. (2010) 65:889–93. doi: 10.1007/s00280-009-1094-6
14. Scarpa A, Chang DK, Nones K, Corbo V, Patch A-M, Bailey P, et al. Whole-genome landscape of pancreatic neuroendocrine tumours. *Nature*. (2017) 543:65–71. doi: 10.1038/nature21063
15. Leung R, Lang B, Wong H, Chiu J, Yat WK, Shek T, et al. Advances in the systemic treatment of neuroendocrine tumors in the era of molecular therapy. *Anticancer Agents Med Chem*. (2013) 13:382–8. doi: 10.2174/1871520611313030002
16. Willems L. PI3K and mTOR signaling pathways in cancer: new data on targeted therapies. *Curr Oncol Rep*. (2012) 14:129–38. doi: 10.1007/s11912-012-0227-y
17. Davis WJ, Lehmann PZ, Li W. Nuclear PI3K signaling in cell growth and tumorigenesis. *Front Cell Dev Biol*. (2015) 3:1–14. doi: 10.3389/fcell.2015.00024
18. Zhang X, Vadas O, Perisic O, Anderson KE, Clark J, Hawkins PT, et al. Structure of lipid kinase p110b/p85b elucidates an unusual SH2-domain-mediated inhibitory mechanism. *Mol Cell*. (2011) 41:567–78. doi: 10.1016/j.molcel.2011.01.026
19. Echeverria I, Liu Y, Gabelli SB, Amzel LM. Oncogenic mutations weaken the interactions that stabilize the p110 a—p85 a heterodimer isn phosphatidylinositol 3—kinase a. *FEBS J*. (2015) 282:3528–42. doi: 10.1111/febs.13365
20. Payne SN, Maher ME, Tran NH, Hey V De, Foley TM, Yueh AE, et al. PIK3CA mutations can initiate pancreatic tumorigenesis and are targetable with PI3K inhibitors. *Oncogenesis*. (2015) 4:e169–10. doi: 10.1038/oncsis.2015.28
21. Hassan B, Akcakanat A, Holder AM, Meric-Bernstam F. Targeting the PI3-kinase/Akt/mTOR signaling pathway. *Surg Oncol Clin N Am*. (2013) 22:641–64. doi: 10.1016/j.soc.2013.06.008
22. Moschetta M, Reale A, Marasco C, Vacca A. CMR. Therapeutic targeting of the mTOR-signaling pathway in cancer: benefits and limitations. *Br J Pharmacol*. (2014) 171:3801–13. doi: 10.1111/bph.12749
23. Yuan R, Kay A, Berg WJ, Lebwohl D. Targeting tumorigenesis : development and use of mTOR inhibitors in cancer therapy. *J Hematol Oncol*. (2009) 2:1–12. doi: 10.1186/1756-8722-2-45
24. Stambolic V, Suzuki A, Pompa L De, Brothers GM, Mirtsos C, Sasaki T, et al. Negative regulation of PKB / Akt-dependent cell survival by the tumor suppressor PTEN. *Cell*. (1998) 95:29–39. doi: 10.1016/S0092-8674(00)81780-8
25. Easton JB, Houghton PJ. mTOR and cancer therapy. *Oncogene*. (2006) 25:6436–46. doi: 10.1038/sj.onc.1209886
26. Land SC, Tee AR. Hypoxia-inducible factor 1α is regulated by the mammalian target of Rapamycin (mTOR) *via* an mTOR signaling motif. *J Biol Chem*. (2007) 282:20534–43. doi: 10.1074/jbc.M611782200
27. Capurso G, Archibugi L. Molecular pathogenesis and targeted therapy of sporadic pancreatic neuroendocrine tumors. *J Hepatobiliary Pancreat Sciepato*. (2015) 22:594–601. doi: 10.1002/jhbp.210
28. Zhang J, Francois R, Iyer R, Seshadri M, Zajac-kaye M, Hochwald SN. Current understanding of the molecular biology of pancreatic neuroendocrine tumors. *J Natl Cancer Inst*. (2013) 105:1005–17. doi: 10.1093/jnci/djt135
29. Shah T, Hochhauser D, Frow R, Quaglia A. Dhillon AP, Caplin ME. Epidermal growth factor receptor expression and activation in neuroendocrine tumours. *J Neuroendocr*. (2006) 18:355–60. doi: 10.1111/j.1365-2826.2006.01425.x
30. Missiaglia E, Dalai I, Barbi S, Beghelli S, Falconi M, Peruta M, et al. Pancreatic endocrine tumors : expression profiling evidences a role for AKT-mTOR pathway. *J Clin Oncol*. (2010) 28:245–55. doi: 10.1200/JCO.2008.21.5988
31. Catena L, Bajetta E, Milione M, Ducceschi M, Valente M, Dominoni F, et al. Mammalian target of rapamycin expression in poorly differentiated endocrine carcinoma: clinical and therapeutic future challenges. *Target Oncol*. (2011) 6:65–8. doi: 10.1007/s11523-011-0171-z
32. Svejda B, Kidd M, Kazberouk A, Lawrence B, Pfragner R. Limitations in small intestinal neuroendocrine tumor therapy by mTor kinase inhibition reflect growth factor—mediated PI3K feedback loop activation *via* ERK1 / 2 and AKT. *Cancer*. (2011) 117:4141–54. doi: 10.1002/cncr.26011
33. Jiao Y, Shi C, Edil BH, Wilde RF De, Klimstra DS, Maitra A, et al. DAXX/ ATRX, MEN1, and mTOR pathway genes are frequently altered in pancreatic neuroendocrine tumors. *Science*. (2011) 331:1199–204. doi: 10.1126/science.1200609
34. Yuan F, Shi M, Ji J, Shi H, Zhou C, Yu Y, et al. KRAS and DAXX / ATRX gene mutations are correlated with the clinicopathological features, advanced diseases, and poor prognosis in Chinese patients

with pancreatic neuroendocrine tumors. *Int J Biol Sci*. (2014) 10:957–65. doi: 10.7150/ijbs.9773
35. Öberg K. Genetics and molecular pathology of neuroendocrine gastrointestinal and pancreatic tumors (gastroenteropancreatic neuroendocrine tumors). *Curr Opin Endocrinol Diabetes Obes*. (2009) 16:72–8. doi: 10.1097/MED.0b013e328320d845
36. Asati V, Mahapatra DK, Bharti SK. European Journal of Medicinal Chemistry PI3K / Akt / mTOR and Ras / Raf / MEK / ERK signaling pathways inhibitors as anticancer agents: structural and pharmacological perspectives. *Eur J Med Chem*. (2016) 109:314–41. doi: 10.1016/j.ejmech.2016.01.012
37. Huang S, Houghton PJ. Resistance to rapamycin : a novel anticancer drug. *Cancer Metastasis*. (2001) 20:69–78. doi: 10.1023/A:1013167315885
38. Grozinsky-glasberg S, Pavel M. Inhibition of mTOR in carcinoid tumors. *Target Oncol*. (2012) 7:189–95. doi: 10.1007/s11523-012-0225-x
39. Duran I, Kortmansky J, Singh D, Hirte H, Kocha W, Goss G, et al. A phase II clinical and pharmacodynamic study of temsirolimus in advanced neuroendocrine carcinomas. *Br J Cancer*. (2006) 95:1148–54. doi: 10.1038/sj.bjc.6603419
40. Hobday TJ, Qin R, Reidy-lagunes D, Moore MJ, Strosberg J, Kaubisch A, et al. Multicenter phase II trial of temsirolimus and bevacizumab in pancreatic neuroendocrine tumors. *J Clin Oncol*. (2014) 32:1–6. doi: 10.1200/JCO.2014.56.2082
41. Capdevila J, Salazar R, Halperín I, Abad A, Yao JC. Innovations therapy : mammalian target of rapamycin (mTOR) inhibitors for the treatment of neuroendocrine tumors. *Cancer Metastasis Rev*. (2011) 30:27–34. doi: 10.1007/s10555-011-9290-3
42. Capozzi M, Caterina I, De Divitiis C, von Arx C, Maiolino P, Tatangelo F, et al. Everolimus and pancreatic neuroendocrine tumors (PNETs): activity, resistance and how to overcome it. *Int J Surg*. (2015) 21:S89–94. doi: 10.1016/j.ijsu.2015.06.064
43. Tabernero J, Rojo F, Calvo E, Burris H, Judson I, Hazell K, et al. Dose- and schedule-dependent inhibition of the mammalian target of rapamycin pathway with everolimus : a phase I tumor pharmacodynamic study in patients with advanced solid tumors. *J Clin Oncol*. (2008) 26:1603–10. doi: 10.1200/JCO.2007.14.5482
44. Yao JC, Shah MH, Ito T, Catherine Lombard Bohas EMW, Van CE, Hobday TJ, et al. Everolimus for advanced pancreatic neuroendocrine tumors. *N Engl Lornal Med*. (2011) 364:514–23. doi: 10.1056/NEJMoa1009290
45. Yao JC, Fazio N, Singh S, Buzzoni R, Carnaghi C, Wolin E, et al. Everolimus for the treatment of advanced, non-functional neuroendocrine tumours of the lung or gastrointestinal tract (RADIANT-4): a randomised, placebo-controlled, phase 3 study. *Lancet*. (2015) 387:1–10. doi: 10.1016/S0140-6736(15)00817-X
46. Verheijen RB, Atrafi F, Schellens JHM, Beijnen JH, Huitema ADR, Mathijssen RHJ. Pharmacokinetic optimization of everolimus dosing in oncology : a randomized crossover trial. *Clin Pharmacokinet*. (2017) 57:637–44. doi: 10.1007/s40262-017-0582-9
47. Rinke A, Mu H, Schade-brittinger C, Klose K, Barth P, Wied M, et al. Placebo-controlled, double-blind, prospective, randomized study on the effect of octreotide LAR in the control oftumor growth in patients with metastatic neuroendocrine midgut tumors: a report from the PROMID study group. *J Clin Oncol*. (2009) 27:4656–63. doi: 10.1200/JCO.2009.22.8510
48. Yao JC, Phan AT, Chang DZ, Wolff RA, Hess K, Gupta S, et al. Efficacy of RAD001 (Everolimus) and octreotide LAR in advanced low- to intermediate-grade neuroendocrine tumors: results of a phase II study. *J Clin Oncol*. (2008) 26:4311–8. doi: 10.1200/JCO.2008.16.7858
49. Yao JC, Catherine Lombard-Bohas EB, Kvols LK, Rougier P, Ruszniewski P, Hoosen S, et al. Daily oral everolimus activity in patients with metastatic pancreatic neuroendocrine tumors after failure of cytotoxic chemotherapy : a phase II trial. *J Clin Oncol*. (2010) 28:69–76. doi: 10.1200/JCO.2009.24.2669
50. Pavel ME, Hainsworth JD, Baudin E, Peeters M, Hörsch D, Winkler RE, et al. Everolimus plus octreotide long-acting repeatable for the treatment of advanced neuroendocrine tumours associated with carcinoid syndrome (RADIANT-2): a randomised, placebo-controlled, phase 3 study. *Lancet*. (2011) 378:2005–12. doi: 10.1016/S0140-6736(11)61742-X
51. Pavel ME, Baudin E, Öberg KE, Hainsworth JD, Voi M, Rouyrre N, et al. Efficacy of everolimus plus octreotide LAR in patients with advanced neuroendocrine tumor and carcinoid syndrome : final overall survival from the randomized, placebo-controlled phase 3 RADIANT-2 study. *Ann Oncol*. (2017) 28:1569–75. doi: 10.1093/annonc/mdx193
52. Bajetta E, Catena L, Fazio N, Pusceddu S, Pamela B, Blanco G, et al. Everolimus in combination with octreotide long-acting repeatable in a first-line setting for patients with neuroendocrine tumors. *Cancer*. (2014) 15:2457–63. doi: 10.1002/cncr.28726
53. Kim HS, Shaib WL, Zhang C, Nagaraju GP. Phase 1b study of pasireotide, everolimus, and selective internal radioembolization therapy for unresectable neuroendocrine tumors with hepatic metastases. *Cancer*. (2018) 124:1992–2000. doi: 10.1002/cncr.31192
54. Kulke MH, Ruszniewski P, Cutsem EV, Lombard-Bohas C, Valle JW, Herder WWD, et al. A randomized, open-label, phase 2 study of everolimus in combination with pasireotide LAR or everolimus alone in advanced, well-differentiated, progressive pancreatic neuroendocrine tumors: COOPERATE-2 trial. *Ann Oncol*. (2017) 28:1309–15. doi: 10.1093/annonc/mdx078
55. Chan JA, Ryan DP, Zhu AX, Abrams TA, Wolpin BM, Malinowski P, et al. Phase I study of pasireotide (SOM 230) and everolimus (RAD001) in advanced neuroendocrine tumors. *Endocr Relat Cancer*. (2012) 19:615–23. doi: 10.1530/ERC-11-0382
56. Chan JA, Mayer RJ, Jackson N, Malinowski P, Regan E, Kulke MH. Phase I study of sorafenib in combination with everolimus (RAD001) in patients with advanced neuroendocrine tumors. *Cancer Chemother Pharmacol*. (2013) 23:1–7. doi: 10.1007/s00280-013-2118-9
57. Lane HA, Wood JM, Mcsheehy PMJ, Allegrini PR, Boulay A, Brueggen J, et al. mTOR inhibitor RAD001 (Everolimus) has antiangiogenic/vascular properties distinct from a VEGFR tyrosine kinase inhibitor. *Clin Cancer Res*. (2009) 15:1612–23. doi: 10.1158/1078-0432.CCR-08-2057
58. Hobday TJ, Rubin J, Holen K, Picus J, Donehower R, Marschke R, et al. MC044h, a phase II trial of sorafenib in patients (pts) with metastatic neuroendocrine tumors (NET): a Phase II Consortium (P2C) study. *J Clin Oncol*. (2007) 25:4504. doi: 10.1200/jco.2007.25.18_suppl.4504
59. Molina AM, Feldman DR, Voss MH, Ginsberg MS, Baum MS, Brocks DR. Phase 1 trial of Everolimus plus sunitinib in patients with metastatic renal cell carcinoma. *Cancer*. (2012) 118:1868–76. doi: 10.1002/cncr.26429
60. Wiedmann MW, Mössner J. Clinical medicine insights : oncology safety and efficacy of sunitinib in patients with unresectable pancreatic neuroendocrine tumors. *Clin Med Insights Oncol*. (2012) 6:381–94. doi: 10.4137/CMO.S7350
61. Motzer RJ, Barrios CH, Kim TM, Falcon S, Cosgriff T, Harker WG, et al. Phase II randomized trial comparing sequential first-line everolimus and second-line sunitinib versus first-line sunitinib and second-line everolimus in patients with metastatic renal cell carcinoma. *J Clin Oncol*. (2014) 32:2765–72. doi: 10.1200/JCO.2013.54.6911
62. Angelousi A, Kamp K, Kaltsatou M, O'Toole D, De Herder W. Sequential everolimus and sunitinib treatment in pancreatic metastatic well-differentiated neuroendocrine tumours resistant to prior treatments. *Neuroendocrinology*. (2017) 105:394–402. doi: 10.1159/000456035
63. Kulke MH, Niedzwiecki D, Foster NR, Fruth B, Kunz PL, Kennecke HF, et al. Randomized phase II study of everolimus (E) vs. everolimus plus bevacizumab (E+B) in patients (Pts) with locally advanced or metastatic pancreatic neuroendocrine tumors (pNET), CALGB 80701 (Alliance). *J Clin Oncol*. (2015) 33:4005. doi: 10.1200/jco.2015.33.15_suppl.4005
64. Chan JA, Blaszkowsky L, Stuart K, Zhu AX. A prospective, phase 1/2 study of everolimus and temozolomide in patients with advanced pancreatic neuroendocrine tumor. *Cancer*. (2013) 119:3212–8. doi: 10.1002/cncr.28142
65. Claringbold PG, Turner JH. Neuroendocrine tumor therapy with lutetium-177-octreotate and everolimus (NETTLE): a phase i study. *Cancer Biother Radiopharm*. (2015) 30:261–9. doi: 10.1089/cbr.2015.1876
66. Xie J, Wang X, Proud CG. mTOR inhibitors in cancer therapy [version 1; referees : 3 approved] Referee Status. *F1000Research*. (2016) 5:1–11. doi: 10.12688/f1000research.9207.1
67. Wolin E, Mita A, Mahipal A, Meyer T, Bendell J, Nemunaitis J, et al. A phase 2 study of an oral mTORC1/mTORC2 kinase inhibitor (CC-223) for non-pancreatic neuroendocrine tumors with or without carcinoid symptoms. *PLoS ONE*. (2019) 14:1–14. doi: 10.1371/journal.pone.0221994
68. Rodrik-Outmezguine VS. Overcoming mTOR resistance mutations with a new-generation mTOR inhibitor. *Nature*. (2016) 534:272–6. doi: 10.1038/nature17963

69. Fan Q, Aksoy O, Wong RA, Okaniwa M, Shokat KM, Weiss WA, et al. A kinase inhibitor targeted to mTORC1 drives regression in glioblastoma article a kinase inhibitor targeted to mTORC1 drives regression in glioblastoma. *Cancer Cell*. (2017) 31:424–35. doi: 10.1016/j.ccell.2017.01.014
70. Moore KN, Bauer TM, Falchook GS, Chowdhury S, Patel C, Neuwirth R, et al. Phase i study of the investigational oral mTORC1/2 inhibitor sapanisertib (TAK-228): tolerability and food effects of a milled formulation in patients with advanced solid tumours. *ESMO Open*. (2018) 3:291. doi: 10.1136/esmoopen-2017-000291
71. Chamberlain CE, German MS, Yang K, Wang J, Vanbrocklin H, Regan M, et al. Cancer biology and translational studies a patient-derived xenograft model of pancreatic neuroendocrine tumors identifies sapanisertib as a possible new treatment for everolimus-resistant tumors. *Cancer Biol Transl Stud.* (2018) 17:1204 doi: 10.1158/1535-7163.MCT-17-1204
72. Aksamitiene E, Kiyatkin A, Kholodenko BN. Cross-talk between mitogenic Ras/MAPK and survival PI3K/Akt pathways: a fine balance. *Biochem Soc Trans*. (2011) 40:139–46. doi: 10.1042/BST20110609
73. Kriegsheim AV, Baiocchi D, Birtwistle M, Sumpton D, Bienvenut W, Morrice N, et al. Cell fate decisions are specified by the dynamic ERK interactome. *Nat Cell Biol*. (2009) 11:1458–64. doi: 10.1038/ncb1994
74. Carracedo A. inhibition of mTORC1 leads to MAPK pathway activation through a PI3K-dependent feedback loop in human cancer. *J Clin Invest*. (2008) 118:3065–74. doi: 10.1172/JCI34739
75. Ruifang M, Jianhui M, Dechang Z, Limin Li HZ. efficacy of combined inhibition of mTOR and ERK/MAPK pathways in treating a tuberous sclerosis complex cell model. *J Genet Genomics.* (2009) 36:355–61. doi: 10.1016/S1673-8527(08)60124-1
76. Wang X, Hawk N, Yue P, Kauh J, Ramalingam SS, Fu H, et al. Overcoming mTOR inhibition-induced paradoxical activation of survival signaling pathways enhances mTOR inhibitors' anticancer efficacy. *Cancer Biol Ther*. (2008) 7:1952–8. doi: 10.4161/cbt.7.12.6944
77. Carew JS, Kelly KR, Nawrocki ST. Mechanisms of mTOR inhibitor resistance in cancer therapy. *Target Oncol.* (2011) 6:17–27. doi: 10.1007/s11523-011-0167-8
78. Zitzmann K, Rüden JV, Brand S, Göke B, Lichtl J, Spöttl G, et al. Compensatory activation of Akt in response to mTOR and Raf inhibitors—a rationale for dual-targeted therapy approaches in neuroendocrine tumor disease. *Cancer Lett*. (2010) 295:100–9. doi: 10.1016/j.canlet.2010.02.018
79. Fazio N. Neuroendocrine tumors resistant to mammalian target of rapamycin inhibitors: a difficult conversion from biology to the clinic. *World J Clin Oncol*. (2015) 6:194–8. doi: 10.5306/wjco.v6.i6.194
80. Reilly KEO, Rojo F, She Q, Reilly KEO, Rojo F, She Q, et al. mTOR inhibition induces upstream receptor tyrosine kinase signaling and activates Akt. *Cancer Res.* (2006) 66:1500–8. doi: 10.1158/0008-5472.CAN-05-2925
81. Zhang H, Griffin JD, Kwiatkowski DJ, Zhang H, Bajraszewski N, Wu E, et al. PDGFRs are critical for PI3K/Akt activation and negatively regulated by mTOR. *J Clin Invest*. (2007) 117:730–8. doi: 10.1172/JCI28984
82. Zhang H, Carpenter CL, David J, Zhang H, Cicchetti G, Onda H, et al. Loss of Tsc1/Tsc2 activates mTOR and disrupts PI3K-Akt signaling through downregulation of PDGFR. *J Clin Invest*. (2003) 112:1223–33. doi: 10.1172/JCI200317222
83. Elke Tatjana Aristizabal Prada GS, Maurer J, Lauseker M, Koziolek EJ, Schrader J, Grossman A, et al. The role of GSK3 and its reversal with GSK3 antagonism in everolimus resistance. *Endocr Relat Cancer*. (2018) 25:893–908. doi: 10.1530/ERC-18-0159
84. Antonuzzo L, Del Re M, Barucca V, Spada F, Meoni G, Restante G, et al. Critical focus on mechanisms of resistance and toxicity of m-TOR inhibitors in pancreatic neuroendocrine tumors. *Cancer Treat Rev*. (2017) 57:28–35. doi: 10.1016/j.ctrv.2017.05.001
85. Beyens M, Vandamme T, Peeters M, Van Camp G, De Beeck KO. Resistance to targeted treatment of gastroenteropancreatic neuroendocrine tumors. *Endocrine-Related Cancer*. (2019) 26:R109–30. doi: 10.1530/ERC-18-0420
86. Karar J, Maity A. PI3K/AKT/mTOR pathway in angiogenesis. *Front Mol Neurosci*. (2011) 4:1–8. doi: 10.3389/fnmol.2011.00051
87. Dormond-meuwly A, Roulin D, Dufour M, Benoit M, Demartines N, Dormond O. The inhibition of MAPK potentiates the anti-angiogenic efficacy of mTOR inhibitors. *Biochem Biophys Res Commun*. (2011) 407:714–9. doi: 10.1016/j.bbrc.2011.03.086
88. Katsha A, Wang L, Arras J. Activation of EIF4E by aurora kinase a depicts a novel druggable axis in everolimus-resistant cancer cells. *Clin Cancer Res*. (2017) 23:3756–68. doi: 10.1158/1078-0432.CCR-16-2141
89. Aguirre D, Boya P, Bellet D, Faivre S, Troalen F, Benard J, et al. Bcl-2 and CCND1/CDK4 expression levels predict the cellular effects of mTOR inhibitors in human ovarian carcinoma. *Apoptosis*. (2004) 9:797–805. doi: 10.1023/B:APPT.0000045781.46314.e2
90. Modlin IM, Kidd M, Malczewska A, Drozdov I, Bodei L, Matar S, et al. The NETest: the clinical utility of multigene blood analysis in the diagnosis and management of neuroendocrine tumors. *Endocrinol Metab Clin N A*. (2018) 47:485–504. doi: 10.1016/j.ecl.2018.05.002
91. Lv Y, Han X, Zhang C, Fang Y, Pu N, Ji Y, et al. Combined test of serum CgA and NSE improved the power of prognosis predicition of NF-pNETs. *Endocr Connect*. (2017) 7:1–34. doi: 10.1530/EC-17-0276
92. Baudin E, Wolin E, Castellano D, Kaltsas G, Panneerselvam A, Tsuchihashi Z, et al. Correlation of PFS with early response of chromogranin A and 5-hydroxyindoleacetic acid levels in Pts with advanced neuroendocrine tumours: phase III RADIANT-2 study results. *Eur J Cancer*. (2011) 47:S460. doi: 10.1016/S0959-8049(11)71875-5
93. Martins D, Spada F, Lambrescu I, Rubino M, Cella C, Gibelli B, et al. Predictive markers of response to everolimus and sunitinib in neuroendocrine tumors. *Target Oncol.* (2017) 12:611–22. doi: 10.1007/s11523-017-0506-5
94. Zatelli MC, Fanciulli G, Malandrino P, Ramundo V, Faggiano A, Colao A. Predictive factors of response to mTOR inhibitors in neuroendocrine tumours. *Endocr Relat Cancer*. (2016) 23:173–83. doi: 10.1530/ERC-15-0413
95. Gelsomino F, Casadei-Gardini A, Caputo F, Rossi G, Bertolini F, Petrachi T, et al. mTOR pathway expression as potential predictive biomarker in patients with advanced neuroendocrine tumors treated with everolimus. *Cancers*. (2020) 12:1201. doi: 10.3390/cancers12051201
96. Meric-bernstam F, Akcakanat A, Chen H, Do K, Sangai T, Adkins F, et al. PIK3CA/PTEN mutations and Akt activation as markers of sensitivity to allosteric mTOR inhibitors. *Clin Cancer Res.* (2012) 18:1777–90. doi: 10.1158/1078-0432.CCR-11-2123
97. Delbaldo C, Albert S, Dreyer C, Sablin M-P, Serova M, Raymond E, et al. Predictive biomarkers for the activity of mammalian target of rapamycin (mTOR) inhibitors. *Target Oncol.* (2011) 6:119–24. doi: 10.1007/s11523-011-0177-6
98. Nicolantonio FD, Biffo S, Bardelli A, Nicolantonio FD, Arena S, Tabernero J, et al. Deregulation of the PI3K and KRAS signaling pathways in human cancer cells determines their response to everolimus. *J Clin Invest*. (2010) 120:2858–66. doi: 10.1172/JCI37539
99. Serra S, Zheng L, Hassan M, Phan AT, Woodhouse LJ, Yao JC, et al. The FGFR4-G388R single-nucleotide polymorphism alters pancreatic neuroendocrine tumor progression and response to mTOR inhibition therapy. *AACR J.* (2012) 12:5683–92. doi: 10.1158/0008-5472.CAN-12-2102
100. Cros J, Moati E, Raffenne J, Hentic O, Svrcek M, Mestier Ld, et al. Gly388Arg FGFR4 polymorphism is not predictive of everolimus efficacy in well-differentiated digestive neuroendocrine tumors. *Neuroendocrinology*. (2016) 103:495–9. doi: 10.1159/000440724
101. Bellister SA, Zhou Y, Sceusi E, Ellis LM, Yao JC. Prediction of prognosis in patients treated with everolimus for extrapancreatic neuroendocrine tumors by a single nucleotide polymorphism in PHLPP2. *J Clin Oncol*. (2013) 31:163. doi: 10.1200/jco.2013.31.4_suppl.163
102. Falletta S, Partelli S, Rubini C, Nann D, Doria A, Marinoni I, et al. mTOR inhibitors response and mTOR pathway in pancreatic neuroendocrine tumors. *Endocr Relat Cancer*. (2016) 23:883–91. doi: 10.1530/ERC-16-0329
103. Grabiner BC, Nardi V, Birsoy K, Possemato R, Shen K, Sinha S, et al. A diverse array of cancer-associated MTOR mutations are hyperactivating and can predict rapamycin sensitivity. *Cancer Discov*. (2014) 4:554–63. doi: 10.1158/2159-8290.CD-13-0929
104. Roviello G, Zanotti L, Venturini S, Bottini A, Generali D. Role of targeted agents in neuroendocrine tumours: results from a meta-analysis. *Cancer Biol Ther*. (2016) 17:883–8. doi: 10.1080/15384047.2016.1210735

105. Kaderli RM, Spanjol M, Kollár A, Bütikofer L, Gloy V, Dumont RA, et al. Therapeutic options for neuroendocrine tumors a systematic review and network meta-analysis. *JAMA Oncol*. (2019) 5:480–9. doi: 10.1001/jamaoncol.2018.6720
106. Ravaud A, Urva SR, Grosch K, Cheung WK, Anak O, Sellami DB. Relationship between everolimus exposure and safety and efficacy: meta-analysis of clinical trials in oncology. *Eur J Cancer*. (2014) 50:486–95. doi: 10.1016/j.ejca.2013.11.022
107. Mujica-Mota R, Varley-Campbell J, Tikhonova I, Cooper C, Griffin E, Haasova M, et al. Everolimus, lutetium-177 DOTATATE and sunitinib for advanced, unresectable or metastatic neuroendocrine tumours with disease progression: a systematic review and cost-effectiveness analysis. *Health Technol Assess*. (2018) 22:1–325. doi: 10.3310/hta22490
108. Lee L, Ito T, Jensen RT. Everolimus in the treatment of neuroendocrine tumors: efficacy, side-effects, resistance, and factors affecting its place in the treatment sequence. *Expert Opin Pharmacother*. (2018) 19:909–28. doi: 10.1080/14656566.2018.1476492
109. Pan J, Bao Q, Enders G. The altered metabolic molecular signatures contribute to the RAD001 resistance in gastric neuroendocrine tumor. *Front Oncol*. (2020) 10:546. doi: 10.3389/fonc.2020.00546

Conflict of Interest: The authors declare that the research was conducted in the absence of any commercial or financial relationships that could be construed as a potential conflict of interest.

frontiers in Endocrinology

ORIGINAL RESEARCH
published: 29 March 2021
doi: 10.3389/fendo.2021.647369

Serum miR-375 for Diagnostic and Prognostic Purposes in Medullary Thyroid Carcinoma

*Simona Censi[1], Loris Bertazza[1], Ilaria Piva[1], Jacopo Manso[1], Clara Benna[2], Maurizio Iacobone[2], Alberto Mondin[1], Mario Plebani[3], Diego Faggian[3], Francesca Galuppini[4], Gianmaria Pennelli[4], Susi Barollo[1] and Caterina Mian[1]**

[1] Endocrinology Unit, Department of Medicine (DIMED), University of Padua, Padua, Italy, [2] Endocrine Surgery Unit, Department of Surgical, Oncological and Gastroenterological Sciences (DiSCOG), University of Padua, Padua, Italy, [3] Laboratory Medicine, Department of Medicine (DIMED), University of Padua, Padua, Italy, [4] Surgical Pathology and Cytopathology Unit, Department of Medicine (DIMED), University of Padua, Padua, Italy

OPEN ACCESS

Edited by:
Enzo Lalli, UMR7275 Institut de pharmacologie moléculaire et cellulaire (IPMC), France

Reviewed by:
Rossella Elisei, University of Pisa, Italy
Mehdi Hedayati, Shahid Beheshti University of Medical Sciences, Iran

***Correspondence:**
Caterina Mian
caterina.mian@unipd.it

Specialty section:
This article was submitted to Cancer Endocrinology, a section of the journal Frontiers in Endocrinology

Received: *29 December 2020*
Accepted: *01 March 2021*
Published: *29 March 2021*

Citation:
Censi S, Bertazza L, Piva I, Manso J, Benna C, Iacobone M, Mondin A, Plebani M, Faggian D, Galuppini F, Pennelli G, Barollo S and Mian C (2021) Serum miR-375 for Diagnostic and Prognostic Purposes in Medullary Thyroid Carcinoma. Front. Endocrinol. 12:647369. doi: 10.3389/fendo.2021.647369

Purpose: Having previously demonstrated that tissue miR-375 expression in medullary thyroid carcinoma (MTC) tissues is linked to prognosis, the aim of this study was to assess the diagnostic and prognostic value of circulating miR-375 levels in MTC patients.

Methods: A series of 68 patients with MTC was retrospectively retrieved and assessed in terms of their clinicopathological characteristics. MiR-375 levels were measured in all patients' presurgical blood samples. Both serum and tissue levels were tested prior to surgery in a subgroup of 57 patients. Serum miR-375 levels were also measured in serum from 49 patients with non-C-cell thyroid nodular diseases (non-CTN), 14 patients with pheochromocytoma, and 19 healthy controls.

Results: Circulating miR-375 levels were 101 times higher in the serum of patients with MTC than in all other patients and controls, with no overlap ($P < 0.01$). No correlation emerged between serum and tissue miR-375 levels. Serum miR-375 levels were higher in MTC patients with N0 than in those with N1 disease ($P = 0.01$), and also in patients who were biochemically cured than in those who were not ($P = 0.02$). In the whole series of patients and controls, calcitonin (CT) and serum miR-375 levels were correlated at diagnosis ($R^2 = 0.40$, $P < 0.01$), but in a U-shaped manner: a positive correlation was found with low CT levels, then the correlation turns negative as CT rises (in MTC patients). A negative correlation was indeed found in MTC patients between serum miR-375 and CT ($R^2 = -0.10$, $P = 0.01$). On ROC curve analysis, a cut-off of 2.1 for serum miR-375 proved capable of distinguishing between MTC patients and the other patients and controls with a 92.6% sensitivity and a 97.6% specificity (AUC: 0.978, $P < 0.01$).

Conclusions: Serum miR-375 levels can serve as a marker in the diagnosis of MTC, with a remarkable specificity. Serum miR-375 also proved a novel marker of prognosis in this disease. Further *in vitro* experiments to corroborate our results are currently underway.

Keywords: miR-375, circulating miRNAs, medullary thyroid cancer, calcitonin, diagnostic marker

INTRODUCTION

Medullary thyroid cancer (MTC) is a neuroendocrine neoplasm arising from thyroid parafollicular C-cells.

Sporadic MTC (sMTC) carries somatic REarranged during Transfection *(RET)* mutations in approximately 50% of cases, with a subset of sporadic and *RET*-negative MTC also carrying a mutation in *RAS* genes (1). It is well known that somatic *RET* mutations point to a poor prognosis in sMTC, and somatic *RAS* mutations to a better prognosis (2). It is therefore useful to assess patients' mutational status for prognostic purposes, and crucial to the choice of new target treatments such as the now-approved tyrosine kinase cabozantinib (3, 4) or the highly selective *RET* inhibitor pralsetinib currently being trialed for use against MTC (5). About 40–60% of sporadic MTCs do not carry any recognized genetic driver, however, making it difficult to establish a patient's prognosis and therapeutic options. In short, the discovery of new molecular changes remains pivotal to improving the prognostic stratification of patients with MTC, and to the search for novel targets for therapy.

The availability of new serum markers would also benefit the diagnosis of MTC. Calcitonin (CT) is a 32-amino-acid monomeric peptide produced by C-cells. It is a sensitive marker for the purposes of tumor diagnostics and prognostics because its serum concentrations correlate directly with the C-cell mass (6). Measuring CT has many pre-analytical, analytical, and post-analytical pitfalls, however, which sometimes make its interpretation difficult, especially in the event of moderately elevated levels (7).

One in four cases of MTC—hereditary MTC, hMTC—arises in the context of an autosomal dominant multiple endocrine neoplasia syndrome type 2 (MEN2), which is caused by *RET* proto-oncogene germline mutations (in both MEN2A and MEN2B) (8). Affected individuals initially develop primary C-cell hyperplasia (CCH), which progresses to early invasive MTC, and eventually to grossly invasive macroscopic MTC. Apart from patients with the *RET* codon M918T mutation (who should undergo thyroidectomy in the first year of life), the age of onset and aggressiveness of MTC varies considerably, even among individuals from the same family (4). Hence the particular interest in finding new serum markers to improve the specificity of patients' diagnosis and prognosis, in both sMTC and hMTC.

MiRNAs are endogenous single-stranded non-coding RNAs that selectively bond to the complementary 3'UTR mRNAs, influencing their cleavage and translation (9) and many studies have documented their involvement in the pathogenesis of cancer, including endocrine tumors (10, 11). MiRNAs can act as "onco-miRNAs" or "oncosuppressor miRNAs," their final biological function being tissue- and context-dependent (12). MiRNAs have also been isolated in biofluids, such as blood serum and plasma, and they have consequently emerged as novel biomarkers for use in cancer diagnostics and prognostics (13, 14–17). They have shown a remarkable stability in clinical samples of plasma and serum (17), possibly overcoming the analytical problems associated with CT measurement.

One of the most promising miRNAs involved in the pathogenesis of MTC is miR-375. A first study by our group demonstrated its overexpression in MTC, with levels 10 times higher than in normal thyroid tissues (18). In a subsequent study focusing on the tissue expression of miR-375 in a larger series of sMTC and hMTC, we confirmed that miR-375 levels are higher in MTC than in normal thyroid tissue, with no overlap in the levels measured between the two entities. We also documented a link between miR-375 tissue expression and the aggressiveness of a tumor's clinicopathological characteristics and patient outcomes at the end of the follow-up. This would suggest a role for miR-375 as an onco-miRNA in the pathogenesis of MTC. Based on these findings in tissue miR-375, the aim of the present study was to examine circulating miR-375 levels, and their possible role in MTC diagnostics and prognostics.

MATERIALS AND METHODS

Patients

A tissue bank has been operating at Padua University Hospital since 2005. Patients undergoing surgery for certain diseases (including nodular thyroid diseases and adrenal diseases) are routinely asked beforehand for permission to collect and store their tissue and serum samples for research purposes (protocol ref. 3388). All patients involved in this study thus gave their informed written consent to the banking of their tissue and serum samples, with the approval of the ethical committee for clinical experimentation at Padua Hospital. This study was conducted in accordance with the Declaration of Helsinki.

The study involved a consecutive series of 69 patients with MTC who underwent surgery between 2007 and 2020 (30 males and 39 females; median age: 55 years; range: 5–87 years). MiR-375 levels were assessed in all patients' serum samples obtained at the time of surgery, before intervention. Analyses were conducted to identify all germinal and somatic *RET* mutations. Both preoperative serum and postoperative MTC tissue samples were available for a subgroup of 57 patients. For this subgroup, tissue miR-375 levels were also measured, and somatic *RET* and *RAS* mutations were sought.

Data were collected on CT levels at diagnosis, TNM staging at diagnosis, and the biochemical cure rate. The median follow-up was 70.5 months (IQR: 29.0–109.0 months).

For comparison, serum miR-375 levels were measured in samples from 49 patients with non-C-cell thyroid nodular diseases (non-CTN) (23 males and 26 females), whose histological diagnoses included: 12 follicular adenomas (FA); 15 hyperplastic nodules (HN); 10 follicular thyroid carcinomas (FTC); and 12 papillary thyroid cancers (PTC). MiR-375 was also assayed in serum samples obtained before adrenal surgery from 14 patients with pheochromocytoma (7 males and 7 females), and in the serum of 19 healthy controls (10 males, 9 females).

RET Germline Mutations and RET/RAS Somatic Mutations

DNA was extracted from all patients' serum samples and tissues frozen after surgery using the DNeasy Blood and Tissue kit

(Qiagen, Milano, Italy), according to the manufacturer's protocol. Analyses were performed by direct sequencing, as described elsewhere (19, 20): for *RET* (NM_020975.4; exons 5, 8, 10, 11, 13, 14, 15, and 16) in 47 tissue samples, and all serum samples; and for *N-RAS* (NM_002524.3; exons 2 and 3), *K-RAS* (NM_033360.2; exons 2 and 3), and *H-RAS* (NM_005343.2; exons 2 and 3) mutations in 42 tissue samples.

miRNA Quantitative Real-Time Polymerase Chain Reaction

Total RNA was extracted from fresh snap-frozen samples of 57 MTC, using the TRIzol reagent as lysis buffer (Invitrogen, Carlsbad, CA, USA) according to the manufacturer's protocol. RNA extractions from serum were performed using the Zymo DirectZol RNA Miniprep Plus Kit (cat. no. R2051) according to the manufacturer's instructions. RNA was quantified by Nanodrop (Thermo-Fisher). CDNA synthesis was done with the TaqMan Advanced miRNA cDNA Synthesis Kit (Applied Biosystems, Milan, Italy).

A real-time quantitative PCR (qRT-PCR) was performed for has-miR-375-3p on the StepOne real-time PCR system using TaqMan advanced miRNA assays, and following the manufacturer's instructions. Normalization was done through the application of the hsa-miR-24-3p. All real-time reactions, including no template controls, were run in triplicate. A pool of cDNA derived from mixed normal human thyroid tissues and serum was used as the calibrator source.

Data were analyzed with the relative quantification (2-ΔΔCt) method, as described elsewhere (21).

Statistical Analysis

The Kolmogorov-Smirnov test showed that the variables were not distributed normally, so data are reported as medians and interquartile ranges (IQR). The Mann-Whitney test was used to analyze the tissue and circulating miR-375 serum levels and gender, lymph node involvement, stage of MTC at diagnosis (I+II *versus* III+IV), biochemical cure, *RAS* somatic mutation, *RET* somatic and germinal mutational status, and dichotomized CT levels. The Mann-Whitney test was also used to investigate the relationships: between CT levels, lymph node involvement, and stage of MTC at diagnosis (I+II *versus* III+IV); and between biochemical cure rate, CT levels, and tumor size. The Kruskal-Wallis test was used to evaluate miR-375 circulating levels with subjects' condition (MTC *versus* non-CTN or pheochromocytoma or healthy controls). Categorical variables (biochemical cure rate, sex, age, and lymph node involvement) were compared with the chi-squared test. A P-value of <0.05 was considered statistically significant.

RESULTS

Patients

Table 1 shows the clinicopathological features of the MTC patients, including their mutational status and biochemical cure rates.

Tissue miR-375 Levels

Tissue miR-375 levels correlated weakly with CT levels at diagnosis (r^2 = 0.095, P = 0.04), and tumor size (r^2 = 0.14, P < 0.01).

Median tissue miR-375 levels were higher in males (0.044, IQR: 0.03–0.14 in males and 0.02, IQR: 0.008–0.06 in females, P = 0.04), in cases with positive lymph nodes (0.07, IQR: 0.03–0.17 in N1 patients; 0.02, IQR: 0.007–0.05 in N0 patients, P = 0.02), in patients with higher tumor stages at diagnosis (0.02, IQR: 0.007–0.05 for stages I+II; 0.08, IQR: 0.03–0.17 for stages III+IV; P = 0.02), and in patients not biochemically cured by the end of the follow-up (0.02, IQR: 0.008–0.03 in those who were biochemically cured; 0.06, IQR: 0.01–0.12 in those who were not; P = 0.03).

No correlations emerged with age at diagnosis (P = 0.42), or with somatic *RET* or *RAS* mutations (P = 0.43 and P = 0.71, respectively).

Circulating miR-375 Levels

Median circulating miR-375 levels were higher in the serum of MTC patients (15.15, IQR: 5.82–36.51) than in the other patients and controls (P < 0.01), with no overlap in the IQR for these two groups' miR-375 levels. The median miR-375 levels in the patients and controls were as follows: non-CTN patients 0.11, IQR: 0.005–0.36; pheochromocytoma patients: 0.002, IQR: 0.001–0.002; and healthy controls 0.84, IQR: 0.55–1.38. When the median values were compared, the MTC patients' miR-375 levels were 101 times higher than in the non-MTC subjects (P < 0.01) (**Figure 1** and **Table 2**).

Intriguingly, no correlation was found between serum and tissue miR-375 levels (P = 0.19).

Considering the MTC patients alone, there was no statistically significant difference in the median serum miR-375 levels by gender, although male patients had higher median levels than females (20.18, IQR: 5.21–40.23 *vs* 12.80, IQR of 6.93–23.26, P = 0.37). Nor was there any significant correlation between

TABLE 1 | Clinicopathological characteristics of the MTC patients enrolled.

	Parameter	Results
Primary cancer size, median, IQR (mm)		13, 8–24
T	1	35/63 (55.6%)
	2	11/63 (17.5%)
	3	16/63 (25.4%)
	4	1/63 (1.6%)
Lymph node involvement	N0	44/65 (67.7%)
	N1a	7/65 (10.8%)
	N1b	14/65 (21.5%)
Tumor stage	I	31/65 (47.7%)
	II	13/65 (20.0%)
	III	7/65 (10.8%)
	IV	14/65 (21.5%)
***RET* germline mutation**	Present	17/69 (24.6%)
	Absent	52/69 (75.4%)
***RET* somatic mutation**	Present	19/47 (40.4%)
	Absent	28/47 (59.6%)
***RAS* somatic mutation**	Present	4/42 (9.5%)
	Absent	38/42 (90.5%)
Biochemical cure	Yes	42/60 (70.0%)
	No	18/60 (30.0%)

serum miR-375 levels and age at diagnosis (P = 0.58) or cancer size (P = 0.92), or between serum miR-375 levels and any presence of somatic *RET/RAS* mutations in MTC tissue (P = 0.35).

Median serum miR-375 levels were higher in patients with hMTC than in those with sMTC (23.77, IQR 15.98–40.81 *vs* 10.72, IQR: 4.18–27.49, P = 0.03), in N0 patients than in N1 patients (18.71, IQR: 9.79–35.12 *vs* 5.70, IQR: 2.48–12.17, P = 0.01), and in patients who were biochemically cured than in those who were not (19.56, IQR: 9.54–40.23 *vs* 4.67, IQR: 24.67–16.11, P = 0.02). There was no difference in the biochemical cure rate between hMTC and sMTC (P = 0.07), though a trend towards a worse prognosis emerged for sMTC: at the end of the follow-up, the biochemical cure rate was 28/44 (63.6%) cases of sMTC *versus* 14/16 (87.5%) cases of hMTC.

A trend towards higher median miR-375 levels was seen in patients with lower tumor stages at diagnosis (19.28, IQR: 9.79–37.4 for patients in stages I+II *vs* 7.45, IQR: 3.12–29.73 for those in stages III+IV), although the difference did not reach statistical significance (P = 0.05).

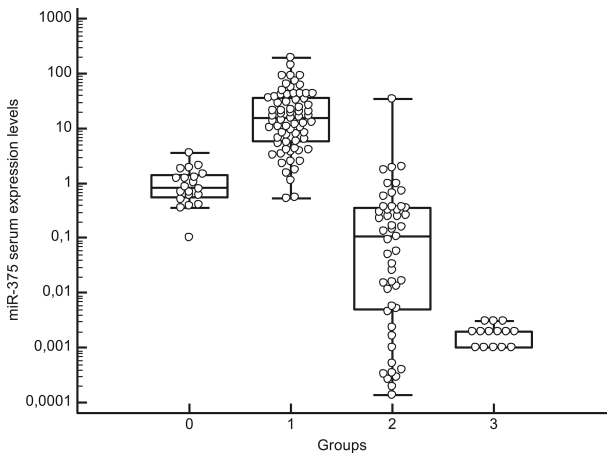

FIGURE 1 | Box-whisker plot graph representing the medians, minimum and maximum values and interquartile ranges (IQR) of serum miR-375 levels in different groups: group 0: healthy subjects, group 1: MTC patients, group 2: patients with thyroid non-C-cell nodular diseases (non-CTN), group 3: pheochromocytoma patients. Values are represented on a logarithmic scale.

TABLE 2 | *Post-hoc* test after Kruskal-Wallis analysis for median circulating miR-375 levels in the different groups: group 0: healthy subjects, group 1: MTC patients, group 2: patients with thyroid non-C-cell nodular diseases (non-CTN), group 3: pheochromocytoma patients.

Factor	n	Average Rank	Different (P < 0.05) from factor nr
0 (healthy subjects)	19	69.40	(1)(2)(3)
1 (MTC)	69	116.17	(0)(2)(3)
2 (non-CTN)	49	40.43	(0)(1)(3)
3 (pheochromocytoma)	14	17.36	(0)(1)(2)

As for CT levels at diagnosis, median CT levels were higher in N1 than in N0 patients, (P< 0.01), in those with higher-stage tumors at diagnosis (stages III+IV) than in those with lower-stage disease (stages I+II) (P< 0.01), and in patients not biochemically cured at the end of the follow-up compared with those biochemically cured (P< 0.01). In the whole series of patients and controls, CT and serum miR-375 levels at diagnosis were correlated (r^2 = +0.40, P< 0.01), but this correlation was linear only up to moderately high CT levels. Then circulating miR-375 levels tended to be lower the higher the CT levels. When only the MTC patients were considered, a weak negative correlation emerged between serum miR-375 levels and CT levels (r^2 = −0.10, P = 0.01) (**Figure 2**).

Receiver operating characteristic (ROC) curve analysis showed that a cut-off of >2.1 for serum miR-375 levels could distinguish between MTC patients and the other subjects with a sensitivity of 92.6%, a specificity of 97.6%, a positive predictive value (PPV) of 96.9%, and a negative predictive value (NPV) of 94.2% (AUC: 0.978, P < 0.01) (**Figure 3**).

Considering only the subjects whose CT levels at diagnosis were <100 ng/L (making a diagnosis of MTC more debatable), the cut-off for discriminating between cases with and without MTC was >0.97 (sensitivity 100%, specificity 93.6%, PPV 84.6%, NPV 100%, AUC 0.983, P< 0.01).

From our ROC curve analysis, it emerged that the best cut-off for serum miR-375 levels capable of identifying a patient with MTC unlikely to be biochemically cured at the end of the follow-up was ≤6.19. This cut-off was not very accurate, however (sensitivity 80.9%, specificity 55.6%, NPV 55.6%, PPV 81.0%, AUC 0.627, P = 0.185). MTC patients with serum miR-375 levels ≤6.19 therefore had a worse prognosis than those with higher levels: in the 60 evaluable MTC patients, 34/42 patients (80.9%) with serum miR-375 levels >6.19 were biochemically cured at the end of the follow-up, while this was true of only 8/18 patients (44.4%) with miR-375 levels below this cut-off (P< 0.01).

DISCUSSION

This study on a large series of subjects with various thyroid diseases demonstrated that circulating miR-375 can be useful in diagnosing MTC as there was no overlap between the levels measured in the groups with and without MTC. A previous study on a more limited series came to the same conclusion: Romeo *et al.* found higher miR-375 levels in the serum of 37 patients with persistent or recurrent metastatic MTC than in healthy controls (22). The same authors also found a greater *in situ* hybridization (ISH) reactivity for miR-375 on formalin-fixed, paraffin-embedded samples of MTC than on samples of CCH, while this reactivity was nil or very low on stromal and follicular thyroid cells. This could mean that miR-375 upregulation is a particular feature of C-cell biology. Having analyzed various benign or malignant thyroid tissues of follicular origin, our data certainly confirm serum miR-375 as a specific marker capable of identifying any cases of MTC. That said, a possible limitation of our study lies in that we were unable to analyze serum miR-375 levels for patients with CCH

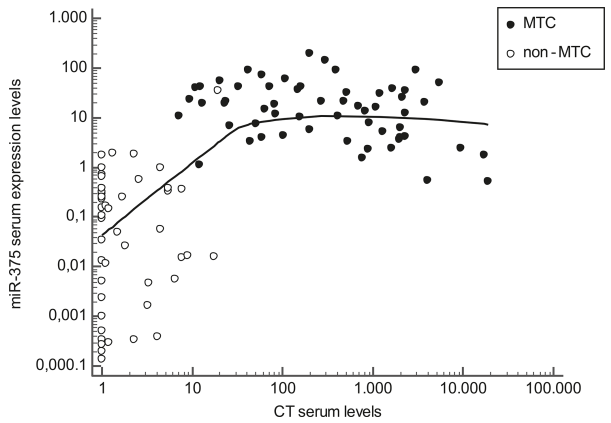

FIGURE 2 | Scatter diagram representing the correlation between calcitonin (CT) serum levels (horizontal axis) and miR-375 serum levels (vertical axis) in MTC patients (black dots) and non-MTC patients (white dots). Values are represented on a logarithmic scale.

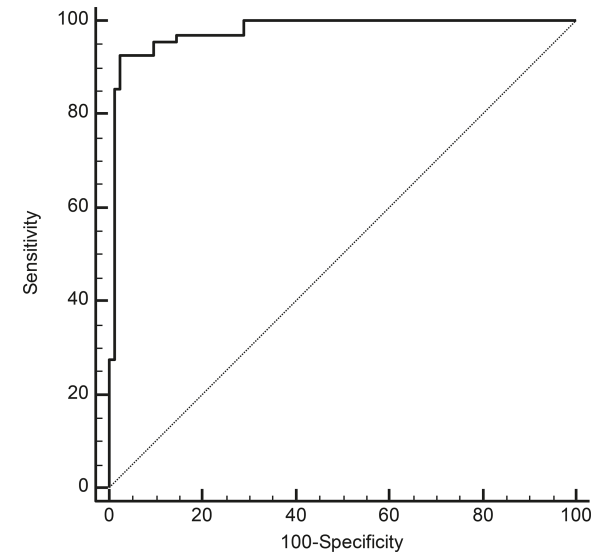

FIGURE 3 | ROC curve analyses to identify the most accurate cut-off for miR-375 serum levels for differentiating between cases with and without MTC ($P < 0.01$; AUC: 0.978).

alone because they do not usually undergo thyroid surgery unless they carry *RET* germline mutations.

Our comprehensive analysis also included some patients with pheochromocytoma in an effort to see if circulating miR-375 could also serve as a marker in the diagnosis of neuroendocrine tumors other than MTC. Serum MiR-375 levels were almost undetectable in the patients with pheochromocytoma, however, thus confirming the specificity of this marker for C-cell neoplasia, at serum level at least. Intriguingly, serum miR-375 levels were found lower in patients with pheochromocytoma, also in comparison with healthy subjects. The reason at the basis of this result remains unknown. Unfortunately, our series did not include MEN2 patients with the contemporary presence of MTC and pheochromocytoma at the time of the withdrawal to understand how serum miR-375 could be found in this very peculiar setting. Further studies are needed to confirm our preliminary findings, testing circulating miR-375 levels in patients with other neuroendocrine tumors.

We identified a cut-off for circulating miR-375 of >2.1 that was able to discriminate between cases with and without MTC with a very good sensitivity and specificity. Serum CT is usually considered highly sensitive, but not very specific for the purposes of diagnosing MTC. In our opinion, miR-375 could be particularly useful in the case of moderately high CT levels and suspected thyroid nodular disease—a situation in which another confirmatory biochemical tool would be helpful for patients' clinical management. In fact, a valid miR-375 cut-off for identifying MTC in subjects with moderately high CT levels (<100 ng/L) was also calculated (miR-375 >0.97).

In short, miR-375 performed well as a diagnostic tool in MTC patients, but further intriguing findings emerged on analyzing the correlations between the levels of miR-375 and CT. In our whole series of patients and controls, CT and miR-375 were directly related up to moderately high CT levels, but then (focusing on MTC sera) became inversely related (the higher the CT levels, the lower the miR-375 levels). Lower miR-375 levels in MTC sera were also associated with a worse prognosis. As mentioned earlier, miR-375 expression was also demonstrated on CCH samples. Pooling all these findings together in a view of neoplastic progression, we suggest that miR-375 upregulation occurs early in the process of C-cell neoplastic transformation, and may indicate an initially greater MTC differentiation that is subsequently lost as the cancer progresses and becomes more aggressive. In fact, high serum miR-375 levels were found in patients with no lymph node involvement and a low tumor stage at diagnosis, who were biochemically cured at the end of the follow-up. Intriguingly, these data contrast with findings at tissue level previously reported both by our group and elsewhere in the literature (23, 24). At tissue level, higher miR-375 levels were associated with more advanced clinicopathological features, and therefore with a tendency towards a more aggressive disease. In the light of this inconsistency vis-à-vis previous results, we also tested tissue miR-375 expression in a subgroup of paired MTC tissues in the present series, confirming that higher tissue miR-375 levels were associated with more advanced disease at diagnosis. As expected, higher CT levels in our series were also associated with higher tumor stages at diagnosis, lymph node involvement, and a lower biochemical cure rate, which goes to show that ours was not an "atypical" MTC series. The reason behind the mismatch between the prognostic significance of miR-375 in tissue and serum is still unclear. It was recently reported that exosomes (extracellular vesicles 30–100 nm in size) carry a non-random cargo of miRNAs, raising the hypothesis that miRNAs could also serve as intercellular paracrine and endocrine communicators. The delivery of miRNAs to surrounding and target tissues may

therefore contribute to creating the milieu for cancer onset and dissemination (25). Exosome release is an active process that involves a number of finely regulated steps, from packaging to surface and adhesion molecules (26). We speculate that, as MTC becomes more aggressive and possibly dedifferentiated, its exosome delivery machine for miR-375 is lost, and levels of the latter in a patient's serum consequently drop. Our findings regarding serum miR-375 levels differ from those obtained in the only other study that analyzed the prognostic value of miR-375 serum levels, in which Romeo *et al.* found higher circulating miR-375 levels in the sera of MTC patients with progressive disease, a greater tumor burden, and metastases. These discrepancies may be due to the marked differences between the two MTC series involved. Our series was tested prior to any surgery, and included cases of both high- and low-risk MTC, whereas Romeo *et al.* analyzed miR-375 on sera collected during the follow-up after surgery, and most of their cases involved persistent and recurrent progressive MTC (22).

To shed light on the possible role of miR-375 in the physiopathology of MTC, we investigated its association with *RET* and *RAS* mutations on a somatic and germinal level. No such associations emerged between somatic *RET* and *RAS* mutations and circulating miR-375 levels, consistently with our previous findings on tissue miR-375 expression levels (23), that we also replicated in the present series on MTC tissues. As regards *RET* germinal mutations, higher serum miR-375 levels were documented in hMTC than in sMTC. This finding should be taken with caution, however, as the data had a low level of statistical significance, whereas stronger data emerged on the association between higher miR-375 levels and higher biochemical cure rates. We surmise that the difference seen in miR-375 levels between hMTC and sMTC in our series could be due to a larger proportion of biochemically cured patients in the former group, rather than to any biological difference at a molecular level in the role of miR-375 role in these two categories of MTC patients.

In conclusion, our findings add to the previously published body of evidence suggesting that miR-375 can play a part in the complex landscape of MTC tumorigenesis. Further data are needed to better understand its role, its interaction with the known pathways involved in MTC, and its consequent diagnostic and prognostic value when measured in a given patient's sera and tissues. Based on these intriguing and promising clinical results, further *in vitro* experiments will be necessary, and are now being conducted by our group. We are confident that a better understanding of the role of miRNAs in MTC could pave the way to the discovery of new molecular targets, especially in *RET*-negative MTC.

DATA AVAILABILITY STATEMENT

The original contributions presented in the study are included in the article/supplementary materials. Further inquiries can be directed to the corresponding author.

ETHICS STATEMENT

The studies involving human participants were reviewed and approved by the ethical committee for clinical experimentation at Padua Hospital. The patients/participants provided their written informed consent to participate in this study.

AUTHOR CONTRIBUTIONS

SC and LB: study concept and design, analysis and interpretation, drafting of the manuscript, and final approval of the version to be published. CM and SB: study concept and design, supervision, final approval of the version to be published, and agreement with all aspects of the work. IP, AM, JM, CB, MI, and FG: substantial contributions to data acquisition and interpretation, critical revision of the manuscript, and final approval of the version to be published. MP and DF: substantial contributions to data acquisition. All authors: final approval of the version to be published, and agreement with all aspects of the work. All authors contributed to the article and approved the submitted version.

ACKNOWLEDGMENTS

This research was conducted using the resources of the Tissue Bank at the 1st Clinical Surgery Unit, University of Padua. We thank Lorenzo Baccarin for her his excellent technical support, and Frances Coburn for text editing.

REFERENCES

1. Ciampi R, Mian C, Fugazzola L, Cosci B, Romei C, Barollo S, et al. Evidence of a low prevalence of ras mutations in a large medullary thyroid cancer series. *Thyroid* (2013) 23:50–7. doi: 10.1089/thy.2012.0207
2. Ciampi R, Romei C, Ramone T, Prete A, Tacito A, Cappagli V, et al. Genetic landscape of somatic mutations in a large cohort of sporadic medullary thyroid carcinomas studied by next-generation targeted sequencing. *iScience* (2019) 20:324–36. doi: 10.1016/j.isci.2019.09.030
3. Elisei R, Schlumberger MJ, Müller SP, Schöffski P, Brose MS, Shah MH, et al. Cabozantinib in progressive medullary thyroid cancer. *J Clin Oncol* (2013) 31:3639–46. doi: 10.1200/JCO.2012.48.4659
4. Wells SA, Asa SL, Dralle H, Elisei R, Evans DB, Gagel RF, et al. Revised American Thyroid Association guidelines for the management of medullary thyroid carcinoma. *Thyroid* (2015) 25:567–610. doi: 10.1089/thy.2014.0335
5. Subbiah V, Gainor JF, Rahal R, Brubaker JD, Kim JL, Maynard M, et al. Precision targeted therapy with BLU-667 for RET-driven cancers. *Cancer Discovery* (2018) 8:836–49. doi: 10.1158/2159-8290.CD-18-0338
6. Machens A, Dralle H. Biomarker-based risk stratification for previously untreated medullary thyroid cancer. *J Clin Endocrinol Metab* (2010) 95:2655–63. doi: 10.1210/jc.2009-2368
7. Censi S, Cavedon E, Fernando SW, Barollo S, Bertazza L, Zambonin L, et al. Calcitonin measurement and immunoassay interference: a case report and literature review. *Clin Chem Lab Med* (2016) 54:1861–70. doi: 10.1515/cclm-2015-1161

8. Leboulleux S, Baudin E, Travagli J-P, Schlumberger M. Medullary thyroid carcinoma. *Clin Endocrinol (Oxf)* (2004) 61:299–310. doi: 10.1111/j.1365-2265.2004.02037.x
9. Zeng Y, Yi R, Cullen BR. MicroRNAs and small interfering RNAs can inhibit mRNA expression by similar mechanisms. *Proc Natl Acad Sci USA* (2003) 100:9779–84. doi: 10.1073/pnas.1630797100
10. Croce CM. Causes and consequences of microRNA dysregulation in cancer. *Nat Rev Genet* (2009) 10:704–14. doi: 10.1038/nrg2634
11. Pallante P, Visone R, Croce CM, Fusco A. Deregulation of microRNA expression in follicular-cell-derived human thyroid carcinomas. *Endocr Relat Cancer* (2010) 17:F91–104. doi: 10.1677/ERC-09-0217
12. Inui M, Martello G, Piccolo S. MicroRNA control of signal transduction. *Nat Rev Mol Cell Biol* (2010) 11:252–63. doi: 10.1038/nrm2868
13. Manso J, Censi S, Mian C. Epigenetic in medullary thyroid cancer: the role of microRNA in tumorigenesis and prognosis. *Curr Opin Oncol* (2021) 33:9–15. doi: 10.1097/cco.0000000000000692
14. Silva J, García V, Zaballos Á, Provencio M, Lombardía L, Almonacid L, et al. Vesicle-related microRNAs in plasma of nonsmall cell lung cancer patients and correlation with survival. *Eur Respir J* (2011) 37:617–23. doi: 10.1183/09031936.00029610
15. Szabó PM, Butz H, Igaz P, Rácz K, Hunyady L, Patócs A. Minireview: Miromics in Endocrinology: a novel approach for modeling endocrine diseases. *Mol Endocrinol* (2013) 27:573–85. doi: 10.1210/me.2012-1220
16. Farazi TA, Hoell JI, Morozov P, Tuschl T. MicroRNAs in human cancer. *Adv Exp Med Biol* (2013) 774:1–20. doi: 10.1007/978-94-007-5590-1_1
17. Mitchell PS, Parkin RK, Kroh EM, Fritz BR, Wyman SK, Pogosova-Agadjanyan EL, et al. Circulating microRNAs as stable blood-based markers for cancer detection. *Proc Natl Acad Sci USA* (2008) 105:10513–8. doi: 10.1073/pnas.0804549105
18. Mian C, Pennelli G, Fassan M, Balistreri M, Barollo S, Cavedon E, et al. MicroRNA profiles in familial and sporadic medullary thyroid carcinoma: preliminary relationships with *RET* status and outcome. *Thyroid* (2012) 22:890–6. doi: 10.1089/thy.2012.0045
19. Mian C, Pennelli G, Barollo S, Cavedon E, Nacamulli D, Vianello F, et al. Combined RET and Ki-67 assessment in sporadic medullary thyroid carcinoma: a useful tool for patient risk stratification. *Eur J Endocrinol* (2011) 164:971–6. doi: 10.1530/EJE-11-0079
20. Pennelli G, Vianello F, Barollo S, Pezzani R, Merante Boschin I, Pelizzo MR, et al. *BRAF* ^{K601E} mutation in a patient with a follicular thyroid carcinoma. *Thyroid* (2011) 21:1393–6. doi: 10.1089/thy.2011.0120
21. Mian C, Barollo S, Pennelli G, Pavan N, Rugge M, Pelizzo MR, et al. Molecular characteristics in papillary thyroid cancers (PTCs) with no 131I uptake. *Clin Endocrinol (Oxf)* (2008) 68:108–16. doi: 10.1111/j.1365-2265.2007.03008.x
22. Romeo P, Colombo C, Granata R, Calareso G, Gualeni AV, Dugo M, et al. Circulating miR-375 as a novel prognostic marker for metastatic medullary thyroid cancer patients. *Endocr Relat Cancer* (2018) 25:217–31. doi: 10.1530/ERC-17-0389
23. Galuppini F, Bertazza L, Barollo S, Cavedon E, Rugge M, Guzzardo V, et al. MiR-375 and YAP1 expression profiling in medullary thyroid carcinoma and their correlation with clinical-pathological features and outcome. *Virchows Arch* (2017) 471:651–8. doi: 10.1007/s00428-017-2227-7
24. Abraham D, Jackson N, Gundara JS, Zhao J, Gill AJ, Delbridge L, et al. MicroRNA profiling of sporadic and hereditary medullary thyroid cancer identifies predictors of nodal metastasis, prognosis, and potential therapeutic targets. *Clin Cancer Res* (2011) 17:4772–81. doi: 10.1158/1078-0432.CCR-11-0242
25. Neviani P, Fabbri M. Exosomic microRNAs in the tumor microenvironment. *Front Med* (2015) 2:47. doi: 10.3389/fmed.2015.00047
26. Raposo G, Stoorvogel W. Extracellular vesicles: exosomes, microvesicles, and friends. *J Cell Biol* (2013) 200:373–83. doi: 10.1083/jcb.201211138

Conflict of Interest: The authors declare that the research was conducted in the absence of any commercial or financial relationships that could be construed as a potential conflict of interest.

frontiers in Endocrinology

ORIGINAL RESEARCH
published: 26 April 2021
doi: 10.3389/fendo.2021.669426

Cytotoxic Effect of Progesterone, Tamoxifen and Their Combination in Experimental Cell Models of Human Adrenocortical Cancer

Elisa Rossini[1], Mariangela Tamburello[1], Andrea Abate[1], Silvia Beretta[1], Martina Fragni[1], Manuela Cominelli[2], Deborah Cosentini[3], Constanze Hantel[4,5], Federica Bono[1], Salvatore Grisanti[3], Pietro Luigi Poliani[2], Guido A. M. Tiberio[6], Maurizio Memo[1], Sandra Sigala[1†] and Alfredo Berruti[3†]*

[1] Department of Molecular and Translational Medicine, Section of Pharmacology, University of Brescia at ASST Spedali Civili di Brescia, Brescia, Italy, [2] Pathology Unit, Department of Molecular and Translational Medicine, University of Brescia at ASST Spedali Civili di Brescia, Brescia, Italy, [3] Medical Oncology Unit, Department of Medical and Surgical Specialties, Radiological Sciences, and Public Health, University of Brescia at ASST Spedali Civili di Brescia, Brescia, Italy, [4] Department of Endocrinology, Diabetology and Clinical Nutrition, University Hospital Zurich (USZ) and University of Zurich (UZH), Zurich, Switzerland, [5] Medizinische Klinik und Poliklinik III, University Hospital Carl Gustav Carus Dresden, Dresden, Germany, [6] Surgical Clinic, Department of Clinical and Experimental Sciences, University of Brescia at ASST Spedali Civili di Brescia, Brescia, Italy

Progesterone (Pg) and estrogen (E) receptors (PgRs and ERs) are expressed in normal and neoplastic adrenal cortex, but their role is not fully understood. In literature, Pg demonstrated cytotoxic activity on AdrenoCortical Carcinoma (ACC) cells, while tamoxifen is cytotoxic in NCI-H295R cells. Here, we demonstrated that in ACC cell models, ERs were expressed in NCI-H295R cells with a prevalence of ER-β over the ER-α.Metastasis-derived MUC-1 and ACC115m cells displayed a very weak ER-α/β signal, while PgR cells were expressed, although at low level. Accordingly, these latter were resistant to the SERM tamoxifen and scarcely sensitive to Pg, as we observed a lower potency compared to NCI-H295R cells in cytotoxicity (IC_{50}: MUC-1 cells: 67.58 μM (95%CI: 63.22–73.04), ACC115m cells: 51.76 μM (95%CI: 46.45–57.67) and cell proliferation rate. Exposure of NCI-H295R cells to tamoxifen induced cytotoxicity (IC_{50}: 5.43 μM (95%CI: 5.18–5.69 μM) mainly involving ER-β, as their nuclear localization increased after tamoxifen: Δ A.U. treated *vs* untreated: 12 h: +27.04% ($p < 0.01$); 24 h: +36.46% ($p < 0.0001$). This effect involved the SF-1 protein reduction: Pg: −36.34 ± 9.26%; tamoxifen: −46.25 ± 15.68% ($p < 0.01$). Finally, in a cohort of 36 ACC samples, immunohistochemistry showed undetectable/low level of ERs, while PgR demonstrated a higher expression. In conclusion, ACC experimental cell models expressed PgR and low levels of ER in line with data obtained in patient tissues, thus limiting the possibility of a clinical approach targeting ER. Interestingly, Pg exerted cytotoxicity also in metastatic ACC cells, although with low potency.

Keywords: adrenocortical carcinoma, ACC cell lines, ACC primary cells, estrogen receptors, progesterone receptors, tamoxifen

OPEN ACCESS

Edited by:
Enzo Lalli,
UMR7275 Institut de pharmacologie moléculaire et cellulaire (IPMC), France

Reviewed by:
Madson Almeida,
University of São Paulo, Brazil
Antonio Marcondes Lerario,
University of Michigan, United States
Barbara Bardoni,
UMR7275 Institut de pharmacologie moléculaire et cellulaire (IPMC), France

****Correspondence:***
Sandra Sigala
sandra.sigala@unibs.it

†These authors share senior authorship

Specialty section:
This article was submitted to Cancer Endocrinology, a section of the journal Frontiers in Endocrinology

Received: *18 February 2021*
Accepted: *06 April 2021*
Published: *26 April 2021*

Citation:
Rossini E, Tamburello M, Abate A, Beretta S, Fragni M, Cominelli M, Cosentini D, Hantel C, Bono F, Grisanti S, Poliani PL, Tiberio GAM, Memo M, Sigala S and Berruti A (2021) Cytotoxic Effect of Progesterone, Tamoxifen and Their Combination in Experimental Cell Models of Human Adrenocortical Cancer. Front. Endocrinol. 12:669426. doi: 10.3389/fendo.2021.669426

INTRODUCTION

Adrenocortical carcinoma (ACC) is a rare and aggressive tumor with an incidence of 0.7–2 new cases per million populations per year (1). Early diagnosis followed by radical surgical resection associated or not with adjuvant mitotane therapy (2, 3) is the only option that can give to ACC patients a chance of cure (4). The standard systemic treatment for advanced/metastatic ACC patients, not eligible to surgery, is mitotane, which is administered either alone or in combination with Etoposide, Doxorubicin, and Cisplatin (EDP-M regimen) (5). Although some pathological responses have been observed (6), the efficacy of EDP-M is limited and most initially responding patients are destined to relapse and die of the disease. Other cytotoxic therapies administered to patients with disease progression to EDP-M did not show a remarkable activity (7, 8). Molecular target therapies, attempted up to now (9), and immunotherapy (10) appeared ineffective.

Progesterone receptors (PgRs) and estrogen receptors (ERs) are expressed at different intensities in both normal and neoplastic adrenal cortex (11); however, the patho-physiological relevance of the steroid receptor expression in the physiological regulation of adrenal cell proliferation is not yet fully understood. In particular, in adulthood, ER-β is expressed in the glomerular and fasciculated area of the adrenal cortex, while at the prepubertal age, it is mainly located in the reticular area (12, 13). The ER-α subtype appears to be poorly expressed. During the course of neoplastic degeneration, there is an unpredictable rearrangement of the expression of these receptors, and data concerning the expression of the ERs are controversial. Indeed, a negativity for ER-α and an increase of the ER-β in the AdrenoCortical Carcinoma (ACC) have been reported by immunohistochemical analysis (11), while a decrease of ER expression has been observed as the ACC progresses (14, 15). Finally, other studies demonstrated low ER-β levels and/or high levels of ER-α in numerous cases of ACC, leading to an increase in the ER-α/ER-β ratio compared to that observed in healthy tissue (13). In the NCI-H295R cells, it was observed that ER-β gene expression is higher compared to ER-α, and the selective estrogen receptor modulator (SERM) 4-OH-tamoxifen inhibits cell proliferation (16).

The expression of ER subtypes varies in different tissues, although they are often co-expressed (17). The traditional paradigm is that ER-α is oncogenic and increases cell survival, while ER-β exerts an opposite role, being protective and pro-apoptotic. This clear distinction, however, cannot be applied for each tissue and cell expressing both ER subtypes; indeed, ER-α has a dominant role in tissues such as the uterus, mammary glands, pituitary, skeletal muscle, adipose, and bone; whereas, ER-β has a major role in the ovary, prostate, lung, cardiovascular, and central nervous systems (17).

PgR expression was as well detected in ACC (11). Recently, our group demonstrated a cytotoxic effect of Pg in ACC cells (18). Pg treatment of NCI-H295R cells induced apoptosis *via* activation of PgR with the involvement of both genomic and non-genomic pathways.

In breast cancer cells, PgR is a transcriptional target of ER, and estrogen is well known to be an important stimulator of PgR synthesis (19). Similar results have been obtained in human endometrial carcinoma (20). Interestingly, in a rare and peculiar setting such as pregnancy in ACC patients, in which there are elevated levels of both Pg and E hormones, their role in the control/progression of the disease is controversial. Indeed a study in 12 pregnant ACC patients concluded that pregnancy is associated with shorter survival and disease-free survival compared to control group (21), while another study on 17 treated ACC patients becoming pregnant during the follow-up, the pregnancy seems to be not associated with worse clinical outcome (22). As the authors correctly pointed out, however, pregnancy-associated ACC tended to be discovered at a more advanced stage. Thus, the possibility of a pregnancy-induced more rapid progression cannot be excluded, and we would like to underline that diagnostic and therapeutic delays probably account for the most severe presentation. Tamoxifen and medroxy-progesterone acetate combined treatment exhibited significant inhibitory growth effect on breast cancer (23), endometrial cancer (24), and cisplatin-resistant ovarian cancer cells (25). This combination therapy appeared to be active in phase II studies enrolling endometrial carcinoma patients (26). These data provided the rationale to explore the cytotoxic interaction between selective estrogen receptor modulators (SERMs), such as tamoxifen, and Pg in ACC.

Here, we explored the possible effect of tamoxifen on ACC cell viability and investigated the additive/synergic cytotoxic activity of tamoxifen and progesterone in *in vitro* ACC experimental cell models.

MATERIALS AND METHODS

Cell Lines

The human NCI-H295R cell line, derived from a primitive ACC in a female patient (27), was obtained from the American Type Culture Collection (ATCC) and cultured as indicated by ATCC. MUC-1 cell line, established form a neck metastasis of an EDP-M treated male patient, was kindly given by Dr. Hantel and cultured as suggested (28). Media and supplements were supplied by Sigma Aldrich Italia, (Milan, Italy).

Primary ACC Cell Culture

Human ACC primary cells were derived from a male patient who underwent surgical removal of metastatic ACC, in progression after EDP-M. The local Ethical Committee approved the project and written informed consent was obtained from the patient. The primary culture ACC115m was obtained as previously described (29) and maintained in MUC-1 medium supplemented with L-Glutamine (2 mM) and amphotericin B (2.5 µg/ml). The clinical characteristics of the patient are reported in **Supplemental Table 1**. Cells were tested for mycoplasma and authenticated from BMR genomics (Padova, Italy).

Immunohistochemistry

Tissue samples were obtained from formalin-fixed and paraffin embedded blocks from surgical samples. 2 μm thick sections were used for routine Hematoxylin and Eosin (H&E) staining and immunohistochemistry using the automatic stainer BenchMark ULTRA IHC/ISH System (Ventana). Diagnosis of cortical cell carcinoma was revised according to the most recent WHO criteria (30). The clinical characteristics of the patient are reported in **Supplemental Table 1**. The following primary antibodies were used: anti-PgR clone 1E2, anti-ER clone SP1. All the primary antibodies were from "ready to use" kits from Ventana. Antigen retrieval was performed by incubation for 64 min for PgR and ER at 95°C in Ultra Cell Conditioning Solution (Ultra CC1, Ventana). Signal was revealed using the ultraView Universal DAB Detection kit (Ventana) followed by diaminobenzydine as chromogen and Hematoxylin for nuclear counterstain. Digital images were acquired by an Olympus XC50 camera mounted on a BX51 microscope (Olympus, Tokyo, Japan) using CellF Imaging software (Soft Imaging System GmbH, Münster, Germany). Expression of PR and ER was semi-quantitatively scored on representative tumor areas based on both percentage [score ranges: 0 (0–5%), 1 (6–29%), 2 (30–69%), 3 (≥70%)] and intensity (score ranges: 0, no expression; 1, weak; 2, moderate; 3, high) of immunoreactive (IR) neoplastic cells.

Immunofluorescence

Cells were grown onto 12 mm poly-L-lysine coated coverslips for 4 days and were then fixed with paraformaldehyde 4% (w/v) (Immunofix, Bio-Optica, Milan, Italy) for 15 min at 4°C and permeabilized with 20% MetOH and 0.1% Triton X-100 in PBS for 10 min. Non-specific binding was blocked by incubation in PBS containing 0.1% Triton X-100 and 0.2% of BSA for 45 min. Cells were incubated with anti-PgR (raised in rabbit, 1:800, Cell Signaling Technology, Denvers, MA, USA), anti-ER-β (raised in rabbit, 1:500, Abcam, Cambridge, United Kingdom) and anti-ER-α (raised in mouse, 1:500, Invitrogen, Carlsbad, CA, USA) primary antibodies o/n at 4°C. After extensive washes, the anti-rabbit Alexa Fluor 488 (green signal) and anti-mouse Alexa Fluor 555 (red signal) (Immunological Sciences, Rome, Italy) secondary antibodies, and Alexa Fluor 647 Phalloidin (Invitrogen) were applied for 1 h at rt. After rinsing in PBS, coverslips were mounted using DAPI-containing Vectashield mounting medium (Vector Laboratories, Burlingame, CA, USA).

Slides were observed by a LSM 880 Zeiss confocal laser microscope equipped with Plan-Apochromat 63×/1.4 numerical aperture oil objective or by a LSM 510 Zeiss confocal laser microscope (Carl Zeiss AG, Oberkochen, Germany) equipped with Plan-Apochromat 63×/1.4 numerical aperture oil objective. Images were then reconstructed using Zeiss ZEN 2.3 Imaging Software (Carl Zeiss). The specific mean fluorescence intensity of the pixels was quantified using ZEN Black software (Carl Zeiss) and/or ImageJ software (Nation Institute of Health. Bethesda, MD, USA). Several fields, randomly chosen, were acquired and analyzed for each experimental condition.

Cell Treatments

Cells were treated with increasing concentrations of progesterone (0.1–160 μM; Merck Serono, Milan, Italy) and tamoxifen (0.1–20 μM; Selleckchem Chemicals-DBA Italia, Segrate, Milan, Italy); both drugs were solubilized in DMSO. Preliminary experiments of concentration–response curves were conducted in the ACC cell cultures in order to establish the optimal drug concentration range and length of treatment. All experiments were conducted in charcoal-dextran-treated serum (CTS).

Measurement of Cell Viability and Proliferation

Cell viability was assessed by 3-(4,5-Dimethyl-2-thiazol)-2,5-diphenyl-2H-tetrazolium bromide (MTT) dye reduction assay as described in Fiorentini et al. (31). Briefly, untreated and drug-treated cells were incubated with MTT dye (at final concentration of 0.5 mg/ml) and solubilized with DMSO. Absorbance was determined at 540/620 nm by a spectrophotometer (GDV, Rome, Italy). Cell proliferation rate was evaluated with TC20 automated cell counter (Bio-Rad Laboratories, Segrate, Milan, Italy). Briefly, cells were grown in 24-well plates, dislodged by trypsinization and suspended in culture medium followed by trypan blue dilution (1:2). The parameter settings were established according to the manufacturer's instructions. 10 μl of sample was loaded into a slide and counted.

Drug Combination Experiments

Combination experiments were performed to evaluate the interaction of Pg and tamoxifen on cell viability according to the Chou and Talalay method (32). Cells were treated for 4 days using increasing concentrations of progesterone (7.4–84.3 μM), tamoxifen (0.8–13.5 μM), and mitotane (1.51–17.21 μM) as single drug and in combination, as recommended for the most efficient data analysis (33). The drug concentration curve for the combination has been designed for each ACC cell model based on the respective IC_{50} of each drug. Data were then converted to Fraction affected (Fa, range from 0 to 1 where Fa = 0 indicating 100% cell viability and Fa = 1 indicating 0% cell viability) and analyzed using the CompuSyn software (ComboSyninc. Paramus, NJ, USA) to calculate the Combination Index (CI). A CI value <1, = 1, and >1 indicates synergism, additive effect, and antagonism respectively.

Quantitative RT-PCR

Gene expression was evaluated by q-RT-PCR (ViiA7, Applied Biosystems, Milan, Italy) using SYBR Green as fluorochrome as described elsewhere (34). Sequences of oligonucleotide primers were reported in **Supplemental Table 2**. Reactions were performed under the following conditions: 1 cycle at 95°C for 10 min, 40 cycles at 95°C for 15 s, 62°C for 1 min. Differences of the threshold cycle (Ct) values between the β actin housekeeping gene and the gene of interest (ΔCt) were then calculated.

miRNA Analysis

Total RNA, including miRNAs, was extracted from cells using the miRNeasy kit (Qiagen, Milan, Italy), and 1 μg was transcribed into cDNA using miScript II RT kit (Qiagen), following the manufacturer's protocol. q-RT-PCR was

performed with a miScript System (Qiagen) (35). Reactions were performed under the following conditions: 95°C 15 min; 94°C 15 s, 55°C 30 s, 70°C 30 s, 40 cycles. Sequences of miR-23 used were: miR23a: 5′AUCACAUUGCCAGGGAUUUCC; miRNA23b: 5′AUCACAUUGCCAGGGAUUACC. Variations in expression of miR-23a/b among different samples were calculated after normalization to U6.

Western Blot

Cells were homogenized in cold RIPA buffer, and total protein concentrations were determined by Bio-Rad Protein Assay (Bio-Rad Laboratories). Proteins (30 μg/lane) were separated by electrophoresis on a 4–12% NuPAGEbis-tris gel system (Life Technologies, Milan, Italy) and electroblotted to a nitrocellulose membrane. Membranes were incubated with an anti-SF1 (0.234 μg/ml; Cell Signaling Technology) and anti-GAPDH (1 μg/ml Merk Millipore, Burlington, MA, USA) primary antibodies according to the manufacturer's instructions. Secondary HRP-labeled anti-mouse and anti-rabbit antibodies (Santa Cruz Biotechnologies, Heidelberg, Germany) were used, and the specific signal was visualized using a Westar ECL Sun Western blot substrate (Cyanagen, Bologna, Italy). Densitometric analysis of the immunoblots was performed using NIH ImageJ Software.

Statistical Analysis

The analysis of the data was carried out by the GraphPad Prism version 5.02 software (GraphPad Software, La Jolla, CA) using the one-way ANOVA with Bonferroni's multiple comparisons test considering $P < 0.05$ as threshold for significant difference. IC_{50} values for each drug were calculated by non-linear regression of the concentration–response curves. All results are expressed as mean ± SEM of three independent experiments, unless otherwise specified. Cytotoxicity experiments were carried out at least three times, each point run in triplicate.

RESULTS

Estrogens in the ACC Cell Models

Due to the suggested different roles of ER in cell viability, we evaluated whether the ER-α and ER-β subtypes were differentially expressed in ACC experimental cell models. ACC cell lines and the ACC115m primary cell culture were then investigated for ER gene and protein subtype expression. Results on gene expression are reported in **Table 1**, while the mRNA translation into the respective protein was demonstrated by immunofluorescence and reported in **Figure 1** and quantified in **Supplemental Figure 1**. Concerning the ACC cell lines, NCI-H295R cells expressed both ER subtypes, although the gene and the protein both indicated a low level of expression with a prevalence of ER-β over the ER-α (**Figure 1A**, **Supplemental Figures 1**, **2**). Metastasis-derived MUC-1 cell line and ACC115m primary culture, displayed a very weak expression of ER-α and ER-β, both at gene (**Table 1**) and protein levels (**Figure 1**; quantified in the **Supplemental Figure 1**). We would like to underline the peculiar sub-cellular localization of the ER subtypes as we can observe a prevalent nuclear localization of ER-β.

TABLE 1 | ER gene expression in ACC cell lines and primary cell culture.

Target gene	NCI-H295R	MUC-1	ACC115m
ER-α	10.88 ± 0.36	>15.00	11.50 ± 0.83
ER-β	9.81 ± 0.38	>15.00	13.43 ± 0.68

Values were reported as ΔCt that are differences of the threshold cycle (Ct) values between the β-actin housekeeping gene and the gene of interest (ΔCt), calculated, as described in Materials and Methods.

NCI-H295R cell line expressed the CYP19A1 enzyme (31) and produced 17β-estradiol (10.01 ± 0.77 ng/ml; **Supplemental Methods**). As it has been shown that exogenous administration induced cell growth [16 and unpublished data], to explore the possible involvement of ERs in ACC cytotoxicity and cell proliferation rate, ACC cells were treated with increasing concentrations of tamoxifen for 4 days and then evaluated for cell viability. The ACC cell line NCI-H295R displayed a concentration-dependent cytotoxicity, with the IC_{50} of 5.43 μM (95% CI: 5.18–5.69 μM) (**Figure 2A**) and the reduction of the cell proliferation rate (**Figure 2B**). MUC-1 cell line and ACC115m primary culture resulted resistant to tamoxifen (**Supplemental Figure 3**), accordingly to the very low ER expression in these ACC cell models. In particular, tamoxifen exposure did not show any effect on cell viability up to 15 μM and then a sharp decrease at 17.5 μM and 20 μM, more evident in ACC115m. Whether this effect is ER-dependent or not needs to be determined.

Tamoxifen Induced ER-β Nuclear Translocation in NCI-H295R Cell Line

To evaluate whether the tamoxifen effect involved a selective subtype, NCI-H295R cells were exposed to the drug IC_{50}, and cells were fixed and analyzed at the confocal microscope at different times. **Figure 3A** shows that tamoxifen treatment induced a time-dependent increase of nuclear signal of ER-β, thus suggesting a significant nuclear translocation after 12 h of drug exposure that was maintained up to 24 h (**Figure 3B**), without any modification of the amount and localization of ER-α (**Supplemental Figure 4**). These results suggested that ER-β could be the subtype mainly involved in the tamoxifen effect.

Pg in the ACC Cell Models

We already demonstrate that NCI-H295R cells express PgR (31) and that Pg exerts a concentration-dependent cytotoxic effect on NCI-H295R cells line as well as in ACC primary cell cultures expressing PgR (18). Here, we confirmed this result in other ACC cell models, studying the Pg effect in metastasis-derived cell models, namely MUC-1 cell line and in ACC115m primary cells. We firstly assessed the PgR expression in these cells by q-RT-PCR. The ΔCt obtained was MUC-1: 12.71 ± 0.62; ACC115m: 10.39 ± 0.04 (cDNA belonging from NCI-H295R cells was used as internal positive control: ΔCt: 9.48 ± 0.57), thus suggesting that PgR gene expression was present. Although a direct relationship between mRNA and proteins cannot be established, a correlation between the gene expression and the immunofluorescent signal in these ACC cell models could be observed. Indeed, PgR signal in MUC-1 cells and ACC115m primary cell culture is weaker compared to NCI-H295R cells.

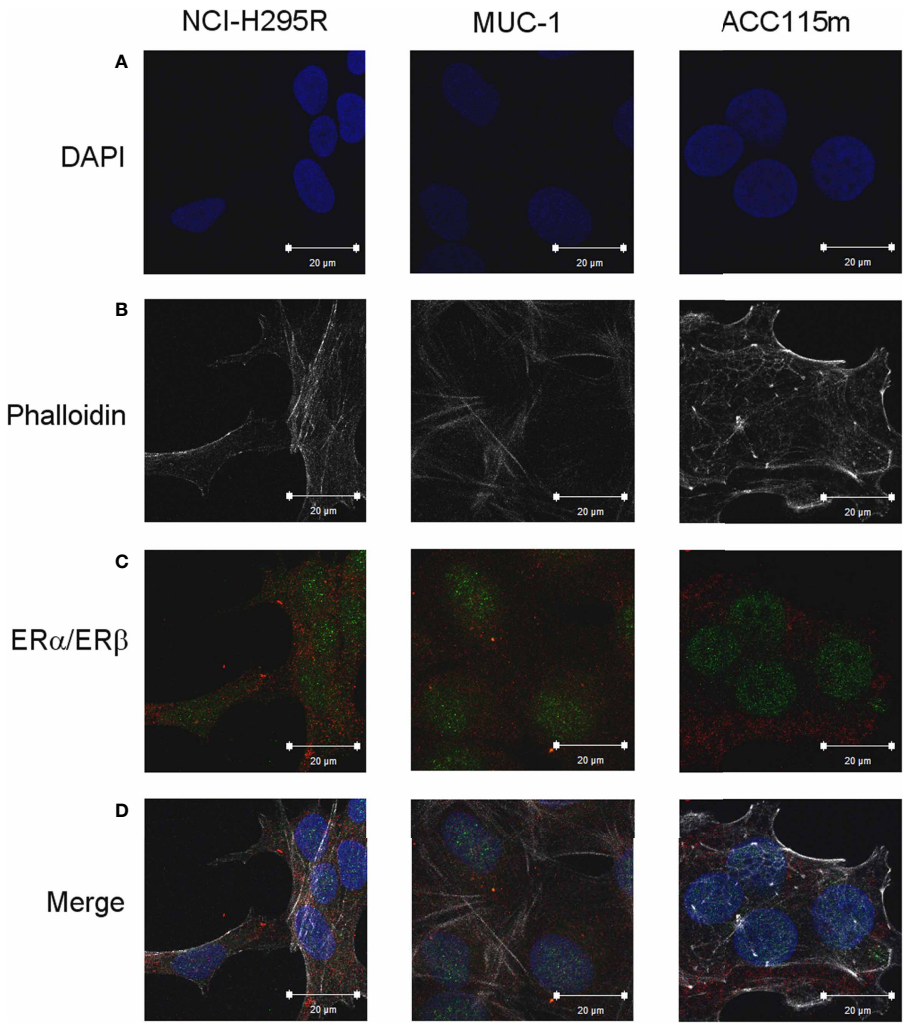

FIGURE 1 | ER expression in NCI-H295R, MUC-1 cell lines and ACC115m primary culture. Cells were seeded on poly-L-lysine pre-treated coverslips following by incubation with DAPI for nuclear staining. Panel **(A)** DAPI; panel **(B)** phalloidin; panel **(C)** ER (red signal: ER-α; green signal: ER-β); panel **(D)** merge. The scale bar of 20 μm is automatically inserted by the software ZEN Black.

These results are reported in **Figure 4** and included NCI-H295R cells as positive control. The immunofluorescence signal quantification is reported in **Supplemental Figure 5**. A modest cytotoxic effect of both ACC cell models derived from metastatic patients was observed when cells were exposed to increasing Pg concentrations, suggesting that these cells were less sensitive to Pg compared to NCI-H295R cells. Indeed, the IC_{50} was 67.58 μM (95% CI: 63.22–73.04 μM) for MUC-1 cells and 51.76 μM (95% CI: 46.45–57.67 μM) for ACC115m cells (**Figure 5A**). Pg treatment affected as well the cell proliferation rate on each ACC cell model as reported in **Figure 5B**.

Effect of Drug Combined Treatment on ACC Cell Viability

Due to the sensitivity of NCI-H295R cell line to both Pg and tamoxifen, we thus evaluated whether the cytotoxic effect of tamoxifen on NCI-H295R cell viability could be enhanced by Pg, applying the Chou–Talalay method for drug combination experiments (32, 33). Cells were exposed to increasing concentrations of tamoxifen (1.2–13.5 μM) and Pg (7.4–84.3 μM) at 1:6.17 fixed molar ratio for 4 days and then analyzed for cell viability by MTT assay (**Figure 6A**). The combination index was then calculated, and the analysis revealed a prevalent antagonist effect when the two drugs were combined (**Figure 6B**). The combination index value for each drug concentration is reported in **Supplemental Table 3**, and the isobolograms are reported in **Supplemental Figure 5**.

Finally, since mitotane is the standard treatment for ACC patients, we then evaluated as well the combined treatment NCI-H295R cell line with tamoxifen and mitotane. Results are reported in **Supplemental Figure 6**, **Supplemental Table 4** and showed that the combination has an additive/synergic effect at low concentrations, while, as the drug concentrations increased, the antagonism prevailed.

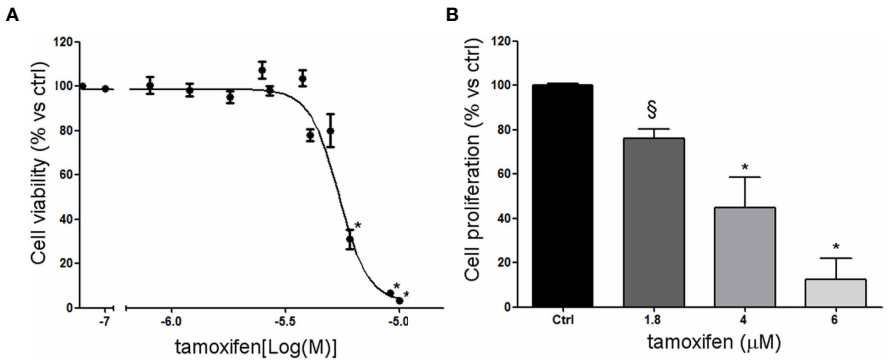

FIGURE 2 | Effect of tamoxifen on NCI-H295R cell viability and proliferation. **(A)** NCI-H295R were treated with increasing concentration of tamoxifen (0.1–20 uM) and cell viability was then evaluated by MTT assay. Results are expressed as percent of viable cells *vs* ctrl ± SEM of three independent experiments run in triplicate. **(B)** NCI-H295R were treated with low, intermediate, and high dose of tamoxifen and then cell proliferation was evaluated by directing counting with trypan blue discrimination. *$P < 0.0001$ *vs* untreated cells; $^{§}P < 0.001$ *vs* untreated cells.

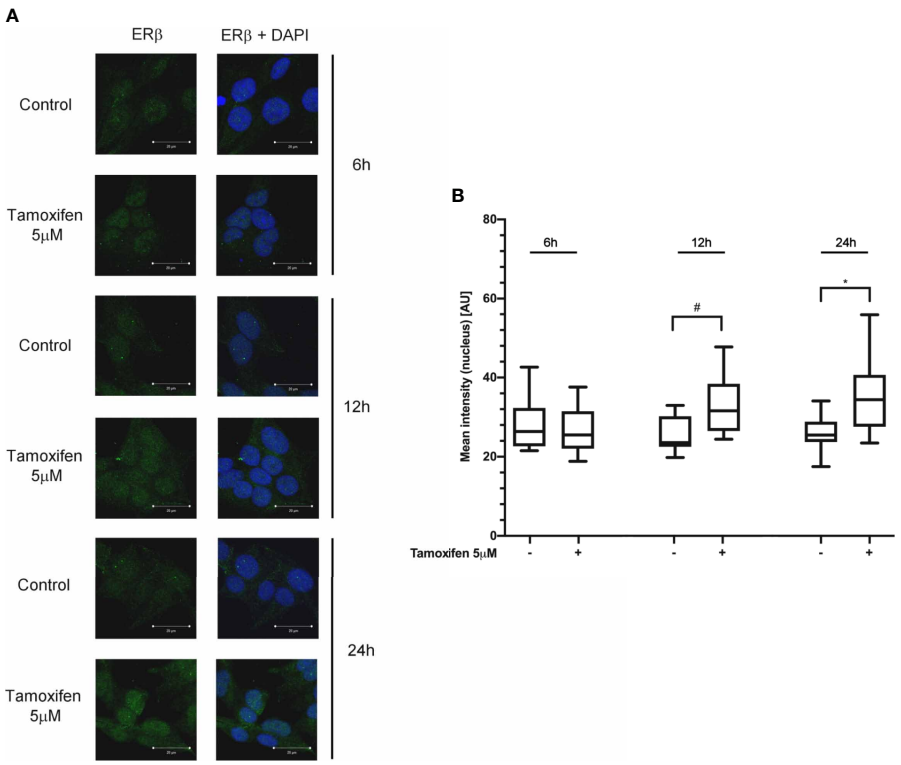

FIGURE 3 | Tamoxifen exposure selectively modified the ER intracellular localization in NCI-H295R cells. **(A)** Cells were treated for different times with tamoxifen IC_{50} value. Slides were observed by a LSM 880 Zeiss confocal laser microscope or by a LSM 510 Zeiss confocal laser microscope (Carl Zeiss with 40× magnification. Images were then reconstructed using Zeiss ZEN 2.3 Imaging Software (Carl Zeiss). On the left the ER-β staining, on the right ER-β + DAPI staining. **(B)** The specific mean fluorescence intensity of the pixels of acquired images was quantified using ZEN Black software (Carl Zeiss). Several fields, randomly chosen, were acquired and then analyzed for each experimental condition. Quantified analysis was conducted by GraphPad Prism 5.02 software. *$P < 0.0001$ *vs* ctrl; $^{#}P < 0.01$ *vs* ctrl.

Pg and Tamoxifen Reduced SF-1 Expression in NCI-H295R Cells

In order to evaluate the functional effect of Pg and tamoxifen in the NCI-H295R cell line, the effect of these drugs on the expression of the adrenal biomarker, namely SF-1, the pleiotropic transcription factor involved as well in the carcinogenesis (36) was studied. Cells were treated with Pg or tamoxifen at their respective IC_{50} for 4 days and then the SF-1

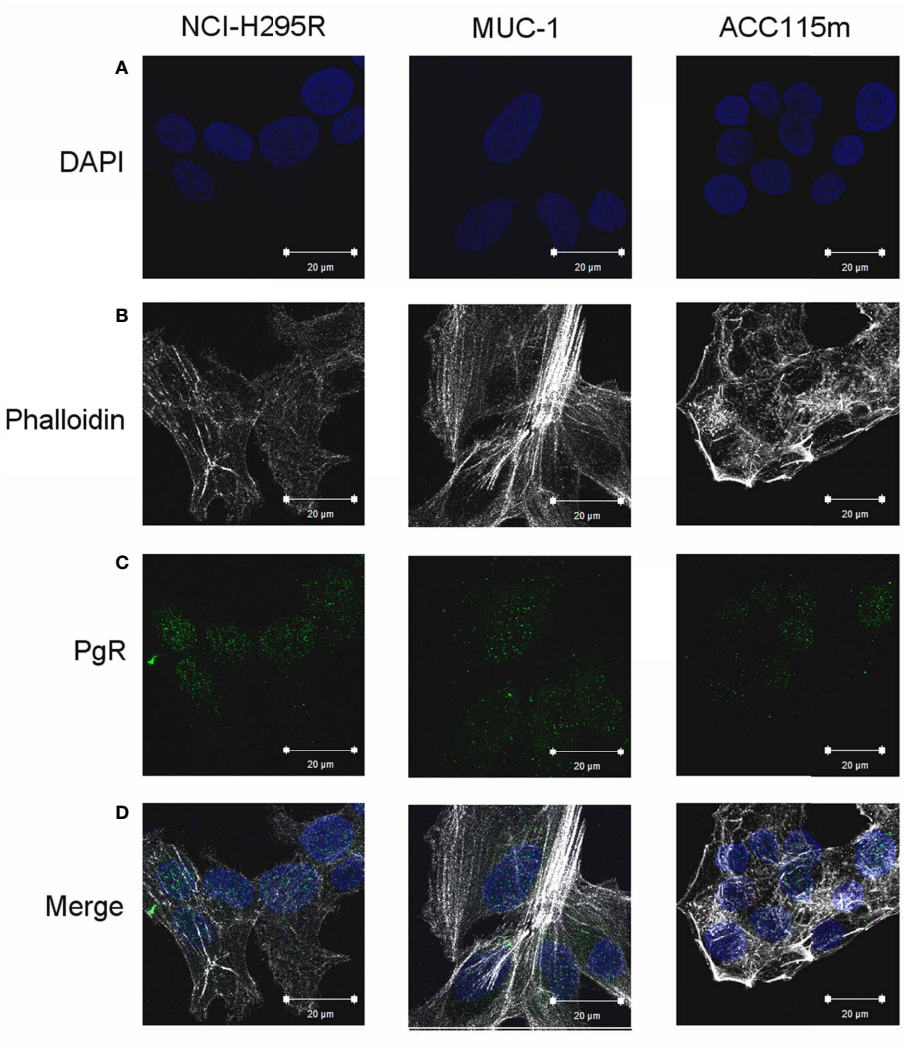

FIGURE 4 | PgR expression in NCI-H295R, MUC-1 cell lines and ACC115m primary culture. Cells were seeded on poly-L-lysine pre-treated coverslips following by incubation with DAPI for nuclear staining. Panel **(A)** DAPI; panel **(B)** phalloidin; panel **(C)**: PgR; panel **(D)**: merge. The scale bar of 20 µm is automatically inserted by the software ZEN Black.

expression was evaluated. Results are reported in **Figure 7**. By q-RT-PCR, after Pg and tamoxifen treatment, no differences in the SF-1 gene expression were detected (not shown), while representative western blots were reported in **Figure 7.1A**. The SF-1 protein expression was modified by both drugs: in particular, as shown in **Figure 7.1B**, Pg treatment induced a significant SF-1 reduction in NCI-H295R cell line (Pg: −36.34% ± 9.26%; tamoxifen: −46.25% ± 15.68%; $P < 0.01$).

In order to explain this phenomenon, we investigated the expression of two miRNAs involved in SF-1 regulation, namely miR23a and miR23b (37). The reduction of SF-1 protein expression seemed to be mediated, at least in part, by the increase of miRNA 23a expression, with an increase compared to untreated cells of up to 1.54 ± 0.11 in Pg-treated cells and of 1.73 ± 0.04 in tamoxifen-treated cells respectively. An increase of miRNA-23b expression was as well observed after tamoxifen treatment (1.51 ± 0.02 compared to untreated cells), while this miRNA did not seem to be involved in the regulation of SF-1 protein expression when NCI-H295R cells are exposed to Pg (**Figure 7.1C**). SF-1 protein expression after Pg and/or tamoxifen IC_{50} treatment was measured also in MUC-1 cell line, but no significant variations were detected (**Figures 7.2A, B**).

PgR and ER Expression in ACC Tissues

Finally, the expression of ER and PgR was studied by immunohistochemistry in 36 paraffin embedded tumor samples belonging to ACC diagnosed patients. Among this cohort, 13 patients were male and 22 female, with an age median of 53 years (range: 16–79 years), 11 of them were cortisol-secreting, while the others were not secreting. Results

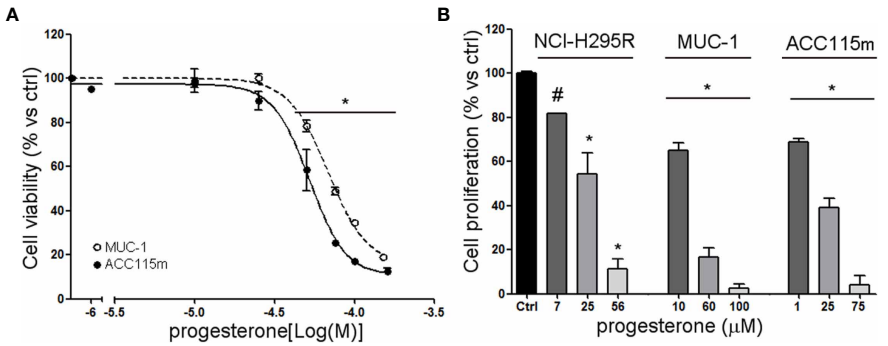

FIGURE 5 | Cytotoxic effect of Pg in ACC cell models. **(A)** MUC-1 cell line and ACC115m primary culture were treated with increasing concentrations of progesterone (0.1–160 uM), then cell viability was analyzed by MTT assay, **(B)** NCI-H295R, MUC-1 cell lines and ACC115m primary culture were treated with low, intermediate, and high dose of Pg, and cell proliferation was analyzed by directing counting with trypan blue discrimination. Results are expressed as percent of viable cells *vs* ctrl ± SEM; *$P < 0.0001$ *vs* untreated cells; #P < 0.01 *vs* untreated cells.

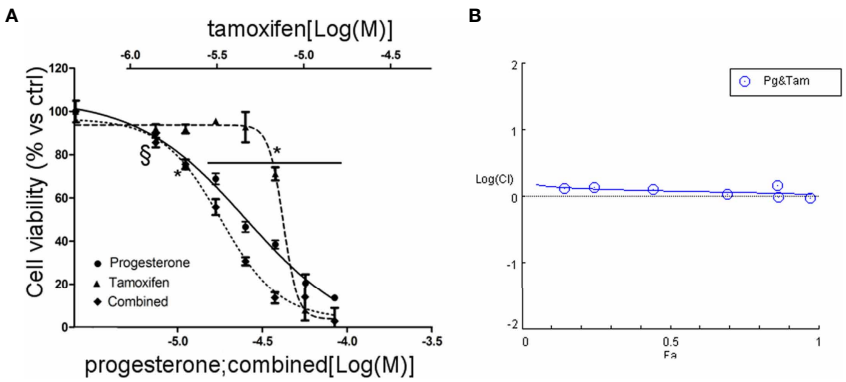

FIGURE 6 | Combined treatment tamoxifen plus Pg in NCI-H295R. **(A)** Concentration–response curve of tamoxifen, Pg, and drug combination in NCI-H295R. Cells were exposed to increasing concentrations of tamoxifen and Pg alone or in combination as described in *Materials and Methods*. Data are expressed as percent of viable cells *vs* ctrl. Data are the mean ± SEM of three independent experiments; *$P < 0.0001$ *vs* untreated cells; §$P < 0.001$ *vs* untreated cells. **(B)** Combination index plot. Cell viability data of panel A were converted to Fa values and analyzed with CompuSyn software.

reported in **Table 2** indicated that ERs were absent or present in a very weak expression, while PgR proteins were expressed, although with a variability within the different samples. In particular, concerning the ER positive cells, we could observe that only three ACC samples displayed a percentage of ER moderately positive cells within the range of 30–69%, while 28 ACC displayed less than 5% ER positive cells, with a null o low intensity. Concerning PgR, they presented an evaluable expression in each sample studied, with only three ACC expressing less than 5% of immunoreactive cells. Indeed, almost half of samples expressed between 30 and 69% of immune positive cells and eight samples up to 36 expressed more than 70% of positive cells. A representative example of immunohistochemistry conducted on some ACC tissues is reported in **Figure 8**. The clinical characteristics are reported in **Supplemental Table 1**. In detail, ACC29 cells showed a tumor with lobulated morphology, moderate atypia and few mitotic figures. This tumor exhibits focal and moderate PgR expression, scant ER IR-cells, and low proliferation index. ACC32 cells presented an epithelioid morphology with higher nuclear atypia and prominent nucleoli. This tumor has few PgR IR cells with faint staining intensity with no ER expression and moderate proliferation index. ACC55 cells showed a solid growth composed of clusters of eosinophilic cells with frequent nuclear atypia and mitotic figures. Tumor has moderate PgR expression with negative ER immunostaining and a labeling index up to 15%. The ACC91 cells had a solid growth composed by poorly cohesive cell clusters with densely eosinophilic cytoplasm, frequent nuclear atypia and mitosis. This tumor has a higher expression of PgR along with moderate expression of ER. Labeling index is higher between these samples, ranging from 15 to 20%.

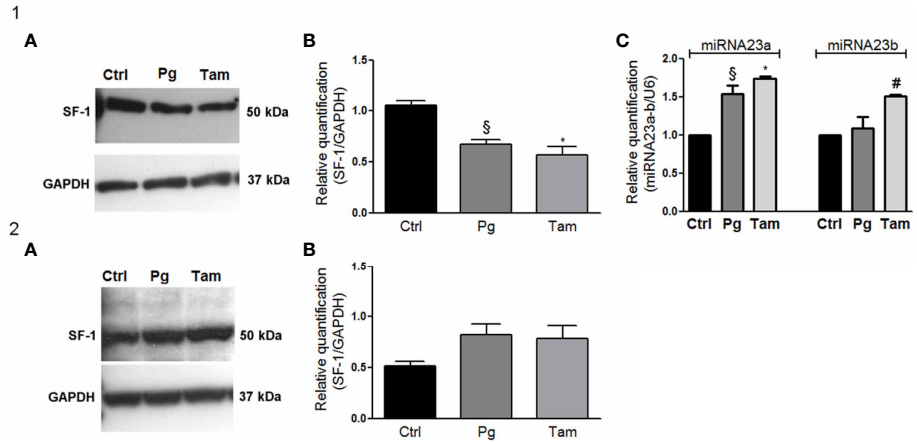

FIGURE 7 | Tamoxifen and Pg reduced the SF-1 expression in NCI-H295R cell line. **(1A)** Representative western blot of SF-1 expression after NCI-H295R tamoxifen IC_{50} and Pg IC_{50} 4 days treatment. **(1B)** Densitometric analysis of SF-1 expression after NCI-H295R drug treatment. Data are expressed as normalized values SF-1/GAPDH and are the mean of three independent experiments. *P < 0.0001 *vs* ctrl; §P < 0.001 *vs* ctrl. **(1C)** NCI-H295R were treated with tamoxifen IC_{50} or Pg IC_{50} for 4 days and then miRNA23a/b expression was investigated. Data are expressed as normalized values on internal control U6 and are the mean of three independent experiments. *P < 0.0001 *vs* ctrl; §P < 0.001 *vs* ctrl; #P < 0.01 *vs* ctrl. **(2A)** Representative western blot of SF-1 expression after MUC-1 tamoxifen IC_{50} and Pg IC_{50} 5 days treatment. **(2B)** Densitometric analysis of SF-1 expression after MUC-1 drug treatment. Data are expressed as normalized values SF-1/GAPDH and are the mean of three independent experiments.

DISCUSSION

In this study, we *in vitro* investigated whether the interplay between ER, PgR, and their ligands may exert a cytotoxic and antiproliferative activity on ACC experimental cell models as it was demonstrated in endocrine-related cancers.

We observed that, although ER expression was relatively low, tamoxifen exerted cytotoxic effect on NCI-H295R cell line, belonging from a primitive ACC, confirming published data (16). Drug exposure led to an increased nuclear localization of ER-β subtype, with no modifications of the ER-α subcellular localization, leading to the hypothesis that the cytotoxic and antiproliferative effects of tamoxifen in ACC cells could be mediated by its ER-β agonist activity, according to previous observations (38). These results are in line with results showing that in breast cancer cell lines stably expressing ER-β, this receptor regulates multiple components normally associated with the suppression of cell proliferation (*i.e.* TGFβ and cell cycle-related genes) (17). Thus, with these results, we supported evidence indicating that ER-β is a protective factor that suppresses uncontrolled proliferation and induces cell differentiation in many tissues and organs, both in physiological condition and in cancer degeneration (17). However, the role of ERs in ACC cell models seemed to be limited to the NCI-H295R cell line, as metastatic derived ACC cell models such as MUC-1 and ACC115m expressed very weak levels of both ER subtypes and were resistant to tamoxifen.

On the same line, this mechanism may have a scarce impact in clinic, as our immunostaining data showed that ER is scarcely expressed in paraffin-embedded ACC tissues as well as we observed in ACC experimental cell models, accordingly with those that detected low expression level of the ER subtypes in ACC.

The amount of ER expression in ACC seemed to decrease as disease progresses, at least in our experimental cell models. Indeed, as already underlined, in EDP-M resistant ACC cells, namely MUC-1 and ACC115m cells, the expression of ER is very low and cells do not respond to the SERM tamoxifen. Accordingly, in our cohort of paraffin-embedded ACC samples, the expression of ER was absent or present in a very weak expression, thus limiting the possibility to explore a clinical approach targeting ER in ACC patients. Another limitation resides in the tamoxifen pharmacokinetic, as the calculated plasma concentration at the steady state after 20 mg tamoxifen for 3 months is about 0.3 μM, that is under the range of concentrations that displayed a cytotoxic effect in our ACC experimental cell models, although tamoxifen presents a distribution volume that is about 50–60 l/kg (39).

Concerning PgR, immunohistochemical analysis of ACC tissues strongly indicated that they are frequently expressed, with a number of samples displaying a high percentage of immunoreactive cells, although with a large variability among samples. Accordingly, in a recent paper, our group demonstrated that exposure to Pg of primary cells derived from PgR expressing ACC (at least 40% of PgR+ cells) resulted in a concentration-dependent increase of cytotoxicity (18) in line with results demonstrating a role this hormone as anti-tumoral drug in different cancers (40–42).

Here, we strengthen the role of PgR in the ACC and the effect of Pg in reducing both cell proliferation and cell viability. This effect seemed to be strictly related to the level of PgR expression, thus the evaluation of the PgR expression during the pathological staging could be of interest, as Pg and its derivative are already part of the cancer supporting care, thus giving the opportunity to have another pharmacological tool over the usual

TABLE 2 | Histological features and expression of PgR and ER in ACC tumor specimens.

code	PgR			ER		
	intensity	% of IR cells	cumulative	intensity	% of IR cells	cumulative
ACC03	1	2	**3**	0	0	**0**
ACC04	2	3	**5**	1	0	**1**
ACC06	1	1	**2**	2	2	**4**
ACC07	2	3	**5**	2	2	**4**
ACC08	1	2	**3**	0	0	**0**
ACC10	3	3	**6**	2	1	**3**
ACC11	2	2	**4**	0	0	**0**
ACC12	1	1	**2**	1	0	**1**
ACC13	1	2	**3**	0	0	**0**
ACC14	1	2	**3**	1	1	**2**
ACC16	2	2	**4**	1	0	**1**
ACC17	1	0	**1**	0	0	**0**
ACC23	1	0	**1**	0	0	**0**
ACC24	2	2	**4**	0	0	**0**
ACC26	1	2	**3**	0	0	**0**
ACC27	1	2	**3**	1	0	**1**
ACC29	2	1	**3**	1	0	**1**
ACC30	2	3	**5**	0	0	**0**
ACC32	1	1	**2**	0	0	**0**
ACC38	2	2	**4**	1	0	**1**
ACC40	1	1	**2**	0	0	**0**
ACC48	1	2	**3**	2	2	**4**
ACC50	1	2	**3**	1	0	**1**
ACC55	1	1	**2**	0	0	**0**
ACC64	2	3	**5**	0	0	**0**
ACC68	2	3	**5**	0	0	**0**
ACC71	2	2	**4**	1	2	**3**
ACC74	2	2	**4**	0	0	**0**
ACC75	1	1	**2**	0	0	**0**
ACC79	1	0	**1**	0	0	**0**
ACC81	2	2	**4**	0	0	**0**
ACC85	1	3	**4**	0	0	**0**
ACC91	2	3	**5**	1	2	**3**
ACC99	1	2	**3**	0	0	**0**
ACC103	1	2	**3**	0	0	**0**
ACC115	1	1	**2**	0	0	**0**

systemic therapy. This hypothesis is now under study in a randomized phase II clinical trial.

The cross-talk between ER/PgR was detectable both at physiological and pathological levels in endocrine tissues and tumors (43). About it, it has been suggested that the combined treatment using drugs targeting ER/PgR could be useful, although the safety profile of the drug combination must be considered (43). Thus, as published data support the rationale for a synergism between anti-E and Pg in inducing an antineoplastic effect, we tested the cytotoxic activity of the combination of tamoxifen and Pg also in ACC experimental model of NCI-H295R cells. Results obtained indicated that the tamoxifen/Pg combination did not result in an either additive or synergic effect; rather the resulting effect was of drug antagonism.

We finally investigated the functional effect of tamoxifen and Pg exposure in ACC cell models, and we observed that both drugs are able to decrease the protein expression of the ACC biomarker SF-1, the transcription factor that is a critical regulator of adrenogonadal development and function (44). SF-1, also known as Ad4-binding protein or NR5A1, binds as a monomer to nuclear receptor half sites on DNA (44), and it plays an important role not only in adrenal steroidogenesis but also in cell adhesion, cell proliferation, apoptosis, and angiogenesis of adrenocortical tumor cells (36). Further, Doghman et al. demonstrated that overexpression of SF-1 in NCI-H295R increases proliferation rate (45). Thus, our results on the downregulation of SF-1 protein expression during the cytotoxic effect of tamoxifen and Pg on NCI-H295R cells found their rationale on the pleiotropic role of SF-1. The reduction of SF-1 protein expression along with a not significant modification of SF-1 mRNA expression induced by both drugs, led us to hypothesize that miRNA regulation of transcriptional capability of mRNA could occurred. It is indeed known that miRNAs, by binding to the 3′-untranslated region of target mRNAs, induced translational repression followed by degradation of approximately one-third of human genes (for an extensive review see: 46). Using computational approaches, it is suggested that each miRNA can bind to hundreds of different mRNAs, which collectively results in an extremely fine regulation of protein transcription (46). Thus, the concept that

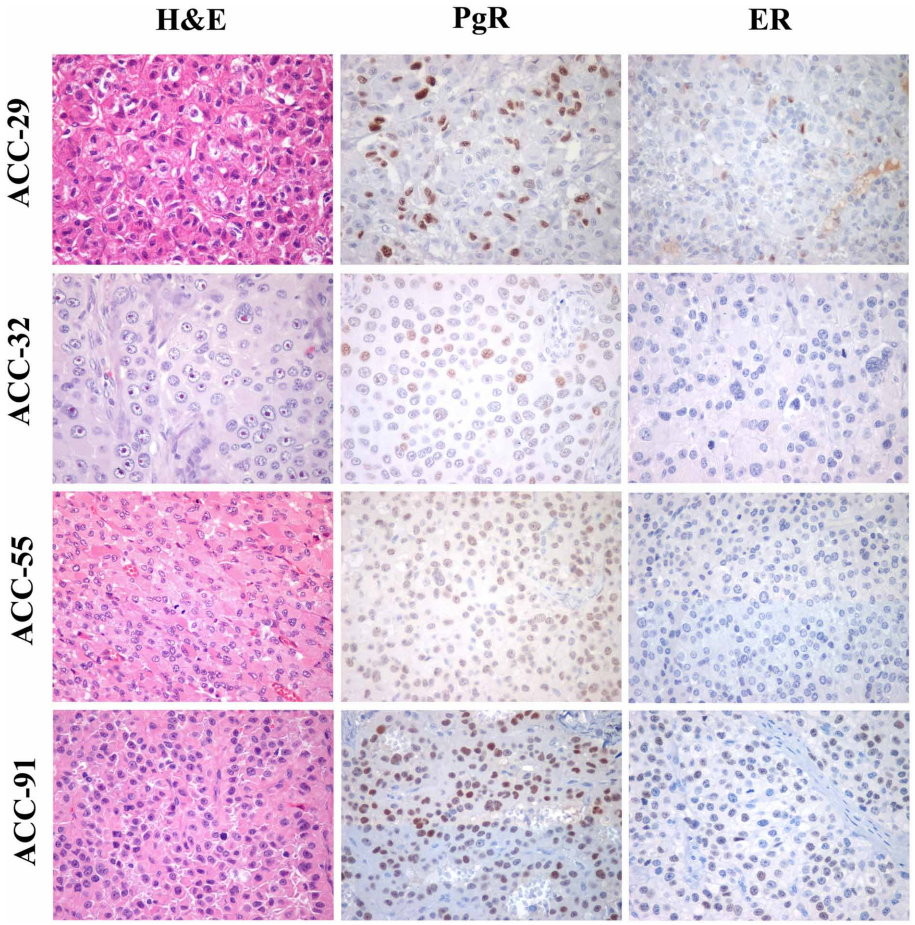

FIGURE 8 | Immunohistochemistry for PgR and ER expression in ACC samples. Left panels show representative H&E-stained section from ACC tumor samples, middle panels PgR and right panels ER immunostainings. All images are from ×40 original magnification.

dysregulation of miRNA expression is linked to cancer is now accepted worldwide. Among the cancer-associated miRNAs, miR23a, one of the most studied miRNAs in different types of cancer, has been found to be involved, together with miR23b, in the regulation of SF-1 protein transcription (37). In NCI-H295R cells, we demonstrated that SF-1 reduction could be mediated, at least in part, by the increase of both miR23a and miR23b. The mechanism underlying this inverse correlation between SF-1 protein and miR23a and miR23b expression is still unknown; however, it has been shown that ER-α binding sites are present in the regulatory region of miR23a (47, 48) and miR23b, along with ER-β binding sites in miR23b regulatory region (49). To our knowledge, no evidence of a direct regulation of Pg on miR23a and miR23b is known at the moment; however, an indirect effect of Pg acting on E-ER-miR23a and miR23b regulation could be as well suggested, as it occurs for a large family of miRNAs in breast cancer (50).

Taken together, these results suggest that SF-1 expression seemed to be regulated by ER and PgR, These data, however, are not exhaustive and the full evidence of the inhibitory effect would require the demonstration of a modulation of the expression of other specific β-catenin target genes in NCI-H295R cells by Pg treatment. These further experiments are outside the scope of the present paper and will be a matter of a future study.

AUTHOR'S NOTE

Part of these results has been presented at the 19th ENS@T Scientific Meeting—6 Nov 2020 ONLINE and accepted for presentation at the 40thNational Meeting of the Italian Society of Pharmacology—9–13 March 2021 Digital Edition.

DATA AVAILABILITY STATEMENT

The original contributions presented in the study are included in the article/**Supplementary Material**. Further inquiries can be directed to the corresponding author.

ETHICS STATEMENT

The studies involving human participants were reviewed and approved by Comitato Etico di Brescia. The patients/participants provided their written informed consent to participate in this study.

AUTHOR CONTRIBUTIONS

Conceptualization, SS, AB, and MF. Methodology, SS, ER, and MT. Formal analysis, AA, E.R, MF, and MC. Investigation, ER, MT, SB, AA, and MC. Writing—original draft preparation, ER, MT, and PP. Writing—review and editing, SS, AB, CH, PP, GT, and MM. Supervision, SS and AB. All authors contributed to the article and approved the submitted version.

FUNDING

This work was funded by: AIRC project IG23009 (PI: AB), local grants from University of Brescia, Fondazione Camillo Golgi, Brescia and F.I.R.M. onlus Foundation, Cremona (Italy). CH received funding by the Uniscientia Foundation (keyword: tumor model).

SUPPLEMENTARY MATERIAL

The Supplementary Material for this article can be found online at: https://www.frontiersin.org/articles/10.3389/fendo.2021.669426/full#supplementary-material

REFERENCES

1. Terzolo M, Daffara F, Ardito A, Zaggia B, Basile V, Ferrari L, et al. Management of Adrenal Cancer: A 2013 Update. *J Endocrinol Invest* (2014) 37(3):207–17. doi: 10.1007/s40618-013-0049-2
2. Terzolo M, Angeli A, Fassnacht M, Daffara F, Tauchmanova L, Conton PA, et al. Adjuvant Mitotane Treatment for Adrenocortical Carcinoma. *N Engl J Med* (2007) 356(23):2372–80. doi: 10.1056/NEJMoa063360
3. Berruti A, Grisanti S, Pulzer A, Claps M, Daffara F, Loli P, et al. Long-Term Outcomes of Adjuvant Mitotane Therapy in Patients With Radically Resected Adrenocortical Carcinoma. *J Clin Endocrinol Metab* (2017) 102(4):1358–65. doi: 10.1210/jc.2016-2894
4. Fassnacht M, Assie G, Baudin E, Eisenhofer G, de la Fouchardiere C, Haak HR, et al. Esmo Guidelines Committee. Electronic Address: Clinicalguidelines@Esmo.Org. Adrenocortical Carcinomas and Malignant Phaeochromocytomas: ESMO-EURACAN Clinical Practice Guidelines for Diagnosis, Treatment and Follow-Up. *Ann Oncol* (2020) 31(11):1476–90. doi: 10.1016/j.annonc.2020.08.2099
5. Fassnacht M, Terzolo M, Allolio B, Baudin E, Haak H, Berruti A, et al. Firm-Act Study Group. Combination Chemotherapy in Advanced Adrenocortical Carcinoma. *N Engl J Med* (2012) 66(23):2189–97. doi: 10.1056/NEJMoa1200966
6. Laganà M, Grisanti S, Cosentini D, Ferrari VD, Lazzari B, Ambrosini R, et al. Efficacy of the EDP-M Scheme Plus Adjunctive Surgery in the Management of Patients With Advanced Adrenocortical Carcinoma: The Brescia Experience. *Cancers (Basel)* (2020) 12(4):941. doi: 10.3390/cancers12040941
7. Cosentini D, Badalamenti G, Grisanti S, Basile V, Rapa I, Cerri S, et al. Activity and Safety of Temozolomide in Advanced Adrenocortical Carcinoma Patients. *Eur J Endocrinol* (2019) 181(6):681–9. doi: 10.1530/EJE-19-0570
8. Sperone P, Ferrero A, Daffara F, Priola A, Zaggia B, Volante M, et al. Gemcitabine Plus Metronomic 5-Fluorouracil or Capecitabine as a Second-/Third-Line Chemotherapy in Advanced Adrenocortical Carcinoma: A Multicenter Phase II Study. *Endocr Relat Cancer* (2010) 17 (2):445–53. doi: 10.1677/ERC-09-0281
9. Fiorentini C, Grisanti S, Cosentini D, Abate A, Rossini E, Berruti A, et al. Molecular Drivers of Potential Immunotherapy Failure in Adrenocortical Carcinoma. *J Oncol* (2019) 1:6072863. doi: 10.1155/2019/6072863
10. Grisanti S, Cosentini D, Laganà M, Volta AD, Palumbo C, Massimo Tiberio GA, et al. The Long and Winding Road to Effective Immunotherapy in Patients With Adrenocortical Carcinoma. *Future Oncol* (2020) 16(36):3017–20. doi: 10.2217/fon-2020-0686
11. de Cremoux P, Rosenberg D, Goussard J, Brémont-Weil C, Tissier F, Tran-Perennou C, et al. Expression of Progesterone and Estradiol Receptors in Normal Adrenal Cortex, Adrenocortical Tumors, and Primary Pigmented Nodular Adrenocortical Disease. *Endocr Relat Cancer* (2008) 15(2):465–74. doi: 10.1677/ERC-07-0081
12. Baquedano MS, Saraco N, Berensztein E, Pepe C, Bianchini M, Levy E, et al. Identification and Developmental Changes of Aromatase and Estrogen Receptor Expression in Prepubertal and Pubertal Human Adrenal Tissues. *J Clin Endocrinol Metab* (2007) 92(6):2215–22. doi: 10.1210/jc.2006-2329
13. Barzon L, Masi G, Pacenti M, Trevisan M, Fallo F, Remo A, et al. Expression of Aromatase and Estrogen Receptors in Human Adrenocortical Tumors. *Virchows Arch* (2008) 452(2):181–91. doi: 10.1007/s00428-007-0542-0
14. Medwid S, Guan H, Yang K. Bisphenol A Stimulates Adrenal Cortical Cell Proliferation Via Erβ-Mediated Activation of the Sonic Hedgehog Signalling Pathway. *J Steroid Biochem Mol Biol* (2018) 178:254–62. doi: 10.1016/j.jsbmb.2018.01.004
15. Shen XC, Gu XC, Qiu YQ, Du CJ Fu YB, Wu JJ. Estrogen Receptor Expression in Adrenocortical Carcinoma. *J Zhejiang Univ Sci B* (2009) 10(1):1–6. doi: 10.1631/jzus.B0820072
16. Montanaro D, Maggiolini M, Recchia AG, Sirianni R, Aquila S, Barzon L, et al. Antiestrogens Upregulate Estrogen Receptor Beta Expression and Inhibit Adrenocortical H295R Cell Proliferation. *J Mol Endocrinol* (2005) 35(2):245–56. doi: 10.1677/jme.1.01806
17. Zhao C, Dahlman-Wright K, Gustafsson J-Å. Estrogen Receptor ß: An Overview and Update. *Nucl Recept Signal* (2008) 6:e003. doi: 10.1621/nrs.06003
18. Fragni M, Fiorentini C, Rossini E, Fisogni S, Vezzoli S, Bonini SA, et al. In Vitro Antitumor Activity of Progesterone in Human Adrenocortical Carcinoma. *Endocrine* (2019a) 63(3):592–601. doi: 10.1007/s12020-018-1795-x
19. Katzenellenbogen BS, Norman MJ. Multihormonal Regulation of the Progesterone Receptor in MCF-7 Human Breast Cancer Cells: Interrelationships Among Insulin/Insulin-Like Growth factor-I, Serum, and Estrogen. *Endocrinology* (1990) 126(2):891–8. doi: 10.1210/endo-126-2-891
20. Carlson JAJr, Allegra JC, Day TGJr, Wittliff JL. Tamoxifen and Endometrial Carcinoma: Alterations in Estrogen and Progesterone Receptors in Untreated Patients and Combination Hormonal Therapy in Advanced Neoplasia. *Am J Obstet Gynecol* (1984) 149(2):149–53. doi: 10.1016/0002-9378(84)90187-x
21. Abiven-Lepage G, Coste J, Tissier F, Groussin L, Billaud L, Dousset B, et al. Adrenocortical Carcinoma and Pregnancy: Clinical and Biological Features and Prognosis. *Eur J Endocrinol* (2010) 163(5):793–800. doi: 10.1530/EJE-10-0412
22. de Corbière P, Ritzel K, Cazabat L, Ropers J, Schott M, Libé R, et al. Pregnancy in Women Previously Treated for an Adrenocortical Carcinoma. *J Clin Endocrinol Metab* (2015) 100(12):4604–11. doi: 10.1210/jc.2015-2341
23. Altinoz MA, Bilir A, Gedikoglu G, Ozcan E, Oktem G, Muslumanoglu M. Medroxyprogesterone and Tamoxifen Augment Anti-Proliferative Efficacy and Reduce Mitochondria-Toxicity of Epirubicin in FM3A Tumor Cells In Vitro. *Cell Biol Int* (2007) 31(5):473–81. doi: 10.1016/j.cellbi.2006.11.013
24. Zaino RJ, Satyaswaroop PG, Mortel R. Hormonal Therapy of Human Endometrial Adenocarcinoma in a Nude Mouse Model. *Cancer Res* (1985) 45(2):539–41.
25. Wen L, Hong D, Yanyin W, Mingyue Z, Baohua L. Effect of Tamoxifen, Methoxyprogesterone Acetate and Combined Treatment on Cellular

Proliferation and Apoptosis in SKOV3/DDP Cells Via the Regulation of Vascular Endothelial Growth Factor. *Arch Gynecol Obstet* (2013) 287(5):997–1004. doi: 10.1007/s00404-012-2664-0
26. Herzog TJ. What is the Clinical Value of Adding Tamoxifen to Progestins in the Treatment [Correction for Treament] of Advanced or Recurrent Endometrial Cancer? *Gynecol Oncol* (2004) 92(1):1–3. doi: 10.1016/j.ygyno.2003.11.014
27. Rainey WE, Saner K, Schimmer BP. Adrenocortical Cell Lines. *Mol Cell Endocrinol* (2004) 228(1-2):23–38. doi: 10.1016/j.mce.2003.12.020
28. Hantel, Shapiro I, Poli G, Chiapponi C, Bidlingmaier M, Reincke M, et al. Targeting Heterogeneity of Adrenocortical Carcinoma: Evaluation and Extension of Preclinical Tumor Models to Improve Clinical Translation. *Oncotarget* (2016) 7(48):79292–304. doi: 10.18632/oncotarget.12685
29. Fragni M, Palma Lopez LP, Rossini E, Abate A, Cosentini D, Salvi V, et al. In Vitro Cytotoxicity of Cabazitaxel in Adrenocortical Carcinoma Cell Lines and Human Adrenocortical Carcinoma Primary Cell Cultures. *Mol Cell Endocrinol* (2019b) 498:110585. doi: 10.1016/j.mce.2019.110585
30. Lloyd RV, Osamura RY, Klöppel G, Rosai J. *Who Classification of Tumours of Endocrine Organs*. Lyon: IARC: WHO (2017).
31. Fiorentini C, Fragni M, Perego P, Vezzoli S, Bonini SA, Tortoreto M, et al. Antisecretive and Antitumor Activity of Abiraterone Acetate in Human Adrenocortical Cancer: A Preclinical Study. *J Clin Endocrinol Metab* (2016) 101(12):4594–602. doi: 10.1210/jc.2016-2414
32. Chou TC, Talalay P. Quantitative Analysis of Dose-Effect Relationships: The Combined Effects of Multiple Drugs or Enzyme Inhibitors. *Adv Enzyme Regul* (1984) 22:27–55. doi: 10.1016/0065-2571(84)90007-4
33. Chou TC. Theoretical Basis, Experimental Design, and Computerized Simulation of Synergism and Antagonism in Drug Combination Studies. *Pharmacol Rev* (2006) 58(3):621–81. doi: 10.1124/pr.58.3.10
34. Fragni M, Bonini SA, Stabile A, Bodei S, Cristinelli L, Simeone C, et al. Inhibition of Survivin is Associated With Zoledronic Acid-Induced Apoptosis of Prostate Cancer Cells. *Anticancer Res* (2016a) 36:913–20.
35. Fragni M, Bonini SA, Bettinsoli P, Bodei S, Generali D, Bottini A, et al. The miR-21/PTEN/Akt Signaling Pathway is Involved in the Anti-Tumoral Effects of Zoledronic Acid in Human Breast Cancer Cell Lines. *Naunyn Schmiedebergs Arch Pharmacol* (2016b) 389(5):529–38. doi: 10.1007/s00210-016-1224-8
36. Lalli E, Doghman M, Latre de Late P, El Wakil A, Mus-Veteau I. Beyond Steroidogenesis: Novel Target Genes for SF-1 Discovered by Genomics. *Mol Cell Endocrinol* (2013) 371(1-2):154–9. doi: 10.1016/j.mce.2012.11.005
37. Shen L, Yang S, Huang W, Xu W, Wang Q, Song Y, et al. MicroRNA23a and microRNA23b Deregulation Derepresses SF-1 and Upregulates Estrogen Signaling in Ovarian Endometriosis. *J Clin Endocrinol Metab* (2013) 98 (4):1575–82. doi: 10.1210/jc.2012-3010
38. Gruvberger-Saal SK, Bendahl PO, Saal LH, Laakso M, Hegardt C, Edén P, et al. Estrogen Receptor Beta Expression is Associated With Tamoxifen Response in ERalpha-negative Breast Carcinoma. *Clin Cancer Res* (2007) 13 (7):1987–94. doi: 10.1158/1078-0432.CCR-06-1823
39. Tamoxifen. *Ibm Micromedex® DRUGDEX® (Electronic Version)* . Greenwood Village, Colorado, USA: IBM Watson Health. Available at: https://www.micromedexsolutions.com/ (Accessed January, 04, 2021).
40. Boonyaratanakornkit V, McGowan E, Sherman L, Mancini MA, Cheskis BJ, Edwards DP. The Role of Extranuclear Signaling Actions of Progesterone Receptor in Mediating Progesterone Regulation of Gene Expression and the Cell Cycle. *Mol Endocrinol* (2007) 21:359–75. doi: 10.1210/me.2006-0337
41. Altinoz MA, Ozpinar A, Elmaci I. Reproductive Epidemiology of Glial Tumors may Reveal Novel Treatments: High-Dose Progestins or Progesterone Antagonists as Endocrino-Immune Modifiers Against Glioma. *Neurosurg Rev* (2019) 42(2):351–69. doi: 10.1007/s10143-018-0953-1
42. Motamed HR, Shariati M, Ahmadi R, Khatamsaz S, Mokhtari M. The Apoptotic Effects of Progesterone on Breast Cancer (MCF-7) and Human Osteosarcoma (MG-636) Cells. *Physiol Int* (2020) 107(3):406–18. doi: 10.1556/2060.2020.00034
43. Truong TH, Lange CA. Deciphering Steroid Receptor Crosstalk in Hormone-Driven Cancers. *Endocrinology* (2018) 159(12):3897–907. doi: 10.1210/en.2018-00831
44. Lalli E. Adrenocortical Development and Cancer: Focus on SF-1. *J Mol Endocrinol* (2010) 44(6):301–7. doi: 10.1677/JME-09-0143
45. Doghman M, Karpova T, Rodrigues GA, Arhatte M, De Moura J, Cavalli LR, et al. Increased Steroidogenic Factor-1 Dosage Triggers Adrenocortical Cell Proliferation and Cancer. *Mol Endocrinol* (2007) 12:2968–87. doi: 10.1210/me.2007-0120
46. Jonas S, Izaurralde E. Towards a Molecular Understanding of MicroRNA-Mediated Gene Silencing. *Nat Rev Genet* (2015) 16(7):421–33. doi: 10.1038/nrg3965
47. Bhat-Nakshatri P, Wang G, Collins NR, Thomson MJ, Geistlinger TR, Carroll JS, et al. Estradiol-Regulated microRNAs Control Estradiol Response in Breast Cancer Cells. *Nucleic Acids Res* (2009) 37(14):4850–61. doi: 10.1093/nar/gkp500
48. Huang FY, Wong DK, Seto WK, Lai CL, Yuen MF. Estradiol Induces Apoptosis Via Activation of miRNA-23a and p53: Implication for Gender Difference in Liver Cancer Development. *Oncotarget* (2015) 6(33):34941–52. doi: 10.18632/oncotarget.5472
49. Paris O, Ferraro L, Grober OM, Ravo M, De Filippo MR, Giurato G, et al. Direct Regulation of microRNA Biogenesis and Expression by Estrogen Receptor Beta in Hormone-Responsive Breast Cancer. *Oncogene* (2012) 31 (38):4196–206. doi: 10.1038/onc.2011.583
50. McFall T, McKnight B, Rosati R, Kim S, Huang Y, Viola-Villegas N, et al. Progesterone Receptor A Promotes Invasiveness and Metastasis of Luminal Breast Cancer by Suppressing Regulation of Critical microRNAs by Estrogen. *J Biol Chem* (2018) 293(4):1163–77. doi: 10.1074/jbc.M117.812438

Conflict of Interest: The authors declare that the research was conducted in the absence of any commercial or financial relationships that could be construed as a potential conflict of interest.

frontiers in Endocrinology

REVIEW
published: 06 May 2021
doi: 10.3389/fendo.2021.678869

Phakomatoses and Endocrine Gland Tumors: Noteworthy and (Not so) Rare Associations

Benjamin Chevalier[1,2†], *Hippolyte Dupuis*[1†], *Arnaud Jannin*[1,2], *Madleen Lemaitre*[1,2], *Christine Do Cao*[1], *Catherine Cardot-Bauters*[1], *Stéphanie Espiard*[1,2,3] *and Marie Christine Vantyghem*[1,2,3*]

[1] Department of Endocrinology, Diabetology and Metabolism, Lille University Hospital, Lille, France, [2] University of Lille, Lille, France, [3] INSERM U1190, European Genomic Institute for Diabetes, Lille, France

OPEN ACCESS

Edited by:
Antongiulio Faggiano, Sapienza University of Rome, Italy

Reviewed by:
Hans Ghayee, University of Florida, United States
Jean-Yves Scoazec, Institut Gustave Roussy, France

***Correspondence:**
Marie Christine Vantyghem
mc-vantyghem@chru-lille.fr

[†]*These authors have contributed equally to this work*

Specialty section:
This article was submitted to Cancer Endocrinology, a section of the journal Frontiers in Endocrinology

Received: *10 March 2021*
Accepted: *15 April 2021*
Published: *06 May 2021*

Citation:
Chevalier B, Dupuis H, Jannin A, Lemaitre M, Do Cao C, Cardot-Bauters C, Espiard S and Vantyghem MC (2021) Phakomatoses and Endocrine Gland Tumors: Noteworthy and (Not so) Rare Associations. Front. Endocrinol. 12:678869. doi: 10.3389/fendo.2021.678869

Phakomatoses encompass a group of rare genetic diseases, such as von Hippel-Lindau syndrome (VHL), neurofibromatosis type 1 (NF1), tuberous sclerosis complex (TSC) and Cowden syndrome (CS). These disorders are due to molecular abnormalities on the RAS-PI3K-Akt-mTOR pathway for NF1, TSC and CS, and to hypoxia sensing for VHL. Phakomatoses share some phenotypic traits such as neurological, ophthalmological and cutaneous features. Patients with these diseases are also predisposed to developing multiple endocrine tissue tumors, e.g., pheochromocytomas/paragangliomas are frequent in VHL and NF1. All forms of phakomatoses except CS may be associated with digestive neuroendocrine tumors. More rarely, thyroid cancer and pituitary or parathyroid adenomas have been reported. These susceptibilities are noteworthy, because their occurrence rate, prognosis and management differ slightly from the sporadic forms. The aim of this review is to summarize current knowledge on endocrine glands tumors associated with VHL, NF1, TSC, and CS, especially neuroendocrine tumors and pheochromocytomas/paragangliomas. We particularly detail recent advances concerning prognosis and management, especially parenchyma-sparing surgery and medical targeted therapies such as mTOR, MEK and HIF-2 α inhibitors, which have shown truly encouraging results.

Keywords: neurofibromatosis type 1, von Hippel-Lindau, Cowden syndrome, tuberous sclerosis complex, pheochromocytoma, paraganglioma, digestive neuroendocrine tumors

Abbreviations: ACTH, adrenocorticotropic hormone; CNS, central nervous system; CS, Cowden syndrome; CT, computerized tomography; ^{18}FDG, ^{18}fluorodeoxyglucose; ^{18}F-DOPA, ^{18}fluoro-dihydroxyphenylalanine; FS, functional syndrome; ^{68}Ga-SSA, ^{68}Ga-somatostatin analogues; GH, growth hormone; HIF, hypoxia-inducible factor; ^{123}I-MIBG, ^{123}I-metaiodobenzylguanidine; APK, mitogen-activated protein kinase; MEN1, multiple endocrine neoplasia type 1; MRI, magnetic resonance imaging; mTOR, mechanistic target of rapamycin; NET, neuroendocrine tumor; NF1, neurofibromatosis type 1; PET-CT, positron emission tomography-computerized tomography; PDGFR α-β, platelet-derived growth factor receptor α-β; PI3K, phosphoinositide 3-kinases; PPGL, pheochromocytoma/paraganglioma; TSC, tuberous sclerosis complex; VEGFR 1-3, vascular endothelial growth factor receptor 1-3; VHL, von Hippel-Lindau disease.

INTRODUCTION

Phakomatoses are a group of systemic diseases linked to ectodermal dysembryogenesis. The term comes from the Greek noun *phakos* (φακός, meaning "lentil" or "spot") and the word termination *-oma* (for "tumor"), which refer to cutaneous birthmarks, i.e. hamartomas. Other cardinal features involve the central nervous system and the eyes (1). The most frequent forms of phakomatoses are:

- neurofibromatosis type 1 (NF1), also known as von Recklinghausen's disease,
- von Hippel-Lindau disease (VHL),
- tuberous systemic complex (TSC),
- and Cowden syndrome (CS).

The prevalence is, however, less than 1/2,000 people. These rare diseases were clinically described in the 19th century by famous physicians such as the pathologist Friedrich Daniel von Recklinghausen, and the ophthalmologist Eugen von Hippel, both from Germany, Arvid Lindau, a Swedish pathologist and Désiré-Magloire Bourneville, a French neurologist. Although the hereditary nature of these syndromes was predicted early on, their molecular basis was only elucidated at the end of the 20th century by means of genetic developments and the characterization of the Ras-PI3K-Akt-mTOR pathway in NF1, TSC, and CS, as well as of the hypoxia signaling pathway in VHL.

Besides classical neurological, ophthalmological and cutaneous features, patients with phakomatoses are predisposed to developing tumors of the endocrine glands, with different spectrums for each disease (**Figure 1**).

After a brief review of the pathophysiology of common forms of phakomatoses, we describe the clinical features of endocrine tumors associated with them and focus on their specific features compared with sporadic counterparts; indeed, time of occurrence, clinical expression and prognosis can differ slightly. We then detail recent advances concerning the management of those tumors, especially focusing on parenchyma-sparing surgery in localized disease and pharmacological therapies targeting mTOR, MEK and HIF2-α in advanced/metastatic disease.

PATHOPHYSIOLOGY AND MOLECULAR BIOLOGY OF PHAKOMATOSES

NF1, TSC and CS are caused by mutations on genes encoding for different components of the MAP kinase and Ras-PI3K-Akt-mTOR pathways (**Figure 2**). The PI3Kinase-Akt pathway is a classical signaling pathway involved in the regulation of metabolic processes, maintenance of the redox balance, and cell survival and growth (2). PI3Kinase is primarily activated by RAS proteins. This family of proteins (HRAS-NRAS-KRAS) also regulates other signaling pathways such as MAP kinase, which is involved in cell proliferation and survival (3). RAS proteins oscillate between active guanosine triphosphate (GTP)-bound and inactive guanosine diphosphate (GDP)-bound states, and deregulation has been observed in various diseases such as cancer or even psychiatric diseases (4).

Downstream from PI3K and Akt is the mTOR pathway, which ultimately leads to the activation of mTOR complexes 1 and 2 (mTORC1 & 2). The mTOR pathway has been highly conserved during evolution and integrates several environmental cues, such as growth factors, amino acids or glucose, in order to guide cellular growth and fate (5). These multi-protein complexes regulate energy metabolism and lipid/protein synthesis and influence cell survival. In human diseases, mTOR deregulation is involved in cancer, diabetes and ageing (6).

Neurofibromatosis Type 1

Neurofibromatosis type 1 (NF1), an autosomal dominant disease, is caused by mutations of the *NF1* gene located on chromosome 17q11.2, which encodes neurofibromin (7). This protein accelerates the conversion of active GTP-bound RAS to inactive GDP-RAS. Consistently, MAP kinase and PI3Kinase-Akt-mTOR are deregulated in NF1 (8, 9).

von Hippel-Lindau Disease

The pathophysiology of another type of phakomatoses, von Hippel-Lindau disease (VHL), is related to a different but major cellular dysfunction: oxygen sensing (10) (**Figure 3**). VHL is an autosomal dominant disease linked to mutations of the *VHL* gene, mapped on chromosome 3p25.3 (11). The VHL protein (pVHL) is part of a multiprotein complex that is also constituted by elongin B and C, Cullin 2 and RBX1, with the whole complex exhibiting E3 ubiquitin ligase properties (12, 13). Under normoxic conditions, hypoxia-inducible factors-α (HIF-α) are hydroxylated on proline residues by prolyl hydroxylase, which allows recognition by pVHL, then ubiquitylation of HIF-2 and subsequent degradation *via* the proteasome (**Figure 3A**). In hypoxic conditions, HIF-α cannot be hydroxylated and recognized by pVHL, and then tend to accumulate, dimerizing with HIF-1 β and activating the transcription of several genes involved in angiogenesis, erythropoiesis, metabolism, cell proliferation, migration and invasion. With *VHL* gene mutations, there is also no possibility of HIF-α degradation even in normoxic conditions, and this create a pseudo-hypoxic state with continuous activity of the HIF-α/HIF-1β heterodimer (**Figure 3B**). Consequently, VHL is crucial in the oxygen sensing process within the body. It also exhibits HIF-independent properties, including assembly and regulation of the extracellular matrix, microtubule stabilization, and regulation of apoptosis.

Tuberous Sclerosis Complex

Tuberous sclerosis complex (TSC), another autosomal dominant disorder, is related to mutations of the *TSC1* or *TSC2* genes, which are located on chromosomes 9q34 and 16p13.3 (14, 15). These genes encode for hamartin and tuberin, respectively, proteins that have the property of directly inhibiting the mTOR protein. Therefore, mutations on *TSC1* or *TSC2* lead to a hyperactive mTOR pathway.

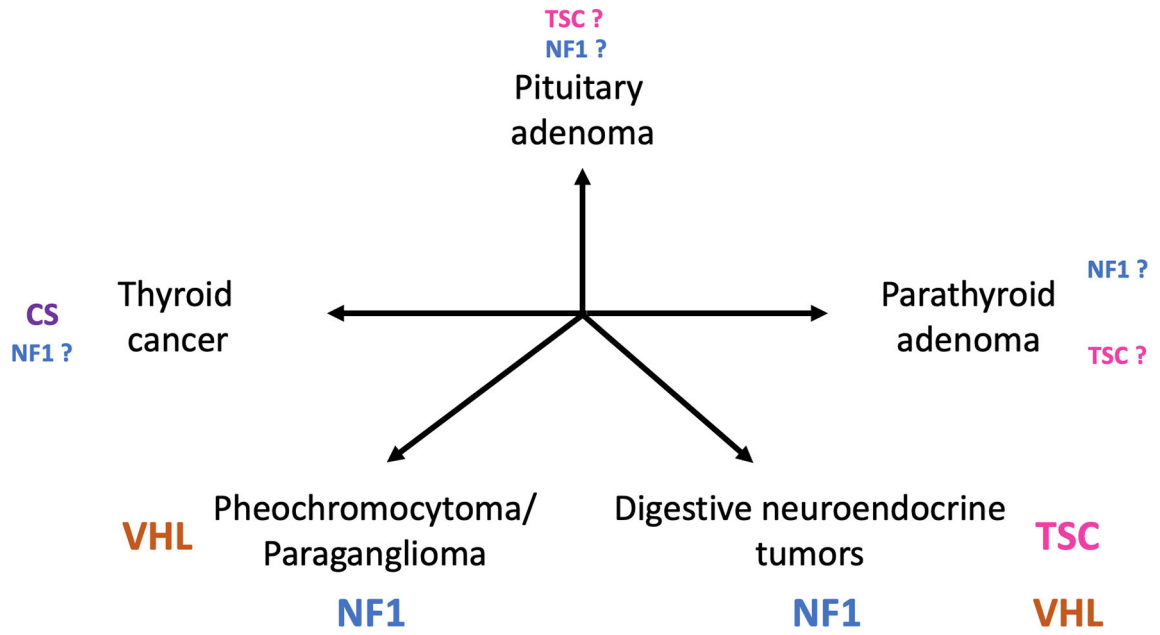

FIGURE 1 | Main tumors of endocrine glands in patients diagnosed with phakomatoses. (TSC, tuberous sclerosis complex; VHL, von Hippel-Lindau disease; NF1, neurofibromatosis type 1; CS, Cowden syndrome).

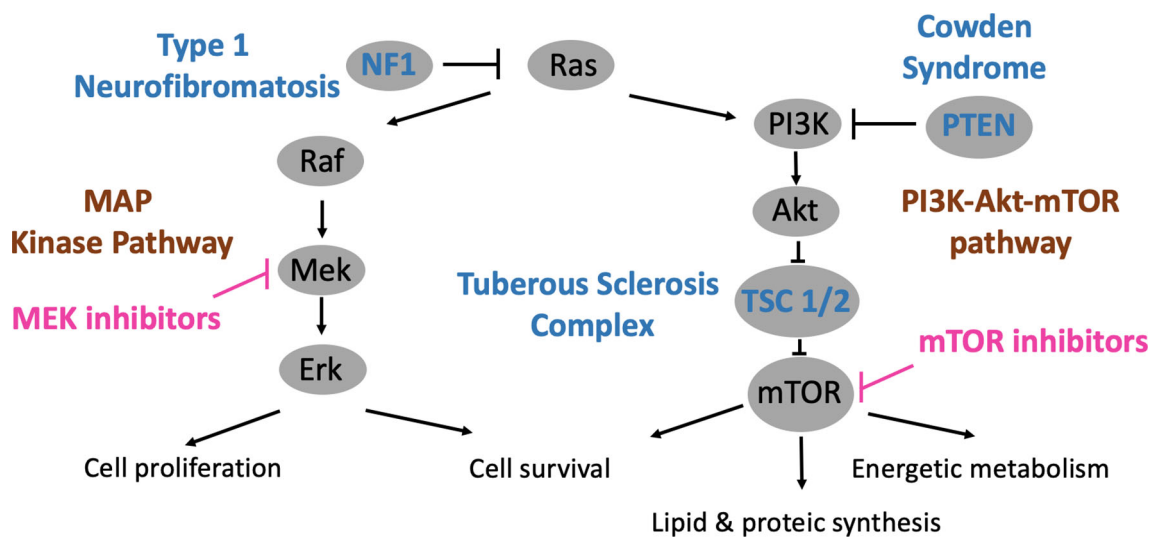

FIGURE 2 | PI3K-Akt-mTOR and MAP kinase pathways, relations with phakomatoses (TSC, NF1 and CS) and therapeutic developments.

Cowden Syndrome

Cowden syndrome (CS), also an autosomal dominant disease, is linked to mutations of the *PTEN* gene, mapped on chromosome 10q23.31 (16). PTEN has the ability to inactivate PI3Kinase, the first kinase that subsequently leads to activation of the mTOR pathway. Consistently, an overactive mTOR pathway is observed when *PTEN* is mutated.

MAIN CLINICAL FEATURES OF PHAKOMATOSES

Neurofibromatosis Type 1

NF1 is the most common form of phakomatoses and affects 1 out of 3000–3500 births worldwide (17). The main symptoms of NF1 are cutaneous, ophthalmological and neurological (**Table 1**). NF1 predisposes to the development of multiple neoplasias including

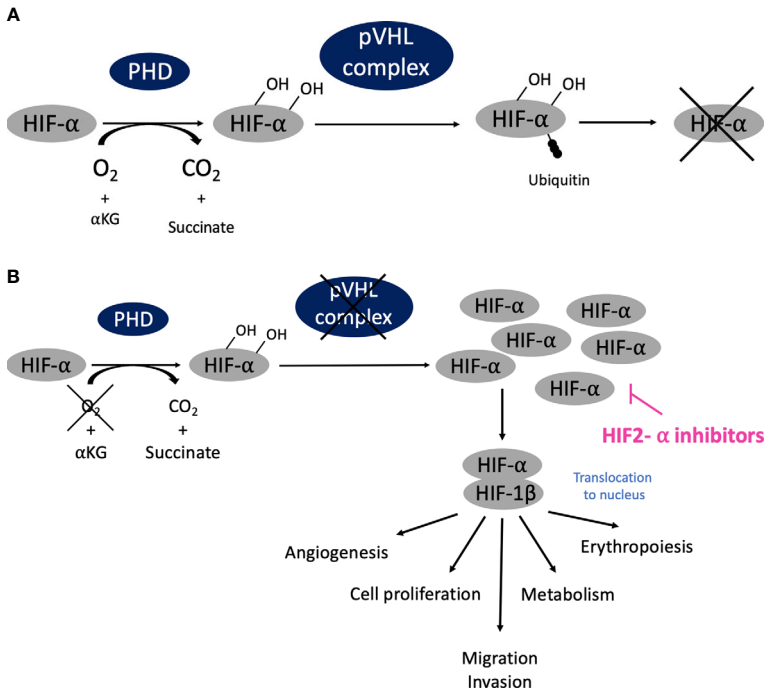

FIGURE 3 | Oxygen sensing pathway, connection with phakomatoses (VHL) and therapeutic developments. **(A)** In normoxic conditions (normal oxygen concentration), HIF-α are hydroxylated on proline residues by prolyl hydroxylase, is then recognized by pVHL complex and ubiquitinated and subsequently degraded *via* the proteasome. **(B)** In hypoxic conditions (low oxygen concentration), HIF-α cannot the be recognized by pVHL and degraded; it accumulates, dimerizes with HIF-1 β, translocates into cellular nucleus and activates transcription of targeted genes. Similarly, when *VHL* is mutated there is also no possibility of HIF-α degradation even in normoxic conditions, and this creates a pseudo-hypoxic state with the HIF-α/HIF-1 β dimer constantly activated, leading to the development of tumor angiogenesis as compensation.

TABLE 1 | Neurofibromatosis type 1 (NF1) diagnostic criteria. Adapted from (18).

Clinical criteria
Two or more of the following:
At least six café-au-lait macules (> 5 mm diameter in pre-pubertal individuals and > 15 mm in post-pubertal individuals)
Freckling in axillary or inguinal regions
Optic nerve glioma
At least two Lisch nodules (iris hamartomas)
At least two neurofibromas of any type, or one plexiform neurofibroma
A distinctive osseous lesion (sphenoid dysplasia or tibial pseudarthrosis)
A first-degree relative with NF1

solid cancers, mainly malignant peripheral nerve sheath tumors, as well as malignant hemopathies (18). Endocrine tumors, mainly pheochromocytoma and digestive neuroendocrine tumors, are also observed. Primary hyperparathyroidism, pituitary adenomas and thyroid cancer have been reported but are indeed very rare and, to date, are not considered as classical phakomatoses-associated endocrine tumors (19).

von Hippel-Lindau Disease

The classical clinical features of VHL disease usually include CNS and/or retinal hemangioblastoma, endolymphatic tumor, clear cell renal carcinoma, and a predisposition for developing cysts, mainly in the kidney and pancreas (**Table 2**). VHL disease occurs in about 1 per 36,000 births, with a penetrance at 65 years estimated at 90%. The disease is due to a *de novo* mutation in 20% of cases. Mosaic mutations can be identified in a minority (5%) of patients (20, 21). The two main endocrine tumors observed in VHL are pheochromocytoma/paraganglioma (PPGL) and pancreatic neuroendocrine tumors (pNETs). VHL disease is classified into two distinct phenotypes, which are based on the absence (type 1) or the presence (type 2) of PPGL. Type 1 VHL affects 80% of patients and is associated with large deletions or truncating mutations, whereas 20% of patients are in the type

TABLE 2 | von Hippel-Lindau disease diagnostic criteria. Adapted from (10).

Clinical diagnosis
Family history of VHL and:
- CNS hemangioblastoma,
- or retinal hemangioblastoma,
- or pheochromocytoma,
-or clear cell renal carcinoma
NO family history of VHL and:
- at least 2 hemangioblastomas
- or at least 2 visceral tumors
- or one hemangioblastoma AND one visceral tumor

CNS, central nervous system.

2 group, which is associated with missense mutations. Subgroups have also been defined within type 2 VHL: type 2a (low risk of renal cancer), type 2b (higher risk of renal cancer) and type 2c (PPGL only).

Tuberous Sclerosis Complex

The classical phenotype of TSC associates cutaneous lesions, neurological features (cortical tubers, subependymal nodules, and subependymal giant cell astrocytomas) and multiple retinal hamartomas (22) (**Table 3**). Its prevalence is estimated at 1/20,000 people. There is no clear genotype-phenotype correlation, but patients with *TSC2* mutations show more severe disease than those with *TSC1* mutations, although it does not involve endocrine tumors. The penetrance is high, with variable expression in the same family. Based on small studies, TSC may be associated with an increased risk of developing digestive neuroendocrine tumors, as well as pituitary and parathyroid adenomas (23).

Cowden Syndrome

The incidence of CS is estimated to be 1/200,000 individuals. Patients with CS classically present with cutaneous features (facial papules, oral mucosal papillomatosis, palmoplantar keratoses), macrocephaly, and Lhermitte-Duclos disease (24) (**Table 4**). They also exhibit a predisposition for developing several types of cancer, the most prevalent being breast, endometrial, renal, colorectal and finally thyroid cancer. Thyroid cancer is typically differentiated, arise from follicular cells and occurs in 20 to 38% of CS patients, with a possible association with promoter or exon 1 mutations (25–28).

TABLE 3 | Tuberous sclerosis complex diagnostic criteria. Adapted from (22).

Genetic diagnostic criteria
The identification of either a TSC1 or TSC2 pathogenic mutation in DNA from normal tissue is sufficient for making a definite diagnosis of tuberous sclerosis complex (TSC).
Clinical diagnostic criteria
Major features
Hypomelanotic macules (3, at least 5-mm diameter)
Angiofibromas (3) or fibrous cephalic plaque
Ungual fibromas (2)
Shagreen patch
Multiple retinal hamartomas
Cortical dysplasia
Subependymal nodules
Subependymal giant cell astrocytoma
Cardiac rhabdomyoma
Lymphangioleiomyomatosis (LAM)
Angiomyolipomas
Minor features
"Confetti" skin lesions
Dental enamel pits (> 3)
Intraoral fibromas (2)
Retinal achromic patch
Multiple renal cysts
Nonrenal hamartomas
Definite diagnosis: Two major features or one major feature with 2 minor features
Possible diagnosis: Either one major feature or 2 minor features

TABLE 4 | Cowden syndrome diagnostic criteria. Adapted from (24).

Pathognomonic features
Adult Lhermitte-Duclos disease (LDD, rare tumor of cerebellum)
Mucocutaneous lesions
Facial trichilemmomas?
Acral keratosis
Papillomatous papules
Mucosal lesions
Major criteria
Breast carcinoma
Thyroid carcinoma (non-medullary), especially follicular thyroid carcinoma
Macrocephaly (occipital frontal circumference ≥ 97th percentile)
Endometrial carcinoma
Minor criteria
Other thyroid lesions (e.g., adenoma, multinodular goiter)
Intellectual Disability (i.e., IQ ≤ 75)
Gastrointestinal hamartomas
Fibrocystic breast disease
Lipomas
Fibromas
Genitourinary tumors (especially renal cell carcinoma)
Genitourinary malformations
Uterine fibroids
Operational diagnosis in an individual (any of the following)
Mucocutaneous lesions alone, if ≥ six facial papules (three of which must be trichilemmomas)
Cutaneous facial papules and oral mucosal papillomatosis
Oral mucosal papillomatosis and acral keratosis
≥ Six palmoplantar keratoses
≥ Two major criteria (one of which must be macrocephaly or LDD)
One major and ≥ three minor criteria
≥ Four minor criteria
Operational diagnosis in a family where one individual has a diagnosis of Cowden syndrome
Any one pathognomonic criterion
Any one major criterion and minor criterion
Two minor criteria
Bannayan-Riley-Ruvalcaba syndrome (overgrowth and hamartomatous disorder with multiple subcutaneous lipomas, macrocephaly and hemangiomas)

PHEOCHROMOCYTOMA/ PARAGANGLIOMA (PPGL) IN PHAKOMATOSES

PPGL arise from adrenal (pheochromocytoma) or extra-adrenal (paraganglioma) chromaffin cells associated with the paravertebral ganglia, and produce one or multiple catecholamines (adrenaline, noradrenaline, dopamine), which results in high blood pressure, palpitations, sweating, headaches, etc. (29, 30). These tumors are usually benign, and malignancy, characterized by distant metastasis, occurs in 8–10% of all PPGL patients: 10% for pheochromocytoma and ~25% for paraganglioma, the difference partially explained by SDH mutations more frequently encountered in paraganglioma (31, 32). Biochemical diagnosis is made with measurements of circulating or urinary catecholamine metabolites (**Table 5**) (33). Half of pheochromocytomas produce significant amounts of adrenaline and are diagnosed by an increase in metanephrines, with a linear relationship between catecholamine concentration and tumor size (34). The other half of pheochromocytomas and extra-adrenal paragangliomas are characterized by a

TABLE 5 | General guidelines for diagnosis and treatment of tumors of endocrine glands.

	Biological investigations	Paraclinical investigations	Treatment
Pheochromocytoma/ Paraganglioma	Plasmatic or urinary catecholamine metabolites (metanephrine, normetanephrine, 3-methoxytyramine)	Imaging: Morphological: CT or MRI, adrenal-specific Functional: ^{18}FDG PET-CT or ^{18}F-DOPA PET-CT or ^{123}I-MIBG scintigraphy or ^{68}Ga-SSA PET-CT	Surgery excision Laparoscopy preferred for abdominal location Adrenal-sparing surgery for bilateral PCC
Gastrointestinal neuroendocrine tumors	- Chromogranin A - Hormones (gastrin, pancreatic polypeptide, insulin, glucagon, somatostatin, VIP, etc.) - In case of carcinoid syndrome: 24-h urinary 5-HIAA, platelet serotonin	Imaging: -CT injected with contrast agent -Abdominal-pelvic MRI injected with Gadolinium to research metastases -Nuclear imaging: ^{68}Ga-SSA PET-CT or ^{18}FDG PET-CT or ^{18}F-DOPA PET-CT If pancreatic tumor -endoscopy - endoscopic ultrasound to perform biopsies	Anti-secretory treatment: - somatostatin analogue, - telotristat (carcinoid), - PPI (gastrinoma), - diazoxide (insulinoma) Surgical excision Metastatic forms: - surgical excision (hepatic metastasis), - chemotherapy, - targeted therapy (e.g., sunitinib, everolimus), - radiometabolic therapy (^{177}Lu-DOTATATE)
Primary hyperparathyroidism	- Blood calcium, phosphate, 25-hydroxy vitamin D, parathyroid hormone - Urinary calcium	Imaging: -Morphological: Cervical US and CT -Functional: ^{99m}Tc-MIBI scintigraphy, F-choline PET	Surgical excision using minimally invasive cervical surgery
Pituitary adenoma	Plasma hormones: cortisol and ACTH at 8 am, 4 pm, 12 am; IGF-1, LH, FSH, estradiol (women); testosterone, SHBG (men); prolactin, TSH, FT4 Dynamic test according to results mainly - 8 am cortisol measurement after 1 mg dexamethasone test at 12 am (if suspicion of hypercortisolism) - OGTT with GH measurement in case of acromegaly suspicion - Intravenous insulin test with GH and cortisol measurement in case of suspicion of hypopituitarism (if no cardiac or neurological impairment)	Imaging: -Morphological: Pituitary MRI -Neuro-ophthalmological examination: e.g., visual fields, Lancaster test	- Somatostatin analogue or dopamine antagonist - Transsphenoidal surgical excision

CT, computed tomography scan; MRI, magnetic resonance imaging; ^{18}FDG, ^{18}Fluorodeoxyglucose; ^{18}F-DOPA, ^{18}Fluoro-dihydroxyphenylalanine; ^{123}I-MIBG, ^{123}I-meta-iodobenzylguanidine; ^{68}Ga-SSA, ^{68}Ga-somatostatin analogues; PCC, pheochromocytoma; VIP, vasoactive intestinal polypeptide; 5-HIAA, 5-hydroxyindolacetic acid; PPI, proton pump inhibitors; ^{177}Lu-DOTATATE, lutetium (^{177}Lu) oxodotreotide; US, ultrasound; ^{99m}Tc-MIBI, Technetium (^{99m}Tc) sestamibi; ACTH, adrenocorticotropic hormone; IGF-1, insulin-like growth factor 1; LH, luteinizing hormone; FSH, follicle-stimulating hormone; SHBG, sex hormone-binding globulin; TSH, thyroid-stimulating hormone; FT4, free thyroxine; GH, growth hormone; OGTT, oral glucose tolerance test.

predominant secretion of noradrenaline (35). Predominant production of dopamine is rare, preferentially encountered in head and neck paragangliomas or in malignant PPGLs (36). Some paragangliomas, especially localized in the head and neck, can also be non-secreting.

NF1

NF1-associated PPGL prevalence varies from 2.9 to 14.6%, with no clear genotype-phenotype association with PPGL risk (37–42). Indeed, in NF1 patients diagnosed with PPGL, the mutational spectrum comprises both intragenic mutations and deletions, with mutations being preferentially located in the cysteine-rich region of the NF1 protein over the RAS-GAP domain (43). The median age at diagnosis is around 40–45 years, which is older than in other genetically-determined PPGLs (44). Most PPGLs are unilateral pheochromocytomas (75%) but bilateral tumors are not rare (up to 17% of cases) and are synchronous in 20 to 40% of cases (38). Paragangliomas are infrequent. In rare cases, mixed tumors can be observed with a ganglioneuroma/ganglioneuroblastoma contingent (45). Gangliocytic paragangliomas can also been observed in ~5% of NF1 patients (46, 47). The catecholamine secretion profile is adrenergic. PPGL tumor size in NF1 (median size 5.8 cm, range 0.8–20 cm) is roughly the same as in sporadic cases. Functional imaging, which is used to investigate bilateral pheochromocytomas and/or paragangliomas and/or metastatic extension, is based on ^{18}F-DOPA PET-CT; second choices include ^{123}I-MIBG scintigraphy or ^{68}Ga-SSA PET-CT (48).

VHL

PPGL, which defines type 2 VHL, is observed in 20–30% of patients (49–51). The youngest patient diagnosed was 4 years old, and the median age at diagnosis is 25–30 years (52). VHL-associated PPGL are mostly pheochromocytomas; paragangliomas account for only 10 to 20% of these chromaffin tumors. The malignancy potential is lower than in sporadic cases, about 5% vs. 10–17% (53). One-third to one-half of patients with PPGLs have synchronous bilateral pheochromocytomas. The median tumor size is smaller than in the sporadic forms, about 30 mm, and this is possibly related to abdominal screening, which allows early diagnosis (49). Accordingly, the release of catecholamines and the prevalence of associated symptoms and hypertension are lower compared

with the sporadic forms (16–55% and 8–46%). VHL-associated PPGL exhibit a specific secretion profile, which is almost exclusively noradrenergic. The absence of adrenaline secretion is due to the epigenetic silencing of phenylethanolamine N-methyltransferase, which catalyzes the production of adrenaline from noradrenaline (54). Functional imaging of PPGL can be performed with various radiopharmaceuticals, which are of particular interest because they can reveal multiple VHL-associated tumors. The recent European Nuclear Medicine Society guidelines prioritized these investigations and, as in NF1 patients, suggested ^{18}F-DOPA PET-CT as first-line imaging for exploring potential bilateral pheochromocytomas and/or extra-adrenal paragangliomas (48, 55). If not available or feasible, ^{123}I-MIBG scintigraphy or ^{68}Ga-SSA PET-CT can be used, with the latter preferred since it also demonstrates great diagnostic performance with regard to neuroendocrine tumors (56).

Treatment of Phakomatoses-Associated PPGLs

Resection of benign PPGLs should be considered in order to limit cardiovascular complications and prevent unexpected death, which can be triggered with the administration of certain drugs (53, 57–60). Of note is that rare bilateral pheochromocytomas have led to adrenal-sparing surgery (61–63). This allows selective removal of the pheochromocytoma and leaves a sufficient amount of adrenal cortex tissue for maintaining corticosteroid independence and avoiding steroid dependence and its associated comorbidities, i.e. increased mortality risk especially in young patients, and deterioration of quality of life (64, 65). The risk is recurrence of the tumor or the occurrence of acute adrenal crisis in case of stress. Procedures can be performed by an open or preferentially laparoscopic approach, at least for lesions < 50 mm, while larger lesions should be removed by total adrenalectomy (66). Preoperative measures have to be taken, especially the introduction/optimization of anti-hypertensive drugs, in order to limit perioperative-associated morbidity and mortality (67).

Few data are currently available on adrenal-sparing surgery and NF1-associated PPGL, possibly because bilateral pheochromocytomas are present in a minority of patients. However, when performed, the procedure is safe and allows exogenous glucocorticoid-independence, with an estimated risk of recurrence between 0 and 10% (38, 68).

A greater number of studies have been dedicated to VHL-associated pheochromocytomas. One such study considered adrenal-sparing surgery in 26 VHL patients, none of whom developed metastatic pheochromocytoma; 11% exhibited local recurrence that could be treated with a second surgical procedure or active surveillance, 11% presented contralateral pheochromocytoma, and finally 11% became steroid-dependent (69). Similar results were published by an international consortium that compared morbidity and mortality among patients with bilateral pheochromocytomas undergoing total or cortical-sparing adrenal surgery. Of the 184 VHL patients included, 56% had bilateral synchronous pheochromocytomas. Cortical-sparing surgery was successful in 87% of procedures, with a 12% risk of ipsilateral recurrence (70). Sixty percent of VHL patients remained steroid-independent. Therefore, this procedure seems particularly recommended, when feasible, in VHL- and NF1-associated pheochromocytomas, and it can be performed in both adult and pediatric populations (71).

There are currently no specific recommendations for the management of rare cases of advanced/malignant VHL- or NF1-associated PPGL that currently do not differ from sporadic cases. Therapeutic options include locoregional therapies, radionuclide therapy and/or chemotherapy (72, 73). Targeted therapies such as sunitinib have been shown to induce a response in a VHL patient with malignant PPGL (74).

Screening and Follow-up of NF1 and VHL-Associated PPGLs

NF1

There are currently no recommendations for systematic screening of PPGL in NF1 patients in childhood, and experts suggest that investigations for PPGL must be done when there is an increase in heart rate and/or blood pressure (**Figure 4**) (75). Likewise, adult guidelines suggest that PPGL should be considered in hypertensive NF1 patients who are over 30 years old, pregnant and/or have catecholamine-related symptoms (76–79). Blood pressure should be evaluated at least annually, but systematic biochemical or morphological PPGL screening in asymptomatic patients with NF1 is not recommended under the current guidelines. Nevertheless, some studies suggest that only consider screening hypertensive patients would fail to recognize the majority of NF1-associated PPGL (80). Furthermore, prospective morphological and biochemical screening in a French series of 156 NF1 patients found a pheochromocytoma prevalence of 7.7% (12 patients), half (n = 6) of whom were secreting, and with only two of them symptomatic (81). This study and others showing the positive impact of genetic testing on the management and outcome of patients with paraganglioma-pheochromocytoma, and the poor prognosis of PPGL during pregnancy suggest that despite current recommendations, a screening for PPGL, at least before pregnancy, would improve the prognosis of these patients (82–85).

VHL

Current Danish and American guidelines as well as French recommendations suggest starting follow-up of VHL patients at a median age of 5 years old, with an annual measurement of plasma or urine metanephrine (**Figure 4**) (86–88). Monitoring of non-invasive imaging can be performed annually from the age of 8 years, initially by ultrasound used first alone, and then alternatively with MRI after the age of 16 years. French guidelines differ slightly and recommend starting abdominal ultrasound at the age of 5 years and the first MRI at 18 years. Functional imaging is useful only when pheochromocytoma is suspected, and it is currently not recommended to repeat it in

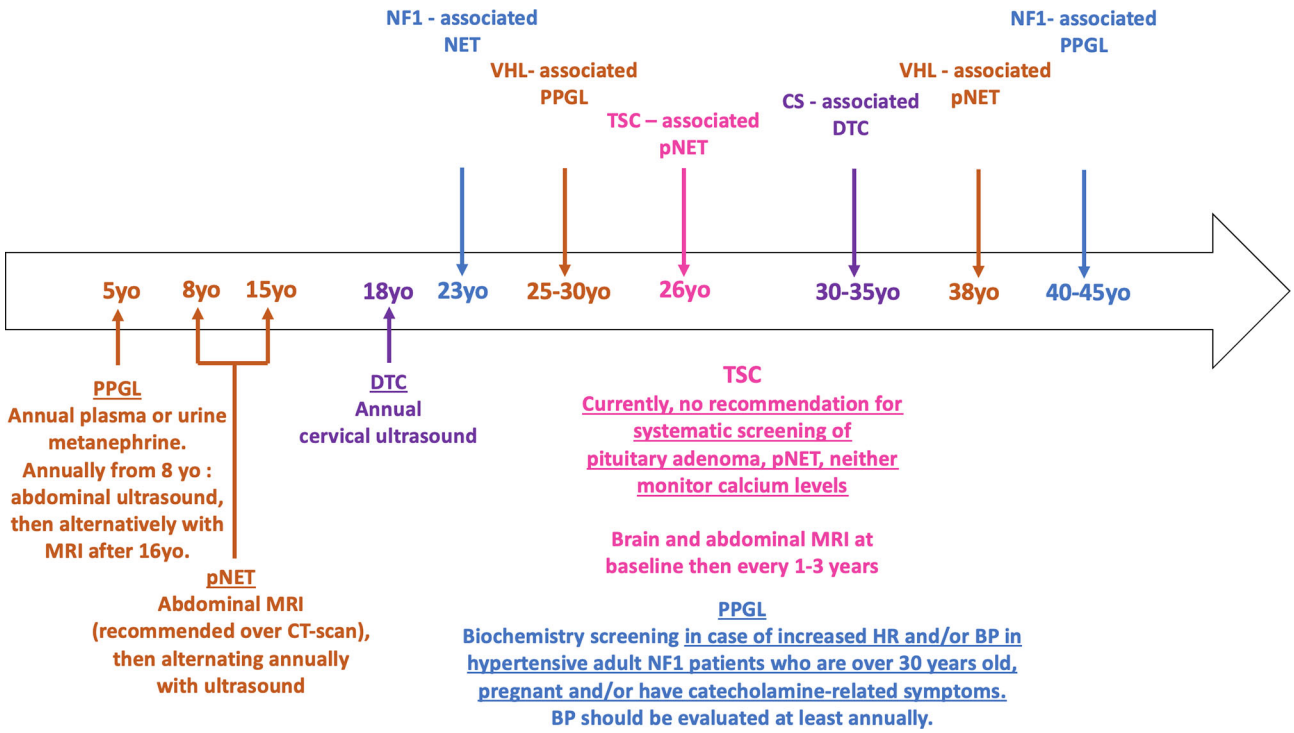

FIGURE 4 | Timeline of phakomatoses-associated endocrine tumors and follow up strategy. The median age of onset of phakomatoses-associated endocrine tumors is shown in the arrow. The various follow up guidelines according to the syndromic presentation are shown below the arrow. **Brown** = VHL; **purple** = CS; **fuchsia** = TSC; **blue** = NF1. HR, heart rate; BP, blood pressure; pNET, pancreatic neuroendocrine tumor; PPGL, pheochromocytoma/paraganglioma; DTC, differentiated thyroid cancer.

asymptomatic patients. Particular attention should be paid to screening before pregnancy.

DIGESTIVE NEUROENDOCRINE NEOPLASMS IN PHAKOMATOSES

Neuroendocrine neoplasms are rare tumors that arise from neuroendocrine cells distributed throughout the entire body (89, 90). Those cells are derived from the embryonic gut (foregut, midgut, hindgut) and can be found in various locations, mainly in the digestive and thoracic regions, with various differentiation and hormonal secretion. Tumor aggressiveness can be assessed according to the WHO grade (grade 1 to 3) based on proliferation index values (Ki-67 and/or mitotic count) (91). Neuroendocrine neoplasms of the gastrointestinal tract comprise neuroendocrine tumors (NETs) and neuroendocrine carcinomas (NECs). Of note, the 2019 WHO classification has modified the cut-off used for the Ki-67 proliferative index to distinguish grade 1 from grade 2 NETs (Ki-67 above or below 3%), emphasized the distinction between grade 3 NETs (low-grade NETs with a high proliferative rate and Ki-67 above 20%) and NECs which are all high grades poorly differentiated aggressive neoplasms (92). Phakomatoses are mainly associated to NETs, which are well differentiated and progress slowly (most of them grade 1) in 85% of cases (93), even if they can be complicated with metastases. Even in metastatic conditions, the median overall survival is typically 5–10 years relative to the location and histological grade in well-differentiated NETs (94–96). In 15% of cases, a functional syndrome (FS) (hypoglycemia, recurrent gastric ulcers, necrolytic migrating erythema) is present, which is related to hormone production (e.g. insulin, gastrin, glucagon). About 4–5% of gastroenteropancreatic tumors arise in the context of an inherited tumor syndrome (mainly MEN1 but also phacomatosis), especially VHL, whereas the incidence of NET is lower in NF1 and TSC. Young age at diagnosis, multiple tumors in multiple organs, and familial history are clinically suggestive of the diagnosis. Neuroendocrine neoplasms in the context of phakomatoses are almost always well-differentiated neuroendocrine tumors. Except in VHL and NF1, tumors themselves do not show specific pathological features (97).

NF1

NF1-associated NETs are rare, and their prevalence is unknown. Most NF1-associated digestive NETs are located on the ampulla of Vater, followed by the duodenum and pancreas (98–100). The youngest published case was diagnosed at 23 years old and the median age at diagnosis is 48 years, which is 15 years younger than in the general population (94, 101). In a series of 58 NF1-

associated NET cases, about 25% (14 cases) were marked with somatostatin antibodies on immunohistochemistry, but only 28% of the patients presented symptoms related to the hormone secretion, i.e. diabetes mellitus, diarrhea, gallstones, and less frequently dyspepsia and hypochlorhydria (102). Gastrinomas and insulinomas have also been observed (103, 104). In NF1, NETs are mostly well-differentiated, rarely multifocal, and can have specific pathological features such as a deceptive tubular/tubuloglandular appearance that can mimic adenocarcinoma. Metastases are present at diagnosis in 14% of reported patients. Specific survival data is not available yet. In a review of 76 published cases, 9% of patients died of NET progression; however, follow-up was short (median 31 months), and the grade as well as median overall survival were unknown. The standard differential diagnosis is gastrointestinal stromal tumors (GISTs), which can also be observed in NF1 patients (105). In this context, the tumors are preferentially located in the ileum/jejunum versus the stomach as in sporadic forms, and most NF1-associated GISTs have a favorable clinical course (106).

VHL

The VHL pancreatic lesions include solid NETs and cystic lesions. Cystic lesions (simple cysts and serous cystadenomas) are generally asymptomatic and do not require any treatment. They must be differentiated from other cystic tumors that have malignant potential, such as intraductal papillary mucin-producing tumors or mucinous cystic tumors. VHL pancreatic neuroendocrine tumors (pNETs) occur in 11–17% of cases and are frequently multifocal (40%) (107–109). In VHL patients, pNETs present with a characteristic microscopic appearance, with finely vacuolated cytoplasm and lipid-rich cells. Patients with missense mutations (type 2 VHL) rather than truncating mutations or large deletions (type 1 VHL) exhibit a higher prevalence of pNETs, with a hotspot on codons 161/67 in exon 3, which could be associated with a higher risk of metastases although the data are discordant (110, 111). Preferential association with PPGL is also discussed (107, 112). The mean age at diagnosis is 35–38 years; not surprisingly and because VHL does not seem to be involved in hormonal secretion, most patients are asymptomatic with nonfunctional tumors. However, ectopic secretion of ACTH with paraneoplastic Cushing syndrome is possible (113). The pathogenesis of VHL pNETs differ from that of MEN1 or sporadic pNETs notably because of:

- upregulation of genes related to hypoxia-inducible factor molecules, angiogenesis, epithelial mesenchymal transition and/or metastasis, cell cycle and growth factors and receptors (114),
- and hypomethylated CpGs, significantly more common in VHL-related versus sporadic and MEN1-related NETs (115).

The presence of local invasion or locoregional/distant metastasis varies between 7.5 and 12.8%; it reaches 20%, however, for the metastatic forms in the largest cohort, which is lower than in other genetic predisposition syndromes or in sporadic forms (112, 116–118). Metastasis is generally associated with pNETs larger than 28 mm, with a doubling time of 22 months vs. 126 months in non-metastatic lesions (111). Morphological investigations of VHL-associated pNETs do not differ from the management of sporadic forms. In the context of VHL, the differential diagnoses of pNETs include serous cystadenoma or metastatic renal cancer lesions (107). Simple cysts are also frequent (up to 75%), whereas cystic aspects of pNET are uncommon (119). Measurement of plasma chromogranin A can be of interest although there are several limitations of this assay, notably the false-positive results due to hypersecretion of gastrin, which is encountered, among other causes, in case of proton pump inhibitor use, or chronic kidney disease that can be associated with VHL (120). Nuclear medicine imaging recommends ^{68}Ga-SSA PET-CT as a first-line investigation, or ^{18}FDG PET-CT in more aggressive pNET cases (48). ^{18}F-DOPA PET-CT is not useful in this context (55). The progression of pNET lesion size is not linear and may include periods of stability or even apparent decrease in size on imaging (121).

pNET-related mortality is not well documented in VHL patients. In two studies focusing on patients presenting with pNETs, tumor-associated mortality was estimated between 6.9 and 9.5%. However, death was associated with pNETs in 29 to 50% of VHL patients (108, 111). Ten-year overall survival is estimated at 50% in non-operated patients with a tumor size greater than 2.8 cm and rises to 94% in operated patients presenting with a pNET size less than 1.5 cm. No correlation was identified between VHL genotype and mortality.

TSC

The link between TSC and digestive NETs, especially pancreatic, is recognized because of the pathogenic role of the mTOR pathway in the development of NETs (122). However, the onset of those tumors in TSC remains low, with an estimated incidence of 1%, which can question the causal relation between these two conditions. Nevertheless, since the availability of medical treatment such as everolimus, their incidence could increase with the morphological follow-up of kidney lesions. Genetic data, available only in a small proportion of reported patients, revealed *TSC2* mutations, most of them in or just upstream of the GTPase-activating protein (GAP) domain (exons 33–36) (123). *TSC1* mutations can also be found, however to a lesser extent (124). The largest study focusing on pNETs in TSC patients (n = 18) found an average age of 26 years at diagnosis, significantly younger than in the sporadic cases; so, development in pediatric age or in young adults should be emphasized (123). pNETs were functional in 44% of patients, mostly due to insulin secretion resulting in hypoglycemia (125). The diagnosis can be challenging because of neurological features in TSC patients with seizures; the seizures may be attributed to neurological lesions, while they are indeed related to underrecognized insulinoma-related hypoglycemia, especially in those patients with intellectual disability. The mean pNET size of 5.1 cm was slightly higher than in sporadic cases, with a cystic aspect in one-third of patients without any multifocality, which is in contrast with other genetic NET predisposition syndromes (126). The proportion of

synchronous metastasis was 13%, which is lower than in sporadic cases. The progression and specific associated mortality are unknown. Finally other locations such as rectal NET have also been described (127).

Treatment of Phakomatoses-Associated Digestive NETs

Treatment of NETs includes the management of tumor volume but also, when present, of the functional syndrome. The risk of resection must always be weighed with the risk of diabetes, especially in case of multiple tumors.

Functional Syndrome

Treatment of the functional syndrome does not differ from that of sporadic tumors, and we will only consider the most frequent secretions. The functional syndrome can be cured with surgical resection of the NET. However, while awaiting surgery and/or in advanced disease, medical treatment can be initiated in order to limit symptoms that may be life-threatening (128). In case of NF1-associated somatostatin-related symptoms, management is not well defined and can include treatment of diabetes, cholecystectomy, and pancreatic enzyme supplementation. Surprisingly, in a few cases the administration of somatostatin analogues can lead to clinical improvement (128–130), although careful monitoring is needed because hypoglycemia may worsen in some patients (131). Insulinoma-induced hypoglycemia can be reversed with small frequent meals and diazoxide. In malignant insulinoma, everolimus and sunitinib as well as pasireotide have been shown to improve glucose levels (132–134).

Antitumor Treatment of NETs

NF1

Treatment of NF1-associated NETs does not differ from the management of sporadic cases, whether or not they are metastatic. Treatment of localized NETs is based on tumor resection, which can be performed endoscopically or surgically according to NET location, size and pathological characteristics (128, 135, 136). In metastatic tumors, MEK inhibitors (selumetinib, trametinib) have shown great benefit in NF1 patients because they inhibit the MAP kinase pathway, which is overactivated due to *NF1* mutation. Indeed, a decrease in the size of low-grade gliomas and plexiform neurofibromas has been reported (137–141). However, there is currently no data in NF1-associated NET patients.

VHL

Treatment of VHL-associated NETs does not differ from the management of sporadic cases. Given the relatively low risk of malignancy and the high frequency of asymptomatic forms, VHL-associated pNETs should not be removed if less than 15 mm in size and slowly progressing at the regular follow-up, with the rare exception of symptomatic forms (142). In case of non-distant metastatic forms, surgery should be considered for tumors with any of the following characteristics: 1) > 2 cm in the head of the pancreas, 2) > 3 cm in the body/tail of the pancreas, 3) doubling time < 500 days, or 4) in case of metastatic locoregional lymph nodes (143, 144). The recommended surgical procedures are enucleation or pancreaticoduodenectomy for pNETs in the pancreatic head relative to the position from the pancreatic duct (145). The risk of this last surgery is associated with a non-negligible morbidity-mortality rate of about 5%, which is much higher than for pancreatic body/tail pNETs in which enucleation or distal or central pancreatectomy should be performed if possible per laparoscopy. Consequently, total pancreatectomy should be discussed only in the very rare cases of symptomatic multifocal pancreatic tumors that cannot be safely enucleated. Post-pancreatectomy diabetes is a classical complication encountered at 10 years in up to 16% of patients after pancreaticoduodenectomy and in 35% after distal pancreatectomy; therefore, physicians and patients should be aware of this risk before validating surgical indication and educate patients to avoid weight gain (146, 147). Islet autotransplantation, now reimbursed through health insurance in France, could be an interesting option for limiting diabetes-associated morbidity; the procedure carries the risk of tumor occurrence in these genetically-determined diseases, although interesting results have been observed in pancreatic adenocarcinoma in an animal model (148, 149).

There is no difference in medical management between VHL-associated and sporadic metastatic pNETs, although antiangiogenic agents have been especially studied because of the specific deregulated angiogenesis mechanism of the disease (128). Nevertheless, there is not yet a direct comparison between VHL-associated and sporadic forms that evaluates the relative efficacy of these drugs. Sunitinib is approved for the management of pNETs and has shown stability in 5 out of 7 cases of VHL-associated pNETs (150, 151). Another study using multiple antiangiogenic treatments (sunitinib, sorafenib, axitinib, pazopanib) showed a partial response in 4 of the 15 VHL patients with cystic or solid pancreatic tumors (152). In a phase 2 trial, 53% of VHL pancreatic lesions responded to pazopanib (anti-VEGFR 1-3, anti-PDGFR α-β, c-KIT), but most of them were serous cystadenomas (153). Interestingly, pazopanib was also shown to reduce the size of renal lesions and hemangioblastomas.

Since the 2010s, specific HIF2-α inhibitors, which showed great benefits in sporadic clear cell renal cell carcinoma in phase1-2 clinical trials, have been undergoing evaluation alone or in combination with immunotherapy and/or antiangiogenic drugs (154). A phase 2 study using the HIF2-α inhibitor MK-6482 in 61 VHL patients with clear cell renal carcinoma and pNETs showed an objective response rate in 64% of pNET cases, with 4 complete responses. The data are not mature yet, but the 12-month progression-free survival rate was 98.3% (155). Therefore, HIF2-α inhibitors could offer promising prospects for VHL metastatic pNETs or even malignant PPGL.

TSC

The management does not differ from the sporadic forms, neither in localized or metastatic disease (128, 156). In advanced disease, mTOR inhibitors such as everolimus, which is used in all NET locations (as second-line treatment), could be of particular interest in TSC patients; however, no studies to date have demonstrated specific efficacy in those patients, except for one case with metastatic pNET and a *TSC2* germline mutation that showed partial response

shortly after the introduction of everolimus. Support for this hypothesis may be found in the results of the EXIST trials using everolimus in other features of TSC, with morphological responses observed in renal angiomyolipoma, subependymal giant cell astrocytomas and cutaneous nodules (157, 158).

Screening and Follow up of Phakomatoses-Associated Digestive NETs

NF1

Due to their rarity, there are currently no follow-up recommendations regarding digestive NETs in NF1 patients, and in particular no recommendations to perform and repeat abdominal imaging or endoscopy in asymptomatic patients (**Figure 4**) (76, 77). Nevertheless, visualization of the pancreas is suggested for morphological investigation of neurofibromas, pheochromocytomas, or GISTs.

VHL

In VHL patients, current surveillance guidelines regarding pNETs and more largely pancreatic lesions suggest first abdominal imaging between 8 and 15 years of age (**Figure 4**) (86, 87). MRI is recommended over CT scan to limit the consequences of repeated ionizing radiation exposure (159). Due to the non-functional characteristic of most pNETs, there is no indication for systematic biological follow-up.

TSC

Finally, there are currently no follow-up recommendations regarding digestive NETs in TSC patients; however, required abdominal imaging for the follow-up of renal angiomyolipoma enables simultaneous visualization of the pancreas and could detect non-functional pNETs at an early stage (**Figure 4**) (160).

PRIMARY HYPERPARATHYROIDISM

NF1

A few cases of primary hyperparathyroidism occurring in NF1 patients have been published (161). The clinical presentation does not differ from that of sporadic cases, and, notably, the diagnosis is not made at a younger age in NF1 patients. Primary hyperparathyroidism is usually associated with a single adenoma, except for few cases of parathyroid carcinoma (162, 163) (**Table 6**). No recurrence has been observed after surgery. Therefore, a causal relationship between hyperparathyroidism and NF1 cannot be assumed.

TABLE 6 | Endocrine tumors and phakomatoses specificities.

	NF1	VHL	TSC
Pheochromocytoma/ Paraglanglioma	Median age 40–45 years	Median age 25–30 years	
	Bilateral in 75% of cases, synchronous in 20% of cases	Bilateral in 15–40% of cases	
	Malignant forms in 10% of cases	Malignant forms in 5% of cases	
	Might be asymptomatic, which does not prevent adrenal crisis		
Gastrointestinal neuroendocrine tumors	Median age 48 years		Median age 26 years
	Location: ampulla of Vater > duodenum > pancreas	Location: pancreas	Location: pancreas
	Secretion: somatostatin (7% of cases), gastrin (5%), insulin (3%)	Multifocal in 40% of cases	Secretion: 40% of cases, mostly insulin
	Metastasis in 14% of cases	Metastasis in 15–20% of cases; malignancy associated with tumor diameter above 28 mm	Synchronous metastasis in 13% of cases
	Treatment does not differ. In metastatic forms, possibility of using targeted therapy (e.g., MEK inhibitors)	Surgical treatment for localized forms (enucleation, pancreaticoduodenectomy). Treatment of metastatic forms does not differ from sporadic tumors, possibility of using targeted therapy (e.g., MEK inhibitors, antiangiogenic agents)	
Primary hyperparathyroidism	9 cases of single adenoma, 1 case of carcinoma, 1 case of multiple adenomas		Only a few cases
	Median age 52 years		Median age 20 years
Pituitary adenoma	20 cases of excess GH, including 15 patients associated with sporadic optic pathway glioma		Rarely associated Secreting (GH, ACTH) or nonfunctional
	Median age 13 years		Median age 35 years

NF1, neurofibromatosis type 1; VHL, von Hippel-Lindau disease; TSC, tuberous sclerosis complex; GH, growth hormone; ACTH, adrenocorticotropic hormone.

TSC

A few cases of parathyroid adenomas have been described in young TSC patients. The occurrence before 20 years of age argues for a causal role of the *TSC* mutation (23, 164). However, recent advances in understanding the biology and pathogenesis of parathyroid adenomas do not seem to involve the mTOR pathway (165). Furthermore, primary hyperparathyroidism is considered the second most common endocrinopathy after diabetes mellitus (166), raising the hypothesis of a coincidental occurrence. However, TSC mutations could also lead to parathyroid adenoma development in an mTOR-independent pathway. In the literature, TSC patients with primary hyperparathyroidism presented symptoms related to hypercalcemia, with one parathyroid lesion at most.

Management

There are no specific recommendations for surgery and management of hyperparathyroidism in phakomatoses.

Screening and Follow up of Phakomatoses-Associated-Primary Hyperparathyroidism

There are currently no recommendations for monitoring calcium levels during the follow-up of NF1 or TSC patients (**Figure 4**).

PITUITARY ADENOMAS

NF1

Pituitary adenomas are rarely reported in NF1 patients, although these genetic mutations are known to predispose patients to this condition (**Table 6**) (167–170). Excess growth hormone (GH) has been observed, notably in patients with central precocious puberty, but it seems to be associated with optic pathway tumors (OPT) rather than pituitary somatotroph adenomas (171, 172). Although the mechanism underlying excess GH in NF1 is still unknown, a loss of somatostatinergic inhibition from OPTs with dysregulation of GH secretion is suspected, particularly in tumors close to the hypothalamic and pituitary regions.

TSC

The association between TSC and pituitary adenomas is still debated. In preclinical models of TSC, such as in an Eker rat with *TSC2* germline mutations, pituitary adenomas were observed in 40–60% of cases, and this was associated with premature death attributed to pituitary hemorrhage (173, 174). However, pituitary adenoma in human TSC patients have rarely been reported (23, 175). As TSC surveillance guidelines suggest repeating a brain MRI every 1 to 3 years because of the risk of astrocytoma, it is unlikely that pituitary adenomas are underdiagnosed (160). When diagnosed, TSC-associated pituitary adenomas are secreting (GH, ACTH) or non-functional tumors, and patients are diagnosed at a relatively young age, before 35 years, compared with sporadic cases.

Management

There is no rationale for managing phakomatoses and especially TSC-associated pituitary adenomas differently from sporadic cases. It should be noted that in *in vitro* situations, everolimus can lead to a significant decrease in cell viability in TSC; however, no human data are currently available (175).

Screening and Follow up of Phakomatoses-Associated-Pituitary Adenoma

There are currently no recommendations for screening of pituitary adenomas in asymptomatic NF1 or TSC patients (**Figure 4**).

THYROID TUMORS

Among cases of phakomatoses, thyroid cancer prevalence is increased in Cowden syndrome. Nevertheless, clinical cases have been reported in NF1.

NF1

The presence of thyroid disease in NF1 may be linked to different mechanisms including autoimmune thyroiditis, metastasis of another cancer, thyroid neurofibromas, and thyroid cancer. The latter is consistent with knowledge that somatic NF1 mutations have been identified in differentiated and anaplastic thyroid carcinoma (176, 177). In exceptional conditions, it can also be favored by GH secretion from pituitary somatotroph adenomas (168). A population-based study estimated the relative risk of NF1 patients developing thyroid cancer to be 4.9 (178). However, only a few cases have been reported in the literature, so a coincidental association cannot be excluded. Different types of thyroid tumors have been reported, such as well-differentiated papillary cancer or medullary thyroid cancer (179–182). Pathologists must be aware of the presence of NF1 because cancer should not be confused with rare intrathyroid neurofibroma (183, 184). Clinical presentation, notably age at diagnosis, does not seem to differ from the usual presentation. Differentiated thyroid cancer can be found through focal hypermetabolism on ^{18}FDG PET-CT that is initially performed to distinguish between neurofibromas and malignant peripheral nerve sheath tumors (185, 186).

Cowden Syndrome

There is a clear molecular rationale linking Cowden syndrome (CS) and differentiated thyroid cancer because mutations resulting in PI3K/Akt pathway activation are known to be involved in thyroid carcinogenesis and cancer progression (176, 187). The diagnosis can be made during childhood or adolescence in 15% of patients, and the majority of CS patients are diagnosed with thyroid cancer before the age of 40 years. The main histological subtypes are papillary carcinoma (classical

and follicular variants) and follicular carcinoma, with a potentially higher prevalence of the latter compared with sporadic forms (14–45% vs. 2%) (188–190). These cancers are often associated with specific pathological features such as multiple adenomatous nodules in the context of lymphocytic thyroiditis (190).

Management

Management of thyroid cancer in NF1 and CS does not differ from that of sporadic cases and includes surgery with or without complementary iodine treatment (191). There is no increased risk of lymph node extension, so systematic lymph node dissection is not recommended and depends on pre-operative ultrasound findings in individual patients. Since a significant proportion of patients with CS also develop nonmalignant thyroid diseases, some authors have suggested prophylactic thyroidectomy (192, 193). However, this procedure is not recommended given the good prognosis of CS-associated thyroid cancer, similar to that of sporadic cases. Recently, a pilot study investigating the benefits of sirolimus, an mTOR inhibitor, in patients with germline *PTEN* mutation demonstrated improvement in skin and gastrointestinal lesions, but there are no data focusing on thyroid cancer (194).

Screening and Follow up of Phakomatoses-Associated Thyroid Cancer

The European guidelines for CS follow-up suggest an systematic surveillance for thyroid cancer by cervical spine ultrasound (**Figure 4**) (195). An annual investigation starting at 18 years of age is proposed, although the levels of evidence supporting those modalities are moderate and some authors suggest beginning surveillance at 10 years of age (196). Indeed, systematic annual ultrasound monitoring could lead to overdiagnosis and excessive thyroidectomy, therefore follow up frequency could be modified based on the first cervical screening results.

There are currently no recommendations for screening of thyroid cancer in asymptomatic NF1 patients.

CONCLUSIONS

Phacomatoses are a group of rare diseases that can be associated with neoplasia of the endocrine glands. Clinicians must be aware of these features. The main tumors are PPGL and digestive, especially pancreatic neuroendocrine tumors. They can occur at a younger age compared with sporadic cases and are more frequently multiple. Usually benign, they can, however, be aggressive, and surveillance guidelines are available for detecting tumors at early stages and limiting associated morbidity and mortality, especially in VHL. Screening for catecholamine secretion in NF1 appears beneficial according to recent data, since these frequently asymptomatic but life-threatening tumors pose a high risk for cardiovascular morbidity and mortality and have a poor maternal-fetal prognosis in case of pregnancy. All secreting pheochromocytomas should be operated, but parenchyma-sparing surgery must be favored to avoid complete adrenal insufficiency in selected cases with bilateral pheochromocytomas. Management of pancreatic NET depends on the size, number, secretion, aggressiveness (Ki-67) and extra-pancreatic extension of the lesions. The treatment (including surveillance) must be discussed in order to limit surgical risk and post-pancreatectomy diabetes. In advanced/metastatic diseases, besides standard treatments, specific therapies that target the underlying genetic abnormality are under investigation. Importantly, those rare patients should be managed and followed by specialized and multidisciplinary teams and networks to weigh the benefit-risk ratio of each therapeutic strategy.

AUTHOR CONTRIBUTIONS

BC and HD wrote the manuscript and are co first authors. AJ, ML, CD, CC-B, and SE contributed to the enrichment and the editing of the manuscript by their comments and remarks. MV supervised the work, wrote and edited the manuscript. All authors contributed to the article and approved the submitted version.

REFERENCES

1. Huson SM, Korf BR. Chapter 121 - The Phakomatoses. In: D Rimoin, R Pyeritz and B Korf, editors. *Emery and Rimoin's Principles and Practice of Medical Genetics*. Oxford: Academic Press (2008). p. 1–45. doi: 10.1016/B978-0-12-383834-6.00128-2
2. Hoxhaj G, Manning BD. The PI3K–AKT Network At the Interface of Oncogenic Signalling and Cancer Metabolism. *Nat Rev Cancer* (2020) 20:74–88. doi: 10.1038/s41568-019-0216-7
3. Gimple RC, Wang X. RAS: Striking At the Core of the Oncogenic Circuitry. *Front Oncol* (2019) 9:965. doi: 10.3389/fonc.2019.00965
4. Simanshu DK, Nissley DV, McCormick F. RAS Proteins and Their Regulators in Human Disease. *Cell* (2017) 170:17–33. doi: 10.1016/j.cell.2017.06.009
5. Saxton RA, Sabatini DM. TOR Signaling in Growth, Metabolism, and Disease. *Cell* (2017) 168:960–76. doi: 10.1016/j.cell.2017.02.004
6. Inoki K, Corradetti MN, Guan K-L. Dysregulation of the TSC-mTOR Pathway in Human Disease. *Nat Genet* (2005) 37:6. doi: 10.1038/ng1494
7. Gutmann DH, Wood DL, Collins FS. Identification of the Neurofibromatosis Type 1 Gene Product. *Proc Natl Acad Sci* (1991) 88:9658–62. doi: 10.1073/pnas.88.21.9658
8. Dasgupta B, Yi Y, Chen DY, Weber JD, Gutmann DH. Proteomic Analysis Reveals Hyperactivation of the Mammalian Target of Rapamycin Pathway in Neurofibromatosis 1–Associated Human and Mouse Brain Tumors. *Cancer Res* (2005) 65:2755–60. doi: 10.1158/0008-5472.CAN-04-4058
9. Johannessen CM, Reczek EE, James MF, Brems H, Legius E, Cichowski K. The NF1 Tumor Suppressor Critically Regulates TSC2 and Mtor. *PNAS* (2005) 102:8573–8. doi: 10.1073/pnas.0503224102
10. Lonser RR, Glenn GM, Walther M, Chew EY, Libutti SK, Linehan WM, et al. Von Hippel-Lindau Disease. *Lancet* (2003) 361:2059–67. doi: 10.1016/S0140-6736(03)13643-4
11. Latif F, Tory K, Gnarra J, Yao M, Duh FM, Orcutt ML, et al. Identification of the Von Hippel-Lindau Disease Tumor Suppressor Gene. *Science* (1993) 260:1317–20. doi: 10.1126/science.8493574
12. Gossage L, Eisen T, Maher ER. VHL, the Story of a Tumour Suppressor Gene. *Nat Rev Cancer* (2015) 15:55–64. doi: 10.1038/nrc3844
13. Richard S, Gardie B, Couvé S, Gad S. Von Hippel–Lindau: How a Rare Disease Illuminates Cancer Biology. *Semin Cancer Biol* (2013) 23:26–37. doi: 10.1016/j.semcancer.2012.05.005
14. The European Chromosome 16 Tuberous Sclerosis Consortium. Identification and Characterization of the Tuberous Sclerosis Gene on

Chromosome 16. *Cell* (1993) 75:1305–15. doi: 10.1016/0092-8674(93)90618-Z
15. Kandt RS, Haines JL, Smith M, Northrup H, Gardner RJM, Short MP, et al. Linkage of an Important Gene Locus for Tuberous Sclerosis to a Chromosome 16 Marker for Polycystic Kidney Disease. *Nat Genet* (1992) 2:37–41. doi: 10.1038/ng0992-37
16. Liaw D, Marsh DJ, Li J, Dahia PLM, Wang SI, Zheng Z, et al. Germline Mutations of the PTEN Gene in Cowden Disease, an Inherited Breast and Thyroid Cancer Syndrome. *Nat Genet* (1997) 16:64–7. doi: 10.1038/ng0597-64
17. Gutmann DH, Ferner RE, Listernick RH, Korf BR, Wolters PL, Johnson KJ. Neurofibromatosis Type 1. *Nat Rev Dis Primers* (2017) 3:17004. doi: 10.1038/nrdp.2017.4
18. National Institutes of Health Consensus Development Conference, Neurofibromatosis: Conference Statement. *Arch Neurol* (1988) 45:575–8. doi: 10.1001/archneur.1988.00520290115023
19. Lodish MB, Stratakis CA. Endocrine Tumours in Neurofibromatosis Type 1, Tuberous Sclerosis and Related Syndromes. *Best Pract Res Clin Endocrinol Metab* (2010) 24:439–49. doi: 10.1016/j.beem.2010.02.002
20. Sgambati MT, Stolle C, Choyke PL, Walther MM, Zbar B, Linehan WM, et al. Mosaicism in Von Hippel–Lindau Disease: Lessons From Kindreds With Germline Mutations Identified in Offspring With Mosaic Parents. *Am J Hum Genet* (2000) 66:84–91. doi: 10.1086/302726
21. Coppin L, Plouvier P, Crépin M, Jourdain A-S, Ait Yahya E, Richard S, et al. Optimization of Next-Generation Sequencing Technologies for Von Hippel Lindau (VHL) Mosaic Mutation Detection and Development of Confirmation Methods. *J Mol Diagn* (2019) 21:462–70. doi: 10.1016/j.jmoldx.2019.01.005
22. Northrup H, Krueger DA, Northrup H, Krueger DA, Roberds S, Smith K, et al. Tuberous Sclerosis Complex Diagnostic Criteria Update: Recommendations of the 2012 International Tuberous Sclerosis Complex Consensus Conference. *Pediatr Neurol* (2013) 49:243–54. doi: 10.1016/j.pediatrneurol.2013.08.001
23. Dworakowska D, Grossman AB. Are Neuroendocrine Tumours a Feature of Tuberous Sclerosis? A Systematic Review. *Endocr Relat Cancer* (2009) 16:45–58. doi: 10.1677/ERC-08-0142
24. Eng C. Will the Real Cowden Syndrome Please Stand Up: Revised Diagnostic Criteria. *J Med Genet* (2000) 37:828–30. doi: 10.1136/jmg.37.11.828
25. Ngeow J, Mester J, Rybicki LA, Ni Y, Milas M, Eng C. Incidence and Clinical Characteristics of Thyroid Cancer in Prospective Series of Individuals With Cowden and Cowden-Like Syndrome Characterized by Germline PTEN, SDH, or KLLN Alterations. *J Clin Endocrinol Metab* (2011) 12:E2063–71. doi: 10.1210/jc.2011-1616
26. Son EJ, Nosé V. Familial Follicular Cell-Derived Thyroid Carcinoma. *Front Endocrinol* (2012) 3:3–61. doi: 10.3389/fendo.2012.00061
27. Bubien V, Bonnet F, Brouste V, Hoppe S, Barouk-Simonet E, David A, et al. High Cumulative Risks of Cancer in Patients With *PTEN* Hamartoma Tumour Syndrome. *J Med Genet* (2013) 50:255–63. doi: 10.1136/jmedgenet-2012-101339
28. Szabo Yamashita T, Baky FJ, McKenzie TJ, Thompson GB, Farley DR, Lyden ML, et al. Occurrence and Natural History of Thyroid Cancer in Patients With Cowden Syndrome. *Eur Thyroid J* (2020) 9:243–6. doi: 10.1159/000506422
29. Alrezk R, Suarez A, Tena I, Pacak K. Update of Pheochromocytoma Syndromes: Genetics, Biochemical Evaluation, and Imaging. *Front Endocrinol* (2018) 9:515. doi: 10.3389/fendo.2018.00515
30. Crona J, Taïeb D, Pacak K. New Perspectives on Pheochromocytoma and Paraganglioma: Toward a Molecular Classification. *Endocr Rev* (2017) 38:489–515. doi: 10.1210/er.2017-00062
31. Hamidi O, Young WF, Iñiguez-Ariza NM, Kittah NE, Gruber L, Bancos C, et al. Malignant Pheochromocytoma and Paraganglioma: 272 Patients Over 55 Years. *J Clin Endocrinol Metab* (2017) 102:3296–305. doi: 10.1210/jc.2017-00992
32. Gimenez-Roqueplo A-P, Favier J, Rustin P, Rieubland C, Crespin M, Nau V, et al. Mutations in the SDHB Gene Are Associated With Extra-adrenal and/or Malignant Phaeochromocytomas. *Cancer Res* (2003) 63:5615–21.
33. Eisenhofer G, Klink B, Richter S, Lenders JW, Robledo M. Metabologenomics of Phaeochromocytoma and Paraganglioma: An Integrated Approach for Personalised Biochemical and Genetic Testing. *Clin Biochem Rev* (2017) 38:69–100.
34. Eisenhofer G, Lenders JW, Goldstein DS, Mannelli M, Csako G, Walther MM, et al. Pheochromocytoma Catecholamine Phenotypes and Prediction of Tumor Size and Location by Use of Plasma Free Metanephrines. *Clin Chem* (2005) 51:735–44. doi: 10.1373/clinchem.2004.045484
35. Kimura N, Miura Y, Nagatsu I, Nagura H. Catecholamine Synthesizing Enzymes in 70 Cases of Functioning and non-Functioning Phaeochromocytoma and Extra-Adrenal Paraganglioma. *Vichows Arch A Pathol Anat* (1992) 421:25–32. doi: 10.1007/BF01607135
36. Rao D, Peitzsch M, Prejbisz A, Hanus K, Fassnacht M, Beuschlein F, et al. Plasma Methoxytyramine: Clinical Utility With Metanephrines for Diagnosis of Pheochromocytoma and Paraganglioma. *Eur J Endocrinol* (2017) 177:103–13. doi: 10.1530/EJE-17-0077
37. Al-Sharefi A, Javaid U, Perros P, Ealing J, Truran P, Nag S, et al. Clinical Presentation and Outcomes of Phaeochromocytomas/Paragangliomas in Neurofibromatosis Type 1. *Eur Endocrinol* (2019) 15:95. doi: 10.17925/EE.2019.15.2.95
38. Gruber LM, Erickson D, Babovic-Vuksanovic D, Thompson GB, Young WF, Bancos I. Pheochromocytoma and Paraganglioma in Patients With Neurofibromatosis Type 1. *Clin Endocrinol* (2017) 86:141–9. doi: 10.1111/cen.13163
39. Walther MM, Herring J, Enquist E, Keiser HR, Linehan WM. Von Recklingausen's Disease and Pheochromocytomas. *J Urol* (2006) 162:1582–6. doi: 10.1016/S0022-5347(05)68171-2
40. Zografos GN, Vasiliadis GK, Zagouri F, Aggeli C, Korkolis D, Vogiaki S, et al. Pheochromocytoma Associated With Neurofibromatosis Type 1: Concepts and Current Trends. *World J Surg Oncol* (2010) 8:14. doi: 10.1186/1477-7819-8-14
41. Opocher G, Conton P, Schiavi F, Macino B, Mantero F. Pheochromocytoma in Von Hippel–Lindau Disease and Neurofibromatosis Type 1. *Fam Cancer* (2005) 4:13–6. doi: 10.1007/s10689-004-6128-y
42. Bausch B, Borozdin W, Neumann HPH. Clinical and Genetic Characteristics of Patients With Neurofibromatosis Type 1 and Pheochromocytoma. *N Engl J Med* (2006) 354:2729–31. doi: 10.1056/NEJMc066006
43. Bausch B, Borozdin W, Mautner VF, Hoffmann MM, Boehm D, Robledo M, et al. Germline *NF1* Mutational Spectra and Loss-of-Heterozygosity Analyses in Patients With Pheochromocytoma and Neurofibromatosis Type 1. *J Clin Endocrinol Metab* (2007) 92:2784–92. doi: 10.1210/jc.2006-2833
44. Moramarco J, El Ghorayeb N, Dumas N, Nolet S, Boulanger L, Burnichon N, et al. Pheochromocytomas are Diagnosed Incidentally and At Older Age in Neurofibromatosis Type 1. *Clin Endocrinol* (2017) 86:332–9. doi: 10.1111/cen.13265
45. Kimura N, Miura Y, Miura K, Takahashi N, Osamura RY, Nagatsu I, et al. Adrenal and Retroperitoneal Mixed Neuroendocrine-Neural Tumors. *Endocr Pathol* (1991) 2:139–47. doi: 10.1007/BF02915454
46. Castoldi L, De Rai P, Marini A, Ferrero S, De Luca VM, Tiberio G. Neurofibromatosis-1 and Ampullary Gangliocytic Paraganglioma Causing Biliary and Pancreatic Obstruction. *Int J Pancreatol* (2001) 29:93–7. doi: 10.1385/IJGC:29:2:093
47. Okubo Y, Yoshioka E, Suzuki M, Washimi K, Kawachi K, Kameda Y, et al. Diagnosis, Pathological Findings, and Clinical Management of Gangliocytic Paraganglioma: A Systematic Review. *Front Oncol* (2018) 8:291. doi: 10.3389/fonc.2018.00291
48. Taïeb D, Hicks RJ, Hindié E, Guillet BA, Avram A, Ghedini P, et al. European Association of Nuclear Medicine Practice Guideline/Society of Nuclear Medicine and Molecular Imaging Procedure Standard 2019 for Radionuclide Imaging of Phaeochromocytoma and Paraganglioma. *Eur J Nucl Med Mol Imaging* (2019) 46:2112–37. doi: 10.1007/s00259-019-04398-1
49. Li SR, Nicholson KJ, Mccoy KL, Carty SE, Yip L. Clinical and Biochemical Features of Pheochromocytoma Characteristic of Von Hippel–Lindau Syndrome. *World J Surg* (2020) 44:570–7. doi: 10.1007/s00268-019-05299-y
50. Aufforth RD, Ramakant P, Sadowski SM, Mehta A, Trebska-McGowan K, Nilubol N, et al. Pheochromocytoma Screening Initiation and Frequency in Von Hippel-Lindau Syndrome. *J Clin Endocrinol Metab* (2015) 100:4498–504. doi: 10.1210/jc.2015-3045
51. Kittah NE, Gruber LM, Bancos I, Hamidi O, Tamhane S, Iñiguez-Ariza N, et al. Bilateral Pheochromocytoma: Clinical Characteristics, Treatment and Longitudinal Follow-Up. *Clin Endocrinol* (2020) 3:288–95. doi: 10.1111/cen.14222

52. Fagundes GFC, Petenuci J, Lourenco DM, Trarbach EB, Pereira MAA, Correa D'Eur JE, et al. New Insights Into Pheochromocytoma Surveillance of Young Patients With VHL Missense Mutations. *J Endocr Soc* (2019) 3:1682–92. doi: 10.1210/js.2019-00225
53. Lenders JWM, Duh Q-Y, Eisenhofer G, Gimenez-Roqueplo A-P, Grebe SKG, Murad MH, et al. Pheochromocytoma and Paraganglioma: An Endocrine Society Clinical Practice Guideline. *J Clin Endocrinol Metab* (2014) 99:1915–42. doi: 10.1210/jc.2014-1498
54. Letouzé E, Martinelli C, Loriot C, Burnichon N, Abermil N, Ottolenghi C, et al. SDH Mutations Establish a Hypermethylator Phenotype in Paraganglioma. *Cancer Cell* (2013) 23:739–52. doi: 10.1016/j.ccr.2013.04.018
55. Weisbrod AB, Kitano M, Gesuwan K, Millo C, Herscovitch P, Nilubol N, et al. Clinical Utility of Functional Imaging With 18F-FDOPA in Von Hippel-Lindau Syndrome. *J Clin Endocrinol Metab* (2012) 97:E613–7. doi: 10.1210/jc.2011-2626
56. Shell J, Tirosh A, Millo C, Sadowski SM, Assadipour Y, Green P, et al. The Utility of 68Gallium-DOTATATE PET/CT in the Detection of Von Hippel-Lindau Disease Associated Tumors. *Eur J Radiol* (2019) 112:130–5. doi: 10.1016/j.ejrad.2018.11.023
57. Lenders JWM, Kerstens MN, Amar L, Prejbisz A, Robledo M, Taieb D, et al. Genetics, Diagnosis, Management and Future Directions of Research of Phaeochromocytoma and Paraganglioma: A Position Statement and Consensus of the Working Group on Endocrine Hypertension of the European Society of Hypertension. *J Hypertens* (2020) 38:1443–56. doi: 10.1097/HJH.0000000000002438
58. Zelinka T, Petrák O, Turková H, Holaj R, Štrauch B, Kršek M, et al. High Incidence of Cardiovascular Complications in Pheochromocytoma. *Horm Metab Res* (2012) 44:379–84. doi: 10.1055/s-0032-1306294
59. Y-Hassan S, Falhammar H. Cardiovascular Manifestations and Complications of Pheochromocytomas and Paragangliomas. *J Clin Med* (2020) 9:2435. doi: 10.3390/jcm9082435
60. Eisenhofer G, Rivers G, Rosas AL, Quezado Z, Manger WM, Pacak K. Adverse Drug Reactions in Patients With Phaeochromocytoma. *Drug Saf* (2007) 30:1031–62. doi: 10.2165/00002018-200730110-00004
61. Rossitti HM, Söderkvist P, Gimm O. Extent of Surgery for Phaeochromocytomas in the Genomic Era. *Br J Surg* (2018) 105:e84–98. doi: 10.1002/bjs.10744
62. Neumann HPH, Bender BU, Reincke M, Eggstein S, Laubenberger J, Kirste G. Adrenal-Sparing Surgery for Phaeochromocytoma. *Br J Surg* (1999) 86:94–7. doi: 10.1046/j.1365-2168.1999.00974.x
63. Castinetti F, Taieb D, Henry JF, Walz M, Guerin C, Brue T, et al. MANAGEMENT OF ENDOCRINE DISEASE: Outcome of Adrenal Sparing Surgery in Heritable Pheochromocytoma. *Eur J Endocrinol* (2016) 174:R9–R18. doi: 10.1530/EJE-15-0549
64. Erichsen MM, Løvås K, Fougner KJ, Svartberg J, Hauge ER, Bollerslev J, et al. Normal Overall Mortality Rate in Addison's Disease, But Young Patients are At Risk of Premature Death. *Eur J Endocrinol* (2009) 160:233–7. doi: 10.1530/EJE-08-0550
65. Tiemensma J, Andela CD, Kaptein AA, Romijn JA, van der Mast RC, Biermasz NR, et al. Psychological Morbidity and Impaired Quality of Life in Patients With Stable Treatment for Primary Adrenal Insufficiency: Cross-Sectional Study and Review of the Literature. *Eur J Endocrinol* (2014) 171:171–82. doi: 10.1530/EJE-14-0023
66. Brauckhoff M. Critical Size of Residual Adrenal Tissue and Recovery From Impaired Early Postoperative Adrenocortical Function After Subtotal Bilateral Adrenalectomy. *Surgery* (2003) 134:1020–7. doi: 10.1016/j.surg.2003.08.005
67. Fang F, Ding L, He Q, Liu M. Preoperative Management of Pheochromocytoma and Paraganglioma. *Front Endocrinol* (2020) 11:586795. doi: 10.3389/fendo.2020.586795
68. Ku YK, Sangla K, Tan YM, Williams DJ. A Case of Using Cortical Sparing Adrenalectomy to Manage Bilateral Phaeochromocytoma in Neurofibromatosis Type 1. *Internal Med J* (2010) 40:239–40. doi: 10.1111/j.1445-5994.2010.02181.x
69. Benhammou JN, Boris RS, Pacak K, Pinto PA, Linehan WM, Bratslavsky G. Functional and Oncologic Outcomes of Partial Adrenalectomy for Pheochromocytoma in Patients With Von Hippel-Lindau Syndrome After At Least 5 Years of Followup. *J Urol* (2010) 184:1855–9. doi: 10.1016/j.juro.2010.06.102
70. Neumann HPH, Tsoy U, Bancos I, Amodru V, Walz MK, Tirosh A, et al. Comparison of Pheochromocytoma-Specific Morbidity and Mortality Among Adults With Bilateral Pheochromocytomas Undergoing Total Adrenalectomy vs Cortical-Sparing Adrenalectomy. *JAMA Netw Open* (2019) 2:e198898. doi: 10.1001/jamanetworkopen.2019.8898
71. Volkin D, Yerram N, Ahmed F, Lankford D, Baccala A, Gupta GN, et al. Partial Adrenalectomy Minimizes the Need for Long-Term Hormone Replacement in Pediatric Patients With Pheochromocytoma and Von Hippel-Lindau Syndrome. *J Pediatr Surg* (2012) 47:2077–82. doi: 10.1016/j.jpedsurg.2012.07.003
72. Fassnacht M, Assie G, Baudin E, Eisenhofer G, de la Fouchardiere C, Haak HR, et al. Adrenocortical Carcinomas and Malignant Phaeochromocytomas: ESMO–EURACAN Clinical Practice Guidelines for Diagnosis, Treatment and Follow-Up. *Ann Oncol* (2020) 31:1476–90. doi: 10.1016/j.annonc.2020.08.2099
73. Otoukesh S, Cooper CJ, Lou W, Mojtahedzadeh M, Nasrazadani A, Wampler M, et al. Combination Chemotherapy Regimen in a Patient With Metastatic Malignant Pheochromocytoma and Neurofibromatosis Type 1. *Am J Case Rep* (2014) 15:123–7. doi: 10.12659/AJCR.890181
74. Jimenez C, Cabanillas ME, Santarpia L, Jonasch E, Kyle KL, Lano EA, et al. Use of the Tyrosine Kinase Inhibitor Sunitinib in a Patient With Von Hippel-Lindau Disease: Targeting Angiogenic Factors in Pheochromocytoma and Other Von Hippel-Lindau Disease-Related Tumors. *J Clin Endocrinol Metab* (2009) 94:386–91. doi: 10.1210/jc.2008-1972
75. Miller DT, Freedenberg D, Schorry E, Ullrich NJ, Viskochil D, Korf BR, et al. Health Supervision for Children With Neurofibromatosis Type 1. *Pediatrics* (2019) 143:e20190660. doi: 10.1542/peds.2019-0660
76. Stewart DR, Korf BR, Nathanson KL, Stevenson DA, Yohay K. Care of Adults With Neurofibromatosis Type 1: A Clinical Practice Resource of the American College of Medical Genetics and Genomics (ACMG). *Genet Med* (2018) 20:671–82. doi: 10.1038/gim.2018.28
77. France Network NF, Bergqvist C, Servy A, Valeyrie-Allanore L, Ferkal S, Combemale P, et al. Neurofibromatosis 1 French National Guidelines Based on an Extensive Literature Review Since 1966. *Orphanet J Rare Dis* (2020) 15:37. doi: 10.1186/s13023-020-1310-3
78. Hirbe AC, Gutmann DH. Neurofibromatosis Type 1: A Multidisciplinary Approach to Care. *Lancet Neurol* (2014) 13:834–43. doi: 10.1016/S1474-4422(14)70063-8
79. Ferner RE, Huson SM, Thomas N, Moss C, Willshaw H, Evans DG, et al. Guidelines for the Diagnosis and Management of Individuals With Neurofibromatosis 1. *J Med Genet* (2006) 44:81–8. doi: 10.1136/jmg.2006.045906
80. Shinall MC, Solórzano CC. Pheochromocytoma in Neurofibromatosis Type 1: When Should it Be Suspected. *Endocr Pract* (2014) 20:792–6. doi: 10.4158/EP13417.OR
81. Képénékian L, Mognetti T, Lifante J-C, Giraudet A-L, Houzard C, Pinson S, et al. Interest of Systematic Screening of Pheochromocytoma in Patients With Neurofibromatosis Type 1. *Eur J Endocrinol* (2016) 175:335–44. doi: 10.1530/EJE-16-0233
82. Cornu E, Motiejunaite J, Belmihoub I, Vidal-Petiot E, Mirabel M, Amar L. Acute Stress Cardiomyopathy: Heart of Pheochromocytoma. *Ann Endocrinol* (2020) S0003–4266(20):30046-9. doi: 10.1016/j.ando.2020.03.011
83. Vermalle M, Tabarin A, Castinetti F. Hereditary Pheochromocytoma and Paraganglioma: Screening and Follow-Up Strategies in Asymptomatic Mutation Carriers. *Ann Endocrinol* (2018) 79:S10–21. doi: 10.1016/S0003-4266(18)31234-4
84. Buffet A, Ben Aim L, Leboulleux S, Drui D, Vezzosi D, Libé R, et al. Positive Impact of Genetic Test on the Management and Outcome of Patients With Paraganglioma and/or Pheochromocytoma. *J Clin Endocrinol Metab* (2019) 104:1109–18. doi: 10.1210/jc.2018-02411
85. Bancos I, Atkinson E, Eng C, Young WF, Neumann HPH, Yukina M, et al. Maternal and Fetal Outcomes in Phaeochromocytoma and Pregnancy: A Multicentre Retrospective Cohort Study and Systematic Review of Literature. *Lancet Diabetes Endocrinol* (2021) 9:13–21. doi: 10.1016/S2213-8587(20)30363-6
86. Rednam SP, Erez A, Druker H, Janeway KA, Kamihara J, Kohlmann WK, et al. Von Hippel–Lindau and Hereditary Pheochromocytoma/Paraganglioma Syndromes: Clinical Features, Genetics, and Surveillance

Recommendations in Childhood. *Clin Cancer Res* (2017) 23:e68–75. doi: 10.1158/1078-0432.CCR-17-0547
87. Binderup ML, Bisgaard ML, Harbud V, Møller HU, Gimsing S, Friis-Hansen L, et al. Danish vHL Coordination Group. Von Hippel-Lindau disease (vHL). National Clinical Guideline for Diagnosis and Surveillance in Denmark. 3rd edition. *Dan Med J* (2013) 60(12):B4763.
88. PREDIR National Reference Center For Rare Cancers. French Recommendations for Clinical Surveillance in Von Hippel Lindau (2018). Available at: http://www.vhlfrance.org/wp-content/uploads/2019/03/Fiche-de-recommandation-surveillance-clinique-VHL-France-du-28-ao%C3%BBt-2018.pdf.
89. Modlin IM, Oberg K, Chung DC, Jensen RT, de Herder WW, Thakker RV, et al. Gastroenteropancreatic Neuroendocrine Tumours. *Lancet Oncol* (2008) 9:61–72. doi: 10.1016/S1470-2045(07)70410-2
90. Rindi G, Wiedenmann B. Neuroendocrine Neoplasia of the Gastrointestinal Tract Revisited: Towards Precision Medicine. *Nat Rev Endocrinol* (2020) 16:590–607. doi: 10.1038/s41574-020-0391-3
91. Nagtegaal ID, Odze RD, Klimstra D, Paradis V, Rugge M, Schirmacher P, et al. The 2019 WHO Classification of Tumours of the Digestive System. *Histopathology* (2020) 76:182–8. doi: 10.1111/his.13975
92. Gill AJ. Why did They Change That? Practical Implications of the Evolving Classification of Neuroendocrine Tumours of the Gastrointestinal Tract. *Histopathology* (2021) 78:162–70. doi: 10.1111/his.14172
93. Lombard-Bohas C, Mitry E, O'Toole D, Louvet C, Pillon D, Cadiot G, et al. Thirteen-Month Registration of Patients With Gastroenteropancreatic Endocrine Tumours in France. *Neuroendocrinology* (2009) 89:217–22. doi: 10.1159/000151562
94. Dasari A, Shen C, Halperin D, Zhao B, Zhou S, Xu Y, et al. Trends in the Incidence, Prevalence, and Survival Outcomes in Patients With Neuroendocrine Tumors in the United States. *JAMA Oncol* (2017) 3:1335. doi: 10.1001/jamaoncol.2017.0589
95. Pape U, Jann H, Müller-Nordhorn J, Bockelbrink A, Berndt U, Willich SN, et al. Prognostic Relevance of a Novel TNM Classification System for Upper Gastroenteropancreatic Neuroendocrine Tumors. *Cancer* (2008) 113:256–65. doi: 10.1002/cncr.23549
96. Yao JC, Hassan M, Phan A, Dagohoy C, Leary C, Mares JE, et al. One Hundred Years After "Carcinoid": Epidemiology of and Prognostic Factors for Neuroendocrine Tumors in 35,825 Cases in the United States. *J Clin Oncol* (2008) 26:3063–72. doi: 10.1200/JCO.2007.15.4377
97. Couvelard A, Scoazec J-Y. Inherited Tumor Syndromes of Gastroenteropancreatic and Thoracic Neuroendocrine Neoplasms. *Ann Pathol* (2020) 40:120–33. doi: 10.1016/j.annpat.2020.01.002
98. Relles D, Baek J, Witkiewicz A, Yeo CJ. Periampullary and Duodenal Neoplasms in Neurofibromatosis Type 1: Two Cases and an Updated 20-Year Review of the Literature Yielding 76 Cases. *J Gastrointest Surg* (2010) 14:1052–61. doi: 10.1007/s11605-009-1123-0
99. Tanaka S, Yamasaki S, Matsushita H, Ozawa Y, Kurosaki A, Takeuchi K, et al. Duodenal Somatostatinoma: A Case Report and Review of 31 Cases With Special Reference to the Relationship Between Tumor Size and Metastasis. *Pathol Int* (2000) 50:146–52. doi: 10.1046/j.1440-1827.2000.01016.x
100. Vanoli A, La Rosa S, Klersy C, Grillo F, Albarello L, Inzani F, et al. Four Neuroendocrine Tumor Types and Neuroendocrine Carcinoma of the Duodenum: Analysis of 203 Cases. *Neuroendocrinology* (2017) 104:112–25. doi: 10.1159/000444803
101. Samonakis DN, Quaglia A, Joshi NM, Tibballs JM, Nagree A, Triantos CK, et al. Obstructive Jaundice Secondary to Neuroendocrine Tumour in a Patient With Von Recklinghausen's Disease. *Eur J Gastroenterol Hepatol* (2005) 17:1229–32. doi: 10.1097/00042737-200511000-00012
102. Sandru F, Carsote M, Valea A, Albu SE, Petca R-C, Dumitrascu MC. Somatostatinoma: Beyond Neurofibromatosis Type 1. *Exp Ther Med* (2020) 4:3383–8. doi: 10.3892/etm.2020.8965
103. Alshikho MJ, Noureldine SI, Talas JM, Nasimian A, Zazou S, Mobaed B, et al. Zollinger-Ellison Syndrome Associated With Von Recklinghausen Disease: Case Report and Literature Review. *Am J Case Rep* (2016) 17:398–405. doi: 10.12659/AJCR.898472
104. Rogers A, Wang LM, Karavitaki N, Grossman AB. Neurofibromatosis Type 1 and Pancreatic Islet Cell Tumours: An Association Which Should be Recognized. *QJM* (2015) 108:573–6. doi: 10.1093/qjmed/hcs203
105. Salvi PF, Lorenzon L, Caterino S, Antolino L, Antonelli MS, Balducci G. Gastrointestinal Stromal Tumors Associated With Neurofibromatosis 1: A Single Centre Experience and Systematic Review of the Literature Including 252 Cases. *Int J Surg Oncol* (2013) 2013:1–8. doi: 10.1155/2013/398570
106. Andersson J, Sihto H, Meis-Kindblom JM, Joensuu H, Nupponen N, Kindblom L-G. NF1-Associated Gastrointestinal Stromal Tumors Have Unique Clinical, Phenotypic, and Genotypic Characteristics. *Am J Surg Pathol* (2005) 29:1170–6. doi: 10.1097/01.pas.0000159775.77912.15
107. Hammel PR, Vilgrain V, Terris B, Penfornis A, Sauvanet A, Correas J, et al. Pancreatic Involvement in Von Hippel–Lindau Disease. *Gastroenterology* (2000) 119:1087–95. doi: 10.1053/gast.2000.18143
108. Corcos O, Couvelard A, Giraud S, Vullierme M-P, O'Toole D, Rebours V, et al. Endocrine Pancreatic Tumors in Von Hippel-Lindau Disease: Clinical, Histological, and Genetic Features. *Pancreas* (2008) 37:85–93. doi: 10.1097/MPA.0b013e31815f394a
109. Blansfield JA, Choyke L, Morita SY, Choyke PL, Pingpank JF, Alexander HR, et al. Clinical, Genetic and Radiographic Analysis of 108 Patients With Von Hippel-Lindau Disease (VHL) Manifested by Pancreatic Neuroendocrine Tumors (PNETs). *Surgery* (2007) 142:814–8.e2. doi: 10.1016/j.surg.2007.09.012
110. Tirosh A, El Lakis M, Green P, Nockel P, Patel D, Nilubol N, et al. In Silico VHL Gene Mutation Analysis and Prognosis of Pancreatic Neuroendocrine Tumors in Von Hippel–Lindau Disease. *J Clin Endocrinol Metab* (2018) 103:1631–8. doi: 10.1210/jc.2017-02434
111. Krauss T, Ferrara AM, Links TP, Wellner U, Bancos I, Kvachenyuk A, et al. Preventive Medicine of Von Hippel–Lindau Disease-Associated Pancreatic Neuroendocrine Tumors. *Endocr Relat Cancer* (2018) 25:783–93. doi: 10.1530/ERC-18-0100
112. Igarashi H, Ito T, Nishimori I, Tamura K, Yamasaki I, Tanaka M, et al. Pancreatic Involvement in Japanese Patients With Von Hippel-Lindau Disease: Results of a Nationwide Survey. *J Gastroenterol* (2014) 49:511–6. doi: 10.1007/s00535-013-0794-1
113. Zhang C, Jin J, Xie J, Ye L, Su T, Jiang L, et al. The Clinical Features and Molecular Mechanisms of ACTH-secreting Pancreatic Neuroendocrine Tumors. *J Clin Endocrinol Metab* (2020) 105:dgaa507. doi: 10.1210/clinem/dgaa507
114. Speisky D, Duces A, Bieche I, Rebours V, Hammel P, Sauvanet A, et al. Molecular Profiling of Pancreatic Neuroendocrine Tumors in Sporadic and Von Hippel-Lindau Patients. *Clin Cancer Res* (2012) 18:2838–49. doi: 10.1158/1078-0432.CCR-11-2759
115. Keutgen XM, Kumar S, Gara S, Boufraqech M, Agarwal S, Hruban RH, et al. Transcriptional Alterations in Hereditary and Sporadic Nonfunctioning Pancreatic Neuroendocrine Tumors According to Genotype. *Cancer* (2018) 124:636–47. doi: 10.1002/cncr.31057
116. Charlesworth M, Verbeke CS, Falk GA, Walsh M, Smith AM, Morris-Stiff G. Pancreatic Lesions in Von Hippel–Lindau Disease? A Systematic Review and Meta-synthesis of the Literature. *J Gastrointest Surg* (2012) 16:1422–8. doi: 10.1007/s11605-012-1847-0
117. Yamasaki I, Nishimori I, Ashida S, Kohsaki T, Onishi S, Shuin T. Clinical Characteristics of Pancreatic Neuroendocrine Tumors in Japanese Patients With Von Hippel-Lindau Disease. *Pancreas* (2006) 33:382–5. doi: 10.1097/01.mpa.0000240604.26312.e4
118. Halfdanarson TR, Rabe KG, Rubin J, Petersen GM. Pancreatic Neuroendocrine Tumors (PNETs): Incidence, Prognosis and Recent Trend Toward Improved Survival. *Ann Oncol* (2008) 19:1727–33. doi: 10.1093/annonc/mdn351
119. Sharma A, Mukewar S, Vege SS. Clinical Profile of Pancreatic Cystic Lesions in Von Hippel-Lindau Disease: A Series of 48 Patients Seen At a Tertiary Institution. *Pancreas* (2017) 46:948–52. doi: 10.1097/MPA.0000000000000875
120. Oberg K, Couvelard A, Delle Fave G, Gross D, Grossman A, Jensen RT, et al. ENETS Consensus Guidelines for the Standards of Care in Neuroendocrine Tumors: Biochemical Markers. *Neuroendocrinology* (2017) 105:201–11. doi: 10.1159/000472254
121. Weisbrod AB, Kitano M, Thomas F, Williams D, Gulati N, Gesuwan K, et al. Assessment of Tumor Growth in Pancreatic Neuroendocrine Tumors in Von Hippel Lindau Syndrome. *J Am Coll Surg* (2014) 218:163–9. doi: 10.1016/j.jamcollsurg.2013.10.025
122. Mafficini A, Scarpa A. Genetics and Epigenetics of Gastroenteropancreatic Neuroendocrine Neoplasms. *Endocr Rev* (2019) 40:506–36. doi: 10.1210/er.2018-00160

123. Larson A, Hedgire S, Deshpande V, Stemmer-Rachamimov A, Harisinghani M, Ferrone C, et al. Pancreatic Neuroendocrine Tumors in Patients With Tuberous Sclerosis Complex. *Clin Genet* (2012) 82:558–63. doi: 10.1111/j.1399-0004.2011.01805.x
124. Mehta S, Rusyn L, Ginsburg H, Hajdu C, Kohn B. Pancreatic Neuroendocrine Tumor in a Young Child With Tuberous Sclerosis Complex 1. *J Endocr Soc* (2019) 3:1201–6. doi: 10.1210/js.2019-00051
125. Borson-Chazot F, Cardot-Bauters C, Mirallie É, Pattou F. Insulinoma of Genetic Aetiology. *Ann Endocrinol* (2013) 74:200–2. doi: 10.1016/j.ando.2013.05.006
126. Crona J, Skogseid B. GEP- NETS UPDATE: Genetics of Neuroendocrine Tumors. *Eur J Endocrinol* (2016) 174:R275–90. doi: 10.1530/EJE-15-0972
127. Kolin DL, Duan K, Ngan B, Gerstle JT, Krzyzanowska MK, Somers GR, et al. Expanding the Spectrum of Colonic Manifestations in Tuberous Sclerosis: L-Cell Neuroendocrine Tumor Arising in the Background of Rectal Pecoma. *Endocr Pathol* (2018) 29:21–6. doi: 10.1007/s12022-017-9497-0
128. Falconi M, Eriksson B, Kaltsas G, Bartsch DK, Capdevila J, Caplin M, et al. Enets Consensus Guidelines Update for the Management of Patients With Functional Pancreatic Neuroendocrine Tumors and Non-Functional Pancreatic Neuroendocrine Tumors. *Neuroendocrinology* (2016) 103:153–71. doi: 10.1159/000443171
129. Angeletti S, Corleto VD, Schillaci O, Marignani M, Annibale B, Moretti A, et al. Use of the Somatostatin Analogue Octreotide to Localise and Manage Somatostatin-Producing Tumours. *Gut* (1998) 42:792–4. doi: 10.1136/gut.42.6.792
130. Hofland J, Kaltsas G, de Herder WW. Advances in the Diagnosis and Management of Well-Differentiated Neuroendocrine Neoplasms. *Endocr Rev* (2020) 41:bnz004. doi: 10.1210/endrev/bnz004
131. Healy ML, Dawson SJ, Murray RML, Zalcberg J, Jefford M. Severe Hypoglycaemia After Long-Acting Octreotide in a Patient With an Unrecognized Malignant Insulinoma. *Internal Med J* (2007) 37:406–9. doi: 10.1111/j.1445-5994.2007.01371.x
132. Baudin E, Caron P, Lombard-Bohas C, Tabarin A, Mitry E, Reznick Y, et al. Malignant Insulinoma: Recommendations for Characterisation and Treatment. *Ann Endocrinol* (2013) 74:523–33. doi: 10.1016/j.ando.2013.07.001
133. Hendren NS, Panach K, Brown TJ, Peng L, Beg MS, Weissler J, et al. Pasireotide for the Treatment of Refractory Hypoglycaemia From Malignant Insulinoma. *Clin Endocrinol* (2018) 88:341–3. doi: 10.1111/cen.13503
134. Kulke MH. A Randomized, Open-Label, Phase 2 Study of Everolimus in Combination With Pasireotide LAR or Everolimus Alone in Advanced, Well-Differentiated, Progressive Pancreatic Neuroendocrine Tumors: COOPERATE-2 Trial. *Ann Oncol* (2017) 28:7. doi: 10.1093/annonc/mdx078
135. de Mestier L, Lepage C, Baudin E, Coriat R, Courbon F, Couvelard A, et al. Digestive Neuroendocrine Neoplasms (NEN): French Intergroup Clinical Practice Guidelines for Diagnosis, Treatment and Follow-Up (SNFGE, GTE, RENATEN, TENPATH, FFCD, GERCOR, UNICANCER, SFCD, SFED, SFRO, SFR). *Dig Liver Dis* (2020) 5:473–92. doi: 10.1016/j.dld.2020.02.011
136. Pavel M, Öberg K, Falconi M, Krenning EP, Sundin A, Perren A, et al. Gastroenteropancreatic Neuroendocrine Neoplasms: ESMO Clinical Practice Guidelines for Diagnosis, Treatment and Follow-Up. *Ann Oncol* (2020) 31:844–60. doi: 10.1016/j.annonc.2020.03.304
137. Klesse LJ, Jordan JT, Radtke HB, Rosser T, Schorry E, Ullrich N, et al. The Use of MEK Inhibitors in Neurofibromatosis Type 1–Associated Tumors and Management of Toxicities. *Oncol* (2020) 7:1109–16. doi: 10.1634/theoncologist.2020-0069
138. Dombi E, Baldwin A, Marcus LJ, Fisher MJ, Weiss B, Kim A, et al. Activity of Selumetinib in Neurofibromatosis Type 1–Related Plexiform Neurofibromas. *N Engl J Med* (2016) 375:2550–60. doi: 10.1056/NEJMoa1605943
139. Banerjee A, Jakacki RI, Onar-Thomas A, Wu S, Nicolaides T, Young Poussaint T, et al. A Phase I Trial of the MEK Inhibitor Selumetinib (AZD6244) in Pediatric Patients With Recurrent or Refractory Low-Grade Glioma: A Pediatric Brain Tumor Consortium (PBTC) Study. *Neuro Oncol* (2017) 19:1135–44. doi: 10.1093/neuonc/now282
140. Fangusaro J, Onar-Thomas A, Young Poussaint T, Wu S, Ligon AH, Lindeman N, et al. Selumetinib in Paediatric Patients With BRAF-aberrant or Neurofibromatosis Type 1-Associated Recurrent, Refractory, or Progressive Low-Grade Glioma: A Multicentre, Phase 2 Trial. *Lancet Oncol* (2019) 20:1011–22. doi: 10.1016/S1470-2045(19)30277-3
141. Gross AM, Wolters PL, Dombi E, Baldwin A, Whitcomb P, Fisher MJ, et al. Selumetinib in Children With Inoperable Plexiform Neurofibromas. *N Engl J Med* (2020) 382:1430–42. doi: 10.1056/NEJMoa1912735
142. de Mestier L, Gaujoux S, Cros J, Hentic O, Vullierme M-P, Couvelard A, et al. Long-Term Prognosis of Resected Pancreatic Neuroendocrine Tumors in Von Hippel-Lindau Disease Is Favorable and Not Influenced by Small Tumors Left in Place. *Ann Surg* (2015) 262:384–8. doi: 10.1097/SLA.0000000000000856
143. Libutti SK, Choyke PL, Bartlett DL, Vargas H, Walther M, Lubensky I, et al. Pancreatic Neuroendocrine Tumors Associated With Von Hippel Lindau Disease: Diagnostic and Management Recommendations. *Surgery* (1998) 124:1153–9. doi: 10.1067/msy.1998.91823
144. Keutgen XM, Hammel P, Choyke PL, Libutti SK, Jonasch E, Kebebew E. Evaluation and Management of Pancreatic Lesions in Patients With Von Hippel–Lindau Disease. *Nat Rev Clin Oncol* (2016) 13:537–49. doi: 10.1038/nrclinonc.2016.37
145. Howe JR, Merchant NB, Conrad C, Keutgen XM, Hallet J, Drebin JA, et al. The North American Neuroendocrine Tumor Society Consensus Paper on the Surgical Management of Pancreatic Neuroendocrine Tumors. *Pancreas* (2020) 49:1–33. doi: 10.1097/MPA.0000000000001454
146. Dai M, Xing C, Shi N, Wang S, Wu G, Liao Q, et al. Risk Factors for New-Onset Diabetes Mellitus After Distal Pancreatectomy. *BMJ Open Diabetes Res Care* (2020) 8:e001778. doi: 10.1136/bmjdrc-2020-001778
147. Maxwell DW, Jajja MR, Galindo RJ, Zhang C, Nadeem SO, Sweeney JF, et al. Post-Pancreatectomy Diabetes Index: A Validated Score Predicting Diabetes Development After Major Pancreatectomy. *J Am Coll Surg* (2020) 230:393–402.e3. doi: 10.1016/j.jamcollsurg.2019.12.016
148. Renaud F, Chetboun M, Thevenet J, Delalleau N, Gmyr V, Hubert T, et al. Safety of Islet Autotransplantation After Pancreatectomy for Adenocarcinoma. *Transplantation* (2019) 103:177–81. doi: 10.1097/TP.0000000000002419
149. Wojtusciszyn A, Branchereau J, Esposito L, Badet L, Buron F, Chetboun M, et al. Indications for Islet or Pancreatic Transplantation: Statement of the TREPID Working Group on Behalf of the Société Francophone Du Diabète (SFD), Société Francaise D'endocrinologie (SFE), Société Francophone De Transplantation (SFT) and Société Française De Néphrologie – Dialyse – Transplantation (SFNDT). *Diabetes Metab* (2019) 45:224–37. doi: 10.1016/j.diabet.2018.07.006
150. Raymond E, Dahan L, Raoul J-L, Bang Y-J, Borbath I, Lombard-Bohas C, et al. Sunitinib Malate for the Treatment of Pancreatic Neuroendocrine Tumors. *N Engl J Med* (2011) 364:501–13. doi: 10.1056/NEJMoa1003825
151. Jonasch E, McCutcheon IE, Waguespack SG, Wen S, Davis DW, Smith LA, et al. Pilot Trial of Sunitinib Therapy in Patients With Von Hippel–Lindau Disease. *Ann Oncol* (2011) 22:2661–6. doi: 10.1093/annonc/mdr011
152. Ma K, Hong B, Zhou J, Gong Y, Wang J, Liu S, et al. The Efficacy and Safety of Tyrosine Kinase Inhibitors for Von Hippel–Lindau Disease: A Retrospective Study of 32 Patients. *Front Oncol* (2019) 9:1122. doi: 10.3389/fonc.2019.01122
153. Jonasch E, McCutcheon IE, Gombos DS, Ahrar K, Perrier ND, Liu D, et al. Pazopanib in Patients With Von Hippel-Lindau Disease: A Single-Arm, Single-Centre, Phase 2 Trial. *Lancet Oncol* (2018) 19:1351–9. doi: 10.1016/S1470-2045(18)30487-X
154. Choueiri TK, Kaelin WG. Targeting the HIF2–VEGF Axis in Renal Cell Carcinoma. *Nat Med* (2020) 26:1519–30. doi: 10.1038/s41591-020-1093-z
155. Jonasch E, Donskov F, Iliopoulos O, Rathmell WK, Narayan V, Maughan BL, et al. Phase II Study of the Oral HIF-2α Inhibitor MK-6482 for Von Hippel-Lindau Disease–Associated Renal Cell Carcinoma. *J Clin Oncol* (2020) 38:5003–3. doi: 10.1200/JCO.2020.38.15_suppl.5003
156. Pavel M, O"Toole D, Costa F, Capdevila J, Gross D, Kianmanesh R, et al. ENETS Consensus Guidelines Update for the Management of Distant Metastatic Disease of Intestinal, Pancreatic, Bronchial Neuroendocrine Neoplasms (NEN) and NEN of Unknown Primary Site. *Neuro endocrinology* (2016) 103:172–85. doi: 10.1159/000443167
157. Franz DN. Efficacy and Safety of Everolimus for Subependymal Giant Cell Astrocytomas Associated With Tuberous Sclerosis Complex (EXIST-1): A Multicentre, Randomised, Placebo-Controlled Phase 3 Trial. *Lancet* (2013) 381:8. doi: 10.1016/S0140-6736(12)61134-9

158. Bissler JJ, Kingswood JC, Radzikowska E, Zonnenberg BA, Frost M, Belousova E, et al. Everolimus for Angiomyolipoma Associated With Tuberous Sclerosis Complex or Sporadic Lymphangioleiomyomatosis (EXIST-2): A Multicentre, Randomised, Double-Blind, Placebo-Controlled Trial. *Lancet* (2013) 381:817–24. doi: 10.1016/S0140-6736(12)61767-X
159. Tirosh A, Journy N, Folio LR, Lee C, Leite C, Yao J, et al. Cumulative Radiation Exposures From CT Screening and Surveillance Strategies for Von Hippel-Lindau–Associated Solid Pancreatic Tumors. *Radiology* (2019) 290:116–24. doi: 10.1148/radiol.2018180687
160. Amin S, Kingswood JC, Bolton PF, Elmslie F, Gale DP, Harland C, et al. The UK Guidelines for Management and Surveillance of Tuberous Sclerosis Complex. *QJM Int J Med* (2019) 112:171–82. doi: 10.1093/qjmed/hcy215
161. Kodama H, Iihara M, Okamoto T, Obara T. Water-Clear Cell Parathyroid Adenoma Causing Primary Hyperparathyroidism in a Patient With Neurofibromatosis Type 1: Report of a Case. *Surg Today* (2007) 37:884–7. doi: 10.1007/s00595-007-3484-x
162. Hayashibara N, Ogawa T, Tsuji E, Oya M, Fujii A. Parathyroid Carcinoma Coincident With Neurofibromatosis Type 1. *J Clin Exp Oncol* (2018) 5:6. doi: 10.4172/2324-9110.1000170
163. Demirjian AN, Grossman JM, Chan JL, Parangi S. Parathyroid Carcinoma and Neurofibromatosis. *Surgery* (2008) 144:827–9. doi: 10.1016/j.surg.2008.07.015
164. Shinzato Y, Ikehara Y. A Case of Tuberous Sclerosis Complex With Concomitant Primary Hyperparathyroidism Due to Parathyroid Adenoma: A Case Report. *World J Surg Oncol* (2015) 13:106. doi: 10.1186/s12957-015-0520-y
165. Brewer K, Costa-Guda J, Arnold A. Molecular Genetic Insights Into Sporadic Primary Hyperparathyroidism. *Endocr Relat Cancer* (2019) 2:R53–72. doi: 10.1530/ERC-18-0304
166. Clarke BL. Epidemiology of Primary Hyperparathyroidism. *J Clin Densitom* (2013) 16:6. doi: 10.1016/j.jocd.2012.11.009
167. Checa Garrido A, del Pozo Picó C. Acromegaly and Type 1 Neurofibromatosis. Is Association of Both Conditions Due to Chance? *Endocrinol Nutr* (2013) 60:144–5. doi: 10.1016/j.endoen.2012.01.014
168. Hozumi K, Fukuoka H, Odake Y, Takeuchi T, Uehara T, Sato T, et al. Acromegaly Caused by a Somatotroph Adenoma in Patient With Neurofibromatosis Type 1. *Endocr J* (2019) 66:853–7. doi: 10.1507/endocrj.EJ19-0035
169. Hannah-Shmouni F, Demidowich AP, Rowell J, Lodish M, Stratakis CA. Large Pituitary Gland With an Expanding Lesion in the Context of Neurofibromatosis 1. *BMJ Case Rep* (2017) 2017:bcr-2017-222411. doi: 10.1136/bcr-2017-222411
170. Lim CT, Korbonits MK. Update on the Clinicopathology of Pituitary Adenomas. *Endocr Pract* (2018) 24:473–88. doi: 10.4158/EP-2018-0034
171. Zacharin M. Precocious Puberty in Two Children With Neurofibromatosis Type I in the Absence of Optic Chiasmal Glioma. *J Pediatr* (1997) 130:155–7. doi: 10.1016/S0022-3476(97)70327-5
172. Cambiaso P, Galassi S, Palmiero M, Mastronuzzi A, Del Bufalo F, Capolino R, et al. Growth Hormone Excess in Children With Neurofibromatosis Type-1 and Optic Glioma. *Am J Med Genet* (2017) 173:2353–8. doi: 10.1002/ajmg.a.38308
173. Yeung RS, Katsetos CD, Klein-Szanto A. Subependymal Astrocytic Hamartomas in the Eker Rat Model of Tuberous Sclerosis. *Am J Pathol* (1997) 151:10.
174. Kenerson H, Dundon TA, Yeung RS. Effects of Rapamycin in the Eker Rat Model of Tuberous Sclerosis Complex. *Pediatr Res* (2005) 57:67–75. doi: 10.1203/01.PDR.0000147727.78571.07
175. Regazzo D, Gardiman MP, Theodoropoulou M, Scaroni C, Occhi G, Ceccato F. Silent Gonadotroph Pituitary Neuroendocrine Tumor in a Patient With Tuberous Sclerosis Complex: Evaluation of a Possible Molecular Link. *Endocrinol Diabetes Metab Case Rep* (2018) 2018. doi: 10.1530/EDM-18-0086
176. Agrawal N, Akbani R, Aksoy BA, Ally A, Arachchi H, Asa SL, et al. Integrated Genomic Characterization of Papillary Thyroid Carcinoma. *Cell* (2014) 159:676–90. doi: 10.1016/j.cell.2014.09.050
177. Kunstman JW, Juhlin CC, Goh G, Brown TC, Stenman A, Healy JM, et al. Characterization of the Mutational Landscape of Anaplastic Thyroid Cancer Via Whole-Exome Sequencing. *Hum Mol Genet* (2015) 24:2318–29. doi: 10.1093/hmg/ddu749
178. Seminog OO, Goldacre MJ. Risk of Benign Tumours of Nervous System, and of Malignant Neoplasms, in People With Neurofibromatosis: Population-Based Record-Linkage Study. *Br J Cancer* (2013) 108:193–8. doi: 10.1038/bjc.2012.535
179. Findakly D, Solsi A, Arslan W. A Novel Combination of Metachronous Primary Malignancies of the Thyroid and Breast in a Patient With Neurofibromatosis Type 1. *Cureus* (2020) 12. doi: 10.7759/cureus.7590
180. Hashiba T, Maruno M, Fujimoto Y, Suzuki T, Wada K, Isaka T, et al. Skull Metastasis From Papillary Thyroid Carcinoma Accompanied by Neurofibromatosis Type 1 and Pheochromocytoma: Report of a Case. *Brain Tumor Pathol* (2006) 23:97–100. doi: 10.1007/s10014-006-0203-z
181. Miyamoto K, Nakamura M, Suzuki K, Katsuki S, Kaki Y, Inoue G, et al. Diagnosis of Neurofibromatosis Type 1 After Rupture of Aneurysm and Consequent Fatal Hemothorax. *Am J Emergency Med* (2020) 38:1543.e3–1543.e5. doi: 10.1016/j.ajem.2020.04.004
182. Ercolino T, Lai R, Giachè V, Melchionda S, Carella M, Delitala A, et al. Patient Affected by Neurofibromatosis Type 1 and Thyroid C-cell Hyperplasia Harboring Pathogenic Germ-Line Mutations in Both NF1 and RET Genes. *Gene* (2014) 536:332–5. doi: 10.1016/j.gene.2013.12.003
183. Anagnostouli M, Piperingos G, Yapijakis C, Gourtzelidis P, Balafouta S, Zournas C, et al. Thyroid Gland Neurofibroma in a NF1 Patient: NF1 and Thyroid Gland. *Acta Neurol Scand* (2002) 106:58–61. doi: 10.1034/j.1600-0404.2002.01159.x
184. Koksal Y, Sahin M, Koksal H, Esen H, Sen M. Neurofibroma Adjacent to the Thyroid Gland and a Thyroid Papillary Carcinoma in a Patient With Neurofibromatosis Type 1: Report of a Case. *Surg Today* (2009) 39:884–7. doi: 10.1007/s00595-008-3946-9
185. van Lierop ZYGJ, Jentjens S, Anten MHME, Wierts R, Stumpel CT, Havekes B, et al. Thyroid Gland ^{18}f-Fdg Uptake in Neurofibromatosis Type 1. *Eur Thyroid J* (2018) 7:155–61. doi: 10.1159/000488706
186. Nishida Y, Ikuta K, Ito S, Urakawa H, Sakai T, Koike H, et al. Limitations and Benefits of FDG-PET/CT in NF1 Patients With Nerve Sheath Tumors: A Cross-Sectional/Longitudinal Study. *Cancer Sci* (2021) 3:1114–22. doi: 10.1111/cas.14802
187. Robbins HL, Hague A. The PI3K/Akt Pathway in Tumors of Endocrine Tissues. *Front Endocrinol* (2016) 6:188. doi: 10.3389/fendo.2015.00188
188. Cameselle-Teijeiro J, Fachal C, Cabezas-Agrícola JM, Alfonsín-Barreiro N, Abdulkader I, Vega-Gliemmo A, et al. Thyroid Pathology Findings in Cowden Syndrome: A Clue for the Diagnosis of the PTEN Hamartoma Tumor Syndrome. *Am J Clin Pathol* (2015) 144:322–8. doi: 10.1309/AJCP84INGJUVTBME
189. Fagin JA, Wells SA. Biologic and Clinical Perspectives on Thyroid Cancer. *N Engl J Med* (2016) 375:1054–67. doi: 10.1056/NEJMra1501993
190. Laury AR, Bongiovanni M, Tille J-C, Kozakewich H, Nosé V. Thyroid Pathology in *PTEN* -Hamartoma Tumor Syndrome: Characteristic Findings of a Distinct Entity. *Thyroid* (2011) 21:135–44. doi: 10.1089/thy.2010.0226
191. Haugen BR, Alexander EK, Bible KC, Doherty GM, Mandel SJ, Nikiforov YE, et al. 2015 American Thyroid Association Management Guidelines for Adult Patients With Thyroid Nodules and Differentiated Thyroid Cancer: The American Thyroid Association Guidelines Task Force on Thyroid Nodules and Differentiated Thyroid Cancer. *Thyroid* 26:1–133. doi: 10.1089/thy.2015.0020
192. Hall JE, Abdollahian DJ, Sinard RJ. Thyroid Disease Associated With Cowden Syndrome: A Meta-Analysis. *Head Neck* (2013) 35:1189–94. doi: 10.1002/hed.22971
193. Milas M, Mester J, Metzger R, Shin J, Mitchell J, Berber E, et al. Should Patients With Cowden Syndrome Undergo Prophylactic Thyroidectomy? *Surgery* (2012) 152:1201–10. doi: 10.1016/j.surg.2012.08.055
194. Komiya T, Blumenthal GM, DeChowdhury R, Fioravanti S, Ballas MS, Morris J, et al. A Pilot Study of Sirolimus in Subjects With Cowden Syndrome or Other Syndromes Characterized by Germline Mutations in *PTEN*. *Oncologist* (2019) 24:1510. doi: 10.1634/theoncologist.2019-0514
195. PHTS Guideline Development Group and The European Reference Network GENTURIS, Tischkowitz M, Colas C, Pouwels S, Hoogerbrugge N. Cancer Surveillance Guideline for Individuals With PTEN Hamartoma Tumour Syndrome. *Eur J Hum Genet* (2020) 28:1387–93. doi: 10.1038/s41431-020-0651-7
196. Jonker LA, Lebbink CA, Jongmans MCJ, Nievelstein RAJ, Merks JHM, Nieveen van Dijkum EJM, et al. Recommendations on Surveillance for Differentiated Thyroid Carcinoma in Children With PTEN Hamartoma Tumor Syndrome. *Eur Thyroid J* (2020) 9:234–42. doi: 10.1159/000508872

Conflict of Interest: The authors declare that the research was conducted in the absence of any commercial or financial relationships that could be construed as a potential conflict of interest.

frontiers in Endocrinology

REVIEW
published: 19 May 2021
doi: 10.3389/fendo.2021.679000

Role of Somatostatin Receptor in Pancreatic Neuroendocrine Tumor Development, Diagnosis, and Therapy

Yuheng Hu[1,2,3,4†], *Zeng Ye*[1,2,3,4†], *Fei Wang*[1,2,3,4], *Yi Qin*[1,2,3,4], *Xiaowu Xu*[1,2,3,4], *Xianjun Yu*[1,2,3,4*] *and Shunrong Ji*[1,2,3,4*]

[1] Department of Pancreatic Surgery, Fudan University Shanghai Cancer Center, Shanghai, China, [2] Department of Oncology, Shanghai Medical College, Fudan University, Shanghai, China, [3] Shanghai Pancreatic Cancer Institute, Shanghai, China, [4] Pancreatic Cancer Institute, Fudan University, Shanghai, China

OPEN ACCESS

Edited by:
Enzo Lalli,
UMR7275 Institut de pharmacologie moléculaire et cellulaire (IPMC), France

Reviewed by:
Erika Peverelli,
University of Milan, Italy
Mauro Cives,
University of Bari Aldo Moro, Italy

***Correspondence:**
Xianjun Yu
yuxianjun@fudanpci.org
Shunrong Ji
jishunrong@fudanpci.org

[†]These authors have contributed equally to this work and share first authorship

Specialty section:
This article was submitted to Cancer Endocrinology, a section of the journal Frontiers in Endocrinology

Received: 10 March 2021
Accepted: 27 April 2021
Published: 19 May 2021

Citation:
Hu Y, Ye Z, Wang F, Qin Y, Xu X, Yu X and Ji S (2021) Role of Somatostatin Receptor in Pancreatic Neuroendocrine Tumor Development, Diagnosis, and Therapy. Front. Endocrinol. 12:679000. doi: 10.3389/fendo.2021.679000

Pancreatic neuroendocrine tumors (pNETs) are rare and part of the diverse family of neuroendocrine neoplasms (NENs). Somatostatin receptors (SSTRs), which are widely expressed in NENs, are G-protein coupled receptors that can be activated by somatostatins or its synthetic analogs. Therefore, SSTRs have been widely researched as a diagnostic marker and therapeutic target in pNETs. A large number of studies have demonstrated the clinical significance of SSTRs in pNETs. In this review, relevant literature has been appraised to summarize the most recent empirical evidence addressing the clinical significance of SSTRs in pNETs. Overall, these studies have shown that SSTRs have great value in the diagnosis, treatment, and prognostic prediction of pNETs; however, further research is still necessary.

Keywords: somatostatin receptor, pancreatic neuroendocrine tumor, somatostatin analog, peptide receptor radionuclide therapy, somatostatin receptor imaging

INTRODUCTION

Pancreatic neuroendocrine tumors (pNETs) originate from the neuroendocrine cells in the pancreas and belong to a group of diverse neuroendocrine neoplasms (NENs) (1). Of all the different types of pancreatic neoplasms, pNETs only account for 1 to 2% and are therefore defined as uncommon tumors with a clinical incidence of <1 patient per 100,000 individuals per year (2). Although considered rare, their clinical incidence has been rising from 0.27 to 1.00 per 100,000 individuals in the last 40 years (3). Furthermore, an increasing number of patients are getting diagnosed in earlier stages, possibly due to improved diagnostic methods, in particular endoscopic and imaging techniques (2). Pancreatic NENs (p-NENs) can be classified into two groups according to the presentation of hormone related symptoms: non-functioning (NF-pNENs) or functioning (F-pNENs). A minor fraction (30%) of pNETs are F-pNENs which may release peptides and hormones, for instance vasoactive intestinal peptide (VIP), gastrin, insulin, glucagon, *etc.* (4). Even though most of the pNETs arise sporadically, they have been associated with genetical conditions as well, including tuberous sclerosis, von Hippel Lindau disease, multiple endocrine neoplasia (MEN)-1 (which is also accountable for <5% of insulinomas and 20–30% of gastrinomas),

and neurofibromatosis-1. According to their pathological features, pNETs have been categorized as follows: grade 1, which has a well-differentiated morphology and Ki-67 <3%; grade 2, which also has a well-differentiated morphology and Ki-67 3–20%; and grade 3, neuroendocrine carcinomas with Ki-67 >20% and poorly differentiated morphology. The World Health Organization (WHO) introduced the following subgroup to a new grading system for pNETs in 2017: well-differentiated neuroendocrine tumors (NETs) with a Ki-67 >20%, defined as grade 3 pNET, which is clearly different from poorly differentiated neuroendocrine carcinoma, defined as grade 3 pNEC (5, 6). The grade and stage of the pNET determine a patient's prognosis. Tumors of less than 2 cm usually have a very good prognosis and indicate an indolent grade or biology (7–10). The majority (>80%) of patients with localized tumors, stage I or II, that qualify for resection are cured by undergoing solely surgery. The survival of grade 1 and grade 2 pNETs has significantly improved over the last thirty years, reflected by an increase of around 2 to 5 years in median overall survival (OS) (3). A less promising prognosis is seen in advanced grade 3 pNETs, although it is still superior to poorly differentiated (grade 3) pNECs, with a 5-year survival rate of approximately 29% (11). Surgery is both the main and most significant treatment as well as the only method to cure pNETs. Patients who are unsuitable for surgery can be offered systemic therapy such as peptide receptor radionuclide therapy (PRRT), chemotherapy, targeted therapy, and somatostatin analog (12).

Somatostatin receptors (SSTRs) belong to the superfamily of G protein-coupled receptors (GPCRs) and can be activated by their ligands to exert their physiological function (13). Knowledge of SSTRs and their activation has increased over the last 20 years as a result of many clinical and translational studies and has led to the development of novel treatments (14). The clear effectiveness of somatostatin (SST) analogs (SSAs) has been demonstrated in the treatment of numerous diseases including pancreatitis, nephro- or retinopathy as complications of obesity and diabetes, some types of pain, inflammation, and acromegaly (excessive growth hormone produced by the body) (15, 16). In addition, one of the unique features of NETs is the overexpression of SSTRs. Diagnostic and treatment approaches targeting SSTR with SSAs have shown advantages and a promising future prospect (17–20). **Figure 1** represents the theranostic significance of SSTRs in patients with NETs.

In this review, we focused on the diagnostic, prognostic, and therapeutic values of SSTRs in the management of pNETs.

BIOLOGY OF SSTRs AND SSAs

Five subtypes of SSTRs have been discovered (13). Receptor sequences for human SSTRs range in length from 364 amino acids for SSTR5 to 418 amino acids for SSTR3. Unfortunately, crystal structures are not yet available for any SSTR (14). The coding sequences of the genes that encode SSTRs are all intronless, with the exception of SSTR2. The SSTR2 gene could be spliced to generate two distinct receptor proteins, SSTR2A and SSTR2B, which are different in carboxyl termini sequence and length. Only human tissues encompass the unspliced variant

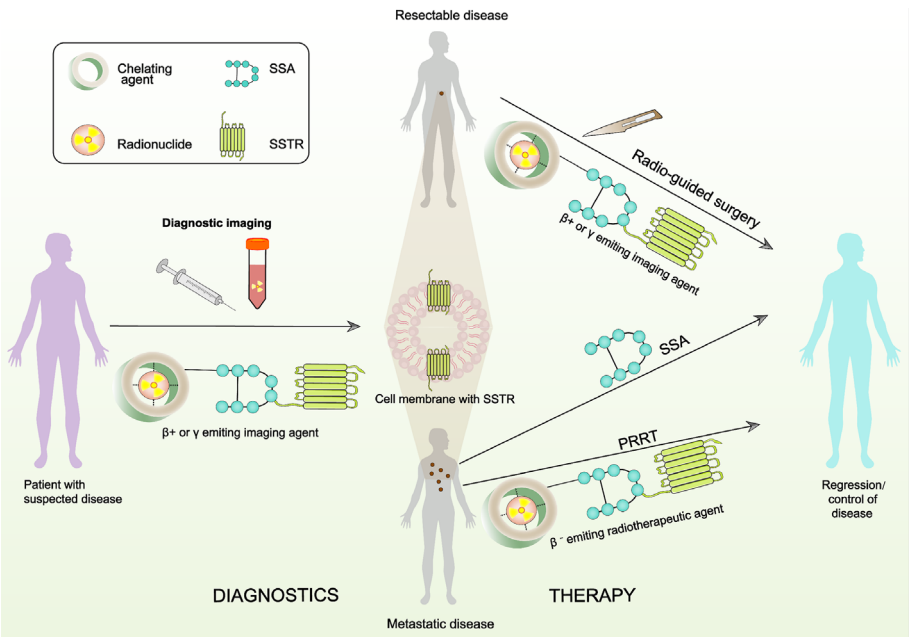

FIGURE 1 | A schematic presentation of theranostics with radiolabeled SSAs that target the SSTRs. The radiopharmaceutical element is comprised of the targeting fraction (SSA) and a chelator that forms a steady composite with the radionuclide. Radiotheranostics consists of diagnostic (panel on the left) and therapeutic (panel on the right) aspects.

of SSTR2A (21). Although SSAs that target SSTR2 and SSTR5 have important therapeutic functions in the treatment of endocrine tumors, it is remarkable that only a few mutations associated with disease have been detected in the somatotropin release-inhibiting factor (SRIF) system, which consist of seven genes (five receptor genes and two peptide precursors). To date, there has been only one report of an acromegaly patient, who is resistant to octreotide treatment and demonstrated a mutation (R240W) of SSTR5 which evidently affected signaling of the receptor (22). SSTR expression can generally be found in tumors and healthy tissues. SSTRs are based in cellular membranes that consist of seven membrane-spanning domains and are connected to the transmembrane potassium ion channels, calcium ion channels, and intracellular enzymes including adenylate cyclase (ACL) and phosphotyrosine phosphatases (PTPs) like phosphotyrosine phosphatase η (PTPη), Src homology phosphatase 1 (SHP1), and Src homology phosphatase 2 (SHP2). After binding to the SST or SSA, intracellular pathways are activated by SSTRs resulting in antiproliferative and antisecretory effects. In addition, activation of SSTR2 and SSTR3 also exert proapoptotic effects as shown in **Figure 2** (23–26).

Natural SST, also referred to as SRIF, is a cyclic polypeptide of which two isotypes exist (SST-14 and SST-28, which consist of a N-terminal extension). SST functions as an internal regulator of inhibition and is part of the neuropeptide family. SST-14 as well as SST-28 possess a high affinity to bind each of the five related subtypes of SSTRs (14). The hypothalamus can secrete SST, which leads to the inhibition of essential hormones, for instance thyroid-stimulating hormone and growth hormone. Whereas in the gastrointestinal tract, the production of gastric acid is controlled by SST as well as inhibition of the secretion of diverse hormones, namely cholecystokinin, gastrin, glucagon, VIP, secretin, insulin, and gastric inhibitory polypeptide (GIP). In addition, SST can also reduce motility in the gastrointestinal tract and contraction in the gallbladder through the reduction of blood flow and inhibition of exocrine pancreatic secretion (23).

The induction of various biological effects following activation of the SSTR resulted in identifying them as important therapeutic targets. However, the use of native SST as *in vivo* therapy is limited because it has a remarkably short half-life. Thus, many different analogs have been developed that could extend the biological actions of SST, prolong its persistence in the body, and often possess increased efficacy. Among these, the very first octapeptide that was developed was octreotide, which could sustain a half-life of 90–120 min following subcutaneous administration. Subsequently, lanreotide and vapreotide were developed, which were cyclooctapeptide SSAs (27). It has been discovered recently that pasireotide (SOM-230) is one of the very first analogs to demonstrate a strong affinity for

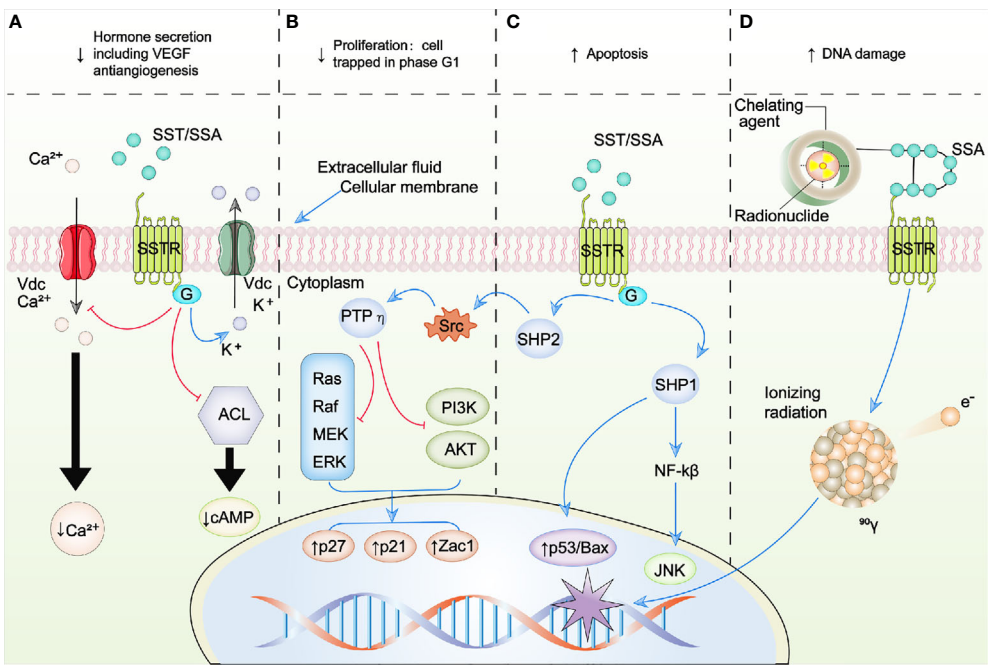

FIGURE 2 | Schematic representation of SSTR-targeted therapy. **(A–C)** represent the intracellular signaling pathways modulated by SSA/SST. **(D)** represents the schematic of peptide receptor radionuclide therapy (PRRT). Blue arrows, activation; red arrows, inhibition; ↑, increase; ↓, decrease; ACL, adenylate cyclase; AKT, protein kinase B; BAX, B-cell lymphoma 2 (BCL2)-associated X protein; Ca2+, calcium; G, G protein; JNK, c-Jun N-terminal kinases; K+, potassium; MEK, mitogen-activated protein kinase kinase; NFκB, nuclear factor kappa B; PI3K, phosphoinositide 3 kinase; PTPη, phosphotyrosine phosphatase η; raf, rapidly accelerated fibrosarcoma kinase; ras, RAS kinase; SHP1, Src homology phosphatase 1; SHP2, Src homology phosphatase 2; Src, Rous sarcoma oncogene; SSAs, somatostatin analogues; SST, somatostatin; SSTR, somatostatin receptor; Vdc, voltage-dependent channel; VEGF, vascular endothelial growth factor; Zac1, zinc finger protein regulator of apoptosis and cell cycle arrest.

the majority of SSTR subtypes, except for SSTR4 (also known as pansomatostatin analog), while octreotide and lanreotide only show a high affinity for SSTR2 and SSTR5 as shown in **Table 1** (29). Consequently, the development of synthetic SSAs promoted the clinical use of radiolabeled SSAs, either in imaging, combined with probes in various clinical practices, or as therapy, with a large number of compounds in clinical research. For instance ^{90}Y or ^{177}Lu-DOTATATE and ^{177}Lu-DOTATOC for PRRT, and SSA labeled with ^{68}Ga, such as DOTATOC, DOTATATE, and DOTANOC for somatostatin receptor imaging (SRI) (30). Each of the SSTRs has a high binding affinity to natural SST28 and SST14, while a significant difference is found in the binding affinity of radiolabeled SSAs and synthetic SSAs as shown in **Table 1** (25, 28).

PROGNOSTIC VALUES OF SSTR EXPRESSION IN pNETs

Since SSTRs are present on the surface of tumor cells, it provides a molecular basis for long-acting SSAs to be implemented in therapy and diagnostics; thus, the assessment of SSTR expression in pNETs could be important for diagnostic purposes and SSA-based treatment strategies. In previous research, the expression of SSTR subtypes in pNETs was studied mainly through immunohistochemical methods or reverse transcription PCR (RT-PCR) and only a few by receptor autoradiography (31–40). Although these studies revealed a heterogeneous SSTR expression pattern, it was confirmed in most studies that SSTR2 is the most commonly expressed subtype in pNET (**Table 2**).

Furthermore, several studies have assessed the potential value of SSTR expression in the prognosis of pNETs. For instance, Okuwaki et al. (41) retrospectively studied 79 pNET patients to evaluate the correlation between outcomes and the intensity of SSTR2a expression (SSTR-2a score from 0 to 3 by immunohistochemistry criteria). The results revealed that the survival rate of patients with a SSTR-2a score of 0 was 58% at 1 year, 51% at 3 years, and 35% at 5 years; patients with a SSTR-2a score of 1 was 88% at 1 year, 74% at 3 years, and 74% at 5 years; patients with a SSTR-2a score of 2 was 94% at 1 year, 80% at 3 years, and 80% at 5 years; and patients with a SSTR-2a score of 3 was 100% at 1 year, 3 years, as well as 5 years. As the results clearly indicate, survival was significantly reduced in patients with a SSTR-2a score of 0 compared to those with a higher SSTR-2a score, implying that assessing the SSTR2 could be valuable in choosing treatment options and estimating future survival. A retrospective study (42) that followed up 116 patients with gastroenteropancreatic neuroendocrine neoplasms (GEP-NENs) showed that the positive expression of SSTR5 and SSTR2 was associated with an improvement in survival. The results indicated that the median OS of patients with a positive expression of SSTR5 and SSTR2 had not been reached yet prior to publication, while the median OS of patients with a negative expression of SSTR5 and SSTR2 was 7.22 and 3.48 years, respectively; however the pNET subgroup was not analyzed exclusively in this study. Another retrospective study, which included 99 pNET patients, demonstrated by univariate analysis that the expression of SSTR2 was correlated to an improvement in OS, with combined survival rates of 97.5% at 1 years, 91.5% at 3 years, and 82.9% at 5 years. In addition, multivariate analysis demonstrated that positive expression of SSTR2 was a greater prognostic indicator of OS than high Ki-67 (43).

Positive expression of SSTR2 (41–44) and SSTR5 (42) has shown a significant correlation with improved OS, indicating its potential value as prognostic marker and imaging, or therapeutic target. However, an agreement on the significance of the expression of SSTR as a prognostic biomarker in pNETs has not been achieved yet and requires additional evaluation in studies of a prospective nature.

SSTR-TARGETED IMAGING IN pNETs

As discussed above, most well-differentiated pNETs contain and overexpress SSTRs (see **Table 2**) that have a higher binding affinity for these SSAs (SSTR2 > SSTR5 and 3, as shown in **Table 1**).

TABLE 1 | Somatostatin Analog Affinities.

Somatostatin analog	Affinity (IC_{50} nM)				
	SSTR1	SSTR2	SSTR3	SSTR4	SSTR5
Octreotide	>1000	0.4–2.1	4.4–34.5	>1,000	5.6–32
Lanreotide	>1000	0.5–1.8	43–107	>1,000	0.6–14
Pasireotide	9.3	1	1.5	>100	0.16
In-DTPA-octreotide	>10,000	22 ± 3.6	182 ± 13	>1,000	237 ± 52
Ga-DOTATOC	>10,000	2.5 ± 0.5	613 ± 140	>1,000	73 ± 21
Ga-DOTANOC	>10,000	1.9 ± 0.4	40.0 ± 5.8	260 ± 74	7.2 ± 1.6
Ga-DOTATATE	>10,000	0.20 ± 0.04	>1,000	300 ± 140	377 ± 18
Y-DOTATOC	>10,000	11 ± 1.7	389 ± 135	>10,000	114 ± 29
Y-DOTATATE	>10,000	1.6 ± 0.4	>1,000	523 ± 239	187 ± 50
Lu-DOTATATE	>1,000	2.0 ± 0.8	162 ± 16	>1,000	>1,000

Data from (25, 28).

All data are mean ± SD; IC_{50}: half maximum inhibitory concentration (IC_{50} depicts the concentration of a drug needed for in vitro inhibition of 50%; the lower the IC_{50}, the stronger the affinity).

TABLE 2 | SSTR expression in p-NETs.

Tumor type	SSTR subtype									
	SSTR1		SSTR2		SSTR3		SSTR4		SSTR5	
	mRNA	Protein	mRNA	Protein	mRNA	Protein	mRNA	Protein	mRNA	Protein
p-NET in general	62%(32)	30%(69)	90%(32)	78%(69)	56%(32)	78%(69)	78%(32)	12%(25)	81%(32)	76%(69)
	62%(21)	36%(25)	86%(21)	76%(25)	86%(21)	40%(25)		52%(199)	86%(21)	56%(25)
		53%(199)		55%(199)		29%(199)				34%(199)
Functioning p-NET										
Gastrinoma		30%(33)		100%(33)		79%(33)				76%(33)
Insulinoma		25%(16)		13%(16)		19%(16)		88%(16)		19%(16)
		31%(36)		58%(36)		78%(36)				78%(36)

The data on mRNA expression is obtained from studies that used RT-PCR (31–34). The data on protein expression is obtained from immunohistochemical studies (35–38, 40) that used SSTR subtype-specific antibodies and receptor autoradiography method with subtype-selective SSTR autoradiography (39). The numbers indicate the percentage of tumors that express the corresponding SSTR subtype amongst the total of tumors investigated; the numbers between parentheses represent the total number of tumors included in these studies.

Therefore, Somatostatin receptor imaging (SRI) combined with radiolabeled SSA (^{111}In-pentetreotide (Octreoscan)/^{68}Ga-DOTA-SSA PET/CT) is increasingly being used as a diagnostic tool when pNET is suspected (45). A review comparing the sensitivity of different imaging methods for pNETs and their metastases in the liver (see **Table 3**) showed that SRI has advantages in sensitivity.

As **Table 3** evidently shows, ^{111}In-pentetreotide has a higher sensitivity overall compared to cross-sectional imaging for the two types of primary pNETs (non-insulinomas) as well as a specific advantage in examining the whole body at once and thereby possibly discovering liver as well as distant metastases (47–51). ^{111}In-pentetreotide has an overall sensitivity in pNET of 60–80% (52). The use of ^{111}In-pentetreotide following cross-sectional imaging led in 39% of patients (with a total range of 16–71%) to an alteration in management (47, 51). Among all the distinct pNETs, SRI is generally not conducted in insulinomas since the sensitivity for ^{111}In-pentetreotide in benign insulinomas is considered as low, due to the low levels or absence of SSTR2 and SSTR5 in these type of tumors (53).

Different studies have used a variety of ^{68}Ga-labeled SSAs (54, 55). These mainly include ^{68}Ga-DOTATATE, ^{68}Ga-DOTATOC, and ^{68}Ga-DOTANOC (54–57). Although these three possess a different affinity for varying subtypes of SSTRs, they do have a high affinity for SSTR2 in common, and reviews including comparative studies have demonstrated that minor or no obvious differences were observed in their performances (53–55, 58, 59). Multiple published studies, in which the findings of ^{68}Ga-DOTA-SSA PET/CT were compared to those of ^{111}In-pentetreotide SPECT/CT in the exact same group of patients, concluded that ^{68}Ga-DOTA-SSA PET/CT had a significantly higher (which varied from 22 to 46%) sensitivity in the patients ^{68}Ga-DOTA-SSA PET/CT 95–100% *vs* SSTR scintigraphy 45–78%) (45, 60–63). It has been recommended most recently to replace SRI with ^{111}In-pentetreotide SPECT/CT by ^{68}Ga-DOTA-SSA PET/CT since it has a higher diagnostic accuracy and sensitivity and requires a smaller dose of radiation (45, 54, 55). However, a recently published meta-analysis, which only included pNET patients, that evaluated the detection of the primary lesion and its primary staging with ^{68}Ga-DOTA-SSA PET/CT demonstrated that the pooled specificity and sensitivity for identifying primary pNET was 95 and 79.6%, respectively (64). This sensitivity was lower compared to the results of other meta-analysis/series, which included patients with different type of NETs, and demonstrated a mean sensitivity of 92% (range between 68 and 100%), a relatively high mean specificity of 88% (range between 50 and 100%), and a high mean accuracy of 93% (range between 90 and 97%) (50, 54, 55, 65–69). These differences might be correlated to the PET/CT's spatial resolution that can cause restriction in the identification of minor pancreatic lesions and the inclusion of higher histopathological grades of pNETs in these studies which could have resulted in an increase of false-negative outcomes due to a lower expression of SSTR (70). Moreover, the inclusion of insulinoma patients could also have contributed to these differences due to their restricted expression of SSTR in

TABLE 3 | The sensitivity of different imaging modalities for pNETs and their metastases in the liver.

Imaging modality	Sensitivity (%)				
	Gastrinoma	Insulinoma	pNET <1.5 cm	pNET >2.5 cm	Liver metastasis
CT scan	5–47	20–63	34	50–94	75–100
MRI	10–44	10–85	34	60–95	67–100
US	0–21	26–50	11–33	30–76	15–77
Angiography	15–51	50–60	30–60	60–90	33–86
EUS	40–63	71–94	40–90	82–100	N/A
^{111}In-pentetreotide	30–32	33–60	29–30	52–96	90–100
^{68}GaDOTATAC PET/CT	68–100	31–90	60–80	68–100	95–100

Data from (46).

pNET, Pancreatic Neuroendocrine Tumor; CT, Computed Tomography; MRI, Magnetic Resonance Imaging; US, Ultrasound; EUS, Endoscopic Ultrasound.

comparison with carcinoids, the most common histopathological subtype of GEP-NET, resulting in the potential reduction of SSTR-PET sensitivity (71).

^{68}Ga-DOTA-SSA PET/CT also has a high sensitivity for identifying metastases in liver, lymph nodes, and distant ones (bone, *etc.*), which has a great influence on treatment, prognosis, and OS (50, 68, 72–75). Various studies (56, 76–79) have demonstrated that the tumor standardized uptake value (SUV) of ^{68}Ga-DOTA-SSA PET/CT is related to progression-free survival (PFS), Ki-67, tumor progression, and tumor grade/differentiation. Another study also found that the SUV of ^{68}Ga-DOTA-SSA PET/CT in NET patients is related to the expression of SSTR2 and can serve as a distinct predictor of OS (44). In addition, it has been demonstrated that the SUV of ^{68}Ga-DOTA-SSA PET/CT correlates with the uptake amount of radioligand in PRRT (80), and a maximum cut-off of 16.4 could predict responding lesions with a specificity of 60% and sensitivity of 95% (81).

SRI has also demonstrated its value in radioguided surgery (RGS). RGS makes use of radiopharmaceuticals that are uptaken by tumor tissues by preference. Studies found that RGS combined with ^{68}Ga-DOTATATE in GEP-NET patients showed feasibilities in guiding the removal of lymph node metastasis and both intraoperative evaluation as well as establishing the correctness of surgical margins. In addition, it could also be valuable in the identification and removal of minor tumors that were invisible or not palpable in recurrent NET patients, in whom the surgical area is covered with scar tissue (82, 83).

These studies suggest that SRI with radiolabeled SSAs have an essential role in identifying the primary tumor, initial staging, restaging, prognosis, intraoperation guidance, and evaluation of the response to treatment in pNET patients. Moreover, SRI can differentiate whether or not patients are suitable for treatment with PRRT. This is a key feature of targeting SSTRs because it provides the opportunity to personalize treatment (also referred to as theranostic approach as shown in **Figure 1**).

SSTR-TARGETED THERAPY IN pNET

The therapeutic value of PRRT and SSAs in NETs relies on the biological foundation of SSTR expression on the NET's surface (see **Figure 2**).

SSA in the Treatment of pNET

Antiproliferative Effects

SSAs function through targeting SSTRs (84). The most studied SSAs are lanreotide autogel and octreotide long-acting release (LAR), which primarily target SSTR5 and SSTR2. Whereas the newest SSA, pasireotide, can target a broader scope of SSTRs, including SSTR1, 2, 3, and 5 as shown in **Table 1** (85, 86). Due to their anti-secretory effects, SSAs were previously only used to regulate symptoms (84). However, at present their anti-proliferative effect has been widely confirmed (87).

The PROMID clinical trial was the first to provide solid evidence of the anti-proliferative effect (88, 89). This study was a double-blind, placebo-controlled, prospective phase III randomized controlled trial (RCT), in which the effect of octreotide LAR was evaluated in patients who had a metastatic or locally advanced, non-treated grade 1 midgut NET, or an idiopathic NET. The results showed that the increase in median time to progression (TTP) of the tumor was clinically and statistically significant (placebo 6 months *vs.* octreotide LAR 14.3 months and hazard ratio (HR) of 0.34 (95%-CI 0.20–0.59; p = 0.000072). The patients in this study who were in the placebo group were permitted to go over to the octreotide LAR group if progression occurred, which is probably the primary cause of TTP differences not resulting in an improvement of the OS. Even though no pNET patients were included in this RCT, the results were still regarded as powerful and led to the addition of octreotide as treatment in pNET patients to the ENETS guidelines (19, 90). This was further confirmed by a few small phase II studies and retrospective series that demonstrated the anti-proliferative effect of octreotide LAR in patients with a pNET, of which a majority were low Ki-67 NETs (as longer lasting responses were observed in patients with a low Ki-67 of less than 10) (91). The CLARINET study was a crucial phase III trial, in which the effects of SSA in pNET patients was evaluated (20, 92–94). This randomized, placebo-controlled, and double-blinded study assessed lanreotide autogel in patients who had metastatic or locally advanced, well-differentiated, and non-functioning (except for gastrinomas) GEP-NETs with a low Ki-67 of less than 10%. The (core) study duration was 96 weeks, which was followed by an open label extension (OLE) component. The majority of the included patients were treatment-naïve (84% in both groups) and were in a steady disease state during baseline (95 and 96% in the placebo and lanreotide group, respectively). The findings demonstrated an advantage in regard to PFS with a HR of 0.58 (95%-CI 0.32–1.04 in the core study) (92) and median PFS of 29.7 months in the pNET group (core study and OLE as a whole). The advantage in PFS was seen irrespective to tumor burden (20). Despite the poor response rate (2%), stabilization of disease was still high (64%), which resulted in a great disease control rate (DCR) of 66%. Data on the patients, during OLE, that crossed over to the lanreotide autogel group due to disease progression under placebo and were initially already in that group without disease progression at week 96 (n = 88) showed that, interestingly, 50% of these patients had pNETs (93). The median PFS of pNET patients was 29.7 months, which was shorter compared to the median PFS of all the included patients (38.5 months) (20). A large number of studies have tried to enhance the anti-tumor ability of SSAs by developing novel SSAs like pasireotide LAR (95) or compounds of SSAs combined with other anti-tumor media like everolimus, as demonstrated in the COOPERATE-1 study (96). However, these studies have not yielded any successful results and the clinical use of SSAs in the treatment of pNETs is, at present, still restricted to single agent approaches.

Anti-Secretory Effects

In patients with malignant insulinoma, SSAs are mainly used as second-line medical therapy to regulate hypoglycemia. A previous study has demonstrated that octreotide can be

successful in regulating hypoglycemia in a majority of insulinoma patients (97). In addition, pasireotide could be considered as an alternative treatment choice in malignant insulinomas and subsequent recurrence of hypoglycemic incidents since it is capable of regulating hypoglycemia in insulinomas that are resistant to other therapies, such as octreotide LAR, everolimus, and chemotherapy (98). However, SSAs can also exacerbate hypoglycemia through the inhibition of counter-regulatory processes, such as GH and glucagon, in insulinomas that do not express SSTRs (99). High dosages of proton pump inhibitors can effectively decrease oversecretion of gastric acid, although it cannot decrease the abnormal increase of enterochromaffin-like (ECL) cells. On the contrary, multiple studies have shown that the use of SSAs, such as lanreotide and octreotide LAR, in type 1 gastric NETs (related to chronic atrophic gastritis) and type 2 (related to the Zollinger–Ellison syndrome) can suppress the secretion of gastrin and decrease the tumor burden. Their results show that in 50–100% of gastrinomas, gastric secretion is either decreased or normalized, which resulted in the stabilization of the tumor in 47–75% of included patients. Furthermore, SSAs may be capable of inhibiting hyperplasia of ECL cells or the growth of type 2 gastric NETs (100–102). Lanreotide and octreotide have demonstrated the ability to quickly reduce diarrhea and migratory necrolytic erythema in glucagonoma patients, despite the sustained rise of glucagon levels in the serum (103–105), whereas pasireotide has been proposed as a suitable treatment approach in first-generation glucagonomas resistant to SSAs. Treatment with octreotide, as an adjuvant, in the rare vipomas was successful in decreasing VIP levels in serum and regulating diarrhea (106–108). Even though it seems contradictory to use SSAs in the treatment of somatostatinomas, a study has shown that octreotide relieved the associated symptoms and successfully decreased the levels of SST in the plasma of three patients (109).

PRRT in the Treatment of pNETs

The effectiveness of PRRT in NETs is based on the biologic foundation of SSTR expression on the NET's surface. PRRT is comprised of a radionuclide (*e.g.*, β-emitters Lutetium-177 [^{177}Lu] and Yttrium-90 [^{90}Y], α-emitter Actinum-225 [^{225}Ac]) which is connected to a chelator (DOTA) that is bound to a SSTR ligand, for instance [Tyr3] octreotide or [Tyr3] octreotate (110). This composite is intravenously given after which the ligand, [Tyr3] octreotate, first connects to the cell surface's SSTR and then supplies emission of β^- radiation with a span of 12 mm for ^{90}Y and 2 mm for ^{177}Lu (111). Among the compounds that have been studied, β-emitters, ^{90}Y-DOTATOC and ^{177}Lu-DOTATATE, have been the most widely used clinically. However, recently several clinical studies using PRRT with α-emitters have demonstrated its strengths compared with β-emitters, which will be discussed below in more details.

Anti-Tumoral Efficacy

It is worth noting that no prospective and randomized phase III trials have been conducted with PRRT in pNETs. Although, the NETTER-1 trial is the biggest study to date that evaluated the effects of PRRT, it unfortunately did not include any pNET patients (18). However, several non-randomized studies have been reviewed and they provided retrospective as well as prospective data on evaluation the use of PRRT with ^{177}Lu-DOTATATE in pNET patients (112, 113). The results showed a median objective response rate (ORR) of 58% (with a range between 13 and 73%), a median DCR of 83% (with a range between 50 and 94%), a median OS between 42 and 71 months, and a median PFS ranging between 25 and 34 months. A retrospectively conducted study including 74 GEP NET patients demonstrated that a more elevated ORR (adjusted SWOG criteria) of 73 *vs* 39% (p = 0.005) was found in pNET patients. This group of patients also seemed to have a longer median OS (57 *vs.* 45 months); however, this finding was only observed in the univariate analysis (p = 0.037) and not in the multivariate analysis (p = 0.173) (112). Another retrospective study that included 310 GEP-NET patients showed that the patients with functional pNETs had a decreased disease-specific survival in comparison to patients with non-functional GEP-NETs (33 *vs.* >48 months, respectively, p = 0.04) (114). These findings were further underwritten by the outcomes of another retrospective study which had 68 patients included. The results demonstrated a poorer median OS in functional pNETs compared to non-functional pNETs with univariate analysis (45 *vs.* 63 months, respectively, p = 0.045); however, these findings did not show statistical significance in the multivariate analysis (p = 0.506) (115).

To date, the largest study that evaluated ^{90}Y-DOTATOC has been a prospective phase II trial in which 342 pNET patients were enrolled (divided in functional pNET, n = 47 and non-functional pNET, n = 295). Nearly 50% of the pNET patients (ORR = 47%, according to the RECIST criteria) had tumor response. In addition, the study revealed a mean OS of 60 months in the group of nonfunctional pNET patients (116).

Although PRRT with β-emitters has shown a good clinical effect, recently, a more promising radionuclide, α-emitters has attracted increased attention in radionuclide therapy (117, 118). Radioisotopes that emit α-particles which have higher energy and shorter penetration range in comparison with β-particles, induce a higher probability of double strand breaks and minimum damage to surrounding healthy tissue (119, 120). These α-emitters have demonstrated promising therapeutic effects in a few pre-clinical *in vitro* (121–123) or *in vivo* (124, 125) studies. Currently, the only clinical experience with ^{213}Bi-DOTATOC included seven patients with advanced NETs with liver metastases who were refractory to treatment with ^{90}Y-DOTATOC or ^{177}Lu-DOTATOC (117). It demonstrated lower toxicity, better specific tumor binding than with β-irradiation, and partial remission of metastases. Two years after receiving ^{213}Bi-DOTATOC targeted alpha therapy (TAT), all seven patients were still alive. A study with another type of α-emitters, ^{225}Ac, had included 10 patients with progressive NETs after β-PRRT. In line with ^{213}Bi, ^{225}Ac-DOTATOC was well tolerated and effective (126). Another recent study with ^{225}Ac-DOTATATE confirmed the potential of these radiotracers

as an additional, and valuable, treatment option for patients who are refractory to ^{177}Lu-DOTATATE therapy. The included 32 patients, who previously received ^{177}Lu-DOTATATE therapy, were treated with ^{225}Ac-DOTATATE. Of them, 24 patients were assessed as responsive, with nine as stabilized disease and 15 partial remissions (127). The clinical experience with TAT in NETs has shown very promising results even in patients refractory to treatment with β-particles. However, further investigations are needed due to the limited amount of clinical evidence.

Efficacy in Hormone-Related Symptoms

There have been two studies that studied PRRT as treatment of gastrinomas (128, 129). In one of these studies 11 gastrinoma patients were assessed, and the results indicated that every patient experienced improvement of their symptoms although, the median OS was just 14 months (129). In contrast, the findings of the other study,which assessed 36 gastrinoma patients, revealed an ORR of 30% as well as a clinically observed response rate of 16% (128). In addition, the median OS was reported to be 45 months in the patients that were considered as responders. In terms of malignant insulinomas, there is a limited amount of data by means of case reports or series that indicate a positive result of PRRT in stabilization of disease as well as hypoglycemia (130, 131). Another recently published retrospective study, which had 34 functional pNET patients with metastasis and persistent hormonal symptoms included in it, reported that most patients (71%) showed a significant improvement in terms of the functional syndrome and 80% of them showed a decrease in the circulating levels of related hormones. Following PRRT, the outcomes demonstrated a median PFS of 18.1 months, which was correlated to a coexisting improvement of quality of life (132).

Overall, PRRT can be considered as a real innovation in the treatment of NETs. Even though randomized and prospective data of PRRT in pNETs is limited, the data that is available today indicates that it is an effective treatment for pNETs and should be studied further.

FUTURE PROSPECTIVE

SSTR Antagonists in Imaging and Therapy

SRI and PRRT use radiolabeled SSAs (see **Table 1**), which are only SSTR agonists as mentioned previously, mainly because it is believed in general that agonists would be the most suitable for imaging since they are internalized, while SSTR antagonists are not (133). It has been uncovered recently that SSTR antagonists with radiolabeling produce more superior imaging than SSTR agonists with radiolabeling (133, 134). A study conducted *in vitro* with SSTR3 antagonists revealed that it detected 76-fold more sites of binding in comparison to the SSTR3 agonist (134). Thereafter, a few studies which only included a minor amount of NET patients (pNETs as well as GI-NETs were included) showed that SSTR2 antagonists with radiolabeling, *i.e.*, ^{111}In-DOTA-BASS and ^{68}Ga-OPS202 (^{68}Ga-NODAGA-JR11), demonstrated more superior imaging of the tumor and higher sensitivity than SSTR2 agonists with radiolabeling (28, 133–136). These results have led to the option of using ^{177}Lu-radiolabeled SSTR2 antagonists in PRRT instead of ^{177}Lu-radiolabeled SSTR2 agonists. The results of another preclinical study (137) conducted *in vivo* with SSTR2 positive cells and in mice with tumors, showed that the tumor uptake was five times more with SSTR2 radiolabeled antagonists, ^{177}Lu-DOTA-JR11, compared to the SSTR2 radiolabeled agonist, ^{177}Lu-DOTA-octreotate, which led to a longer delay in growth. When research using these two SSTR2 radiolabeled compounds were expanded to four advanced NET patients (134), the ^{177}Lu-DOTA-JR11 provided 1.7–10.6-fold higher tumor uptake dose compared to the agonist, ^{177}Lu-DOTA-octreotate, which resulted in a partial remission in half of the enrolled patients. These findings indicate that SSTR2 radiolabeled antagonists have the potential of being an improved agent in comparison to SSTR2 radiolabeled agonists in pNET/NET imaging and PRRT.

CONCLUSION

Although pNET is a highly heterogeneous disease, SSTR is expressed in most pNETs, which provides the opportunity for promising approaches and strategies in diagnosing, treating, and predicting the prognosis of pNET patients. In the previous few decades magnificent progress has been made in the clinical significance of SSTRs in pNETs. SRI and therapies with radiolabeled SSA have shown significant value in clinical practice and has been recommended in various guidelines. However, an even more promising agent, namely radiolabeled somatostatin antagonists, has shown its superiority compared with agonists. Despite the accumulation of evidence that SSTR-targeted or related therapies (*e.g.*, SSAs and SSTR-targeted PRRT) are safe and effective options for refractory or unresectable pNETs, most SSTR-targeted therapies target SSTR2, and for those SSTR2-negative patients, more effective therapeutic approaches targeting other SSTRs are urgently needed. More and larger randomized prospective trials, conducted in multiple centers with a long-term follow-up are desperately needed as well. In addition, research deciphering crystal structures for the five SSTRs are also needed, in particular to uncover the exact signaling pathways of SSTR ligands and SSAs that underlie its antitumor effects and to facilitate the development of novel SSTR subtype-selective agents, along with the detection and selection of appropriate candidate patients who could benefit from these therapies.

AUTHOR CONTRIBUTIONS

SJ conceived of the presented idea. YH and ZY wrote the manuscript. FW and YQ searched the literature. XX and XY supervised the project. All authors contributed to the article and approved the submitted version.

FUNDING

This work was supported by grants from National Science Foundation of China (No.81871950 and 81972250); Scientific Innovation Project of Shanghai Education Committee (2019-01-07-00-07-E00057); and National Science Foundation for Distinguished Young Scholars of China [81625016], Shanghai Municipal Commission of Health and Family Planning (No. 2018YQ06).

REFERENCES

1. Alsidawi S, Westin GFM, Hobday TJ, Halfdanarson TR. Pancreatic Neuroendocrine Tumors: A Population-Based Analysis of Epidemiology and Outcomes. *J Clin Oncol* (2017) 35(4_suppl):401–. doi: 10.1200/JCO.2017.35.4_suppl.401
2. Hallet J, Law CHL, Cukier M, Saskin R, Liu N, Singh S. Exploring the Rising Incidence of Neuroendocrine Tumors: A Population-Based Analysis of Epidemiology, Metastatic Presentation, and Outcomes. *Cancer* (2015) 121 (4):589–97. doi: 10.1002/cncr.29099
3. Dasari A, Shen C, Halperin D, Zhao B, Zhou SH, Xu Y, et al. Trends in the Incidence, Prevalence, and Survival Outcomes in Patients With Neuroendocrine Tumors in the United States. *JAMA Oncol* (2017) 3 (10):1335–42. doi: 10.1001/jamaoncol.2017.0589
4. Ito T, Lee L, Jensen RT. Treatment of Symptomatic Neuroendocrine Tumor Syndromes: Recent Advances and Controversies. *Expert Opin Pharmacother* (2016) 17(16):2191–205. doi: 10.1080/14656566.2016.1236916
5. Kim JY, Hong S-M, Ro JY. Recent Updates on Grading and Classification of Neuroendocrine Tumors. *Ann Diagn Pathol* (2017) 29:11–6. doi: 10.1016/j.anndiagpath.2017.04.005
6. Choe J, Kim KW, Kim HJ, Kim DW, Kim KP, Hong S-M, et al. What Is New in the 2017 World Health Organization Classification and 8th American Joint Committee on Cancer Staging System for Pancreatic Neuroendocrine Neoplasms? *Korean J Radiol* (2019) 20(1):5–17. doi: 10.3348/kjr.2018.0040
7. Marchegiani G, Landoni L, Andrianello S, Masini G, Cingarlini S, D'Onofrio M, et al. Patterns of Recurrence After Resection for Pancreatic Neuroendocrine Tumors: Who, When, and Where? *Neuroendocrinology* (2019) 108(3):161–71. doi: 10.1159/000495774
8. Teo RYA, Teo TZ, Tai DWM, Tan DM, Ong S, Goh BKP. Systematic Review of Current Prognostication Systems for Pancreatic Neuroendocrine Neoplasms. *Surgery* (2019) 165(4):672–85. doi: 10.1016/j.surg.2018.10.031
9. Landoni L, Marchegiani G, Pollini T, Cingarlini S, D'Onofrio M, Capelli P, et al. The Evolution of Surgical Strategies for Pancreatic Neuroendocrine Tumors (Pan-Nens) Time-trend and Outcome Analysis From 587 Consecutive Resections at a High-volume Institution. *Ann Surg* (2019) 269(4):725–32. doi: 10.1016/j.pan.2018.05.377
10. Sallinen VJ, Le Large TTY, Tieftrunk E, Galeev S, Kovalenko Z, Haugvik SP, et al. Prognosis of Sporadic Resected Small (<= 2 Cm) Nonfunctional Pancreatic Neuroendocrine Tumors - a Multi-Institutional Study. *HPB (Oxford)* (2018) 20(3):251–9. doi: 10.1016/j.hpb.2017.08.034
11. Basturk O, Yang ZH, Tang LH, Hruban RH, Adsay V, McCall CM, et al. The High-grade (Who G3) Pancreatic Neuroendocrine Tumor Category is Morphologically and Biologically Heterogenous and Includes Both Well Differentiated and Poorly Differentiated Neoplasms. *Am J Surg Pathol* (2015) 39(5):683–90. doi: 10.1097/PAS.0000000000000408
12. Pavel M, Öberg K, Falconi M, Krenning E, Sundin A, Perren A, et al. Gastroenteropancreatic Neuroendocrine Neoplasms: ESMO Clinical Practice Guidelines for Diagnosis, Treatment and Follow-Up. *Ann Oncol: Off J Eur Soc Med Oncol* (2020) 31(7):844–60. doi: 10.1016/j.annonc.2020.03.304
13. Patel Y, Srikant C. Somatostatin Receptors. *Trends Endocrinol Metabol: TEM* (1997) 8(10):398–405. doi: 10.1016/S1043-2760(97)00168-9
14. Günther T, Tulipano G, Dournaud P, Bousquet C, Csaba Z, Kreienkamp HJ, et al. International Union of Basic and Clinical Pharmacology. CV. Somatostatin Receptors: Structure, Function, Ligands, and New Nomenclature. *Pharmacol Rev* (2018) 70(4):763–835. doi: 10.1124/pr.117.015388
15. Weckbecker G, Lewis I, Albert R, Schmid H, Hoyer D, Bruns C. Opportunities in Somatostatin Research: Biological, Chemical and Therapeutic Aspects. *Nat Rev Drug Discovery* (2003) 2(12):999–1017. doi: 10.1038/nrd1255
16. Rai U, Thrimawithana TR, Valery C, Young SA. Therapeutic Uses of Somatostatin and its Analogues: Current View and Potential Applications. *Pharmacol Ther* (2015) 152:98–110. doi: 10.1016/j.pharmthera.2015.05.007
17. Baumann T, Rottenburger C, Nicolas G, Wild D. Gastroenteropancreatic Neuroendocrine Tumours (GEP-NET) - Imaging and Staging. *Best Pract Res Clin Endocrinol Metab* (2016) 30(1):45–57. doi: 10.1016/j.beem.2016.01.003
18. Strosberg J, El-Haddad G, Wolin E, Hendifar A, Yao J, Chasen B, et al. Phase 3 Trial of Lu-Dotatate for Midgut Neuroendocrine Tumors. *New Engl J Med* (2017) 376(2):125–35. doi: 10.1056/NEJMoa1607427
19. Pavel M, O'Toole D, Costa F, Capdevila J, Gross D, Kianmanesh R, et al. Enets Consensus Guidelines Update for the Management of Distant Metastatic Disease of Intestinal, Pancreatic, Bronchial Neuroendocrine Neoplasms (NEN) and NEN of Unknown Primary Site. *Neuroendocrinology* (2016) 103(2):172–85. doi: 10.1159/000443167
20. Wolin EM, Pavel M, Cwikla JB, Phan AT, Raderer M, Sedlackova E, et al. Final Progression-Free Survival (PFS) Analyses for Lanreotide Autogel/Depot 120 Mg in Metastatic Enteropancreatic Neuroendocrine Tumors (Nets): The CLARINET Extension Study. *J Clin Oncol* (2017) 35:4089. doi: 10.1200/JCO.2017.35.15_suppl.4089
21. Vanetti M, Kouba M, Wang X, Vogt G, Höllt V. Cloning and Expression of a Novel Mouse Somatostatin Receptor (SSTR2B). *FEBS Lett* (1992) 311 (3):290–4. doi: 10.1016/0014-5793(92)81122-3
22. Ballare E, Persani L, Lania AG, Filopanti M, Giammona E, Corbetta S, et al. Mutation of Somatostatin Receptor Type 5 in an Acromegalic Patient Resistant to Somatostatin Analog Treatment. *J Clin Endocrinol Metab* (2001) 86(8):3809–14. doi: 10.1210/jcem.86.8.7787
23. Lamberts SW, van der Lely AJ, de Herder WW, Hofland LJ. Octreotide. *New Engl J Med* (1996) 334(4):246–54. doi: 10.1056/NEJM199601253340408
24. Dasgupta P. Somatostatin Analogues: Multiple Roles in Cellular Proliferation, Neoplasia, and Angiogenesis. *Pharmacol Ther* (2004) 102 (1):61–85. doi: 10.1016/j.pharmthera.2004.02.002
25. Barbieri F, Bajetto A, Pattarozzi A, Gatti M, Würth R, Thellung S, et al. Peptide Receptor Targeting in Cancer: The Somatostatin Paradigm. *Int J Pept* (2013) 2013:926295. doi: 10.1155/2013/926295
26. Abdel-Rahman O, Lamarca A, Valle JW, Hubner RA. Somatostatin Receptor Expression in Hepatocellular Carcinoma: Prognostic and Therapeutic Considerations. *Endocr Relat Cancer* (2014) 21(6):R485–93. doi: 10.1530/ERC-14-0389
27. Patel Y. Somatostatin and its Receptor Family. *Front Neuroendocrinol* (1999) 20(3):157–98. doi: 10.1006/frne.1999.0183
28. Fani M, Nicolas GP, Wild D. Somatostatin Receptor Antagonists for Imaging and Therapy. *J Nucl Med* (2017) 58(Suppl 2):61s–6s. doi: 10.2967/jnumed.116.186783
29. Schmid HA. Pasireotide (SOM230): Development, Mechanism of Action and Potential Applications. *Mol Cell Endocrinol* (2008) 286(1-2):69–74. doi: 10.1016/j.mce.2007.09.006
30. Ambrosini V, Fani M, Fanti S, Forrer F, Maecke H. Radiopeptide Imaging and Therapy in Europe. *J Nucl Med: Off Publ Soc Nucl Med* (2011) 52 (Supplement 2):42S–55S. doi: 10.2967/jnumed.110.085753
31. Nakayama Y, Wada R, Yajima N, Hakamada K, Yagihashi S. Profiling of Somatostatin Receptor Subtype Expression by Quantitative PCR and Correlation With Clinicopathological Features in Pancreatic Endocrine Tumors. *Pancreas* (2010) 39(8):1147–54. doi: 10.1097/MPA.0b013e3181e78120
32. O'Toole D, Saveanu A, Couvelard A, Gunz G, Enjalbert A, Jaquet P, et al. The Analysis of Quantitative Expression of Somatostatin and Dopamine Receptors in Gastro-Entero-Pancreatic Tumours Opens New Therapeutic Strategies. *Eur J Endocrinol* (2006) 155(6):849–57. doi: 10.1530/eje.1.02307
33. Jaïs P, Terris B, Ruszniewski P, LeRomancer M, Reyl-Desmars F, Vissuzaine C, et al. Somatostatin Receptor Subtype Gene Expression in Human

Endocrine Gastroentero-Pancreatic Tumours. *Eur J Clin Invest* (1997) 27 (8):639–44. doi: 10.1046/j.1365-2362.1997.1740719.x
34. Papotti M, Bongiovanni M, Volante M, Allìa E, Landolfi S, Helboe L, et al. Expression of Somatostatin Receptor Types 1-5 in 81 Cases of Gastrointestinal and Pancreatic Endocrine Tumors. A Correlative Immunohistochemical and Reverse-Transcriptase Polymerase Chain Reaction Analysis. *Virchows Archiv: An Int J Pathol* (2002) 440(5):461–75. doi: 10.1007/s00428-002-0609-x
35. Kulaksiz H, Eissele R, Rössler D, Schulz S, Höllt V, Cetin Y, et al. Identification of Somatostatin Receptor Subtypes 1, 2A, 3, and 5 in Neuroendocrine Tumours With Subtype Specific Antibodies. *Gut* (2002) 50(1):52–60. doi: 10.1136/gut.50.1.52
36. Zamora V, Cabanne A, Salanova R, Bestani C, Domenichini E, Marmissolle F, et al. Immunohistochemical Expression of Somatostatin Receptors in Digestive Endocrine Tumours. *Digestive Liver Dis: Off J Ital Soc Gastroenterol Ital Assoc Study Liver* (2010) 42(3):220–5. doi: 10.1016/j.dld.2009.07.018
37. Fjällskog M, Ludvigsen E, Stridsberg M, Oberg K, Eriksson B, Janson E. Expression of Somatostatin Receptor Subtypes 1 to 5 in Tumor Tissue and Intratumoral Vessels in Malignant Endocrine Pancreatic Tumors. *Med Oncol (Northwood London England)* (2003) 20(1):59–67. doi: 10.1385/MO:20:1:59
38. Song KB, Kim SC, Kim JH, Seo DW, Hong SM, Park KM, et al. Prognostic Value of Somatostatin Receptor Subtypes in Pancreatic Neuroendocrine Tumors. *Pancreas* (2016) 45(2):187–92. doi: 10.1097/MPA.0000000000000493
39. Reubi J, Waser B. Concomitant Expression of Several Peptide Receptors in Neuroendocrine Tumours: Molecular Basis for *In Vivo* Multireceptor Tumour Targeting. *Eur J Nucl Med Mol Imag* (2003) 30(5):781–93. doi: 10.1007/s00259-003-1184-3
40. Portela-Gomes G, Stridsberg M, Grimelius L, Rorstad O, Janson E. Differential Expression of the Five Somatostatin Receptor Subtypes in Human Benign and Malignant Insulinomas - Predominance of Receptor Subtype 4. *Endocr Pathol* (2007) 18(2):79–85. doi: 10.1007/s12022-007-0014-8
41. Okuwaki K, Kida M, Mikami T, Yamauchi H, Imaizumi H, Miyazawa S, et al. Clinicopathologic Characteristics of Pancreatic Neuroendocrine Tumors and Relation of Somatostatin Receptor Type 2A to Outcomes. *Cancer* (2013) 119(23):4094–102. doi: 10.1002/cncr.28341
42. Wang Y, Wang W, Jin K, Fang C, Lin Y, Xue L, et al. Somatostatin Receptor Expression Indicates Improved Prognosis in Gastroenteropancreatic Neuroendocrine Neoplasm, and Octreotide Long-Acting Release is Effective and Safe in Chinese Patients With Advanced Gastroenteropancreatic Neuroendocrine Tumors. *Oncol Lett* (2017) 13(3):1165–74. doi: 10.3892/ol.2017.5591
43. Shreya M, dRP R, Preetjote G, Juliana A, Lisa DU, Anubhav M, et al. Somatostatin Receptor SSTR-2a Expression is a Stronger Predictor for Survival Than Ki-67 in Pancreatic Neuroendocrine Tumors. *Medicine* (2015) 94(40):e1281. doi: 10.1097/MD.0000000000001281
44. Brunner P, Jörg A-C, Glatz K, Bubendorf L, Radojewski P, Umlauft M, et al. The Prognostic and Predictive Value of Sstr-Immunohistochemistry and Sstr-Targeted Imaging in Neuroendocrine Tumors. *Eur J Nucl Med Mol Imag* (2017) 44(3):468–75. doi: 10.1007/s00259-016-3486-2
45. Graham MM, Gu X, Ginader T, Breheny P, Sunderland JJ. Ga-68-DOTATOC Imaging of Neuroendocrine Tumors: A Systematic Review and Metaanalysis. *J Nucl Med* (2017) 58(9):1452–8. doi: 10.2967/jnumed.117.191197
46. Lee L, Ito T, Jensen RT. Imaging of Pancreatic Neuroendocrine Tumors: Recent Advances, Current Status, and Controversies. *Expert Rev Anticancer Ther* (2018) 18(9):837–60. doi: 10.1080/14737140.2018.1496822
47. Barrio M, Czernin J, Fanti S, Ambrosini V, Binse I, Du L, et al. The Impact of Somatostatin Receptor-Directed PET/CT on the Management of Patients With Neuroendocrine Tumor: A Systematic Review and Meta-Analysis. *J Nucl Med* (2017) 58(5):756–61. doi: 10.2967/jnumed.116.185587
48. van Essen M, Sundin A, Krenning EP, Kwekkeboom DJ. Neuroendocrine Tumours: The Role of Imaging for Diagnosis and Therapy. *Nat. Rev. Endocrinol.* (2014) 10(2):102–14. doi: 10.1038/nrendo.2013.246
49. Gibril F, Reynolds JC, Doppman JL, Chen CC, Venzon DJ, Termanini B, et al. Somatostatin Receptor Scintigraphy: Its Sensitivity Compared With That of Other Imaging Methods in Detecting Primary and Metastatic Gastrinomas - a Prospective Study. *Ann Intern Med* (1996) 125(1):26–+. doi: 10.7326/0003-4819-125-1-199607010-00005
50. Gibril F, Doppman JL, Reynolds JC, Chen CC, Sutliff VE, Yu F, et al. Bone Metastases in Patients With Gastrinomas: A Prospective Study of Bone Scanning, Somatostatin Receptor Scanning, and Magnetic Resonance Image in Their Defection, Frequency, Location, and Effect of Their Detection on Management. *J Clin Oncol* (1998) 16(3):1040–53. doi: 10.1200/JCO.1998.16.3.1040
51. Gibril F, Jensen R. Diagnostic Uses of Radiolabelled Somatostatin Receptor Analogues in Gastroenteropancreatic Endocrine Tumours. *Digestive Liver Dis: Off J Ital Soc Gastroenterol Ital Assoc Study Liver* (2004) 36(Supplement 1):S106–20. doi: 10.1016/j.dld.2003.11.024
52. Sundin A, Arnold R, Baudin E, Cwikla JB, Eriksson B, Fanti S, et al. Enets Consensus Guidelines for the Standards of Care in Neuroendocrine Tumors: Radiological, Nuclear Medicine and Hybrid Imaging. *Neuroendocrinology* (2017) 105(3):212–44. doi: 10.1159/000471879
53. Dromain C, Deandreis D, Scoazec JY, Goere D, Ducreux M, Baudin E, et al. Imaging of Neuroendocrine Tumors of the Pancreas. *Diagn Interv Imaging* (2016) 97(12):1241–57. doi: 10.1016/j.diii.2016.07.012
54. Ito T, Jensen RT. Molecular Imaging in Neuroendocrine Tumors: Recent Advances, Controversies, Unresolved Issues, and Roles in Management. *Curr Opin Endocrinol Diabetes Obes* (2017) 24(1):15–24. doi: 10.1097/MED.0000000000000300
55. Ambrosini V, Morigi JJ, Nanni C, Castellucci P, Fanti S. Current Status of PET Imaging of Neuroendocrine Tumours (18F FDOPA, 68Ga Tracers, 11C/18F -HTP). *Q J Nucl Med Mol Imaging* (2015) 59(1):58–69.
56. Wild D, Bomanji JB, Benkert P, Maecke H, Ell PJ, Reubi JC, et al. Comparison of Ga-68-DOTANOC and Ga-68-DOTATATE Pet/Ct Within Patients With Gastroenteropancreatic Neuroendocrine Tumors. *J Nucl Med* (2013) 54(3):364–72. doi: 10.2967/jnumed.112.111724
57. Johnbeck CB, Knigge U, Kjaer A. PET Tracers for Somatostatin Receptor Imaging of Neuroendocrine Tumors: Current Status and Review of the Literature. *Future Oncol* (2014) 10(14):2259–77. doi: 10.2217/fon.14.139
58. Velikyan I, Sundin A, Sorensen J, Lubberink M, Sandstrom M, Garske-Roman U, et al. Quantitative and Qualitative Intrapatient Comparison of Ga-68-DOTATOC and Ga-68-DOTATATE: Net Uptake Rate for Accurate Quantification. *J Nucl Med* (2014) 55(2):204–10. doi: 10.2967/jnumed.113.126177
59. Yang J, Kan Y, Ge BH, Yuan L, Li C, Zhao W. Diagnostic Role of Gallium-68 DOTATOC and Gallium-68 Dotatate PET in Patients With Neuroendocrine Tumors: A Meta-Analysis. *Acta Radiol* (2014) 55(4):389–98. doi: 10.1177/0284185113496679
60. Van Binnebeek S, Vanbilloen B, Baete K, Terwinghe C, Koole M, Mottaghy FM, et al. Comparison of Diagnostic Accuracy of In-111-pentetreotide SPECT and Ga-68-DOTATOC Pet/Ct: A Lesion-by-Lesion Analysis in Patients With Metastatic Neuroendocrine Tumours. *Eur Radiol* (2016) 26 (3):900–9. doi: 10.1007/s00330-015-3882-1
61. Deppen SA, Liu E, Blume JD, Clanton J, Shi C, Jones-Jackson LB, et al. Safety and Efficacy of Ga-68-DOTATATE PET/CT for Diagnosis, Staging, and Treatment Management of Neuroendocrine Tumors. *J Nucl Med* (2016) 57 (5):708–14. doi: 10.2967/jnumed.115.163865
62. Sadowski SM, Neychev V, Millo C, Shih J, Nilubol N, Herscovitch P, et al. Prospective Study of Ga-68-DOTATATE Positron Emission Tomography/Computed Tomography for Detecting Gastro-Entero-Pancreatic Neuroendocrine Tumors and Unknown Primary Sites. *J Clin Oncol* (2016) 34(6):588–+. doi: 10.1200/JCO.2015.64.0987
63. Lee I, Paeng JC, Lee SJ, Shin CS, Jang J-Y, Cheon GJ, et al. Comparison of Diagnostic Sensitivity and Quantitative Indices Between Ga-68-Dotatoc PET/CT and In-111-Pentetreotide SPECT/CT in Neuroendocrine Tumors: A Preliminary Report. *Nucl Med Mol Imaging* (2015) 49(4):284–90. doi: 10.1007/s13139-015-0356-y
64. Bauckneht M, Albano D, Annunziata S, Santo G, Guglielmo P, Frantellizzi V, et al. Somatostatin Receptor Pet/Ct Imaging for the Detection and Staging of Pancreatic Net: A Systematic Review and Meta-Analysis. *Diagn (Basel Switzerland)* (2020) 10(8):598. doi: 10.3390/diagnostics10080598
65. Deppen SA, Blume J, Bobbey AJ, Shah C, Graham MM, Lee P, et al. Ga-68-DOTATATE Compared With In-111-DTPA-Octreotide and Conventional Imaging for Pulmonary and Gastroenteropancreatic Neuroendocrine Tumors: A Systematic Review and Meta-Analysis. *J Nucl Med* (2016) 57 (6):872–8. doi: 10.2967/jnumed.115.165803
66. Skoura E, Michopoulou S, Mohmaduvesh M, Panagioddis E, Al Harbi M, Toumpanakis C, et al. The Impact of Ga-68-DOTATATE Pet/Ct Imaging on

Management of Patients With Neuroendocrine Tumors: Experience From a National Referral Center in the United Kingdom. *J Nucl Med* (2016) 57 (1):34–40. doi: 10.2967/jnumed.115.166017
67. Mojtahedi A, Thamake S, Tworowska I, Ranganathan D, Delpassand ES. The Value of Ga-68-DOTATATE PET/CT in Diagnosis and Management of Neuroendocrine Tumors Compared to Current FDA Approved Imaging Modalities: A Review of Literature. *Am J Nucl Med Mol Imaging* (2014) 4 (5):426–34.
68. Merola E, Pavel ME, Panzuto F, Capurso G, Cicchese N, Rinke A, et al. Functional Imaging in the Follow-Up of Enteropancreatic Neuroendocrine Tumors: Clinical Usefulness and Indications. *J Clin Endocrinol Metab* (2017) 102(5):1486–94. doi: 10.1210/jc.2016-3732
69. Sa de Camargo Etchebehere EC, Santos A, Gumz B, Vicente A, Hoff PG, Corradi G, et al. Ga-68-DOTATATE PET/CT, Tc-99m-HYNIC-Octreotide SPECT/CT, and Whole-Body Mr Imaging in Detection of Neuroendocrine Tumors: A Prospective Trial. *J Nucl Med* (2014) 55(10):1598–604. doi: 10.2967/jnumed.114.144543
70. Modlin I, Oberg K, Chung D, Jensen R, de Herder W, Thakker R, et al. Gastroenteropancreatic Neuroendocrine Tumours. *Lancet Oncol* (2008) 9 (1):61–72. doi: 10.1016/S1470-2045(07)70410-2
71. Zimmer T, Stölzel U, Bäder M, Koppenhagen K, Hamm B, Buhr H, et al. Endoscopic Ultrasonography and Somatostatin Receptor Scintigraphy in the Preoperative Localisation of Insulinomas and Gastrinomas. *Gut* (1996) 39 (4):562–8. doi: 10.1136/gut.39.4.562
72. Klimstra DS. Pathologic Classification of Neuroendocrine Neoplasms. *Hematol Oncol Clin North Am* (2016) 30(1):1–+. doi: 10.1016/j.hoc.2015.08.005
73. Ito T, Igarashi H, Jensen RT. Zollinger-Ellison Syndrome: Recent Advances and Controversies. *Curr Opin Gastroenterol* (2013) 29(6):650–61. doi: 10.1097/MOG.0b013e328365efb1
74. Metz DC, Jensen RT. Gastrointestinal Neuroendocrine Tumors: Pancreatic Endocrine Tumors. *Gastroenterology* (2008) 135(5):1469–92. doi: 10.1053/j.gastro.2008.05.047
75. Schraml C, Schwenzer NF, Sperling O, Aschoff P, Lichy MP, Mueller M, et al. Staging of Neuroendocrine Tumours: Comparison of Ga-68 DOTATOC Multiphase PET/CT and Whole-Body MRI. *Cancer Imaging* (2013) 13 (1):63–72. doi: 10.1102/1470-7330.2013.0007
76. Sharma P, Naswa N, Suman SKC, Alvarado LA, Dwivedi AK, Yadav Y, et al. Comparison of the Prognostic Values of Ga-68-DOTANOC PET/CT and F-18-FDG PET/CT in Patients With Well-Differentiated Neuroendocrine Tumor. *Eur J Nucl Med Mol Imag* (2014) 41(12):2194–202. doi: 10.1007/s00259-014-2850-3
77. Panagiotidis E, Alshammari A, Miehopoulou S, Skoura E, Naik K, Maragkoudakis E, et al. Comparison of the Impact of Ga-68-DOTATATE and F-18-FDG PET/CT on Clinical Management in Patients With Neuroendocrine Tumors. *J Nucl Med* (2017) 58(1):91–6. doi: 10.2967/jnumed.116.178095
78. Campana D, Ambrosini V, Pezzilli R, Fanti S, Labate A, Santini D, et al. Standardized Uptake Values of (68)Ga-DOTANOC PET: A Promising Prognostic Tool in Neuroendocrine Tumors. *J Nucl Med: Off Publ Soc Nucl Med* (2010) 51(3):353–9. doi: 10.2967/jnumed.109.066662
79. Ambrosini V, Campana D, Polverari G, Peterle C, Diodato S, Ricci C, et al. Prognostic Value of Ga-68-DOTANOC Pet/Ct SUVmax in Patients With Neuroendocrine Tumors of the Pancreas. *J Nucl Med* (2015) 56(12):1843–8. doi: 10.2967/jnumed.115.162719
80. Ezziddin S, Opitz M, Attassi M, Biermann K, Sabet A, Guhlke S, et al. Impact of the Ki-67 Proliferation Index on Response to Peptide Receptor Radionuclide Therapy. *Eur J Nucl Med Mol Imag* (2011) 38(3):459–66. doi: 10.1007/s00259-010-1610-2
81. Kratochwil C, Stefanova M, Mavriopoulou E, Holland-Letz T, Dimitrakopoulou-Strauss A, Afshar-Oromieh A, et al. SUV of Ga-68 Dotatoc-Pet/Ct Predicts Response Probability of PRRT in Neuroendocrine Tumors. *Mol Imag Biol* (2015) 17(3):313–8. doi: 10.1007/s11307-014-0795-3
82. El Lakis M, Gianakou A, Nockel P, Wiseman D, Tirosh A, Quezado M, et al. Radioguided Surgery With Gallium 68 Dotatate for Patients With Neuroendocrine Tumors. *JAMA Surg* (2019) 154(1):40–5. doi: 10.1001/jamasurg.2018.3475
83. Sadowski S, Millo C, Neychev V, Aufforth R, Keutgen X, Glanville J, et al. Feasibility of Radio-Guided Surgery With^{68} Gallium-DOTATATE in Patients With Gastro-Entero-Pancreatic Neuroendocrine Tumors. *Ann Surg Oncol* (2015) 22:S676–82. doi: 10.1245/s10434-015-4857-9
84. Stueven AK, Kayser A, Wetz C, Amthauer H, Wree A, Tacke F, et al. Somatostatin Analogues in the Treatment of Neuroendocrine Tumors: Past, Present and Future. *Int J Mol Sci* (2019) 20(12):3049. doi: 10.3390/ijms20123049
85. Toumpanakis C, Caplin ME. Update on the Role of Somatostatin Analogs for the Treatment of Patients With Gastroenteropancreatic Neuroendocrine Tumors. *Semin Oncol* (2013) 40(1):56–68. doi: 10.1053/j.seminoncol.2012.11.006
86. Kvols LK, Oberg KE, O'Dorisio TM, Mohideen P, de Herder WW, Arnold R, et al. Pasireotide (SOM230) Shows Efficacy and Tolerability in the Treatment of Patients With Advanced Neuroendocrine Tumors Refractory or Resistant to Octreotide LAR: Results From a Phase II Study. *Endocr Relat Cancer* (2012) 19(5):657–66. doi: 10.1530/ERC-11-0367
87. Garcia-Carbonero R, Sorbye H, Baudin E, Raymond E, Wiedenmann B, Niederle B, et al. Enets Consensus Guidelines for High-Grade Gastroenteropancreatic Neuroendocrine Tumors and Neuroendocrine Carcinomas. *Neuroendocrinology* (2016) 103(2):186–94. doi: 10.1159/000443172
88. Rinke A, Mueller H-H, Schade-Brittinger C, Klose K-J, Barth P, Wied M, et al. Placebo-Controlled, Double-Blind, Prospective, Randomized Study on the Effect of Octreotide LAR in the Control of Tumor Growth in Patients With Metastatic Neuroendocrine Midgut Tumors: A Report From the PROMID Study Group. *J Clin Oncol* (2009) 27(28):4656–63. doi: 10.1200/JCO.2009.22.8510
89. Rinke A, Wittenberg M, Schade-Brittinger C, Aminossadati B, Ronicke E, Gress TM, et al. Placebo-Controlled, Double-Blind, Prospective, Randomized Study on the Effect of Octreotide LAR in the Control of Tumor Growth in Patients With Metastatic Neuroendocrine Midgut Tumors (Promid): Results of Long-Term Survival. *Neuroendocrinology* (2017) 104(1):26–32. doi: 10.1159/000443612
90. Falconi M, Eriksson B, Kaltsas G, Bartsch D, Capdevila J, Caplin M, et al. Enets Consensus Guidelines Update for the Management of Patients With Functional Pancreatic Neuroendocrine Tumors and Non-Functional Pancreatic Neuroendocrine Tumors. *Neuroendocrinology* (2016) 103 (2):153–71. doi: 10.1159/000443171
91. Jann H, Denecke T, Koch M, Pape UF, Wiedenmann B, Pavel M. Impact of Octreotide Long-Acting Release on Tumour Growth Control as a First-Line Treatment in Neuroendocrine Tumours of Pancreatic Origin. *Neuroendocrinology* (2013) 98(2):137–43. doi: 10.1159/000353785
92. Caplin ME, Pavel M, Cwikla JB, Phan AT, Raderer M, Sedlackova E, et al. Lanreotide in Metastatic Enteropancreatic Neuroendocrine Tumors. *New Engl J Med* (2014) 371(3):224–33. doi: 10.1056/NEJMoa1316158
93. Caplin M, Pavel M, Ćwikła J, Phan A, Raderer M, Sedláčková E, et al. Anti-Tumour Effects of Lanreotide for Pancreatic and Intestinal Neuroendocrine Tumours: The CLARINET Open-Label Extension Study. *Endocr Relat Cancer* (2016) 23(3):191–9. doi: 10.1530/ERC-15-0490
94. Phan AT, Dasari A, Liyanage N, Cox D, Lowenthal SP, Wolin EM. Tumor Response in the CLARINET Study of Lanreotide Depot vs. Placebo in Patients With Metastatic Gastroenteropancreatic Neuroendocrine Tumors (GEP-NETs). *J Clin Oncol* (2016) 34(4_suppl):434–. doi: 10.1200/jco.2016.34.4_suppl.434
95. Cives M, Kunz PL, Morse B, Coppola D, Schell MJ, Campos T, et al. Phase II Clinical Trial of Pasireotide Long-Acting Repeatable in Patients With Metastatic Neuroendocrine Tumors. *Endocr Relat Cancer* (2015) 22(1):1–9. doi: 10.1530/ERC-14-0360
96. Kulke MH, Ruszniewski P, Van Cutsem E, Lombard-Bohas C, Valle JW, De Herder WW, et al. A Randomized, Open-Label, Phase 2 Study of Everolimus in Combination With Pasireotide LAR or Everolimus Alone in Advanced, Well-Differentiated, Progressive Pancreatic Neuroendocrine Tumors: COOPERATE-2 Trial. *Ann Oncol* (2017) 28(6):1309–15. doi: 10.1093/annonc/mdx078
97. Vezzosi D, Bennet A, Rochaix P, Courbon F, Selves J, Pradere B, et al. Octreotide in Insulinoma Patients: Efficacy on Hypoglycemia, Relationships With Octreoscan Scintigraphy and Immunostaining With anti-sst2A and Anti-Ssts Antibodies. *Eur J Endocrinol* (2005) 152(5):757–67. doi: 10.1530/eje.1.01901
98. Tirosh A, Stemmer SM, Solomonov E, Elnekave E, Saeger W, Ravkin Y, et al. Pasireotide for Malignant Insulinoma. *Horm-Int J Endocrinol Metab* (2016) 15(2):271–6. doi: 10.14310/horm.2002.1639

99. Maton P. Use of Octreotide Acetate for Control of Symptoms in Patients With Islet Cell Tumors. *World J Surg* (1993) 17(4):504–10. doi: 10.1007/BF01655110
100. Tomassetti P, Migliori M, Caletti GC, Fusaroli P, Corinaldesi R, Gullo L. Treatment of Type II Gastric Carcinoid Tumors With Somatostatin Analogues. *New Engl J Med* (2000) 343(8):551–4. doi: 10.1056/NEJM200008243430805
101. Tomassetti P, Campana D, Piscitelli L, Mazzotta E, Brocchi E, Pezzilli R, et al. Treatment of Zollinger-Ellison Syndrome. *World J Gastroenterol* (2005) 11 (35):5423–32. doi: 10.3748/wjg.v11.i35.5423
102. Prommegger R, Bale R, Ensinger C, Sauper T, Profanter C, Knoflach M, et al. Gastric Carcinoid Type I Tumour: New Diagnostic and Therapeutic Method. *Eur J Gastroenterol Hepatol* (2003) 15(6):705–7. doi: 10.1097/00042737-200306000-00020
103. Tomassetti P, Migliori M, Corinaldesi R, Gullo L. Treatment of Gastroenteropancreatic Neuroendocrine Tumours With Octreotide LAR. *Aliment Pharmacol Ther* (2000) 14(5):557–60. doi: 10.1046/j.1365-2036.2000.00738.x
104. Wermers RA, Fatourechi V, Wynne AG, Kvols LK, Lloyd RV. The Glucagonoma Syndrome - Clinical and Pathologic Features in 21 Patients. *Medicine* (1996) 75(2):53–63. doi: 10.1097/00005792-199603000-00002
105. Casadei R, Tomassetti P, Rossi C, la Donna M, Migliori M, Marrano D. Treatment of Metastatic Glucagonoma to the Liver: Case Report and Literature Review. *Ital J Gastroenterol Hepatol* (1999) 31(4):308–12.
106. Ghaferi AA, Chojnacki KA, Long WD, Cameron JL, Yeo CJ. Pancreatic VIPomas: Subject Review and One Institutional Experience. *J Gastrointest Surg* (2008) 12(2):382–93. doi: 10.1007/s11605-007-0177-0
107. Song S, Shi R, Li B, Liu Y. Diagnosis and Treatment of Pancreatic Vasoactive Intestinal Peptide Endocrine Tumors. *Pancreas* (2009) 38(7):811–4. doi: 10.1097/MPA.0b013e3181b2bc7c
108. Nakayama S, Yokote T, Kobayashi K, Hirata Y, Hiraiwa T, Komoto I, et al. Vipoma With Expression of Both VIP and VPAC1 Receptors in a Patient With WDHA Syndrome. *Endocrine* (2009) 35(2):143–6. doi: 10.1007/s12020-009-9146-6
109. Angeletti S, Corleto VD, Schillaci O, Marignani M, Annibale B, Moretti A, et al. Use of the Somatostatin Analogue Octreotide to Localise and Manage Somatostatin-Producing Tumours. *Gut* (1998) 42(6):792–4. doi: 10.1136/gut.42.6.792
110. van der Zwan WA, Bodei L, Mueller-Brand J, de Herder WW, Kvols LK, Kwekkeboom DJ. Gep-Nets UPDATE Radionuclide Therapy in Neuroendocrine Tumors. *Eur J Endocrinol* (2015) 172(1):R1–R8. doi: 10.1530/EJE-14-0488
111. Garkavij M, Nickel M, Sjogreen-Gleisner K, Ljungberg M, Ohlsson T, Wingardh K, et al. Lu-177- DOTA0,Tyr3 Octreotate Therapy in Patients With Disseminated Neuroendocrine Tumors: Analysis of Dosimetry With Impact on Future Therapeutic Strategy. *Cancer* (2010) 116(4):1084–92. doi: 10.1002/cncr.24796
112. Ramage J, Naraev BG, Halfdanarson TR. Peptide Receptor Radionuclide Therapy for Patients With Advanced Pancreatic Neuroendocrine Tumors. *Semin Oncol* (2018) 45(4):236–48. doi: 10.1053/j.seminoncol.2018.08.004
113. Starr JS, Sonbol MB, Hobday TJ, Sharma A, Kendi AT, Halfdanarson TR. Peptide Receptor Radionuclide Therapy for the Treatment of Pancreatic Neuroendocrine Tumors: Recent Insights. *Oncol Targets Ther* (2020) 13:3545–55. doi: 10.2147/OTT.S202867
114. Kwekkeboom DJ, de Herder WW, Kam BL, van Eijck CH, van Essen M, Kooij PP, et al. Treatment With the Radiolabeled Somatostatin Analog Lu-177-DOTA(0), Tyr(3) Octreotate: Toxicity, Efficacy, and Survival. *J Clin Oncol* (2008) 26(13):2124–30. doi: 10.1200/JCO.2007.15.2553
115. Ezziddin S, Khalaf F, Vanezi M, Haslerud T, Mayer K, Al Zreiqat A, et al. Outcome of Peptide Receptor Radionuclide Therapy With Lu-177-octreotate in Advanced Grade 1/2 Pancreatic Neuroendocrine Tumours. *Eur J Nucl Med Mol Imag* (2014) 41(5):925–33. doi: 10.1007/s00259-013-2677-3
116. Imhof A, Brunner P, Marincek N, Briel M, Schindler C, Rasch H, et al. Response, Survival, and Long-Term Toxicity After Therapy With the Radiolabeled Somatostatin Analogue Y-90-DOTA -TOC in Metastasized Neuroendocrine Cancers. *J Clin Oncol* (2011) 29(17):2416–23. doi: 10.1200/JCO.2010.33.7873
117. Kratochwil C, Giesel F, Bruchertseifer F, Mier W, Apostolidis C, Boll R, et al. ^{213}Bi-DOTATOC Receptor-Targeted Alpha-Radionuclide Therapy Induces Remission in Neuroendocrine Tumours Refractory to Beta Radiation: A First-in-Human Experience. *Eur J Nucl Med Mol Imag* (2014) 41(11):2106–19. doi: 10.1007/s00259-014-2857-9
118. Morgenstern A, Apostolidis C, Kratochwil C, Sathekge M, Krolicki L, Bruchertseifer F. An Overview of Targeted Alpha Therapy With Actinium and Bismuth. *Curr Radiopharmaceut* (2018) 11(3):200–8. doi: 10.2174/1874471011666180502104524
119. Brons S, Jakob B, Taucher-Scholz G, Kraft G. Heavy Ion Production of Single- and Double-Strand Breaks in Plasmid DNA in Aqueous Solution. *Physica Med: PM: An Int J Devoted Appl Phys Med Biol: Off J Ital Assoc Biomed Phys (AIFB)* (2001) 17(Suppl. 1):217–8.
120. Kim Y, Brechbiel M. An Overview of Targeted Alpha Therapy. *Tumour Biol: J Int Soc Oncodevelopmental Biol Med* (2012) 33(3):573–90. doi: 10.1007/s13277-011-0286-y
121. Nayak T, Norenberg J, Anderson T, Atcher R. A Comparison of High-Versus Low-Linear Energy Transfer Somatostatin Receptor Targeted Radionuclide Therapy *In Vitro*. *Cancer Biother Radiopharmaceut* (2005) 20(1):52–7. doi: 10.1089/cbr.2005.20.52
122. Nayak T, Norenberg J, Anderson T, Prossnitz E, Stabin M, Atcher R. Somatostatin-Receptor-Targeted Alpha-Emitting 213Bi is Therapeutically More Effective Than Beta(-)-Emitting 177Lu in Human Pancreatic Adenocarcinoma Cells. *Nucl Med Biol* (2007) 34(2):185–93. doi: 10.1016/j.nucmedbio.2006.11.006
123. Chan H, de Blois E, Morgenstern A, Bruchertseifer F, de Jong M, Breeman W, et al. In Vitro Comparison of 213Bi- and 177Lu-Radiation for Peptide Receptor Radionuclide Therapy. *PloS One* (2017) 12(7):e0181473. doi: 10.1371/journal.pone.0181473
124. Norenberg J, Krenning B, Konings I, Kusewitt D, Nayak T, Anderson T, et al. 213Bi-[DOTA0, Tyr3]octreotide Peptide Receptor Radionuclide Therapy of Pancreatic Tumors in a Preclinical Animal Model. *Clin Cancer Res: An Off J Am Assoc Cancer Res* (2006) 12:897–903. doi: 10.1158/1078-0432.CCR-05-1264
125. Miederer M, Henriksen G, Alke A, Mossbrugger I, Quintanilla-Martinez L, Senekowitsch-Schmidtke R, et al. Preclinical Evaluation of the Alpha-Particle Generator Nuclide 225Ac for Somatostatin Receptor Radiotherapy of Neuroendocrine Tumors. *Clin Cancer Res: An Off J Am Assoc Cancer Res* (2008) 14(11):3555–61. doi: 10.1158/1078-0432.CCR-07-4647
126. Zhang J, Singh A, Kulkarni H, Schuchardt C, Müller D, Wester H, et al. From Bench to Bedside-The Bad Berka Experience With First-in-Human Studies. *Semin Nucl Med* (2019) 49(5):422–37. doi: 10.1053/j.semnuclmed.2019.06.002
127. Ballal S, Yadav M, Bal C, Sahoo R, Tripathi M. Broadening Horizons With Ac-DOTATATE Targeted Alpha Therapy for Gastroenteropancreatic Neuroendocrine Tumour Patients Stable or Refractory to Lu-DOTATATE PRRT: First Clinical Experience on the Efficacy and Safety. *Eur J Nucl Med Mol Imag* (2020) 47(4):934–46. doi: 10.1007/s00259-019-04567-2
128. Dumont RA, Seiler D, Marincek N, Brunner P, Radojewski P, Rochlitz C, et al. Survival After Somatostatin Based Radiopeptide Therapy With Y-90-DOTATOC vs. Y-90-DOTATOC Plus Lu-177-DOTATOC in Metastasized Gastrinoma. *Am J Nucl Med Mol Imaging* (2015) 5(1):46–55.
129. Grozinsky-Glasberg S, Barak D, Fraenkel M, Walter MA, Mueller-Brand J, Eckstein J, et al. Peptide Receptor Radioligand Therapy is an Effective Treatment for the Long-Term Stabilization of Malignant Gastrinomas. *Cancer* (2011) 117(7):1377–85. doi: 10.1002/cncr.25646
130. van Schaik E, van Vliet EI, Feelders RA, Krenning EP, Khan S, Kamp K, et al. Improved Control of Severe Hypoglycemia in Patients With Malignant Insulinomas by Peptide Receptor Radionuclide Therapy. *J Clin Endocrinol Metab* (2011) 96(11):3381–9. doi: 10.1210/jc.2011-1563
131. Magalhães D, Sampaio IL, Ferreira G, Bogalho P, Martins-Branco D, Santos R, et al. Peptide Receptor Radionuclide Therapy With (177)Lu-DOTA-TATE as a Promising Treatment of Malignant Insulinoma: A Series of Case Reports and Literature Review. *J Endocrinol Invest* (2019) 42(3):249–60. doi: 10.1007/s40618-018-0911-3
132. Zandee WT, Brabander T, Blazevic A, Kam BLR, Teunissen JJM, Feelders RA, et al. Symptomatic and Radiological Response to Lu-177-DOTATATE for the Treatment of Functioning Pancreatic Neuroendocrine Tumors. *J Clin Endocrinol Metab* (2019) 104(4):1336–44. doi: 10.1210/jc.2018-01991
133. Wild D, Fani M, Behe M, Brink I, Rivier JEF, Reubi JC, et al. First Clinical Evidence That Imaging With Somatostatin Receptor Antagonists is Feasible. *J Nucl Med* (2011) 52(9):1412–7. doi: 10.2967/jnumed.111.088922
134. Wild D, Fani M, Fischer R, Del Pozzo L, Kaul F, Krebs S, et al. Comparison of Somatostatin Receptor Agonist and Antagonist for Peptide Receptor

Radionuclide Therapy: A Pilot Study. *J Nucl Med* (2014) 55(8):1248–52. doi: 10.2967/jnumed.114.138834

135. Nicolas G, Schreiter N, Kaul F, Uiters J, Bouterfa H, Kaufmann J, et al. Sensitivity Comparison of Ga-OPS202 and Ga-DOTATOC PET/CT in Patients With Gastroenteropancreatic Neuroendocrine Tumors: A Prospective Phase Ii Imaging Study. *J Nucl Med: Off Publ Soc Nucl Med* (2018) 59(6):915–21. doi: 10.2967/jnumed.117.199760
136. Nicolas G, Beykan S, Bouterfa H, Kaufmann J, Bauman A, Lassmann M, et al. Safety, Biodistribution, and Radiation Dosimetry of Ga-OPS202 in Patients With Gastroenteropancreatic Neuroendocrine Tumors: A Prospective Phase I Imaging Study. *J Nucl Med: Off Publ Soc Nucl Med* (2018) 59(6):909–14. doi: 10.2967/jnumed.117.199737
137. Dalm S, Nonnekens J, Doeswijk G, de Blois E, van Gent D, Konijnenberg M, et al. Comparison of the Therapeutic Response to Treatment With a 177Lu-Labeled Somatostatin Receptor Agonist and Antagonist in Preclinical Models. *J Nucl Med: Off Publ Soc Nucl Med* (2016) 57(2):260–5. doi: 10.2967/jnumed.115.167007

Conflict of Interest: The authors declare that the research was conducted in the absence of any commercial or financial relationships that could be construed as a potential conflict of interest.

frontiers in Endocrinology

ORIGINAL RESEARCH
published: 24 May 2021
doi: 10.3389/fendo.2021.667798

Effects of Sorafenib, a Tyrosin Kinase Inhibitor, on Adrenocortical Cancer

*Lidia Cerquetti[1], Barbara Bucci[2], Salvatore Raffa[3], Donatella Amendola[2], Roberta Maggio[1], Pina Lardo[1], Elisa Petrangeli[4], Maria Rosaria Torrisi[3], Vincenzo Toscano[1], Giuseppe Pugliese[1] and Antonio Stigliano[1]**

[1] Endocrinology, Department of Clinical and Molecular Medicine, Sant'Andrea Hospital Rome, Sapienza University of Rome, Rome, Italy, [2] Clinic Pathology Unit, San Pietro Hospital Fatebenefratelli, Rome, Italy, [3] Department of Clinical and Molecular Medicine, Sant'Andrea Hospital Rome, Sapienza University of Rome, Rome, Italy, [4] Department of Molecular Medicine Rome, Sapienza University of Rome, Rome, Italy

The lack of an effective medical treatment for adrenocortical carcinoma (ACC) has prompted the search for better treatment protocols for ACC neoplasms. Sorafenib, a tyrosine kinase inhibitor has exhibited effectiveness in the treatment of different human tumors. Therefore, the aim of this study was to understand the mechanism through which sorafenib acts on ACC, especially since treatment with sorafenib alone is sometimes unable to induce a long-lasting antiproliferative effect in this tumor type. The effects of sorafenib were tested on the ACC cell line H295R by evaluating cell viability, apoptosis and VEGF receptor signaling which was assessed by analyzing VE-cadherin and β-catenin complex formation. We also tested sorafenib on an *in vitro* 3D cell culture model using the same cell line. Apoptosis was observed after sorafenib treatment, and coimmunoprecipitation data suggested that the drug prevents formation VEGFR-VE-cadherin and β-catenin proteins complex. These results were confirmed both by ultrastructural analysis and by a 3D model where we observed a disaggregation of spheres into single cells, which is a crucial event that represents the first step of metastasis. Our findings suggest that although sorafenib induces apoptotic cell death a small portion of cells survive the treatment and have characteristics of a malignancy. Based on our data we recommend against the use of sorafenib in patients with ACC.

Keywords: adrenal cancer, neoangiogenesis, sorafenib, apoptosis, intercellular junctions, spheroids, matrix metalloproteinase-9, epithelium-mesenchymal transition

OPEN ACCESS

Edited by:
Barbara Altieri, University Hospital of Wuerzburg, Germany

Reviewed by:
Vincenzo Pezzi, University of Calabria, Italy
Giulia Cantini, University of Florence, Italy

***Correspondence:**
Antonio Stigliano
antonio.stigliano@uniroma1.it

Specialty section:
This article was submitted to Cancer Endocrinology, a section of the journal Frontiers in Endocrinology

Received: *14 February 2021*
Accepted: *29 March 2021*
Published: *24 May 2021*

Citation:
Cerquetti L, Bucci B, Raffa S, Amendola D, Maggio R, Lardo P, Petrangeli E, Torrisi MR, Toscano V, Pugliese G and Stigliano A (2021) Effects of Sorafenib, a Tyrosin Kinase Inhibitor, on Adrenocortical Cancer. Front. Endocrinol. 12:667798. doi: 10.3389/fendo.2021.667798

INTRODUCTION

Adrenocortical carcinoma (ACC) is a rare and malignant endocrine tumor with a worldwide incidence of approximately two cases per million people per year (1). The long term therapeutic results are limited and are largely dependent on tumor stage. Surgery is the treatment of choice for patients with primary and secondary tumors and for local recurrence (2).

Moreover several cytotoxic agents have been used as monotherapies or have been used in combination to treat advanced disease, and mitotane is the only available adrenal specific treatment for ACC; however, since it exerts a cytotoxic effect it has limited utility (3). Because of the lack of

effective treatments for this cancer, efforts to improve medical protocols for ACC are continually sought out.

Sorafenib is an inhibitor of several receptor tyrosine kinases involved in the neoangiogenesis process, including Vascular-Endothelial Growth Factor Receptors-2 (VEGFR2) and 3 (VEGFR3), and Platelet-Derived Growth Factor (PDGF). In preclinical models, it has shown efficacy against a wide variety of tumors such as breast, colon, and pancreas carcinoma (4, 5). It has been shown to block tumor angiogenesis by inhibiting serine/threonine kinases and block cell proliferation by inducing apoptosis in different human tumor cell lines (6, 7).

Since sorafenib showed a broad spectrum of antitumor activity in preclinical studies (8–10), multiple clinical trials have been undertaken to further investigate the role of this drug alone or in combination with several chemotherapies for cancer treatment. For its antineoplastic abilities, sorafenib (Nexavar, BAY43-9006, Bayer Pharmaceuticals Corp., West Haven, CT and Onyx Pharmaceuticals Corp., Emeryville, CA) has been approved by the Food and Drug Administration (FDA) for the treatment of advanced kidney and hepatocellular cancer.

Since ACC shows high levels of vascular endothelial growth factor (VEGF) (1, 11), some studies have focused on assessing the activity of sorafenib both in preclinical tumor models and in patients with adrenocortical cancer.

Mariniello et al. (12) reported the effects of sorafenib and everolimus, a mTOR inhibitor used as an anti-cancer therapy, alone or in combination in the SW13 and H295R cell lines and in a xenograft ACC model respectively. The authors demonstrated that the drug combination produced marked synergistic growth inhibition, in comparison to single agent therapy, suggesting that simultaneous inhibition of several signaling pathways may be a more effective anticancer strategy than using a single agent (12). They observed a great apoptotic effect in SW13 and H295R cells after sorafenib treatment and a significant mass reduction with increased survival particularly in SW13 xenograft model undergoing the combined sorafenib and everolimus treatment (12). Based on these results the authors concluded by proposing that the combination of molecular targeted agents may have both antiangiogenic and direct antitumor effects, thus representing a new therapeutic tool for the treatment of ACC.

In contrast, the results of the phase II study, published by Berruti et al. (13), reported the effects of metronomic administration of chemotherapeutic paclitaxel and antiangiogenic sorafenib in patients affected by advanced ACC. They observed clear disease development with a dramatic tumor progression and a significant increase in neoplastic lesions that occurred at a much higher and faster rate than the months before the start of the trial, forcing them to suspend experimentation before the end of the study. The authors concluded that, despite the antiproliferative effects observed with sorafenib in the preclinical model, treatment in patients with advanced ACC should not be recommended.

Finally, O'Sullivan and colleagues (14), demonstrated limited sorafenib effectiveness in ACC patients. After exposure of the tyrosine kinase inhibitor, the patients did not have any objective response evaluation criteria in the solid tumors response. The authors conclude that future trials are needed that target other molecular pathways in ACC.

In the present study we aimed to understand the detailed mechanism of the cytotoxic effects of sorafenib that were observed both in preclinical and clinical studies related to ACC. For this purpose we evaluated the effect of sorafenib *in vitro* by using the H295R ACC cell line, which is a monolayer culture, and in a 3D cell culture model, that is intended to mimic the structure, activity and extracellular environment of an *in vivo* tumor (15).

MATERIALS AND METHODS

Cell Culture and Treatments

The H295R (CRL-2128) cell line, was cultured to confluence in DMEM F-12 medium (Sigma-Aldrich, St.Louis, MO,USA). The medium was supplemented with transferrin (5 μg/ml; Sigma-Aldrich, Milan, Italy), sodium selenite (5 ng/ml; Sigma-Aldrich, Italy), L-glutamine (2.5 mM; Life-Technologies, Inc., Paisley, UK), and antibiotics (50 μg/ml streptomycin, 50 IU/ml penicillin) (Life-Technologies). H295R cells were mycoplasma free and were maintained at 37°C in a humidified atmosphere of 5% CO_2 and 95% air. Cells were treated with sorafenib at a concentration of 5 μM which was chosen based on a dose response curve (data not shown).

Trypan Blue Analysis

Cell number was determined using a hemocytometer, and viability was assessed by the ability to exclude trypan blue. After trypsinization, cells were suspended in phosphate-buffered saline (PBS) and mixed with an equal volume of 0.4% trypan blue in PBS and the percentage of stained cells was determined.

Cell Cycle Analysis in Flow Cytometric Analysis

The cell cycle was studied by using bromodeoxyuridine incorporation (BrdU; Sigma-Aldrich, USA). Briefly, cells were pulsed with BrdU at a final concentration of 10 μM for 15 min. Pulse-labeling experiments were performed by adding 10 μM BrdU to the medium during the last 30 min before analysis. After 30 min, the cells were harvested, washed once in PBS, fixed in 70% ethanol and stored at 4°C before analysis. Samples were then incubated with a mouse monoclonal anti-BrdU antibody (Roche Diagnostics, Milan, Italy) in complete medium containing 20% FCS and 0.06% Tween 20 (Calbiochem, San Diego, CA, USA) at room temperature for 1 h. After washing in PBS, cells were incubated with FITC-conjugated rabbit anti-mouse IgG 1:20 (DAKO, Glostrup, Denmark) in PBS for 1 h. Finally, cells were stained with a solution containing 5 μg/mL PI and 75 KU/mL RNase in PBS for 3 h, the top line of the cytograms represent BrdU-positive cells.

Quantification of Apoptosis by Flow Cytometry

Apoptosis induction was evaluated by terminal deoxynucleotidyl transferase-mediated dUTP nick end labeling (TUNEL) assay (Roche Diagnostics) by using flow cytometry (FCM). Briefly,

trypsinised adherent cells and floating cells were pooled, washed once with PBS (Lonza, Basel, Switzerland) and fixed in 4% paraformaldehyde (Sigma-Aldrich, Italy) for 30 min. Samples were then permeabilized in 0.1% Triton X-100 (Sigma-Aldrich, Italy) and 0.1% sodium citrate (Sigma-Aldrich, Italy) and washed with PBS (Lonza). Each sample was incubated in a 50 µl reaction mixture (Terminal deoxynucleotidyl Transferase, TdT, and fluorescein-dUTP) for 1 h at 37°C, washed with PBS (Lonza) and then measured by FCM at 24, 48 and 72 h.

Gelatin Zymography of Matrix Metalloproteinase-9

Levels of matrix metalloproteinase-9 (MMP-9) expression in H295R cells were analyzed by SDS-PAGE gelatin zymography as reported by Baragi VM et al. (16). Briefly, when cells were 80% confluent, they were treated with 5 µM sorafenib for 72 h, washed twice, trypsinized and subjected to electrophoresis under non-reducing conditions *via* 10% SDS-PAGE copolymerized with 1 mg/ml gelatin as a substrate. After the gel was washed with 2% Triton X-100 solution to remove SDS, it was incubated in activation buffer (50 mM Tris, 5 mM $CaCl_2$, 0.5 uM $ZnCl_2$, pH 7.4) for 24 h at 37°C. Gels were then stained with 0.05% Coomassie brilliant blue R-250 and destained in acetic acid. Not stained regions of the gel corresponding to the active MMP-2 and MMP-9 were quantified by densitometry using ImageJ analysis.

Western Blotting Analysis

Cellular lysates were sonicated on ice, clarified by centrifugation at 20.000 g and stored at –80°C. An aliquot of the cell lysates was used to evaluate the protein content by colorimetric assay. A total of 50 µg of protein content was electrophoresed on a 10% polyacrylamide gel in the presence of SDS and then was transferred onto a nitrocellulose membrane. Blots were blocked for 1 h at room temperature with 5% nonfat dry milk in Tween-PBS buffer. Treated and untreated cells were incubated with the following antibodies: anti-vimentin 1:200 (Santa Cruz Biotechnology, CA, US) anti-MMP-9 1:200 (Santa Cruz Biotechnology, CA, US), anti-N cadherin 1:100 (Santa Cruz Biotechnology, CA, US), anti-Vinculin 1:4000 (Sigma Aldrich, MO, US). The visualization of the antigens was performed by enhanced chemiluminescent detection reagents by ECL. The analysis of bands was performed with ImageJ software (Image Processing and analysis in Java).

Flow Cytometric Immunofluorescence

Cultured cells were harvested and the expression of cell surface markers was analysed by indirect immunofluorescence using a FACS Calibur cytofluorimeter (Becton Dickinson, Franklin Lakes, NJ, USA). For indirect immunofluorescence, cells were incubated with primary antibodies specific for N-Cadherin (1:100), VE-Cadherin (1:500), VEGFR2 (1:250), pVEGFR2 (1:500) and β-Catenin (1:500) (Santa Cruz Biotechnology, CA, US) for 1 h on ice and then incubated with a secondary FITC-conjugated antibody for 50 min on ice and immediately analyzed by FCM.

Coimmunoprecipitation

H295R cell pellets were resuspended in a low stringency cell lysis solution (NP40 1%, leupeptin 1µg/ml, pepstatin 1µg/ml, aprotinin 2 µg/ml, phenylmethylsulphonylfluoride 0.2 mM, sodium fluoride 10 mM). Then, the samples were sonicated for 10 s (Branson sonifier 150, Carouge, Switzerland). Preclearing of the lysates was performed by adding protein A to the extracts and mixing for 1h at 4°C. After preclearing, the supernatant was again incubated with protein A and with VEGFR2 at 4°C overnight. Immunocomplexes were washed three times with the low stringency lysis solution and were resolved by SDS-PAGE. Following the transfer to membranes, proteins were detected both by a VE-Cadherin and a β-Catenin horseradish peroxidase-linked secondary antibody. The anti-VEGFR2 antibody was used to normalize the amount of immunocomplex for quantification. The visualization of the antigens was performed by enhanced chemiluminescent detection. The analysis of bands was performed with ImageJ software (Image Processing and analysis in Java).

Conversion of H295R Into Spheres Cells

H295R cells were plated in non-adherent conditions: serum-free cell culture medium (Gibco, Gaithersburg, MD, USA), supplemented with 20 ng/ml epidermal growth factor (EGF) (Sigma-Aldrich, USA), 40 ng/ml bFGF (Sigma-Aldrich, USA) and B27 (Gibco), and 2 µg/ml heparin in 60 mm low-attachment culture dishes at a density of 1.9×10^6 cells/dish. After four days of seeding, the cells formed primary floating sphere-like structures. These structures grew rapidly until day 7. At this time, before the obtained sphere-like structures became necrotic, we harvested them and resuspended them in Accutase enzymatic solution (Gibco) for five minutes at 37°C and then mechanically dissociated them into a single cell suspension. The cells were reseeded in the same non-adherent conditions as above, and secondary spheres were allowed to form.

Morphometric Analysis of H295R Spheroids

For the three-dimensional (3D) morphological analysis of H295R spheroids, samples were examined under an Axiovert 200 inverted microscope (Zeiss, Oberkochen, Germany) equipped with differential interference contrast (DIC) optics. For quantitative image analysis, digital micrographs of at least 300 multicellular structures and single floating cells for each condition were randomly captured from three different experiments using an AxioCam MRm CCD camera (Zeiss). The projected area (A), perimeter (P) and two orthogonal diameters (a and b) were measured for each multicellular structure using Axiovision software (Zeiss). Sphericity, volume and size were subsequently calculated according to the previously proposed methods (17–19).

The sphericity of each structure was expressed by calculating the shape factor: $\Phi = \frac{\pi\sqrt{\frac{4A}{\pi}}}{P}$.

The volume (μm^3) was corrected for shape factor (SFC) and calculated by applying: $V = \Phi\frac{4\pi}{3}(\frac{P}{2\pi})^3$.

The size (μm) was determined by calculating the geometric mean diameter: $D_G = \sqrt{ab}$.

All 3D cellular structures were also categorized according to their morphology and classified as follows: tight spheroids (densely packed spheres with almost indiscernible individual cells), irregular aggregates (two or more cells organized in loose or compact aggregates that do not form the typical spheroid structure) and single floating cells.

Transmission Electron Microscopy

H295R monolayer and spheroid cultures, treated or not as described above, were washed three times with PBS and fixed with 2% glutaraldehyde in PBS for 2 h at 4°C. Samples were postfixed with 1% osmium tetroxide in veronal acetate buffer (pH 7.4) for 1 h at 25°C, stained with uranyl acetate (5 mg/ml) for 1 h at 25°C, dehydrated in acetone and embedded in Epon 812 (EMbed 812, Electron Microscopy Science, Hatfield, PA, USA). Ultrathin sections, unstained or poststained with uranyl acetate and lead hydroxide, were examined under a Morgagni 268D transmission electron microscope (TEM) (FEI, Hillsboro, OR, USA) equipped with a Mega View II charge-coupled device camera (SIS, Soft Imaging System GmbH, Munster, Germany) and analyzed with AnalySIS software (SIS).

Statistical Methods

To compare variables that do not assume a Gaussian distribution, a Mann-Whitney nonparametric test was used. The data are presented with the Tukey box-and-whisker plot, where the central box represents the interquartile ranges (IR; 25th to 75th percentile), the middle line represents the median, and the horizontal lines represent the minimum and the maximum value of observation range. The values are expressed as the median ± IR. To compare variables that assume a normal distribution, Student's T tests were used. The values are expressed as the mean ± SE (standard error) from three independent experiments. A chi-square test was used to compare categorical variables. P values <0.05 were assumed to be statistically significant.

RESULTS

Sorafenib Reduced Cancer Cell Proliferation

To assess the effects of sorafenib on cancer cell proliferation, H295R cells were treated with 5 μM of sorafenib for 72 h. As shown in **Figure 1A** the drug exposure showed a 24% inhibition

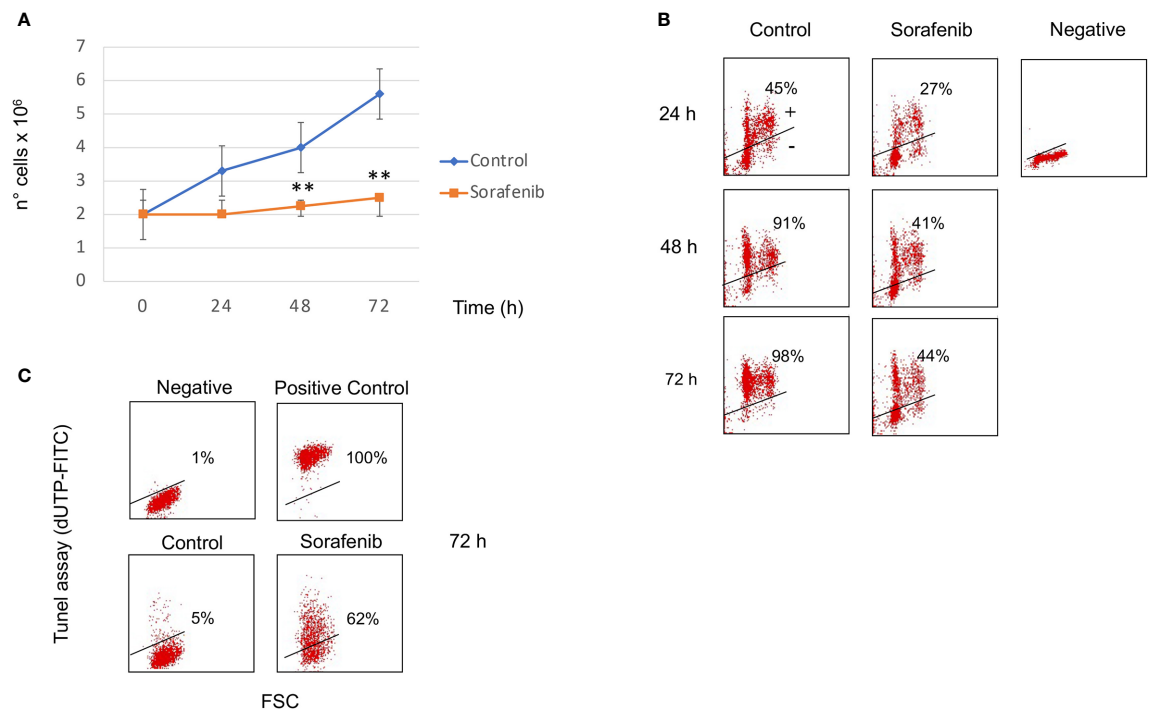

FIGURE 1 | Sorafenib inhibits cell growth and cell proliferation. Viability curves of untreated and treated H295R cells with 5 μM sorafenib for 72 hours. Cell growth inhibition progressively increases and, at the highest concentration at 72 h, reaches 42% of inhibition after sorafenib treatment. The results represent the mean ± s.d. of three independent experiments done in duplicate. A comparison of the individual treatment was conducted by using ANOVA followed by the Tukey–Kramer *post hoc* test. $^{**}P$ <0.01 vs Ctrl **(A)**. Analysis of BrdU incorporation in control and in treated cells for 24h, 48h and 72 hours respectively. In samples treated with sorafenib about 40% BrdU incorporation was evident at 48-72 h of treatment. Representative results are shown, and were quantified from three independent experiments; each group was analyzed in duplicate **(B)**. TUNEL assay to evaluate induction of apoptotic cell death in H295R cells by sorafenib treatment. Flow cytometric analysis of untreated and treated cells with sorafenib for 72 h. At this time 62% of treated cells were dUTP-FITCH positive revealing apoptotic cell death. Similar results were obtained in three independent experiments **(C)**.

of cell growth at 48 h, increasing 42% after 72 h compared to untreated cells ($p<0.01$). Cell viability in treated and untreated cells was assessed by trypan blue exclusion test to determine if cell viability was maintained after sorafenib treatment. We observed an integrity of the cell membrane after drug exposure, infact no alteration of cellular viability was observed during sorafenib treatment (data not shown), meaning that sorafenib did not induce toxicity.

BrdU incorporation was performed to determine if sorafenib treatment affected the cell cycle as well. **Figure 1B** shows that about 40% BrdU incorporation was evident at 48-72 h of treatment while in untreated cells incorporation was 91% and 98% after 48 h and 72 h respectively. These results suggest that the sorafenib used in this study successfully inhibited the growth of H295R cells according to a previous study (12).

Sorafenib Induced Apoptosis in H295R Cells

To evaluate whether cell growth inhibition was attributed to apoptotic death we performed the TUNEL assay analyzed by FCM analysis. As evidenced in **Figure 1C**, sorafenib was able to induce apoptotic cell death (62% vs untreated cells) which was consistent with data from Mariniello and colleagues (12). They estimated an apoptotic percentage of 43% after sorafenib treatment in the same cell model.

Sorafenib Inhibited Cell Proliferation and Did Not Affect VEGFR2 Expression

To investigate whether the effects of sorafenib on cell growth inhibition were correlated with the modulation of VEGFR2 protein, we assessed protein expression by immunofluorescence. The results obtained, revealed that the expression of the VEGFR2 protein did not significantly change after 72 h of sorafenib treatment. On the contrary the drug was able to increase p-VEGFR2 after the same time (approximately 50% vs untreated cells) ($p<0.05$) (**Figures 2A** and **5A**).

Then, we investigated whether VE-cadherin and β-catenin, whose action is mediated by the establishment of cadherin-based junctions, could be involved in the anti-proliferative and anti-angiogenic effects of sorafenib (20). As highlighted in **Figure 2A** the expression level of both VE-cadherin and β-catenin is similar to the levels observed for each in untreated cells. These results demonstrate that the effects of sorafenib on cell proliferation did not interfere with the expression levels of VEGFR2, VE-cadherin and β-catenin.

Sorafenib Interfered With Intercellular Junctions

Although we did not observe a change in VEGFR2, VE-cadherin and β-catenin protein expression following sorafenib treatment, we wanted to test whether the drug interfered with the formation of the protein complex, which is involved in the proliferative

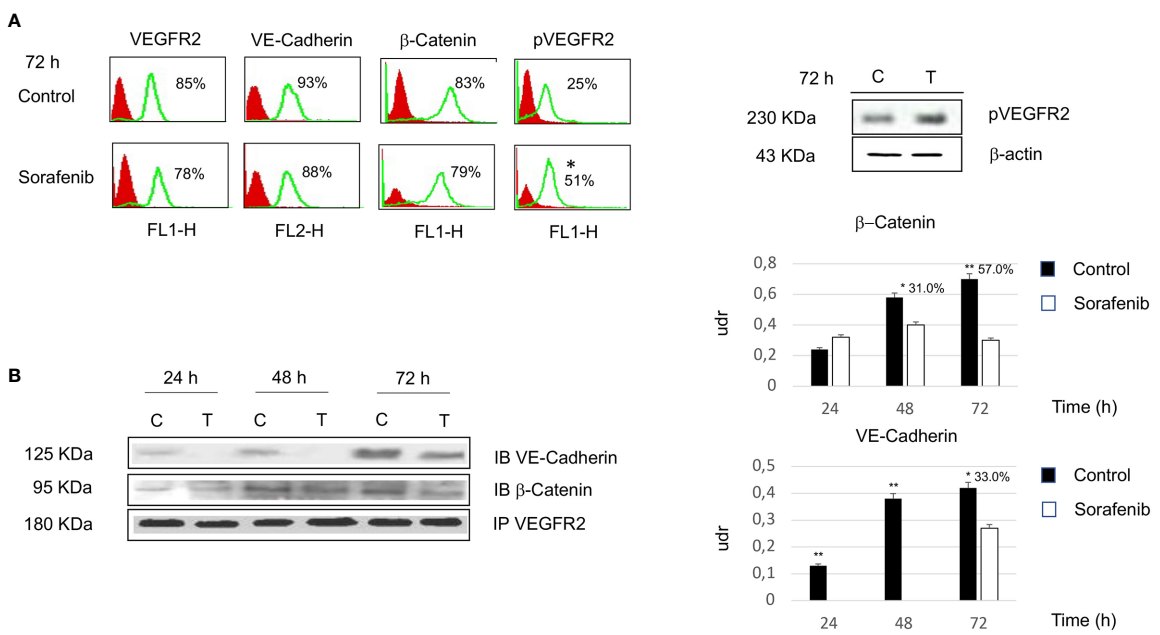

FIGURE 2 | Flow cytometry analysis of VEGFR2, VE-cadherin, β-catenin and pVEGFR2 in untreated and sorafenib treated H295R cells. Only pVEGFR2 was significant in sorafenib treated sample ($p<0.05$). Western blot analysis of pVEGFR2 at 72 h is shown on the side **(A)**. Coimmunoprecipitations of VE-Cadherin and β-Catenin with VEGFR2. On the right, graph bars corresponding to densitometric analysis of β-Catenin and VE-Cadherin. Next to the bar graphs are reported the percentage of coprecipitate proteins at 24, 48 and 72 h. The samples treated with sorafenib and marked on top of the bar are considered statistically significant (*$p<0.05$;**$p<0.01$) **(B)**. The values of flow cytometry analysis and coimmunoprecipitations are expressed as the mean ± SE (standard error) from three independent experiments.

and angiogenetic processes. Thus coimmunoprecipitation experiments were performed using H295R cells to determine the effects of sorafenib on intercellular junctions.

As shown in **Figure 2B**, VE-cadherin did not coprecipitate with VEGFR2 at 24 and 48 h. Moreover, we observed that 33% of the protein was in complex after 72 h of sorafenib treatment ($p<0.05$). In contrast changes in protein-protein interactions after sorafenib treatment were evidenced for β-catenin, in fact a 31% and 57% of the protein was in complex with VEGFR2 at 48 h ($p<0.05$) and 72 h ($p<0.01$) respectively. These data could indicate that sorafenib destabilizes the protein-protein interactions of a complex that is implicated in intercellular junctions.

Sorafenib Affected the Ability of H295R Cultures to Grow as Tight Spheroids

To analyze the 3D morphology and assess the morphometric parameters of H295R spheroids grown in sphere medium with or without sorafenib, DIC microscopy and digital image analysis techniques were performed as described in the *Materials and Methods*. Untreated H295R cultures (control) displayed a typical spheroid pattern of growth with densely packed spheres; in contrast, the H295R cell growth in the presence of sorafenib was characterized by a higher number of irregular multicellular aggregates (**Figures 3A, B**). In fact, the sphericity index of multicellular structures was significantly higher in untreated cultures with a shape factor of $\varphi = 0.90$ vs 0.85 in treated H295R cultures cells; also the percentage of tight spheroids was higher in untreated cultures (16.7% vs 6.7%; $p<0.001$) with fewer irregular aggregate compared with those of H295R cultures cells treated with sorafenib (3.1% vs 15.2%; $p<0.01$) (**Figure 3C** and **Table 1**).

Morphometric analysis of tight spheroids revealed that size and SFC volume in untreated cultures were characterized by a higher size and volume of tight spheroids compared to what was observed in the treated H295R cells ($p<0.001$) (**Figure 3D** and **Table 1**).

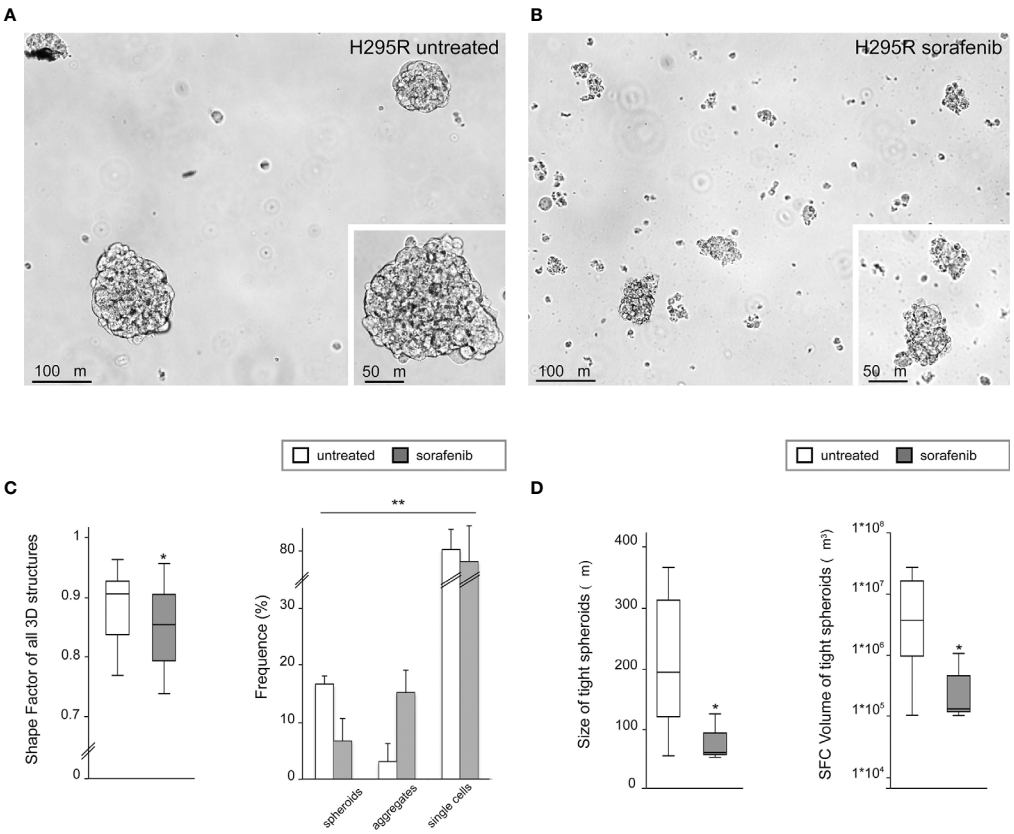

FIGURE 3 | Three-dimensional and morphometric analysis of H295R spheroid growth in sphere medium with or without sorafenib. Differential interference contrast microscopy of H295R cell cultures: typical spheroid pattern of growth in untreated H295R cultures **(A)** and multicellular aggregates in H295R cultures cell growth treated with sorafenib **(B)**. Morphometric analysis of all multicellular structures from treated or untreated H295R cells: the box-and-whisker plot of shape factor shows a higher sphericity index for the spheroids derived from H295R untreated cultures (control) than for those from the treated cultures. The central box represents the interquartile ranges, the middle line represents the median and the horizontal lines represent the minimum and the maximum value of the observation range (Mann-Whitney test: *$p<0.001$). The results reported in the graph represent the mean values ± standard error (chi-squared test: **$p<0.01$) **(C)**. Morphometric analysis of tight spheroids from treated or untreated H295R cells: the box-and-whisker plots of size and SFC volume show a significant difference in untreated and treated cultures H295R cells (Mann-Whitney test: *$p<0.001$) **(D)**.

TABLE 1 | Morphological characterization and morphometric analysis of three-dimensional multicellular structures obtained from H295R cells cultured in sphere medium with or without sorafenib.

	All 3D structures	Tight spheroids				Irregular aggregates				Single floating cells
	Shape Factor† (IR)	Frequency (% ± SE)	Shape Factor† (IR)	Volume‡ (IR)	Size° (IR)	Frequency (%± SE)	Shape Factor† (IR)	Volume‡ (IR)	Size° (IR)	Frequency (% ± SE)
H295R untreated	0.90 Φ (0.83–0.92)	16.7 ± 3.8	0.93 Φ (0.91–0.95)	$3.7x10^6$ µm^3 ($0.9–22.7x10^6$)	194 µm (121–312)	3.1 ± 3.9	0.83 Φ (0.79–0.89)	$7.2x10^5$ µm^3 ($0.3–7.4x10^6$)	111.5 µm (80–236.8)	80.2 ± 6.2
H295R sorafenib treated	0.85 Φ (0.79–0.90)*	6.7 ± 1.4**	0.91 (0.90–0.93)^	$1.3x10^5$ µm^3 ($1.1–4.5x10^5$)*	63 µm (59–95)*	15.2 ± 3.1**	0.81 Φ (0.77–0.86)**	$2.3x10^5$ µm^3 ($1.3–5.2x10^5$)*	76.5 µm (65–100.5)^	78.1 ± 3.5**

†Shape Factor for spherical shape = 1; ‡Volume: parameter based on project area and correct for Shape Factor Φ; °Size: parameter based on geometric mean diameter of the multicellular structures (see Materials and Methods).

Statistics (vs H295R untreated):

^p=Not Significant (Mann–Whitney test);*p<0.001 (Mann-Whitney test); **p<0.01 (chi-square test).

The sphericity index of multicellular structures was significantly higher in untreated vs treated cultures (p<0.01); the percentage of tight spheroids was higher in untreated cultures (p<0.001) with fewer irregular aggregate compared with those of H295R cultures cells treated with sorafenib (p<0.01). Size and SFC volume in untreated cultures showed a higher size and volume of tight spheroids compared to treated H295R cells (p<0.001).

Sorafenib Induced Cellular Damage in H295R Cells

To further characterize the morphological changes related to the sorafenib 5 µM treatment, the ultrastructural features of H295R monolayer and spheroid cultures were analyzed by TEM analysis at 72 h. The untreated H295R monolayers (**Figures 4A–C**) and spheroids (**Figures 4D, E**) had nuclei that were rounded or occasionally lobulated, and finely dispersed chromatin and prominent nucleoli. The cytoplasm displayed numerous rod-shaped or elongated mitochondria, variable amounts of organelles, a prominent Golgi apparatus, many cytoplasmic vesicles and a well-developed rough endoplasmic reticulum. Areas similar to tight junctions, as well as intermediate junctions and some tight junction-like regions were visible.

In contrast, the sorafenib-treated H295R monolayers (**Figures 4F–H**) and spheroids (**Figures 4I–K**) exhibited several ultrastructural characteristics of cellular damage. Apoptotic nuclei with areas of marginal, dense stained chromatin and nuclear fragmentation were visible. Most of the mitochondrial structures appeared swollen with a subtotal loss of internal cristae, while large vacuoles, swollen cisternae of endoplasmic reticulum and myelinic bodies (histological artefact) were also noticeable. Treated H295R spheroids did not exhibit classical junctional complexes and even exhibited few intermediate-like junctions.

Sorafenib Treatment Promoted Tumor Progression and Invasiveness in the H295R Cell Line

Surprisingly, our study demonstrated an increase in p-VEGFR2 after 72 h of sorafenib treatment (approximately 50% vs untreated cells) (**Figures 2A** and **5A**). These results prompted us to verify whether sorafenib could paradoxically promote tumor progression. Thus, we determined the expression level of N-cadherin and vimentin, which are prognostic markers of tumor progression. As evidenced in **Figure 5B** the N-cadherin expression level, measured by immunofluorescence staining, showed an upregulation of approximately 10% compared to untreated cells. A similar increase was also observed for the level of vimentin (10% vs untreated cells) analyzed by Western blot (**Figure 5C**). Both of these results were observed after 72 h of sorafenib treatment. Finally, to evaluate the involvement of drug treatment on tumor invasiveness, we performed Western blot analyses of MMP-9 protein. As shown in **Figure 6A** sorafenib treatment induced an increase in the protein level of approximately 10% over the levels observed in the untreated cells. A similar result was obtained by zymographyc analysis, confirming up-regulation of the protein expression level of by approximately 10% (**Figure 6B**). All these data demonstrated that sorafenib failed to have an antiproliferative effect on a small population of tumor cells with tumor aggressiveness features.

DISCUSSION

Sorafenib is an inhibitor of several receptor tyrosine kinases involved in neovascularization, including VEGFR2, VEGFR3, and platelet-derived growth factor (5); it has shown efficacy against a wide variety of tumors in preclinical models, such as breast, colon, and pancreas carcinoma, and it has been approved for the treatment of hepatocellular carcinoma (9, 21). The mechanism of antineoplastic action of sorafenib lies primarily in its induction of apoptosis (7). Since sorafenib showed a broad spectrum of antitumor activity in preclinical studies (10–12), multiple clinical trials have been undertaken to further investigate its role, either alone or in combination with different chemotherapies for the treatment of several neoplasms (4, 6, 8, 10). Because of its activities, sorafenib has been approved by the FDA for the treatment of patients with advanced renal cell carcinoma, unresectable hepatocellular carcinoma and locally recurrent or metastatic, progressive differentiated thyroid carcinoma refractory to radioactive iodine treatment.

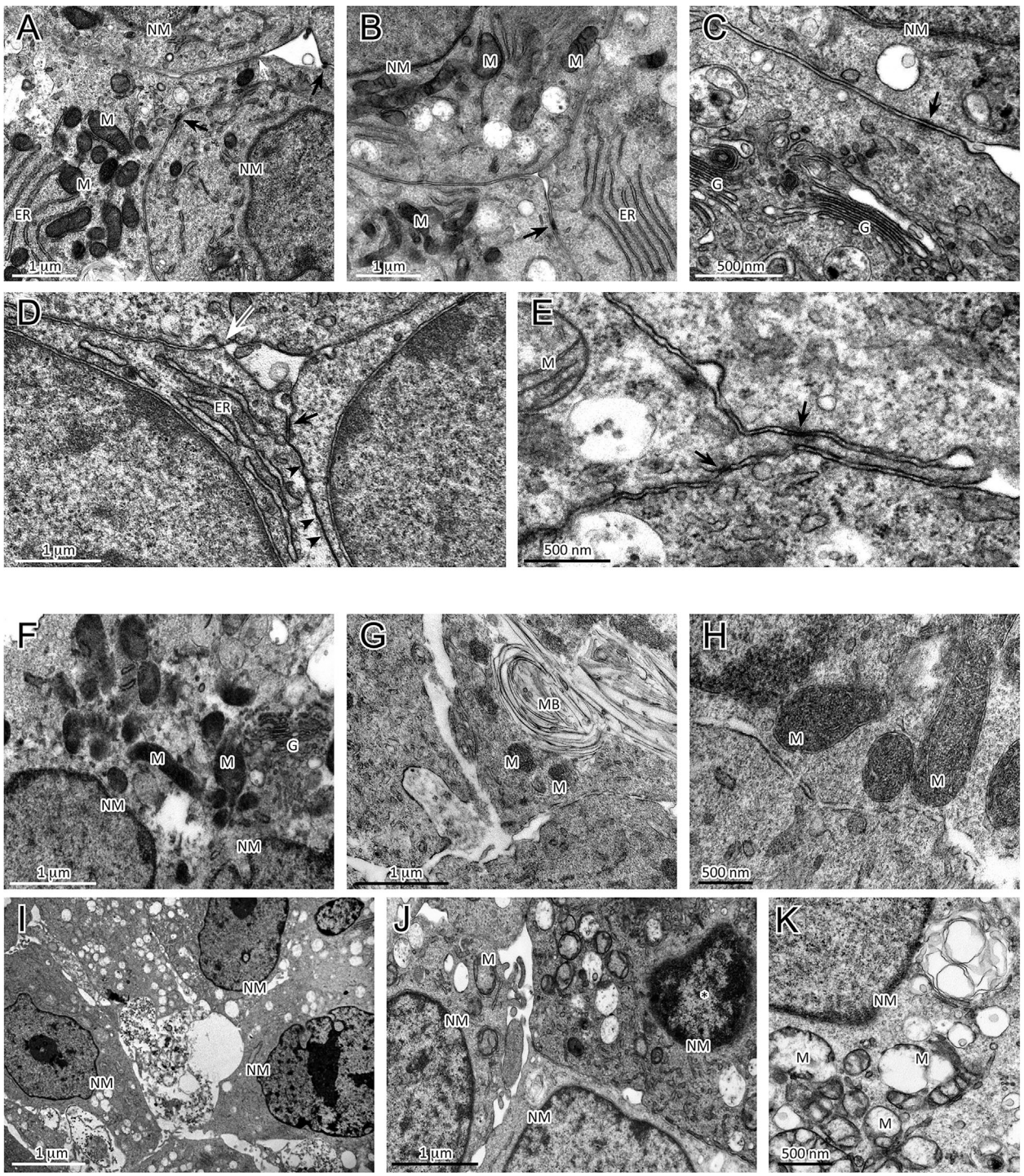

FIGURE 4 | Analysis of ultrastructural features of cellular damage induced by sorafenib 5 µM at 72 h in H295R cultures. The H295R untreated monolayers **(A–C)** and spheroids **(D, E)** show nuclei with finely dispersed chromatin and prominent nucleoli, and cytoplasms with numerous mitochondria, a variable number of organelles, a prominent Golgi apparatus, many vesicles and a well-developed rough endoplasmic reticulum. Areas similar to tight junctions (white arrow), intermediate junctions (black arrows) and some tight junction-like regions (black arrowheads) are visible. Sorafenib treated H295R monolayers **(F–H)** and spheroid **(I–K)** cultures displayed apoptotic nuclei with areas of marginal and dense stained chromatin (**J**, asterisk) and nuclear and cellular fragmentation. The mitochondria are swollen and exhibit a loss of internal cristae. Cytoplasmatic vacuolization, swelling of rough endoplasmic reticulum cisternae and myelinic bodies were observed. H295R-treated spheroids show only a few intermediate-like junctions. Legend: NM, Nuclear membrane, M, Mitochondrion; ER, Endoplasmic reticulum; G, Golgi complex; MB, Myelinic body (considered as histological artifact).

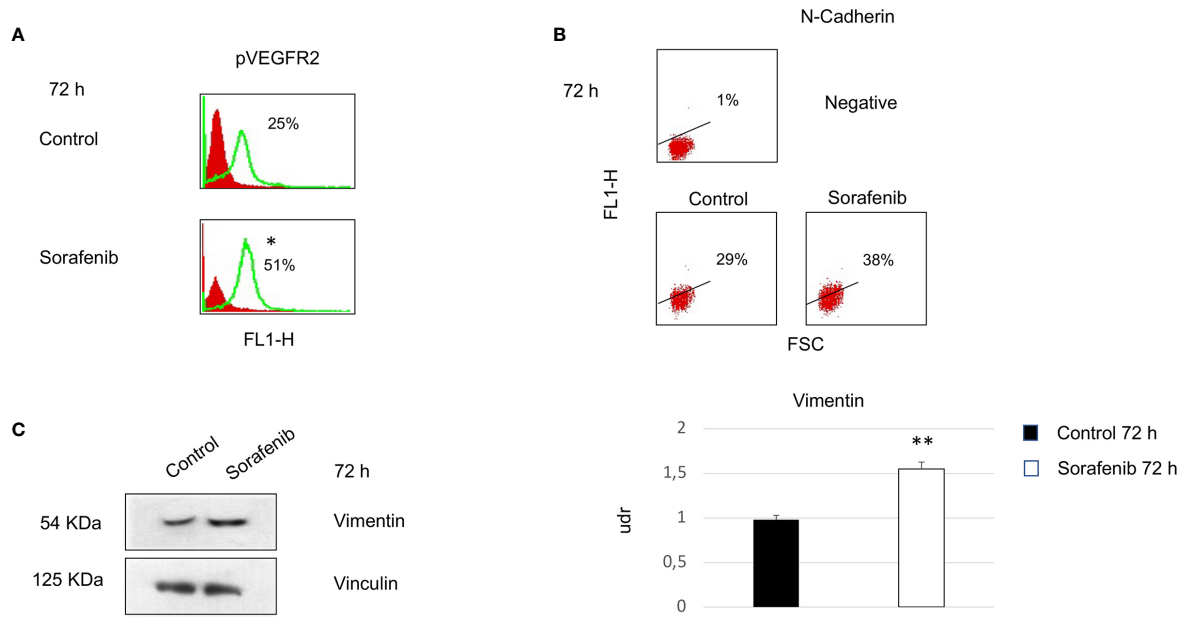

FIGURE 5 | Cells were analyzed at 72 h after sorafenib treatment. Indirect immunofluorescence was analyzed by flow cytometric histograms for pVEGFR2 (particular of **Figure 2A**) (*p<0.05) **(A)** and by dot plot for N-cadherin in sorafenib-treated and untreated cells **(B)**. Western blot analyses of Vimentin and Vinculin were performed with 50 µg of protein from untreated and treated cells (**p<0.01) **(C)**. Proteins were resolved by 10% SDS-PAGE to anable analyses with the anti-vimentin or anti-vinculin antibodies.

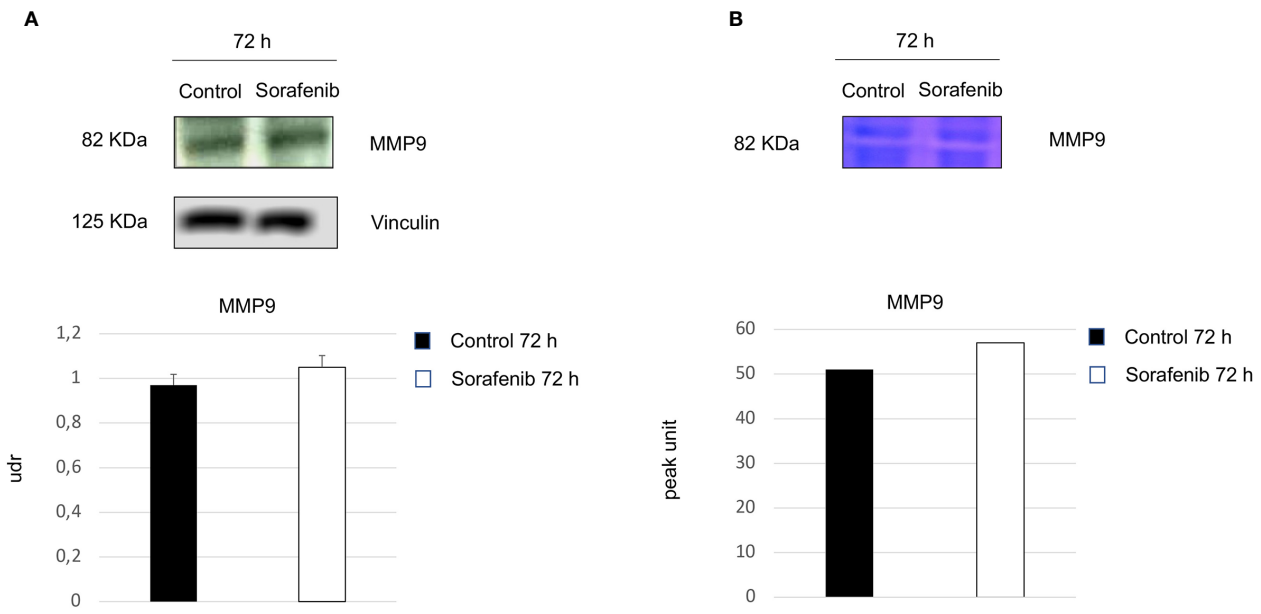

FIGURE 6 | Role of sorafenib treatment in tumor invasiveness. MMP9 protein levels were detected by Western blot **(A)**. Zymographyc analysis confirmed the protein activity **(B)**. Below are shown bar graphs expressing the protein expression of MMP9 (on the left) and MMP9 activity (on the right). The results reported in the graph represent the mean values ± standard error. Densitometry summarizes the results obtained in three independent experiments.

Despite the antineoplastic effects described for sorafenib, some patients may exhibit neoplastic progression during therapy with this drug as demonstrated by the comparison of the progression-free survival curves between treated patients and controls (22, 23).

Finally, numerous animal studies have also suggested that antiangiogenesis drugs may, in certain situations, actually accelerate metastatic spread which is recognized as a new form of adaptive resistance used by cancer cells (23, 24).

ACC is a highly vascularized neoplasia (1, 11) and metronomic chemotherapy is thought to be effective against ACC mainly by inhibiting tumor angiogenesis. Moreover, the antiangiogenic activity of metronomic chemotherapy can be theoretically increased by the concomitant administration of an antiangiogenetic drug (25). Therefore, there is a strong rationale for testing the combination of a metronomic chemotherapy with antiangiogenetic drugs in the management of ACC.

Berruti et al. tested the combination of daily sorafenib and weekly paclitaxel therapy in patients with progressive metastatic ACC in progression following treatment with mitotane in combination with one or two chemotherapy lines (13); the test was carried out as a multicenter, prospective phase II trial. The results of this study documented a progressive disease in nine consecutive patients at the first restaging dose after 2 months, which led to the interruption of the clinical trial. Furthermore in many patients, the tumor progression was dramatic, and the increase in the size of the tumor lesions was faster than it was in the months before the trial. These data suggest that this combination therapy may have paradoxically favored tumor progression. Although the data regarding the progression of tumors during treatment with sorafenib can be found in the literature (22–24) there is little data available regarding the mechanism by which sorafenib can elicit a malignant phenotype. In this regard the primary objective of our study was to determine whether sorafenib was able to induce a malignant phenotype in ACC *in vitro*.

For this purpose we conducted experiments in both 2D monolayer and 3D models. We chose a new approach, *in vitro* 3D cultures, since it represents an additional step that can bridge the gap between conventional 2D monolayer cultures and animal models. Additionally, this approach is especially useful for studying the invasive proprieties and metastatic potential of tumor cells, thus facilitating the development and screening of new drugs (17, 18, 26).

The results obtained from our study demonstrated that sorafenib induces cell growth inhibition due to a significant increase in apoptosis. The treatment also caused a destabilization of intercellular junctions by altering the formation of the protein scaffold; this alteration was revealed by coimmunoprecipitation experiments, in which an absence of the complex formation between VE-cadherin and β-catenin was evident after sorafenib exposure. Furthermore, we used ultrastructure analysis to demonstrate the disaggregation of the spheres into single cells after sorafenib treatment.

However, following treatment, we noticed an increase in the amount of the phosphorylated form of VEGFR2. This result contrasts with a well-known effects of sorafenib, which is interference with the angiogenetic process, leading to a reduction in VEGFR expression. These steps are crucial for tumor growth, progression, and metastasis. These apparently contradictory results have been observed by other authors and support both the resistance to sorafenib that occurs in some cancers and the lack of long-term response to sorafenib treatment (27–29).

This prompted us to investigate the molecular processes and the angiogenetic factors associated with tumor progression.

Tumor spheroid cell culture models have been used to study the responses of ACC to sorafenib treatment. H295R cells have the capacity to form spheroids, as reported by Lichtenauer and colleagues (30). The ability to form spheroid colonies is a recognized method used to identify cancer stem cells displaying an enhanced tumorigenic ability (31). This specific cell population is thought to be closely linked to the epithelium-mesenchymal transition (EMT), which is defined as crucial in metastatic spread and in tumor recurrence (32, 33). In cancer, EMT is associated with poor survival for the patients and seems to be a key step in the development of metastasis (32), since cells lose their polarity and cell-to-cell contacts and therefore become more motile (33, 34).

Evidence that exposure to sorafenib leads to EMT in ACC neoplasms come from analyzing some of the markers involved in this transition, such as N-cadherin and vimentin. Our results showed an increased expression level of both of these proteins. We noticed that only a small percentage of cells (approximately 10%) revealed disregulation of this protein as revealed by FACS analysis and by densitometric analysis of the proteins.

Furthermore, in our study, we observed that although sorafenib induced apoptosis, a small percentage of cells appeared to be resistant to treatment and exhibited the features of invasive phenotype, as evidenced by increased levels of MMP-9 after sorafenib treatment. MMP-9 is recognized as an enhancer protein in the metastatic process. Therefore it is clear that this population of cells is resistant to treatment and shows features of invasiveness and malignancy. Our results were in agreement with those described by van Malenstein et al. (35) who reported a direct effect of sorafenib on the epithelial cells by inducing a malignant phenotype. It was also demonstrated that sorafenib targets cofilin, which negatively regulates the polymerization of actin to disrupt the cytoskeleton, and cause cells detachment (36). Our results, which are in accordance with previous studies performed and are confirmed by Berruti's clinical trial could explain why sorafenib treatment elicits a malignant phenotype, in patients with ACC to cause poor and devastating results. Based on these data, we warn against the clinical use of sorafenib as a therapeutic strategy for the treatment of ACC.

DATA AVAILABILITY STATEMENT

The original contributions presented in the study are included in the article/supplementary material. Further inquiries can be directed to the corresponding author.

AUTHOR CONTRIBUTIONS

LC and AS conceived the original idea. LC, BB, DA, SR, PL, and RM carried out the experiments. LC, BB, and AS wrote the

manuscript with support from SR. EP, MT, and AS supervised the project. VT and GP performed data curation. AS funding acquisition. All authors contributed to the article and approved the submission version.

FUNDING

This work was supported by Sapienza University of Rome "Progetti d'Ateneo": grant No. RM1181643692671C (to AS).

REFERENCES

1. Else T, Kim AC, Sabolch A, Raymond VM, Kandathil A, Caoili EM, et al. Adrenocortical Carcinoma. *Endocr Rev* (2014) 35(2):282–326. doi: 10.1210/er.2013-1029
2. Crucitti F, Bellantone R, Ferrante A, Boscherini M, Crucitti P. The Italian Registry for Adrenal Cortical Carcinoma: Analysis of a Multiinstitutional Series of 129 Patients. The Acc Italian Registry Study Group. *Surgery* (1996) 119:161–70. doi: 10.1016/s0039-6060(96)80164-4
3. Stigliano A, Chiodini I, Giordano R, Faggiano A, Canu L, Della Casa S, et al. Management of Adrenocortical Carcinoma: A Consensus Statement of the Italian Society of Endocrinology (Sie). *J End Invest* (2016) 39:103–21. doi: 10.1007/s40618-015-0349-9
4. Wilhelm SM, Carter C, Tang L, Wilkie D, Mcnabola A, Rong H, et al. Bay43-9006 Exhibits Broad Spectrum Oral Antitumor Activity and Targets the RAF/MEK/ERK Pathway and Receptor Tyrosine Kinases Involved in Tumor Progression and Angiogenesis. *Cancer Res* (2004) 64:7099–109. doi: 10.1158/0008-5472.CAN-04-1443
5. Hasskarl J. Sorafenib. *Cancer Res* (2010) 184:61–70. doi: 10.1007/978-3-642-01222-8_5
6. Rahmani M, Davis EM, Bauer C, Dent P, Grant S. Apoptosis Induced by the Kinase Inhibitor Bay 43-9006 in Human Leukemia Cells Involves Down-Regulation of Mcl-1 Throug Inhibiton of Translation. *J Biol Chem* (2005) 280:35217–27. doi: 10.1074/jbc.M506551200
7. Yu C, Bruzek LM, Meng XW, Gores GJ, Carter CA, Kaufmann SH, et al. The Role of Mcvl-1 Down Regulation in the Proapototic Activity of the Multikinase Inhibitor Bay 43-9006. *Oncogene* (2005) 24:6861–9. doi: 10.1038/sj.onc.1208841
8. Llovet JM, Di Bisceglie AM, Bruix J, Kramer BS, Lencioni R, Zhu AX, et al. Design and Endpoints of Clinical Trials in Hepatocellular Carcinoma. *J Natl Cancer Inst* (2008) 100:698–711. doi: 10.1093/jnci/djn134
9. Llovet JM, Ricci S, Mazzaferro V, Hilgard P, Gane E, Blanc JF, et al. Sorafenib in Advanced Hepatocellular Carcinoma. *N Engl J Med* (2008) 359:378–90. doi: 10.1056/NEJMoa0708857
10. Cheng AL, Kang YK, Chen Z, Tsao CJ, Qin S, Kim JS, et al. Efficacy and Safety of Sorafenib in Patients in the Asia-Pacific Region With Advanced Hepatocellular Carcinoma: A Phase III Randomised, Double-Blind, Placebocontrolled Trial. *Lancet Oncol* (2009) 10:25–34. doi: 10.1016/S1470-2045(08)70285-7
11. Bernini GP, Moretti A, Bonadio AG, Menicagli M, Viacava P, Naccarato AG, et al. Angiogenesis in Human Normal and Pathologic Adrenal Cortex. *J Clin Endocrinol Metab* (2002) 287:4961–5. doi: 10.1210/jc.2001-011799
12. Mariniello B, Rosato A, Zuccolotto G, Rubin B, Cicala MV, Finco I, et al. Combination of Sorafenib and Everolimus Impacts Therapeutically on Adrenocortical Tumor Models. *End Relat Canc* (2012) 4:527–39. doi: 10.1530/ERC-11-0337
13. Berruti A, Sperone P, Ferrero A, Germano A, Ardito A, Priola AM, et al. Phase II Study of Weekly Paclitaxel and Sorafenib as Second/Third-Line Therapy in Patients With Adrenocortical Carcinoma. *Eur J Endocrinol* (2012) 3:451–8. doi: 10.1530/EJE-11-0918
14. O'Sullivan C, Edgerly M, Velarde M, Wilkerson ,J, Venkatesan AM, Pittaluga S, et al. The VEGF Inhibitor Axitinib has Limited Effectiveness as a Therapy for Adrenocortical Cancer. *J Clin Endocrinol Metab* (2014) 4:1291–7. doi: 10.1210/jc.2013-2298
15. Leonard F, Collnot EM, Lehr CM. A Three-Dimensional Coculture of Enterocyte, Monocyte and Dendritic Cells to Model Inflamed Intestinal Mucosa In Vitro. *Mol Pharm* (2010) 7:2103–19. doi: 10.1021/mp1000795
16. Baragi VM, Shaw ,BJ, Renkiewicz RR, Kuipers PJ, Welgus HG, Mathrubutham M, et al. A Versatile Assay for Gelatinases Using Succinylated Gelatin. *Matrix Biol* (2000) 3:267–73. doi: 10.1016/s0945-053x(00)00086-x
17. Kelm JM, Timmins NE, Brown CJ, Fussenegger M, Nielsen LK. Method for Generation of Homogeneous Multicellular Tumor Spheroids Applicable to a Wide Variety of Cell Types. *Biotechnol Bioeng* (2003) 83:173–80. doi: 10.1002/bit.10655
18. Vinci M, Gowan S, Boxall F, Patterson L, Zimmermann M, Court W, et al. Advances in Establishment and Analysis of Three-Dimensional Tumor Spheroid-Based Functional Assays for Target Validation and Drug Evaluation. *BMC Biol* (2012) 10:29. doi: 10.1186/1741-7007-10-29
19. Noto A, Raffa S, De Vitis C, Roscilli G, Malpicci D, Coluccia P, et al. Stearoyl-CoA Desaturase-1 is a Key Factor for Lung Cancer-Initiating Cells. *Cell Death Dis* (2013) 4:e947. doi: 10.1038/cddis.2013.444
20. Caveda L, Martin-Padura I, Navarro P. Inhibition of Cultured Cell Growth by Vascular Endothelial Cadherin (Cadherin-5/VE-Cadherin). *J Clin Invest* (1996) 98:886 –93. doi: 10.1172/JCI118870
21. Keating GM, Santoro A. Sorafenib: A Review of its Use in Advanced Hepatocellular Carcinoma.21. *Drugs* (2009) 69:223–40. doi: 10.2165/00003495-200969020-00006
22. Paez-Ribes M, Allen E, Hudock J, Takeda T, Okuyama H, Vinals F, et al. Antiangiogenic Therapy Elicits Malignant Progression of Tumors to Increased Local Invasion and Distant Metastasis. *Cancer Cell* (2009) 15:220–31. doi: 10.1016/j.ccr.2009.01.027
23. Ebos ,JM, Lee CR, Cruz-Munoz W, Bjarnason GA, Christensen JG, Kerbel RS. Accelerated Metastasis After Short-Term Treatment With a Potent Inhibitor of Tumor Angiogenesis. *Cancer Cell* (2009) 15:232–9. doi: 10.1016/j.ccr.2009.01.021
24. Zhang W, Sun HC, Wang WQ, Zhang QB, Zhuang PY, Xiong YQ, et al. Sorafenib Down-Regulates Expression of HTATIP2 to Promote Invasiveness and Metastasis of Orthotopic Hepatocellular Carcinoma Tumors in Mice. *Gastroenterology* (2012) 143:1641–1649. 24. doi: 10.1053/j.gastro.2012.08.032.
25. Loges S, Mazzone M, Hohensinner P, Carmeliet P. Silencing or Fueling Metastasis With VEGF Inhibitors: Antiangiogenesis Revisited. *Cancer Cell* (2009) 15:167–70. doi: 10.1016/j.ccr.2009.02.007
26. Zietarska M, Maugard CM, Filali-Mouhim A, Alam-Fahmy M, Tonin PN, Provencher DM, et al. Molecular Description of a 3D In Vitro Model for the Study of Epithelial Ovarian Cancer (EOC). *Mol Carcinog* (2007) 46:872–85. doi: 10.1002/mc.20315
27. Hora C, Romanque P, Dufour JFF. Effect of Sorafenib on Murine Liver Regeneration. *Hepatology* (2011) 53(2):577–86. doi: 10.1002/hep.24037
28. Lewandowski RJ, Andreoli JM, Stickey R, Kellini J,R, Gabr A, Baker T, et al. Angiogenic Response Following Radioembolization: Results From a Randomized Pilot Study of Yttrium-90 With or Without Sorafenib. *J Vasc Interv Radiol* (2016) 27(9):1329–36. doi: 10.1016/j.jvir.2016.03.043
29. Wang Z, Dai J, Yan J, Zhang Y, Yin Z. Targeting EZH2 as a Novel Therapeutic Strategy for Sorafenib-Resistant Thyroid Carcinoma. *J Cell Mol Med* (2019) 23:4770–8. doi: 10.1111/jcmm.14365
30. Lichtenauer UD, Shapiro I, Osswald A, Meurer S, Kulle A, Reincke M, et al. Characterization of NCI-H295R Cells as an In Vitro Model of Hyperaldosteronism. *Horm Metab Res* (2013) 45:124–9. doi: 10.1055/s-0032-1323810
31. Kasper S. Identification, Characterization, and Biological Relevance of Prostate Cancer Stem Cells From Clinical Specimens. *Urol Oncol* (2009) 27:301–3. doi: 10.1016/j.urolonc.2008.12.012
32. Thiery JP. Epithelial–Mesenchymal Transitions in Tumour Progression. *Nat Rev Cancer* (2002) 2:442–54. doi: 10.1038/nrc822
33. Mani SA, Guo W, Liao MJ, Eaton EN, Ayyanan A, Zhou AY, et al. The Epithelial-Mesenchymal Transition Generates Cells With Properties of Stem Cells. *Cell* (2008) 133:704–15. doi: 10.1016/j.cell.2008.03.027

34. Bremnes RM, Veve R, Hirsch FR, Franklin WA. The E-cadherin Cell-Cell Adhesion Complex and Lung Cancer Invasion Metastasis and Prognosis. *Lung Cancer* (2002) 36:115–24. doi: 10.1016/s0169-5002(01)00471-8
35. van Malenstein H, Dekervel J, Verslype C, Van Cutsem E, Windmolders P, Nevens F, et al. Long-Term Exposure to Sorafenib of Liver Cancer Induces Resistance With Epithelial-to-Mesenchymal Transition, Increased Invasion and Risk of Rebound Growth. *Cancer Lett* (2013) 329:74–83. doi: 10.1016/j.canlet.2012.10.021
36. Wang Z, Wang M, Carr BI. Involvement of Receptor Tyrosine Phosphatase DEP-1 Mediated 36. PI3K-cofilin Signaling Pathway in Sorafenib-Induced Cytoskeletal Rearrangement in Hepatoma Cells. *J Cell Physiol* (2010) 224:559–65. doi: 10.1002/jcp.22160

Conflict of Interest: The authors declare that the research was conducted in the absence of any commercial or financial relationships that could be construed as a potential conflict of interest.

frontiers in Endocrinology

ORIGINAL RESEARCH
published: 14 June 2021
doi: 10.3389/fendo.2021.672319

Adrenocortical Carcinoma Steroid Profiles: *In Silico* Pan-Cancer Analysis of TCGA Data Uncovers Immunotherapy Targets for Potential Improved Outcomes

João C. D. Muzzi[1,2,3], *Jessica M. Magno*[2,3], *Milena A. Cardoso*[2,3], *Juliana de Moura*[1], *Mauro A. A. Castro*[2] *and Bonald C. Figueiredo*[3,4*]

[1] Laboratório de Imunoquímica (LIMQ), Pós-Graduação em Microbiologia, Parasitologia e Patologia, Departamento de Patologia Básica, Universidade Federal do Paraná (UFPR), Curitiba, Brazil, [2] Laboratório de Bioinformática e Biologia de Sistemas, Pós-Graduação em Bioinformática, Universidade Federal do Paraná (UFPR), Curitiba, Brazil, [3] Instituto de Pesquisa Pelé Pequeno Príncipe, Oncology Division, Curitiba, Brazil, [4] Centro de Genética Molecular e Pesquisa do Câncer em Crianças (CEGEMPAC), Molecular Oncology Laboratory, Curitiba, Brazil

OPEN ACCESS

Edited by:
Barbara Altieri,
University Hospital of Wuerzburg, Germany

Reviewed by:
Prathibha Ranganathan,
Centre for Human Genetics (CHG), India
Laura-Sophie Landwehr,
University Hospital of Wuerzburg, Germany

***Correspondence:**
Bonald C. Figueiredo
bonaldf@yahoo.com.br

Specialty section:
This article was submitted to Cancer Endocrinology, a section of the journal Frontiers in Endocrinology

Received: 25 February 2021
Accepted: 05 May 2021
Published: 14 June 2021

Citation:
Muzzi JCD, Magno JM, Cardoso MA, de Moura J, Castro MAA and Figueiredo BC (2021) Adrenocortical Carcinoma Steroid Profiles: In Silico Pan-Cancer Analysis of TCGA Data Uncovers Immunotherapy Targets for Potential Improved Outcomes. Front. Endocrinol. 12:672319. doi: 10.3389/fendo.2021.672319

Despite progress in understanding the biology of adrenocortical carcinoma (ACC), treatment options have not dramatically changed in the last three decades, nor have we learned how to avoid some of its long-term side effects. Our goal was to improve the understanding of immune pathways that may include druggable targets to enhance immune responses of patients with ACC, focusing on immune evasion and the activation of immune cells against ACC. Our strategy was aimed at improving insight regarding gene expression without steroid interference. Using approaches based on high and low steroid phenotypes (HSP and LSP, respectively), we characterized immune pathways using The Cancer Genome Atlas (TCGA) ACC cohort data. Although previous studies have suggested that patients with ACC receive minimal benefit from immunotherapy, high expression of immune modulators was noted in patients with LSP, suggesting the activation of these biomarkers may be an important adjuvant therapy target after clearance of excess glucocorticoids. In addition, patients with LSP ACC had higher immune cell infiltration than patients with HSP ACC and other cancer subtypes. Our findings can be summarized as follows (1): we confirmed and improved the definition of two immune response pathways to ACC (HSP and LSP) based on *in silico* transcriptome analysis (2), we demonstrated the steroid profile should be considered, otherwise analyses of ACC immune characteristics can generate confounding results (3), among the overexpressed immunotherapy targets, we demonstrated that LSP was rich in *PDCD1LG2* (*PD-L2*) and both HSP and LSP overexpressed *CD276* (*B7-H3*), which was associated with resistance to anti-PD1 therapy and may have accounted for the modest results of previous clinical trials, and (4) identification of patients with LSP or HSP ACC can be used to help determine whether immunotherapy should be used. In conclusion, we highlighted the differences between LSP and HSP, drawing attention to

potential therapeutic targets (*CD276*, *PDCD1*, and *PDCD1LG2*). Treatments to reduce immune evasion, as well as the use of other natural and pharmacological immune activators, should include prior pharmacological inhibition of steroidogenesis. Attempts to combine these with tumor cell proliferation inhibitors, if they do not affect cells of the immune system, may produce interesting results.

Keywords: adrenocortical carcinoma, steroidogenesis, PD-1/PD-L1/PD-L2, *PDCD1/CD274/PDCD1LG2*, B7-H3, *CD276*, CD8+ T lymphocytes

INTRODUCTION

Adrenocortical carcinoma (ACC) is a rare highly aggressive malignancy of which >80% are steroidogenic (1–4). Overt hypercortisolism is observed in 37.6% (197/524) of adults with ACC, excluding cases with elevated cortisol levels without clinical manifestations, which may also have some molecular impact (4). The phenotypes seen with molecular changes in ACC may be largely derived from the dominant co-secretion of cortisol and androgens. These differences in combinations of steroid underlie the importance of defining steroid phenotypes and identifying the relevant genetic alterations that characterize the various immune system profiles observed.

Pan-genomic and molecular characterizations of ACC have been the focus of diverse studies in an attempt to establish useful classifications for prognosis or therapy. Zheng et al. (5) suggested the differentiation of patients with ACC based on three CpG island hypermethylated phenotype (CIMP) statuses: high, intermediate, and low. To date, CIMP is the most robust biomarker for ACC pan-molecular subgroups (6). Despite providing meaningful prognosis, this classification cannot be translated into determining optimal target treatment options (6, 7). Besides DNA methylation status, other molecular strategies have been used to characterize ACC subtypes (5, 8, 9). Based on transcriptome profiling, de Reyniès et al. (8) and Giordano et al. (9) defined two ACC subgroups, C1A and C1B, while Zheng et al. (5) clustered ACC mRNA-seq data in two subgroups with a high steroid phenotype (HSP) and low steroid phenotype (LSP), separating the expression pattern of genes in the steroid synthesis pathway. This was further refined into four subgroups: HSP (n = 25), HSP + proliferation (n = 22), LSP (n = 27), and LSP + proliferation (n = 4). The proliferation profile was mainly associated with HSP, whereas the LSP + proliferation was restricted to only four cases in The Cancer Genome Atlas (TCGA) cohort (n = 78). These four subgroups demonstrated a high overlap of C1A and C1B subtypes, with most HSP patients classified as C1A and LSP patients classified as C1B (5). Zheng and colleagues found an immune signature associated with the LSP profile upon comparison of immune-suppressed ACC with strong steroidogenesis (5).

Landmark studies have extensively focused on profiling biomarkers and cells associated with cancer immunity with extensive immunogenomic analysis of tumors (10, 11). Thorsson et al. (11) provided new insights into the immune landscape of cancers using TCGA data. Assembling all ACC cases without consideration of more specific clinical or steroidal phenotypes, ACC was found to exhibit the second lowest leukocyte fraction among the cancer types studied (11). These investigators analyzed over 10,000 TCGA tumors and using cluster analysis of a robust list of immune expression signatures reported by other studies proposed six immune subtypes with specific features and prognoses: C1, wound healing; C2, IFN-γ dominant; C3, inflammatory; C4, lymphocyte depleted; C5, immunologically quiet; and C6, TGF-ß dominant (11). Based on the dominant sample characteristics, they proposed the ACCs in the TCGA database (patient ages ranging from 14 to 77 years) fit better within the C4 immune subtype, with a more prominent macrophage signature, suppression of T helper type 1 (Th1) cells, and a high M2 response (11). These cancers are among those with the least favorable outcome. This immunosuppressed profile is associated with hypercortisolism and low survival in the majority of adult patients with ACC (12), while younger children with a dominant androgen steroid phenotype have a better prognosis (13, 14).

As tumors grow, they acquire mutations. These mutations may impair the function of the immune system in ACC subtypes (with both low and high steroidogenesis). These genetic changes include mutations in driver genes, DNA damage, copy number variation, aneuploidy, loss of heterozygosity, intratumor heterogeneity, and decreased telomere length (5, 15). Consequently, overall survival (OS) analyses are frequently less accurate in ACC cases because of the complex interactions between these changes in the tumor and the immune system (16). The worse prognosis for adults with ACC is explained by molecular differences and the higher frequency of elevated glucocorticoids (17–19). After C4 (49 of the 78 ACC cases), the second most common immune subtype was C3, found in 23 of the 78 ACC cases, predominantly in LSP (16/31). The C3 immune subtype is represented by an inflammatory response with higher presence of Th1 and Th17 responses and a balanced presence of macrophages and lymphocytes. In a pan-cancer analysis, the C3 immune subtype presented the best prognosis. The other six ACC cases were C5 (n = 3) and one each of subtypes C1, C2, and C6.

Lymphocyte expression signature, high number of unique T-cell receptor clonotypes, cytokines produced by activated CD4+ Th1 and Th17 lymphocytes, and M1 macrophages, which secrete pro-inflammatory cytokines and chemokines, are associated with improved OS in some cancer subtypes (11). The ability to kill transformed cells is essential for an effective anti-tumor response by the immune system. This ability relies on the cytotoxic activity of natural killer (NK) cells and CD8+ T lymphocytes (CD8+TL) (20).

Activated NK cells are able to recruit dendritic cells and elicit an antitumor T-cell response (21). The presence of activated tumor-infiltrating CD8+TL in human cancers is associated with improved prognosis, expression of specific antigens, and increased immune-cancer interactions (10). For example, there is a positive correlation between melanoma-associated antigen 3 (*MAGEA3*) expression and CD8+TL infiltration in melanoma, explaining the success of the *MAGEA3*-based vaccine (22). Another successful example of immunomodulation is the stimulation of blood cells with bacille Calmette-Guérin (BCG) or recombinant BCG to enhance the expression of CD25 and CD69 on human CD4+ T cells, a highly effective immunotherapeutic agent against bladder cancer (23, 24). Interestingly, most patients with bladder cancer are diagnosed in their seventies when the immune system may be impaired (25). Similarly, more than 50% of adults with ACC are diagnosed in patients 50 years or older (26). As CD8+TL are crucial for protective immunity, it is vital to identify candidate activators of the host immune response to cancer. Specific driver mutations (e.g., *TP53*) are correlated with higher leukocyte levels across all cancers (11). This is not the case in pediatric ACC with the germline *TP53* R337H variant, where higher CD8+TL infiltration is associated with other factors, such as stage 1 and diagnosis at a younger age (14). This is in line with the observed changes in the immune infiltrate composition at each tumor stage, where there is a decrease in T-cell density and an increase in T-follicular helper cells and innate immune cells with tumor progression (27).

T-cell activation requires two distinct signaling pathways, one mediated by the binding of T-cell receptor (TCR) with an antigen bound major histocompatibility complex (MHC) and the second by the binding of CD28 to T cells with B7-1 (CD80) or B7-2 (CD86) of antigen-presenting cells (28). In addition to B7-1 and B7-2, other B7 family proteins interact with other T-cell membrane molecules and may act as co-inhibitors, such as B7-H1, which is well known as programmed cell death ligand 1 (PD-L1), B7-DC, which is known as programmed cell death ligand 2 (PD-L2), and B7-H3 (CD276), among others (29). Blockade of immune checkpoint evasion was expected to provide a more effective treatment for patients with ACC. However, the use of antibodies targeting programmed cell death 1 (PD-1) expressed by T cells (30–32) or PD-L1 (33) is associated with poor efficacy. In the latter study (33), 50% of patients were under concomitant treatment with mitotane to block immunosuppressive glucocorticoids. However, this study did not consider the possibility of evasion through PD-1/PD-L2. Despite these setbacks, other approaches have been suggested to overcome the reported modest responses (7, 34).

The impact of excess steroids on the immune system interaction with ACC tumors, including a complete understanding of the related molecular profiles, has not been fully evaluated. Our aim was to perform a comprehensive and translational analysis of ACC immune biomarkers to identify those that could predict a favorable outcome with and without steroid interference. We evaluated possible modifiers of immune evasion (*CD274* that encodes PD-L1 and *PDCD1LG2* that encodes PD-L2), and investigated how these ligands correlate with *CD8B* expression in ACC, revisiting TCGA cohort data and the molecular steroidogenic classification established by Zheng et al. (5). Considering the hypothesis that HSP has a worse prognosis because of its effect on the immune system, we discuss strategies, supported by prior studies, for downregulating steroid biosynthesis before using possible immune activators.

MATERIALS AND METHODS

Data Sources

Data sources used in this study were obtained from the ACC cohort in TCGA (5). Inclusion criteria, quality control, and characterization of these participants were previously described (5). The data are available on the National Cancer Institute (NCI) Genomic Data Commons (GDC) Data Portal (https://gdc.cancer.gov/about-data/publications/acc_2016). The transcriptome profiles of 78 patients with ACC for whom the steroid phenotype was available were used for the subsequent analysis. This group included 31 men and 47 women with a mean age of 46.7 years (range, 14–77 years). Based on mRNA data, the patients were classified as HSP (n = 25), HSP + Proliferation (n = 22), LSP (n = 27), and LSP + Proliferation (n = 4) (5). For the current study, we used only the steroid phenotype classification, HSP (n = 47) and LSP (n = 31). Clinical data were obtained using the R/Bioconductor package TCGABiolinks v 2.18.0 (35–37) from the GDC Data Portal. History of excessive hormone expression was downloaded from the GDC Data Portal and classified as (i) Cortisol Excess (n = 32) for patients with a history of excess Cortisol (n = 15), Mineralocorticoids|Cortisol (n = 1), and Androgen|Cortisol (n = 16); (ii) Mineralocorticoids Excess (n = 4) for patients with a history of Mineralocorticoids (n = 3) and Mineralocorticoids|Cortisol (n = 1); and (iii) Sexual Hormone Excess (n = 28) for patients with a history of excess Androgen (n = 8), Androgen|Cortisol (n = 16), Androgen|Estrogen (n = 2), and Estrogen (n = 2). There were no notations on hormone levels for 5 patients.

The data on immune characteristics were obtained from Thorsson et al. (11) (https://www.cell.com/cms/10.1016/j.immuni.2018.03.023/attachment/1b63d4bc-af31-4a23-99bb-7ca23c7b4e0a/mmc2) and xCell immune infiltrate cell scores were downloaded from TIMER2.0 (http://timer.cistrome.org/infiltration_estimation_for_tcga.csv.gz) (10, 38, 39). For comparison between two steroid groups, data were filtered using the patients' barcodes.

The study was approved by the Ethics Committee of Pequeno Príncipe Hospital and National Research Ethics Committee (CAAE number 50622315.0.0000.0097), without use of a consent form as it involved only anonymous public data from the original cohorts deposited at TCGA.

Leukocyte Fraction and Immune Infiltrate Comparison

Leukocyte fractions data for pan-cancer analysis were extracted from Thorsson et al. (11). The study included 11,080 patients from TCGA of which 10,448 were annotated with a leukocyte

fraction. TCGA studies were used and were arranged by median leukocyte fraction values. For grouping based on the ACC steroid phenotype, patients from this cohort were selected according to their barcode identifiers.

Previous studies used two methods to estimate immune cell infiltration in the ACC cohort: xCell (38) scores using a marker-gene-based approach, inferred by Sturm et al. (39), and Cibersort using a deconvolution-based approach (40), calculated by Thorsson et al. (11). A more detailed evaluation on the limitations and characteristics of these approaches has been reviewed by Sturm et al. (39).

The immune cell proportions based on Cibersort estimations were multiplied by the leukocyte fraction, resulting in a final score that could be used for intra- and inter-sample comparisons, as previously described (11). For the ACC cohort analysis, scores of CD8+TL and activated NK cells were used for pan-cancer comparisons, while the scores for all 22 cell types were used for intra-cohort analysis. For pan-cancer comparisons, the barcodes were merged with the Thorsson dataset, and xCell results for CD8+TL and NK cells of the TCGA study and were grouped and ordered by median values. For comparisons within the ACC cohort, samples were filtered for all xCell infiltrate estimates by patient barcodes. Beyond cell estimations, xCell offers microenvironment, immune, and stroma scores. However, the enrichment scores do not allow for a comparison between different cell types of the same sample, but does allow for comparison of the same cell type between different samples. Accordingly, the two groups of patients could be compared using this method, but the relative abundance of each cell type within a patient could not be compared.

The Wilcoxon test was used to compare the xCell and Cibersort immune infiltrate scores between the HSP and LSP groups. The R package ComplexHeatmap v 2.6.2 (41) was used for heatmap construction. Column-wise z-scores were calculated for the immune cell scores, and maximum and minimum values were limited to +2 and −2, respectively. Samples were clustered for immune characteristics and cell scores scaled data in a semi-supervised manner using the McQuitty and Euclidean distance methods.

RNA-seq Filtering, Processing, and Differential Expression (DE)

High-throughput sequencing (HTSeq) mRNA data were obtained for the 78 ACC patients with steroid phenotype characterization using the R package TCGAbiolinks v 2.18.0 (35–37) and SummarizedExperiment v 1.20.0 (42). The 56,457 transcripts were filtered for protein-coding genes using EnsembleDb version 101 and notated using AnnotationHub R package v 2.22.0 (43). The genes with a sum of zero counts were excluded, resulting in the inclusion of 19,169 genes. The two steroid phenotype groups underwent DE analysis using the R package DESeq2 v 1.30.0 as previously described (44). P-values were calculated using Wald's test and adjusted with Benjamini–Hochberg estimation. The gene count expression matrix was normalized by variance-stabilizing transformation using the DESeq2 package. Three genes had duplicated symbol names (*PINX1, TMSB15B*, and *MATR3*). To differentiate these three genes, we added an underscore after the first entry in the DE results.

Enrichment Analysis

After ordering based on adjusted p-values, the ranked genes list underwent gene set enrichment analysis (GSEA) with the Coincident Extreme Ranks in Numerical Observations (CERNO) test (45, 46) using the R package tmod v 0.46.2, as previously described (46, 47). The CERNO test is an application of modified Fisher p-value integration for creating a GSEA ranked list, which avoids the arbitrary choice of a p-value or log-fold change threshold (46). Two gene sets were used for the enrichment analysis. Hallmark gene sets were obtained from MSigDb v7.1 (https://data.broadinstitute.org/gsea-msigdb/msigdb/release/7.1/msigdb_v7.1.xml) (48, 49) and blood transcriptional modules (BTM) (50) were obtained from the tmod R package. The hallmark gene set is comprised of 50 modules summarizing the molecular signature database gene sets and reducing redundancy (49). These modules are divided into eight categories: cellular component, development, DNA damage, immune, metabolic, pathway, proliferation, and signaling. The other gene set consists of 334 BTMs combining information about adaptive and innate immune responses.

Expression of Immune Modulators and Immune Checkpoints

Expression profiles of the immunomodulatory genes listed by Thorsson et al. (11) (https://www.cell.com/cms/10.1016/j.immuni.2018.03.023/attachment/8d3ffc74-4db4-4531-a4ad-389dfc8bb7ec/mmc7.xlsx) were obtained from a variance stabilizing transformation gene expression matrix. Of the 75 immune modulators, only one (*C10orf54*) was not found in the expression matrix. *CSF2* expression was added based on the study by Wang et al. (51), which showed its importance for dendritic cell recruitment in poorly immunogenic tumors. Adjusted p-values for the findings from the DE analysis were used for comparison between groups. The R package ComplexHeatmap v 2.6.2 (41) was used for heatmap construction, column-wise z-scores were calculated for immune modulator gene expressions, and maximum and minimum values were limited to +2 and −2, respectively. Columns were arranged following the order of the semi-supervised clusters of immune characteristics and cell scores determined previously. For expression of immune checkpoint genes *CD8B*, *CD274* (*PD-L1)*, and *PDCD1LG2* (*PD-L2)*, Pearson's correlation coefficients and p-values were calculated and the confidence interval was inferred based on Fisher's Z transformation.

Leukocyte Fractions and Mutations in the ACC Cohort

Pan-Cancer Atlas data from TCGA regarding ACC patients with mutations in *TP53* (n = 16), *CTNNB1* (n = 13), and *MEN1* (n = 7) were obtained from the cBioPortal (https://www.cbioportal.org/) and merged with the leukocyte fraction information. Comparison

between patients with and without mutations in these driver genes was performed using the Wilcoxon test.

Extracellular Communication Networks in Immune Subtypes

Extracellular communication networks were inferred based on the study by Thorsson et al. (11) and the data for the TCGA ACC cohort were obtained from iAtlas (https://isb-cgc.shinyapps.io/shiny-iatlas/). The networks involved ligand-receptor, cell-receptor, and cell-ligand pairs described by Ramilowski et al. (52) and enhanced by Thorsson et al. (11). Nodes with more than 50% abundance and concordance interaction greater than 2.5 were chosen as the C3 and C4 immune subtypes. The networks were reconstructed using R packages igraph v 1.2.6 and RedeR v 1.38.0 (53). The node line width varies proportionally to the abundance score and the edge width varies proportionally to the concordance.

A batch corrected and normalized gene expression matrix for the 11,060 TCGA samples was downloaded from the Supplemental Data of Hoadley et al. (54) (https://api.gdc.cancer.gov/data/9a4679c3-855d-4055-8be9-3577ce10f66e). The matrix was filtered for the 25 ligands and receptors present in the C3 and C4 networks. Samples were selected from primary tumors only and duplicate entries were removed. The matrix was merged with the Thorsson dataset according to the participant barcode. Gene expression data were ranked from lowest to highest counts for each gene, and patients were divided into terciles (low, intermediate, and high) and filtered for the ACC patients' barcodes.

Survival Analysis

The prognostic impact of LSP (n = 31) versus HSP (n = 47), immune subtype C3 (n = 23) versus C4 (n = 49), and LSP + Immune Subtype C3 (n = 16) versus other configurations (n = 62) were evaluated using Kaplan-Meier analysis for OS and progression-free interval (PFI) using R packages survival v3.2-7 (55, 56) and survminer v0.4.8. P-values were calculated using the log-rank test.

Statistical Analysis

Q values and false discovery rate (FDR) quantities were calculated using R package qvalue v2.20.0 (57). For DE results, q-values were calculated based on π estimation. Due to the small number of p-values available for π estimation, the q-value was determined using Benjamini-Hochberg estimation for enrichment analysis.

RESULTS

Pan-Cancer Comparison Showed Significant Immune Infiltrates in Patients With LSP ACC

ACC had one of the lowest immune infiltrate profiles in the TCGA pan-cancer comparison (**Figure 1A**). However, when

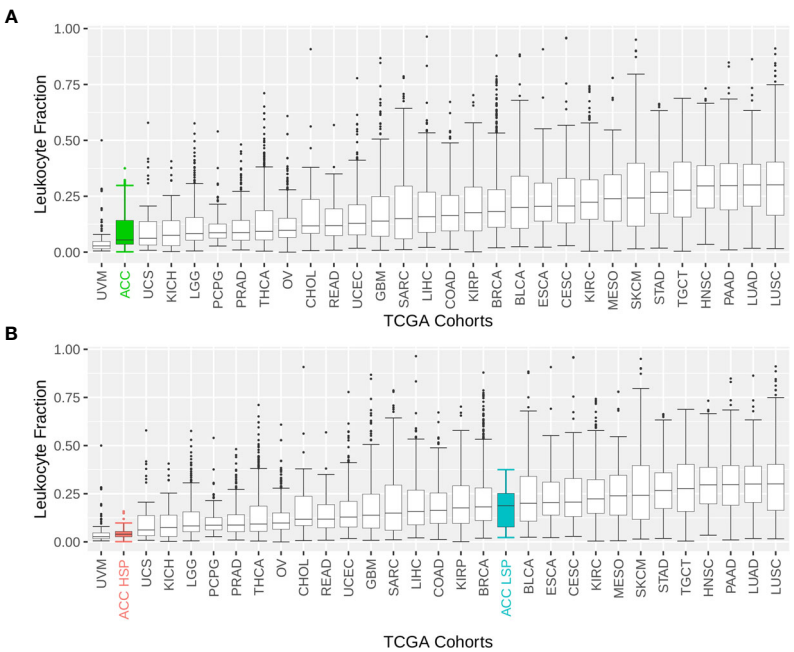

FIGURE 1 | Boxplot of the leukocyte fraction in the tumor microenvironment of 30 TCGA solid tumors. The leukocyte fraction was inferred by Thorsson et al. (11) for 10,448 participants included in The Cancer Genome Atlas (TCGA) database using molecular methods and compared with hematoxylin and eosin stained images, which demonstrated good correlation. Participants were grouped by TCGA cohort. The boxplot shows the median and interquartile range (IQR) for the leukocyte fraction of each cohort. Whiskers are set at 1.5 IQR and outliers (above and below the 1.5 IQR) are presented as points. TCGA cohorts were ordered by median values. **(A)** Patients with adrenocortical carcinoma (ACC) are represented as one group. **(B)** Patients with ACC are divided according to steroid phenotypes.

distinguishing by steroid profiles, patients with LSP ACC had considerable leukocyte infiltration, placing them in the top 40% of tumor types (**Figure 1B**). This was also seen with CD8+TL and NK cells infiltrates, as measured by the Cibersort and xCell scores (**Figures 2A–D**).

The main clinical characteristics of HSP and LSP are shown in **Table 1**. Cortisol was the most frequently elevated hormone (57.4% in HSP and 16.1% in LSP) compared to less frequently observed sex steroids, mineralocorticoids, and others, as described by Zheng et al. (5). The prognostic differences were remarkable, with only 3 death events (9.7%) in patients with LSP versus 24 (51.1%) in patients with HSP. This was in addition to a higher proportion of advanced cancer stages observed in the HSP group, which may have been associated with a higher proliferation rate.

Immune Activation Was Enriched in Patients With LSP ACC

The results from the DE analysis of LSP versus HSP are presented in **Figure 3**. The order is based on LSP versus HSP and is used in all analyses presented in this study. Opposite

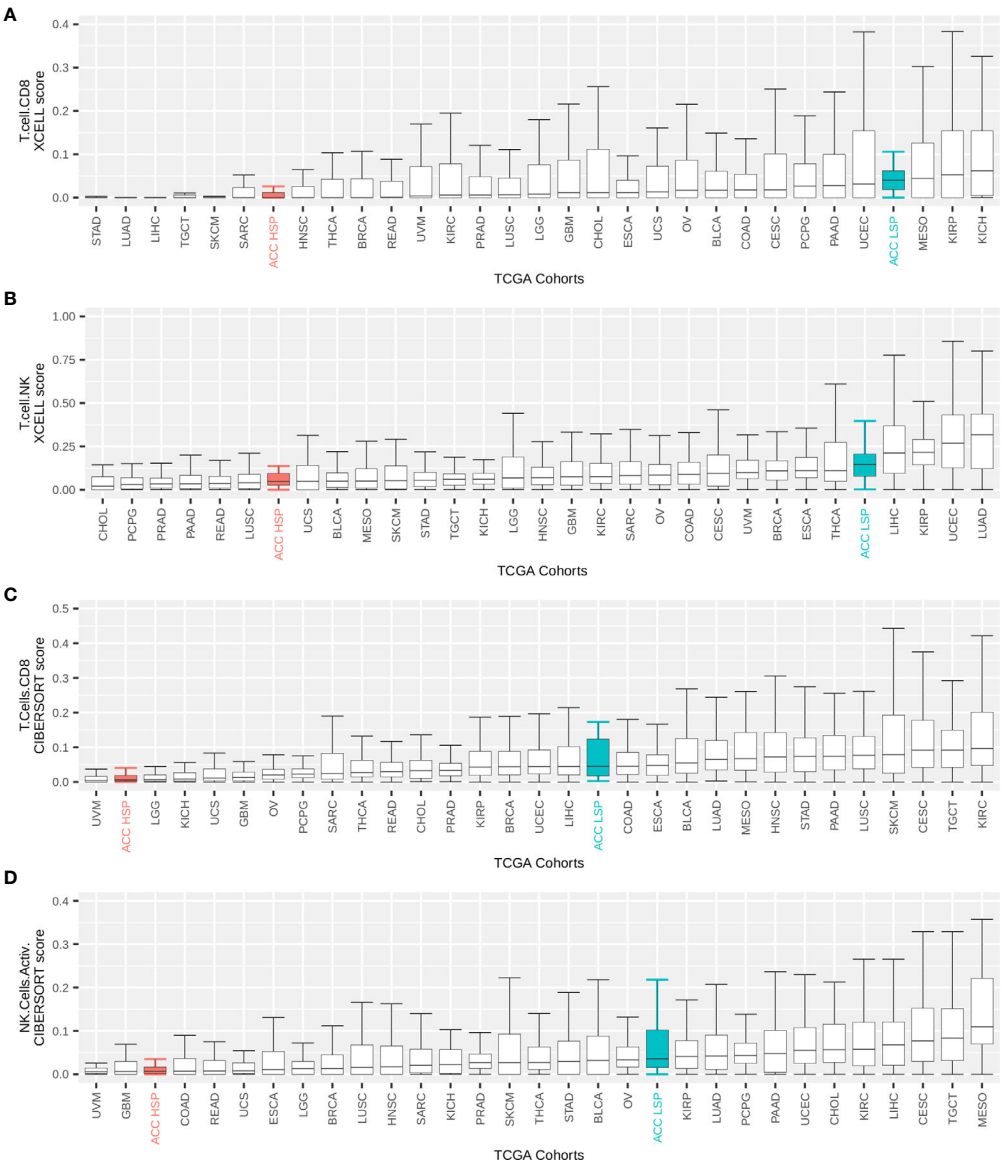

FIGURE 2 | TCGA pan-cancer comparison of immune infiltrates. Immune infiltrate scores (y-axis) were rescaled to range from 0 to 1. The maximum on the y-axis is independently set for each plot for better visualization. Participants were grouped by TCGA cohort and the boxplot shows median and IQR for immune cell infiltrate scores of each cohort. Whiskers are set at 1.5 IQR and outliers (above and below the 1.5 IQR) are not shown. TCGA cohorts were ordered by median values. Patients with ACC were divided according to steroid phenotypes **(A, B)** xCell scores for CD8+ T cells and T natural killer (NK) cells inferred by Sturm et al. (39). **(C, D)** Cibersort scores for activated CD8+ T cells and NK cells as inferred by Thorsson et al. (11) and multiplied by the leukocyte fraction as described by these authors.

TABLE 1 | Clinical data.

	HSP	LSP
Total (Dead)	47 (24)	31 (3)
Mean Age ± SD	46.5 ± 17	48.5 ± 14.3
Males	16 (9)	15 (2)
Mean age ± SD	46 ± 14.6	52.9 ± 11
Females	31 (15)	16 (1)
Mean age ± SD	46.8 ± 18.3	44.3 ± 16.1
High Proliferation	22 (15)	4 (2)
Tumor Stage		
Stage I	3 (1)	6 (0)
Stage II	18 (6)	19 (1)
Stage III	12 (6)	4 (1)
Stage IV	12 (10)	2 (1)
Hormone Excess		
Cortisol	27 (14)	5 (1)
Mineralocorticoids	3 (1)	1 (0)
Sexual	20 (14)	8 (1)
Immune Subtype		
C1	1 (1)	0 (0)
C2	0 (0)	1 (1)
C3	7 (3)	16 (0)
C4	37 (19)	12 (1)
C5	2 (1)	1 (0)
C6	0 (0)	1 (1)

The total number of patients for each clinical category for the Low Steroid Phenotype (LSP) and High Steroid Phenotype (HSP) is shown with the number of dead patients in parenthesis. The mean age of participants with the standard deviation (SD) is shown for both groups and subdivided into males and females. All clinical data were retrieved from Zheng et al. (5) and the immune subtype classification from Thorsson et al. (11). Proliferation is bipartite as presented by Zheng et al. (5) based on transcriptomic classification and associated with markers such KI67 and BUB1.

values for the log-fold change would have been determined if HSP versus LSP was used. The full DE results are available in **Supplementary Table 1**.

Enrichment analysis using the hallmark gene sets is presented in **Figure 4A** and **Supplementary Table 2**. Most gene sets were enriched for genes related mainly to the immune response and were upregulated in LSP and downregulated in HSP. The gene sets significantly enriched with genes downregulated in LSP and upregulated in HSP were associated with estrogen response, cholesterol homeostasis, and hedgehog signaling (**Figure 4A**), which was consistent with the steroidogenic profile used for the DE analysis.

As the immune response was strongly associated with the different steroid phenotypes, we conducted GSEA with the BTMs described by Li et al. (50). In general, modules associated with T lymphocytes and NK cells, monocytes, and antigen presentation displayed the strongest association with ranked genes, especially those upregulated in LSP. With exception of the "Cell Cycle and Transcription" module, most immune modules were markedly enriched with genes up-regulated in LSP and down-regulated in HSP, with some modules such as "Enriched in Antigen Presentation (II)" and "Leukocyte Activation and Migration" fully represented by DE genes up-regulated in LSP (**Figure 4B**).

Enrichment of T Cells, Monocytes, and Cytolytic Activity in LSP ACC

The column-wise z-scores for the xCell and Cibersort results for TCGA ACC patients are presented in **Figure 5A**. Both methods found a higher immune cell presence in patients with LSP compared to those in patients with HSP, which appeared immunosuppressed. Not all cell types identified using one method were present in the results obtained using the other method, indicating differences in some specificities. Consistent with the BTM enrichment analysis (**Figure 4B**), the presence of monocytes and T cells differed significantly between the two steroid phenotypes (**Figures 5A, B**). As xCell detected NK cells in only a few samples and Cibersort differentiated resting NK cells from activated NK cells but did not distinguish between subtypes of CD8+ T cells, the last two panels of **Figure 5B** show a boxplot comparison of the xCell T NK cells and the Cibersort activated NK cells. Because xCell generates arbitrary scores, y values were rescaled to a range of 0 to 1. Most discrepancies between the xCell and Cibersort scores were observed for B cells, plasma cells, naive CD4+ T cells, and eosinophils, which may have been a result of the spillover effect from the methods (39).

LSP Was Associated With an Inflammatory Immune Response and HSP With a Lymphocyte Depleted Microenvironment

According to the classification by Thorsson et al. (11), ACC patients fit mainly into the C4 subtype (n = 46), with a subset of patients in C3 subtype (n = 23), where C3 seemed to be associated with LSP (n = 16) and C4 with HSP (n = 37) (**Table 1** and **Figure 5A**). Only one participant each fit into the C1, C2, and C6 subtypes, and three patients presented with a C5 subtype profile. Density plots show the distribution of C3 and C4 ACC patients separated into the steroid phenotypes based on monocyte, CD8+TL, and NK cell scores (**Figure 5B**).

The higher immune activation of patients with LSP ACC was also seen in the expression of immunomodulator genes (**Figure 6A**). Patients with LSP had a higher expression pattern of immune activators and inhibitors compared to patients with HSP. From the immune characteristics analyzed by Thorsson et al. (11), the differences between LSP and HSP were significant for leukocyte fraction, lymphocyte infiltration score, and macrophage regulation (**Figure 6B**), which demonstrates immune activation and recruitment in patients with LSP, in contrast with the immunosuppressed tumor microenvironment (TME) seen in patients with HSP.

Thorsson et al. (11) also evaluated the T-cell receptor (TCR) and B-cell receptor (BCR) repertoire. However, this information for most patients with ACC unfortunately could not be retrieved from bulk mRNA sequencing, probably due to the small numbers of these cell fractions in the TME. For instance, only 5 of 78 patients had information regarding BCR (3 LSP and 2 HSP) and 37 regarding TCR (21 LSP and 16 HSP) of which 16 had a 0 score on TCR Shannon entropy (3 LSP and 13 HSP).

Steroid Phenotype Generated a Confounding Effect on the Correlation Between Leukocyte Fraction and Driver Gene Mutations

Thorsson et al. (11) reported that mutations in driver genes are significantly correlated with the leukocyte fraction. Among driver

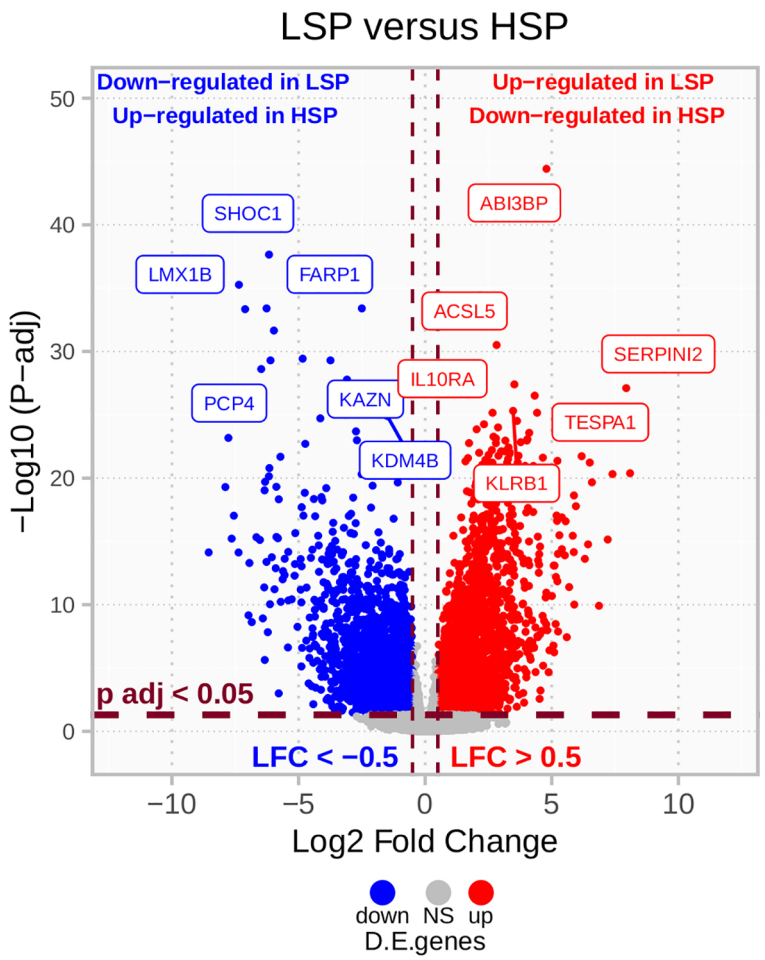

FIGURE 3 | LSP *versus* HSP DE in TCGA ACC cohort (n = 78). After filtering for protein-coding genes and excluding those with sums of zero counts, a total of 19,169 genes were used for a LSP *versus* HSP differential expression (DE) analysis. P-values were calculated using the Wald's test and adjusted using Benjamini-Hochberg estimation. Genes with absolute log2 fold change lower than 0.5 and adjusted p-value greater than 0.05 are colored in gray. Above these cut-offs, genes upregulated in LSP and downregulated in HSP are indicated in red and genes downregulated in LSP and upregulated in HSP are indicated in blue.

genes, the most common mutations found in the ACC cohort were in *TP53* (n = 16), *CTNNB1* (n = 13), and *MEN1* (n = 7); however, these mutations were mainly present in patients with HSP (n = 13 of 16, n = 13 of 13, and n = 6 of 7, respectively). It was not possible to determine whether differences in the leukocyte fraction were caused by the mutations or due to the steroid phenotype. Using the Wilcoxon test to evaluate the differences in the leukocyte fraction based on the presence or absence of these mutations resulted in p-values of 1.8×10^{-1}, 3.8×10^{-2}, and 4.8×10^{-1} for *TP53*, *CTNNB1*, and *MEN1*, respectively.

Extracellular Communication Networks and Possible Immunotherapy Targets Associated With Steroid Phenotypes

Based on the study by Thorsson et al. (11), two extracellular communication networks were reconstructed for ACC subtypes C3 and C4 with 50% abundance and 2.5 concordance thresholds (**Figure 7A**). A small network was also obtained for the C5 subtype with these parameters centered on macrophages; however, as it contained only 3 patients and was not further considered in the current study. The abundance was representative of the prevalence of the node in the samples (%), while concordance was relative to the concordance to discordance ratio (a pair with concordant high or low expression versus a pair with distinct expression patterns in each sample).

The nodes in the C3 and C4 networks were used to compare all TCGA participants. The ACC patient classification is shown in **Figure 7B**. Most ACC patients, despite phenotype distinction, were in the top third group for expression of *CD276 (B7-H3)*, *GPC1*, vascular endothelial growth factor A (*VEGFA)*, vascular endothelial growth factor B (*VEGFB)*, and vascular endothelial growth factor receptor 1 *(VEGFR1) FLT1* (**Figure 7B**).

Despite its greater representativity in the ACC cohort (49 of 78 patients), C4 formed a smaller network (**Figure 7A**) with generally lower abundance and weaker connections. Curiously, a

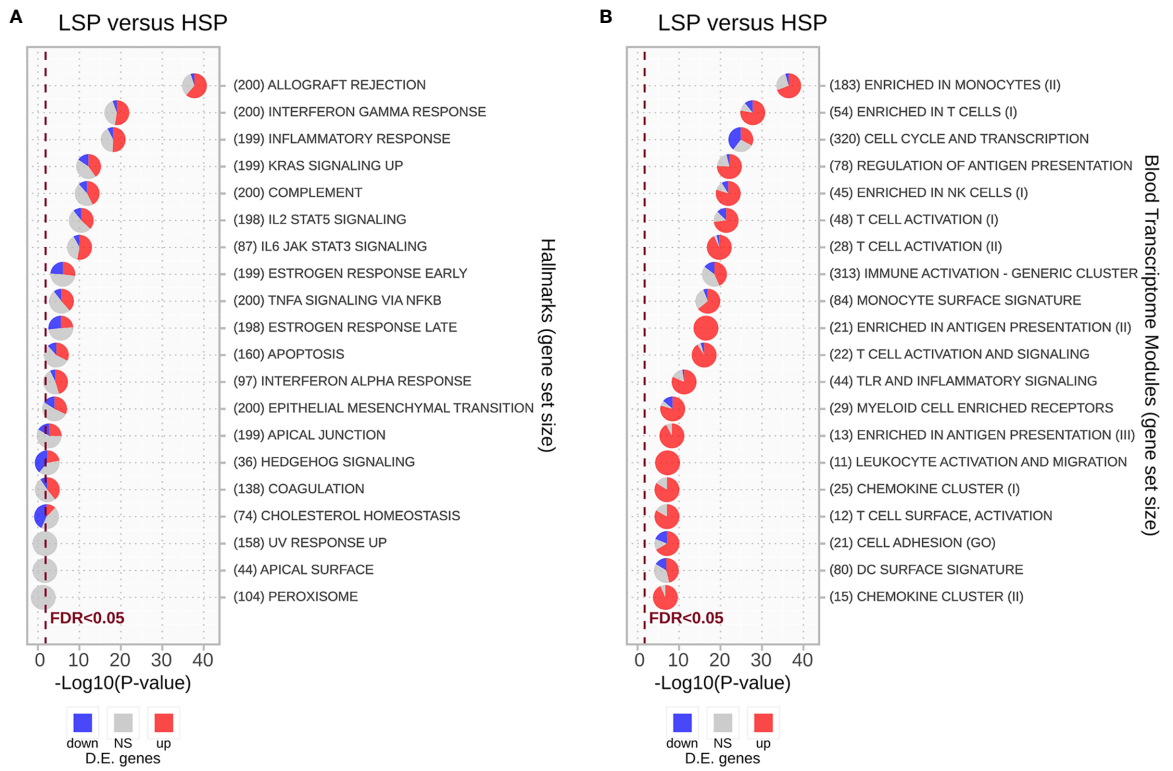

FIGURE 4 | Enrichment analysis for differentially expressed genes using the CERNO test. The CERNO test was applied to the differentially expressed genes using the hallmark gene sets **(A)** and blood transcriptome modules (BTMs) **(B)**. The modules are ordered according to the adjusted p-values and are considered non-significant based on a false discovery rate (FDR) of 0.05. The number of genes in each module is presented before the module names in brackets. The charts are colored based on the DE results: red for module genes upregulated in low steroid phenotype (LSP) and downregulated in high steroid phenotype (HSP), gray for module genes with no significant p-value, and blue for module genes down-regulated in LSP and upregulated in HSP.

high abundance of *TNFSF9* (*4-1BB-L)*, commonly expressed by antigen-presenting cells, was found to be related to the C4 network, but not its receptor *TNFRSF9* (*4-1BB)*, which is normally expressed in CD8+ T cells.

In the C3 network, which was mainly associated with patients with LSP (**Figure 7A**), antigen presentation molecules and some of their receptors were prominently present. It is noteworthy that *PDCD1LG2 (PD-L2)*, but not *CD274* (*PD-L1)*, appeared in good concordance with its receptor *PDCD1 (PD-1)*. Interestingly, a relative positive correlation was observed between *CD8B* and *CD274* expression, but it was more evident between *CD8B* and *PDCD1LG2* expression (**Figure 8**).

Finally, *CD276 (B7-H3)* and *FLT1* (*VEGFR1)* were present in abundance in both networks. *CD276* was in concordance with CD8+ T cells in C3 and in concordance with dendritic cells in C4, while *FLT1* was in concordance with *VEGFA* in C4 and in concordance with *VEGFB* in C3.

Steroid Phenotype Was More Predictable of Outcome Than Immune Subtype Alone

Based on Kaplan-Meier analysis, LSP presented better outcomes, both in OS ($p = 2 \times 10^{-4}$) and PFI (p-value $< 1 \times 10^{-4}$) (**Figure 9A**). When comparing the C3 and C4 immune subtypes, a slightly better prognosis was seen for C3 ($p = 3.2 \times 10^{-2}$ for OS and $p = 4.7 \times 10^{-2}$ for PFI) (**Figure 9B**). The separation between C3 and patients with LSP from the other configurations showed a significant difference in survival analysis ($p = 4.5 \times 10^{-3}$ for OS and $p = 7.1 \times 10^{-3}$ for PFI) (**Figure 9C**).

DISCUSSION

We present a complementary approach to the analyses of the pioneering studies by Zheng et al. (5) and Thorsson et al. (11) and revisit the potential biomarkers underlying the immunological processes in ACC, considering important contributions from previous studies (7–9, 12). The interplay between steroid production and the immune response in ACC has been a topic of recent studies (5, 12, 14, 18, 19). We have uncovered further interesting findings from the ACC datasets, deepened the investigation of immune pathways, and revealed possible druggable targets that may guide the selection criteria for ACC-targeted immunotherapy.

We demonstrated the immune system capabilities were dramatically better in patients with LSP (**Figures 1** and **2**), which is in agreement with studies describing the immune

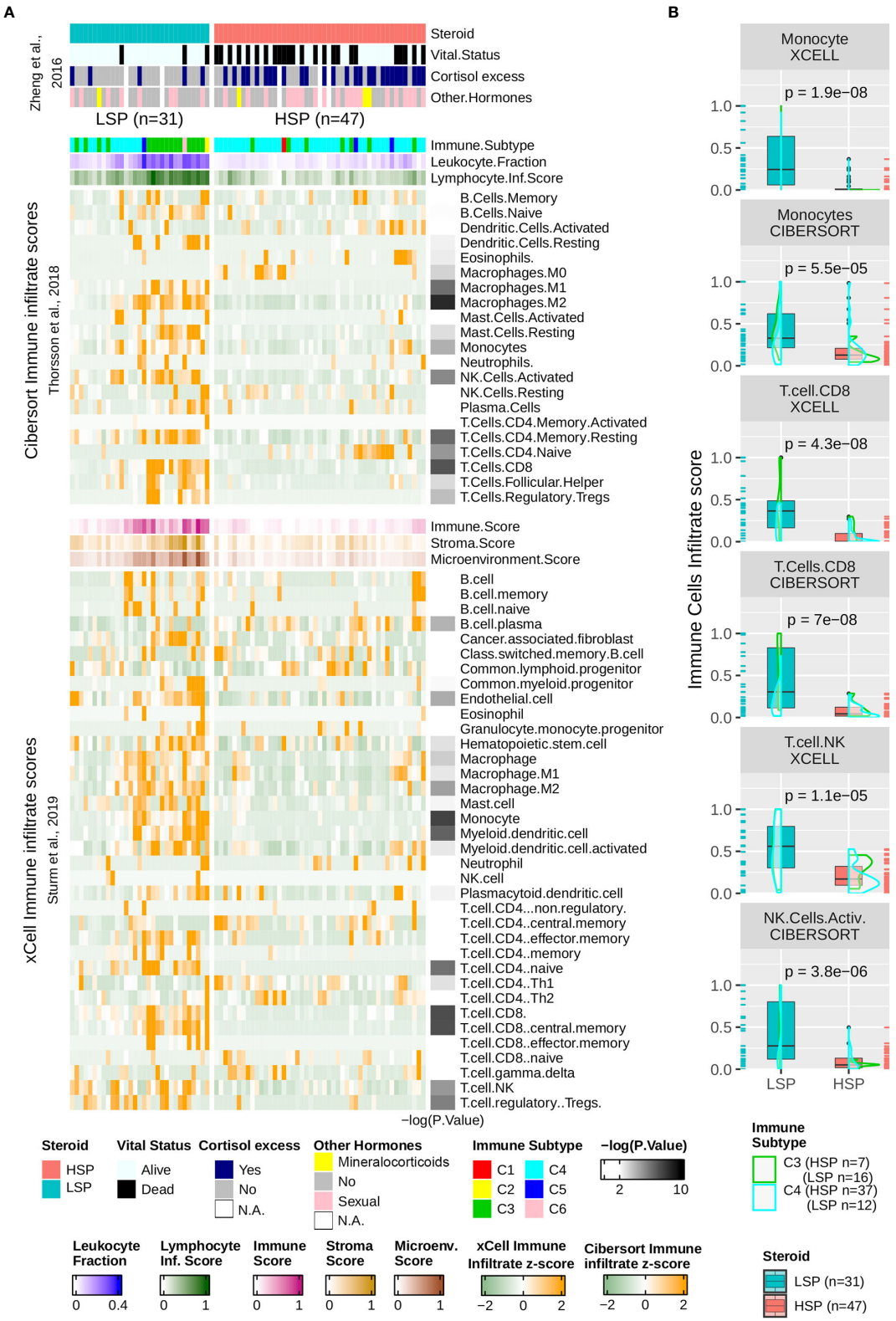

FIGURE 5 | Continued

FIGURE 5 | Immune infiltrate comparison. **(A)** Heatmap with column-wise z-scores for TCGA ACC immune infiltrates as inferred by Sturm et al. (39) using xCell and by Thorsson et al. (11) using Cibersort. Maximum and minimum z-scores for the color gradient were set at +2 and –2 standard deviations from the mean. Each column represents a patient and columns were subjected to semi-supervised clustering. In addition to the immune infiltrate, Thorsson et al. (11) presented a classification of six immune subtypes (C1–C6) and inferred the leukocyte fraction and a molecular signature associated with the lymphocyte infiltrate score. xCell provides a stroma, immune, and microenvironment score in addition to the immune cell infiltrate. Lymphocyte infiltrate, immune, stroma, and microenvironment scores were rescaled to a range of 0 to 1. The clinical information was provided by Zheng et al. (5) and appears in the top annotation rows. The p-value calculated using the Wilcoxon test comparing LSP and HSP for each cell type is represented in the right as a color gradient ranging from 2 to 10 for –log10 (p-value), values lesser than 2 are set as white. **(B)** Boxplot comparing LSP and HSP in terms of monocytes, CD8+ T cells (xCell and Cibersort), T natural killer (NK) cells (xCell), and activated NK cells (Cibersort). All scores (y-axis) are rescaled from 0 to 1. The density plot shows the distribution according to the immune subtypes: C3 (green) and C4 (cyan). Each sample is shown in a rug plot and colored according to the HSP and LSP classification. The p-value calculated using the Wilcoxon test comparing both phenotypes is shown above each pair of boxplots.

suppression caused by excess glucocorticoids (12). This higher immune activation seen in a subset of patients with ACC was in contrast with worst outcomes previously demonstrated for ACC in a pan-cancer analysis of solid tumors, which considered all patients with ACC without distinction of subtypes (5, 11). Our analyses, which considered steroid phenotype, improved our understanding of how the immune system reacts to ACC.

The immune cell composition in the TME is associated with important prognostic and therapeutic characteristics (14, 39). Our analysis of TME was based on scores inferred by previous studies (11, 39) and used two different methods, xCell and Cibersort, to detect immune cells according to bulk RNA-seq data. Some observed divergences (e.g., native CD4+ T cells) may be explained by limitation of the methods, such as background prediction or the spillover effect, as discussed by Sturm et al. (39). However, a higher immune cell infiltrate was observed in general for patients with LSP compared with that for patients with HSP (**Figures 5A, B**). Furthermore, both methods showed a significantly higher presence of cells associated with cytotoxic activity (**Figure 5B**), such as CD8+ T cells ($p = 4.3 \times 10^{-8}$ for xCell and $p = 7 \times 10^{-8}$ for Cibersort scores), T NK cells ($p = 1.1 \times 10^{-5}$ for xCell scores), and activated NK cells ($p = 3.8 \times 10^{-6}$ for Cibersort scores).

Notably, we observed an activation of immune system-related genes (**Figure 6A**), as well as expression of immune evasion-related genes in patients with LSP (**Figures 6A** and **8**). We also demonstrated a positive correlation between *CD8B* and *CD274 (PD-L1)* expression ($R = 0.61$, $p = 1 \times 10^{-11}$) and *CD8B* and *PDCD1LG2* (*PD-L2)* ($R = 0.77$, $p = 8.6 \times 10^{-18}$) (**Figure 8**). This may indicate that selective pressure induced enhanced immune evasion by tumor cells, which is in agreement with recent studies (51). PD-1/PD-L1-related and PD-1/PD-L2-related immune escape mechanisms are known to downregulate the CD8+ T-cell activation process. *CD274* is expressed by other immune cells in greater a proportion than that of *PDCD1LG2* expression (58), which may help explain why the dispersion seen in scatter plots was more evident for *CD274*. In addition, patients with HSP ACC overall presented lower levels of *CD8B* and *CD274/PDCD1LG2* expression compared to those of patients with LSP ACC. However, the positive correlation observed between *CD8B* and *CD274/PDCD1LG2* expression may imply that following glucocorticoid suppression, mechanisms of immune evasion may be induced in patients with HSP ACC. The correlation between CD8+TL and PD-L1 expression levels cannot be determined using immunohistochemistry (14, 59). However, findings from a previous study (59) and our current study suggest that PD-L2 plays a greater role than that of PD-L1 in ACC cells (**Figure 6A**). Nevertheless, this hypothesis has not been assessed in a clinical trial. Anti-PD-1 clinical trials conducted without inhibiting steroidogenesis (30–32) may have had modest results due to the immune suppression caused by hormone production in the TME. On the other hand, Le Tourneau et al. (33) evaluated the concomitant suppression of steroidogenesis with and without mitotane administration. However, only anti-PD-L1 was used in their study and they did not consider the possibility of PD-L2 being an important immune checkpoint in ACC.

In agreement with recent findings showing that 90% of ACC samples (n = 48) were positive for B7-H3 (*CD276*) in immunohistochemical assays (60), our analysis demonstrated that *CD276* overexpression was detected in both LSP and HSP. Remarkably, its expression was considered high in a pan-cancer comparison of most ACC patients (**Figure 7B**). Moreover, *CD276* overexpression has been implicated in resistance to anti-PD1 therapies (61–63). B7-H3 is a member of the B7 ligand family and is a recent and attractive target for antibody-based immunotherapy. B7-H3 is differentially overexpressed in malignant cells at high frequency (60% of 25,000 tumor samples), is detected at low levels in normal tissues, and probably has an inhibitory role in adaptive immunity, suppressing T-cell activation and proliferation (60–62). B7-H3 modulates T-cell responses, but unlike PD-1 and CTLA-4, may inhibit T-cell activation, possibly by interacting with tumor necrosis family receptors (64). However, other investigators believe the B7-H3 receptor remains unknown (61). Recent studies have shown that blocking B7-H3 results in a response of tumor resistance to treatments with anti-PD1/PD-L1 antibodies (61). Yonesaka et al. (63) demonstrated the dual blockade of B7-H3 and PD-L1 enhances the antitumor reaction compared to that of PD-L1 blockade alone, which may indicate a role of B7-H3 overexpression in immune evasion. These findings suggest that anti-B7-H3 combined with anti-PD-1/PD-L1 antibody therapy is a promising approach for B7-H3-expressing cancers, such as ACC. In addition to *CD276* (B7-H3), *FLT1* (VEGFR1) appeared in both C3 and C4 networks (**Figure 7A**) and was highly expressed in ACC compared with that in other cancers (**Figure 7B**). This may imply a role in angiogenesis, which has been described as an important pathway in ACC (65, 66). However, clinical trials to date using VEGFR inhibitors for ACC have demonstrated limited results (67, 68).

In contrast to *CD276* (B7-H3) and *FLT1* (VEGFR1), *BTLA*, interleukin 10 (*IL10*), IL10 receptor subunit alpha *(IL10RA)*, integrin beta chain-2 (*ITGB2*), *CD274* (*PD-L1*), and *PDCD1LG2*

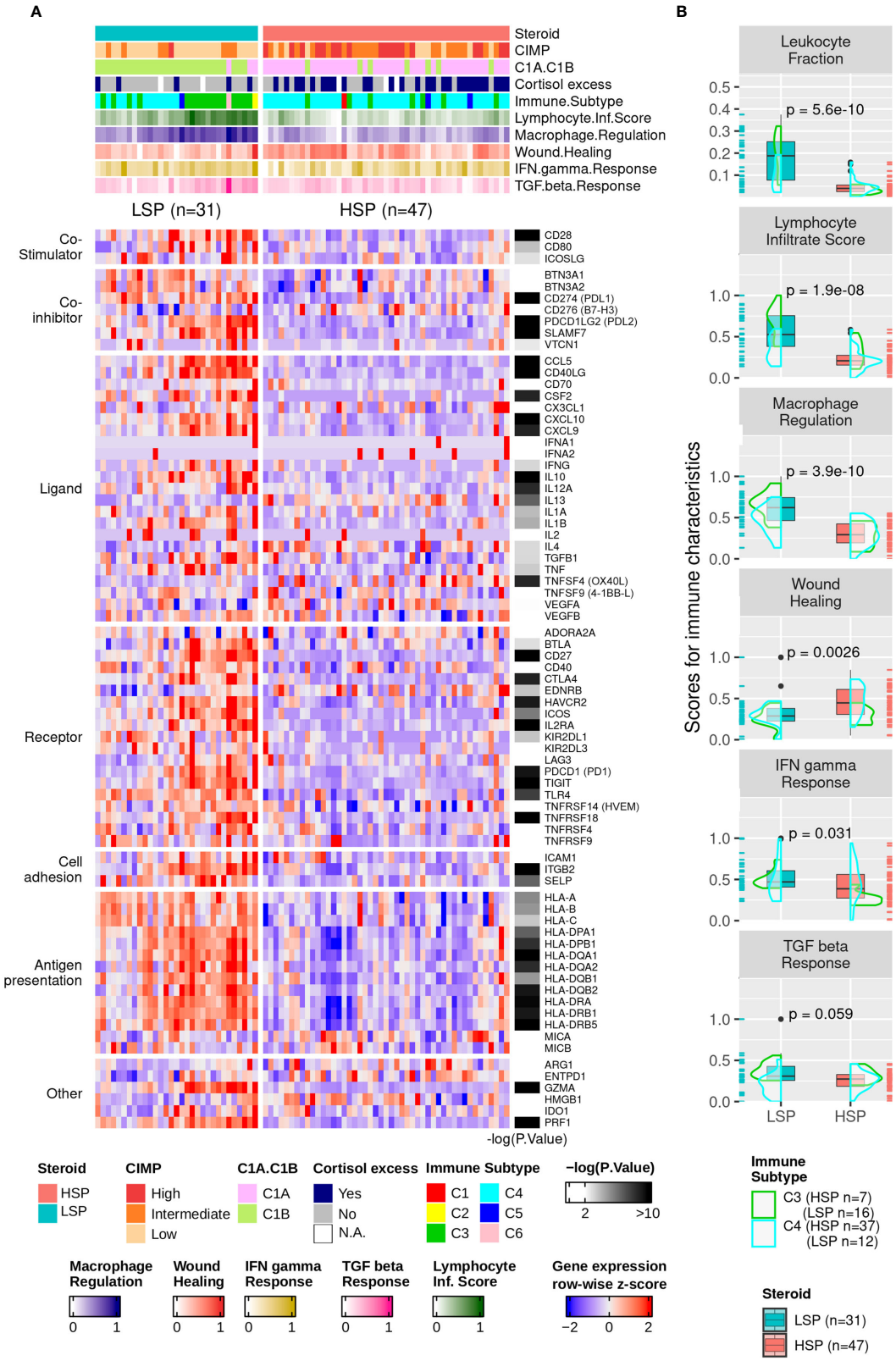

FIGURE 6 | Continued

FIGURE 6 | Gene expression of immune modulators and Thorsson and colleagues' immune signatures. **(A)** Heatmap with column-wise z-scores for expression of immune modulator genes. The maximum and minimum z-scores for the color gradient is set at +2 and –2 standard deviations from the mean. Each column represents a patient. The order from **Figure 5A** was maintained. The p-value for the DE analysis for each gene determined using the Wald's test is represented in the right. The –log10 (p-value) color gradient is set as white up to the minimum value of 2 and the maximum is set to 10; however, its range exceeds 20 for *GZMA, CCL5*, and *CD40LG*. The absolute p-values for all differentially expressed genes can be found in **Supplementary Table 1**. *Clinical cortisol excess and the molecular classification were described by Zheng et al. (5) and presented in the top annotation. **Immune subtype classification and the five molecular immune signatures rescaled to a range of 0 to 1 were according to Thorsson et al. (11) and are shown in the top annotation. **(B)** Boxplot comparing LSP and HSP for leukocyte fractions and the five immune signatures associated with lymphocyte infiltrate scores, macrophage regulation, wound healing, IFN-γ response, and TGF-ß response according to Thorsson et al. (11). The scores for each of the five signatures are rescaled to a range of 0 to 1 (y-axis). The density plot shows the distribution according to the immune subtypes C3 (green) and C4 (cyan). Each sample is shown in a rug plot and colored according to HSP and LSP classification. The p-value calculated using Wilcoxon test comparing both phenotypes is shown above each pair of boxplots.

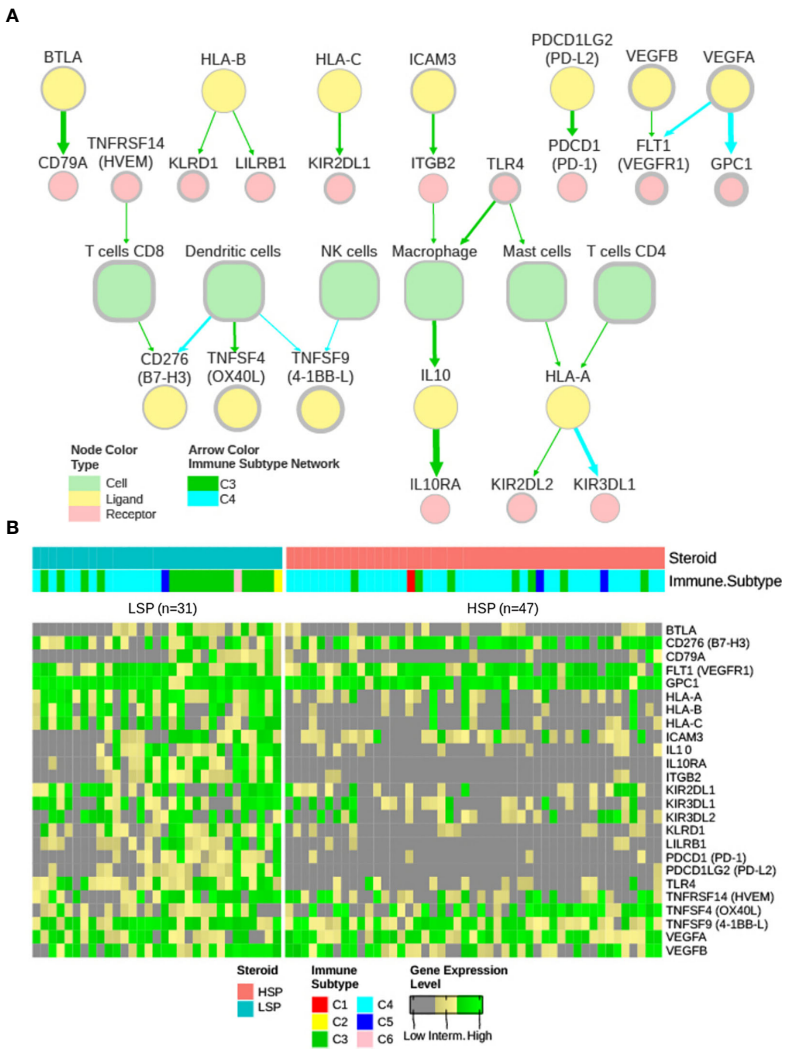

FIGURE 7 | iAtlas explorer-extracellular communication network. **(A)** The extracellular communication network according to Thorsson et al. (11) and available on CRI Atlas (https://isb-cgc.shinyapps.io/shiny-iatlas/) was reconstructed for the C3 and C4 patients of TCGA ACC cohort. Nodes with greater than 50% abundance and a concordance interaction larger than 2.5 were selected. The node line width varies proportionally to abundance and the edge width varies proportionally to concordance. Green arrows represent interactions of C3 patients and cyan arrows represent interactions of C4 patients. Node colors represent immune cells (light green), receptors (pink), and ligands (yellow). **(B)** The receptors and ligands present in the network were evaluated based on gene expression levels in a pan-cancer comparison. Gene expression of the 25 nodes in the network were ranked among 9,361 primary tumor samples available in the TCGA database and classified as low (grey), intermediate (yellow), or high (green) expression level based on ranking terciles. Each column represents a patient with ACC. Column order is maintained from **Figures 5A** and **6A** heatmaps. Steroid phenotype and immune subtype classifications are indicated in the top annotation.

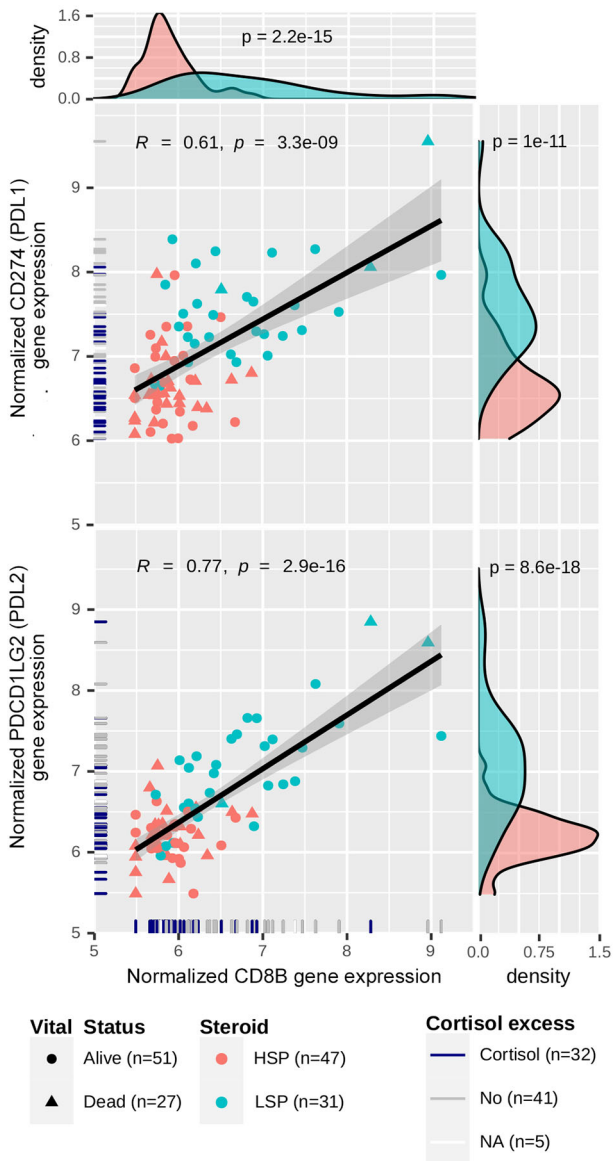

FIGURE 8 | Correlation between *CD274/PDCD1LG2* and *CD8B* expression. Gene expression levels for *CD274, PDCD1LG2* and *CD8B* were normalized using a variance-stabilizing transformation from DESeq2 R package. Pearson's correlation coefficients and p-values are shown in the scatter plots, as well as the regression line. The confidence interval was inferred using Fisher's Z transform. Point colors are set according to the steroid phenotype: salmon for HSP and blue for LSP. Point shapes are set according to the patient's vital status: triangles for dead and circles for alive. In the rug plot, navy blue indicates the presence of cortisol excess, gray indicates absence, and white indicates non-annotated patients regarding cortisol levels. In the density plot, p-values determined using Wald's test for DE analysis between LSP and HSP is shown.

(*PD-L2*) are significantly downregulated in HSP (**Supplementary Table 1**, **Figures 6A** and **7B**). Similar to PD-1 and CTLA-4, BTLA is an immune checkpoint associated with suppression of the immune response and its blockade has been related to a reduction of ovarian carcinoma *via* the regulation of IL6 and IL10 (69). IL10 mediates immunosuppressive signals through its interaction with IL10 receptors, leading to inhibition of synthesis of proinflammatory cytokines (70). Integrins, such as ITGB2, play significant roles in cellular adhesion and cell surface signaling, and also participate in leukocyte adhesion and extravasation to inflame tissues, and mediate the formation of immunological synapses (71).

Curiously, *TNFSF9 (4-1BB-L)* was present at a surprisingly high abundance in ACC when compared to that of other TCGA tumor types, but not its receptor *TNFRSF9* (*4-1BB)*, which was present mainly on CD8+ T cells, (**Figure 7B**). In the C4 network,

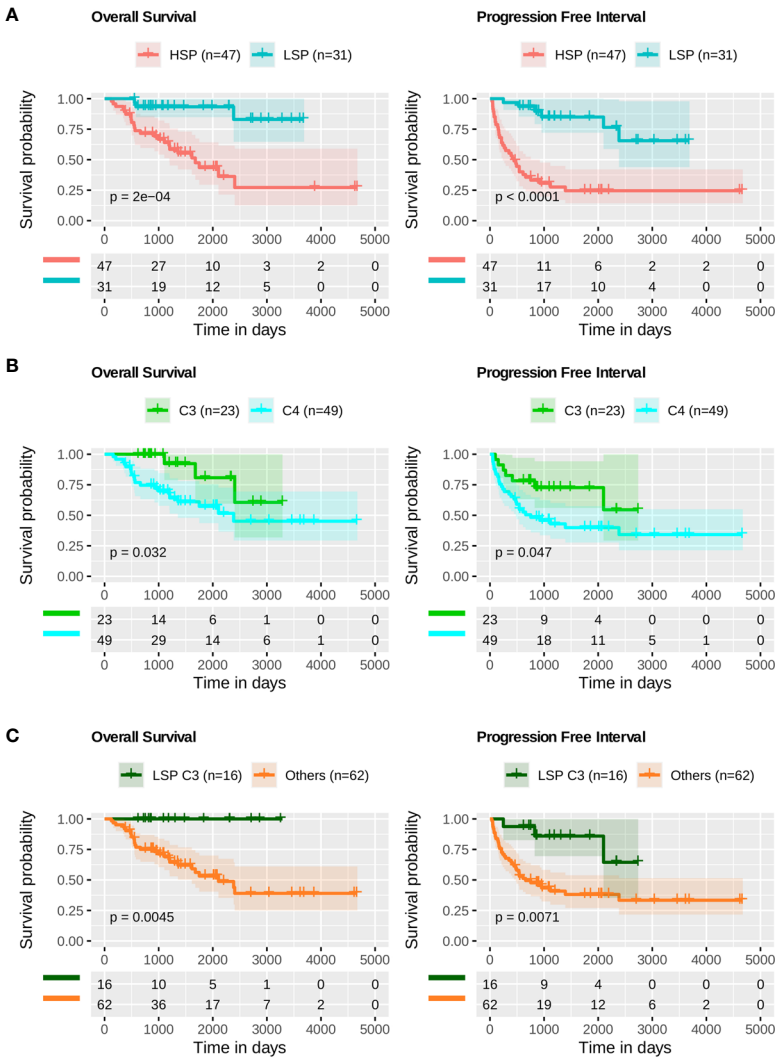

FIGURE 9 | Survival analysis. Kaplan-Meier analysis for overall survival (OS) and progression free interval (PFI) of ACC profiles. The p-value was calculated using a log-rank test and the confidence interval is shown. Below each plot a survival table with the absolute number of participants over time. **(A)** OS and PFI for LSP (n = 31) versus HSP (n = 47). **(B)** OS and PFI for immune subtype C3 (n = 23) versus immune subtype C4 (n = 49). **(C)** OS and PFI for LSP and C3 patients (n = 16) versus other combinations (LSP C2, C4, C5, and C6, or HSP C1, C3, C4, and C5; total n = 62).

TNFSF9 appeared in concordance with dendritic and NK cells (**Figure 7A**). TNFSF9 is commonly expressed by antigen-presenting cells and its interaction with its receptor TNFRSF9 tends to stimulate T cells and cytotoxic activity, demonstrating strong anti-tumor activity (72). Although the use of TNFSF9 analogues as an immunotherapy strategy has been considered (73), the relatively low level expression of its receptor TNFRSF9 on T cells may limit the efficacy of this type of treatment. Understanding the role of *TNFSF9* overexpression in ACC may be a subject of future studies.

Classification of ACC into subgroups based on methylation profiles, which was also proposed by Zheng et al. (5), appears to be robust as reviewed by Crona and Beuschlein (6). However, despite providing good clinical prognostic indications, this classification has not resulted in novel treatment possibilities for each of the groups (6, 7, 74). One strong point of our current study using the molecular classification of steroidal profiles was the possibility of separating the immune activation profile of tumor subtypes. This is in agreement with the suggestion by Fiorentini et al. (7) that patients who may benefit from immunotherapies should be selected based on some type of molecular classification. We believe that separation based on steroid profiles may provide useful information regarding this criterion. Furthermore, the LSP classification successfully grouped all patients with higher expression of immune modulator genes, in addition to higher leukocyte fractions. Remarkably, the immune activation distinction was not clear when using the classification of cases based solely on clinical parameters, that is, hypercortisolism

versus non-hypercortisolism (data not shown). This was despite its good correlation with HSP (Fisher's exact test, $p = 2.55 \times 10^{-4}$). In addition, the available HSP data are associated with downregulation of the immune system, higher tumor proliferation, and worst prognosis (75).

Genomic and epigenetic changes frequently occur in ACC, in both childhood (15, 76) and adulthood (5, 75, 77) cases. However, the TCGA ACC cohort is mainly limited to adults (median age, 46 years). The accumulation of these alterations may alter lymphocyte recruitment (11) and drive a higher proliferation profile, which would consequently result in a worse prognosis. It is currently not clear if the anti-tumor immune response is not strong enough to surpass tumor proliferation or if there is a surge in proliferation due to the immunosuppressed TME.

Interestingly, it was not possible to determine a clear correlation between leukocyte fraction and mutations in driver gene known to impact the immune response. This could have been due to the small number of patients with these mutations, as well as the fact that most of these patients were from the immunosuppressed HSP group. In analysis of the whole cohort (LSP + HSP patients) *CTNNB1* mutations were noted only in patients of the HSP group and they demonstrated a weak negative correlation with leukocyte fraction ($p = 3.8 \times 10^{-2}$ on Wilcoxon test). However, when analyzing only the HSP group, the presence of *CTNNB1* mutations did not demonstrate any significant impact on leukocyte fraction ($p = 9.9 \times 10^{-1}$ on Wilcoxon test), indicating the weak correlation observed was mainly due to the steroid phenotype. This indicates the steroid phenotype should be taken into account during immune response analysis of ACC. Failing to do so may generate confounding effects.

When comparing the inflammatory C3 and lymphocyte-depleted C4 immune signatures, we found a slightly better survival for C3 ($p = 3.2 \times 10^{-2}$ for OS and $p = 4.7 \times 10^{-2}$ for PFI; log-rank test) (**Figure 9B**). In the pan-cancer analysis performed by Thorsson and colleagues, C3 had a significantly better outcome than that of C4; however, the steroid phenotype provides more characteristics regarding tumor aggressiveness and outcome prognosis in ACC than that of the C3-C4 signatures. For example, there were no death events among the 16 patients with C3 LSP, whereas there were 3 deaths among the 7 patients with C3 HSP (42.9%). Furthermore, among the 12 patients with C4 LSP, only 1 died (8.33%) compared with 19 deaths in the group of 37 patients with C4 HSP (51,35%). When distinguishing C3 and C4 patients within the steroid phenotypes (density plots in **Figures 5B**, **6B**), differences were observed in LSP C3 versus C4, especially in the leukocyte fraction and lymphocyte infiltration scores; however, HSP C3 versus C4 does not in general present great distinction. Considering there were only seven patients with HSP C3, the steroid phenotype distinguished some immune features better than that of the C1–C6 subtype classification alone.

In addition to differences in the targeted immune checkpoints, a crucial difference affecting the success of immunotherapies for other tumors (22–24, 78) and the modest results of immunotherapy in ACC, such as less than 15% of patients with ACC benefiting from PD-1 or PD-L1 inhibition (30–33), seems to be the immunosuppressive and anti-inflammatory effects of intratumoral glucocorticoids (12). Among potential prognostic factors, CD3+ and CD8+ cytotoxic T lymphocytes were found in 84% of 146 patients with ACC and were associated with overall and recurrence-free survival (12). This parameter could be further improved by blocking steroidogenesis in combination with different immune checkpoint inhibitors. Patients with tumor progression and mitotane-resistance may still benefit from a reduction in the dose aiming for steroidogenesis blockade. One important feature of mitotane treatment is the ability to block steroid biosynthesis at lower daily doses and with less toxic side effects (approximately <10 μg/mL of plasma) (79). Future studies may investigate if this blockade is adequate to induce an efficient immune response.

Despite the reduced number of cases, we found evidence of considerable immune cell infiltrates within LSP and sought to characterize the interactions and networks in order to identify transcriptomic biomarkers associated with significant immune activation. Our analysis also exploited target immune modulators that may regulate potential pathways associated with the anti-tumor response. Our analysis framework had limitations as it relied on a small number of accessible profiles and a simple binary change (LSP and HSP) where HSP combined different steroid subtypes that could not be identified using only the clinical manifestations of hypercortisolism. It is important to note that the activation of steroid biosynthesis pathways seen in HSP was based on a transcriptome profile, which may imply a possible hormone excess in the TME had not been related to clinical manifestations. Our experimental design using a probabilistic approach to identify potential targets for immunotherapy was restricted to *in silico* findings. Despite the rationale, this may not be translatable to *in vivo* assays. Further work is needed to fully understand the possibility of changing the outcome of ACC immunotherapy, which may start with the selection of patients with LSP ACC and the inhibition of steroidogenesis in patients with HSP ACC. Despite significant progress in identifying immunogenic biomarkers in ACC through evaluation of the TCGA cohort (5), there are still many limitations and puzzles to be solved. Additional efforts beyond RNAseq analyses are needed to validate functional studies to define the key pathways in a larger number of patients with LSP ACC. Considering we are still in the early stage of understanding the B7-H3 network, it is important to define the actual B7-H3 receptor in order to fully understand this pathway in ACC.

CONCLUSIONS

An important frontier of ACC therapeutics to improve the anti-tumor activity of the immune system starts explicitly by modeling steroidogenic differences. The analytical approach we describe herein requires further studies to ascertain the possible

druggable role of B7-H3 in relation to PD1-PDL1/PDL2 in ACC. Our present approach was unable to predict improved outcomes of immunotherapy; however, it points to possible selection criteria and potential targets. Future work should confirm these findings using a larger cohort, in addition to including pre-clinical or clinical trials.

CODE AVAILABILITY AND REPRODUCIBILITY

All scripts, datasets, software and algorithms used to generate results, figures, and tables for this study are available on the GitHub repository (https://github.com/sysbiolab/Sup_Material_Muzzi2021) and **Supplementary Tables 3** and **4**.

DATA AVAILABILITY STATEMENT

The original contributions presented in the study are included in the article/**Supplementary Material**. Further inquiries can be directed to the corresponding author.

ETHICS STATEMENT

The studies involving human participants were reviewed and approved by Pequeno Príncipe Ethics Committee. Written informed consent from the participants' legal guardian/next of kin was not required to participate in this study in accordance with the national legislation and the institutional requirements.

AUTHOR CONTRIBUTIONS

All authors made substantial contributions to the conception of the work. JCDM was responsible for data acquisition and analysis. MAAC contributed to the acquisition of data and method analyses. All authors contributed to data interpretation. JCDM and BF wrote the first draft of the manuscript. JMM and MAC helped in code review and creating the public repository. All authors contributed to the article and approved the submitted version.

FUNDING

JCDM, JMM, and MAC receive scholarships from the BIG DATA innovation program from the Associação Hospitalar de Proteção à Infância Raul Carneiro-AHPIRAC (2020). MAAC and JM are funded by the Conselho Nacional de Desenvolvimento Científico e Tecnológico (CNPq).

ACKNOWLEDGMENTS

Data used in this manuscript were obtained from The Cancer Genome Atlas (TCGA) ACC database. We are grateful to AHPIRAC for the scientific editing support.

SUPPLEMENTARY MATERIAL

The Supplementary Material for this article can be found online at: https://www.frontiersin.org/articles/10.3389/fendo.2021.672319/full#supplementary-material

REFERENCES

1. Allolio B, Fassnacht M. Adrenocortical Carcinoma: Clinical Update. *J Clin Endocrinol Metab* (2006) 91:2027–37. doi: 10.1210/jc.2005-2639
2. Libè R, Fratticci A, Bertherat J. Adrenocortical Cancer: Pathophysiology and Clinical Management. *Endocr Relat Cancer* (2007) 14:13–28. doi: 10.1677/erc.1.01130
3. Fassnacht M, Kroiss M, Allolio B. Update in Adrenocortical Carcinoma. *J Clin Endocrinol Metab* (2013) 98:4551–64. doi: 10.1210/jc.2013-3020
4. Berruti A, Fassnacht M, Haak H, Else T, Baudin E, Sperone P, et al. Prognostic Role of Overt Hypercortisolism in Completely Operated Patients With Adrenocortical Cancer. *Eur Urol* (2014) 65:832–38. doi: 10.1016/j.eururo.2013.11.006
5. Zheng S, Cherniack AD, Dewal N, Moffitt RA, Danilova L, Murray BA, et al. Comprehensive Pan-Genomic Characterization of Adrenocortical Carcinoma. *Cancer Cell* (2016) 29:723–36. doi: 10.1016/j.ccell.2016.04.002
6. Crona J, Beuschlein F. Adrenocortical Carcinoma — Towards Genomics Guided Clinical Care. *Nat Rev Endocrinol* (2019) 15:548–60. doi: 10.1038/s41574-019-0221-7
7. Fiorentini C, Grisanti S, Cosentini D, Abate A, Rossini E, Berruti A, et al. Molecular Drivers of Potential Immunotherapy Failure in Adrenocortical Carcinoma. *J Oncol* (2019) 2019:6072863. doi: 10.1155/2019/6072863
8. de Reyniès A, Assié G, Rickman DS, Tissier F, Groussin L, René-Corail F, et al. Gene Expression Profiling Reveals a New Classification of Adrenocortical Tumors and Identifies Molecular Predictors of Malignancy and Survival. *J Clin Oncol* (2009) 27:1108–15. doi: 10.1200/JCO.2008.18.5678
9. Giordano TJ, Kuick R, Else T, Gauger PG, Vinco M, Bauersfeld J, et al. Molecular Classification and Prognostication of Adrenocortical Tumors by Transcriptome Profiling. *Clin Cancer Res* (2009) 15:668–76. doi: 10.1158/1078-0432.CCR-08-1067
10. Li B, Severson E, Pignon J-CC, Zhao H, Li T, Novak J, et al. Comprehensive Analyses of Tumor Immunity: Implications for Cancer Immunotherapy. *Genome Biol* (2016) 17:174. doi: 10.1186/s13059-016-1028-7
11. Thorsson V, Gibbs DL, Brown SD, Wolf D, Bortone DS, Ou Yang TH, et al. The Immune Landscape of Cancer. *Immunity* (2018) 48:812–30.e14. doi: 10.1016/j.immuni.2018.03.023
12. Landwehr L-S, Altieri B, Schreiner J, Sbiera I, Weigand I, Kroiss M, et al. Interplay Between Glucocorticoids and Tumor-Infiltrating Lymphocytes on the Prognosis of Adrenocortical Carcinoma. *J Immunother Cancer* (2020) 8:e000469. doi: 10.1136/jitc-2019-000469
13. Michalkiewicz E, Sandrini R, Figueiredo B, Miranda ECMM, Caran E, Oliveira-Filho AG, et al. Clinical and Outcome Characteristics of Children With Adrenocortical Tumors: A Report From the International Pediatric Adrenocortical Tumor Registry. *J Clin Oncol* (2004) 22:838–45. doi: 10.1200/JCO.2004.08.085
14. Parise IZS, Parise GA, Noronha L, Surakhy M, Woiski TD, Silva DB, et al. The Prognostic Role of CD8+ T Lymphocytes in Childhood Adrenocortical Carcinomas Compared to Ki-67, Pd-1, PD-L1, and the Weiss Score. *Cancers (Basel)* (2019) 11:1730. doi: 10.3390/cancers11111730
15. Pinto EM, Chen X, Easton J, Finkelstein D, Liu Z, Pounds S, et al. Genomic Landscape of Paediatric Adrenocortical Tumours. *Nat Commun* (2015) 6:6302. doi: 10.1038/ncomms7302

16. Finn OJ. Cancer Immunology. *N Engl J Med* (2008) 358:2704–15. doi: 10.1056/NEJMra072739
17. Custódio G, Komechen H, Figueiredo FRO, Fachin ND, Pianovski MAD, Figueiredo BC. Molecular Epidemiology of Adrenocortical Tumors in Southern Brazil. *Mol Cell Endocrinol* (2012) 351:44–51. doi: 10.1016/j.mce.2011.10.019
18. Vanbrabant T, Fassnacht M, Assie G, Dekkers OM. Influence of Hormonal Functional Status on Survival in Adrenocortical Carcinoma: Systematic Review and Meta-Analysis. *Eur J Endocrinol* (2018) 179:429–36. doi: 10.1530/EJE-18-0450
19. Lalli E, Figueiredo BC. Pediatric Adrenocortical Tumors: What They Can Tell Us on Adrenal Development and Comparison With Adult Adrenal Tumors. *Front Endocrinol (Lausanne)* (2015) 6:23. doi: 10.3389/fendo.2015.00023
20. Prager I, Liesche C, van Ooijen H, Urlaub D, Verron Q, Sandström N, et al. NK Cells Switch From Granzyme B to Death Receptor–Mediated Cytotoxicity During Serial Killing. *J Exp Med* (2019) 216:2113–27. doi: 10.1084/jem.20181454
21. Cursons J, Souza-Fonseca-Guimaraes F, Foroutan M, Anderson A, Hollande F, Hediyeh-Zadeh S, et al. A Gene Signature Predicting Natural Killer Cell Infiltration and Improved Survival in Melanoma Patients. *Cancer Immunol Res* (2019) 7:1162–74. doi: 10.1158/2326-6066.CIR-18-0500
22. Drake CG, Lipson EJ, Brahmer JR. Breathing New Life Into Immunotherapy: Review of Melanoma, Lung and Kidney Cancer. *Nat Rev Clin Oncol* (2014) 11:24–37. doi: 10.1038/nrclinonc.2013.208
23. Rodriguez D, Goulart C, Pagliarone AC, Silva EP, Cunegundes PS, Nascimento IP, et al. *In Vitro* Evidence of Human Immune Responsiveness Shows the Improved Potential of a Recombinant Bcg Strain for Bladder Cancer Treatment. *Front Immunol* (2019) 10:1460. doi: 10.3389/fimmu.2019.01460
24. Pettenati C, Ingersoll MA. Mechanisms of BCG Immunotherapy and its Outlook for Bladder Cancer. *Nat Rev Urol* (2018) 15:615–25. doi: 10.1038/s41585-018-0055-4
25. Hong H, Wang Q, Li J, Liu H, Meng X, Zhang H. Aging, Cancer and Immunity. *J Cancer* (2019) 10:3021–7. doi: 10.7150/jca.30723
26. Wasserman JD, Zambetti GP, Malkin D. Towards an Understanding of the Role of p53 in Adrenocortical Carcinogenesis. *Mol Cell Endocrinol* (2012) 351:101–10. doi: 10.1016/j.mce.2011.09.010
27. Bindea G, Mlecnik B, Tosolini M, Kirilovsky A, Waldner M, Obenauf AC, et al. Spatiotemporal Dynamics of Intratumoral Immune Cells Reveal the Immune Landscape in Human Cancer. *Immunity* (2013) 39:782–95. doi: 10.1016/j.immuni.2013.10.003
28. Rieder SA, Wang J, White N, Qadri A, Menard C, Stephens G, et al. B7-H7 (HHLA2) Inhibits T-cell Activation and Proliferation in the Presence of TCR and CD28 Signaling. *Cell Mol Immunol* (2020). doi: 10.1038/s41423-020-0361-7
29. Greenwald RJ, Freeman GJ, Sharpe AH. The B7 Family Revisited. *Annu Rev Immunol* (2005) 23:515–48. doi: 10.1146/annurev.immunol.23.021704.115611
30. Carneiro BA, Konda B, Costa RB, Costa RLB, Sagar V, Gursel DB, et al. Nivolumab in Metastatic Adrenocortical Carcinoma: Results of a Phase 2 Trial. *J Clin Endocrinol Metab* (2019) 104:6193–200. doi: 10.1210/jc.2019-00600
31. Raj N, Zheng Y, Kelly V, Katz SS, Chou J, Do RKG, et al. Pd-1 Blockade in Advanced Adrenocortical Carcinoma. *J Clin Oncol* (2020) 38:71–80. doi: 10.1200/JCO.19.01586
32. Habra MA, Stephen B, Campbell M, Hess K, Tapia C, Xu M, et al. Phase II Clinical Trial of Pembrolizumab Efficacy and Safety in Advanced Adrenocortical Carcinoma. *J Immunother Cancer* (2019) 7:253. doi: 10.1186/s40425-019-0722-x
33. Le Tourneau C, Hoimes C, Zarwan C, Wong DJ, Bauer S, Claus R, et al. Avelumab in Patients With Previously Treated Metastatic Adrenocortical Carcinoma: Phase 1b Results From the JAVELIN Solid Tumor Trial. *J Immunother Cancer* (2018) 6:111. doi: 10.1186/s40425-018-0424-9
34. Cosentini D, Grisanti S, Volta AD, Laganà M, Fiorentini C, Perotti P, et al. Immunotherapy Failure in Adrenocortical Cancer: Where Next? *Endocr Connect* (2018) 7:E5–8. doi: 10.1530/EC-18-0398
35. Colaprico A, Silva TC, Olsen C, Garofano L, Cava C, Garolini D, et al. Tcgabiolinks: An R/Bioconductor Package for Integrative Analysis of TCGA Data. *Nucleic Acids Res* (2016) 44:e71. doi: 10.1093/nar/gkv1507
36. Silva TC, Colaprico A, Olsen C, D'Angelo F, Bontempi G, Ceccarelli M, et al. Tcga Workflow: Analyze Cancer Genomics and Epigenomics Data Using Bioconductor Packages. *F1000Research* (2016) 5:1542. doi: 10.12688/f1000research.8923.2
37. Mounir M, Lucchetta M, Silva TC, Olsen C, Bontempi G, Chen X, et al. New Functionalities in the TCGAbiolinks Package for the Study and Integration of Cancer Data From GDC and Gtex. *PloS Comput Biol* (2019) 15:e1006701. doi: 10.1371/journal.pcbi.1006701
38. Aran D, Hu Z, Butte AJ. xCell: Digitally Portraying the Tissue Cellular Heterogeneity Landscape. *Genome Biol* (2017) 18:220. doi: 10.1186/s13059-017-1349-1
39. Sturm G, Finotello F, Petitprez F, Zhang JD, Baumbach J, Fridman WH, et al. Comprehensive Evaluation of Transcriptome-Based Cell-Type Quantification Methods for Immuno-Oncology. *Bioinformatics* (2019) 35:i436–45. doi: 10.1093/bioinformatics/btz363
40. Newman AM, Liu CL, Green MR, Gentles AJ, Feng W, Xu Y, et al. Robust Enumeration of Cell Subsets From Tissue Expression Profiles. *Nat Methods* (2015) 12:453–7. doi: 10.1038/nmeth.3337
41. Gu Z, Eils R, Schlesner M. Complex Heatmaps Reveal Patterns and Correlations in Multidimensional Genomic Data. *Bioinformatics* (2016) 32:2847–9. doi: 10.1093/bioinformatics/btw313
42. Morgan M, Obenchain V, Hester J, Pagès H. Summarizedexperiment: SummarizedExperiment Container. In: *R package version 1.20.0* (2020). doi: 10.18129/B9.bioc.SummarizedExperiment
43. Morgan M, Shepherd L. Annotationhub: Client to Access AnnotationHub Resources. In: *R package, version 2.22.0* (2020). doi: 10.18129/B9.bioc.AnnotationHub
44. Love MI, Huber W, Anders S. Moderated Estimation of Fold Change and Dispersion for RNA-seq Data With Deseq2. *Genome Biol* (2014) 15:550. doi: 10.1186/s13059-014-0550-8
45. Yamaguchi KD, Ruderman DL, Croze E, Wagner TC, Velichko S, Reder AT, et al. Ifn-β-Regulated Genes Show Abnormal Expression in Therapy-Naïve Relapsing–Remitting MS Mononuclear Cells: Gene Expression Analysis Employing All Reported Protein–Protein Interactions. *J Neuroimmunol* (2008) 195:116–20. doi: 10.1016/j.jneuroim.2007.12.007
46. Weiner J3rd, Domaszewska T. Tmod: An R Package for General and Multivariate Enrichment Analysis. *PeerJ* (2016) 4:1–9. doi: 10.7287/peerj.preprints.2420
47. Zyla J, Marczyk M, Domaszewska T, Kaufmann SHE, Polanska J, Weiner J. Gene Set Enrichment for Reproducible Science: Comparison of CERNO and Eight Other Algorithms. *Bioinformatics* (2019) 35:5146–54. doi: 10.1093/bioinformatics/btz447
48. Subramanian A, Tamayo P, Mootha VK, Mukherjee S, Ebert BL, Gillette MA, et al. Gene Set Enrichment Analysis: A Knowledge-Based Approach for Interpreting Genome-Wide Expression Profiles. *Proc Natl Acad Sci* (2005) 102:15545–50. doi: 10.1073/pnas.0506580102
49. Liberzon A, Birger C, Thorvaldsdóttir H, Ghandi M, Mesirov JP, Tamayo P. The Molecular Signatures Database Hallmark Gene Set Collection. *Cell Syst* (2015) 1:417–25. doi: 10.1016/j.cels.2015.12.004
50. Li S, Rouphael N, Duraisingham S, Romero-Steiner S, Presnell S, Davis C, et al. Molecular Signatures of Antibody Responses Derived From a Systems Biology Study of Five Human Vaccines. *Nat Immunol* (2014) 15:195–204. doi: 10.1038/ni.2789
51. Wang H, Najibi AJ, Sobral MC, Seo BR, Lee JY, Wu D, et al. Biomaterial-Based Scaffold for in Situ Chemo-Immunotherapy to Treat Poorly Immunogenic Tumors. *Nat Commun* (2020) 11:5696. doi: 10.1038/s41467-020-19540-z
52. Ramilowski JA, Goldberg T, Harshbarger J, Kloppmann E, Lizio M, Satagopam VP, et al. A Draft Network of Ligand–Receptor-Mediated Multicellular Signalling in Human. *Nat Commun* (2015) 6:7866. doi: 10.1038/ncomms8866
53. Castro MA, Wang X, Fletcher MN, Meyer KB, Markowetz F. Reder: R/Bioconductor Package for Representing Modular Structures, Nested Networks

and Multiple Levels of Hierarchical Associations. *Genome Biol* (2012) 13:R29. doi: 10.1186/gb-2012-13-4-r29
54. Hoadley KA, Yau C, Hinoue T, Wolf DM, Lazar AJ, Drill E, et al. Cell-of-Origin Patterns Dominate the Molecular Classification of 10,000 Tumors From 33 Types of Cancer. *Cell* (2018) 173:291–304. doi: 10.1016/j.cell.2018.03.022
55. Therneau T. A Package for Survival Analysis in R. In: *R package version 3.2-7* (2020). Available at: https://cran.r-project.org/package=survival.
56. Therneau TM, Grambsch PM. *Modeling Survival Data: Extending the Cox Model*. New York, NY: Springer New York (2000). doi: 10.1007/978-1-4757-3294-8
57. Storey J, Bass A, Dabney A, Robinson D. *Qvalue: Q-value Estimation for False Discovery Rate Control R Package Version 2.22.0*. (2020). doi: 10.18129/B9.bioc.qvalue.
58. Monaco G, Lee B, Xu W, Mustafah S, Hwang YY, Carré C, et al. Rna-Seq Signatures Normalized by Mrna Abundance Allow Absolute Deconvolution of Human Immune Cell Types. *Cell Rep* (2019) 26:1627–40.e7. doi: 10.1016/j.celrep.2019.01.041
59. Tierney JF, Vogle A, Poirier J, Min IM, Finnerty B, Zarnegar R, et al. Expression of Programmed Death Ligand 1 and 2 in Adrenocortical Cancer Tissues: An Exploratory Study. *Surgery* (2019) 165:196–201. doi: 10.1016/j.surg.2018.04.086
60. Liang J, Liu Z, Pei T, Xiao Y, Zhou L, Tang Y, et al. Clinicopathological and Prognostic Characteristics of CD276 (B7-H3) Expression in Adrenocortical Carcinoma. *Dis Markers* (2020) 2020:1–10. doi: 10.1155/2020/5354825
61. Kontos F, Michelakos T, Kurokawa T, Sadagopan A, Schwab JH, Ferrone CR, et al. B7-H3: An Attractive Target for Antibody-based Immunotherapy. *Clin Cancer Res* (2021) 27:1227–35. doi: 10.1158/1078-0432.CCR-20-2584
62. Flem-Karlsen K, Fodstad Ø, Tan M, Nunes-Xavier CE. B7-H3 in Cancer – Beyond Immune Regulation. *Trends Cancer* (2018) 4:401–4. doi: 10.1016/j.trecan.2018.03.010
63. Yonesaka K, Haratani K, Takamura S, Sakai H, Kato R, Takegawa N, et al. B7-H3 Negatively Modulates CTL-Mediated Cancer Immunity. *Clin Cancer Res* (2018) 24:2653–64. doi: 10.1158/1078-0432.CCR-17-2852
64. Loos M, Hedderich DM, Friess H, Kleeff J. B7-H3 and Its Role in Antitumor Immunity. *Clin Dev Immunol* (2010) 2010:1–7. doi: 10.1155/2010/683875
65. Xu Y, Zhu Y, Shen Z, Sheng J, He H, Ma G, et al. Significance of Heparanase-1 and Vascular Endothelial Growth Factor in Adrenocortical Carcinoma Angiogenesis: Potential for Therapy. *Endocrine* (2011) 40:445–51. doi: 10.1007/s12020-011-9502-1
66. Pereira SS, Costa MM, Guerreiro SG, Monteiro MP, Pignatelli D. Angiogenesis and Lymphangiogenesis in the Adrenocortical Tumors. *Pathol Oncol Res* (2018) 24:689–93. doi: 10.1007/s12253-017-0259-6
67. O'Sullivan C, Edgerly M, Velarde M, Wilkerson J, Venkatesan AM, Pittaluga S, et al. The VEGF Inhibitor Axitinib has Limited Effectiveness as a Therapy for Adrenocortical Cancer. *J Clin Endocrinol Metab* (2014) 99:1291–7. doi: 10.1210/jc.2013-2298
68. Berruti A, Sperone P, Ferrero A, Germano A, Ardito A, Priola AM, et al. Phase II Study of Weekly Paclitaxel and Sorafenib as Second/Third-Line Therapy in Patients With Adrenocortical Carcinoma. *Eur J Endocrinol* (2012) 166:451–8. doi: 10.1530/EJE-11-0918
69. Chen Y-L, Lin H-W, Chien C-L, Lai Y-L, Sun W-Z, Chen C-A, et al. BTLA Blockade Enhances Cancer Therapy by Inhibiting IL-6/IL-10-induced Cd19high B Lymphocytes. *J Immunother Cancer* (2019) 7:313. doi: 10.1186/s40425-019-0744-4
70. Pestka S, Krause CD, Sarkar D, Walter MR, Shi Y, Fisher PB. Interleukin-10 and Related Cytokines and Receptors. *Annu Rev Immunol* (2004) 22:929–79. doi: 10.1146/annurev.immunol.22.012703.104622
71. Rojas K, Baliu-Piqué M, Manzano A, Saiz-Ladera C, García-Barberán V, Cimas FJ, et al. In Silico Transcriptomic Mapping of Integrins and Immune Activation in Basal-like and HER2+ Breast Cancer. *Cell Oncol* (2021). doi: 10.1007/s13402-020-00583-9
72. Vinay DS, Kwon BS. 4-1BB Signaling Beyond T Cells. *Cell Mol Immunol* (2011) 8:281–4. doi: 10.1038/cmi.2010.82
73. Chester C, Sanmamed MF, Wang J, Melero I. Immunotherapy Targeting 4-1BB: Mechanistic Rationale, Clinical Results, and Future Strategies. *Blood* (2018) 131:49–57. doi: 10.1182/blood-2017-06-741041
74. Jasim S, Habra MA. Management of Adrenocortical Carcinoma. *Curr Oncol Rep* (2019) 21:20. doi: 10.1007/s11912-019-0773-7
75. Assié G, Letouzé E, Fassnacht M, Jouinot A, Luscap W, Barreau O, et al. Integrated Genomic Characterization of Adrenocortical Carcinoma. *Nat Genet* (2014) 46:607–12. doi: 10.1038/ng.2953
76. Figueiredo BC, Stratakis CA, Sandrini R, DeLacerda L, Pianovsky MAD, Giatzakis C, et al. Comparative Genomic Hybridization Analysis of Adrenocortical Tumors of Childhood 1. *J Clin Endocrinol Metab* (1999) 84:1116–21. doi: 10.1210/jcem.84.3.5526
77. Kjellman M, Kallioniemi OP, Karhu R, Höög A, Farnebo LO, Auer G, et al. Genetic Aberrations in Adrenocortical Tumors Detected Using Comparative Genomic Hybridization Correlate With Tumor Size and Malignancy. *Cancer Res* (1996) 56:4219–23.
78. Hodi FS, O'Day SJ, McDermott DF, Weber RW, Sosman JA, Haanen JB, et al. Improved Survival With Ipilimumab in Patients With Metastatic Melanoma. *N Engl J Med* (2010) 363:711723. doi: 10.1056/NEJMoa1003466
79. Zancanella P, Pianovski MAD, Oliveira BH, Ferman S, Piovezan GC, Lichtvan LL, et al. Mitotane Associated With Cisplatin, Etoposide, and Doxorubicin in Advanced Childhood Adrenocortical Carcinoma. *J Pediatr Hematol Oncol* (2006) 28:513–24. doi: 10.1097/01.mph.0000212965.52759.1c

Conflict of Interest: The authors declare the current research was conducted in the absence of any commercial or financial relationships that could be construed as a potential conflict of interest.

frontiers in Endocrinology

ORIGINAL RESEARCH
published: 23 June 2021
doi: 10.3389/fendo.2021.698862

Circulating Fascin 1 as a Promising Prognostic Marker in Adrenocortical Cancer

Giulia Cantini[1]*, *Laura Fei*[1], *Letizia Canu*[1,2], *Giuseppina De Filpo*[1,2], *Tonino Ercolino*[2], *Gabriella Nesi*[3], *Massimo Mannelli*[1] and *Michaela Luconi*[1]

[1] Endocrinology Unit, Department of Experimental and Clinical Biomedical Sciences, University of Florence, Florence, Italy, [2] Endocrinology Unit, Careggi University Hospital, Florence, Italy, [3] Department of Health Science, University of Florence, Florence, Italy

Fascin-1 (FSCN1) is an actin-bundling protein associated with an invasive and aggressive phenotype of several solid carcinomas, as it is involved in cell cytoskeleton rearrangement and filopodia formation. Adrenocortical carcinoma (ACC) is a rare endocrine malignancy characterized by poor prognosis, particularly when metastatic at diagnosis. Radical resection is the only therapeutic option for ACC patients in addition to the adjuvant treatment with mitotane. Novel specific biomarkers suggestive of tumor progression to refine diagnosis and prognosis of patients with advanced ACC are urgently needed. ACC intratumoral FSCN1 has previously been suggested as a valid prognostic marker. In the present study, we identified FSCN1 in the bloodstream of a small cohort of ACC patients (n = 27), through a specific ELISA assay for human FSCN1. FSCN1 can be detected in the serum, and its circulating levels were evaluated in pre-surgery samples, which resulted to be significantly higher in ACC patients from stage I/II and stage III/IV compared with nontumoral healthy controls (HC, n = 4, FI: 5.5 ± 0.8, P<0.001, and 8.0 ± 0.5, $P < 0.001$ for stage I/II and stage III/IV group *vs* HC, respectively). In particular, FSCN1 levels were significantly higher in advanced stage versus stage I/II (22.8 ± 1.1 *vs* 15.8 ± 1.8 ng/ml, $P < 0.005$, respectively). Interestingly, circulating levels of pre-surgical FSCN1 can significantly predict tumor progression/recurrence (Log rank = 0.013), but not the overall survival (Log rank=0.317), in patients stratified in high/low PreS FSCN1. In conclusion, these findings—though very preliminary—suggest that circulating FSCN1 may represent a new minimally-invasive prognostic marker in advanced ACC, in particular when measured before surgery enables histological diagnosis.

Keywords: fascin actin-bundling protein 1, circulating biomarker, prognosis, advanced adrenocortical carcinoma, liquid biopsy

OPEN ACCESS

Edited by:
Barbara Altieri, University Hospital of Wuerzburg, Germany

Reviewed by:
Leonardo Guasti, Queen Mary University of London, United Kingdom
Antonio Stigliano, Sapienza University of Rome, Italy

***Correspondence:**
Giulia Cantini
giulia.cantini@unifi.it

Specialty section:
This article was submitted to Cancer Endocrinology, a section of the journal Frontiers in Endocrinology

Received: *22 April 2021*
Accepted: *07 June 2021*
Published: *23 June 2021*

Citation:
Cantini G, Fei L, Canu L, De Filpo G, Ercolino T, Nesi G, Mannelli M and Luconi M (2021) Circulating Fascin 1 as a Promising Prognostic Marker in Adrenocortical Cancer. Front. Endocrinol. 12:698862. doi: 10.3389/fendo.2021.698862

INTRODUCTION

Adrenocortical carcinoma (ACC) is a rare, heterogeneous endocrine tumor often characterized by poor prognosis and aggressive behavior when metastatic at diagnosis. Unfortunately, selective and effective therapies are not available, making the radical resection of the tumor mass (R0) and adjuvant administration of the adrenolytic drug mitotane (MTT) the only therapeutic strategy for ACC

patients (1, 2). It has been shown that treatment with MTT improves the overall survival (OS) both in adjuvant regimen and in particular in advanced stages in association with cytotoxic agents (etoposide, doxorubicin, and cisplatinum) (1, 2). Characterization of specific and sensitive tumor markers capable of anticipating the diagnosis and also displaying a prognostic power is urgently needed, in particular for those cancers that, such as ACC, are often difficult to be studied because of their rarity.

Over the last 5 years, fascin-1 (FSCN1), a globular actin-binding protein, has emerged as an interesting novel biomarker for the most aggressive human carcinomas (3). Immunohistochemical studies have demonstrated that FSCN1 overexpression in the tumor correlates with a decreased OS and with different aspects of carcinoma invasiveness (3–7). Our previous findings have shown that FSCN1 is differentially expressed between normal adrenals and ACCs (6). More recently, we have demonstrated that the quantitative FSCN1 expression, detected by immunohistochemistry and quantitative RT-PCR in the tumor mass, may also represent a prognostic biomarker able to implement the predictive power of the current ACC histological classification (7), as high expression levels of FSCN1 positively associated with the invasive characteristics of ACC (7).

In the present study, we went further in the validation of FSCN1 biomarker in ACC, assessing whether FSCN1 was also detectable in the bloodstream of ACC patients and maintained its prognostic value, as in the tumor.

TABLE 1 | Clinical characteristics of the ACC cohort.

ACC PATIENT COHORT (N=27)	
AGE (ys)	50 ± 12 *(19-67)*
SEX (% male)	14 (52)
BMI (kg/m^2)	25.9 ± 5.8 *(19.4-44.9)*
SECRETION	
Non-secreting	7 (26)
Glucocorticoids	10 (37)
Sex steroids	7 (26)
Mineralcorticoids	1 (4)
NA	2 (7)
DIAMETER (cm)	9.4 ± 5.3 *(2-18)*
STAGE	
I	6 (22)
II	10 (37)
III	8 (30)
IV	3 (11)
WEISS score	6.0 ± 1.9 *(3-8)*
KI-67 LI (%)	21.0 ± 18.2 *(1-70)*
Resection status R0	23 (85)
R>0	4 (15)
Disease free survival time (months)	43.9 ± 36.6 *(0-116)*
Overall survival time (months)	53.9 ± 29.9 *(9-116)*

Anthropometric data and clinical features are reported for the analyzed cohort of ACC patients. Data are expressed as mean ± SD for parametric continuous variables (age, BMI, tumor diameter, Ki67 LI %) and for Weiss, and as absolute number and percentage of patients for the other non-continuous variables (sex, stages, secretion type, resection status). Data intervals (min-max) are indicated in italics in brackets.
NA, not available.

MATERIALS AND METHODS

Patients and Ethical Approval

The study includes 27 patients affected by ACC, enrolled and evaluated at Careggi University Hospital in Florence, whose clinical characteristics are detailed in **Table 1**. All patients underwent surgical removal of the tumor mass at our hospital, and a repository of tissue specimen and blood samples has been created. Tumor samples were snap-frozen and stored at −80°C until protein extraction (7). All patients gave their written informed consent to the study, which was approved by the local ethical committee (Prot.2017-277 BIO 59/11, 27/09/2017). Matched or unmatched blood samples were selected—where available—from 9 and 26 ACC patients before (PreS) and after surgery (PostS), respectively, and stored at −20°C until the ELISA assay was performed. Two different control groups were used in the study: obese subjects with type 2 diabetes (T2D) (n = 8; mean age, 42 ± 10; mean BMI, 40.5 ± 3.1; 12.5% male) and healthy non-tumoral non-obese/T2D subjects (n = 4; mean age, 52 ± 10; mean BMI, 23.5 ± 2.3; 25% male).

The histopathological parameters (KI-67-LI, Weiss score) reported in **Table 1** have been evaluated by the referent pathologist (GN) at our center (8), whereas the clinical data of the ACC patients were provided by the referent endocrinologists (MM, LC, GDF).

Tumor Lysates

Tumor samples were homogenized by mechanical disruption with Ultraturrax T10 basic IKA (Werke Gmbh & Co, Staufen, Germany) in radioimmunoprecipitation assay lysis buffer [RIPA: 20 mM Tris, pH 7.4, 150 mM NaCl, 0.5% Triton-100, 1 mM Na_3VO_4, 1 mM phenylmethylsulfonylfluoride (PMSF)]. After protein measurement using the Bradford method, equal amounts of proteins for each tissue sample (50 μg) were loaded onto the ELISA plate as detailed below.

Blood Sample Collection and Separation

For each subject, blood was collected, and serum was obtained after centrifugation at 3000 rpm for 10 min at 4°C.

ELISA Assay

FSCN1 was measured in the serum of the three groups: healthy non-tumoral non-obese/nondiabetic subjects, obese/diabetic subjects, and ACC patients using Human Fascin-1 ELISA kit (#MBS764737, MyBioSource Inc, Southern California, San Diego, USA). The sensitivity (0.469 ng/ml), the detection range (0.78-50 ng/ml), and specificity are according to the manufacturer. The intra-assay and inter-assay coefficients of variation were <8% and <10%, respectively. The obtained results were expressed as ng/ml, except for FSCN1 measured in tissue lysates, which is reported as pg/μg.

Briefly, all the buffers and reagents were equilibrated at room temperature (RT), and standard curve has been prepared and aliquoted into the plate together with the control. Blood samples previously centrifuged at 4,000 rpm at 4°C for 10 min to avoid debris, or 50 μg of tissue lysates were diluted in the specific buffer supplied in the kit and incubated in the pre-coated plate containing the anti-FSCN1 antibody for 90 min at a temperature of 37°C. After performing a series of washes with washing buffer, standards, controls, and samples were incubated with the biotinylated

antibody for 60 min at 37°C. After washing, streptavidin conjugated to HRP was added for 30 min at 37°C. Following incubation in the dark with the TMB substrate for 15 to 30 min at 37°C and after adding the Stop Solution, the optical density (OD) was measured at 450 nm using a spectrophotometer (VICTOR multilabel plate reader; Perkin-Elmer). The absorbance values of the sample were interpolated on a standard curve to obtain the relative concentrations.

Statistical Analysis

Statistical analysis was performed using SPSS software 27.0 (Statistical Package for the Social Sciences, Chicago, US) for Windows. The Kolmogorov-Smirnov's test was used to verify normal distribution of data. Results are expressed as mean ± SE, unless otherwise stated. One-way analysis of variance (ANOVA) followed by the Dunnett's *post hoc* test was applied for multiple comparison, whereas Student's t-test was used for comparison of two classes of data. A P value <0.05 was considered statistically significant.

Correlation analyses were carried out Pearson's/Spearman's test for parametric/nonparametric continuous variables, respectively. Overall survival (OS) and disease-free survival (DFS) are defined as the probability (ranging from 0 to 1) that a patient diagnosed with the disease is still alive (OS) or is free from the disease (DFS) at a time point from surgery. Survival analysis was estimated through the Kaplan-Meier method, and differences between groups were assessed by Log rank test. Univariate and multivariate Cox regression analyses of DFS in patients stratified for the indicated factors in high and low classes for PreS FSCN1 levels and PostS FSCN1 levels were performed by SPSS.

RESULTS

FSCN1 Detection in Blood Samples of ACC Patients

FSCN1 levels were measured in the serum samples of 27 ACC patients and compared with measurements obtained in the serum samples of non-tumoral obese/T2D patients (n=8) and non-tumoral/non-obese/non-T2D subjects (n=4). Clinical characteristics of ACC patients are reported in **Table 1**. Metastasis and relapse were present in 10 (37%) of 27 patients, whereas death occurred in 4 (15%) of 27 patients. Circulating FSCN1 levels in blood samples collected before surgery of ACC patients (stage I/II and stage III/IV) were significantly higher than those in the serum samples of the two cohorts of non-tumoral control subjects (fold increase, FI: 5.5 ± 0.5, P<0.0001 and 8.0 ± 0.5, P<0.0001 for stage I/II and stage III/IV group *vs* healthy controls, respectively; FI: 2.4 ± 0.4, P<0.01 and 3.5 ± 0.2, P<0.001 for stage I/II and stage III/IV group *vs* obese/T2D subjects, respectively; **Figure 1A**). A statistically significant positive correlation was found between serum concentration of FSCN1 and FSCN1 levels in tumor tissues of the 10 ACC patients analyzed by ELISA technique (**Figure 1B**). When compared between stages in ACC patients, FSCN1 levels resulted significantly elevated in serum samples collected before surgery from stage III/IV patients compared with those measured for stage I/II (**Figure 1C**). Interestingly, after the surgical resection of the tumor mass, FSCN1 concentration in serum samples collected close to the surgery (PostS < 12 months from surgery) was significantly decreased in stage III/IV group only, and was raised again toward pre-surgery levels at a longer follow up (PostS ≥ 12 months from surgery). No differences in FSCN1 levels between pre- and post-surgery samples were evident in stage I/II group. The mean follow-up time interval at which serum samples were taken after surgery in ACC patients stratified in low/high stages is shown in **Figure 1D**.

Clinical Significance of Circulating FSCN1 in ACC Patients

To investigate the predictive power of circulating levels of FSCN1 in the tumor progression, we evaluated any association between pre-surgery FSCN1 concentrations and clinical characteristics of ACC patients (see **Table 1**). A statistically significant positive association was found between pre-surgery levels of FSCN1 and stage (r=0.784, p=0.012, **Figure 2A**), whereas pre-surgery FSCN1 negatively correlated with DFS time (r=-0.695, p=0.038, **Figure 2B**).

We analyzed the prognostic power of circulating FSCN1 levels for DFS and OS by applying Kaplan-Meier analysis to ACC patients stratified by PreS FSCN1 levels. When patients were dichotomized in low (≤ 21.49 ng/ml) and high (>21.49 ng/ml) FSCN1 levels in PreS serum samples, according to the median value of pre-surgery FSCN1, FSCN1 levels significantly predicted DFS (Log-rank=0.013, **Figure 3A**), but not OS (Log-rank=0.317, **Figure 3B**). Metastasis and relapse were present in 4 (44%) of 9 patients, whereas death occurred in 2 (22%) of 9 patients. Both DFS time (49.6 ± 18.2 *vs.* 5.25 ± 5.25 months, p=0.070, Student's t test) and OS time (59.2 ± 17.4 *vs.* 23.5 ± 5.6 months, p=0.111) were longer in the low compared to the high PreS FSCN1 level groups, although the differences were not statistically significant. PostS FSCN1 levels showed no significant predictive power for either DFS or OS when patients were stratified in high and low PostS FSCN1 levels (on the median value of PostS FSCN1 level distribution). Multivariate Cox regression analysis of DFS indicated that PreS FSCN1 remained the only statistically significant predictive factor when adjusted for PostS FSCN1 and resection status (**Table 2**).

DISCUSSION

Circulating tumor markers represent a potential clue of the tumor presence obtained with minimally invasive procedures, such as blood drawn compared with intratumor markers obtained by invasive biopsies or tumor removal and, therefore, may constitute a valuable tool for patient diagnosis, prognosis, and monitoring. The most recent ACC guidelines suggest the importance of potential integration of the classical clinical parameters defined for this cancer with the molecular analysis to improve the management of this rare and aggressive endocrine tumor (9). However, despite the significant advances in characterizing the molecular intratumor landscape of ACC (10, 11), there is still a great need of developing biomarkers for early diagnosis, as the tumor histological assessment remains, until now, the gold standard for ACC diagnosis (12).

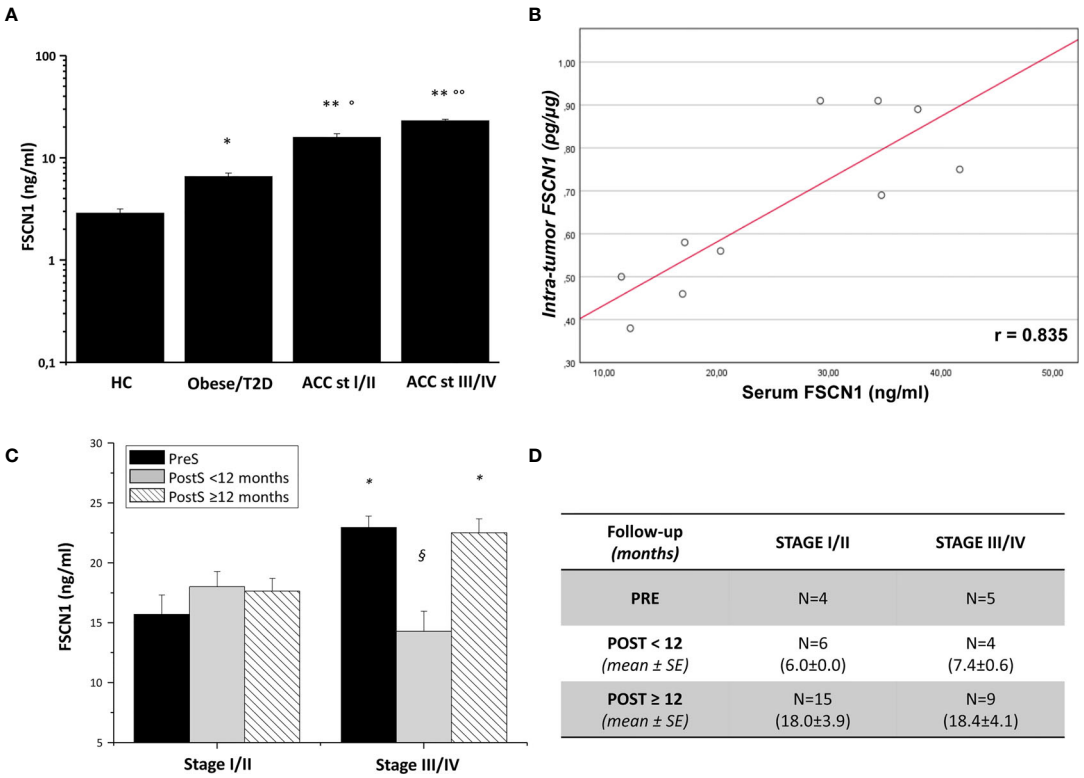

Follow-up *(months)*	STAGE I/II	STAGE III/IV
PRE	N=4	N=5
POST < 12 *(mean ± SE)*	N=6 (6.0±0.0)	N=4 (7.4±0.6)
POST ≥ 12 *(mean ± SE)*	N=15 (18.0±3.9)	N=9 (18.4±4.1)

FIGURE 1 | FSCN1 detection in blood samples of ACC patients. **(A)** Quantitative evaluation of FSCN1 concentrations in pre-operative serum samples of ACC patients compared to obese/diabetic and healthy controls (HC). Data are expressed as mean ± SE of circulating FSCN1 levels measured in at least n=3 independent measurements. Statistical significance obtained by One-way ANOVA followed by Dunnett's Post-hoc test: *P < 0.01, **P < 0.0001 *vs* HC, °P<0.01, °°P<0.001 *vs* Obese/T2D. **(B)** A statistically significant positive linear correlation was found between FSCN1 detected in serum samples and in tumor tissue samples, r=0.835, R^2 = 0.698, p=0.002, n=10. **(C)** Circulating FSCN1 levels were measured in patients with stage III/IV compared to stage I/II in pre-surgery (PreS) samples and after surgery at early (PostS <12 months) and long term (PostS ≥12 months) follow-up. Data are expressed as mean ± SE of protein levels in at least n= 3 independent measurements. Statistical significance obtained by One-way ANOVA followed by Dunnett's Post-hoc: *P < 0.005 stage I/II *vs* III/IV; §P < 0.001 PreS *vs* PostS. **(D)** The table shows the number of patients with PreS, PostS<12, and PostS≥12 samples and their follow-up time for post-surgery sampling (mean ± SE). In stage I/II group all patients had a R=0 resection status, while for stage III/IV group n=4 patients had R>0 in the PreS and PostS groups.

In the present paper, we demonstrated that FSCN1 levels are measurable in the bloodstream of ACC patients and are significantly higher than those measured in healthy non-tumoral subjects, reflecting the higher intratumoral levels of FSCN1 compared with normal adrenals (6, 7). Furthermore, we found a positive correlation between FSCN1 levels measured in serum and in the primary ACC mass. The levels found in non-tumoral patients in our studies are in agreement with those reported in similar studies performed in healthy subjects (13) and in other cancers (14) and lower than 10 ng/ml. Moreover, serum FSCN1 levels were significantly higher in ACC patients compared with obese/T2D patients, who have higher levels of FSCN1, probably due to kidney overload/damage associated to diabetes, as already demonstrated in renal injury associated with renal transplantation (15). These findings suggest that the high levels of FSCN1 may be indicative of an adrenal tumor, although a differential diagnostic power cannot be claimed, as circulating FSCN1 levels have not been measured in different types of adrenal tumors, such as pheochromocytoma and adrenocortical adenoma.

It is still unclear if FSCN1 release in the bloodstream is an active or a passive process from the tumor mass; and its potential role in the bloodstream is still unknown. FSCN1 was discovered as an actin-bundling protein responsible of promoting migration through its localization in cell microspikes, filopodia, and actin-based protrusions (5). Although this protein can also be expressed in normal tissues, recent studies have shown that FSCN1 is up-regulated in many types of metastatic tumors, and its expression correlates with enhanced aggressiveness, poor prognosis, and reduced survival (4, 5, 7, 16). Selective block of FSCN1 in the tumor has been recently described to inhibit the metastatic process and stimulate anti-tumor immune responses in several mouse models of solid tumors (17).

Significantly elevated concentrations of serum FSCN1 have been described in head and neck cancer (HNC) patients (18) and in non-small cell lung cancer (NSCLC) patients (14, 19) compared with healthy controls. In addition, similar to what has been found in NSCLC patients (14, 19), we showed here that serum FSCN1 levels in pre-surgery samples are significantly higher in advanced stage-

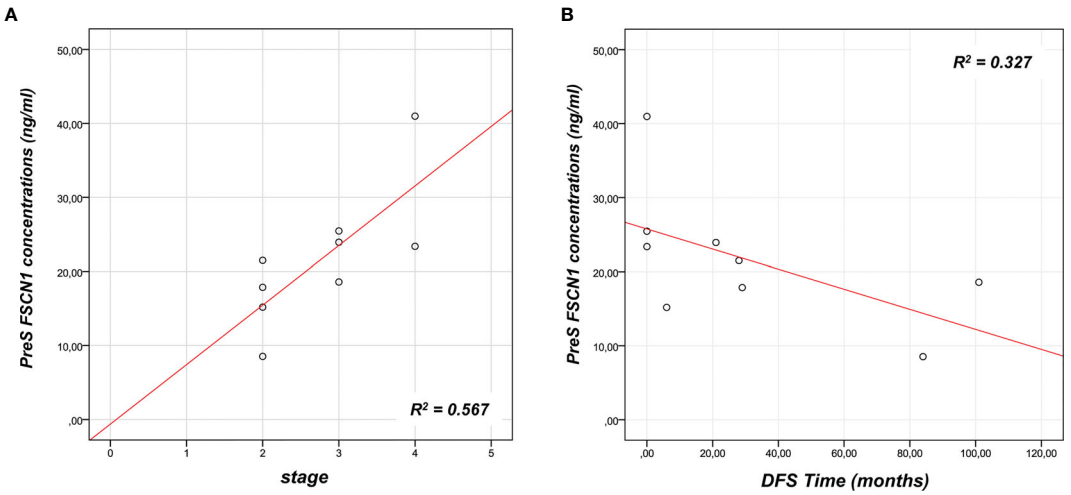

FIGURE 2 | Association between FSCN1 levels and ACC parameters. A statistically significant positive linear correlation was found between pre-surgery FSCN1 concentrations (PreS) and stage - r=0.784, R^2 = 0.567, p=0.012, n=9 **(A)**, and a statistically significant negative linear correlation with the disease-free survival time - r=- 0.695, R^2 = 0.327, p=0.038, n=9 **(B)**.

patients. This is the first study also assessing serum levels of FSCN1 after the removal of the tumor mass. Although in stage I/II patients, FSCN1 levels did not significantly differ before and after surgery, in stage III/IV patients, also including R>0 masses, there was a significant drop in FSCN1 soon after the surgery followed by a return back to the levels similar to presurgery. Of note, the decrease observed did not reach FSCN1 levels as low as those in nontumoral conditions, but resembled the levels found in stage I/II. This behavior might be explained by a reduction in the active release of FSCN1 from the primary mass after its removal, which might characterize advanced ACC, followed by a return to the pre-surgery levels once the tumor progresses or relapses. The low but stable levels found in stage I/II, which, nevertheless, are higher than those found in nontumoral subjects, might be a marker of the condition of the adrenal tumor, which also remains after the mass removal. A passive leakage from the remaining epithelia or the damaged kidney may be hypothesized, as suggested by the rather high levels of circulating FSCN1 found in obese/diabetic subjects with kidney sufferance.

In our analysis, we found a positive correlation between Pre-S serum FSCN1 levels and stage, as well as a negative relationship with the DFS time, reflecting our previous findings (7) that FSCN1 expression in the tumor mass is associated with disease progression and worse prognosis. These results suggest that circulating

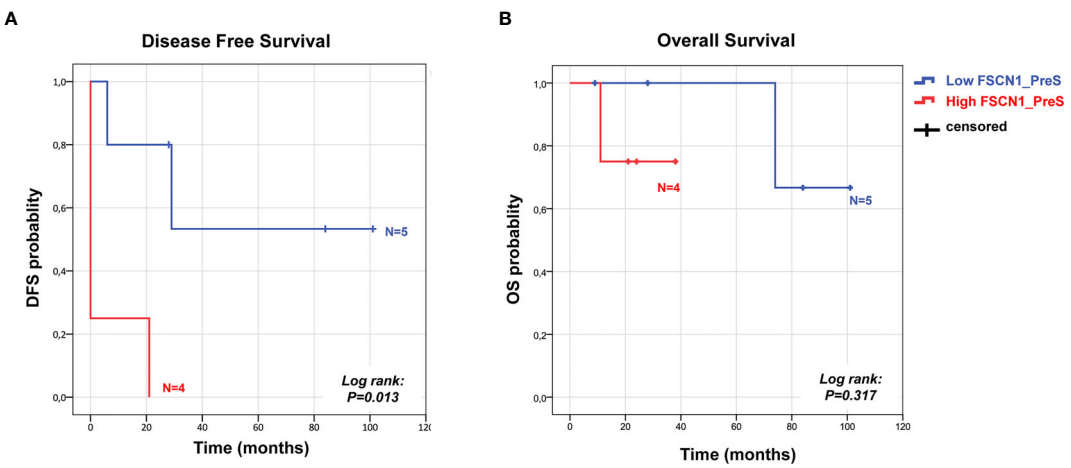

FIGURE 3 | Survival predictive power of pre-surgery serum FSCN1 levels in ACC. Kaplan Meier analysis of DFS **(A)** and OS **(B)** in n=9 ACC patients stratified in two classes according to low and high FSCN1 preS serum concentrations (cut off=21.49 ng/ml, pre-surgery FSCN1 median value). Statistical significance is indicated by Log-rank.

TABLE 2 | PreS levels are the best predictor of DFS.

	Univariate			Multivariate		
	HR	**95%CI**	**P**	**HR**	**95%CI**	**P**
PreS FSCN1 high *vs* low	9.4	0.98-90.4	*0.05*	10.7	1.0-113	*0.049*
PostS FSCN1 high *vs* low	0.3	0.04-1.9	0.181	0.2	0.3-1.8	0.161
Resection status R>0 *vs* R=0	3.8	0.5-27.3	0.181	4.4	0.6-35.5	0.161

Univariate and Multivariate Cox regression analyses of DFS in patients stratified for the indicated factors in high and low classes for PreS FSCN1 levels and PostS FSCN1 levels (according to the median value of FSCN1 distributions in serum samples drawn before and after surgery).
HR, hazard ratio; CI, confidence interval.

pre-surgery FSCN1, as found in liquid biopsy, may represent a valid prognostic marker of advanced ACC.

Circulating FSCN1 may be somehow involved in tumor progression, namely in the metastatic process, as well as in tumor relapse, supported by the evidence that FSCN1 in pre-surgery samples is predictive of DFS but not of the OS. Of note, this information is obtained through a minimally invasive procedure, such as a blood sample before surgery, thus allowing the histopathological diagnosis of ACC on the removed tumor mass.

We acknowledge some limitations in our study, such as the small number of patients for PreS FSCN1 analysis, as this study was retrospectively performed, and PreS samples were not available for all the 27 patients who were tested for FSCN1 following surgery. Therefore, a different number of PreS and PostS measurements were available, and it was not always possible to evaluate FSCN1 levels in pre- and post-surgery paired serum for each patient. Other factors that might affect the analysis are the heterogeneity of ACC patients' adjuvant treatments, which were not only limited to mitotane alone but also included EDP chemotherapy and radiotherapy (20).

Serum tumor markers have been widely used in diagnosis, prognosis, and treatment monitoring of several solid cancers (19, 21), although they might not be always sensitive enough for early diagnosis of the disease or for monitoring tumor evolution (21). A different approach reported in the literature involves the research of circulating autoantibodies against FSCN1 instead of measuring serum FSCN1 levels, even though this alternative strategy might lack sensitivity (21). However, this approach might be of a potential value in ACC, as previously demonstrated for another potential marker of ACC, FATE-1 (22).

Blood samples are a rich source of tumor material and the liquid biopsy is rapidly emerging as a minimal-invasive and powerful tool for diagnosis and prognosis of solid cancers.

In conclusion, our preliminary findings suggest that the measurements of circulating FSCN1 may represent an innovative minimally invasive marker of advanced ACC, in particular when measured before surgery can provide material for the histological diagnosis. The proposed marker can provide additional information to be used to refine ACC patients' management. Validation of the data of our preliminary study in extended cohorts of ACC patients is mandatory.

DATA AVAILABILITY STATEMENT

The raw data supporting the conclusions of this article will be made available by the authors, without undue reservation.

ETHICS STATEMENT

The studies involving human participants were reviewed and approved by the local ethical committee (Prot.2017-277 BIO 59/11, 27/09/2017). The patients/participants provided their written informed consent to participate in this study.

AUTHOR CONTRIBUTIONS

GC: study concept and design, analysis and interpretation, drafting of the manuscript, writing—review and editing, and final approval of the version to be published. LF and TE: substantial contributions to data acquisition. LC and GDF: data curation. GN: data interpretation. MM: substantial contributions to critical revision of the manuscript, and final approval of the version to be published. ML: study concept and design, supervision, writing—review and editing, final approval of the version to be published, agreement with all aspects of the work, and funding acquisition. All authors: final approval of the version to be published, and agreement with all aspects of the work. All authors contributed to the article and approved the submitted version.

FUNDING

This work was supported by Associazione Italiana Ricerca sul Cancro (AIRC) Investigator Grant to ML (grant IG2015-17691); Seventh Framework Program (FP7/2007-2013) under grant agreement 259735 ENS@T-Cancer.

ACKNOWLEDGMENTS

GC, LF, LC, GDF, TE, GN, MM, and ML are members of the European Network for the Study of Adrenal Tumors (ENS@T).

REFERENCES

1. De Filpo G, Mannelli M, Canu L. Adrenocortical Carcinoma: Current Treatment Options. *Curr Opin Oncol* (2021) 33(1):16–22. doi: 10.1097/CCO.0000000000000695
2. Puglisi S, Calabrese A, Basile V, Ceccato F, Scaroni C, Simeoli C, et al. Mitotane Concentrations Influence the Risk of Recurrence in Adrenocortical Carcinoma Patients on Adjuvant Treatment. *J Clin Med* (2019) 8(11):1850. doi: 10.3390/jcm8111850
3. Liu H, Zhang Y, Li L, Cao J, Guo Y, Wu Y, et al. Fascin Actin-Bundling Protein 1 in Human Cancer: Promising Biomarker or Therapeutic Target? *Mol Ther Oncolytics* (2021) 20:240–64. doi: 10.1016/j.omto.2020.12.014
4. Tan VY, Lewis SJ, Adams JC, Martin RM. Association of Fascin-1 With Mortality, Disease Progression and Metastasis in Carcinomas: A Systematic Review and Meta-Analysis. *BMC Med* (2013) 11(52):52. doi: 10.1186/1741-7015-11-52
5. Hashimoto Y, Kim DJ, Adams JC. The Roles of Fascins in Health and Disease. *J Pathol* (2011) 224(3):289–300. doi: 10.1002/path.2894
6. Poli G, Ceni E, Armignacco R, Ercolino T, Canu L, Baroni G, et al. 2d-DIGE Proteomic Analysis Identifies New Potential Therapeutic Targets for Adrenocortical Carcinoma. *Oncotarget* (2015) 6(8):5695–706. doi: 10.18632/oncotarget.3299
7. Poli G, Ruggiero C, Cantini G, Canu L, Baroni G, Armignacco R, et al. Fascin-1 Is a Novel Prognostic Biomarker Associated With Tumor Invasiveness in Adrenocortical Carcinoma. *J Clin Endocrinol Metab* (2019) 104(5):1712–24. doi: 10.1210/jc.2018-01717
8. Salvianti F, Canu L, Poli G, Armignacco R, Scatena C, Cantini G, et al. New Insights in the Clinical and Translational Relevance of miR483-5p in Adrenocortical Cancer. *Oncotarget* (2017) 8(39):65525–33. doi: 10.18632/oncotarget.19118
9. Fassnacht M, Dekkers OM, Else T, Baudin E, Berruti A, de Krijger R, et al. European Society of Endocrinology Clinical Practice Guidelines on the Management of Adrenocortical Carcinoma in Adults, in Collaboration With the European Network for the Study of Adrenal Tumors. *Eur J Endocrinol* (2018) 179(4):G1–46. doi: 10.1530/EJE-18-0608
10. Armignacco R, Cantini G, Canu L, Poli G, Ercolino T, Mannelli M, et al. Adrenocortical Carcinoma: The Dawn of a New Era of Genomic and Molecular Biology Analysis. *J Endocrinol Invest* (2018) 41(5):499–507. doi: 10.1007/s40618-017-0775-y
11. Crona J, Beuschlein F. Adrenocortical Carcinoma - Towards Genomics Guided Clinical Care. *Nat Rev Endocrinol* (2019) 15(9):548–60. doi: 10.1038/s41574-019-0221-7
12. Lalli E, Luconi M. The Next Step: Mechanisms Driving Adrenocortical Carcinoma Metastasis. *Endocr Relat Cancer* (2018) 25(2):R31–48. doi: 10.1530/ERC-17-0440
13. Porav-Hodade D, Martha O, Balan D, Tataru S, Hutanu A, Sin A, et al. Fascin is Secreted in Male's Serum: Results of a Pilot Study. *Futur Sci OA* (2018) 4(3):FSO273. doi: 10.4155/fsoa-2017-0098
14. Yang L, Teng Y, Han TP, Li FG, Yue WT, Wang ZT. Clinical Significance of Fascin-1 and Laminin-5 in Non-Small Cell Lung Cancer. *Genet Mol Res* (2017) 16(2). doi: 10.4238/gmr16029617
15. Jacobs-Cacha C, Torres IB, Lopez-Hellin J, Cantarell C, Azancot MA, Roman A, et al. Fascin-1 Is Released From Proximal Tubular Cells in Response to Calcineurin Inhibitors (Cnis) and Correlates With Isometric Vacuolization in Kidney Transplanted Patients. *Am J Transl Res* (2017) 9(9):4173–83.
16. Han S, Huang J, Liu B, Xing B, Bordeleau F, Reinhart-King CA, et al. Improving Fascin Inhibitors to Block Tumor Cell Migration and Metastasis. *Mol Oncol* (2016) 10(7):966–80. doi: 10.1016/j.molonc.2016.03.006
17. Wang Y, Song M, Liu M, Zhang G, Zhang X, Li MO, et al. Fascin Inhibitor Increases Intratumoral Dendritic Cell Activation and Anti-Cancer Immunity. *Cell Rep* (2021) 35(1):108948. doi: 10.1016/j.celrep.2021.108948
18. Lee LY, Chen YJ, Lu YC, Liao CT, Chen IH, Chang JT, et al. Fascin is a Circulating Tumor Marker for Head and Neck Cancer as Determined by a Proteomic Analysis of Interstitial Fluid From the Tumor Microenvironment. *Clin Chem Lab Med* (2015) 53(10):1631–41. doi: 10.1515/cclm-2014-1016
19. Teng Y, Xu S, Yue W, Ma L, Zhang L, Zhao X, et al. Serological Investigation of the Clinical Significance of Fascin in non-Small-Cell Lung Cancer. *Lung Cancer* (2013) 82(2):346–52. doi: 10.1016/j.lungcan.2013.08.017
20. Cantini G, Canu L, Armignacco R, Salvianti F, De Filpo G, Ercolino T, et al. Prognostic and Monitoring Value of Circulating Tumor Cells in Adrenocortical Carcinoma: A Preliminary Monocentric Study. *Cancers (Basel)* (2020) 12(11):3176. doi: 10.3390/cancers12113176
21. Chen WX, Hong XB, Hong CQ, Liu M, Li L, Huang LS, et al. Tumor-Associated Autoantibodies Against Fascin as a Novel Diagnostic Biomarker for Esophageal Squamous Cell Carcinoma. *Clin Res Hepatol Gastroenterol* (2017) 41(3):327–32. doi: 10.1016/j.clinre.2016.10.011
22. Doghman-Bouguerra M, Finetti P, Durand N, Parise IZS, Sbiera S, Cantini G, et al. Cancer-Testis Antigen Fate1 Expression in Adrenocortical Tumors Is Associated With A Pervasive Autoimmune Response and Is A Marker of Malignancy in Adult, But Not Children, Acc. *Cancers (Basel)* (2020) 12(3):689. doi: 10.3390/cancers12030689

Conflict of Interest: The authors declare that the research was conducted in the absence of any commercial or financial relationships that could be construed as a potential conflict of interest.

frontiers in Endocrinology

REVIEW
published: 22 July 2021
doi: 10.3389/fendo.2021.672499

Are Markers of Systemic Inflammatory Response Useful in the Management of Patients With Neuroendocrine Neoplasms?

Elisa Giannetta[1], Anna La Salvia[2], Laura Rizza[3], Giovanna Muscogiuri[4], Severo Campione[5], Carlotta Pozza[1], Annamaria Anita LIvia Colao[6] and Antongiulio Faggiano[7] on behalf of NIKE*

[1] Department of Experimental Medicine, "Sapienza" University of Rome, Rome, Italy, [2] Department of Oncology, University Hospital 12 de Octubre, Madrid, Spain, [3] Endocrinology Unit, Department of Oncology and Medical Specialities, AO San Camillo-Forlanini, Rome, Italy, [4] Endocrinology Unit Department of Clinical Medicine and Surgery, University Federico II School of Medicine, Naples, Italy, [5] A. Cardarelli Hospital, Naples Department of Advanced Diagnostic-Therapeutic Technologies and Health Services Section of Anatomic Pathology, Naples, Italy, [6] Department of Clinical Medicine and Surgery, University "Federico II", Naples, Italy, [7] Department of Clinical and Molecular Medicine, Endocrine-Metabolic Unit, Sant'Andrea University Hospital "Sapienza" University of Rome, Rome, Italy

OPEN ACCESS

Edited by:
Roberta Malaguarnera, Kore University of Enna, Italy

Reviewed by:
Paula Jimenez Fonseca, Hospital Universitario Central de Asturias, Spain
Jean-Yves Scoazec, Institut Gustave Roussy, France

***Correspondence:**
Elisa Giannetta
elisa.giannetta@uniroma1.it

Specialty section:
This article was submitted to Cancer Endocrinology, a section of the journal Frontiers in Endocrinology

Received: *25 February 2021*
Accepted: *03 May 2021*
Published: *22 July 2021*

Citation:
Giannetta E, La Salvia A, Rizza L, Muscogiuri G, Campione S, Pozza C, Colao AAL and Faggiano A (2021) Are Markers of Systemic Inflammatory Response Useful in the Management of Patients With Neuroendocrine Neoplasms? Front. Endocrinol. 12:672499. doi: 10.3389/fendo.2021.672499

Given the increasing incidence of neuroendocrine neoplasms (NENs) over the past few decades, a more comprehensive knowledge of their pathophysiological bases and the identification of innovative NEN biomarkers represents an urgent unmet need. There is still little advance in the early diagnosis and management of these tumors, due to the lack of sensible and specific markers with prognostic value and ability to early detect the response to treatment. Chronic systemic inflammation is a predisposing factor for multiple cancer hallmarks, as cancer proliferation, progression and immune-evading. Therefore, the relevance of inflammatory biomarkers has been identified as critical in several types of tumours, including NENs. A bidirectional relationship between chronic inflammation and development of NENs has been reported. Neuroendocrine cells can be over-stimulated by chronic inflammation, leading to hyperplasia and neoplastic transformation. As the modulation of inflammatory response represents a therapeutic target, inflammatory markers could represent a promising new key tool to be applied in the diagnosis, the prediction of response to treatment and also as prognostic biomarkers in NENs field. The present review provides an overview of the pre-clinical and clinical data relating the potentially usefulness of circulating inflammatory markers: neutrophil-lymphocyte ratio (NLR), platelet-lymphocyte ratio (PLR), cytokines and tissue inflammatory markers (PD-1/PD-L1), in the management of NENs. (1) NLR and PLR have both demonstrated to be promising and simple to acquire biomarkers in patients with advanced cancer, including NEN. To date, in the context of NENs, the prognostic role of NLR and PLR has been confirmed in 15 and 4 studies, respectively. However, the threshold value, both for NLR and PLR, still remains not defined. (2) Cytokines seem to play a central role in NENs tumorigenesis. In particular, IL-8 levels seems to be a good predictive marker of response to anti-angiogenic treatments. (3) PD-1 and PD-L1

expression on tumour cells and on TILs, have demonstrated to be promising predictive and prognostic biomarkers in NENs. Unfortunately, these two markers have not been validated so far and further studies are needed to establish their indications and utility.

Keywords: neuroendocrine neoplasms, neutrophil-lymphocyte ratio, platelet-lymphocyte ratio, PD-L1, early response, cytokines, VEGF

INTRODUCTION

The physiopathological association between chronic inflammation and cancer has been established for a long time (1–3). Although chronic inflammatory milieu could contribute to the development of cancer, several studies reported that tumor itself could begin and keep an inflammatory process up. A change in a set of cytokines and chemokines has been reported in studies regarding stomach (4), liver (5, 6), lung (7), esophagus (8), breast (9), and prostate cancer (10). These findings could be of interest to identify not only potential pathogenetic mechanisms but also novel diagnostic/prognostic markers (11). In this view, recent studies analyzed the immunophenotypes of cancer cells and cancer stromal cells in terms of usefulness as prognostic factors, showing the prognostic values of podoplanin-positive cancer-associated fibroblasts (CAFs) for patients with high-grade neuroendocrine carcinomas (HG-NEC) of the lung (12).

An important hallmark of cancer is that it can escape immune attack; therefore, chronic cancer-related inflammation could be considered as an attempt of immunosuppression mechanisms mediated primarily by immature myeloid-derived suppressor cells to block the development of cancer (13, 14). The fascinating link between inflammation and the field of neuroendocrinology has also been evaluated (15, 16). A bidirectional action between neuroendocrine stimuli and macrophage function in the development of innate and adaptive immune responses was described (17), suggesting a potential involvement of inflammation in the development of neuroendocrine neoplasms (NENs).

Neuroendocrine cells can be over-stimulated by chronic inflammation, which leads to hyperplasia and neoplastic transformation (18).

Research efforts have shown that NENs of gastroentero-pancreatic tract (GEP-NENs) occur more frequently in the settings of chronic inflammation. Indeed, it was shown that enteroendocrine cells can be hyperstimulated by chronic inflammation, which leads to their hyperplasia and neoplastic transformation (19–21).

Despite the progress in the understanding of NEN molecular biology, we are still far from the identification of markers able to detect the tumor at an early stage as well as to predict disease relapse after treatments.

As the modulation of inflammatory response represents a therapeutic target, changes of inflammatory markers may potentially represent in the future new biomarkers, which beyond the RECIST criteria, could eventually be helpful in the follow up of patient with NENs treated with targeted therapies.

This review investigated a panel of inflammatory response markers apparently heterogeneous but sharing the feature to be readily available and inexpensive diagnostic and prognostic factors in NENs.

PROGNOSTIC VALUE OF NEUTROPHIL-TO-LYMPHOCYTE RATIO AND PLATELET-TO-LYMPHOCYTE RATIO FOR PATIENTS WITH NEN

The recent advent of detecting systemic inflammation levels through non-invasive blood tests, has opened the possibility of studying inflammatory processes at baseline and monitoring the course of cancer disease, in order to stratify patients according to their prognosis and to achieve a personalized approach (22). In this context, two *ratios*, neutrophil-lymphocyte ratio (NLR, calculated as the neutrophil count divided by the lymphocyte count) and platelet-lymphocyte ratio (PLR, obtained by dividing the platelet count by the absolute number of lymphocytes), have demonstrated to be powerful biomarkers for patients with cancer (23, 24). Notably, both NLR and PLR, are non-invasive, rapid, simple to acquire and inexpensive markers, thus, they could have a potential for widespread clinical use.

High NLR has been associated with poor clinical outcome in several tumor types (25). The underlying mechanism has not completely been elucidated, so far. Preclinical studies have shown that neutrophilia, which is a direct expression of systemic inflammation, represses the cytolytic activity of immune cells, such as lymphocytes, activated T cells, and natural killer cells (26). Additionally, tumor-associated neutrophils (TANs) have been demonstrated to promote tumor progression acting as pro-angiogenic agents (27), by a high expression of different pro-angiogenic factors as vascular endothelial growth factor (VEGF), Interleukin 1 beta (IL-1β) and Integrin Subunit Beta 1 (ITGB1) (28). Several studies have also reported that TANs are associated with an elevated expression of matrix metallopeptidase-9 (MMP-9), favoring angiogenesis through the MMP-9-VEGF axis (28).

PLR has arisen as a useful marker of systemic inflammation, metabolic syndrome and prothrombotic state and it is regarded as a promising biomarker in cancer patients (24, 29). Alterations in PLR have also been associated with other markers of systemic inflammation, particularly with NLR. Even in this case, as for NLR, the molecular mechanism has not been fully understood yet. Platelets represent an essential storage for secreted growth factors (as VEGF or platelet-derived growth factor, PDGF).

In that way, platelets play a key role in regulating tumor angiogenesis, cell proliferation, migration, and metastasis (30, 31).

Therefore, despite the encouraging data about the clinical relevance and prognostic implication of NLR and PLR as biomarkers in cancer patients, some limitations still exist. For instance, a unique cut-off value of these two inflammatory *ratios* has not been established. Another open issue is to determine the best timing for dosing NLR and PLR, given the dynamic nature of this measures that change over times and that could be altered in relation to the administration of systemic treatments or because of other clinical conditions (as sepsis and septic shock) (32).

Clinical Evidence in NENs

To date, several studies have been published about the role of the two ratios, NLR and PLR, in NENs. The available data are summarized in **Table 1**.

In 2016 the Izmir Oncology Group Study retrospectively investigated the prognostic role of baseline NLR and PLR in 132 GEP-NENs patients. The included patients were equally distributed according to grading (31.1% G1, 33.3% G2, 35.6% G3). Embryonic origin was foregut in 87 cases, midgut in 20 cases and hindgut in 25. Primary site was pancreas in 50 cases and gastro-enteric tract in 82. 62 were metastatic patients. NLR and PLR were significantly higher in high grade NENs (0.0001), in metastatic patients (0.0001) and in those of foregut origin (0.0001). Patients with pancreatic NENs had higher NLR and PLR compared to those with gastrointestinal NENs (0.0001). Finally, higher NLR and PLR were negatively associated to progression-free survival (PFS) (0.0001), while no overall survival (OS) data were provided (13).

Another study, by Cao et al., evaluated the prognostic role of preoperative NLR in 147 gastric NENs (g-NENs) patients that underwent to radical surgery. Of them, 27 (18.4%) patients were gastric neuroendocrine tumors (g-NETs), 48 (32.7%) with gastric neuroendocrine carcinoma (g-NEC), and 72 (48.9%) with gastric mixed adenoneuroendocrine carcinoma (g-MANEC). Among these patients, 97 (66.0%) received adjuvant chemotherapy. Moreover, 147 healthy controls were enrolled. Significantly higher value of NLR was detected in patients with g-NENs compared to controls ($P < 0.001$). Furthermore, the NLR was an independent prognostic factor of relapse free survival (RFS) and OS ($p<0.05$ for both outcome measures), and, along with Ki67, positively correlated with liver metastases and negatively correlated with recurrence time (16).

One year later, a retrospective study aimed to evaluate the role of preoperative NLR as prognostic marker, was performed by Arima et al. (15). All the 58 pancreatic NENs patients included in the analysis, underwent curative pancreatic resection. Among these 58 patients, 46 were well differentiated G1 pancreatic neuroendocrine tumors (pNETs) and 31 were no-functioning tumors. The median NLR of all pNENs 58 patients was 2.18. A high preoperative NLR was significantly associated with higher tumor size ($p= 0.0015$) and grade 3 ($p< 0.0001$). In this analysis, the authors were able to identify a cut off value of NLR ≥2.4, that resulted associated to a worst OS ($P = 0.0481$) and RFS ($P < 0.0001$) and to an increased risk of postoperative recurrence ($p= 0.0035$).

In the same year, other three similar retrospective analysis were performed. All these three studies included G1, G2 and G3 pNENs. The first, included a population of 95 operated pancreatic NENs (33). Among these patients, 52 (54.7%) were G1 NET, 32 (33.7%) G2 NET, and 11 (11.6%) G3 NEC. A significant association was found between high NLR and advanced T stage, nodal metastasis, and advanced grade ($p< 0.05$ for all variables). High NLR value was confirmed as an independent prognostic factor for lymph-node metastasis by multivariate logistic regression (Hazard ratio (HR) 6.74; $p=0.02$)). NLR higher than 1.4 correlated with decreased RFS ($p < 0.05$). A second study, by Zhou B et al., evaluated both NLR and PLR in 172 patients with pNENs (34). 73 (42.4%) were G1 pNETs, 76 (44.2%) G2, and 23 (13.4%) G3 pancreatic NEC. 150 cases (87.2%) had stage I-II disease. 166 patients (96.5%), underwent R0 resection and 6 cases received palliative surgery (3.5%). In the study were enrolled also 172 healthy volunteers. A cut-off for NLR was identified as 2.31, for PLR was 151.4. NLR and PLR were significantly higher in the patients than in controls (all $p<0.001$). At univariate analysis an increased NLR and PLR correlated with advanced stage, high grade, and R1 resection (all $p<0.05$). High NLR or PLR had shorter OS (HR=4.907, $p<0.001$ and HR=3.307, $p=0.003$, respectively) and disease-free survival, DFS (HR=4.143, $p<0.001$ and HR=2.617, $p=0.001$, respectively) than patients with a low NLR or PLR). However, at multivariant analysis, only NRL remained significant as independent prognostic factor in terms of OS (HR=4.47, $p=0.006$) and DFS (HR=2.531, $p=0.015$). The third study, by Zhou et al., analyzed preoperative NLR and PLR in a population of 101 surgically removed pNENs (35). In this study, cutoff values were 1.80 for NLR and 168.25 for PLR. PLR and NLR were significantly higher in those patients with lymph-nodes metastases ($p<0.05$). At multivariable analysis, NLR ($p= 0.017$) correlated with lymph-nodes metastases. High NLR or PLR had shorter DFS ($p=0.007$ and $p<0.001$, respectively).

One year later, in 2018, a prospective study evaluating the role of NLR (calculated at baseline and preoperatively) and PLR (calculated at the time of enrollment for all patients, as well as preoperatively for patients who underwent resection with curative intent) in 97 pNENs, was published (37). The authors found that NLR higher than a cut-off values of 2.3 was a negative prognostic factor in terms PFS (HR 2.53, $p = 0.038$) and at multivariant analysis PLR > 160.9 resulted independently associated with reduced PFS (HR 5.86, $p=0.023$).

Another interesting retrospective study evaluated the role of NLR in a population of 26 completely resected large cells neuroendocrine carcinomas (LCNEC) (36). Notably, at multivariate analysis, a preoperative NLR value > 1.7 was confirmed as an independent prognostic factor for OS (HR 8.559, $p = 0.011$).

McDermott and colleagues, instead, investigated the prognostic value of NLR in 262 stage IV patients with liver metastases from different primary origins (GEP and pulmonary primary tumor), who were treated with transarterial chemoembolization (TACE) (38). As a result, pre-TACE NLR > 4 was associated with shorter OS

TABLE 1 | Prognostic values of Neutrophil-Lymphocyte Ratio (NLR) and Platelet-to-Lymphocyte Ratio (PLR) in NENs patients.

Author, year	Mean age	Primary site	Grade	TNM stage	Metastasis	NLR cut-off	PLR
Salman T. et al. (13)	56.7	GEP-NENs	1-2-3	1-2-3-4	Metastatic & Non-metastatic	**2.17** Pretreatment NLR >2.17->shorter median PFS (11.1 months) NLR ≤ 2.17 ->longer median PFS (22.2 months) p = 0.001	**181.5** Pretreatment PLR >181.5 ->shorter median PFS (11.2 months) PLR ≤ 181.5 -> longer median PFS (21.9 months) p = 0.001
Cao L-L. et al. (16)	58	Gastric NENs	1-2-3	1-2-3-4	Metastatic & Non-metastatic	**2.20** Preoperative NLR>2.20 correlates with a shorter reccurence time, RFS and OS (p<0.01) NLR >2.20 associated with both liver metastasis and peritoneal metastasis (P < 0.05)	/
Arima K.et al. (15)	58	Pancreatic-NENs	1-2-3	/	Metastatic & Non-metastatic	**2.40** Preoperative NLR>2.40 -> shorter RFS (<0.05) shorter OS (<0.0001) and postoperative liver metastasis (p<0.0001)	/
Tong Z. et al. (33)	54.4	Pancreatic-NENs	1-2-3	1-2-3-4	Metastatic & Non-metastatic	**1.40** Preoperative NLR > 1.4-> shorter RFS (p < 0.05).	/
Zhou B. et al. (34)	52.9	Pancreatic-NENs	1-2-3	1-2-3-4	Metastatic & Non-metastatic	**2.31** NLR > 2.31-> shorter OS (HR=4.907, p<0.001) NLR > 2.31-> shorter DFS (HR=4.143, p<0.001)	**151.4** PLR> 151.4 -> shorter OS (HR=3.307, p=0.003) PLR > 151.4 -> shorter DFS (HR=2.617, p=0.001)
Zhou B. et al. (35)	53	Non- functioning Pancreatic-NENs	1-2-3	1-2-3-4	Metastatic & Non-metastatic	**1.80** NLR > 1.80-> shorter DFS (p=0.007)	**168.25** PLR > 168.25-> shorter DFS (p<0.001)
Okui M. et al. (36)	68.8	LCNEC	3	1-2-3	Non metastatic	**1.7** NLR value > 1.7 -> shorter OS (HR 8.559, p = 0.011).	/
Gaitanidis A. et al. (37)	52	Pancreatic-NENs	1-2-3	/	Metastatic & Non-metastati	**2.3** NLR> 2.3 -> shorter PFS (HR 2.53, p = 0.038)	**160.9** PLR > 160.9 -> shorter PFS (HR 5.86, p=0.023).
McDermott SM. et al. (38)	57	GEP, colorectal and lung NENs	1-2-3	4	Metastatic	**4** NLR>4-> shorter OS (p=0.005).	/
Zou J. et al. (39)	65	GEP, colorectal and other NENs	1-2-3	4	Metastatic & Non-metastatic	**2.8** NLR> 2.8 -> shorter OS (p = 0.03)	/
Panni RZ. et al. (40)	57.5	Pancreatic-NENs	1-2-3	1-2-3	Non-metastatic	**3.7** NLR> 3.7 -> shorter RFS (HR 1.79, p=0.01) and shorter OS (HR 2.04, p=0.01)	/
Harimoto N. et al. (41)	61	Pancreatic-NENs	1-2-3	1-2-3	Non-metastatic	**3.4** NLR> 3.4 -> shorter RFS (HR 31.75, p=0.03)	/
Pozza A. et al. (42)	70, 66, 63.5	Foregut, Midgut and hindgut NEN	1-2-3	1-2-3-4	Metastatic & Non-metastatic	**2.6** NLR> 2,6 -> shorter OS (HR 4.71, p=0.02)	Not significant association with OS
Zhou B. et al. (43)	60	Pancreatic-NENs	1-2-3	1-2-3-4	Metastatic & Non-metastatic	**3.1** NLR> 3.1 -> shorter DFS (p<0.001) and OS (p=0.002)	/
Zhou W. et al. (44)	53	Pancreatic-NENs	1-2-3	1-2-3-4	Metastatic & Non-metastatic	**1.9** NLR> 1.9 -> shorter RFS (p=0.046) and in OS (p=0.032).	/

GEP, gastro-entero-pancreatic; HR, hazard ratio; NEC, neuroendocrine carcinomas; NENs, neuroendocrine neoplasms; PFS, progression free survival; RFS, recurrence free survival; OS, overall survival.

(p=0.005). Additionally, pre-TACE NLR and 6-months post-TACE NLR resulted independently associated with OS on multivariant analysis (HR 1.4 p=0.030 and HR 1.7 0.007, respectively).

Another study focused on locally advanced and metastatic patients was performed in 2019 by the group of Zou and colleagues (39). In this case, were included 135 G1, G2 and G3 NENs of different primary origin. At univariate analysis, NLR > 2.8 correlated with OS (p=0.003), but the statistical significance was not confirmed at multivariant analysis.

Additionally, a year later in 2019, four retrospective analyses, which investigated the prognostic role of inflammatory markers in surgically removed pNENs patients were published. The first of them, included 620 non metastatic G1, 2 and 3 patients (40). With a cut-off of NLR of 3.7, the authors demonstrated a significative impact on RFS (HR 1.79, p=0.01) and OS (HR 2.04, p=0.01). The second study, by Harimoto N and colleagues, included 55 pNEN patients (41) and showed a negative prognostic role (in terms of RFS) for NLR>3.4, on univariate (HR 12.62, p<0.01) and multivariate analysis (HR 31.75, p=0.03). The third analysis was conducted on 64 operated pNENs (43). In this study, high NLR correlated with poor OS and DFS compared to patients with a low NLR score (p < 0.001). In the multivariate analysis, high NLR resulted an independent prognostic factor in terms of OS and DFS for pNENs of the head (p=0.002 and p<0.001, respectively). The fourth study, by Zhou W et al., included 174 pNENs (44). Even in this case, the prognostic role for NLR, with a cut-off of 1.9, was confirmed at univariant analysis, both in RFS (p=0.046) and in OS (p=0.032). However, multivariate analysis did not confirm that the NLR had an independent prognostic impact".

Finally, a study on 48 G1, G2 and G3 NENs of different primary origins, but all surgically removed, was carried on by an Italian group (42). By a threshold value for NLR of 2.6, at the multivariable analysis high NLR was confirmed to have a significant impact on OS (HR 4.71, p = 0.02).

Future Directions

Proinflammatory signals promote tumorigenesis and neoplastic progression, but their origins and downstream effects remain unclear. Given the pooled data of these studies about NLR and PLR, that confirm their role, these two inflammatory biomarkers could potentially represent innovative prognostic factors for NENs. In fact, both NLR and PLR are rapid, easy to measure, and cheap to obtain from routinary blood tests. In the analyzed studies both of them have been demonstrated to correlate with RFS and OS. Additionally, their combination with other markers such as proliferation index (ki67) and for example lymph node ratio, in order to obtain nomograms, has demonstrated to have a higher power to predict clinical outcomes of NEN patients (45). Polymorphonuclear neutrophils (PMN) also represent critical innate immune effector cells that either protect the host or exacerbate organ dysfunction by migrating to injured or inflamed tissues. Pathways including neuroendocrine and innate and acquired immune systems regulates PMN mobilization. In this view there is still no evidence of an accumulation of PMN in the NENs, but this aspect deserves to be examined (46).

However, there are many limitations of these data and some open questions. First of all, almost all the studies considered are retrospective and the sample size is quite often little. Furthermore, both the cut-off value used, and the population included is highly heterogeneous. Unfortunately, considering these issues a strong recommendation to the direct application in the clinical practice of NLR or PLR, couldn't be given. However, the data presented are promising and should be confirmed in further prospective study, given the striking need to find new biomarkers in the field of NENs in order to better stratify patients by prognosis and to improve the personalization of therapeutic strategy.

CIRCULATING CYTOKINES AS POSSIBLE BIOMARKERS OF THERAPEUTIC RESPONSE IN PATIENTS WITH NEN

The key molecular links between inflammation and cancer involve the canonical nuclear factor kappa-light-chain-enhancer of activated B cells (NF-kB) activation and Signal transducer and activator of transcription 3 (STAT3) pathways (47). NF-κB and STAT3 signaling pathways control genes necessary for angiogenesis (mainly VEGF) and influence the ability of tumor cells to invade and metastasize (48, 49). As a rule, most proinflammatory cytokines including tumor necrosis factor α (TNF-α), interleukin 6 (IL-6) and interleukin 17 (IL-17), produced by either the host immune system or the tumor cells themselves, promote tumor progression. In turn, pro-apoptotic TNF-related apoptosis-inducing ligand (TRAIL) and anti-inflammatory cytokines such as Interleukin 10 (IL-10) and transforming growth factor beta (TGF-β) usually lead to tumor suppression (50).

Clinical Evidences in NEN

The role of cytokines (such as IL-1) in NENs differentiation has been demonstrated (51). Furthermore, Interleukin 2 (IL-2) has an established role in the regulation of the neuroendocrine system and in gastrointestinal hormone synthesis and secretion (52). Although normal pancreatic cells do not express Interleukin 8 (IL-8), pNENs show increased expression of IL-8 and its receptors, especially C-X-C Motif Chemokine Receptor 2 (CXCR2) (53, 54). In low-grade pNENs, normal circulating Placental Growth Factor (PlGF) values are associated with better survival, while in low-grade small intestinal NENs (SI-NENs) is an independent prognostic factor for shorter time-to-progression (55). The overexpression of VEGF promotes the growth of human NENs in part through up-regulation of angiogenesis (56). Low-grade NENs can synthesize, store and secrete VEGF, while, in HG-NENs this process is inconstant and heterogeneous. This feature is part of the so-called "neuroendocrine paradox": in pNENs the density of the vascular network reflects the rate of differentiation rather than of aggressiveness: most is the vascularization, less the aggressiveness, and more differentiated pNEN are the less angiogenic. In this view, a recent study analyzing 60 resected HG-NEC of the lung (37 LCNECs and 23 Small Cell Lung Carcinomas -SCLCs), revealed the presence of

stromal cells within vascular invasion was not significant predictor for recurrence. This suggests that the roles of intravascular stromal cells in HG-NEC metastasis are less, raise an "alarm" against overemphasis of stromal cell-targeting therapy (57).

Then, there is a strong rationale for supporting the use of angiogenesis inhibitor in well differentiated rather than poorly differentiated NENs. By contrast HG-pNENs are particularly active in terms of angiogenesis, meaning endothelial cell proliferation and abnormal vasculature (58).

In this view, cytokines panel represents an interesting tool in NENs, needing for framing. Cigrovski Berkovic et al. proposed a model of different cytokine genotypes and corresponding high serum values that regulate GEP-NEN etiopathogenesis (19).

Finally, Pavel et al. (59) showed that the circulating levels of VEGF and IL-8 are associated with tumor progression in patients with advanced NEC and might qualify as markers of prognosis and therapy control. Angiogenin and basic fibroblast growth factor (bFGF) levels do not correlate with tumor growth and with patient survival.

The prognostic utility of systemic inflammatory markers in NENs' patients after therapy is still debated. The first-in-human trial of sunitinib (SUN) (60) included an analysis of plasma levels of VEGF and its soluble receptor, sVEGFR-2, of twenty-eight cancer patients (among them 4 patients were NENs), both pretreatment and after 28 days of treatment. VEGF concentrations increased slightly during the first month of SUN, while the plasma mean sVEGFR-2 decreased, demonstrating a targeted effect of the drug. Comparable findings were observed in another study on patients with metastatic NENs (61). After 28 days of SUN administration, VEGF levels increased more than 3-fold over baseline in about half of all patients, while sVEGFR-2 and sVEGFR-3 levels decreased by ≥ 30% in about 60% and 70% of all patients, respectively. Levels returned to baseline after two weeks of therapy interruption. Furthermore, IL8 values raised 2.2-fold average by the end of SUN cycle 1, and a larger increase was proportional to the tumor size reduction. This increase in IL-8 levels during SUN treatment can represent a mechanism of drug resistance, as also reported by Huang (62) in renal clear-cell carcinomas (RCC) cell lines. In addition, Zurita et al. (63) report that, at four weeks of the first cycle, SUN treatment is associated with significant increases from baseline in VEGF, IL-8, and stromal cell-derived factor-1 (SDF-1a) (also known as C-X-C motif chemokine 12, CXCL12), and with reduction in sVEGFR-2 and sVEGFR-3 with no difference between 66 pNENs and 39 carcinoid tumors. No significant associations have been found between soluble protein levels and clinical benefit response or PFS in pNENs, while high sVEGFR-3 and IL-8 levels correlated with shorter PFS and shorter OS in carcinoid tumors. Additionally, recent data come from the Spanish prospective SALSUN clinical trial enrolling well-differentiated pancreatic neuroendocrine tumors treated with sunitinib (PMID: 30651923). In this study, two SNPs in the VEGFR-3 gene, rs307826 and rs307821, predicted lower OS, with HR 3.67 and with HR 3.84, respectively. IL-6 was associated with increased mortality: HR 1.06, and osteopontin was associated with shorter PFS: HR 1.087, independently of Ki-67 value. Furthermore, levels of osteopontin remained higher at the end of the study in patients considered non-responders: 38.5 ng/mL *vs.* responders: 18.7 ng/mL, p-value=0.039. Dynamic upward variations were also observed with respect to IL-8 levels in sunitinib-refractory individuals: 28.5 pg/mL at baseline *vs.* 38.3 pg/mL at 3 months, p-value=0.024. In the RADIANT-3 phase III randomized clinical trial (64), baseline and post-treatment VEGF, PIGF, bFGF, sVEGFR-1, and sVEGFR-2 values were investigated in advanced pNENs' patients treated with everolimus (EVE) 10 mg/die. In relation to the placebo, EVE treatment leads a significant and progressive reduction in sVEGFR-2 and an early but not significant decrease in PIGF. No significant differences in circulating concentrations of VEGF or sVEGFR-1 were observed. These data suggest a possible antiangiogenic effect of EVE as consequence of mTOR inhibition.

With regard to somatostatin analogs and interferon, in 36 patients with metastatic or unresectable carcinoid tumors (65), treatment with PEG interferon + depot Octreotide was associated with a significant increase in plasma Interleukin 18 (IL-18) and a significant reduction in plasma bFGF. No significant changes in the same plasma cytokines were associated with bevacizumab + depot octreotide therapy. Bevacizumab therapy resulted in objective responses, reduction of tumor blood flow, and longer PFS in patients with carcinoid than PEG interferon treatment. Finally, eight patients with NENs present lower VEGF plasma levels and reduced VEGF mRNA levels and microvessel density in liver metastasis biopsy material after IFN-α treatment (66). **Table 2** summarized circulating cytokine trend in response to different treatment approaches.

Future Perspectives

Cytokines seem to play a central role in NEN tumorigenesis. The observation that the modulation of IL-1 was positively related to a decrease in Chromogranin A (CgA) and a parallel increase in Carcinoembryonic antigen (CEA) secretion, suggest the key role of cytokines in NEN progression (51).

Together, the main results of the studies with large sample size suggest that the VEGF-pathway proteins and IL-8 are possible markers of prognosis and/or SUN treatment benefit in patients with GEP-NENs. Particularly, the IL-8 increase can represent a potential predictor of SUN response (61–63). VEGF, sVGEFR-2 and -3 changes can be new SUN's biological activity biomarkers in NENs, confirming that SUN's activity is mediated by the VEGF signaling pathway (60, 61, 63). Routine use of these circulating cytokines, in NEN patients' clinical practice for SUN, is hopeful. Owing to the limited number of patients, further studies are needed to confirm the SDF-1α role in resistance to antiangiogenic SUN therapy.

A cross-talk between pro-inflammatory and angiogenic chemokines is described (67, 68). Interleukin-8 is an inflammatory cytokine upregulated in both cancer and chronic inflammatory diseases. Moreover, IL-8 is a chemokine that increases endothelial permeability during early stages of angiogenesis. IL-8 expression was inducible by hypoxia due to VEGF inhibition. In this view targeting both VEGF and IL8 it may be possible to achieve greater therapeutic efficacy.

As regard EVE treatment, except sVEGFR-2 and PIGF significant reduction, there are no significant differences in

TABLE 2 | Circulating cytokines trend according to different treatments.

		Treatment	N° pts	Tumor types	Tumor site	Tumor stage	Author, Year
VEGF	↑	SUN	4	NEN	digestive system (1/4 rectum)	advanced	Faivre S. (60)
VEGFR-2	↓	SUN	4	NEN	digestive system (1/4 rectum)		
VEGF	↑	SUN	109	NEN	pancreas	advanced	Bello CL. (61)
sVEGFR-2	↓	SUN	109	NEN	pancreas		
sVEGFR-3	↓	SUN	109	NEN	pancreas		
IL8	↑	SUN	109	NEN	pancreas		
VEGF	↑	SUN	65	NEN	pancreas	advanced	Zurita AJ. (63)
			35	carcinoid	foregut, midgut, hindgut		
IL-8	↑	SUN	66	NEN	pancreas		
			36	carcinoid	foregut, midgut, hindgut		
SDF-1a	↑	SUN	11	NEN	pancreas		
			10	carcinoid	foregut, midgut, hindgut		
sVEGFR-2	↓	SUN	65	NEN	pancreas		
			37	carcinoid	foregut, midgut, hindgut		
sVEGFR-3	↓	SUN	64	NEN	pancreas		
			34	carcinoid	foregut, midgut, hindgut		
PlGF	↓	EVE	393	NEN	pancreas	low – intermediate; advanced (unresectable or metastatic)	Yao JC. (64)
sVEGFR1	=	EVE	393	NET	pancreas		
sVEGFR2	↓	EVE	390	NET	pancreas		
VEGF	=	EVE	393	NET	pancreas		
bFGF	=	EVE	393	NET	pancreas		
IL18	↑	PEG-IFN + OCT-LAR	22	carcinoid	foregut (3/22); midgut (11/22); hindgut (4/22); unknown (4/11).	low – intermediate; advanced (unresectable or metastatic)	Yao JC. (65)
bFGF	↓	PEG-IFN + OCT-LAR	22	carcinoid	foregut (3/22); midgut (11/22); hindgut (4/22); unknown (4/11).		
IL18	=	BEV + OCT-LAR	22	carcinoid	foregut (3/22); midgut (13/22); unknown (6/11).	low – intermediate; advanced (unresectable or metastatic)	Yao JC. (65)
bFGF	=	BEV + OCT-LAR	22	carcinoid	foregut (3/22); midgut (13/22); unknown (6/22).		
VEGF	↓	IFN-α	8	carcinoid	midgut	advanced (metastatic)	von Marschall Z. (66)

VEGF, vascular endothelial growth factor; sVEGFR, soluble vascular endothelial growth factor receptor; IL, interleukin; SDF-1a, stromal cell-derived factor 1; PlGF, placental growth factor; bFGF, basic fibroblast growth factor; SUN, sunitinib; EVE, everolimus; IFN-α, interferon α; PEG-IFN, peglyated interferon; OCT-LAR, depot long-acting octreotide; BEV, bevacizumab; NENs, neuroendocrine neoplasms; NET, neuroendocrine tumors; pts, patients.

VEGF-pathway circulating proteins (64). These data suggest a possible antiangiogenic effect of EVE as a consequence of mTOR inhibition. Probably, other NENs biomarkers [such as Neuron-specific enolase (NSE) and CgA)] have a better prognostic value than the inflammatory cytokines in terms of survival and/or response to EVE treatment.

Given the strong rationale for using anti-angiogenic therapy for several tumors, basic and clinical research has shown a growing interest in investigating new related pathways (69). Tie2-expressing monocytes/macrophages (TEMs), Tie2 and VEGFR2 are highly expressed on stromal cells of the tumor microenvironment, especially on endothelial cells. Certain cancers, such as melanomas and gliomas, have been shown to lead to increased circulating Tie2+ monocytes and their recruitment to distal metastatic sites or anti-VEGF-treated gliomas (70). Recently an *in vitro* study proposed that modulation of Tie2+ proangiogenic macrophages through rebastinib, could possibly control tumor angiogenesis and lymphangiogenesis involved in cancer cell intravasation and metastasis in a model of pNENs (71). Our suggestion is that by identifying proinflammatory pathways in NENs we could extrapolate a set of prognostic markers useful in the management of NENs.

PREDICTIVE AND PROGNOSTIC VALUE OF PD1 AND PD-L1 FOR PATIENTS WITH NEN

A key role in the immune-escape process is related to the interaction between programmed cell death protein 1 receptor

(PD1) present on the surface of T lymphocytes and its ligand (PD-L1) on the surface of tumoral cells. PD-L1, by binding to PD-1, activate an inhibitory signal that avoids the destruction of cancer cells by host immune system.

In oncology, several compounds have been developed that act on this mechanism, and they are defined as Immune Checkpoint Inhibitors (ICIs). ICIs are monoclonal antibodies that bind to PD-1 (as Nivolumab and Pembrolizumab) or PD-L1 (as Atezolizumab, Avelumab and Durvalumab), respectively. The outcome of both bonds is to prevent the interaction between PD-1 and PD-L1 from blocking the T lymphocytes capable of attacking and eliminating tumour cells.

Immunotherapy acting through inhibition of PD1 and PD-L1 was firstly introduced with encouraging results in melanoma and non-small cell lung carcinomas (NSCLC), by using nivolumab and pembrolizumab, and now its use is widening in many other malignant tumors (72). To date, tissue expression of PD-L1 is tested by immunohistochemistry (IHC) and evaluated by microscopic assessment in all non-operable NSCLC, where the rate of expression in neoplastic cells can predict treatment response and its efficacy, indicating the place of pembrolizumab in the therapeutic algorithm (73, 74).

In the context of NENs, the potential efficacy of ICIs was investigated, at first, in HG, poorly differentiated NEC. HG-NEC are aggressive tumors, associated with a dismal prognosis (of approximately 10-12 months). The standard of care for this subgroup, still remains chemotherapy, which is associated with rapid but not long-lasting responses. Unfortunately, no targeted agents nor innovative approaches have been validated for NEC, so far. However, a rationale for the use of PD1 and PD-L1 inhibitors in this setting exists and it is represented by their high tumor mutational burden (TMB) (above all of SCLC), if compared to other type of cancer. Therefore, different ICIs have been tested in HG-NEC, confirming their activity. Some key examples are represented by skin Merkel cell carcinoma and SCLC, which almost always do not achieve durable remission with chemo- and radiotherapy, while the introduction of new therapies showed excellent and more durable responses (75, 76). In both cases, Merkel carcinoma and SCLC, ICIs have been approved and are currently used in daily clinical practice (77, 78).

However, the optimal selection of patients with HG-NEC as candidate for PD1 and PD-L1 inhibitors is still debated and immunohistochemical evaluation may not be alone satisfactory (76, 79–81).

On the other hand, for well-differentiated, low-grade NET, given their nature of more indolent tumors, with a very low TMB, and considering their relative favorable prognosis in the majority of cases, the potential activity of immune-checkpoint inhibition has not been established, so far. The current guidelines recommend surgery as the only curative treatment for early stages. For locally advanced inoperable or metastatic patients, depending on some essential clinic-pathologic features of each case (primary tumor localization, expression of somatostatin receptors on cell surface, ki67 value, presence of symptoms and tumor burden), the therapeutic armamentarium includes a great variety of active treatments as SSA (Octreotide or Lanreotide), targeted agents (i.e. the mTOR inhibitor EVE and the anti-angiogenetic drug SUN), peptide receptor radionuclide therapy (PRRT) or chemotherapy (82). All these treatments could be used individually or combined, and their sequence is decided case per case within the multidisciplinary-NEN dedicated tumor boards. However, the potential activity of ICIs in NET is still an open and challenging issue and hopefully the results of the studies currently ongoing in this field, could allow to define a role for this strategy.

Clinical Evidence in NEN

As previously reported, a role for ICIs in HG-NEN is a promising therapeutic weapon. Unfortunately, no predictive biomarkers of response to anti-PD1/PDL1 therapy, have been established yet. It is well known that tissue expression and tissue localization (membrane of tumor cells or tumor-infiltrating immune cells, TILs) are both important for the access to the therapy (83). Therefore, the predictive value of PD-L1 expression in tumor cells and TILs by IHC has been investigated within several clinical trials for ICIs, for which different assays with specific IHC platforms were used. Of these, different PD-L1 IHC assays have been validated for the corresponding ICI. Not all laboratories, however, are equipped with dedicated platforms, and many laboratories are used to prepare house assays. Additionally, has been showed that the different available antibodies anti PD-L1 for IHC use are highly heterogeneous in their sensitivity to tumor cells expression or to TILs (83).

In this context, several authors have published results of PD-L1 tissue expression in lung NENs in the last years. The available data are summarized in **Table 3**. We will comment some of the most relevant papers, on lung NENs (84–90, 95, 96) as well as in Merkel cell carcinoma (92). In 2015, Schultheis and colleagues, were the first who investigated PD-1 and PD-L1 IHC expression in 61 SCLC. No expression in cancer cells was detected.

In 2017, Inamura reported a PD-L1 positivity in 25 cases (21%) of a population of 74 SCLC and 41 LCNEC. The multivariant analysis confirmed PD-L1 expression on tumoral cells as an independent positive prognostic factor (HR=0.29; p=0.0006) in lung HG-NENs. In 2018, Eichhorn and colleagues performed a retrospective analysis of PD-L1 expression by IHC in tumoral cells and microenvironment, in a population of 76 LCNECs. The authors found positivity for PD-L1 (positivity was defined as the presence of PD-L1 in >1% of cells) only in tumor cells in 17 cases and only in the tumor microenvironment in 16 cases, while in 12 cases PD-L1 was positive in both cell types. A statistically significant difference in survival was observed comparing the cases with PD- L1 positive tumor/negative immune-cell infiltrate and PD- L1 negative tumor/positive immune-cell infiltrate, being the first associated with a worse prognosis (5-year Tumor-specific survival, TSS: 0% *vs.* 60%; $p < 0.017$). This observation was confirmed in 2019, by Xu Y, who reported that PD-L1 expression on tumoral cells was as an independent prognostic factor for OS (HR=2.55, p =0.017) in a population of 60 SCLC patients. The same conclusions came from a more recent study, published in 2020 by Sun C and his colleagues. This analysis included 102 surgically removed stage I,

TABLE 3 | Prognostic values of programmed cell death protein 1 receptor (PD1) and programmed death-ligand 1 (PD-L1) in NENs patients.

Author, year	Number of patients	Diagnosis	Tumor Grade	Metastasis	PD1/PDL1 and patients outcome
Lung origin					
Fan et al. (84)	80	22 NET, 48 SCLC, 10 LCNEC	1-2-3	Metastatic & Non-metastatic	The expression of PD1 in TILs was independently associated with OS (HR 0.367, p=0.001)
Kim et al. (85)	192	120 SCLC, 72 LCNEC	3	Metastatic & Non-metastatic	No relationship between PD-L1 expression on TCs and survival. Patients with PD-L1 expression on TILs had longer PFS than those without PD-L1 expression on TILs (11.3 *vs* 7.0 months, p=0.02)
Kasajima et al. (86)	242	57 NET, 127 SCLC, 58 LCNEC	1-2-3	Metastatic & Non-metastatic	For SCLC/LCNEC patients: PD-L1 positivity in TILs correlated with prolonged OS (p<0.01, HR 0.4)
Inamura et al. (87)	115	74 SCLC and 41 LCNEC	3	Metastatic & Non-metastatic	PD-L1 expression on TCs was an independent positive prognostic factor (p=0.0006, HR=0.29)
Eichhorn et al. (88)	76	LCNEC	3	Metastatic & Non-metastatic	PD-L1 expression on TCs and negative on TILs was associated with a worse prognosis (5-year TSS: 0% *vs* 60%; p<0.017)
Xu Y. et al. (89)	60	SCLC	3	Non-metastatic	PD-L1 expression on TCs was a negative independent prognostic factor for OS (HR=2.55, p =0.017)
Sun C. et al. (90)	102	SCLC	3	Non-metastatic	PD-L1 positive on TILs was associated with better RFS (p=0.004)
Merkel cell carcinoma					
Wehkamp et al. (91)	39	NEC	3	Metastatic & Non-metastatic	Shorter mOS for PD-1 positive patients (23.2 months *vs* 61.6 months, p=0.35); shorter mOS for PD-L1+ patients (PD-L1+ 24.7 *vs* PD-L1- 61.6 months, p = 0.86)
Giraldo et al. (92)	26	NEC	3	Metastatic	Higher density of expression on tumoral cells for PD-1 (median cells/mm2, 70.7 *vs* 6.7, p=0.03) and PD-L1 (855.4 *vs* 245.0, p=0.02) in responders *vs* not responders to pembrolizumab
GEP origin					
Wang et al. (93)	120	NENs	1-2-3	Metastatic & Non-metastatic	PD-L1 resulted an independent prognostic factor for OS
Bösch et al. (94)	244	NENs	1-2-3	Metastatic & Non-metastatic	PD-1 positive *vs* negative (44.5 months *vs* 53.8) and PD-L1 positive *vs* negative (46 months *vs* 51.9) had a negative impact on OS (p< 0.05, in both cases)

GEP, gastro-entero-pancreatic; HR, hazard ratio; LCNEC, large cell neuroendocrine lung carcinomas; NEC, neuroendocrine carcinomas; NENs, neuroendocrine neoplasms; NET, neuroendocrine tumors; NS, not specified; mOS, median overall survival; OS, overall survival; PFS, progression free survival; SCLC, small cell lung carcinomas; RFS, relapse free survival; TILs, tumor-infiltrating lymphocytes; TCs, tumor cells; TSS, tumor-specific survival; vs, versus.

II and III SCLC.". 40.2% and 37.3% of cases were detected to present a positivity on TILs for PD-1 and PD-L1, respectively. Only 3.9% of tumor cells resulted positive for PD-L1. TILs positive cases for PD-L1 presented better RFS (p=0.004). In the same direction, Fan Y. et al. demonstrated that the expression of PD1 in TILs remained independently associated with survival (HR, 0.367; p=0.001) in a population of 80 lung NENs (22 NET, 48 SCLC and 10 LCNEC).

Figure 1 shows a case of SCLC, followed at the Department of Advanced Diagnostic-therapeutic technologies and health services Section of Anatomic Pathology (A. Cardarelli Hospital, Naples, Italy), where PD-L1 positivity was limited to TIL, while tumor cells were negative (**Figure 1**).

Among Merkel cell carcinoma, in a very interesting study 39 patients were analyzed for immunohistochemical PD-1, PD-L1 and nerve growth factor (NGF) expression. These variables were correlated with clinic and pathological features, showing that PD-L1 and NGF are co-expressed on spindle cells in the microenvironment. Authors suggested that this co-expression might be a link of the microenvironment to the tropomyosin receptor kinase A (TrkA)-positive tumor cells, representing a critical mechanism for tumor growth and lack of response to anti-PD-1/L1 treatment, requiring to be investigated in further studies (91). Another study, by Giraldo et al, included 26 advanced Merkel cell carcinomas and investigated PD-1 and PD-L1 expression in order to determine their role as predictive biomarkers of response to ICIs. In this case, all the patients received treatment with Pembrolizumab. Higher density of expression on tumoral cells for PD-1 and PD-L1 were detected in responders versus not responders to the therapy (median cells/mm2, 70.7 *vs*. 6.7, p=0.03; and 855.4 *vs*. 245.0, p=0.02, respectively).

Additionally, PD-L1 expression has been also related to TMB (85) and tumor inflammation (86). Kim H.S. et al. found that the PD-1/PD-L1 pathway is activated in the microenvironment of pulmonary HG-NEN and correlated with a higher TMB, both in SCLC and LCNEC. Moreover, Kasajima et al. found an increased PD-L1 expression in TIL both in SCLC and LCNEC with a higher tumor associated inflammation and T cell CD8+.

Furthermore, in other HG NEN, beyond SCLC and Merkel cell carcinoma (that are the two fields in which ICIs have demonstrated their activity), PD-1 and PD-L1 are also under evaluation as potentially useful biomarkers.

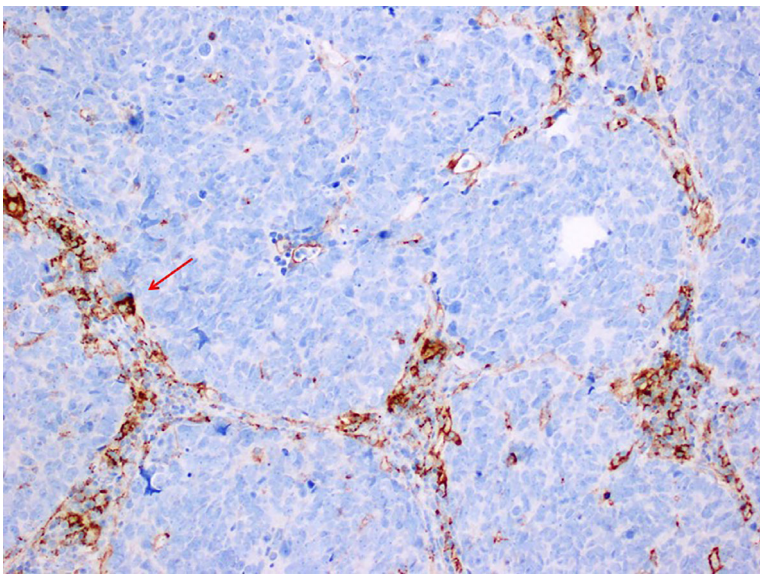

FIGURE 1 | Immunohistochemistry stain, antibody anti PD-L1, SP263 VENTANA 200X MAGNIFICATION in a case of Small Cell Lung Carcinoma. PD-L1 positivity is limited to tumor infiltrating lymphocytes that lie between the nest of tumor cells, that are negative to PD-L1.

Among GEP-NEN, only few studies about the evaluation of PD-L1 by IHC have been published so far. In 2017, Cavalcanti and colleagues, studied the expression of this tissue marker in 57 G1, G2 and G3 extrapulmonary-NENs (85, 97, 98). The authors found a significant correlation between PD-L1 expression by tumor cells and immune infiltrates and G3 of WHO classification (p=0.001), while it was not associated with gender, primary site, or number of metastatic sites. The next year, Lamarca et al., evaluated PD-L1 expression in 62 well-differentiated, G1 or G2 Si-NETs. PD-L1 was studied in tumoral cells as well as in TILs (85, 97, 98). PD-L1 expression was positive in 12.8% of cases and in 24.3% of TILs. PD-1 was expressed in 22.8% of TILs. Furthermore, the results obtained by IHC were confirmed with RT-qPCR. This technique detected higher expression levels of PD-L1 (p=0.007) and PD-1 (p=0.001) in samples positive by IHC compared to negative by IHC. In 2019, Wang and colleagues (93), investigated the positivity for PD-1/PD-L1 in 120 GEP-NENs. In this study, PD-L1 was expressed in 52.5% of the tumor cells, while PD-L1 was positive in 55.8% of TILs. At multivariate analysis, PD-L1 resulted an independent prognostic factor in this population. Additionally, Bösch and colleagues, included 244 pancreatic and G1, G2 and G3 SI-NEN patients (94). In this study, PD-1/PD-L1 were analysed on TILs, where a high PD-1 expression was demonstrated in 35 samples (16.1%), and a high PD-L1 expression was evidenced in 20 cases (8.7%). A significant negative impact on OS for PD-1 and PD-L1 positivity was demonstrated ($p< 0.05$, in both cases).

Future Directions

The rationale of investigating PD-1 and PD-L1 expression in NENs is represented by the clinical need to find predictive biomarkers of response to ICIs. However, the role of PD-1 and PD-L1 tissue testing (in tumoral cells as well as in TILs) in defining the access to immunotherapy in NENs is still uncertain (87, 96).

The majority of the available supporting data are in the field of HG-NEN, as previously reported in detail. To date, skin Merkel cell carcinoma should be considered a paradigm for the efficacy of immunotherapy in NENs. However, PD-1 and PD-L1 tissue testing has not been validated as a fundamental predictive marker for patients selection (75). Also, in SCLC ICIs treatment has been approved, but even in this case the debate regarding predictive biomarkers of response is still an open issue (76). Among GEP-NEN, only a couple of studies have been carried on.Taking all the results together, PD-1 and PD-L1 expression appear to possibly have a role as negative prognostic biomarkers. However, further prospective studies, aimed to determine the epidemiology and the role as predictive or prognostic markers in NENs should be highly encouraged.

CONCLUSIONS

NENs are a complex family of tumors, extremely heterogeneous in terms of primary origin of the tumor, tumor morphology (from well differentiated to poorly differentiated forms), proliferation index, clinical presentation and prognosis. To date, several treatments are available for NENs, including SSA, PRRT, targeted agents, chemotherapy, surgery and locoregional approaches. However, despite a clear role for inflammation in cancer and in NENs, only few immunotherapy agents have been approved (mainly in Merkel cell carcinoma and in SCLC) and

above all no specific biomarkers capable of early predicting response to these agents, have been validated so far.

NLR and PLR and pro-inflammatory cytokines could represent a new tool for the early management of NENs. However, future studies adopting a prospective and matched study design need to confirm the role of inflammatory markers in NENs diagnosis, response evaluation, prognosis, and follow-up.

In conclusion, this panel of circulating inflammatory markers, correlated where possible with tissue markers, may be of utility if integrated in a cluster as biomarkers for targeted therapies response in clinical practice.

AUTHOR CONTRIBUTIONS

EG, AS, LR, GM, SC, and AF selected the issue, researched studies from databases, and independently analyzed published data. EG, AS, LR, GM, SC, CP, and AF contributed to the final version of the manuscript. EG, CP, and AF performed quality control checks on extracted data. AC verified the analytic method and supervised the planned systemic review of literature. SC conceived the figure extracting images from his analysis of a case. All authors contributed to the article and approved the submitted version.

FUNDING

Ministerial research project PRIN2017Z3N3YC

ACKNOWLEDGMENTS

This review is part of the 'NIKE' project (Neuroendocrine tumors Innovation Knowledge and Education) led by Prof Annamaria Colao and Dr Antongiulio Faggiano, which aims at increasing the knowledge on NETs. We would like to acknowledge all the Collaborators of this project: Albertelli M. (Genova), Bianchi A. (Roma), Circelli L. (Napoli), De Cicco F. (Napoli), Dicitore A. (Milano), Di Dato C. (Roma), Di Molfetta S. (Bari), Fanciulli G. (Sassari), Ferraù F. (Messina), Gallo M. (Torino), Grossrubatscher E. (Milano), Guadagno E. (Napoli), Guarnotta V. (Palermo), Lo Calzo F. (Napoli), Kara E. (Udine), Malandrino P. (Catania), Messina E. (Messina), Modica R. (Napoli), Pizza G. (Napoli), Razzore P. (Torino), Rubino M. (Milano), Ruggeri R.M. (Messina), Sciammarella C. (Napoli), Vitale G. (Milano), Zatelli M.C. (Ferrara). We would like to thank Marie-Hélène Hayles for revision of the English text. We wish to thank the NETTARE Unit—NeuroEndocrine Tumor TAsk foRcE of "Sapienza" University of Rome, Italy, led by Prof. Andrea Lenzi, Prof. Antongiulio Faggiano, Prof. Elisa Giannetta and Prof. Andrea M. Isidori.

REFERENCES

1. Landskron G, de la Fuente M, Thuwajit P, Thuwajit C, Hermoso MA. Chronic Inflammation and Cytokines in the Tumor Microenvironment. *J Immunol Res* (2014) 2014:149185. doi: 10.1155/2014/149185
2. Mostofa AG, Punganuru SR, Madala HR, Al-Obaide M, Srivenugopal KS. The Process and Regulatory Components of Inflammation in Brain Oncogenesis. *Biomolecules* (2017) 7(2):34. doi: 10.3390/biom7020034
3. Yu S, Wang Y, Jing L, Claret FX, Li Q, Tian T, et al. Autophagy in the "Inflammation-Carcinogenesis" Pathway of Liver and HCC Immunotherapy. *Cancer Lett* (2017) 411:82–9. doi: 10.1016/j.canlet.2017.09.049
4. Raja UM, Gopal G, Shirley S, Ramakrishnan AS, Rajkumar T. Immunohistochemical Expression and Localization of Cytokines/Chemokines/Growth Factors in Gastric Cancer. *Cytokine* (2017) 89:82–90. doi: 10.1016/j.cyto.2016.08.032
5. Liepelt A, Tacke F. Stromal Cell-Derived Factor-1 (SDF-1) as a Target in Liver Diseases. *Am J Physiol Gastrointestinal liver Physiol* (2016) 311(2):G203–9. doi: 10.1152/ajpgi.00193.2016
6. Elia G, Fallahi P. Hepatocellular Carcinoma and CXCR3 Chemokines: A Narrative Review. *La Clin Terapeutica* (2017) 168(1):e37–41. doi: 10.7417/CT.2017.1980
7. Altundag O, Altundag K, Morandi P, Gunduz M. Cytokines and Chemokines as Predictive Markers in non-Small Cell Lung Cancer Patients With Brain Metastases. *Lung Cancer* (2005) 47(2):291–2. doi: 10.1016/j.lungcan.2004.09.003
8. Lukaszewicz-Zajac M, Mroczko B, Szmitkowski M. Chemokines and Their Receptors in Esophageal Cancer–the Systematic Review and Future Perspectives. *Tumour Biol: J Int Soc Oncodev Biol Med* (2015) 36(8):5707–14. doi: 10.1007/s13277-015-3705-7
9. King J, Mir H, Singh S. Association of Cytokines and Chemokines in Pathogenesis of Breast Cancer. *Prog Mol Biol Trans Sci* (2017) 151:113–36. doi: 10.1016/bs.pmbts.2017.07.003
10. Mukherjee S, Siddiqui MA, Dayal S, Ayoub YZ, Malathi K. Epigallocatechin-3-Gallate Suppresses Proinflammatory Cytokines and Chemokines Induced by Toll-Like Receptor 9 Agonists in Prostate Cancer Cells. *J Inflammation Res* (2014) 7:89–101. doi: 10.2147/JIR.S61365
11. Samarendra H, Jones K, Petrinic T, Silva MA, Reddy S, Soonawalla Z, et al. A Meta-Analysis of CXCL12 Expression for Cancer Prognosis. *Br J Cancer* (2017) 117(1):124–35. doi: 10.1038/bjc.2017.134
12. Takahashi A, Ishii G, Kinoshita T, Yoshida T, Umemura S, Hishida T, et al. Identification of Prognostic Immunophenotypic Features in Cancer Stromal Cells of High-Grade Neuroendocrine Carcinomas of the Lung. *J Cancer Res Clin Oncol* (2013) 139(11):1869–78. doi: 10.1007/s00432-013-1502-5
13. Salman T, Kazaz SN, Varol U, Oflazoglu U, Unek IT, Kucukzeybek Y, et al. Prognostic Value of the Pretreatment Neutrophil-To-Lymphocyte Ratio and Platelet-To-Lymphocyte Ratio for Patients With Neuroendocrine Tumors: An Izmir Oncology Group Study. *Chemotherapy* (2016) 61(6):281–6. doi: 10.1159/000445045
14. Franco AT, Corken A, Ware J. Platelets at the Interface of Thrombosis, Inflammation, and Cancer. *Blood* (2015) 126(5):582–8. doi: 10.1182/blood-2014-08-531582
15. Arima K, Okabe H, Hashimoto D, Chikamoto A, Nitta H, Higashi T, et al. Neutrophil-To-Lymphocyte Ratio Predicts Metachronous Liver Metastasis of Pancreatic Neuroendocrine Tumors. *Int J Clin Oncol* (2017) 22(4):734–9. doi: 10.1007/s10147-017-1111-4
16. Cao LL, Lu J, Lin JX, Zheng CH, Li P, Xie JW, et al. A Novel Predictive Model Based on Preoperative Blood Neutrophil-to-Lymphocyte Ratio for Survival Prognosis in Patients With Gastric Neuroendocrine Neoplasms. *Oncotarget* (2016) 7(27):42045–58. doi: 10.18632/oncotarget.9805
17. Jurberg AD, Cotta-de-Almeida V, Temerozo JR, Savino W, Bou-Habib DC, Riederer I. Neuroendocrine Control of Macrophage Development and Function. *Front Immunol* (2018) 9:1440. doi: 10.3389/fimmu.2018.01440
18. Ruszniewski P, Delle Fave G, Cadiot G, Komminoth P, Chung D, Kos-Kudla B, et al. Well-Differentiated Gastric Tumors/Carcinomas. *Neuroendocrinology* (2006) 84(3):158–64. doi: 10.1159/000098007
19. Cigrovski Berkovic M, Cacev T, Catela Ivkovic T, Zjacic-Rotkvic V, Kapitanovic S. New Insights Into the Role of Chronic Inflammation and Cytokines in the Etiopathogenesis of Gastroenteropancreatic Neuroendocrine Tumors. *Neuroendocrinology* (2014) 99(2):75–84. doi: 10.1159/000362339
20. Le Marc'hadour F, Bost F, Peoc'h M, Roux JJ, Pasquier D, Pasquier B. Carcinoid Tumour Complicating Inflammatory Bowel Disease. A Study of

Two Cases With Review of the Literature. *Pathol Res Pract* (1994) 190 (12):1185–92; discussion 93-200. doi: 10.1016/S0344-0338(11)80445-0
21. Cadden I, Johnston BT, Turner G, McCance D, Ardill J, McGinty A. An Evaluation of Cyclooxygenase-2 as a Prognostic Biomarker in Mid-Gut Carcinoid Tumours. *Neuroendocrinology* (2007) 86(2):104–11. doi: 10.1159/000107555
22. Dolan RD, McSorley ST, Horgan PG, Laird B, McMillan DC. The Role of the Systemic Inflammatory Response in Predicting Outcomes in Patients With Advanced Inoperable Cancer: Systematic Review and Meta-Analysis. *Crit Rev Oncol Hematol* (2017) 116:134–46. doi: 10.1016/j.critrevonc.2017.06.002
23. Guthrie GJ, Charles KA, Roxburgh CS, Horgan PG, McMillan DC, Clarke SJ. The Systemic Inflammation-Based Neutrophil-Lymphocyte Ratio: Experience in Patients With Cancer. *Crit Rev Oncol Hematol* (2013) 88(1):218–30. doi: 10.1016/j.critrevonc.2013.03.010
24. Templeton AJ, Ace O, McNamara MG, Al-Mubarak M, Vera-Badillo FE, Hermanns T, et al. Prognostic Role of Platelet to Lymphocyte Ratio in Solid Tumors: A Systematic Review and Meta-Analysis. *Cancer Epidemiol Biomarkers Prev* (2014) 23(7):1204–12. doi: 10.1158/1055-9965.EPI-14-0146
25. McMillan DC. The Systemic Inflammation-Based Glasgow Prognostic Score: A Decade of Experience in Patients With Cancer. *Cancer Treat Rev* (2013) 39 (5):534–40. doi: 10.1016/j.ctrv.2012.08.003
26. Mantovani A, Allavena P, Sica A, Balkwill F. Cancer-Related Inflammation. *Nature* (2008) 454(7203):436–44. doi: 10.1038/nature07205
27. Huo X, Li H, Li Z, Yan C, Agrawal I, Mathavan S, et al. Transcriptomic Profiles of Tumor-Associated Neutrophils Reveal Prominent Roles in Enhancing Angiogenesis in Liver Tumorigenesis in Zebrafish. *Sci Rep* (2019) 9(1):1509. doi: 10.1038/s41598-018-36605-8
28. Imtiyaz HZ, Simon MC. Hypoxia-Inducible Factors as Essential Regulators of Inflammation. *Curr Top Microbiol Immunol* (2010) 345:105–20. doi: 10.1007/82_2010_74
29. Deryugina EI, Zajac E, Juncker-Jensen A, Kupriyanova TA, Welter L, Quigley JP. Tissue-Infiltrating Neutrophils Constitute the Major *In Vivo* Source of Angiogenesis-Inducing MMP-9 in the Tumor Microenvironment. *Neoplasia* (2014) 16(10):771–88. doi: 10.1016/j.neo.2014.08.013
30. Gay LJ, Felding-Habermann B. Contribution of Platelets to Tumour Metastasis. *Nat Rev Cancer* (2011) 11(2):123–34. doi: 10.1038/nrc3004
31. Goubran HA, Stakiw J, Radosevic M, Burnouf T. Platelets Effects on Tumor Growth. *Semin Oncol* (2014) 41(3):359–69. doi: 10.1053/j.seminoncol.2014.04.006
32. Liu Y, Zheng J, Zhang D, Jing L. Neutrophil-Lymphocyte Ratio and Plasma Lactate Predict 28-Day Mortality in Patients With Sepsis. *J Clin Lab Anal* (2019) 33(7):e22942. doi: 10.1002/jcla.22942
33. Tong Z, Liu L, Zheng Y, Jiang W, Zhao P, Fang W, et al. Predictive Value of Preoperative Peripheral Blood Neutrophil/Lymphocyte Ratio for Lymph Node Metastasis in Patients of Resectable Pancreatic Neuroendocrine Tumors: A Nomogram-Based Study. *World J Surg Oncol* (2017) 15(1):108. doi: 10.1186/s12957-017-1169-5
34. Zhou B, Zhan C, Wu J, Liu J, Zhou J, Zheng S. Prognostic Significance of Preoperative Neutrophil-To-Lymphocyte Ratio in Surgically Resectable Pancreatic Neuroendocrine Tumors. *Med Sci Monit* (2017) 23:5574–88. doi: 10.12659/MSM.907182
35. Zhou B, Deng J, Chen L, Zheng S. Preoperative Neutrophil-to-Lymphocyte Ratio and Tumor-Related Factors to Predict Lymph Node Metastasis in Nonfunctioning Pancreatic Neuroendocrine Tumors. *Sci Rep* (2017) 7 (1):17506. doi: 10.1038/s41598-017-17885-y
36. Okui M, Yamamichi T, Asakawa A, Harada M, Saito M, Horio H. Prognostic Significance of Neutrophil-Lymphocyte Ratios in Large Cell Neuroendocrine Carcinoma. *Gen Thorac Cardiovasc Surg* (2017) 65(11):633–9. doi: 10.1007/s11748-017-0804-y
37. Gaitanidis A, Patel D, Nilubol N, Tirosh A, Sadowski S, Kebebew E. Markers of Systemic Inflammatory Response are Prognostic Factors in Patients With Pancreatic Neuroendocrine Tumors (PNETs): A Prospective Analysis. *Ann Surg Oncol* (2018) 25(1):122–30. doi: 10.1245/s10434-017-6241-4
38. McDermott SM, Saunders ND, Schneider EB, Strosberg D, Onesti J, Dillhoff M, et al. Neutrophil Lymphocyte Ratio and Transarterial Chemoembolization in Neuroendocrine Tumor Metastases. *J Surg Res* (2018) 232:369–75. doi: 10.1016/j.jss.2018.06.058
39. Zou J, Li Q, Kou F, Zhu Y, Lu M, Li J, et al. Prognostic Value of Inflammation-Based Markers in Advanced or Metastatic Neuroendocrine Tumours. *Curr Oncol* (2019) 26(1):e30–e8. doi: 10.3747/co.26.4135
40. Panni RZ, Lopez-Aguiar AG, Liu J, Poultsides GA, Rocha FG, Hawkins WG, et al. Association of Preoperative Monocyte-to-Lymphocyte and Neutrophil-to-Lymphocyte Ratio With Recurrence-Free and Overall Survival After Resection of Pancreatic Neuroendocrine Tumors (US-NETSG). *J Surg Oncol* (2019) 120(4):632–8. doi: 10.1002/jso.25629
41. Harimoto N, Hoshino K, Muranushi R, Hagiwara K, Yamanaka T, Ishii N, et al. Prognostic Significance of Neutrophil-Lymphocyte Ratio in Resectable Pancreatic Neuroendocrine Tumors With Special Reference to Tumor-Associated Macrophages. *Pancreatology* (2019) 19(6):897–902. doi: 10.1016/j.pan.2019.08.003
42. Pozza A, Pauletti B, Scarpa M, Ruffolo C, Bassi N, Massani M. Prognostic Role of Neutrophil-to-Lymphocyte Ratio and Platelet-to-Lymphocyte Ratio in Patients With Midgut Neuroendocrine Tumors Undergoing Resective Surgery. *Int J Colorectal Dis* (2019) 34(11):1849–56. doi: 10.1007/s00384-019-03356-5
43. Zhou B, Zhan C, Xiang J, Ding Y, Yan S. Clinical Significance of the Preoperative Main Pancreatic Duct Dilation and Neutrophil-to-Lymphocyte Ratio in Pancreatic Neuroendocrine Tumors (PNETs) of the Head After Curative Resection. *BMC Endocr Disord* (2019) 19(1):123. doi: 10.1186/s12902-019-0454-4
44. Zhou W, Kuang T, Han X, Chen W, Xu X, Lou W, et al. Prognostic Role of Lymphocyte-to-Monocyte Ratio in Pancreatic Neuroendocrine Neoplasms. *Endocr Connect* (2020) 9(4):289–98. doi: 10.1530/EC-19-0541
45. Cao LL, Lu J, Lin JX, Zheng CH, Li P, Xie JW, et al. Nomogram Based on Tumor-Associated Neutrophil-to-Lymphocyte Ratio to Predict Survival of Patients With Gastric Neuroendocrine Neoplasms. *World J Gastroenterol* (2017) 23(47):8376–86. doi: 10.3748/wjg.v23.i47.8376
46. Liu Y, Yuan Y, Li Y, Zhang J, Xiao G, Vodovotz Y, et al. Interacting Neuroendocrine and Innate and Acquired Immune Pathways Regulate Neutrophil Mobilization From Bone Marrow Following Hemorrhagic Shock. *J Immunol* (2009) 182(1):572–80. doi: 10.4049/jimmunol.182.1.572
47. Grivennikov SI, Greten FR, Karin M. Immunity, Inflammation, and Cancer. *Cell* (2010) 140(6):883–99. doi: 10.1016/j.cell.2010.01.025
48. Huang S. Regulation of Metastases by Signal Transducer and Activator of Transcription 3 Signaling Pathway: Clinical Implications. *Clin Cancer Res: Off J Am Assoc Cancer Res* (2007) 13(5):1362–6. doi: 10.1158/1078-0432.CCR-06-2313
49. Naugler WE, Karin M. NF-kappaB and Cancer-Identifying Targets and Mechanisms. *Curr Opin Genet Dev* (2008) 18(1):19–26. doi: 10.1016/j.gde.2008.01.020
50. Lin WW, Karin M. A Cytokine-Mediated Link Between Innate Immunity, Inflammation, and Cancer. *J Clin Invest* (2007) 117(5):1175–83. doi: 10.1172/JCI31537
51. Abdul M, Hoosein N. Relationship of the Interleukin-1 System With Neuroendocrine and Exocrine Markers in Human Colon Cancer Cell Lines. *Cytokine* (2002) 18(2):86–91. doi: 10.1006/cyto.2001.1019
52. Qian BF, El-Salhy M, Melgar S, Hammarstrom ML, Danielsson A. Neuroendocrine Changes in Colon of Mice With a Disrupted IL-2 Gene. *Clin Exp Immunol* (2000) 120(3):424–33. doi: 10.1046/j.1365-2249.2000.01255.x
53. Hussain F, Wang J, Ahmed R, Guest SK, Lam EW, Stamp G, et al. The Expression of IL-8 and IL-8 Receptors in Pancreatic Adenocarcinomas and Pancreatic Neuroendocrine Tumours. *Cytokine* (2010) 49(2):134–40. doi: 10.1016/j.cyto.2009.11.010
54. Tecimer T, Dlott J, Chuntharapai A, Martin AW, Peiper SC. Expression of the Chemokine Receptor CXCR2 in Normal and Neoplastic Neuroendocrine Cells. *Arch Pathol Lab Med* (2000) 124(4):520–5. doi: 10.5858/2000-124-0520-EOTCRC
55. Hilfenhaus G, Gohrig A, Pape UF, Neumann T, Jann H, Zdunek D, et al. Placental Growth Factor Supports Neuroendocrine Tumor Growth and Predicts Disease Prognosis in Patients. *Endocr Relat Cancer* (2013) 20 (3):305–19. doi: 10.1530/ERC-12-0223
56. Zhang J, Jia Z, Li Q, Wang L, Rashid A, Zhu Z, et al. Elevated Expression of Vascular Endothelial Growth Factor Correlates With Increased Angiogenesis and Decreased Progression-Free Survival Among Patients With Low-Grade Neuroendocrine Tumors. *Cancer* (2007) 109(8):1478–86. doi: 10.1002/cncr.22554
57. Sekihara K, Hishida T, Ikemura S, Saruwatari K, Morise M, Kuwata T, et al. The Association of Intravascular Stromal Cells With Prognosis in High-Grade

Neuroendocrine Carcinoma of the Lung. *J Cancer Res Clin Oncol* (2016) 142 (5):905–12. doi: 10.1007/s00432-015-2098-8
58. Cella CA, Minucci S, Spada F, Galdy S, Elgendy M, Ravenda PS, et al. Dual Inhibition of mTOR Pathway and VEGF Signalling in Neuroendocrine Neoplasms: From Bench to Bedside. *Cancer Treat Rev* (2015) 41(9):754–60. doi: 10.1016/j.ctrv.2015.06.008
59. Pavel ME, Hassler G, Baum U, Hahn EG, Lohmann T, Schuppan D. Circulating Levels of Angiogenic Cytokines can Predict Tumour Progression and Prognosis in Neuroendocrine Carcinomas. *Clin Endocrinol* (2005) 62(4):434–43. doi: 10.1111/j.1365-2265.2005.02238.x
60. Faivre S, Delbaldo C, Vera K, Robert C, Lozahic S, Lassau N, et al. Safety, Pharmacokinetic, and Antitumor Activity of SU11248, a Novel Oral Multitarget Tyrosine Kinase Inhibitor, in Patients With Cancer. *J Clin Oncol: Off J Am Soc Clin Oncol* (2006) 24(1):25–35. doi: 10.1200/JCO.2005.02.2194
61. Bello CDSE, Friece C, Smeraglia J, Sherman L, TyeC. Baum L, Meropol NJ, et al. Analysis of Circulating Biomarkers of Sunitinib Malate in Patients With Unresectable Neuroendocrine Tumors (NET): VEGF, IL-8, and Soluble VEGF Receptors 2 and 3. *J Clin Oncol* (2006) 4045(18_suppl.). doi: 10.1200/jco.2006.24.18_suppl.4045
62. Huang D, Ding Y, Zhou M, Rini BI, Petillo D, Qian CN, et al. Interleukin-8 Mediates Resistance to Antiangiogenic Agent Sunitinib in Renal Cell Carcinoma. *Cancer Res* (2010) 70(3):1063–71. doi: 10.1158/0008-5472.CAN-09-3965
63. Zurita AJ, Khajavi M, Wu HK, Tye L, Huang X, Kulke MH, et al. Circulating Cytokines and Monocyte Subpopulations as Biomarkers of Outcome and Biological Activity in Sunitinib-Treated Patients With Advanced Neuroendocrine Tumours. *Br J Cancer* (2015) 112(7):1199–205. doi: 10.1038/bjc.2015.73
64. Yao JC, Pavel M, Lombard-Bohas C, Van Cutsem E, Voi M, Brandt U, et al. Everolimus for the Treatment of Advanced Pancreatic Neuroendocrine Tumors: Overall Survival and Circulating Biomarkers From the Randomized, Phase III RADIANT-3 Study. *J Clin Oncol: Off J Am Soc Clin Oncol* (2016) 34(32):3906–13. doi: 10.1200/JCO.2016.68.0702
65. Yao JC, Phan A, Hoff PM, Chen HX, Charnsangavej C, Yeung SC, et al. Targeting Vascular Endothelial Growth Factor in Advanced Carcinoid Tumor: A Random Assignment Phase II Study of Depot Octreotide With Bevacizumab and Pegylated Interferon Alpha-2b. *J Clin Oncol: Off J Am Soc Clin Oncol* (2008) 26(8):1316–23. doi: 10.1200/JCO.2007.13.6374
66. von Marschall Z, Scholz A, Cramer T, Schafer G, Schirner M, Oberg K, et al. Effects of Interferon Alpha on Vascular Endothelial Growth Factor Gene Transcription and Tumor Angiogenesis. *J Natl Cancer Inst* (2003) 95(6):437–48. doi: 10.1093/jnci/95.6.437
67. Marques P, Barry S, Carlsen E, Collier D, Ronaldson A, Awad S, et al. Chemokines Modulate the Tumour Microenvironment in Pituitary Neuroendocrine Tumours. *Acta Neuropathol Commun* (2019) 7(1):172. doi: 10.1186/s40478-019-0830-3
68. Petreaca ML, Yao M, Liu Y, Defea K, Martins-Green M. Transactivation of Vascular Endothelial Growth Factor Receptor-2 by Interleukin-8 (IL-8/CXCL8) is Required for IL-8/CXCL8-Induced Endothelial Permeability. *Mol Biol Cell* (2007) 18(12):5014–23. doi: 10.1091/mbc.e07-01-0004
69. Smith BD, Kaufman MD, Leary CB, Turner BA, Wise SC, Ahn YM, et al. Altiratinib Inhibits Tumor Growth, Invasion, Angiogenesis, and Microenvironment-Mediated Drug Resistance *via* Balanced Inhibition of MET, TIE2, and VEGFR2. *Mol Cancer Ther* (2015) 14(9):2023–34. doi: 10.1158/1535-7163.MCT-14-1105
70. Gabrusiewicz K, Liu D, Cortes-Santiago N, Hossain MB, Conrad CA, Aldape KD, et al. Anti-Vascular Endothelial Growth Factor Therapy-Induced Glioma Invasion is Associated With Accumulation of Tie2-Expressing Monocytes. *Oncotarget* (2014) 5(8):2208–20. doi: 10.18632/oncotarget.1893
71. Harney AS, Karagiannis GS, Pignatelli J, Smith BD, Kadioglu E, Wise SC, et al. The Selective Tie2 Inhibitor Rebastinib Blocks Recruitment and Function of Tie2(Hi) Macrophages in Breast Cancer and Pancreatic Neuroendocrine Tumors. *Mol Cancer Ther* (2017) 16(11):2486–501. doi: 10.1158/1535-7163.MCT-17-0241
72. Gong J, Chehrazi-Raffle A, Reddi S, Salgia R. Development of PD-1 and PD-L1 Inhibitors as a Form of Cancer Immunotherapy: A Comprehensive Review of Registration Trials and Future Considerations. *J Immunother Cancer* (2018) 6(1):8. doi: 10.1186/s40425-018-0316-z
73. Fusi A, Festino L, Botti G, Masucci G, Melero I, Lorigan P, et al. PD-L1 Expression as a Potential Predictive Biomarker. *Lancet Oncol* (2015) 16 (13):1285–7. doi: 10.1016/S1470-2045(15)00307-1
74. Udall M, Rizzo M, Kenny J, Doherty J, Dahm S, Robbins P, et al. PD-L1 Diagnostic Tests: A Systematic Literature Review of Scoring Algorithms and Test-Validation Metrics. *Diagn Pathol* (2018) 13(1):12. doi: 10.1186/s13000-018-0689-9
75. Palla AR, Doll D. Immunotherapy in Merkel Cell Carcinoma: Role of Avelumab. *ImmunoTargets Ther* (2018) 7:15–9. doi: 10.2147/ITT.S135639
76. Saito M, Shiraishi K, Goto A, Suzuki H, Kohno T, Kono K. Development of Targeted Therapy and Immunotherapy for Treatment of Small Cell Lung Cancer. *Jpn J Clin Oncol* (2018) 48(7):603–8. doi: 10.1093/jjco/hyy068
77. Femia D, Prinzi N, Anichini A, Mortarini R, Nichetti F, Corti F, et al. Treatment of Advanced Merkel Cell Carcinoma: Current Therapeutic Options and Novel Immunotherapy Approaches. *Target Oncol* (2018) 13 (5):567–82. doi: 10.1007/s11523-018-0585-y
78. Yang S, Zhang Z, Wang Q. Emerging Therapies for Small Cell Lung Cancer. *J Hematol Oncol* (2019) 12(1):47. doi: 10.1186/s13045-019-0736-3
79. Gadgeel SM, Pennell NA, Fidler MJ, Halmos B, Bonomi P, Stevenson J, et al. Phase II Study of Maintenance Pembrolizumab in Patients With Extensive-Stage Small Cell Lung Cancer (SCLC). *J Thorac Oncol: Off Publ Int Assoc Study Lung Cancer* (2018) 13(9):1393–9. doi: 10.1016/j.jtho.2018.05.002
80. Pakkala S, Owonikoko TK. Immune Checkpoint Inhibitors in Small Cell Lung Cancer. *J Thorac Dis* (2018) 10(Suppl 3):S460–S7. doi: 10.21037/jtd.2017.12.51
81. Weber MM, Fottner C. Immune Checkpoint Inhibitors in the Treatment of Patients With Neuroendocrine Neoplasia. *Oncol Res Treat* (2018) 41(5):306–12. doi: 10.1159/000488996
82. Pavel M, Valle JW, Eriksson B, Rinke A, Caplin M, Chen J, et al. ENETS Consensus Guidelines for the Standards of Care in Neuroendocrine Neoplasms: Systemic Therapy - Biotherapy and Novel Targeted Agents. *Neuroendocrinology* (2017) 105(3):266–80. doi: 10.1159/000471880
83. Sholl LM, Aisner DL, Allen TC, Beasley MB, Borczuk AC, Cagle PT, et al. Programmed Death Ligand-1 Immunohistochemistry–A New Challenge for Pathologists: A Perspective From Members of the Pulmonary Pathology Society. *Arch Pathol Lab Med* (2016) 140(4):341–4. doi: 10.5858/arpa.2015-0506-SA
84. Fan Y, Ma K, Wang C, Ning J, Hu Y, Dong D, et al. Prognostic Value of PD-L1 and PD-1 Expression in Pulmonary Neuroendocrine Tumors. *OncoTargets Ther* (2016) 9:6075–82. doi: 10.2147/OTT.S115054
85. Kim HS, Lee JH, Nam SJ, Ock CY, Moon JW, Yoo CW, et al. Association of PD-L1 Expression With Tumor-Infiltrating Immune Cells and Mutation Burden in High-Grade Neuroendocrine Carcinoma of the Lung. *J Thorac Oncol: Off Publ Int Assoc Study Lung Cancer* (2018) 13(5):636–48. doi: 10.1016/j.jtho.2018.01.008
86. Kasajima A, Ishikawa Y, Iwata A, Steiger K, Oka N, Ishida H, et al. Inflammation and PD-L1 Expression in Pulmonary Neuroendocrine Tumors. *Endocr Relat Cancer* (2018) 25(3):339–50. doi: 10.1530/ERC-17-0427
87. Inamura K, Yokouchi Y, Kobayashi M, Ninomiya H, Sakakibara R, Nishio M, et al. Relationship of Tumor PD-L1 (CD274) Expression With Lower Mortality in Lung High-Grade Neuroendocrine Tumor. *Cancer Med* (2017) 6(10):2347–56. doi: 10.1002/cam4.1172
88. Eichhorn F, Harms A, Warth A, Muley T, Winter H, Eichhorn ME. PD-L1 Expression in Large Cell Neuroendocrine Carcinoma of the Lung. *Lung Cancer* (2018) 118:76–82. doi: 10.1016/j.lungcan.2018.02.003
89. Xu Y, Cui G, Jiang Z, Li N, Zhang X. Survival Analysis With Regard to PD-L1 and CD155 Expression in Human Small Cell Lung Cancer and a Comparison With Associated Receptors. *Oncol Lett* (2019) 17(3):2960–8. doi: 10.3892/ol.2019.9910
90. Sun C, Zhang L, Zhang W, Liu Y, Chen B, Zhao S, et al. Expression of PD-1 and PD-L1 on Tumor-Infiltrating Lymphocytes Predicts Prognosis in Patients With Small-Cell Lung Cancer. *OncoTargets Ther* (2020) 13:6475–83. doi: 10.2147/OTT.S252031
91. Wehkamp U, Stern S, Kruger S, Weichenthal M, Hauschild A, Rocken C, et al. Co-Expression of NGF and PD-L1 on Tumor-Associated Immune Cells in the Microenvironment of Merkel Cell Carcinoma. *J Cancer Res Clin Oncol* (2018) 144(7):1301–8. doi: 10.1007/s00432-018-2657-x
92. Giraldo NA, Nguyen P, Engle EL, Kaunitz GJ, Cottrell TR, Berry S, et al. Multidimensional, Quantitative Assessment of PD-1/PD-L1 Expression in

Patients With Merkel Cell Carcinoma and Association With Response to Pembrolizumab. *J Immunother Cancer* (2018) 6(1):99. doi: 10.1186/s40425-018-0404-0

93. Wang C, Yu J, Fan Y, Ma K, Ning J, Hu Y, et al. The Clinical Significance of PD-L1/PD-1 Expression in Gastroenteropancreatic Neuroendocrine Neoplasia. *Ann Clin Lab Sci* (2019) 49(4):448–56.
94. Bosch F, Bruwer K, Altendorf-Hofmann A, Auernhammer CJ, Spitzweg C, Westphalen CB, et al. Immune Checkpoint Markers in Gastroenteropancreatic Neuroendocrine Neoplasia. *Endocr Relat Cancer* (2019) 26(3):293–301. doi: 10.1530/ERC-18-0494
95. Tsuruoka K, Horinouchi H, Goto Y, Kanda S, Fujiwara Y, Nokihara H, et al. PD-L1 Expression in Neuroendocrine Tumors of the Lung. *Lung Cancer* (2017) 108:115–20. doi: 10.1016/j.lungcan.2017.03.006
96. Schultheis AM, Scheel AH, Ozretic L, George J, Thomas RK, Hagemann T, et al. PD-L1 Expression in Small Cell Neuroendocrine Carcinomas. *Eur J Cancer* (2015) 51(3):421–6. doi: 10.1016/j.ejca.2014.12.006
97. Cavalcanti E, Armentano R, Valentini AM, Chieppa M, Caruso ML. Role of PD-L1 Expression as a Biomarker for GEP Neuroendocrine Neoplasm Grading. *Cell Death Dis* (2017) 8(8):e3004. doi: 10.1038/cddis.2017.401
98. Lamarca A, Nonaka D, Breitwieser W, Ashton G, Barriuso J, McNamara MG, et al. PD-L1 Expression and Presence of TILs in Small Intestinal Neuroendocrine Tumours. *Oncotarget* (2018) 9(19):14922–38. doi: 10.18632/oncotarget.24464

Conflict of Interest: The authors declare that the research was conducted in the absence of any commercial or financial relationships that could be construed as a potential conflict of interest.

GLOSSARY

bFGF	basic fibroblast growth factor
CAFs	cancer-associated fibroblasts
CEA	carcinoembryonic antigen
CgA	chromogranin A
DFS	disease-free survival
EVE	everolimus
g-NENs	gastric neuroendocrine neoplasms
g-NEC	gastric neuroendocrine carcinoma
g-MANEC	gastric mixed adenoneuroendocrine carcinoma
GEP	gastroenteropancreatic
HG-NEC	high-grade neuroendocrine carcinomas
HR	hazard ratio
ICIs	Immune Checkpoint Inhibitors
IL-1β	Interleukin 1 beta
IL-2	Interleukin 2
IL-6	Interleukin 6
IL-8	Interleukin 8
IL-10	Interleukin 10
IL-17	Interleukin 17
IL-18	Interleukin 18
IHC	immunohistochemistry
ITGB1	Integrin Subunit Beta 1
LCNEC	large cell neuroendocrine lung carcinomas
MMP-9	matrix metallopeptidase-9
NECs	neuroendocrine carcinomas
NENs	neuroendocrine neoplasms
NETs	neuroendocrine tumors
NF-κb	nuclear factor kappa-light-chain-enhancer of activated B cells
NLR	neutrophil-lymphocyte ratio
NSCLC	non-small cell lung carcinomas
NGF	nerve growth factor
NSE	Neuron-specific enolase
OS	overall survival
pNENs	pancreatic NENs
PNETs	pancreatic NETs
PlGF	Placental Growth Factor
PD-1	programmed cell death protein 1 receptor
PD-L1	programmed death-ligand 1
PDGF	platelet-derived growth factor
PFS	progression-free survival
PLR	platelet-lymphocyte ratio
PRRT	Peptide receptor radionuclide therapy
SCLC	small cell lung carcinomas
SSA	somatostatin analogues inhibitors
STAT3	signal transducer and activator of transcription 3
SDF-1a	stromal cell-derived factor-1
SUN	sunitinib
RCC	renal clear-cell carcinomas
RFS	relapse free survival
TANs	tumor-associated neutrophils
TACE	transarterial chemoembolization
TEMs	Tie2-expressing monocytes/macrophages
TGF-β	Transforming growth factor beta
TILs	tumor-infiltrating immune cells
TMB	tumor mutational burden
TNF-α	tumor necrosis factor
TRAIL	TNF-related apoptosis-inducing ligand
TRKA	tropomyosin receptor kinase A
VEGF	vascular endothelial growth factor

frontiers in Endocrinology

ORIGINAL RESEARCH
published: 12 August 2021
doi: 10.3389/fendo.2021.712107

FGF-Receptors and PD-L1 in Anaplastic and Poorly Differentiated Thyroid Cancer: Evaluation of the Preclinical Rationale

*Pia Adam[1], Stefan Kircher[2,3], Iuliu Sbiera[1], Viktoria Florentine Koehler[4,5], Elke Berg[4], Thomas Knösel[6], Benjamin Sandner[7], Wiebke Kristin Fenske[7,8], Hendrik Bläker[9], Constantin Smaxwil[10], Andreas Zielke[10], Bence Sipos[11], Stephanie Allelein[12], Matthias Schott[12], Christine Dierks[13], Christine Spitzweg[4], Martin Fassnacht[1,3] and Matthias Kroiss[1,3,4]*on behalf of the German Study Group for Rare Malignant Tumors of the Thyroid and Parathyroid Glands*

[1] Department of Internal Medicine I, Division of Endocrinology/Diabetology, University of Würzburg, Würzburg, Germany, [2] Institute of Pathology Würzburg, University of Würzburg, Würzburg, Germany, [3] Comprehensive Cancer Center Mainfranken, University of Würzburg, Würzburg, Germany, [4] Department of Internal Medicine IV, University Hospital of Munich, LMU Munich, Munich, Germany, [5] Department of Medicine I, Goethe University Hospital, Frankfurt, Germany, [6] Institute of Pathology LMU, University Hospital of Munich, LMU Munich, Munich, Germany, [7] Department of Internal Medicine III, University Hospital of Leipzig, Leipzig, Germany, [8] Department of Internal Medicine I, Division of Endocrinology/Diabetology, University of Bonn, Bonn, Germany, [9] Institute of Pathology Leipzig, University Hospital of Leipzig, Leipzig, Germany, [10] Department of Endocrine Surgery, Diakonie-Klinikum Stuttgart, Stuttgart, Germany, [11] Medical Oncology and Pulmonology, University Hospital, Tübingen, Germany, [12] Division for Specific Endocrinology, Medical Faculty, University of Düsseldorf, Düsseldorf, Germany, [13] Department of Internal Medicine IV, Division of Oncology and Hematology, University of Halle (Saale), Halle (Saale), Germany

Background: Treatment options for poorly differentiated (PDTC) and anaplastic (ATC) thyroid carcinoma are unsatisfactory and prognosis is generally poor. Lenvatinib (LEN), a multi-tyrosine kinase inhibitor targeting fibroblast growth factor receptors (FGFR) 1-4 is approved for advanced radioiodine refractory thyroid carcinoma, but response to single agent is poor in ATC. Recent reports of combining LEN with PD-1 inhibitor pembrolizumab (PEM) are promising.

Materials and Methods: Primary ATC (n=93) and PDTC (n=47) tissue samples diagnosed 1997-2019 at five German tertiary care centers were assessed for PD-L1 expression by immunohistochemistry using Tumor Proportion Score (TPS). FGFR 1-4 mRNA was quantified in 31 ATC and 14 PDTC with RNAscope *in-situ* hybridization. Normal thyroid tissue (NT) and papillary thyroid carcinoma (PTC) served as controls. Disease specific survival (DSS) was the primary outcome variable.

Results: PD-L1 TPS≥50% was observed in 42% of ATC and 26% of PDTC specimens. Mean PD-L1 expression was significantly higher in ATC (TPS 30%) than in PDTC (5%; $p<0.01$) and NT (0%, $p<0.001$). 53% of PDTC samples had PD-L1 expression ≤5%. FGFR mRNA expression was generally low in all samples but combined FGFR1-4 expression was significantly higher in PDTC and ATC compared to NT (each $p<0.001$). No impact of PD-L1 and FGFR 1-4 expression was observed on DSS.

OPEN ACCESS

Edited by:
Antongiulio Faggiano, Sapienza University of Rome, Italy

Reviewed by:
Franco Fulciniti, Istituto cantonale di patologia, Switzerland
Vincenzo Marotta, Istituto Nazionale Tumori Fondazione G. Pascale (IRCCS), Italy

***Correspondence:**
Matthias Kroiss
Matthias.kroiss@med.lmu.de

Specialty section:
This article was submitted to Cancer Endocrinology, a section of the journal Frontiers in Endocrinology

Received: *19 May 2021*
Accepted: *26 July 2021*
Published: *12 August 2021*

Citation:
Adam P, Kircher S, Sbiera I, Koehler VF, Berg E, Knösel T, Sandner B, Fenske WK, Bläker H, Smaxwil C, Zielke A, Sipos B, Allelein S, Schott M, Dierks C, Spitzweg C, Fassnacht M and Kroiss M (2021) FGF-Receptors and PD-L1 in Anaplastic and Poorly Differentiated Thyroid Cancer: Evaluation of the Preclinical Rationale. Front. Endocrinol. 12:712107. doi: 10.3389/fendo.2021.712107

Conclusion: High tumoral expression of PD-L1 in a large proportion of ATCs and a subgroup of PDTCs provides a rationale for immune checkpoint inhibition. FGFR expression is low thyroid tumor cells. The clinically observed synergism of PEM with LEN may be caused by immune modulation.

Keywords: tyrosine kinase inhibitor (TKI), immune checkpoint inhibitor (ICI), immunohistochemistry, immunotherapy, PD-L1, FGFR

INTRODUCTION

Anaplastic (ATC) and poorly differentiated thyroid carcinoma (PDTC) are orphan diseases which account for 1-2% and 2-15% % among all thyroid malignancies (1, 2). While treatment of DTC is well established and 5-year survival rates are above 90% (3), the management of PDTC and ATC is unsatisfactory and prognosis generally poor with a median overall survival of only six months for ATC patients (4, 5). Current guidelines recommend surgery in ATC cases (stage IVA and IVB) and a careful evaluation of surgical options in stage IVC cases (6). Surgery can be followed by additive chemoradiation therapy to improve locoregional control and overall outcome (7, 8). Nonsurgical treatment options include chemotherapy, palliative radiotherapy, systemic therapy or best supportive care (6). The combination of BRAF inhibitor dabrafenib and MEK inhibitor trametinib for BRAF V600E-mutated ATC poses a recent breakthrough with an overall response rate of 69% (9, 10). For stage IVC non-BRAF V600E-mutated cases guidelines recommend evaluation of PD-L1 status and treatment with checkpoint inhibitors as an alternative to chemotherapy and/or radiation (6). The prognosis of PDTC is more favorable with a 5-year survival rate of 66% because some PDTC are accessible to radioiodine treatment (11, 12). Secondary resistance to radioiodine therapy limit a curative approach in advanced cases (13). Lenvatinib (LEN) is a multi-tyrosine kinase inhibitor (TKI) of VEGFR1-3, FGFR1-4, PDGFR-α, RET and c-kit and approved for the treatment of progressive radioiodine refractory DTC and radioiodine refractory PDTC (14). Nevertheless, important practical issues in the use of tyrosine kinase inhibitors are still unsolved (15, 16).

In an observational study Iwasaki et al. compared treatment with LEN (n=16) and palliative therapy (n=16) in 32 stage IVC ATC patients. The median overall survival (OS) time of patients treated with LEN was 4.2 months while patients receiving palliative therapy had a median overall survival of only 2.0 months (17). In a very recent study of post-marketing registry data, LEN showed an objective response in 44% of ATC patients which was, however, short-lived with a median overall survival of 101 days (18).

Although many of the TKIs currently used in the treatment of thyroid carcinomas refractory to radioiodine share common, e.g., antiangiogenetic TKI activity it has been speculated that the superior clinical response of LEN in these rare thyroid carcinomas may be attributable to its ability to also target FGFR 1-4 (19).

A study that used immunohistochemistry to investigate FGFR4 expression in 12 ATC patients suggested that FGFR4 expression may predict response to LEN (20).

The immune checkpoint inhibitor (ICI) pembrolizumab (PEM) is a programmed death 1 (PD-1) inhibitor approved for numerous types of cancer such as non-small cell lung carcinoma (NSCLC), renal cell carcinoma (RCC), hepatocellular carcinoma (HCC) and head and neck squamous cell cancer (HNSCC) (21–24). Tumoral tissue expression of its ligand PD-L1 as assessed by immunohistochemistry has been proposed as a biomarker and for some tumor entities disease-specific cut-offs have been suggested (25). As part of a phase I/II study 42 ATC patients were treated with PD-1 inhibitor spartalizumab and showed higher response rates in PD-L1-positive versus PD-L1 negative ATC patients with highest rate of response in patients with PD-L1 ≥ 50% (26). In ATC, a phase II trial of single agent PEM or a combination with chemoradiotherapy was prematurely terminated due to rapid fatal outcome in the three patients investigated (27). Trials in multiple disease entities are ongoing including a trial in patients with radioiodine refractory thyroid carcinoma without prior TKI treatment from which preliminary positive results have been reported (NCT02973997).

Addition of PEM after prior failure to TKI therapy with LEN, dabrafenib alone or in combination with trametinib has been reported in a retrospective single center study. Partial response (PR) was seen in 43% but with a very short median PFS of 3 months and a median overall survival (OS) of 7 months only (8). In a recent series of metastatic ATC and PDTC negative for the BRAF V600E mutation, 8 patients received a combination therapy of LEN and PEM for a maximum of 40 months after failing chemotherapy, radiation or radioiodine therapy. The combination treatment was not only well tolerated with 50% (3/6) of ATC patients still on therapy at data cutoff but also led to complete response (CR) in 66% (4/6) of ATC patients after 7, 10 and 12 months and PR in 75% of patients after three to four months of treatment (28). Range of PD-L1 expression was 1%-90% and patients with a PD-L1 expression greater than 50% (5/8) responded best to combination therapy (28). There was no association of PD-1 expression or frequency of tumor infiltrating lymphocytes (TILs) with treatment response (28).

The primary aim of this study is to evaluate a potential molecular rationale for a treatment of ATC and PDTC patients with lenvatinib, pembrolizumab or a combination of both. Secondary aims were the investigation of FGFR and PD-L1 expression as prognostic markers and potential marker of treatment response. As an exploratory aim, we describe the

clinical benefit of patients treated with these substances as a monotherapy or in a combined regimen.

MATERIALS AND METHODS

Setting

This study was conducted as part of the German Study Group for rare malignant tumors of the thyroid and parathyroid glands. The study was approved by the ethics committee of the University of Würzburg (96/13) and subsequently by the ethics committees of all participating centers. All patients provided written informed consent. Prospectively and retrospectively collected data and formalin-fixed paraffin embedded (FFPE) tissue samples of patients diagnosed with ATC and PDTC between 1997 and 2019 were obtained from five German tertiary care centers.

Samples and Data Acquisition

Adult patients with local diagnosis of ATC or PDTC at histopathologic examination of sections or biopsy of the primary tumor were eligible. Archival anonymized papillary thyroid carcinoma (PTC) and normal thyroid (NT) tissue from the institute of pathology, University of Würzburg, served as control.

Clinical data such as the date of diagnosis, tumor stage at initial diagnosis, treatments including surgical interventions, radioiodine treatment and systemic therapies (e.g., cytotoxic chemotherapy, radiotherapy, TKI- and/or ICI-therapy), metastatic sites and number of treatment lines, were recorded by trained personnel at all sites. Tumor stage was recorded according to UICC classification (TNM Classification of Malignant Tumours, 8th edition, 2017) and determined for PDTC and ATC respectively.

Study endpoints were disease-related death or time interval from diagnosis to last follow-up alive. Treatment and follow-up of patients was done according to standard of care at participating centers.

Histopathological Review

The diagnosis of ATC and PDTC in archival FFPE tissue samples (n=140) was verified by a single endocrine pathologist (SK). According to the current WHO Classification of Tumours of Endocrine organs (4th edition, volume 10, 2017).

Immunohistochemistry

All specimens were processed by immunohistochemistry and RNAscope® *in situ* hybridization within two weeks after sectioning. Full FFPE sections of primary tumor tissue (n=93 ATC; n=47 PDTC) mounted on slides were deparaffinized, rehydrated and antigen retrieval was performed in target retrieval solution (Target Retrieval Solution, Citrate pH 6.1 [10x], Dako, CA, USA; 1:10 dilution) under pressure for 4 minutes. Following deparaffinization, steps were carried out with a Freedom EVO 200 base unit (TECAN Trading AG, Switzerland). Tissue sections were incubated with primary antibody (PD-L1 [28-8] rabbit monoclonal antibody 438R-15-ASR; Cell Marque, CA, USA; 1:100 dilution; Antibody Diluent, Dako REAL) for 1h at RT. Signal amplification was achieved by the HRP Kit (HPR HiDef 2-Step Polymer Detection Kit, medac GmbH, Germany) for 40 min and developed for 10 min with Histofine (Histofine DAB-2V, Nichirei Biosciences Inc., Japan). Nuclei were counterstained using Mayer's hematoxylin for 3 min and blued for 10 min in running tap water. Following dehydration, slides were mounted by a Tissue-Tek (Sakura Finetek, Inc., CA, USA).

RNAscope *In Situ* Hybridization

Given the limited reliability of immunohistochemistry for FGFRs due to their high degree of homology, RNAscope was used to study expression of FGFR 1-4. Tumor samples (ATC: n=31; PDTC: n=14) were cut to 2-µm thickness, deparaffinized in xylene, and rehydrated in a graded alcohol series. Fixation, permeabilization and protease digestion were achieved by treatment with hydrogen peroxide (322335, Advanced Cell Diagnostics [ACDbio], CA, USA) at RT for 10 min, target retrieval reagent (322000, ACDbio) under pressure for 15 min and protease plus (322331, ACDbio) at 40°C for 20 min. FGFR 1-4 probes (Hs-FGFR1, 310071; Hs-FGFR2, 311171; Hs-FGFR3, 310791; Hs-FGFR4-CD5, 412301, ACDbio) were then hybridized at 40°C for 2h. Slides were treated with Amplifier 1 (322311, ACDbio) and Amplifier 3 (22313, ACDbio) at 40°C for 45 min, with Amplifier 2 (322312, ACDbio) and Amplifier 4 (322314, ACDbio) at 40°C for 20 min, and with Amplifier 5 (322315, ACDbio) for 1h and Amplifier 6 (322316, ACDbio) for 20 min at RT. In between the amplification steps, slides were washed in wash buffer (310091, ACDbio) for 4 min, each. Equal volumes of DAB-A (DAB-A, 320052, ACDbio) and DAB-B (DAB-B, 320053, ACDbio) were mixed and pipetted on the slides. After incubation at RT for 10 minutes slides were put in hematoxylin, dehydrated and mounted.

Semi-Quantitative Analysis of PD-L1 and FGFR 1-4 Expression

PD-L1 slides were visually scored using an AxioScope.A1 microscope (Carl Zeiss AG, Germany). PD-L1 expression was evaluated using a semi-quantitative scoring system based on the proportion of stained tumor cells according to Tumor Proportion Score (TPS).

FGFR1-4 images were assessed with Aperio VERSA microscope (Leica Biosystems, Germany). Manual counting of cell nuclei and RNA was performed with ImageJ-win64 (Fiji, GitHub enterprise, CA, USA), and quantified as the number of FGFR 1-4 mRNA per cell.

Statistical Analysis

DSS from diagnosis was estimated using the Kaplan-Meier method and groups were compared by the log-rank test. For data with non-normal distribution we used Mann-Whitney

U test. Kruskal-Wallis test was used for comparison among groups for non-nominal distributed variables. Assessment of risk factors was performed by using the Cox proportional hazard regression model (forward and backward step-up regression). P values <0.05 were considered statistically significant. Statistical analyses were performed with SPSS Version 26 (IBM, Chicago, IL, USA). GraphPad Prism 7.0 (GraphPad Software, San Diego, CA, USA) and Microsoft Office Excel 2010 were used for graphical presentation and additional analyses.

RESULTS

Clinical Characteristics

93 patients (40 male, 53 female) with histological evidence of ATC and 47 patients (17 male, 30 female) with poorly differentiated thyroid carcinoma treated at five German tertiary care centers were included. Baseline clinical characteristics of the study population are shown in **Table 1**. In brief, median age at primary diagnosis of ATC patients was 69 years (range 29-95) and 63 years (range 16-86) for patients with PDTC. At the time of initial diagnosis 47 patients with ATC (51%) and 13 patients with PDTC (28%) had local regional lymph node metastases. Disease was restricted to the thyroid gland (stage IVA) at diagnosis in one single ATC patient whereas 52% had distant metastasis (stage IVC). 15 PDTC patients had distant metastases at first diagnosis, four of whom were <55 years (UICC stage II) and 11 aged ≥55 years (UICC stage IVB).

Expression of PD-L1 in ATC and PDTC

The proportion of PD-L1 expression in tumor cells differed widely both in ATC and PDTC samples (**Figure 1**) and was heterogeneous within samples which is accounted for in the semiquantitative TPS. Median PD-L1 TPS was 30% (range 0-95) in ATC (n=93) compared to 5% (range 0-95) in PDTC (n=47, p<0.01, **Figure 2**) and was significantly higher in ATC (p<0.0001) and PDTC (p<0.001) compared to normal thyroid tissue samples (n=30). 39 (42%) of ATC samples and 12 (26%) of PDTC specimens expressed PD-L1 in ≥50% of tumor cells, while none of the PTC samples showed PD-L1 TPS of ≥50%. 27% of ATC samples and 53% of PDTC samples had PD-L1 TPS ≤5%. PD-L1 expression could not be detected in normal thyroid tissue (n=30). Differentiated PTC specimens (n=21) showed median PD-L1 expression of 10% (range 0-30).

Expression of FGFR 1-4 in ATC and PDTC

Expression of FGFR mRNA was generally low in all investigated samples (**Figure 3**). Median expression of FGFR 1 was 1.06 (range 0.16-5.42) mRNA/cell for ATC (n=31) tissue, 0.81 (range 0.18-1.87) mRNA/cell for PDTC (n=14) specimens, and 0.5 (range 0.15-0.97) mRNA/cell for PTC (n=5) tissue (**Figure 4**). Data on FGFR 2 and 3 are shown in **Table 2**. FGFR 4 exhibited the lowest median expression in all types of thyroid carcinoma (ATC: 0.14 mRNA/cell; PDTC: 0.24 mRNA/cell; PTC: 0.08 mRNA/cell). In comparison to normal thyroid tissue, panFGFR expression (sum of FGFR1–4) was significantly higher in ATC (p<0.001) and PDTC (p<0.0001) tissue (**Figure 4**). Median panFGFR expression was 2 mRNAs/cell in ATC and 3 mRNAs/cell in PDTC tissue. Normal thyroid tissue (n=8) expressed FGFR 1-4 at lowest levels with median expression of 0.0 mRNA/cell, respectively. FGFR 1-4 expression was not significantly different between ATC/PDTC and PTC tissue specimens.

Disease-Specific Survival and Tumor-Specific Therapy

83 patients (89%) died due to ATC, 3 (3%) patients with ATC deceased due to causes other than ATC and 7 (8%) patients were still alive at last follow-up. 14 PDTC patients (30%) died from advanced PDTC. In 2 PDTC patients the cause of death was unknown and 31 (66%) were still alive at last follow-up. In 4 (4%) ATC and 4 (9%) PDTC patients, there was no evidence of disease at last follow-up indicating complete remission. Median overall survival was 6.4 months for patients diagnosed with ATC and

TABLE 1 | Patient characteristics of the study cohort.

Patient characteristics	No. of patients ATC (%)	No. of patients PDTC (%)
Number of patients	93	47
Male sex	40 (43)	17 (36)
Median age at diagnosis (range), in years	69 (29-95)	63 (16-86)
Median size of primary tumor (range), in mm	55 (8-105)	46.5 (12-95)
Not reported	18 (19)	5 (11)
Initial tumor stage		
T		
pT1	1 (1)	2 (4)
pT2	1 (1)	10 (21)
pT3	11 (12)	24 (51)
pT4	78 (84)	10 (21)
pTx	2 (2)	1 (2)
N		
pN0	19 (20)	19 (40)
pN1	47 (51)	13 (28)
pNx	27 (29)	15 (32)
M		
cM0	32 (34)	26 (55)
cM1	48 (52)	15 (32)
cMx	13 (14)	6 (13)
UICC		
I	–	13 (28)
II	–	17 (36)
III	–	3 (6)
IVA	1 (1)	2 (4)
IVB	41 (44)	11 (23)
IVC	48 (52)	–
Not available	3 (3)	1 (2)
Sites of metastases at baseline		
local regional lymph nodes	47 (51)	13 (28)
mediastinal lymph nodes	11 (12)	0 (0)
lung	41 (44)	13 (28)
liver	5 (5)	0 (0)
bone	9 (10)	3 (6)
pleura	2 (2)	3 (6)
heart	1 (1)	0 (0)
adrenal gland	1 (1)	0 (0)
thymus	0 (0)	1 (2)
brain	0 (0)	0 (0)

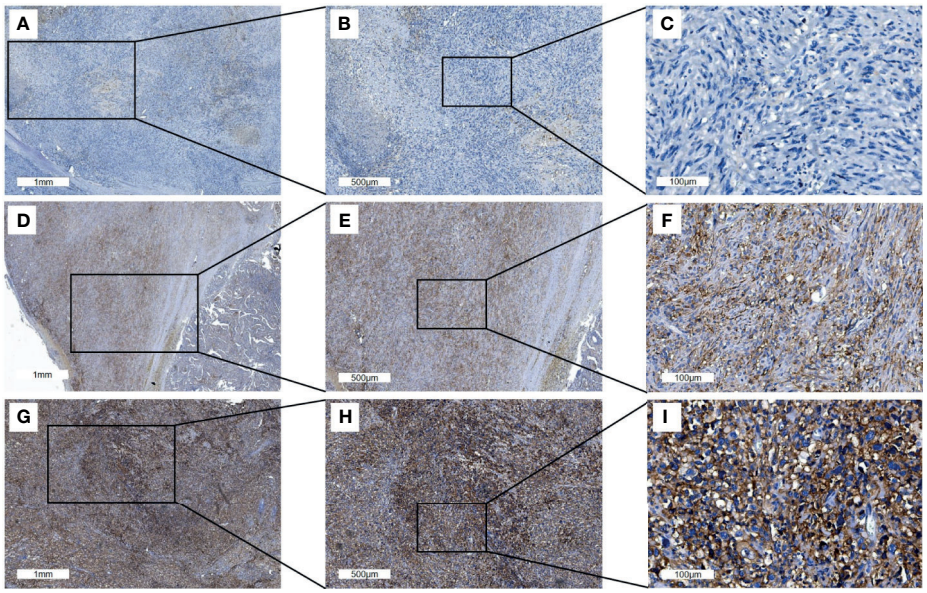

FIGURE 1 | Representative PD-L1 immunohistochemistry staining of full ATC FFPE sections. Three different tissue samples stained with PD-L1 antibody are shown with an overview of the tissue sample (**A, D, G**; scale bars: 1mm), at 2x magnification (**B, E, H**; scale bars: 500µm) and 10x magnification (**C, F, I**; scale bars: 100µm). The PD-L1 TPS in **(A–C)** is 1% and 50% in D-F while 95% in **(G–I)**.

29.1 months for patients diagnosed with PDTC. Disease-specific survival was 5.4 (ATC) and 24.0 months (PDTC) in a median follow-up of 6 (ATC) and 28 (PDTC) months.

Therapy With TKI and/or ICI

Tumor-specific therapy was consistent with previous publications on ATC (4) and is summarized in **Table 3**. Targeted therapies with tyrosine kinase inhibitors (TKI) and/or immune checkpoint inhibitors (ICI) were administered in 15 (16%) of ATC and 13 (28%) of PDTC patients. Patients were treated with LEN (n=3 ATC, n=9 PDTC), PEM (n=2 ATC, n=1 PDTC), LEN + PEM (n=1 ATC, n=2 PDTC) and other TKIs (n=10 ATC; n=8 PDTC). Two PDTC patients received three different lines of targeted therapy, another two PDTC patients were treated with two different TKIs (LEN followed by sorafenib and LEN followed by cabozantinib), and one ATC and one PDTC patient received two lines of targeted therapy.

ATC patient #1 (TPS: 10%, panFGFR expression: 2.8 mRNA/cell) patient received LEN (dose varying from 8 mg to 14 mg) after failure of RCT with partial remission (PR) as best overall response (BOR). LEN monotherapy was followed by LEN and PEM combination therapy (doses 4 mg and 200 mg respectively) with stable disease (SD) as BOR (PFS until after last-follow-up: 9.9 months).

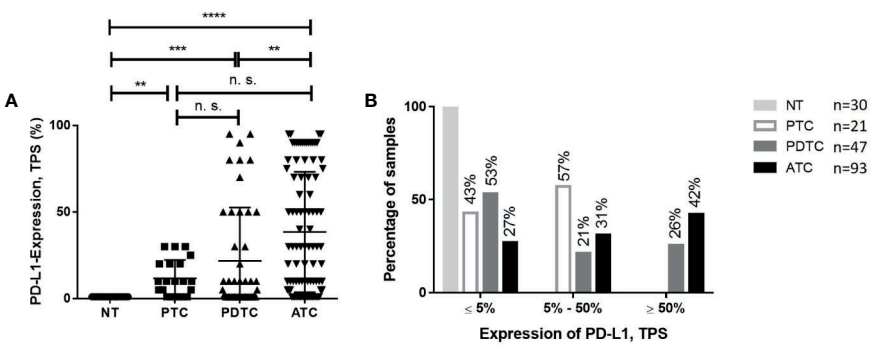

FIGURE 2 | Comparison of PD-L1 expression in ATC or PDTC and PTC or NT. **(A)** PD-L1 expression as assessed by TPS was significantly higher in ATC compared to PDTC and tumor specimens compared to normal thyroid (NT). No significant differences (n. s. = not significant) could be observed in ATC and PTC and PDTC and PTC. **(B)** Proportion of PD-L1 TPS categories in PDTC and ATC. 42% of ATC and 26% of PDTC specimen show PD-L1 TPS ≥50%. **p < 0.01, ***p < 0.001, ****p < 0.0001.

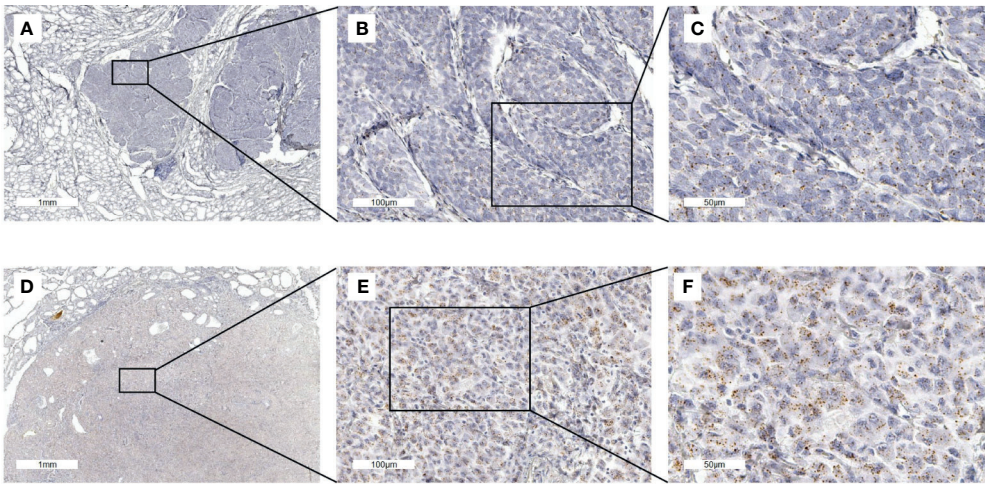

FIGURE 3 | FGFR1 mRNA *in situ* hybridization staining of full ATC and PDTC FFPE sections. **(A–C)** FGFR1 RNAscope *in situ* hybridization in a PDTC tissue sample. FGFR1 expression is 1.9 mRNA/nucleus. **(D–F)** FGFR1 expression in an ATC tissue sample (5.4 mRNA/nucleus).

ATC patient #2 (TPS: 10%) experienced SD by PEM monotherapy (dose: 200 mg every 3 weeks) with a PFS of 22.4 months. PEM treatment was followed by a combination of paclitaxel (80mg every week) and PEM for 3.0 months. The patient deceased one month after termination of treatment.

ATC patient #3 (TPS: 1%, panFGFR expression: 1.0 mRNA/cell) consecutively received LEN and PEM as single agents each with PD as BOR. The PFS for LEN and PEM treatment was 1.7 and 2.3 months, respectively.

In a fourth ATC patient (TPS: 95%, panFGFR expression: 3.1 mRNA/cell), treatment with LEN and PEM was started after failure of RCT five days before the patient deceased and hence is considered unevaluable.

ATC patient #5 (TPS: 70%, panFGFR expression: 1.0 mRNA/cell) received LEN (dose:24 mg) after failure of RCT with a PFS of 4.4 months with PD as BOR.

PDTC patient #6 (TPS: 50%, panFGFR expression not available) who was radioiodine refractory at diagnosis received LEN combined to PEM as first line treatment. Best response was SD and the patient received this combination for 21.5 months until progression occurred. Treatment was then switched to LEN and everolimus.

PDTC patient #7 (TPS: 30%, panFGFR expression 2.83 mRNA/cell) was treated with LEN, best response was SD and PFS 13.7 months. Everolimus was added to the therapy which resulted in SD for 9.7 months. Later, PEM was added to everolimus and LEN with PD after 1.8 months. The patient was still alive at last follow-up.

In a third (#8) PDTC patient (TPS: 90%, panFGFR expression not available) treatment was started with PEM as part of a clinical trial (Keynote 158) and discontinued 4 months later due to PD. Outside of the study, the patient received LEN and is

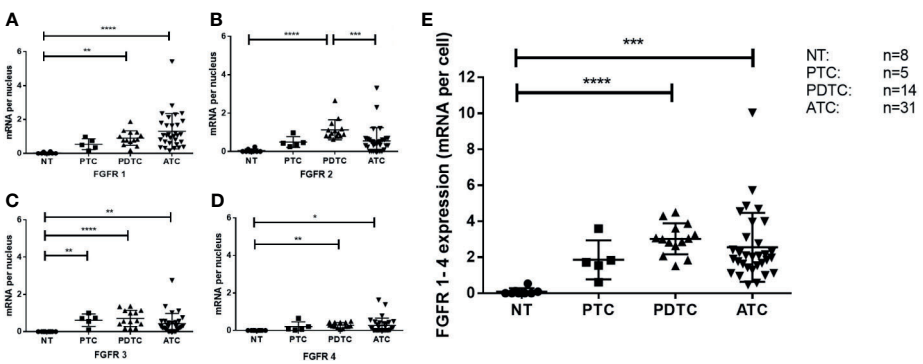

FIGURE 4 | FGFR expression in ATC, PDTC, PTC and NT. FGFR1 **(A)**, FGFR2 **(B)**, FGFR3 **(C)** and FGFR4 **(D)** was detected at low levels in all samples studied. Significant differences are indicated. Combined scoring of FGFR1-4 expression in ATC and PDTC **(E)** is significantly higher compared to normal thyroid (NT) tissue. *p < 0.1, **p < 0.01, ***p < 0.001, ****p < 0.0001.

TABLE 2 | Median expression of FGFR 1-4 in ATC, PDTC and PTC.

FGFR expression (mRNA/cell)	ATC (n=31)		PDTC (n=14)	PTC (n=8)	*P* (Kruskal-Wallis)
FGFR 1 (range)	1.06 (0.16-5.32)		0.81 (0.18-1.87)	0.5 (0.15-0.97)	0.079
P (Kruskal-Wallis*)		*P*=1.0			
FGFR 2 (range)	0.38 (0.0-3.3)		0.96 (0.64-2.65)	0.43 (0.25-0.97)	**<0.0001**
P (Kruskal-Wallis*)		***P*=0.001**			
FGFR 3 (range)	0.31 (0.0-2.75)		0.58 (0.14-1.36)	0.71 (0.09-1.0)	**0.042**
P (Kruskal-Wallis*)		*P*=0.168			
FGFR 4 (range)	0.14 (0.0-1.62)		0.24 (0.06-0.49)	0.08 (0.02-0.65)	0.169
P (Kruskal-Wallis*)		*P*=0.296			
panFGFR (range)	2.03 (0.47-10.03)		3.02 (1.52-4.5)	1.72 (0.61-3.6)	0.058
P (Kruskal-Wallis*)		*P*=0.532			

**p-values of Bonferroni testing for pairwise comparisons between ATC and PDTC are indicated.*

TABLE 3 | Therapeutic regimens in patients with ATC or PDTC.

Therapeutic regimen	No. of patients ATC (%)	No. of patients PDTC (%)
Primary surgery		
One-stage thyroidectomy	39 (42)	21 (45)
Two-stage thyroidectomy	7 (8)	12 (26)
Hemithyroidectomy	21 (23)	9 (19)
debulking surgery	13 (14)	0 (0)
biopsy	8 (9)	0 (0)
only explorative surgery	5 (5)	3 (6)
Not reported	0 (0)	2 (4)
Resection status		
R0	11 (12)	25 (53)
R1	37 (40)	10 (21)
R2	34 (37)	2 (4)
Rx	11 (12)	10 (21)
Radioiodine treatment (RIT)	6 (7)	36 (77)
Median number of RIT (range)	1 (1-1)	1 (1-11)
Median cum. Dose (GBq) (range)	3.36 (2.7-7.4)	6.65 (1.2-74.2)
Dose not available	1 (1)	0 (0)
Radiochemotherapy (RCT)	38 (42)	4 (9)
not available	2 (2)	0 (0)
External beam radiation		
Neck region	79 (85)	16 (34)
Local palliative	52 (56)	7 (15)
Median cum. Dose (Gy) (range)	55.0 (4-105.6)	60.5 (50.4-120)
Dose not available	6 (7)	1 (2)
Distant metastases	17 (18)	12 (26)
Chemotherapy*	48 (53)	6 (13)
Not reported	2 (2)	0 (0)
Doxorubicin weekly	10 (11)	1 (2)
Paclitaxel weekly	8 (9)	0 (0)
Cisplatin	3 (3)	0 (0)
Paclitaxel + carboplatin	22 (24)	5 (11)
Paclitaxel + pemetrexed	6 (7)	2 (4)
Doxorubicin based*	10 (11)	0 (0)
Other	4 (0)	0 (0)
unknown	2 (2)	0 (0)
More than one chemotherapeutic regimen	13 (14)	2 (4)
Tyrosine kinase inhibitor (TKI) and/or immune checkpoint inhibitor (ICI) therapy	15 (16)	13 (28)
Lenvatinib	3 (3)	9 (19)
Pembrolizumab	2 (2)	1 (2)
Lenvatinib + pembrolizumab	1 (1)	2 (4)
Other#	10 (11)	8 (17)
more than one therapy	1 (1)	5 (11)

**Chemotherapy other than monotherapy with doxorubicin weekly.*
**Vemurafenib, Sunitinib, Cabozantinib, Pazopanib, Imatinib, Nivolumab.*

still alive with SD as BOR after data cut-off (PFS until after last follow-up: 38.6 months).

PDTC patient #9 (TPS: 50%, panFGFR expression: 3.1 mRNA/cell) first received LEN (dose: 10 mg) with PR as BOR and PFS of 7.6 months followed by sorafenib (400 mg) for 3.0 months. Treatment was continued with LEN and PEM combination therapy with PR as BOR and a PFS of 6.6 months. Later the patient continued treatment with PEM monotherapy for 2.8 months.

PDTC patient #10 (TPS: 1%, panFGFR expression: 2.6 mRNA/cell) first received LEN (max. dose: 20 mg) with mixed response (MR) as BOR. Treatment was terminated due to adverse events with PFS of 5.7 months. LEN treatment was then followed by sorafenib (dose: 800 mg) for 1.7 months which was followed by chemotherapy.

Primary LEN monotherapy (max. dose: 14 mg) was also administered to PDTC patient #11 (TPS: 1%, panFGFR expression: 4.5 mRNA/cell) for 26.1 months. PEM was added shortly after imaging showed PD, but the patient deceased one month later.

The PFS and treatment response of the different patients treated with PEM alone in combination with LEN is depicted in **Figure 5**. Patients with moderate or high expression showed longer PFS.

Four additional PDTC patients were treated with LEN monotherapy. One patient (TPS: 5%, panFGFR expression: 2.1 mRNA/cell) received LEN 24 mg (PFS: 10.5 months) with SD followed by cabozantinib. Another patient (TPS: 80%) received LEN (max. dose: 24 mg) after RCT treatment, but deceased one month after initiation. A third patient (TPS: 10%) was treated with LEN for 8.9 months and died 8 days later and a fourth patient (TPS: 10%) received LEN (max. dose: 24 mg) for 19.7 months at last follow-up after data cut-off and is still alive with SD.

Prognostic Factors of Disease Specific Survival in ATC and PDTC

The association of clinical factors with DSS in ATC and PDTC is summarized in **Table 4**, respectively. In PDTC where prognostic factors are ill described, UICC stage I, II or III compared to IV, and use of RIT were associated with a significantly longer DSS. Treatment with external beam radiation therapy (EBRT) or

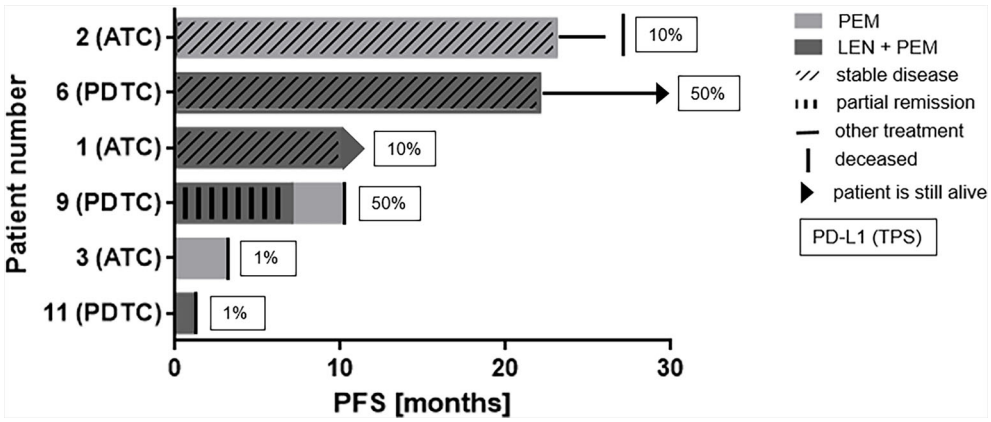

FIGURE 5 | Swim lane plot demonstrating PFS on PEM or the combination of LEN and PEM: Figure shows data before and after data cut-off. Patients 6 and 1 are still alive with patient 1 still receiving LEN + PEM. Exact date of progress or exact treatment duration was not reported because PD was always followed by change of therapeutic regimen or death. Progressive disease was the best response in patients 9 and 3 while on PEM monotherapy and in patient 11 receiving LEN + PEM.

chemotherapy was associated with a significantly longer DSS in ATC while the opposite was observed in PDTC, where the use of EBRT and chemotherapy most likely indicate aggressive clinical course.

Considering PD-L1 TPS ≤ 5% as low, 6-49% intermediate and 50-100% as high expression, we did not observe significant differences of DSS among patients with ATC (p=0.495) or PDTC (p=0.496) patients (**Figure 6**). Using established cut-offs associated with response to PEM in NSCLC (scores from 0-49%: low; scores from 50-100%: high) no significant differences in DSS were observed as well (**Supplementary Figure 1**). We likewise did not find a prognostic relevance of FGFR1-4 expression for DSS (**Supplementary Figure 2**).

DISCUSSION

In this large multicenter analysis of prospectively and retrospectively collected clinical data and tissue specimens we systematically investigated the expression of the immune checkpoint molecule PD-L1 in the orphan diseases PDTC and ATC. We found variable expression in both types of aggressive thyroid malignancies with a significantly higher expression in ATC *vs.* PDTC. Importantly, while more than half of the PDTC samples showed a TPS below 5%, only 21% of ATC had PD-L1 below that arbitrary threshold. Of note, TPS of at least 1% was observed in all PDTC and ATC. In normal thyroid tissue, PD-L1 was absent but it was present at low levels in differentiated papillary thyroid carcinoma.

While clinical observations and small published studies suggested the expression of PD-L1 in the majority of ATC, we are not aware of a similarly large study on this topic (29, 30). Further strengths of our analysis are the systematic staining and evaluation at a single institution by a specialized endocrine pathologist and the systematic verification of diagnoses which is not the case in other series or was not reported (8). Overall, the presence of high PD-L1 expression in a substantial proportion of ATC and PDTC indicates a rationale for treatment with immune checkpoint inhibitors targeting the PD-1/PD-L1 axis. Our study is unable to support, however, a specific cut-off that would govern treatment with immune checkpoint inhibitors such as PEM. The TPS has been established as a response marker primarily for non-small cell lung cancer (NSCLC) and treatment of squamous cell head and neck cancer. In a retrospective analysis of ATC patients treated with kinase inhibitors and PEM progressive disease was observed in patients with PD-L1 TPS of 5%, 30% and 80% while a partial response was demonstrated in five patients, four of whom had PD-L1 TPS available with scores of >95%, 90%, 20% and >10% (8). Our data showed higher median PD-L1 expression in PTC than in PDTC (TPS 30% and 5% respectively), but range of PD-L1 expression in PDTC was much broader compared to PTC samples. PD-L1 expression has been reported for PTC tissue with and without lymphoid thyroiditis. PTC specimens with lymphoid thyroiditis showed higher expression of PD-L1 (39,1%) in comparison to PTC tissue without lymphoid thyroiditis (6,9%) (31). A review on the expression of PD-L1 in PTC tissue demonstrated significant association of PD-L1 expression with reduced disease-free survival (DFS), but not OS (32). We did not find any impact of PD-L1 expression on DSS. This is not surprising since the vast majority of patients did not receive PD-1/PD-L1 directed therapy. Hence, PD-L1 is not a prognostic marker but possibly a marker of treatment response in ATC and PDTC. Accordingly, a recently published ATC cohort from a phase I/II trial treated with spartalizumab, a PD-1 inhibitor, demonstrated objective response exclusively in patients with detectable PD-L1 expression (26). Guidelines recommend the evaluation of PD-L1 status in stage IVC ATC cases with lack of BRAF V600E mutation (6). Detection of high PD-L1 expression can be followed by treatment with immune checkpoint inhibitors and can be an alternative to chemotherapy and/or radiation (6).

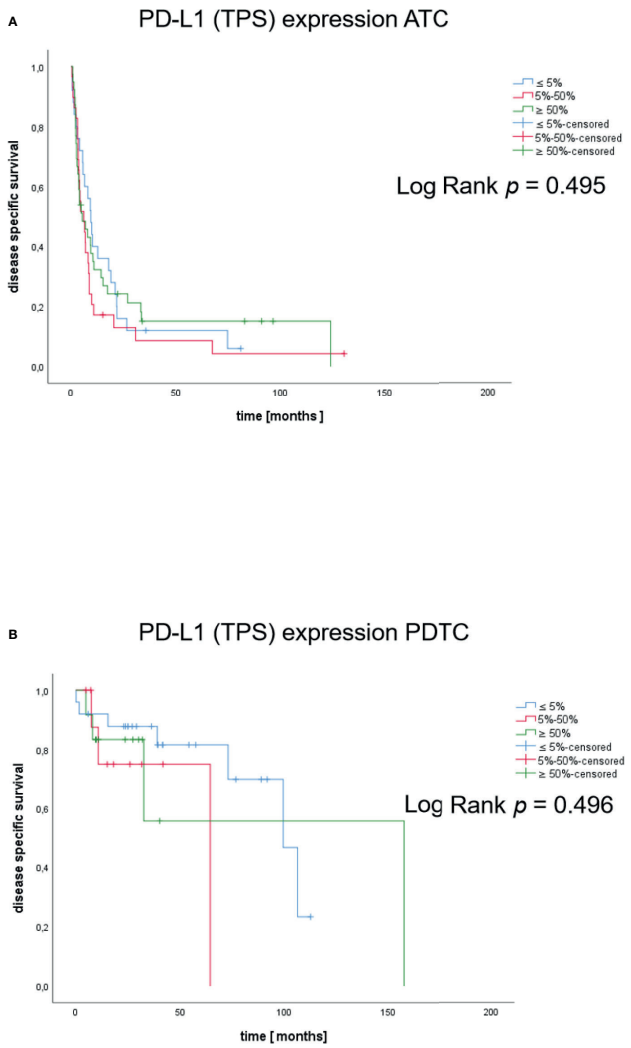

FIGURE 6 | Kaplan-Meier plots of DSS in patients according to PD-L1 expression. Disease specific survival of ATC **(A)** and PDTC **(B)** patients with TPS categories ≤5%, 5-50%, ≥50%).

The rationale to combine PD-L1 with LEN is supported by preclinical observations in an immunocompetent mouse model (33). The authors demonstrated profound changes of the immune microenvironment: LEN led to a pronounced increase in tumor-infiltrating immune cells, tumor-associated macrophages but also a pronounced increase of peripheral and tumoral polymorphonuclear myeloid derived suppressor cells (PMN-MDSC). The authors concluded that LEN exerts both pro-inflammatory and anti-inflammatory immune effects. By experimentally reducing the number of immunosuppressive PMN-MDSC the authors showed increased antitumoral efficacy of LEN alone and inhibition of the PD-1/PD-L1 axis was likewise associated with a decrease of immunosuppressive cell types. There is currently limited evidence of a direct immunomodulatory effect of LEN. Given the poor clinical response of ATC to VEGFR-directed TKI such as sorafenib, pazopanib and sunitinib, we reasoned that expression of the LEN targets FGFR1-4 on tumor cells may contribute to the specific antitumoral response of LEN monotherapy and in combination with immune checkpoint inhibitors. While immunohistochemistry of FGFR4 only has been used in one series (20) we consider our approach with RNAscope® *in situ* hybridization more reliable because it is not susceptible to cross-reactivity of FGFR antibodies in immunohistochemistry and permits the quantification of individual FGFRs. We found extremely low expression of all FGFR in the samples studied. FGFR1 was expressed at highest levels in PDTC and ATC compared to normal thyroid and PTC samples. Overall, we found significantly higher expression of the combination of FGFR1-4 in PDTC and ATC compared to normal thyroid but not to PTC. Tumor infiltrating leukocytes did not express FGFR1-4. Although we cannot exclude that the low expression of FGFR1-4 is still biologically relevant, we conclude that tumoral FGFRs are unlikely to be involved in the immunostimulatory action of LEN.

Our study of PD-L1 and FGFR1-4 expression in ATC and PDTC has some limitations: First, our study is – in part - retrospective in nature. Thus, selection bias confounds the association of treatment factors with prognosis and is the cause of the shorter DSS in PDTC patients receiving chemotherapy or EBRT. On the other hand, radioiodine positive PDTC have an inherently better prognosis.

Second, only few patients were treated with LEN or PEM (12 and 3 respectively) and even fewer patients were primarily treated with a combined regimen (n=3). It is therefore impossible to define cut-off values of response. Third, the tumor mutational burden and the LEN targets c-kit, RET, VEGFR 1-3 or PDGFR-α were not analyzed because we considered FGFR as the most relevant drug-specific target molecules. Indeed it has been suggested that beyond the actual tumoral angiogenesis, patient factors may contribute to the antitumoral effects observed with multi-kinase inhibitors such as LEN but also sorafenib (34, 35).

Finally, although relatively large for the rarity of the disease, the number of PDTC patients is still limited and no specific selection of PDTCs refractory to RIT was applied.

Together with the available preclinical data, our findings suggest that the immunostimulatory effect of LEN in ATC and the promising finding of clinical activity associated with this drug may be conferred by direct effects on circulating immune cells. It is noteworthy that the combination of LEN and PEM has been approved for the treatment of endometrial cancer and is under study in a broad spectrum of tumors (36). Markers of treatment response are yet to be discovered.

CONCLUSION

Our study of the expression of PD-L1 and FGFR 1-4 in ATC and PDTC supports the use of immune checkpoint inhibitors in the majority of ATC and some PDTC with high PD-L1 expression

TABLE 4 | Impact of PD-L1 expression and clinical parameters on disease specific death from ATC.

Prognostic factors	Univariate analysis			Multivariate analysis		
	HR	95% CI	P (log rank)	HR	95% CI	P (cox regression)
ATC						
Pretreatment factors						
Sex						
Male (n=40)						
Female (n=53)			0.82			
Age at diagnosis (years)						
<69 (n=46)						
≥69 (n=47)	1.689	1.091-2.614	**0.017**	1.724	0.958-3.104	0.069
UICC						
IVB (n=41)						
IVC (n=48)	1.886	1.200-2.966	**0.005**	2.068	1.244-3.438	**0.005**
PD-L1			0.495			
≤5% (n=25)						
5%-50% (n=29)						
≥50% (n=39)						
Complete local resection			0.392			
Yes (n=11)						
No (n=71)						
Treatment factors						
External beam radiation						
No (n=14)						
Yes (n=79)	0.503	0.277-0.915	**0.021**	0.463	0.228-0.941	**0.033**
External beam radiation						
<55 Gy (n=36)						
≥55 Gy (n=37)			0.117			
Chemotherapy						
No (n=43)						
Yes (n=48)	0.619	0.399-0.962	**0.031**	0.582	0.335-1.011	0.055
PDTC						
Pretreatment factors						
Sex						
Male (n=17)						
Female (n=30)			0.338			
Age at diagnosis (years)						
<63 (n=23)						
≥63 (n=24)			0.48			
UICC						
I, II and III (n=33)						
IVA and IVC (n=13)	3.176	1.002-10.060	**0.04**	2.984	0.907-9.819	0.072
PD-L1			0.496			
≤5% (n=25)						
5%-50% (n=10)						
≥50% (n=12)						
Complete local resection						
Yes (n=12)			0.119			
No (n=25)						
Treatment factors						
Radioiodine treatment						
No (n=11)					0.07-2.177	
Yes (n=36)	0.148	0.038-0.517	**0.001**	0.284		0.284
Radioiodine treatment						
<6.65 GBq (n=18)						
≥6.65 GBq (n=18)			0.601			
External beam radiation						
No (n=31)					0.512-12.702	
Yes (n=16)	4.065	1.180-14.001	**0.016**	2.55		0.253
External beam radiation						
<60.5 Gy (n=7)						
≥60.5 Gy (n=8)			0.531			
Chemotherapy						
No (n=41)					0.367-8.626	
Yes (n=6)	4.291	1.050-17.537	**0.027**	1.779		0.475

**p-values of Bonferroni testing for pairwise comparisons between ATC and PDTC are indicated.*

although the role of PD-L1 expression for treatment decisions remains to be established. Tumoral FGFR expression is similarly low in ATC and PDTC and likely not the principal target of lenvatinib. In the light of the clinical response of ATC to combined LEN and immune checkpoint inhibitor treatment, we suggest a yet unknown tumoral LEN target or a LEN target not expressed in the tumor to be relevant for the clinically observed drug synergism. We propose to study peripheral immune cells and tumor infiltrating leukocytes systematically in clinical trials to identify markers of treatment response and better understand the mechanistic basis of combination therapy.

DATA AVAILABILITY STATEMENT

The original contributions presented in the study are included in the article/**Supplementary Material**, further inquiries can be directed to the corresponding author.

ETHICS STATEMENT

Written informed consent was obtained from the individual(s) for the publication of any potentially identifiable images or data included in this article.

AUTHOR CONTRIBUTIONS

MK, MF, CSp, CD, MS, and AZ designed the study. PA, SK, and IS performed experiments. SK, VK, EB, TK, BSa, WF, HB, CSm, AZ, BSi, SA, MS, CD, CSp, MF, and MK provided samples and data. PA and MK analyzed the data. PA, SK, VK, BSi, AZ, MF, and MK interpreted the data. PA and MK wrote a manuscript draft. All authors contributed to the article and approved the submitted version.

FUNDING

This work was supported – in part - by the Else Kröner Fresenius Stiftung, grant number 2016-A96.

ACKNOWLEDGMENTS

The authors wish to thank all patients, their families and caregivers for providing clinical data and tumor sections for this study. The authors thank Bianca Schlierf, Nathalie Schwenk, Martina Zink, Ramona Walter and Johanna Vogt for excellent technical support and Dr. Isabel Weigand for critical reading of the manuscript. This work has been carried out with the help of the Interdisciplinary Bank of Biomaterials and Data of the University Hospital of Würzburg and the Julius- Maximilians-University of Würzburg (IBDW) (37).

SUPPLEMENTARY MATERIAL

The Supplementary Material for this article can be found online at: https://www.frontiersin.org/articles/10.3389/fendo.2021.712107/full#supplementary-material

Supplementary Figure 1 | Kaplan-Meier plots of DSS in patients according to PD-L1 expression. Disease specific survival of ATC **(A)** and PDTC **(B)** patients with TPS categories <50% and ≥50%).

Supplementary Figure 2 | Kaplan-Meier plots of DSS in patients according to panFGFR expression. Disease specific survival of ATC **(A)** and PDTC **(B)** patients with mean panFGFR expression (2 mRNA/cell [ATC], 3 mRNA/cell [PDTC]).

REFERENCES

1. Jemal A, Bray F, Center MM, Ferlay J, Ward E, Forman D. Global Cancer Statistics. *CA Cancer J Clin* (2011) 61(2):69–90. doi: 10.3322/caac.20107
2. Sanders EMJr., LiVolsi VA, Brierley J, Shin J, Randolph GW. An Evidence-Based Review of Poorly Differentiated Thyroid Cancer. *World J Surg* (2007) 31(5):934–45. doi: 10.1007/s00268-007-9033-3
3. Owens PW, McVeigh TP, Fahey EJ, Bell M, Quill DS, Kerin MJ, et al. Differentiated Thyroid Cancer: How Do Current Practice Guidelines Affect Management? *Eur Thyroid J* (2018) 7(6):319–26. doi: 10.1159/000493261
4. Wendler J, Kroiss M, Gast K, Kreissl MC, Allelein S, Lichtenauer U, et al. Clinical Presentation, Treatment and Outcome of Anaplastic Thyroid Carcinoma: Results of a Multicenter Study in Germany. *Eur J Endocrinol* (2016) 175(6):521–9. doi: 10.1530/EJE-16-0574
5. Maniakas A, Dadu R, Busaidy NL, Wang JR, Ferrarotto R, Lu C, et al. Evaluation of Overall Survival in Patients With Anaplastic Thyroid Carcinoma, 2000-2019. *JAMA Oncol* (2020) 6(9):1397–1404. doi: 10.1001/jamaoncol.2020.3362
6. Bible KC, Kebebew E, Brierley J, Brito JP, Cabanillas ME, Clark TJJr., et al. 2021 American Thyroid Association Guidelines for Management of Patients With Anaplastic Thyroid Cancer. *Thyroid* (2021) 31(3):337–86. doi: 10.1089/thy.2020.0944
7. Smallridge RC, Copland JA. Anaplastic Thyroid Carcinoma: Pathogenesis and Emerging Therapies. *Clin Oncol (R Coll Radiol)* (2010) 22(6):486–97. doi: 10.1016/j.clon.2010.03.013
8. Iyer PC, Dadu R, Gule-Monroe M, Busaidy NL, Ferrarotto R, Habra MA, et al. Salvage Pembrolizumab Added to Kinase Inhibitor Therapy for the Treatment of Anaplastic Thyroid Carcinoma. *J Immunother Cancer* (2018) 6(1):68. doi: 10.1186/s40425-018-0378-y
9. Ferrari SM, Elia G, Ragusa F, Ruffilli I, La Motta C, Paparo SR, et al. Novel Treatments for Anaplastic Thyroid Carcinoma. *Gland Surg* (2020) 9(Suppl 1): S28–s42. doi: 10.21037/gs.2019.10.18
10. Subbiah V, Kreitman RJ, Wainberg ZA, Cho JY, Schellens JHM, Soria JC, et al. Dabrafenib and Trametinib Treatment in Patients With Locally Advanced or Metastatic BRAF V600-Mutant Anaplastic Thyroid Cancer. *J Clin Oncol* (2018) 36(1):7–13. doi: 10.1200/JCO.2017.73.6785
11. Thiagarajan S, Yousuf A, Shetty R, Dhar H, Mathur Y, Nair D, et al. Poorly Differentiated Thyroid Carcinoma (PDTC) Characteristics and the Efficacy of Radioactive Iodine (RAI) Therapy as an Adjuvant Treatment in a Tertiary Cancer Care Center. *Eur Arch Otorhinolaryngol* (2020) 277(6):1807–14. doi: 10.1007/s00405-020-05898-9
12. Lee DY, Won JK, Lee SH, Park DJ, Jung KC, Sung MW, et al. Changes of Clinicopathologic Characteristics and Survival Outcomes of Anaplastic and Poorly Differentiated Thyroid Carcinoma. *Thyroid* (2016) 26(3):404–13. doi: 10.1089/thy.2015.0316

13. Tumours WHOCo. "WHO Classification of Tumours of Endocrine Organs". In: RV Lloyd, RY Osamura, G Klöppel and J Rosai, editors. *World Health Organization Classification of Tumours, 4th ed*. Lyon: International Agency for Research on Cancer IARC (2017). p. 100–6.
14. Schlumberger M, Tahara M, Wirth LJ, Robinson B, Brose MS, Elisei R, et al. Lenvatinib Versus Placebo in Radioiodine-Refractory Thyroid Cancer. *N Engl J Med* (2015) 372(7):621–30. doi: 10.1056/NEJMoa1406470
15. Marotta V, Sciammarella C, Vitale M, Colao A, Faggiano A. The Evolving Field of Kinase Inhibitors in Thyroid Cancer. *Crit Rev Oncol Hematol* (2015) 93(1):60–73. doi: 10.1016/j.critrevonc.2014.08.007
16. Marotta V, Chiofalo MG, Di Gennaro F, Daponte A, Sandomenico F, Vallone P, et al. Kinase-Inhibitors for Iodine-Refractory Differentiated Thyroid Cancer: Still Far From a Structured Therapeutic Algorithm. *Crit Rev Oncol Hematol* (2021) 162:103353. doi: 10.1016/j.critrevonc.2021.103353
17. Iwasaki H, Toda S, Suganuma N, Murayama D, Nakayama H, Masudo K. Lenvatinib vs. Palliative Therapy for Stage IVC Anaplastic Thyroid Cancer. *Mol Clin Oncol* (2020) 12(2):138–43. doi: 10.3892/mco.2019.1964
18. Takahashi S, Tahara M, Ito K, Tori M, Kiyota N, Yoshida K, et al. Safety and Effectiveness of Lenvatinib in 594 Patients With Unresectable Thyroid Cancer in an All-Case Post-Marketing Observational Study in Japan. *Adv Ther* (2020) 37(9):3850–62. doi: 10.1007/s12325-020-01433-8
19. Dai S, Zhou Z, Chen Z, Xu G, Chen Y. Fibroblast Growth Factor Receptors (FGFRs): Structures and Small Molecule Inhibitors. *Cells* (2019) 8(6):614. doi: 10.3390/cells8060614
20. Yamazaki H, Yokose T, Hayashi H, Iwasaki H, Osanai S, Suganuma N, et al. Expression of Fibroblast Growth Factor Receptor 4 and Clinical Response to Lenvatinib in Patients With Anaplastic Thyroid Carcinoma: A Pilot Study. *Eur J Clin Pharmacol* (2020) 76(5):703–9. doi: 10.1007/s00228-020-02842-y
21. Stuhler V, Maas JM, Rausch S, Stenzl A, Bedke J. Immune Checkpoint Inhibition for the Treatment of Renal Cell Carcinoma. *Expert Opin Biol Ther* (2020) 20(1):83–94. doi: 10.1080/14712598.2020.1677601
22. Garon EB, Rizvi NA, Hui R, Leighl N, Balmanoukian AS, Eder JP, et al. Pembrolizumab for the Treatment of non-Small-Cell Lung Cancer. *N Engl J Med* (2015) 372(21):2018–28. doi: 10.1056/NEJMoa1501824
23. Ferris RL, Licitra L. PD-1 Immunotherapy for Recurrent or Metastatic HNSCC. *Lancet* (2019) 394(10212):1882–4. doi: 10.1016/S0140-6736(19)32539-5
24. Finn RS, Ryoo BY, Merle P, Kudo M, Bouattour M, Lim HY, et al. Pembrolizumab As Second-Line Therapy in Patients With Advanced Hepatocellular Carcinoma in KEYNOTE-240: A Randomized, Double-Blind, Phase III Trial. *J Clin Oncol* (2019) Jco1901307:193–202. doi: 10.1200/JCO.19.01307
25. Yu Y, Zeng D, Ou Q, Liu S, Li A, Chen Y, et al. Association of Survival and Immune-Related Biomarkers With Immunotherapy in Patients With Non-Small Cell Lung Cancer: A Meta-Analysis and Individual Patient-Level Analysis. *JAMA Netw Open* (2019) 2(7):e196879. doi: 10.1001/jamanetworkopen.2019.6879
26. Capdevila J, Wirth LJ, Ernst T, Ponce Aix S, Lin CC, Ramlau R, et al. PD-1 Blockade in Anaplastic Thyroid Carcinoma. *J Clin Oncol* (2020) 38(23):2620–7. doi: 10.1200/JCO.19.02727
27. Chintakuntlawar AV, Yin J, Foote RL, Kasperbauer JL, Rivera M, Asmus E, et al. A Phase 2 Study of Pembrolizumab Combined With Chemoradiotherapy as Initial Treatment for Anaplastic Thyroid Cancer. *Thyroid* (2019) 29(11):1615–22. doi: 10.1089/thy.2019.0086
28. Dierks C, Seufert J, Aumann K, Ruf J, Klein C, Kiefer S, et al. The Lenvatinib/Pembrolizumab Combination is an Effective Treatment Option for Anaplastic and Poorly Differentiated Thyroid Carcinoma. *Thyroid* (2021) 31(7):1076–85. doi: 10.1089/thy.2020.0322
29. Bastman JJ, Serracino HS, Zhu Y, Koenig MR, Mateescu V, Sams SB, et al. Tumor-Infiltrating T Cells and the PD-1 Checkpoint Pathway in Advanced Differentiated and Anaplastic Thyroid Cancer. *J Clin Endocrinol Metab* (2016) 101(7):2863–73. doi: 10.1210/jc.2015-4227
30. Zwaenepoel K, Jacobs J, De Meulenaere A, Silence K, Smits E, Siozopoulou V, et al. CD70 and PD-L1 in Anaplastic Thyroid Cancer - Promising Targets for Immunotherapy. *Histopathology* (2017) 71(3):357–65. doi: 10.1111/his.13230
31. Fadia M, Fookeerah P, Ali S, Shadbolt B, Greenaway T, Perampalam S. PD-L1 Expression in Papillary Thyroid Cancer With and Without Lymphocytic Thyroiditis: A Cross Sectional Study. *Pathology* (2020) 52(3):318–22. doi: 10.1016/j.pathol.2019.11.007
32. Girolami I, Pantanowitz L, Mete O, Brunelli M, Marletta S, Colato C, et al. Programmed Death-Ligand 1 (PD-L1) Is a Potential Biomarker of Disease-Free Survival in Papillary Thyroid Carcinoma: A Systematic Review and Meta-Analysis of PD-L1 Immunoexpression in Follicular Epithelial Derived Thyroid Carcinoma. *Endocr Pathol* (2020) 31(3):291–300. doi: 10.1007/s12022-020-09630-5
33. Gunda V, Gigliotti B, Ashry T, Ndishabandi D, McCarthy M, Zhou Z, et al. Anti-PD-1/PD-L1 Therapy Augments Lenvatinib's Efficacy by Favorably Altering the Immune Microenvironment of Murine Anaplastic Thyroid Cancer. *Int J Cancer* (2019) 144(9):2266–78. doi: 10.1002/ijc.32041
34. Marotta V, Sciammarella C, Capasso M, Testori A, Pivonello C, Chiofalo MG, et al. Preliminary Data of VEGF-A and VEGFR-2 Polymorphisms as Predictive Factors of Radiological Response and Clinical Outcome in Iodine-Refractory Differentiated Thyroid Cancer Treated With Sorafenib. *Endocrine* (2017) 57(3):539–43. doi: 10.1007/s12020-016-1200-6
35. Marotta V, Sciammarella C, Capasso M, Testori A, Pivonello C, Chiofalo MG, et al. Germline Polymorphisms of the VEGF Pathway Predict Recurrence in Nonadvanced Differentiated Thyroid Cancer. *J Clin Endocrinol Metab* (2017) 102(2):661–71. doi: 10.1210/jc.2016-2555
36. Hao Z, Wang P. Lenvatinib in Management of Solid Tumors. *Oncologist* (2020) 25(2):e302–e10. doi: 10.1634/theoncologist.2019-0407
37. Geiger J, Both S, Kircher S, Neumann M, Rosenwald A, Jahns R. Hospital-Integrated Biobanking as a Service – The Interdisciplinary Bank of Biomaterials and Data Wuerzburg (Ibdw). *Open J Bioresour* (2018) 5:6. doi: 10.5334/ojb.38

Conflict of Interest: The authors declare that the research was conducted in the absence of any commercial or financial relationships that could be construed as a potential conflict of interest.

Publisher's Note: All claims expressed in this article are solely those of the authors and do not necessarily represent those of their affiliated organizations, or those of the publisher, the editors and the reviewers. Any product that may be evaluated in this article, or claim that may be made by its manufacturer, is not guaranteed or endorsed by the publisher.

frontiers in Endocrinology

ORIGINAL RESEARCH
published: 07 September 2021
doi: 10.3389/fendo.2021.722656

Plasma Metabolome Profiling for the Diagnosis of Catecholamine Producing Tumors

Juliane März[1], Max Kurlbaum[1,2], Oisin Roche-Lancaster[3,4,5], Timo Deutschbein[1,6], Mirko Peitzsch[7], Cornelia Prehn[8], Dirk Weismann[1], Mercedes Robledo[9,10], Jerzy Adamski[11,12,13], Martin Fassnacht[1,2,14], Meik Kunz[3,15†] and Matthias Kroiss[1,2,16*†]*

[1] Department of Internal Medicine I, Division of Endocrinology and Diabetes, University Hospital, University of Würzburg, Würzburg, Germany, [2] Core Unit Clinical Mass Spectrometry, University Hospital, Würzburg, Germany, [3] Chair of Medical Informatics, Friedrich-Alexander University (FAU) of Erlangen-Nürnberg, Erlangen, Germany, [4] Department of Pediatrics and Adolescent Medicine, University Hospital Erlangen, Erlangen, Germany, [5] Comprehensive Cancer Center Erlangen-Europäische Metropolregion Nürnberg (CCC ER-EMN), Erlangen, Germany, [6] Medicover Oldenburg Medizinisches Versorgungszentrum (MVZ), Oldenburg, Germany, [7] Institute of Clinical Chemistry and Laboratory Medicine, University Hospital Carl Gustav Carus at Technische Universität (TU) Dresden, Dresden, Germany, [8] Metabolomics and Proteomics Core, Helmholtz Zentrum München, German Research Center for Environmental Health, Neuherberg, Germany, [9] Hereditary Endocrine Cancer Group, Spanish National Cancer Research Center, Madrid, Spain, [10] Hereditary Endocrine Cancer Group, Spanish National Cancer Research Center and Centro de Investigación Biomédica en Red de Enfermedades Raras (CIBERER), Madrid, Spain, [11] Institute of Experimental Genetics, Helmholtz Zentrum München, German Research Center for Environmental Health, Neuherberg, Germany, [12] Department of Biochemistry, Yong Loo Lin School of Medicine, National University of Singapore, Singapore, Singapore, [13] Institute of Biochemistry, Faculty of Medicine, University of Ljubljana, Ljubljana, Slovenia, [14] Cancer Center Mainfranken, University of Würzburg, Würzburg, Germany, [15] Fraunhofer Institute of Toxicology and Experimental Medicine, Hannover, Germany, [16] Department of Internal Medicine IV, University Hospital Munich, Ludwig-Maximilians-Universität München, Munich, Germany

OPEN ACCESS

Edited by:
Antongiulio Faggiano, Sapienza University of Rome, Italy

Reviewed by:
Valentina Vaira, University of Milan, Italy
Paraskevi Xekouki, University of Crete, Greece

***Correspondence:**
Matthias Kroiss
matthias.kroiss@med.uni-muenchen.de
Max Kurlbaum
Kurlbaum_m1@ukw.de

†These authors have contributed equally to this work

Specialty section:
This article was submitted to Cancer Endocrinology, a section of the journal Frontiers in Endocrinology

Received: *10 June 2021*
Accepted: *09 August 2021*
Published: *07 September 2021*

Citation:
März J, Kurlbaum M, Roche-Lancaster O, Deutschbein T, Peitzsch M, Prehn C, Weismann D, Robledo M, Adamski J, Fassnacht M, Kunz M and Kroiss M (2021) Plasma Metabolome Profiling for the Diagnosis of Catecholamine Producing Tumors. Front. Endocrinol. 12:722656. doi: 10.3389/fendo.2021.722656

Context: Pheochromocytomas and paragangliomas (PPGL) cause catecholamine excess leading to a characteristic clinical phenotype. Intra-individual changes at metabolome level have been described after surgical PPGL removal. The value of metabolomics for the diagnosis of PPGL has not been studied yet.

Objective: Evaluation of quantitative metabolomics as a diagnostic tool for PPGL.

Design: Targeted metabolomics by liquid chromatography-tandem mass spectrometry of plasma specimens and statistical modeling using ML-based feature selection approaches in a clinically well characterized cohort study.

Patients: Prospectively enrolled patients (n=36, 17 female) from the Prospective Monoamine-producing Tumor Study (PMT) with hormonally active PPGL and 36 matched controls in whom PPGL was rigorously excluded.

Results: Among 188 measured metabolites, only without considering false discovery rate, 4 exhibited statistically significant differences between patients with PPGL and controls (histidine p=0.004, threonine p=0.008, lyso PC a C28:0 p=0.044, sum of hexoses p=0.018). Weak, but significant correlations for histidine, threonine and lyso PC a C28:0 with total urine catecholamine levels were identified. Only the sum of hexoses (reflecting glucose) showed significant correlations with plasma metanephrines. By using ML-based feature selection approaches, we identified diagnostic signatures which all

exhibited low accuracy and sensitivity. The best predictive value (sensitivity 87.5%, accuracy 67.3%) was obtained by using Gradient Boosting Machine Modelling.

Conclusions: The diabetogenic effect of catecholamine excess dominates the plasma metabolome in PPGL patients. While curative surgery for PPGL led to normalization of catecholamine-induced alterations of metabolomics in individual patients, plasma metabolomics are not useful for diagnostic purposes, most likely due to inter-individual variability.

Keywords: adrenal, pheochromocytoma, paraganglioma, targeted metabolomics, mass spectronomy, catecholamines, machine learning, feature selection

INTRODUCTION

Pheochromocytomas and paragangliomas (PPGL) are defined as catecholamine-producing tumors that arise from chromaffin cells (1). Pheochromocytomas represent more than 80% of all PPGL and are located in the adrenal medulla whereas paraganglioma arise from paravertebral sympathetic ganglia and are most frequently located in the abdomen, chest, and pelvis (2). Paragangliomas deriving from parasympathetic tissue in the head and neck rarely produce hormones (1–3). Predisposing germline mutations, extra-adrenal location, and dopaminergic phenotype are the most relevant risk factors for malignancy (4, 5). Current data suggest that germline mutations are present in up to 40% of all patients with PPGL, with 18 susceptibility genes identified so far. Mutations are most frequently found in genes encoding subunits of succinate dehydrogenase (SDH), von Hippel-Lindau gene (VHL) and rearranged during transfection (RET) gene. As the presence of a germ line mutation was found to be an important factor of prognosis of affected patients, testing is recommended (5–8).

Catecholamine excess leads to a variety of well-known but unspecific symptoms such as hypertension, palpitation, headache and pallor (1, 9) and causes cardio- and cerebrovascular complications. The measurement of plasma free metanephrine (MN), normetanephrine (NMN) and methoxytyramine (MTY) is now a cornerstone of diagnosis and follow-up in clinical practice, providing high diagnostic accuracy when adequate pre-analytics, analytics and reference ranges are applied (2, 10, 11). In recent years mass spectrometry has become the gold standard due to its high analytic sensitivity and specificity (12) not limited on quantification of established markers but showing additionally its usefulness to identify tissue metabolomic profiles *via* MALDI-MSI (13). Nevertheless, the diagnosis of PPGL remains challenging and is often delayed due to lack of consideration of PPGL (4). In addition there is a high risk of false positive test results when strict pre-analytical conditions are not followed.

Metabolomics is the screening for characteristic substances in body fluids and tissue, which serve as direct marker of biochemical activity because they are not exposed to epigenetic regulation and post-translational modifications like proteins or genes and therefore reflect the individual phenotype (14). Untargeted metabolomics allows the identification of numerous molecules without prior knowledge of their presence in predefined groups but has the disadvantage of generating mostly qualitative information on target molecules. On the other hand, quantitation of previously specified molecules is possible by targeted metabolomics. Still, the number of metabolites is typically limited to substances that are precisely characterized by their chemical structure and molecular mass.

In a targeted metabolomics approach, we recently identified significant intra-individual metabolic alterations in patients with PPGL before *vs.* after tumor removal and demonstrated that several of those are related to cardiovascular risk (15). Characterization of the metabolic profile in patients with PPGL might help to understand the metabolic effects of excessive catecholamine levels and harbor additional diagnostic potential.

The aim of our study was to characterize differences in plasma metabolic profile between patients with PPGL and controls with consideration of the secretory phenotype. We applied tandem mass spectrometry using a targeted metabolomics approach and logistic regression modeling to identify discriminative pattern potentially useful for diagnostic workup of PPGL.

Abbreviations: a, acyl; aa, diacyl; ae, acyl-alkyl; C x:y, indicates the lipid chain composition where "x" is the number of carbons and "y" the number of bonds; C, carbon; DA, dopamine; ELA, Elastic net; EPI, epinephrine; FDR, false discovery rate; FIA, flow injection analysis; GBM, Gradient Boosting Machine; H1, sum of hexoses; IQR, interquartile range; LC-MS/MS, liquid chromatography tandem mass spectrometry; LLOQ, lower limit of quantification; LOD, lower limit of detection; lysoPC, lysophosphatidylcholine; MN, metanephrine; MTY, methoxytyramine; NE, norepinephrine; NMN, normetanephrine; PC, phosphatidylcholine; PMT, Prospective Monoamine-producing Tumor Study; PPGL, pheochromocytoma/paraganglioma; SDH, succinate dehydrogenase; SM, sphingolipids; SVM, Support Vector Machine; UHLPC, ultra-high performance liquid chromatography.

SUBJECTS AND METHODS

Subjects

Patients with suspected PPGL were recruited from a single center participating in the Prospective Monoamine-Producing tumor (PMT) study, which has been described in detail previously (2). The diagnosis of PPGL was based on biochemical assessment, imaging, and histology. Follow-up ruled out the presence of PPGLs in patients who served as controls. The latter were matched for sex and age at the date of sampling according to

patient data. The study protocol was approved by the Ethics Committee of the University Hospital Würzburg (104/11). All patients provided written informed consent.

Sample Collection

Plasma samples were collected as described elsewhere (2). Briefly, blood was drawn in the morning after an overnight fast for at least 8h and in a supine position for at least 30 minutes. Patients were instructed to refrain from alcohol, nicotine, decaffeinated and caffeinated beverages for 12 hours as well as avoid acetaminophen five days before sample collection (16). Blood was collected into EDTA or heparinized tubes and placed on ice before centrifugation at 20°C for five minutes at 4000 rpm. Plasma was aliquoted and the samples were stored at -80°C until assayed. Urine collection was performed according to the PMT protocol.

Mass Spectrometry

Plasma free metanephrines and urine catecholamines were measured as previously described (17–19).

Targeted metabolomics was performed by using the AbsoluteIDQ™-p180 Kit (Biocrates Life Sciences AG, Innsbruck, Austria). The method has been described in detail previously (15, 20, 21) and complies with EMA "Guideline on bioanalytical method validation" (July 21st 2011).The measurement consists of a ultra-high performance liquid chromatography (UHPLC) separation step and a flow injection analysis (FIA) step, both followed by mass spectrometry analyses (LC-MS/MS and FIA-MS/MS). This method enables for measurement of a total of 188 metabolites, of which 42 are included in the LC-MS/MS part (21 amino acids, 21 biogenic amines) and 146 metabolites in the FIA-MS/MS protocol (40 acylcarnitines including free carnitine, 38 phosphatidylcholines with acyl/acyl side chains [PCaa], 38 phosphatidylcholines with acyl/alkyl side chains [PCae], 14 lysophosphatidylcholines [lysoPC], 15 sphingolipids [SM] and the sum of hexoses [H1]).

A volume of 10 µl plasma was used and prepared according to the manufacturer's manual. Internal standards served as reference for quantification, human reference plasma was included into each batch to ensure quality control, comparability between batch measurements, and normalization of the data (20). Metabolite concentrations are given in µmol/l. LC-MS/MS and FIA-MS/MS were performed by using SCIEX QTRAP® 4500MD MS-system (SCIEX, Darmstadt, Germany) coupled to an Agilent 1290 Infinity UHPLC-system (Agilent, Santa Clara, USA). Analyst® software version 1.6.3 MD (SCIEX, Darmstadt, Germany) was used for data procession. Data was validated and processed with MetIDQ™ software version 5.5.4-DB100 Boron-2623 (Biocrates Life Sciences AG, Innsbruck, Austria).

Genetics

Genetic data were retrieved from patient records or provided by the CNIO institute in Madrid as a part of the PMT study. Targeted next generation sequencing assay, Sanger sequencing and multiplex ligation-dependent probe amplification or custom array comparative genomic hybridization for deletion detection (22, 23) were applied as appropriate.

Statistical Analysis

Baseline data are shown as frequencies for categorical variables and as medians with interquartile range (IQR) for numerical variables. Malignancy was defined as the presence of metastases in non-chromaffin organs. The secretory phenotype of PPGL was characterized as noradrenergic and adrenergic according to an established algorithm which has been descripted in detail elsewhere (24). Metabolites with more than 40% of concentrations below the lower limit of quantification (LLOQ) and samples with more than 40% of analytes lower than the lower limit of detection (LOD) were excluded from further analysis. In the remaining metabolites, the non-valid values measured below LLOQ and LOD were left unchanged and included in further analyses. Values with no detectable signal were replaced by (LOD/ $\sqrt{2}$) x (random number between 0.75-1.25) (25). To detect metabolic alterations associated with catecholamine excess, metabolite values in PPGL and controls were compared. Subgroups were analyzed after stratification for sex (males *vs.* females), BMI ($\leq$ 25 kg/m^2 *vs* > 25 kg/m^2) and secretory phenotype (adrenergic *vs*. noradrenergic). Comparisons between groups were analyzed using the Mann-Whitney-U test, significance was defined as p-value <0.05. The calculation of false discovery rate (FDR) corrected p-values was performed according to the method of Benjamini and Hochberg (26). Spearman test was used for correlations between metabolite and catecholamine concentrations. Statistical analyses were performed by SPSS version 25 (IMP, New York, USA) and Prism 7.05 (GraphPad, San Diego, CA, USA), for principal component analysis, MetaboAnalyst (4.0) was used.

Logistic Regression Modelling

Feature selection models were developed by applying the machine learning methods Elastic net (ELA), Support Vector Machine (SVM) and Gradient Boosting Machine (GBM) using the caret package version 6.0.84. The analysis was done in R (version 3.5.3; script is given online). The data set was normalized using the PreProcess function of the caret package (version 6.0.84). We split the dataset in a training (80%) and validation/test (20%) dataset. We tested each model using repeated 10-fold cross-validation. The variables were selected using the impact that they had on the predictive power of the different models. The models were compared using the predictive values accuracy (correct classification) and kappa (inter-rater reliability; classification including random chance normalization). Identified variables were further analysed using a Wilcoxon test to determine if there is a systematic difference between the conditions (class: PPGL *vs.* control).

RESULTS

Patients Characteristics

The study workflow is depicted in **Figure 1**. 36 patients with confirmed PPGL prior any specific treatment and controls matched for sex and age at date of sample were selected (**Table 1**). In controls, PPGL was suspected based on the

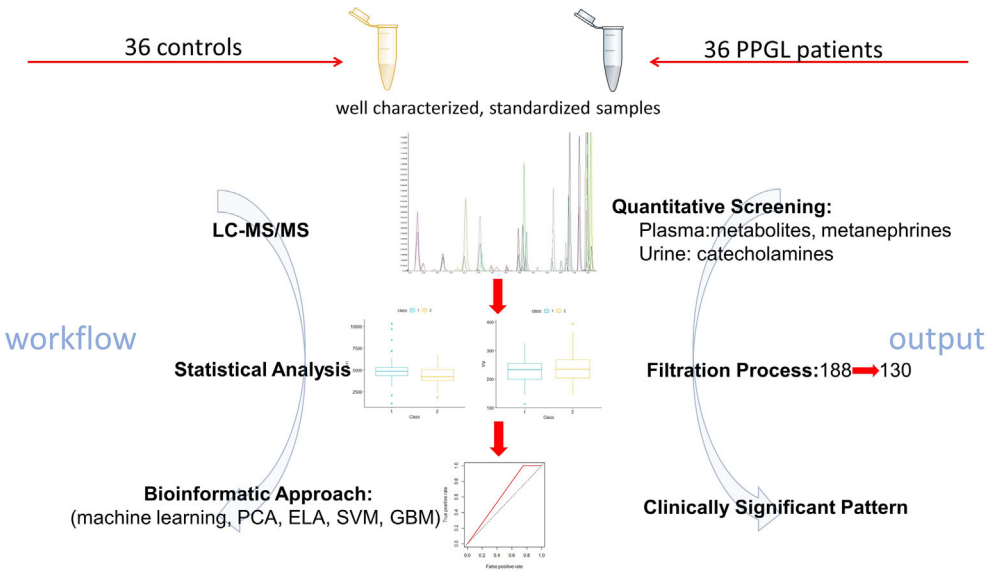

FIGURE 1 | Summary of the workflow leading to identification of significant metabolites *via* liquid chromatography tandem mass spectrometry (LC-MS/MS), in pheochromocytoma and paraganglioma (PPGL),The bioinformatic approach included Elastic net (ELA), Gradient Boosting Machine (GBM), Support Vector Machine (SVM) and Principal component analysis (PCA) approaches.

incidental finding of an adrenal mass upon imaging for an unrelated condition (n=21), signs and symptoms suggestive for PPGL (n=9) or therapy resistant hypertension (n=6) but excluded by normal follow-up biochemistry, negative imaging, resolved signs and symptoms or an alternative diagnosis (17). Other endocrinological causes for resistant hypertension or adrenal incidentalomas such as hyperaldosteronism, acromegaly, hyperthyroidism, hyperparathyroidism, or Cushing's syndrome were excluded in all subjects.

Complete urinary catecholamine data (31/36 controls, 27/36 PPGL) and genetic data (33/36 PPGL) were available in a subset of individuals. There were no statistically significant differences between groups concerning age and time between sampling and measurement of metabolomics while a statistically significant difference in Body mass index (in kg/m^2) was present in PPGL (25.2 [23.6–26.7]) *vs* controls (28.6 [26.0–31.2], p=0.043). Plasma markers of catecholamine excess were significantly increased in PPGL.

Targeted Metabolomics PPGL *vs.* Controls

Overall, 130 of 188 measured metabolites were included in the statistical analysis (**Supplemental Data**). However, only when p-values were not corrected for FDR, four of them showed significantly different concentrations between the two groups. In PPGL *vs.* controls (**Figure 2**) the amino acids histidine (75.40 [61.03-87.05] *vs.* 86.40 [75.63-96.35] µmol/l, p=0.004) and threonine (105.00 [88.57-125.00] *vs.* 128.00 [93.32-147.50] µmol/l, p=0.008) were significantly lower, while lyso PC a C28:0 (0.11 [0.10-0.12] *vs.* 0.12 [0.11-0.14] µmol/l, p=0.044) was only slightly decreased. On the opposite, the sum of hexoses was significantly higher in PPGL patients compared to controls (4844.00 [4325.50-5364.50] *vs.* 4215.50 [3791.00-5086.00] µmol/l, p=0.018). The plasma concentrations of biogenic amines, acylcarnitines, and sphingolipids were comparable between PPGL and controls.

Correlation With Plasma Metanephrine and Urine Catecholamine Values

The association of metabolic changes with catecholamine excretion has already been demonstrated (15). Therefore, we correlated altered metabolites with urinary catecholamines, which represent the biologically active form, and MN, NMN and MTY in plasma as non-functional disease markers (**Table 2** and **Figure 3**). Histidine showed a significant negative correlation with plasma NMN and plasma MTY, as well as with urine free epinephrine (EPI) and urine free dopamine (DA). Threonine was negatively correlated with plasma MTY, urine free norepinephrine (NE), and urine free EPI. LysoPC a C28:0 was negatively associated with urine free DA, whereas the sum of hexoses showed a positive correlation with all plasma metanephrines and with urine free NE. Furthermore, Histidine, threonine and lysoPC C:28 revealed a negative correlation with the total urinary catecholamines.

Subgroup Analyses

Despite the small group sizes, we also explored differences in subgroups. However, these were significant only without FDR correction. If only males were taken into account (n=19), patients with PPGL had lower levels of threonine (102.00 [85.50-127.00] *vs.* 132.00 [104.00-156.00] µmol/l, p=0.008) and higher levels of H1 (4845.00 [4489.00-5285.00] *vs.* 4079.00 [3789.00-5131.00] µmol/l, p=0.050) than controls. In addition,

TABLE 1 | Patient characteristics stratified by patients and controls.

	PPGL	Controls	P value
Subjects, n	36	36	
Females, n (%)	17 (47)	17 (47)	
Extra-adrenal tumor location, n (%)	7 (19)		
Malignant tumor, n (%)	11 (31)		
Tumor size, d [cm]	4.1 (3.3-6.1)		
BMI, [kg/m^2]	25.2 (23.6-26.7)	28.6 (26.0-31.2)	0.043
AHT, n (%)	14 (39)	24 (67)	
Diabetes mellitus, n (%)	6 (17)		
Adrenergic phenotype, n (%)	15 (42)		
PHEO, n	15		
PGL, n	0		
Follow-up			
6 months, n (%)		18 (50)	
24 months, n (%)		11 (31)	
Plasma data (n=72)			
Time between sampling and metabolomics measurement (days)	1164 (922-1407)	1211 (976-1447)	0.971
Age at date of sample	50.7 (41.7-61.4)	50.9 (43.7-62.2)	0.884
MN [pg/ml]	66.7 (31.0-596.2)	28.4 (21.0-45.4)	<0.001
NMN [pg/ml]	1144.4 (561.4-2327.8)	82.8 (62.3-121.7)	<0.001
MTY [pg/ml]	14.1 (7.8-111.6)	5.5 (3.4-8.8)	<0.001
Urine data (n=58)]			
Age at date of sample	53.7 (43.3-61.7)	52.5 (46.8-62.9)	0.953
Free NE [µg/day]	75.0 (38.0-160.9)	20.6 (15.0-37.9)	<0.001
Free EPI [µg/day]	9.6 (2.8-34.6)	4.0 (2.3-5.9)	0.011
Free DA [µg/day]	217.1 (144.3-288.0)	218.5 (165.1-249.8)	0.767
Genetic screening (germline) [N=33]			
Unknown	3		
Wild type	24		
SDHB	2		
NF1	3		
VHL	1		
Antihypertensive medication, n (%)			
Alpha-blocker	14 (39)	10 (27)	
Beta-blocker	16 (44)	12 (33)	
Diuretics	5 (14)	5 (14)	
ACE-inhibitor/AT1-antagonist	10 (27)	8 (22)	
Calcium channel blocker	5 (14)	10 (27)	

Numerical variables data are represented as median with range (inter-quartile) in brackets. For categorical variables, absolute and percentage values are given.
AHT, arterial hypertension; BMI, body mass index; DA, dopamine; EPI, epinephrine; MN, metanephrine; MTY, 3-methoxytyramine; NE, norepinephrine; NMN, normetanephrine; PPGL, pheochromocytoma/paraganglioma.

alterations in three additional metabolites were present: Lyso PC a C16:1 showed lower levels in PPGL (1.68 [1.09-1.79] *vs.* 1.89 [1.54-2.16] µmol/l, p=0.025), whilst PC ae C30:2 and SM (OH) C14:1 had significantly higher levels compared to controls (0.07 [0.06-0.08] *vs.* 0.06 [0.06-0.07] µmol/l, p=0.040 and 4.77 [3.20-5.43] *vs.* 3.46 [2.59-4.38] µmol/l, p=0.040).

In the subgroup with BMI below or equal 25 kg/m^2 the PPGL patients (n=22) exhibited lower level of histidine (75.20 [64.35-85.90] *vs.* 87.50 [82.40-103.00] µmol/l, p=0.006) and higher level of H1 (4773.00 [4357.00-5311.50] *vs.* 4146.00 [3789.00-4428.00] µmol/l, p=0.003) than controls (n=15). In the subgroup with BMI above 25 kg/m^2 PPGL patients (n=12) had higher level of SM OH C22:1 (7.09 [5.49-8.29] *vs.* 5.88 [4.81-6.64] µmol/l, p=0.048) and SM OH C22:2 (5.66 [5.16-6.81] *vs.* 4.90 [3.94-5.51] µmol/l, p=0.036). Octadecenoylcarnitine (0.099 [0.088-0.131] *vs.* 0.135 [0.102-0.203] µmol/l, p=0.048), octadecadienylcarnitine 0.029 [0.023-0.034] *vs.* 0.035 [0.029-0.064] µmol/l, p=0.044) and histidine 71.10 [58.80-85.17] *vs.* 84.20 [71.50-93.80] µmol/l, p=0.036), were lower in PPGL patients than in controls (n=20), The same applies for ornithine (60.75 [54.10-71.30] *vs.* 92.60 [58.10-124.50] µmol/l, p=0.036) and threonine (98.85 [85.50-122.25] vs. 127.00 [93.33-153.50] µmol/l, p=0.036).

Female PPGL patients exhibited higher levels of lysoPC a C20:4 (3.95 [3.50-4.95] *vs.* 2.62 [2.44-3.54] µmol/l, p=0.006), PC aa C36:4 (203.00 [165.00-249.50] *vs.* 160.00 [124.00-211.00] µmol/l, p=0.041) and PC aa C38:4 (94.10 [77.35-107.00] *vs.* 82.60 [64.40-91.55] µmol/l, p=0.049) as well as lower values of PC ae C38:1 (0.37 [0.28-1.24] *vs.* 0.71 [0.47-1.69] µmol/l, p=0.022) and histidine (64.10 [56.70-78.30] *vs.* 85.90 [71.70-104.50] µmol/l, p=0.001).

Analyzing only the subgroup of adrenergic phenotypes, we found increased levels of glycin (221.00 [182.00-373.00] *vs.* 167.00 [145.00-192.00] µmol/l, p=0.007) and lysoPC a C20:4 (4.00 [3.37-5.18] *vs.* 3.10 [2.46-4.04] µmol/l, p=0.019] combined with decreased levels of lysoPC a C28:0 (0.11 [0.08-0.11] *vs.* 0.13 [0.11-0.14] µmol/l, p=0.026) in patients with PPGL compared to controls. Histidine, which had lower levels in the entire group as

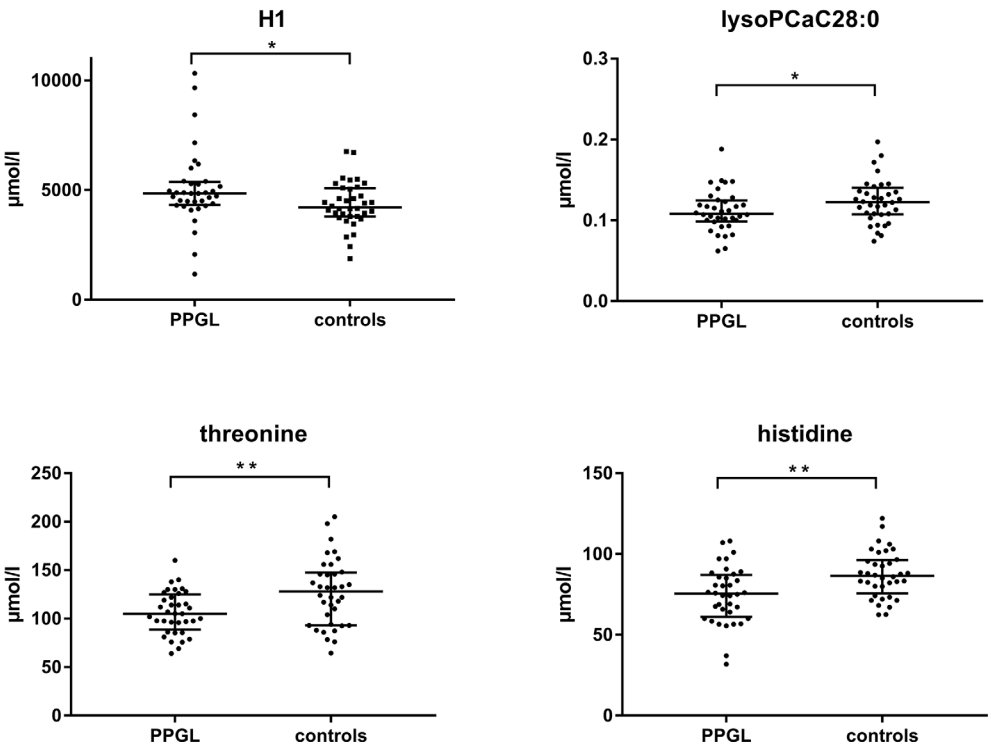

FIGURE 2 | Scatter plot of median plasma levels from metabolites measured by LC-MS/MS with significant differences between PPGL patients and controls. (Mann-Whitney-U-test, $p < 0.05$). H1, sum of hexoses; lysoPC, lysophosphatidylcholine; PPGL, pheochromocytoma and paraganglioma. *<0.05, **<0.01.

well as in females, showed also lower concentrations in adrenergic phenotypes (69.00 [58.40-76.10] *vs*. 85.10 [71.30-93.60] µmol/l, p=0.004). In PPGL with noradrenergic phenotype we found lower concentrations of C0 (35.60 [28.70-41.15] *vs*. 43.00 [34.05-48.70] µmol/l, p=0.042), asparagine (37.20 [32.00-41.95] *vs*. 42.00 [38.65-48.05] µmol/l, p=0.013), threonine (112.00 [96.20-127.50] *vs*. 133.00 [120.00-151.00] µmol/l, p=0.002) and ADMA (0.51 [0.39-0.80] *vs*. 0.62 [0.55-0.91] µmol/l, p=0.048).

Feature Selection Using Machine Learning Techniques and Principal Component Analysis

The machine learning models GBM, ELA, and SVM were run to determine features which are important to class prediction. Each of the models was run with 10-fold cross-validation on the training dataset, the features which contributed most to class prediction were obtained and the models were compared based on their estimated performance. The GBM, ELA and SVM had an estimated accuracy of 0.67, 0.53 and 0.53 respectively (Kappa: GBM 0.33, ELA 0.06 and SVM 0.08; **Figure 4A**). ELA and SVM selected 20 variables, whereas the GBM only selected 9 variables (**Figure 4B**). The GBM had the best estimated predictive value of which hexose showed the largest contribution to diagnosis, calculated using an out-of-bag estimate of the improvement in predictive performance. Comparing the selected variables, only H1 was shared between the 3 modelling algorithms. Furthermore, for GBM each of the selected variables was evaluated for difference (**Supplemental Data**), which found that only the H1 predictor has a significant difference between the two classes. Testing for the class prediction in the validation dataset showed limited predictive value for all models.

Similar analyses were also preformed to select predictors of catecholamine producing tumor types (pheo *vs*. PGL *vs*. control) phenotypes (adrenergic *vs*. noradrenergic *vs*. control) and malignancy (benign *vs*. malignant *vs*. control). The predictors that were selected in all these cases were the same as from the initial analysis, but further investigation of the distribution of the predictors showed a much weaker difference between the groups (diagnosis, phenotype and malignancy) when compared with the distribution between the difference classes (PPGL *vs*. control). GBM selected the same variables in each section (**Supplemental Data**). However, accuracy was always lower than 60%. The most commonly selected variable H1 showed difference between different analyses in phenotype p=0.10 between control and adrenergic/noradrenergic, but p=0.68 between the two states. In malignancy we calculated p=0.11 between benign and control and p=0.08 between benign and malignant, but p=0.76 between control and malignant.

The score plots obtained from principal component analysis models after logarithmic normalization of the entire dataset and subgroup (adrenergic, noradrenergic) demonstrated that the groups were not well discriminated (**Supplemental Data**).

TABLE 2 | Plasma levels of significant altered metabolites ($p \leq 0.05$) in patients with PPGL in comparison to controls including subgroup analysis and the correlation with free plasma metanephrines and 24h urinary free catecholamine excretion values.

	PPGL	Controls	P value	Correlations (Spearman r_s)						
				Plasma			Urine			
				NMN	MN	MTY	NE	EPI	DA	total catecholamine
All patients										
Histidine	75.40 (61.03-87.05)	86.40 (75.63-96.35)	0.004	**-0.287**	-0.219	**-0.242**	-0.239	**-0.408**	**-0.300**	**-0.407**
Threonine	105.00 (88.57-125.00)	128.00 (93.32-147.50)	0.008	-0.229	-0.054	**-0.266**	**-0.255**	**-0.304**	-0.161	**-0.275**
lysoPC a C28:0	0.11 (0.10-0.12)	0.12 (0.11-0.14)	0.044	-0.169	-0.147	-0.144	-0.212	-0.219	**-0.260**	**-0.269**
Hexose	4844.00 (4325.50-5364.50)	4215.50 (3791.00-5086.00)	0.018	**0.337**	**0.276**	**0.339**	**0.437**	0.145	-0.046	0.221
Males										
Threonine	102.00 (85.50-127.00)	132.00 (104.00-156.00)	0.008	**-0.328**	-0.206	-0.226	-0.269	**-0.345**	-0.085	-0.212
lysoPC a C16:1	1.68 (1.09-1.79)	1.89 (1.54-2.16)	0.025	-0.295	0.163	-0.147	-0.329	0.042	-0.102	-0.184
PC ae C30:2	0.07 (0.06-0.08)	0.06 (0.06-0.07)	0.040	0.244	-0.168	0.071	0.185	-0.181	-0.208	-0.040
SM (OH) C14:1	4.77 (3.20-5.43)	3.46 (2.59-4.38)	0.040	0.266	-0.157	-0.060	0.071	-0.151	-0.253	-0.084
Hexose	4845.00 (4489.00-5285.00)	4079.00 (3789.00-5131.00)	0.050	**0.381**	0,068	0.306	**0.425**	-0.020	-0.097	0.206
Females										
Histidine	64.10 (56.70-78.30)	85.90 (71.70-104.50)	0.001	**-0.428**	-0.339	-0.301	-0.364	**-0.434**	0.294	**-0.479**
lysoPC a C20:4	3.95 (3.50-4.95)	2.62 (2.44-3.54)	0.006	**0.471**	0.273	**0.438**	**0.537**	**0.412**	0.302	**0.538**
PC aa C36:4	203.00 (165.00-249.50)	160.00 (124.00-211.00)	0.041	**0.356**	**0.514**	**0.525**	0.117	0.022	-0.256	-0.123
PC aa C38:4	94.10 (77.35-107.00)	82.60 (64.40-91.55)	0.049	0.325	**0.535**	**0.508**	0.120	0.197	-0.093	0.002
PC ae C38:1	0.37 (0.28-1.24)	0.71 (0.47-1.69)	0.022	**-0.368**	**-0.474**	-0.137	-0.353	**-0.531**	-0.048	-0.048
Adrenergic										
Glycin	221.00 (182.00-373.00)	167.00 (145.00-192.00)	0.007	**0.464**	**0.490**	0.258	0.280	0.376	0.108	0.297
Histidine	69.00 (58.40-76.10)	85.10 (71.30-93.60)	0.004	**-0.597**	**-0.494**	**-0.535**	**-0.412**	**-0.499**	-0.315	**-0.459**
lysoPC a C20:4	3.99 (3.37-5.18)	3.10 (2.46-4.04)	0.019	0.353	0.317	0.082	**0.461**	**0.477**	0.087	0.283
LysoPC a C28:0	0.11 (0.08-0.11)	0.13 (0.11-0.14)	0.026	**-0.371**	-0.236	-0.336	-0.345	-0.327	-0.211	-0.297
Noradrenergic										
C0	35.60 (28.70-41.15)	43.00 (34.05-48.70)	0.042	-0.226	0.201	-0.234	-0.114	-0.089	-0.342	-0.290
Asparagine	37.20 (32.00-41.95)	42.00 (38.65-48.05)	0.013	-0.252	0.129	-0.124	-0.254	-0.060	-0.116	-0.193
Threonine	112.00 (96.20-127.50)	133.00 (120.00-151.00)	0.002	**-0.344**	0.064	**-0.351**	**-0.472**	-0.199	-0.307	**-0.494**
ADMA	0.51 (0.39-0.80)	0.62 (0.55-0.91)	0.048	-0.258	-0.041	-0.132	**-0.399**	-0.029	-0.001	-0.195

Plasma levels of significant altered metabolites are given in µmol/l. Metabolomics data is expressed as median with range (inter-quartile) in brackets. Mann-Whitney-U test was performed, and p-values (two-tailed) are reported. The r_s-value represents the Spearman correlation coefficient. Significant correlations are marked bold.
DA, dopamine; EPI, epinephrine; MN, metanephrine; MTY, 3-methoxytyramine; NE, norepinephrine; NMN, normetanephrine; PHEO, pheochromocytoma; PGL, paraganglioma; PPGL, pheochromocytoma/paraganglioma.

DISCUSSION

In our study 36 PPGL patients and matched controls were analyzed with targeted metabolomics. Despite the highly standardized sampling conditions and quantitative liquid chromatography-tandem mass spectrometry, we only found metabolites with significant differences between PPGL patients and matched controls when no correction for FDR was performed. After correction for multiple comparisons, the statistical significance was not retained for all metabolites. Classifying substances as significant without FDR-correction was reasonable in our preliminary setting as the focus was to identify potentially relevant metabolites, which have to be validated in further studies. In this approach it may be preferable to explore leads that may turn out to be wrong than loosing promising markers in early state by stringent statistical criteria, as has been argued by others (27). By using machine learning, we failed to establish metabolic signatures associated with PPGL diagnosis, indicating little value of such targeted metabolomics approach for diagnostic purposes in PPGL at variance to plasma metanephrin, normetanephrin and 3-methoxytyramin which have proven excellent sensitivity and specificity when performed with appropriate preanalytics, analytics and reference intervals.

It is well known that catecholamine excess leads to a diabetogenic state (15, 28–30) and we accordingly found higher levels of hexoses in PPGL patients. This reflects increased glycogen catabolism, glucagon release and gluconeogenesis finally leading to the high prevalence of diabetes mellitus (21-37%) in PPGL patients.

Erlic et al. compared the same metabolite spectrum in PPGL patients before and post-surgery and found lower histidine levels in preoperative samples (15). A low histidine level is linked to type 2 diabetes, increased inflammation and cardiovascular disease (31–33), potentially explaining (at least in part) such effects in PPGL patients (31–34).

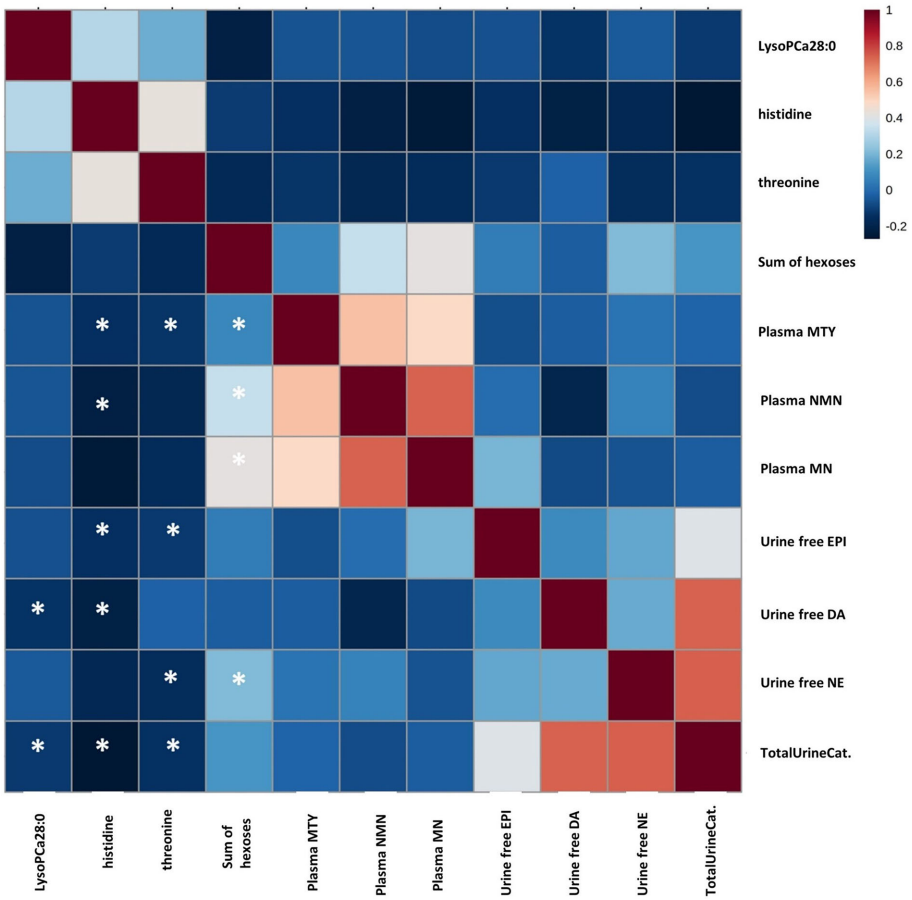

FIGURE 3 | Correlation between plasma concentrations of metanephrine, normetanephrine, and methoxytyramine, 24h urine concentrations of catecholamines, and plasma concentrations of significantly altered metabolites in PPGL patients. Spearmen-coefficient r_s is presented by color coding (positive correlation: red; negative correlation: blue). An Asterisk indicates a statistically significant correlation at the level of ($p < 0.05$). DA, dopamine; EPI, epinephrine; MN, metanephrine; MTY, methoxytyramine; NE, norepinephrine; TotalUrineCat, Total urine catecholamines.

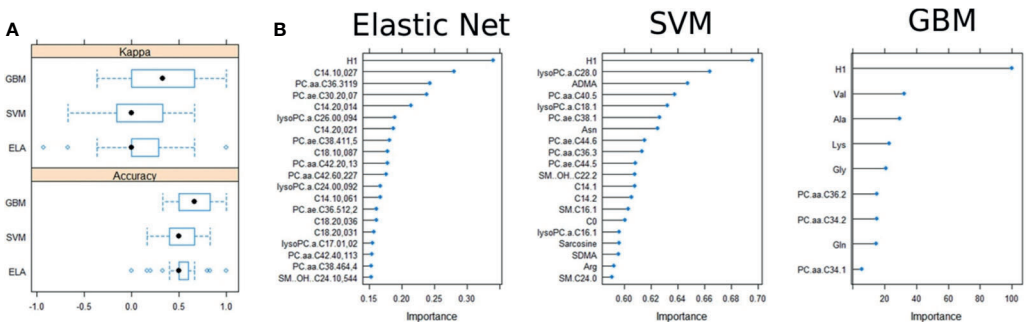

FIGURE 4 | Variable selection in the training dataset. **(A)** Accuracy and Kappa comparisons of the three models used in feature selection. **(B)** Importance of the variable selection and out-of-bag predictive performance estimation.

The negative correlation of histidine with plasma NMN and MTY, urine free EPI and DA in our cohort suggests a catabolic phenotype which has been linked to proinflammatory mediators as well (35). In this regard it is noteworthy that BMI was significantly lower in patients compared to controls. While one may argue that this reflects an imbalance in the matching of base line characteristics, it may rather reflect the catabolic effect of PPGL.

Sex specific differences in metabolic pattern found by Erlic et al. by comparing intra-individual metabolite profiles prior and after surgical tumor removal were confirmed here even if the results should be treated with caution due to the small number of patients in the subgroups (15).

Significant changes between PPGL and controls observed in threonine and histidine are in accordance with other studies that focused on cancer (36, 37). For example, Miyagi et al. also showed decreased levels of histidine in patients with gastric, colorectal, lung and breast cancer, while threonine was lower in gastric as well as colorectal cancer and higher in bronchial carcinoma. The mechanistic background and clinical significance are still subject of discussion (37).

ML approaches imply the need for a substantial amount of data for the development of clinical useful diagnostic models, thus limits the application potential in rare diseases such as PPGL. We overcome this by combining statistical correlation analysis with 3 different feature selection algorithm and applied several validation steps such as data splitting and 10-fold cross-validation on a non-linear and large dimensional variable (130 metabolites) dataset (38). However, even the best performing model (GBM with 9 selected metabolites) showed low predictive values within the test dataset. The GBM model shows a higher sensitivity (87.5%) compared to the other models but was outperformed by ELA and SVM in terms of specificity. Given the low accuracy and no significant p-value, the models show low ability to distinguish between PPGL and control. Similarly, model selection based on diagnosis, phenotype and malignancy predictors showed a much weaker difference between the groups (accuracy always <60%). Given the small size of the disease subsets and the poor significance found in the distributions between each group subset, the confidence with which the features can be used to differentiate between the different group subsets was limited.

It might be argued that a larger study has enabled us to identify a distinct phenotype using ML-based selection approaches which then could possibly include a larger number of features under study. We do not share this point of view because any test applied in PPGL for diagnostic purposes requires a much higher sensitivity and specificity compared to that found in our pilot study to be clinically meaningful. This is particularly true when the generally low pre-test likelihood of a PPGL and the prevalence of diabetes and catabolism in an unselected population is considered. Consequently, a further analysis of the total cohort of the PMT study regarding this pilot study does not seem reasonable.

PPGL-associated mutations in genes involved in the Krebs cycle and electron transport chain have shown to translate into characteristic tumoral metabolic changes (39). Tumors caused by mutations in the SDH genes that belong to this cluster 1 tumors exhibit an increased succinate fumarate ratio in tumor tissue (23, 40, 41) which leads to a pseudo-hypoxic phenotype that downstream activates hypoxia induced factor signaling and angiogenesis.

Recently, Wallace et al. showed that assessment of Krebs cycle related metabolites by using LC-MS/MS in addition to immunohistochemistry improved the diagnosis of SDH impairment at a functional level (42). These tumoral metabolic pathway alterations translate into characteristic secretory pattern of catecholamine metabolites which contribute to the diagnosis of malignancy (39, 43–46). Of note, they also appear to have therapeutic relevance (39, 43–45).

Taken together, we confirmed previous findings of metabolic alterations caused by PPGL related catecholamine excess by comparing PPGL patients and controls. We applied machine learning algorithms, but these failed to provide feature-selection signatures that may be useful for PPGL diagnosis in clinical routine. Still, our study broadens and complements the understanding of changes in the metabolic profile of patients with PPGL.

DATA AVAILABILITY STATEMENT

The raw data supporting the conclusions of this article will be made available by the authors, without undue reservation.

ETHICS STATEMENT

The studies involving human participants were reviewed and approved by Ethics committee of the Medical Faculty, University of Würzburg. Written informed consent to participate in this study was obtained from all study participants and, in the case of minors, from their legal representatives.

AUTHOR CONTRIBUTIONS

JM: Data acquisition, data analysis, data interpretation, and writing of first paper draft. MK: Conception of the work, data acquisition, data analysis, writing of first paper draft, and revising the work critically for important intellectual content. OR-L: Data analysis, data interpretation, writing of first paper draft, and revising the work. TD: Data interpretation and revising the work critically for important intellectual content. MP: Data acquisition, data analysis, data interpretation, and revising the work critically for important intellectual content. CP: Data acquisition and revising the work critically for important intellectual content. DW: Revising the work critically for important intellectual content. MR: Data acquisition and revising the work critically for important intellectual content. JA: Data acquisition and revising the work critically for important intellectual content. MF: Planning and design of the work and revising the work critically for important intellectual content. MKu: Data analysis, data interpretation, and drafting and revising it critically for important intellectual content. MKr: Conception, planning and design of the work, data analysis, data interpretation, drafting and revising it critically for important intellectual content, important intellectual content. MKu and MKr contributed equally to this study. All authors contributed to the article and approved the submitted version.

FUNDING

This work was supported by the German Research Council (DFG) project 314061271 (SFB/CRC Transregio 205: The adrenal – central relay in health and disease).

ACKNOWLEDGMENTS

We thank Sabine Kendl for expert technical assistance. Funding by the German Federal Ministry of Education and Research (BMBF) is acknowledged (CompLS program grant 031L0262C and Era-Net grant 01KT1801 to MKu). OR-L acknowledges the Schickedanz Kinderkrebsstiftung.

SUPPLEMENTARY MATERIAL

The Supplementary Material for this article can be found online at: https://www.frontiersin.org/articles/10.3389/fendo.2021.722656/full#supplementary-material

REFERENCES

1. Lenders JW, Eisenhofer G, Mannelli M, Pacak K. Phaeochromocytoma. *Lancet* (2005) 366(9486):665–75. doi: 10.1016/S0140-6736(05)67139-5
2. Eisenhofer G, Prejbisz A, Peitzsch M, Pamporaki C, Masjkur J, Rogowski-Lehmann N, et al. Biochemical Diagnosis of Chromaffin Cell Tumors in Patients at High and Low Risk of Disease: Plasma Versus Urinary Free or Deconjugated O-Methylated Catecholamine Metabolites. *Clin Chem* (2018) 64(11):1646–56. doi: 10.1373/clinchem.2018.291369
3. Whalen RK, Althausen AF, Daniels GH. Extra-Adrenal Pheochromocytoma. *J Urol* (1992) 147(1):1–10. doi: 10.1016/S0022-5347(17)37119-7
4. Lenders JWM, Eisenhofer G. Update on Modern Management of Pheochromocytoma and Paraganglioma. *Endocrinol Metab (Seoul)* (2017) 32(2):152–61. doi: 10.3803/EnM.2017.32.2.152
5. Lenders JWM, Kerstens MN, Amar L, Prejbisz A, Robledo M, Taieb D, et al. Genetics, Diagnosis, Management and Future Directions of Research of Phaeochromocytoma and Paraganglioma: A Position Statement and Consensus of the Working Group on Endocrine Hypertension of the European Society of Hypertension. *J Hypertens* (2020) 38(8):1443–56. doi: 10.1097/HJH.0000000000002438
6. Favier J, Amar L, Gimenez-Roqueplo AP. Paraganglioma and Phaeochromocytoma: From Genetics to Personalized Medicine. *Nat Rev Endocrinol* (2015) 11(2):101–11. doi: 10.1038/nrendo.2014.188
7. Dahia PL. Pheochromocytoma and Paraganglioma Pathogenesis: Learning From Genetic Heterogeneity. *Nat Rev Cancer* (2014) 14(2):108–19. doi: 10.1038/nrc3648
8. Plouin PF, Amar L, Dekkers OM, Fassnacht M, Gimenez-Roqueplo AP, Lenders JW, et al. European Society of Endocrinology Clinical Practice Guideline for Long-Term Follow-Up of Patients Operated on for a Phaeochromocytoma or a Paraganglioma. *Eur J Endocrinol* (2016) 174(5): G1–G10. doi: 10.1530/EJE-16-0033
9. Geroula A, Deutschbein T, Langton K, Masjkur J, Pamporaki C, Peitzsch M, et al. Pheochromocytoma and Paraganglioma: Clinical Feature-Based Disease Probability in Relation to Catecholamine Biochemistry and Reason for Disease Suspicion. *Eur J Endocrinol* (2019) 181(4):409–20. doi: 10.1530/EJE-19-0159
10. Rao D, Peitzsch M, Prejbisz A, Hanus K, Fassnacht M, Beuschlein F, et al. Plasma Methoxytyramine: Clinical Utility With Metanephrines for Diagnosis of Pheochromocytoma and Paraganglioma. *Eur J Endocrinol* (2017) 177 (2):103–13. doi: 10.1530/EJE-17-0077
11. Eisenhofer G. Screening for Pheochromocytomas and Paragangliomas. *Curr Hypertens Rep* (2012) 14(2):130–7. doi: 10.1007/s11906-012-0246-y
12. Weismann D, Peitzsch M, Raida A, Prejbisz A, Gosk M, Riester A, et al. Measurements of Plasma Metanephrines by Immunoassay vs Liquid Chromatography With Tandem Mass Spectrometry for Diagnosis of Pheochromocytoma. *Eur J Endocrinol* (2015) 172(3):251–60. doi: 10.1530/EJE-14-0730
13. Murakami M, Sun N, Greunke C, Feuchtinger A, Kircher S, Deutschbein T, et al. Mass Spectrometry Imaging Identifies Metabolic Patterns Associated With Malignant Potential in Pheochromocytoma and Paraganglioma. *Eur J Endocrinol* (2021) 185(1):179–91. doi: 10.1530/EJE-20-1407
14. Patti GJ, Yanes O, Siuzdak G. Innovation: Metabolomics: The Apogee of the Omics Trilogy. *Nat Rev Mol Cell Biol* (2012) 13(4):263–9. doi: 10.1038/nrm3314
15. Erlic Z, Kurlbaum M, Deutschbein T, Nolting S, Prejbisz A, Timmers H, et al. Metabolic Impact of Pheochromocytoma/Paraganglioma: Targeted Metabolomics in Patients Before and After Tumor Removal. *Eur J Endocrinol* (2019) 181(6):647–57. doi: 10.1530/EJE-19-0589
16. Galetta F, Franzoni F, Bernini G, Poupak F, Carpi A, Cini G, et al. Cardiovascular Complications in Patients With Pheochromocytoma: A Mini-Review. *BioMed Pharmacother* (2010) 64(7):505–9. doi: 10.1016/j.biopha.2009.09.014
17. Peitzsch M, Prejbisz A, Kroiss M, Beuschlein F, Arlt W, Januszewicz A, et al. Analysis of Plasma 3-Methoxytyramine, Normetanephrine and Metanephrine by Ultraperformance Liquid Chromatography-Tandem Mass Spectrometry: Utility for Diagnosis of Dopamine-Producing Metastatic Phaeochromocytoma. *Ann Clin Biochem* (2013) 50(Pt 2):147–55. doi: 10.1258/acb.2012.012112
18. Peitzsch M, Pelzel D, Glockner S, Prejbisz A, Fassnacht M, Beuschlein F, et al. Simultaneous Liquid Chromatography Tandem Mass Spectrometric Determination of Urinary Free Metanephrines and Catecholamines, With Comparisons of Free and Deconjugated Metabolites. *Clin Chim Acta* (2013) 418:50–8. doi: 10.1016/j.cca.2012.12.031
19. Peitzsch M, Adaway JE, Eisenhofer G. Interference From 3-O-Methyldopa With Ultra-High Performance LC-MS/MS Measurements of Plasma Metanephrines: Chromatographic Separation Remains Important. *Clin Chem* (2015) 61(7):993–6. doi: 10.1373/clinchem.2015.239962
20. Zukunft S, Sorgenfrei M, Prehn C, Moller G, Adamski J. Targeted Metabolomics of Dried Blood Spot Extracts. *Chromatographia* (2013) 76 (19-20):1295–305. doi: 10.1007/s10337-013-2429-3
21. Siskos AP, Jain P, Romisch-Margl W, Bennett M, Achaintre D, Asad Y, et al. Interlaboratory Reproducibility of a Targeted Metabolomics Platform for Analysis of Human Serum and Plasma. *Anal Chem* (2017) 89(1):656–65. doi: 10.1021/acs.analchem.6b02930
22. Curras-Freixes M, Pineiro-Yanez E, Montero-Conde C, Apellaniz-Ruiz M, Calsina B, Mancikova V, et al. Pheoseq: A Targeted Next-Generation Sequencing Assay for Pheochromocytoma and Paraganglioma Diagnostics. *J Mol Diagn* (2017) 19(4):575–88. doi: 10.1016/j.jmoldx.2017.04.009
23. Richter S, Gieldon L, Pang Y, Peitzsch M, Huynh T, Leton R, et al. Metabolome-Guided Genomics to Identify Pathogenic Variants in Isocitrate Dehydrogenase, Fumarate Hydratase, and Succinate Dehydrogenase Genes in Pheochromocytoma and Paraganglioma. *Genet Med* (2019) 21(3):705–17. doi: 10.1038/s41436-018-0106-5
24. Pamporaki C, Hamplova B, Peitzsch M, Prejbisz A, Beuschlein F, Timmers H, et al. Characteristics of Pediatric vs Adult Pheochromocytomas and Paragangliomas. *J Clin Endocrinol Metab* (2017) 102(4):1122–32. doi: 10.1210/jc.2016-3829
25. Xia J, Psychogios N, Young N, Wishart DS. Metaboanalyst: A Web Server for Metabolomic Data Analysis and Interpretation. *Nucleic Acids Res* (2009) 37 (Web Server issue):W652–60. doi: 10.1093/nar/gkp356
26. Benjamini Y, Drai D, Elmer G, Kafkafi N, Golani I. Controlling the False Discovery Rate in Behavior Genetics Research. *Behav Brain Res* (2001) 125(1-2):279–84. doi: 10.1016/S0166-4328(01)00297-2
27. Rothman KJ. No Adjustments Are Needed for Multiple Comparisons. *Epidemiology* (1990) 1(1):43–6. doi: 10.1097/00001648-199001000-00010
28. Leroy ED, James JR, Semans H, Howard JE. Adrenal Medullary Tumor (Pheochromocytoma) and Diabetes Mellitus; Disappearance of Diabetes

After Removal of the Tumor. *Ann Internal Med* (1944) 20(5):815–21. doi: 10.003-4819-20-5-815
29. McCullagh EP, Engel WJ. Pheochromocytoma With Hypermetabolism: Report of Two Cases. *Ann Surg* (1942) 116(1):61–75. doi: 10.1097/00000658-194207000-00008
30. Mesmar B, Poola-Kella S, Malek R. The Physiology Behind Diabetes Mellitus in Patients With Pheochromocytoma: A Review of the Literature. *Endocrine Pract* (2017) 23(8):999–1005. doi: 10.4158/EP171914.RA
31. Du SS, Sun SH, Liu L, Zhang Q, Guo FC, Li CL, et al. Effects of Histidine Supplementation on Global Serum and Urine H-1 NMR-Based Metabolomics and Serum Amino Acid Profiles in Obese Women From a Randomized Controlled Study. *J Proteome Res* (2017) 16(6):2221–30. doi: 10.1021/acs.jproteome.7b00030
32. Mong MC, Chao CY, Yin MC. Histidine and Carnosine Alleviated Hepatic Steatosis in Mice Consumed High Saturated Fat Diet. *Eur J Pharmacol* (2011) 653(1-3):82–8. doi: 10.1016/j.ejphar.2010.12.001
33. Hasegawa S, Ichiyama T, Sonaka I, Ohsaki A, Okada S, Wakiguchi H, et al. Cysteine, Histidine and Glycine Exhibit Anti-Inflammatory Effects in Human Coronary Arterial Endothelial Cells. *Clin Exp Immunol* (2012) 167(2):269–74. doi: 10.1111/j.1365-2249.2011.04519.x
34. Bosanska L, Petrak O, Zelinka T, Mraz M, Widimsky J, Haluzik M. The Effect of Pheochromocytoma Treatment on Subclinical Inflammation and Endocrine Function of Adipose Tissue. *Physiol Res* (2009) 58(3):319–25. doi: 10.33549/physiolres.931483
35. Torres KCL, Antonelli LRV, Souza ALS, Teixeira MM, Dutra WO, Gollob KJ. Norepinephrine, Dopamine and Dexamethasone Modulate Discrete Leukocyte Subpopulations and Cytokine Profiles From Human PBMC. *J Neuroimmunol* (2005) 166(1-2):144–57. doi: 10.1016/j.jneuroim.2005.06.006
36. Kobayashi T, Nishiumi S, Ikeda A, Yoshie T, Sakai A, Matsubara A, et al. A Novel Serum Metabolomics-Based Diagnostic Approach to Pancreatic Cancer. *Cancer Epidemiol Biomarkers Prev* (2013) 22(4):571–9. doi: 10.1158/1055-9965.EPI-12-1033
37. Miyagi Y, Higashiyama M, Gochi A, Akaike M, Ishikawa T, Miura T, et al. Plasma Free Amino Acid Profiling of Five Types of Cancer Patients and Its Application for Early Detection. *PloS One* (2011) 6(9). doi: 10.1371/journal.pone.0024143
38. Vey J, Kapsner LA, Fuchs M, Unberath P, Veronesi G, Kunz M. A Toolbox for Functional Analysis and the Systematic Identification of Diagnostic and Prognostic Gene Expression Signatures Combining Meta-Analysis and Machine Learning. *Cancers (Basel)* (2019) 11(10). doi: 10.3390/cancers11101606
39. Buffet A, Burnichon N, Favier J, Gimenez-Roqueplo AP. An Overview of 20 Years of Genetic Studies in Pheochromocytoma and Paraganglioma. *Best Pract Res Clin Endocrinol Metab* (2020) 34(2). doi: 10.1016/j.beem.2020.101416
40. Lendvai N, Pawlosky R, Bullova P, Eisenhofer G, Patocs A, Veech RL, et al. Succinate-to-Fumarate Ratio as a New Metabolic Marker to Detect the Presence of SDHB/D-Related Paraganglioma: Initial Experimental and Ex Vivo Findings. *Endocrinology* (2014) 155(1):27–32. doi: 10.1210/en.2013-1549
41. Richter S, Peitzsch M, Rapizzi E, Lenders JW, Qin N, de Cubas AA, et al. Krebs Cycle Metabolite Profiling for Identification and Stratification of Pheochromocytomas/Paragangliomas Due to Succinate Dehydrogenase Deficiency. *J Clin Endocrinol Metab* (2014) 99(10):3903–11. doi: 10.1210/jc.2014-2151
42. Wallace PW, Conrad C, Bruckmann S, Pang Y, Caleiras E, Murakami M, et al. Metabolomics, Machine Learning and Immunohistochemistry to Predict Succinate Dehydrogenase Mutational Status in Phaeochromocytomas and Paragangliomas. *J Pathol* (2020) 251(4):378–87. doi: 10.1002/path.5472
43. Tevosian SG, Ghayee HK. Pheochromocytomas and Paragangliomas. *Endocrinol Metab Clinics North America* (2019) 48(4):727–50. doi: 10.1016/j.ecl.2019.08.006
44. Matlac DM, Vanova KH, Bechmann N, Richter S, Folberth J, Ghayee HK, et al. Succinate Mediates Tumorigenic Effects via Succinate Receptor 1: Potential for New Targeted Treatment Strategies in Succinate Dehydrogenase Deficient Paragangliomas. *Front Endocrinol* (2021) 12:129. doi: 10.3389/fendo.2021.589451
45. Fankhauser M, Bechmann MN, Lauseker M, Goncalves J, Favier J, Klink B, et al. Synergistic Highly Potent Targeted Drug Combinations in Different Pheochromocytoma Models Including Human Tumor Cultures. *Endocrinology* (2019) 160(11):2600–17. doi: 10.1210/en.2019-00410
46. Eisenhofer G, Klink B, Richter S, Lenders JW, Robledo M. Metabologenomics of Phaeochromocytoma and Paraganglioma: An Integrated Approach for Personalised Biochemical and Genetic Testing. *Clin Biochem Rev* (2017) 38(2):69–100.

Conflict of Interest: The authors declare that the research was conducted in the absence of any commercial or financial relationships that could be construed as a potential conflict of interest.

Publisher's Note: All claims expressed in this article are solely those of the authors and do not necessarily represent those of their affiliated organizations, or those of the publisher, the editors and the reviewers. Any product that may be evaluated in this article, or claim that may be made by its manufacturer, is not guaranteed or endorsed by the publisher.

frontiers in Endocrinology

CASE REPORT
published: 19 October 2021
doi: 10.3389/fendo.2021.760154

New Regions With Molecular Alterations in a Rare Case of Insulinomatosis: Case Report With Literature Review

Kirill Anoshkin[1], Ivan Vasilyev[2], Kristina Karandasheva[1], Mikhail Shugay[3,4,5], Valeriya Kudryavtseva[1,3], Alexey Egorov[2], Larisa Gurevich[6], Anna Mironova[2], Alexey Serikov[2], Sergei Kutsev[1] and Vladimir Strelnikov[1]*

[1] Laboratory of Epigenetics, Research Centre for Medical Genetics, Moscow, Russia, [2] I.M. Sechenov First Moscow State Medical University, Moscow, Russia, [3] Pirogov Russian National Research Medical University, Moscow, Russia, [4] Shemyakin-Ovchinnikov Institute of Bioorganic Chemistry, Russian Academy of Science, Moscow, Russia, [5] Privolzhsky Research Medical University, Nizhny Novgorod, Russia, [6] Morphological Department of Oncology, M.F. Vladimirsky Moscow Regional Research and Clinical Institute, Moscow, Russia

OPEN ACCESS

Edited by:
Antongiulio Faggiano, Sapienza University of Rome, Italy

Reviewed by:
Jean-Yves Scoazec, Institut Gustave Roussy, France
Giovanni Vitale, University of Milan, Italy

***Correspondence:**
Kirill Anoshkin
anoshkinki@gmail.com

Specialty section:
This article was submitted to Cancer Endocrinology, a section of the journal Frontiers in Endocrinology

Received: *17 August 2021*
Accepted: *28 September 2021*
Published: *19 October 2021*

Citation:
Anoshkin K, Vasilyev I, Karandasheva K, Shugay M, Kudryavtseva V, Egorov A, Gurevich L, Mironova A, Serikov A, Kutsev S and Strelnikov V (2021) New Regions With Molecular Alterations in a Rare Case of Insulinomatosis: Case Report With Literature Review. Front. Endocrinol. 12:760154. doi: 10.3389/fendo.2021.760154

Insulinomatosis is characterized by monohormonality of multiple macro-tumors and micro-tumors that arise synchronously and metachronously in all regions of the pancreas, and often recurring hypoglycemia. One of the main characteristics of insulinomatosis is the presence of insulin-expressing monohormonal endocrine cell clusters that are exclusively composed of proliferating insulin-positive cells, are less than 1 mm in size, and show solid islet-like structure. It is presumed that insulinomatosis affects the entire population of β-cells. With regards to molecular genetics, this phenomenon is not related to mutation in *MEN1* gene and is more similar to sporadic benign insulinomas, however, at the moment molecular genetics of this disease remains poorly investigated. NGS sequencing was performed with a panel of 409 cancer-related genes. Results of sequencing were analyzed by bioinformatic algorithms for detecting point mutations and copy number variations. DNA copy number variations were detected that harbor a large number of genes in insulinoma and fewer genes in micro-tumors. qPCR was used to confirm copy number variations at *ATRX*, *FOXL2*, *IRS2* and *CEBPA* genes. Copy number alterations involving *FOXL2*, *IRS2*, *CEBPA* and *ATRX* genes were observed in insulinoma as well as in micro-tumors samples, suggesting that alterations of these genes may promote malignization in the β-cells population.

Keywords: neuroendocrine tumors, FOXL2, IRS2, CEBPA, copy number variation, insulinomatosis

INTRODUCTION

Multiple insulinomas are most common in MEN1 syndrome, however, several studies show that they can also occur sporadically, albeit very rarely, and are referred to insulinomatosis (1–3). Term "insulinomatosis" was introduced and described by Anlauf et al. (1). It is characterized by monohormonality of multiple macrotumors and microtumors that arise synchronously and

metachronously in all regions of the pancreas, rare of metastases, and often recurring hypoglycemia. In addition, one of the main characteristics of insulinomatosis is the presence of insulin-expressing monohormonal endocrine cell clusters that are exclusively composed of proliferating insulin-positive cells, are less than 1 mm in size, and show solid islet-like structure. Authors suggested that insulinomatosis affects the entire population of β-cells (1, 2). With regards to molecular genetics, this phenomenon is not related to mutation in *MEN1* gene and is more similar to sporadic benign insulinomas, however, large-scale molecular genetic studies on this disease have not yet been carried out (1). Here we present a very rare case of insulinomatosis in a patient with hypoglycemia syndrome and without known hereditary syndromes.

CASE PRESENTATION

A male in his 60s with clinical signs of hypoglycemia was admitted to the surgical department of Sechenov University. The patient signed informed agreement to undergo diagnostic procedures and treatment, as well as to participate in the study, and for the presentation of clinical and molecular data in scientific and medical literature. This case report was approved by the local Ethics Committee at the Research Centre for Medical Genetics, Moscow, Russia.

The history of the disease is about 6 years with fasting serum glucose 2.7-3.7 mmol/l compensated by sugar intake. The 72-hour fasting test was negative. The past medical history is significant for combination treatment for laryngeal carcinoma T2N0M0, stage II. Currently there are no signs of recurrence. CT scan of the abdomen shows heterogeneous hypervascular soft tissue mass up to 26 mm suspicious for neuroendocrine tumor (NET), located within the tail of the pancreas, with a well-defined cystic component attached to the splenic artery and vein without invasion. Hypervascular lesions of up to 5 mm without clear borders are detected within the surrounding parenchyma of the pancreatic tail.

Treatment

Based on the obtained diagnostic data, the multidisciplinary board was held, implying the participation of surgical oncologist, medical oncologist, pathologist and radiation oncologist. Taking into account tumor size more than 2 cm and hypoglycemia syndrome radical pancreatic resection was planned. A distal spleen-preserving pancreatectomy was performed.

Outcome

Taking into account multiple microadenomas in the pancreatic parenchyma the recurrence rate of the hyperinsulinemic hypoglycemia is relatively high. Thus, patient is examined every 3-6 month. In our case there are no signs of hypoglycemia and no pancreatic tumors on imaging during 30 months of follow-up by CT and PET-CT scanning.

Microscopy and Immunohistochemistry

Microscopic examination showed well differentiated neuroendocrine tumor with 2 mitoses and no necrosis in 10 HPF. There are multiple large microadenomas in the surrounding pancreatic tissue. Tumor cells are positive for synaptophysin and chromogranin A, as well as for insulin (**Figures 1A, B**). There is no expression of glucagon, somatostatin and pancreatic polypeptide. Ki-67 is less than 1.5%, Grade 1. The cells of microadenomas express insulin and are negative for glucagon and somatostatin (**Figures 1C, D**).

MATERIALS AND METHODS

DNA Extraction

Macrodissection of tumors was performed under guidance of pathologist. DNA was extracted from four formalin-fixed, paraffin-embedded (FFPE) tumor tissues by using GeneRead DNA FFPE kit (Qiagen, Germany), and from whole peripheral blood by using standard phenol-chloroform extraction protocol. One tumor sample was insulinoma, three others were small proliferative insulin-expressing monohormonal endocrine cell clusters (IMECCs).

NGS Sequencing

Next generation sequencing (NGS) was performed by using Ion AmpliSeq targeted amplification technology with AmpliSeq Comprehensive Cancer Panel (Thermo Fisher Scientific, United States) with exon coverage of 409 oncogenes and tumor suppressor genes.

Bioinformatic Analysis

The bioinformatic workflow for sequencing data analysis was based on Torrent Suite software (version 5.10.1). Annotation was performed by ANNOVAR (4). CNVs were called using CNVpanelizer R package (version 1.22.0) ran with default parameters (5). Putative CNV status is assigned when there is a significant difference between observed copy number and the one expected from the bootstrapped distribution. A reliable CNV is called when the upper bound of the copy number ratio is below the lower bound of background (noise) copy number for deletion or when the lower bound of the copy number ratio is above the upper bound of background (noise) copy number for amplification.

Sanger Sequencing

Sanger sequencing was performed for detection of the Trp372Arg mutation in *YY1* gene. PCR was performed in 25 μl reactions. The reaction mixture for PCR consisted of the following reagents: 8% glycerol, 68 mM Tris-HCl with pH 8.3, 17 mM $(NH_4)_2SO_4$, 0.01% Tween-20, 0.1 mg/ml BSA, 0.2 mM each dNTP, 1.5 units Taq polymerase, 0.12 pM each primer, 2.5 mM $MgCl_2$. On top, 40-60 μl of mineral oil was layered. PCR reaction was performed with the following parameters: 95°C for 5 min, followed by 30 cycles of 95°C for 40 seconds, 61°C for 40 seconds and 72°C for 40 seconds. Final elongation was at 72°C for 5 minutes. Sanger sequencing was performed on ABI3500 according to the manufacturer's protocol (Thermo Fisher, USA). Sequencing results were analyzed in Chromas software and compared to GenBank database using the BLAST algorithm. Primer sequences for Trp372Arg are listed in **Table 1**.

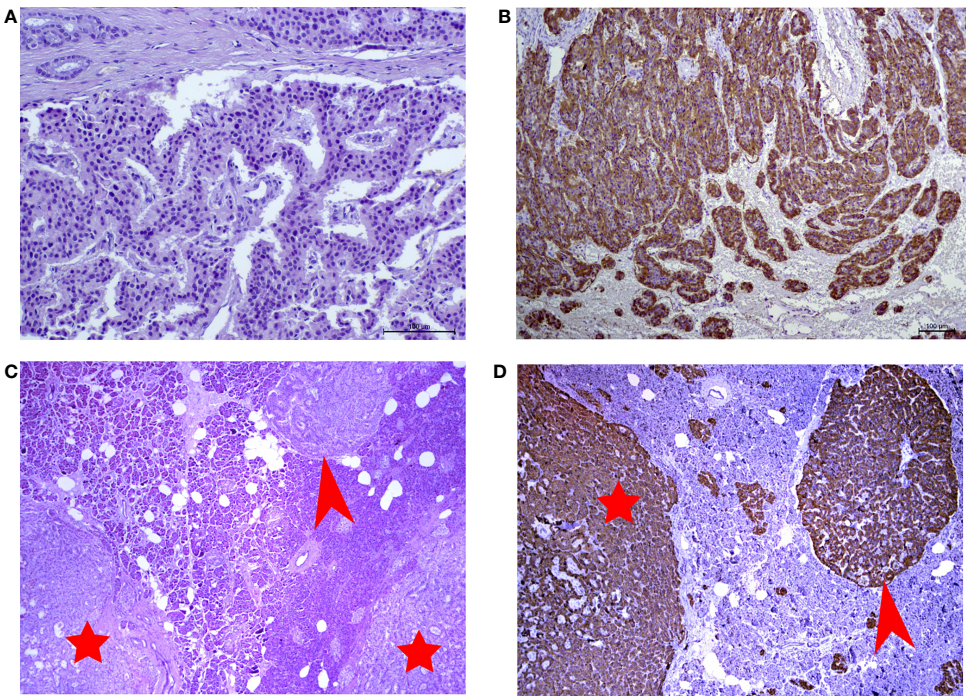

FIGURE 1 | **(A)** Hematoxylin and eosin (H&E)-stained slide of insulinoma (x250 magnification). **(B)** Immunohistochemical reaction with antibodies to insulin in insulinoma (x125 magnification). **(C)** Hematoxylin and eosin (H&E)-stained slide of microtumors (x10 magnification). **(D)** Immunohistochemical reaction with antibodiesto insulin in microadenoma (x10 magnification). Red arrows point to insulin-producing microadenomas. Red stars indicate the microtumors.

TABLE 1 | Primer sequences for Trp372Arg and qPCR confirmations (genome assembly GRCh37/hg19).

Amplicon name	Forward primer	Reverse primer
	Primers for Trp372Arg in YY1 gene	
Y1_372	GGGTCTGGTCAGAGTTGCTG	CCATCGAAGGGGCACACATA
	Primers for qPCR	
B2M	TGCTGTCTCCATGTTTGATGTATCT	TCTCTGCTCCCCACCTCTAAGT
ATRXex1	TGTCGGCTTCTGTGATTGCT	TTTGAGCTGTGGGGAGGTTC
ATRXex9	CTTTCCCCGCCTGAGTCTTT	GGTGAGCAGGATGAGTCACA
CEBPA	ACAAACAAGGCTGAGGGTCC	GTGGGTCAGCTCTGAGGATG
IRS2ex1	GTTGAGGTAGTCCCCGTTGG	GAGGACAGTGGGTACATGCG
IRS2ex2	CGACAGCCCTCCAATCAAGT	ACCAGTGTGTGGCAGTTCTC
FOXL2	ACACACGTATTGGTCCGTCC	GTGCAGTCCATGGCTAGACG

Quantitative PCR

Quantitative PCR (qPCR) is one of the methods that are widely used to detect copy number changes. This method is preferable due to its low consumable and instrumentation costs, high sensitivity and fast development time of assay (6–9). qPCR was performed to confirm the results of CNVPanelizer packages for *CEBPA* and *FOXL2* gene, the first and the second exons of *IRS2* gene and the first and the ninth exons of *ATRX* gene.

The qPCR mixes were prepared according to the GenPak PCR Core protocol (Isogene Lab ltd, Russia) in 20 µl reactions containing 1 ng genomic DNA and using SYBR green as a reporter and ROX as a reference dyes. All qPCR reactions were run in triplicate on a QuantStudio 5 Real-Time PCR System for Human Identification (Thermo Fisher Scientific, USA). The PCR conditions were as follows: 95°C for 5 min, followed by 40 cycles of 95°C for 20 seconds, 60°C for 20 seconds and 72°C for 20 seconds. Data were analyzed by the ΔΔCt method (10). The relative copy number was estimated by comparison with a normal blood control DNA sample. We used the *B2M* housekeeping gene as an endogenous control. Primer sequences for qPCR are shown in **Table 1**.

RESULTS

Sanger Sequencing

Point mutation Trp372Arg (Chr14:100,743,807, hg19) in *YY1* gene was not found in the tested samples.

Next Generation Sequencing

Median NGS read coverage was 486x, 461x, 471x, 454x for four tumor samples and 217x for a blood sample.

Single Nucleotide Variations

No pathogenic point mutations associated with any genetic syndrome including MEN1 were found in blood, neither pathogenic point mutations in tumor samples.

Copy Number Variations

CNVs in Tumors

CNVPanelizer in total has detected 54 genes within CNV regions, where 51, 14 and 4 genes were found in insulinoma, IMECCs #1 and #3, respectively (**Figure 2**). By using ONgene (11) and TSGgene (12) databases that aggregate information about oncogenes and tumor suppressor genes respectively, we identified several oncogenes and tumor suppressor genes with different CNV status in our tumor samples.

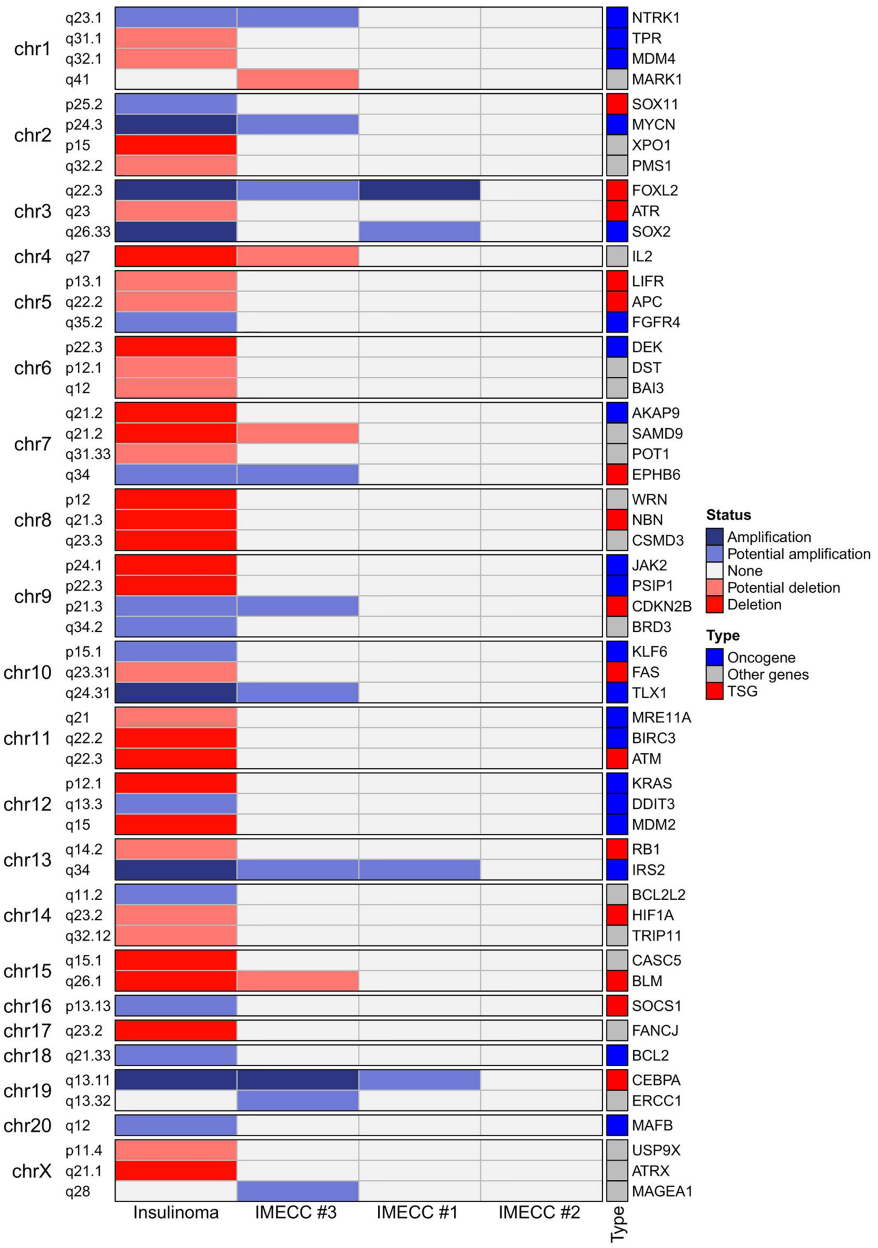

FIGURE 2 | Heatmap of the results of CNVPanelizer.

In insulinoma sample, ten oncogenes (*BCL2*, *DDIT3*, *FGFR4*, *IRS2*, *KLF6*, *MAFB*, *MYCN*, *NTRK1*, *SOX2* and *TLX1*) were with either putative or reliable status of gain, and nine tumor suppressor genes (*APC*, *ATM*, *ATR*, *BLM*, *FAS*, *HIF1A*, *LIFR*, *NBN* and *RB1*) were with putative or reliable status of loss.

With regards to IMECCs, in IMECC #1 sample two oncogenes, *SOX2* and *IRS2*, were with putative status of gain. In IMECC #3 four oncogenes, *IRS2*, *MYCN*, *NTRK1*, *TLX1*, were with putative status of gain and one tumor suppressor gene, *BLM*, with putative status of loss. In IMECC #2 according to CNVPanelizer no CNVs were detected.

With regards to the most common genes that mutate in pancreatic neuroendocrine neoplasms (panNENs) (*MEN1*, *ATRX* and *DAXX*) only loss of *ATRX* was detected in insulinoma sample. Visualizing the results of CNVPanelizer on genome coordinates (hg19) we have noticed that in the insulinoma sample the data for the first exon of *ATRX* was higher (shown in red rectangle) than the reference values, whereas the downstream exons were lower (**Figure 3**).

Recurrent CNVs

According to the results of CNVPanelizer, amplifications of *FOXL2*, *IRS2* and *CEBPA* genes were found in all samples except IMECC #2, (**Figure 2**). However, visualization of CNVPanelizer results (**Figure 3**) showed that in *IRS2* gene the second exon was lower in all tested samples including IMECC #2 compared to reference data, suggesting its loss.

Quantitative PCR

Gain status was confirmed in all samples for *FOXL2* gene. For *CEBPA*, only in insulinoma and IMECC #1 gain status was confirmed (p-value <0.001 and <0.01 respectively).

Amplification of the first exon of the *IRS2* gene was also confirmed in all samples (p-value <0.001 for all samples). However, the data on the second exon was various. Results qPCR with CNVPanelizer matched only in insulinoma sample (p-value <0.01).

Amplification of the first exon of *ATRX* in insulinoma sample that we noticed on CNVPanelizer was confirmed with a statistical significance of p-value < 0.01. The downstream loss of *ATRX* which we checked in the ninth exon was also confirmed with statistical significance of p-value < 0.05. These results show that CNVPanelizer can reliably detect CNVs in separate exons.

DISCUSSION

In this study, we describe genetic alterations in tumors that refer to such rare phenomenon as insulinomatosis in a patient without known hereditary syndromes.

Pancreatic Neuroendocrine Neoplasms

Pancreatic neuroendocrine neoplasms (panNENs or pNENs) are rare tumors of the pancreas that account for up to 2% of all pancreatic neoplasms. However, based on autopsy studies, prevalence of panNENs has been reported to be up to 10% (13). The 2017 World Health Organization classification divided panNENs into two categories, well-differentiated pancreatic neuroendocrine tumors (panNETs or PNETs) and poorly differentiated pancreatic neuroendocrine carcinomas (panNECs) (14). In the vast majority PNETs occur sporadically (~90%), but up to 5-10% are associated with genetic syndromes like multiple endocrine neoplasia type 1, neurofibromatosis type I,

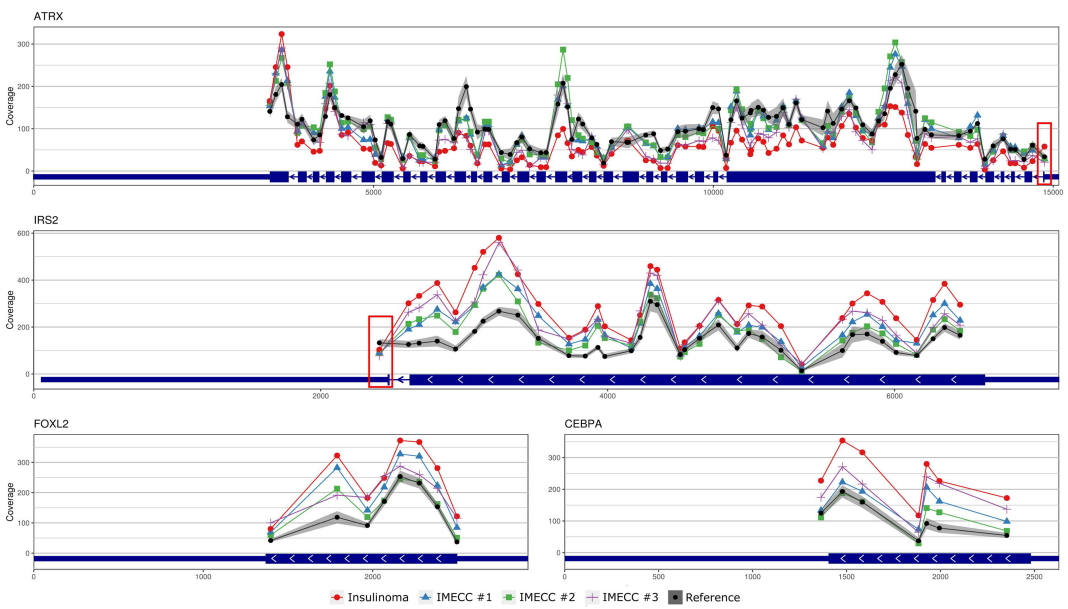

FIGURE 3 | Visualization of CNVPanelizer results on genomic coordinates (genome assembly GRCh37/hg19) of the genes *ATRX*, *IRS2*, *FOXL2* and *CEBPA*.

Von Hippel–Lindau syndrome and tuberous sclerosis complex (15). The most common functioning PNETs are insulinomas with an incidence of 4-7 per 100,000 persons per year (16–18). Most of insulinomas, more than 90%, are benign. Insulinomas are composed of producing beta cells that are actively secreting a large amount of insulin that results in episodic hyperinsulinemia and is the most frequent cause of persistent hyperinsulinemic hypoglycemia (1). In addition to Ki-67, which differentiates malignant and benign nature, tumor size is critical for survival rate prognosis. Thus, insulinomas >2 cm in diameter have a 10-year survival rate nearer to 30%, whereas for those <2 cm, the survival rate is close to 100% (19).

Molecular Genetics of Tumors in Insulinomatosis

The molecular genetic of insulinomatosis is yet to be understood. This phenomenon is not related to mutation in *MEN1* gene and is more similar to sporadic benign insulinomas (1). In insulinomas, mutations in *MEN1*, *ATRX* and *DAXX* that are often mutated in all PNETs occur in no more than 10 percent: 3%, 8% and 3%, respectively (20). In addition many other genes were seen to be mutated in insulinomas (20, 21) and several regions with amplification (7p, 3p, 5q and 13q) were identified as early events and may be involved in tumorogenesis (22). However, the most common mutation in insulinoma is a gain of function mutation Trp372Arg in *YY1* gene that occurs in 30% in Asian population and in 13% in Caucasian (German) population (23, 24). Mutation Trp372Arg increases the activity of YY1 as transcription factor, which results in greater transcription of *IDH3A*, *UCP2* and increases the expression of *ADCY1* and *CACNA2D2* which regulate the insulin secretion (22). It is assumed that mutations in *YY1* gene are driver mutations for insulinomas (25). In our case of insulinoma, we did not find Trp372Arg mutation in the *YY1* gene nor mutations in *MEN1* or *DAXX*, however, loss of *ATRX* was found and confirmed by qPCR (**Figures 2**–**4**).

As for other CNVs, alterations were found in 13q34 (amplification of *IRS2*), 13q14.2 (loss of *RB1*) and 5q22.2 (loss of *APC*) (**Figures 2**, **3**). With regards to the precursor lesions of PNETs, the information about their molecular genetic profile is very limited. Microadenomas are shown to harbor mutations in *MEN1* (13, 14, 26, 27). Hadano et al. in their work showed that sporadic microadenomas have a significantly lower expression of ATRX and overexpression of cytokeratin-19 (CK19) compared to hyperplasia of pancreatic islet cells (13). In our studied samples of micro-tumors, we have not found alteration in *MEN1*, but gain status in *IRS2*, *FOXL2* and *CEBPA* genes was found, suggesting that they can play a role in the development of micro- to macro-tumors, to wit insulinomas, and, accordingly, insulinomatosis.

Common Features and Filiation Between Micro- and Macro-Tumors

Besides the identity in monohormonality, our macro and micro-tumors samples share CNVs that harbor the same genes, *CEBPA*, *FOXL2* and *IRS2*. CCAAT enhancer-binding protein alpha (CEBPA) and Forkhead Box L2 (FOXL2) are known for being able to arrest or suppress cell proliferation respectively (28–30).

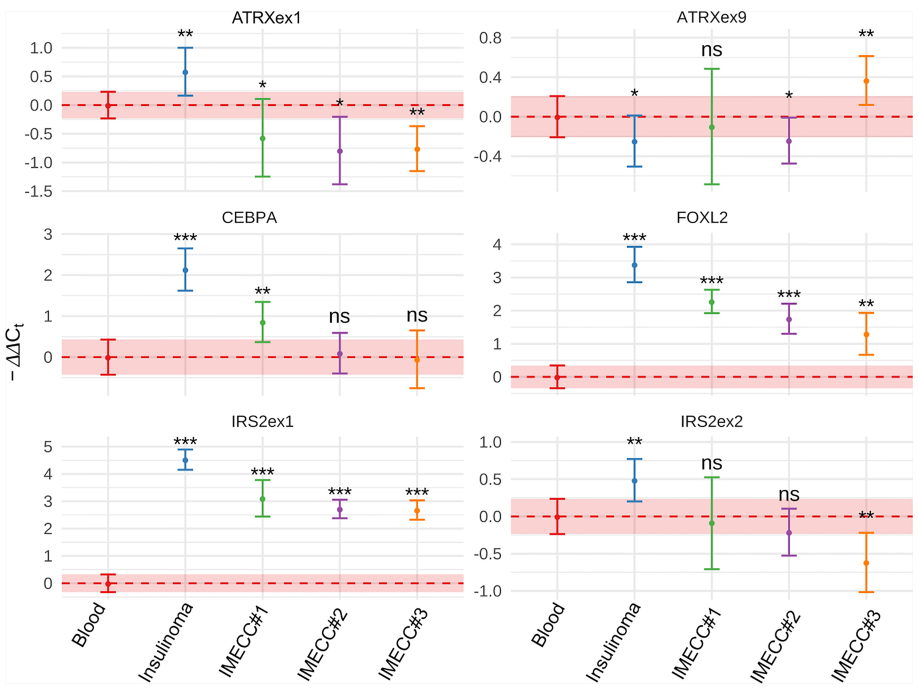

FIGURE 4 | Results of qPCR in blood, insulinoma and IMECCs by using ΔΔCt method. *p-value < 0.05. **p-value < 0.01. ***p-value < 0.001. ns, not significant.

The IRS2 (Insulin receptor substrate 2) protein plays an important role in the response to stimuli for cytokines and growth factors, like insulin and insulin-like growth factor 1, and promotes proliferation and survival of normal and cancer cells by mediating signaling from INSR, IGF1R, EPOR, MPL, VEGFR, LEP, GH and IFNB1/IFNG proteins. The stimulation of insulin receptor results in IRS2 association with the p85 subunit of PI3K and GRB2, activating the PI3K/AKT/MTOR and MAPK pathways and leading to proliferation and differentiation (31, 32).

It was shown that increased expression of CEBPA is involved in apoptosis of pancreatic β-cells exposed to proinflammatory cytokines IL1β, IFNγ, and TNFα (33). Also it was shown that CEBPA induce the transdifferentiation of B cells into macrophages, and in co-expression with the transcription factors Oct4 (Pou5f1), Sox2, Klf4 and Myc enhances reprogramming into induced pluripotent stem cells (34).

Mohanty in his work showed that overexpression of IRS2 stimulates proliferation of β-cells and increases insulin secretion. It also protects β-cells from d-glucose-induced apoptosis. On the contrary, the repression of IRS2 in INS-1 cells leads to downregulation of proliferation (35).

As insulinomatosis seems to be a disease that affects the entire population of β-cells, we can assume that this triad of genes, *CEBPA*, *FOXL2* and *IRS2*, participates in the disturbance of morphogenesis of β-cells, although of course, this statement requires more detailed investigations.

CONCLUSION

Despite the fact that detection of cancer associated CNVs has traditionally been performed by microarray techniques, NGS-based bioinformatic methods are actively developing and becoming increasingly popular due to cost-efficiency. However, the NGS-based bioinformatics results still need to be confirmed with other molecular approaches. On the other hand, molecular approaches such as qPCR are sensitive to the quality of material, which can be challenging when the samples are from FFPE tissues.

Here we described a rare case of insulinomatosis with novel CNVs that are seen in multiple micro-tumors and a macro-tumor and harbor *CEBPA*, *FOXL2* and *IRS2* genes that can be involved in pancreatic neuroendocrine tumor pathogenesis, specifically insulinomatosis, and can provide new insights into the disturbance of morphogenesis of β-cells.

DATA AVAILABILITY STATEMENT

The datasets presented in this study can be found in online repositories. The names of the repository/repositories and accession number(s) can be found below: https://www.ncbi.nlm.nih.gov/, PRJNA752875.

ETHICS STATEMENT

The studies involving human participants were reviewed and approved by Ethics Committee at the Research Centre for Medical Genetics, Moscow, Russia. The patients/participants provided their written informed consent to participate in this study. Written informed consent was obtained from the individual(s) for the publication of any potentially identifiable images or data included in this article.

AUTHOR CONTRIBUTIONS

IV, AS, and AV performed the surgical operation. LG performed the microscopy and immunohistochemistry. KA performed the DNA extraction, NGS, bioinformatics analysis, Sanger sequencing, and literature review. KK performed bioinformatics analysis and data visualization. LK and KA performed qPCR analysis. MS performed statistical analysis of qPCR results and assisted with bioinformatic analysis of CNV data. AE, SK, and VS administered the project. All authors contributed to the article and approved the submitted version.

FUNDING

The research was carried out within the state assignment of Ministry of Science and Higher Education of the Russian Federation for RCMG. Statistical analysis in this work was supported by the Grant of the Government of the Russian Federation № 14.W03.31.0005.

ACKNOWLEDGMENTS

We would like to thank the staff of the Shared Resource Centre "Genome" of FSBI RCMG for the help with sequencing. Also, we would like to thank Sandugash Tasmukanova for assistance with manuscript preparation (translation).

REFERENCES

1. Anlauf M, Bauersfeld J, Raffel A, Koch CA, Henopp T, Alkatout I, et al. Insulinomatosis. *Am J Surg Pathol* (2009) 33(3):339–46. doi: 10.1097/PAS.0b013e3181874eca
2. Perren A, Anlauf M, Henopp T, Rudolph T, Schmitt A, Raffel A, et al. Multiple Endocrine Neoplasia Type 1 (MEN1): Loss of One MEN1 Allele in Tumors and Monohormonal Endocrine Cell Clusters But Not in Islet Hyperplasia of the Pancreas. *J Clin Endocrinol Metab* (2007) 92(3):1118–28. doi: 10.1210/jc.2006-1944
3. Babic B, Keutgen X, Nockel P, Miettinen M, Millo C, Herscovitch P, et al. Insulinoma Due to Multiple Pancreatic Microadenoma Localized by Multimodal Imaging. *J Clin Endocrinol Metab* (2016) 101(10):3559–63. doi: 10.1210/jc.2016-2717
4. Wang K, Li M, Hakonarson H. ANNOVAR: Functional Annotation of Genetic Variants From High-Throughput Sequencing Data. *Nucleic Acids Res* (2010) 38(16):e164–4. doi: 10.1093/nar/gkq603
5. Oliveira C, Wolf T. *CNVPanelizer: Reliable CNV Detection in Targeted Sequencing Applications* (2021).

6. D'haene B, Vandesompele J, Hellemans J. Accurate and Objective Copy Number Profiling Using Real-Time Quantitative PCR. *Methods* (2010) 50 (4):262–70. doi: 10.1016/j.ymeth.2009.12.007
7. Daniell TJ, Davidson J, Alexander CJ, Caul S, Roberts DM. Improved Real-Time PCR Estimation of Gene Copy Number in Soil Extracts Using an Artificial Reference. *J Microbiol Methods* (2012) 91(1):38–44. doi: 10.1016/j.mimet.2012.07.010
8. Weaver S, Dube S, Mir A, Qin J, Sun G, Ramakrishnan R, et al. Taking qPCR to a Higher Level: Analysis of CNV Reveals the Power of High Throughput qPCR to Enhance Quantitative Resolution. *Methods* (2010) 50(4):271–6. doi: 10.1016/j.ymeth.2010.01.003
9. Ponchel F, Toomes C, Bransfield K, Leong FT, Douglas SH, Field SL, et al. Real-Time PCR Based on SYBR-Green I Fluorescence: An Alternative to the TaqMan Assay for a Relative Quantification of Gene Rearrangements, Gene Amplifications and Micro Gene Deletions. *BMC Biotechnol* (2003) 3(1):1–13. doi: 10.1186/1472-6750-3-18
10. Livak KJ, Schmittgen TD. Analysis of Relative Gene Expression Data Using Real-Time Quantitative PCR and the 2–ΔΔct Method. *Methods* (2001) 25 (4):402–8. doi: 10.1006/meth.2001.1262
11. Liu Y, Sun J, Zhao M. ONGene: A Literature-Based Database for Human Oncogenes. *J Genet Genomics* (2017) 44(2):119–21. doi: 10.1016/j.jgg.2016.12.004
12. Zhao M, Kim P, Mitra R, Zhao J, Zhao Z. TSGene 2.0: An Updated Literature-Based Knowledgebase for Tumor Suppressor Genes. *Nucleic Acids Res* (2016) 44:1023–31. doi: 10.1093/nar/gkv1268
13. Hadano A, Hirabayashi K, Yamada M, Kawanishi A, Takanashi Y, Kawaguchi Y, et al. Molecular Alterations in Sporadic Pancreatic Neuroendocrine Microadenomas. *Pancreatology* (2016) 16(3):411–5. doi: 10.1016/j.pan.2016.01.011
14. Khanna L, Prasad SR, Sunnapwar A, Kondapaneni S, Dasyam A, Tammisetti VS, et al. Pancreatic Neuroendocrine Neoplasms: 2020 Update on Pathologic and Imaging Findings and Classification. *RadioGraphics* (2020) 40(5):1240–62. doi: 10.1148/rg.2020200025
15. Jeune F, Taibi A, Gaujoux S. Update on the Surgical Treatment of Pancreatic Neuroendocrine Tumors. *Scand J Surg* (2020) 109(1):42–52. doi: 10.1177/1457496919900417
16. AIRTUM Working Group, Busco S, Buzzoni C, Mallone S, Trama A, Castaing M, et al. Italian Cancer Figures–Report 2015: The Burden of Rare Cancers in Italy. *Epidemiol Prev* (2016) 40(1 Suppl 2):1–120. doi: 10.19191/EP16.1S2.P001.035
17. Dasari A, Shen C, Halperin D, Zhao B, Zhou S, Xu Y, et al. Trends in the Incidence, Prevalence, and Survival Outcomes in Patients With Neuroendocrine Tumors in the United States. *JAMA Oncol* (2017) 3 (10):1335–42. doi: 10.1001/jamaoncol.2017.0589
18. Lawrence B, Gustafsson BI, Chan A, Svejda B, Kidd M, Modlin IM. The Epidemiology of Gastroenteropancreatic Neuroendocrine Tumors. *Endocrinol Metab Clin N Am* (2011) 40(1):1–18. doi: 10.1016/j.ecl.2010.12.005
19. Guilmette JM, Nosé V. Neoplasms of the Neuroendocrine Pancreas: An Update in the Classification, Definition, and Molecular Genetic Advances. *Adv Anat Pathol* (2019) 26(1):13–30. doi: 10.1097/PAP.0000000000000201
20. Stevenson M, Lines KE, Thakker RV. Molecular Genetic Studies of Pancreatic Neuroendocrine Tumors. *Endocrinol Metab Clin N Am* (2018) 47(3):525–48. doi: 10.1016/j.ecl.2018.04.007
21. Tate JG, Bamford S, Jubb HC, Sondka Z, Beare DM, Bindal N, et al. COSMIC: The Catalogue Of Somatic Mutations In Cancer. *Nucleic Acids Res* (2019) 47 (D1):D941–7. doi: 10.1093/nar/gky1015
22. Hong X, Qiao S, Li F, Wang W, Jiang R, Wu H, et al. Whole-Genome Sequencing Reveals Distinct Genetic Bases for Insulinomas and Non-Functional Pancreatic Neuroendocrine Tumours: Leading to a New Classification System. *Gut* (2020) 69 (5):877–87. doi: 10.1136/gutjnl-2018-317233
23. Cao Y, Gao Z, Li L, Jiang X, Shan A, Cai J, et al. Whole Exome Sequencing of Insulinoma Reveals Recurrent T372R Mutations in YY1. *Nat Commun* (2013) 4(1):2810. doi: 10.1038/ncomms3810
24. Lichtenauer UD, Di Dalmazi G, Slater EP, Wieland T, Kuebart A, Schmittfull A, et al. Frequency and Clinical Correlates of Somatic Ying Yang 1 Mutations in Sporadic Insulinomas. *J Clin Endocrinol Metab* (2015) 100(5):E776–82. doi: 10.1210/jc.2015-1100
25. Cromer MK, Choi M, Nelson-Williams C, Fonseca AL, Kunstman JW, Korah RM, et al. Neomorphic Effects of Recurrent Somatic Mutations in Yin Yang 1 in Insulin-Producing Adenomas. *Proc Natl Acad Sci* (2015) 112(13):4062–7. doi: 10.1073/pnas.1503696112
26. Anlauf M, Schlenger R, Perren A, Bauersfeld J, Koch CA, Dralle H, et al. Microadenomatosis of the Endocrine Pancreas in Patients With and Without the Multiple Endocrine Neoplasia Type 1 Syndrome. *Am J Surg Pathol* (2006) 30(5):560–74. doi: 10.1097/01.pas.0000194044.01104.25
27. Anlauf M, Perren A, Klöppel G. Endocrine Precursor Lesions and Microadenomas of the Duodenum and Pancreas With and Without MEN1: Criteria, Molecular Concepts and Clinical Significance. *Pathobiology* (2007) 74(5):279–84. doi: 10.1159/000105810
28. Timchenko NA, Harris TE, Wilde M, Bilyeu TA, Burgess-Beusse BL, Finegold MJ, et al. CCAAT/enhancer Binding Protein Alpha Regulates P21 Protein and Hepatocyte Proliferation in Newborn Mice. *Mol Cell Biol* (1997) 17(12):7353–61. doi: 10.1128/MCB.17.12.7353
29. Harris TE, Albrecht JH, Nakanishi M, Darlington GJ. CCAAT/Enhancer-Binding Protein-α Cooperates With P21 to Inhibit Cyclin-Dependent Kinase-2 Activity and Induces Growth Arrest Independent of DNA Binding. *J Biol Chem* (2001) 276(31):29200–9. doi: 10.1074/jbc.M011587200
30. Liu X-L, Meng Y-H, Wang J-L, Yang B-B, Zhang F, Tang S-J. FOXL2 Suppresses Proliferation, Invasion and Promotes Apoptosis of Cervical Cancer Cells. *Int J Clin Exp Pathol* (2014) 7(4):1534–43.
31. Patti M-E, Sun X-J, Bruening JC, Araki E, Lipes MA, White MF, et al. 4ps/Insulin Receptor Substrate (IRS)-2 Is the Alternative Substrate of the Insulin Receptor in IRS-1-Deficient Mice (∗). *J Biol Chem* (1995) 270(42):24670–3. doi: 10.1074/jbc.270.42.24670
32. Velloso LA, Folli F, Perego L, Saad MJA. The Multi-Faceted Cross-Talk Between the Insulin and Angiotensin II Signaling Systems. *Diabetes Metab Res Rev* (2006) 22(2):98–107. doi: 10.1002/dmrr.611
33. Barbagallo D, Giuseppe Condorelli A, Piro S, Parrinello N, Fløyel T, Ragusa M, et al. CEBPA Exerts a Specific and Biologically Important Proapoptotic Role in Pancreatic β Cells Through Its Downstream Network Targets. *Mol Biol Cell* (2014) 25:2333–41. doi: 10.1091/mbc.e14-02-0703
34. Di Stefano B, Sardina JL, van Oevelen C, Collombet S, Kallin EM, Vicent GP, et al. C/Ebpα Poises B Cells for Rapid Reprogramming Into Induced Pluripotent Stem Cells. *Nature* (2014) 506(7487):235–9. doi: 10.1038/nature12885
35. Mohanty S, Spinas GA, Maedler K, Zuellig RA, Lehmann R, Donath MY, et al. Overexpression of IRS2 in Isolated Pancreatic Islets Causes Proliferation and Protects Human β-Cells From Hyperglycemia-Induced Apoptosis. *Exp Cell Res* (2005) 303(1):68–78. doi: 10.1016/j.yexcr.2004.09.011

Conflict of Interest: The authors declare that the research was conducted in the absence of any commercial or financial relationships that could be construed as a potential conflict of interest.

Advantages of publishing in Frontiers

OPEN ACCESS
Articles are free to read for greatest visibility and readership

FAST PUBLICATION
Around 90 days from submission to decision

HIGH QUALITY PEER-REVIEW
Rigorous, collaborative, and constructive peer-review

TRANSPARENT PEER-REVIEW
Editors and reviewers acknowledged by name on published articles

Frontiers
Avenue du Tribunal-Fédéral 34
1005 Lausanne | Switzerland

Visit us: www.frontiersin.org
Contact us: frontiersin.org/about/contact

REPRODUCIBILITY OF RESEARCH
Support open data and methods to enhance research reproducibility

DIGITAL PUBLISHING
Articles designed for optimal readership across devices

FOLLOW US
@frontiersin

IMPACT METRICS
Advanced article metrics track visibility across digital media

EXTENSIVE PROMOTION
Marketing and promotion of impactful research

LOOP RESEARCH NETWORK
Our network increases your article's readership